VOLUME 120 NUMBER 3

# THE ASTROPHYSICAL JOURNAL

AN INTERNATIONAL REVIEW OF SPECTROSCOPY AND ASTRONOMICAL PHYSICS

## NOVEMBER 1954


SPECTROSCOPIC OBSERVATIONS OF AE AQUARII . . . *Alfred H. Joy* 377
THE ROTATIONAL VELOCITIES OF A-, F-, AND G-TYPE GIANT STARS *J. B. Oke and Jesse L. Greenstein* 384
THE ATMOSPHERE OF THE I COMPONENT OF EPSILON AURIGAE *Robert P. Kraft* 391
THE COMPOSITION OF THE PLANETARY NEBULA NGC 7027 . . *Lawrence H. Aller* 401
MAGNITUDES AND COLOR INDICES OF EXTRAGALACTIC NEBULAE DETERMINED PHOTOELECTRICALLY . . . *Edison Pettit* 413
PHOTOELECTRIC MEASUREMENTS OF EXTRAGALACTIC NEBULAE *C. J. van Houten, J. H. Oort, and W. A. Hiltner* 439
INTERSTELLAR POLARIZATION OF 405 STARS . . . *W. A. Hiltner* 454
A STUDY OF THE DISTRIBUTION OF RELATIVELY COOL STARS IN THE MILKY WAY . . . *J. J. Nassau and V. M. Blanco* 464
REDDENED EARLY M- AND S-TYPE STARS NEAR THE GALACTIC EQUATOR *J. J. Nassau, V. M. Blanco, and W. W. Morgan* 478
CLASSIFICATION OF THE S-TYPE STARS . . . *Philip C. Keenan* 484
SPECTRAL CLASSIFICATION WITH EXCEEDINGLY LOW DISPERSION *W. W. Morgan, A. B. Meinel, and Hugh M. Johnson* 506
IDENTIFICATION OF THE YELLOW CORONAL LINE *Charlotte Pecker, Donald E. Billings, and Walter Orr Roberts* 509
THE SOLAR PHOTOSPHERIC GRADIENT . . . *S. W. Henriksen* 521
PHOTOMETRIC STUDIES OF ASTEROIDS. II . . . *Ingrid Groeneveld and Gerard P. Kuiper* 529
PHOTOMETRIC STUDIES OF ASTEROIDS. III. THE LIGHT-CURVE OF 44 NYSA *Albert V. Shatzel* 547
PHOTOMETRIC STUDIES OF ASTEROIDS. IV. THE LIGHT-CURVES OF CERES, HEBE, FLORA, AND KALLIOPE . . . *Imam I. Ahmad* 551
A NEW $O_2$ BAND IN THE INFRARED AURORAL SPECTRUM *J. W. Chamberlain, C. Y. Fan, and A. B. Meinel* 560
VARIATIONS IN THE AURORAL SPECTRUM . . . *C. Y. Fan and D. H. Schulte* 563
ON THE PRODUCTION OF AURORAL ARCS BY INCIDENT PROTONS *Joseph W. Chamberlain* 566
THE PHYSICAL THEORY OF METEORS. VI. THE LIGHT-CURVE . . . *Allan F. Cook* 572
RADIATIVE EQUILIBRIUM IN A HYDROGEN ATMOSPHERE. I . . . *Allan F. Cook* 578
ON THE DYNAMICAL STABILITY OF MAGNETIC STARS . . . . *G. R. Burbidge* 589

NOTES

SPECTRUM OF NOVA OPHIUCHUS 1952 . . . *W. A. Hiltner* 596
A NOTE ON THE REPORTED COLOR-INDEX EFFECT OF DISTANT GALAXIES *H. Bondi, T. Gold, and D. W. Sciama* 597
OBSERVATIONAL STATUS OF THE COLOR-EXCESS EFFECT IN DISTANT GALAXIES *A. E. Whitford* 599
EAST-WEST MOTION OF AURORAE . . . *J. H. Meek* 602
DETERMINATION OF THE POLE OF ROTATION OF VENUS . . . *Gerard P. Kuiper* 603

ABSTRACTS OF ASTROPHYSICAL JOURNAL: SUPPLEMENT SERIES

THE INDEX OF CLUMPINESS OF THE DISTRIBUTION OF IMAGES OF GALAXIES *Jerzy Neyman, Elizabeth L. Scott, and C. D. Shane* 606
THE SPECTRUM OF THE *CN* MOLECULE . . . *A. E. Douglas and P. M. Routly* 607
ERRATUM . . . 607
INDEX . . . 609


THE UNIVERSITY OF CHICAGO PRESS
CHICAGO, ILLINOIS, U.S.A.

November 1954 Vol. 120, No. 3

# THE ASTROPHYSICAL JOURNAL

## AN INTERNATIONAL REVIEW OF SPECTROSCOPY AND ASTRONOMICAL PHYSICS

Founded in 1895 by George E. Hale and James E. Keeler

Published in Collaboration with the American Astronomical Society

S. CHANDRASEKHAR
*Managing Editor*

GERARD P. KUIPER
*Associate Editor*

Yerkes Observatory of the University of Chicago

EDITORIAL BOARD

MARTIN SCHWARZSCHILD, JR. (1954-58)
Princeton University Observatory

G. HERZBERG (1952-56)
National Research Council, Ottawa

H. W. BABCOCK (1953-57)
Mount Wilson Observatory of the Carnegie Institution of Washington

FRED L. WHIPPLE (1952-54)
Harvard College Observatory

C. D. SHANE (1952-55)
Lick Observatory, University of California

The Astrophysical Journal is published bimonthly by the University of Chicago at the University of Chicago Press, 5750 Ellis Avenue, Chicago 37, Illinois, during January, March, May, July, September, and November. ¶Two volumes are published per year, one beginning with the January issue and the other beginning with the July issue. The subscription price is $6.00 per volume or $12.00 per year; the price of single copies is $3.00. (Orders for service of less than a volume will be charged at the single copy rate.) ¶Postage is prepaid by the publishers on all orders from the United States and its possessions. No extra charge is made for postage to countries in the Pan American Postal Union. ¶Postage is charged extra as follows: for Canada, 20 cents per volume, 40 cents per year (total $6.20 per volume, $12.40 per year); on single copies 5 cents (total $3.05); for all other countries in the Postal Union, 40 cents per volume, 75 cents per year (total $6.40 per volume, $12.75 per year), on single copies 10 cents (total $3.10). ¶Subscriptions are payable in advance. Please make all remittances payable to The University of Chicago Press, in United States currency or its equivalent by postal or express money orders or bank drafts.

The following is an authorized agent:

For the British Commonwealth, except North America and Australasia: The Cambridge University Press, Bentley House, 200 Euston Road, London, N.W. 1, England. Prices of yearly subscriptions and of single copies may be had on application.

Claims for missing numbers should be made within the month following the regular month of publication. The publishers expect to supply missing numbers free only when losses have been sustained in transit, and when the reserve stock will permit.

Business correspondence should be addressed to The University of Chicago Press, Chicago 37, Illinois.

Communications for the editors and manuscripts should be addressed to: S. Chandrasekhar, Editor of THE ASTROPHYSICAL JOURNAL, Yerkes Observatory, Williams Bay, Wisconsin.

Line drawings and photographs should be made by the author, and all marginal notes such as co-ordinates, wave lengths, etc., should be included in the cuts. It will not be possible to set up such material in type.

One copy of the corrected galley proof should be returned as soon as possible to the editor, Yerkes Observatory, Williams Bay, Wisconsin. Authors should take notice that the manuscript will not be sent to them with the proof.

The cable address is "Observatory, Williamsbay, Wisconsin."

The articles in this journal are indexed in the *International Index to Periodicals*, New York, N.Y.

Applications for permission to quote from this journal should be addressed to The University of Chicago Press, and will be freely granted.

Microfilms of complete journal volumes are available to regular subscribers only and may be obtained at the end of the year. Orders and inquiries should be addressed to University Microfilms, 313 North First Street, Ann Arbor, Michigan.

Notice to subscribers: If you change your address, please notify us and your local postmaster immediately.

Entered as second-class matter, July 31, 1950, at the Post-Office at Chicago, Ill., under the Act of March 3, 1879.
Acceptance for mailing at special rate of postage provided for in United States Postal Act of October 3, 1917, Section 1103, amended February 28, 1925.

Copyright 1954 by the University of Chicago.

[PRINTED IN U.S.A.]

# THE ASTROPHYSICAL JOURNAL

AN INTERNATIONAL REVIEW OF SPECTROSCOPY AND ASTRONOMICAL PHYSICS

VOLUME 120 NOVEMBER 1954 NUMBER 3


## SPECTROSCOPIC OBSERVATIONS OF AE AQUARII


ALFRED H. JOY

Mount Wilson and Palomar Observatories



*Received May 24, 1954*



ABSTRACT

More than 100 spectrograms of AE Aquarii were obtained in the years 1943–1953. The absorption spectrum is dK0. Strong emission lines of *H*, *He*, and *Ca* II, 20 A in width, are present, accompanied at times by a continuum which indicates a high-temperature source. From the velocities of the dark and bright lines the elements of the orbits corresponding to two components of a spectroscopic binary were determined. The velocity range is more than 300 km/sec for the red star in a period of 0.701024 day, and the masses are nearly equal. The eccentricity is small. The absolute magnitude of the red star is +6.0. The hot star is somewhat fainter. The velocity-curve of the K0 star cannot be accounted for by a simple elliptical motion, but the deviations may result from illumination on one side by the hot primary and rotation somewhat faster than that necessary to keep the same face toward the other star. SS Cyg and RU Peg are probably similar to AE Aqr.


The spectrum of AE Aquarii was first observed by A. A. Wachmann (1931) on four objective-prism spectrograms of the Bergedorf *Spectraldurchmusterung*. The plates were obtained in the years 1923, 1929, and 1930. His estimate of spectral type, Md, based on the presence of strong emission lines, led to the presumption that the star was a long-period variable, and it was so designated in general variable-star catalogues until 1948.

Photographic observations by E. Zinner (1938) between 1929 and 1937 revealed that the light varied irregularly between 11.0 and 11.7 mag., except that on a few occasions the maxima reached 9.7 mag. Three of these outbursts occurred at intervals of about 371 days. He suggested that the variation was of the U Geminorum type.

Violent nova-like eruptions of this kind occur infrequently in AE Aquarii, but variations, probably semiregular in character, of about ½ mag. and several hours' duration, are often observed (Alden 1947; Henize 1949; Gaposchkin 1949*a*, *b*; Mayall 1951, 1952, 1954). Upon these are superimposed sharp flares lasting only a few minutes which are of sufficient intensity to double the total light of the star (Lenouvel 1952; Lenouvel and Golay 1953; Chiabetta 1953). Such variations are so frequent and sudden that they can be adequately followed only by the use of photoelectric methods. The changes in brightness are rapid and complex far beyond our previous experience with stellar variation.

In 1943 A. N. Vyssotsky reported in a personal letter that he had found strong bright *Ca* II (H and K), as well as hydrogen emission, in objective-prism spectra of the star. Mount Wilson spectrograms (Joy 1943), taken in 1943, showed clearly that the spectrum resembled that of SS Cygni at minimum light.

TABLE I

VELOCITY OBSERVATIONS OF AE AQUARII

| PLATE | J. D. 2430000+ | Phase Days | Absorption Velocity km/sec | WIDE EMISSION No. Lines | Int. | Velocity km/sec |
|---|---|---|---|---|---|---|
| E 951 | 0979.764 | 0.172 | +90 | - | 3 | - |
| γ 25495 | 0982.771 | .375 | -162 | 2 | 3 | +22 |
| E 986 | 1011.685 | .548 | -166 | 4 | 2 | +70 |
| 991 | 1012.622 | .082 | + 74 | 2 | 3 | -42 |
| 996 | 1019.694 | .145 | + 52 | 4 | 3 | -216 |
| E 1002 | 1020.638 | .387 | -179 | 4 | 3 | +20 |
| 1015 | 1034.649 | .378 | -187 | 5 | 3 | +35 |
| 1019 | 1035.669 | .696 | + 3 | 4 | 3 | -75 |
| γ 25664 | 1038.639 | .161 | + 68 | - | 2 | - |
| E 1086 | 1240.959 | .587 | -200 | 5 | 2 | +61 |
| E 1089 | 1241.944 | .169 | + 90 | 3 | 3 | -118 |
| 1152 | 1309.678 | .606 | -199 | - | 1 | - |
| 1155 | 1309.903 | .129 | +144 | 2 | 1 | -190 |
| 1158 | 1310.677 | .202 | + 88 | 2 | 1 | -174 |
| 1159 | 1310.722 | .247 | +106 | 3 | 1 | -159 |
| E 1161 | 1310.816 | .341 | - 98 | 2 | 1 | +46 |
| 1162 | 1310.856 | .381 | -177 | 3 | 1 | +86 |
| 1163 | 1310.897 | .422 | -196 | 4 | 1 | +88 |
| 1164 | 1310.938 | .463 | -186 | 3 | 2 | +114 |
| 1166 | 1311.667 | .491 | -180 | - | 1 | - |
| E 1167 | 1311.715 | .540 | -213 | 4 | 3 | +77 |
| 1168 | 1311.765 | .590 | -179 | 3 | 3 | +41 |
| 1170 | 1312.740 | .162 | +104 | 3 | 2 | -154 |
| 1171 | 1312.826 | .249 | + 55 | 3 | 3 | -161 |
| 1172 | 1312.885 | .308 | - | 3 | 3 | -41 |
| E 1178 | 1327.663 | .364 | - | 2 | 2 | +88 |
| 1179 | 1327.715 | .416 | -166 | 4 | 3 | +84 |
| 1180 | 1327.764 | .464 | -199 | - | 0 | - |
| 1182 | 1328.653 | .652 | -150 | 3 | 2 | +39 |
| 1183 | 1328.701 | .000 | - 58 | 3 | 1 | -28 |
| E 1184 | 1328.745 | .044 | + 39 | 3 | 2 | -123 |
| 1185 | 1328.788 | .086 | + 86 | 3 | 3 | -183 |
| 1188 | 1329.665 | .263 | + 68 | 3 | 3 | -140 |
| 1189 | 1329.706 | .304 | + 25 | 2 | 3 | -83 |
| 1193 | 1330.824 | .020 | + 59 | 3 | 3 | -26 |
| E 1194 | 1330.861 | .057 | + 84 | 2 | 3 | -103 |
| 1197 | 1331.653 | .147 | + 83 | - | 1 | - |
| 1198 | 1331.699 | .193 | +108 | 3 | 2 | -198 |
| 1199 | 1331.743 | .238 | + 70 | 3 | 3 | -178 |
| 1200 | 1331.781 | .275 | + 1 | 4 | 3 | -159 |
| γ 26198 | 1339.766 | .549 | -191 | - | 3 | - |
| 26202 | 1340.729 | .110 | + 88 | 1 | 3 | -101 |
| 26208 | 1341.745 | .425 | -209 | 3 | 3 | +98 |
| 26215 | 1342.732 | .010 | 0 | 3 | 2 | - 2 |
| 26220 | 1355.685 | .344 | - 81 | 2 | 3 | -30 |
| γ 26241 | 1360.638 | .390 | -122 | 4 | 3 | +56 |
| 26242 | 1360.735 | .487 | -223 | 2 | 2 | +137 |
| E 1501 | 1711.867 | .407 | -229 | 4 | 2 | +83 |
| 1504 | 1712.641 | .480 | -190 | 4 | 2 | +81 |
| 1505 | 1712.701 | .540 | -224 | 4 | 2 | +88 |

TABLE I (Cont'd)

| | | | | | | | |
|---|---|---|---|---|---|---|---|
| E | 1506 | 1712.764 | .602 | - 90 | 4 | 3 | +30 |
| | 1514 | 1742.635 | .329 | - 96 | 3 | 2 | -49 |
| | 1520 | 1744.634 | .225 | + 74 | 3 | 3 | -201 |
| | 1521 | 1744.690 | .281 | - 57 | 4 | 3 | -41 |
| γ | 27172 | 1755.657 | .032 | + 34 | 2 | 3 | -77 |
| E | 1723 | 2009.971 | .575 | -124 | - | 1 | - |
| | 1726 | 2010.867 | .069 | + 48 | 2 | 1 | -116 |
| | 1727 | 2010.917 | .119 | +100 | 3 | 2 | -155 |
| | 1728 | 2010.969 | .171 | + 86 | 3 | 2 | -182 |
| γ | 27836 | 2022.834 | .119 | + 48 | 1 | 2 | -186 |
| E | 1732 | 2039.712 | .172 | + 74 | 3 | 2 | -138 |
| | 1734 | 2039.955 | .415 | -223 | 4 | 1 | +109 |
| | 1735 | 2040.770 | .529 | -212 | 2 | 3 | +48 |
| | 1758 | 2081.754 | .152 | + 83 | 4 | 3 | -194 |
| | 1858 | 2376.958 | .226 | + 39 | 2 | 2 | -158 |
| E | 1860 | 2377.851 | .418 | -145 | 2 | 3 | +60 |
| γ | 28970 | 2458.717 | .656 | - 51 | 4 | 2 | -37 |
| | 29047 | 2465.751 | .690 | + 39 | - | 2 | - |
| | 29619 | 2718.911 | .079 | + 27 | - | 2 | - |
| | 29620 | 2718.959 | .127 | + 97 | - | 2 | - |
| E | 2626 | 4521.946 | .080 | + 67 | 2 | 2 | -28 |
| | 2633 | 4523.960 | .693 | - 11 | 3 | 2 | -62 |
| | 2636 | 4524.881 | .211 | + 87 | 2 | 2 | -124 |
| | 2637 | 4524.964 | .294 | - 5 | 3 | 3 | -101 |
| | 2638 | 4526.928 | .155 | + 97 | 2 | 3 | -195 |
| E | 2653 | 4556.919 | .002 | + 9 | 4 | 3 | -24 |
| | 2654 | 4556.975 | .058 | + 71 | 3 | 3 | -172 |
| | 2658 | 4557.906 | .288 | + 43 | - | 2 | - |
| | 2659 | 4557.944 | .326 | - 63 | 2 | 2 | + 2 |
| | 2660 | 4557.982 | .364 | -138 | 4 | 3 | +80 |
| E | 2667 | 4558.953 | .634 | - 65 | - | 1 | - |
| | 2668 | 4558.985 | .666 | + 3 | - | 0 | - |
| | 2674 | 4559.983 | .262 | + 11 | 3 | 3 | -187 |
| | 2678 | 4576.815 | .270 | + 53 | - | 2 | - |
| | 2679 | 4576.851 | .306 | - 25 | 2 | 2 | +16 |
| E | 2680 | 4576.888 | .343 | - 92 | 4 | 3 | +24 |
| | 2681 | 4576.931 | .385 | -156 | 3 | 2 | +113 |
| | 2682 | 4576.975 | .429 | -203 | 4 | 3 | +80 |
| | 2684 | 4577.750 | .503 | -198 | 4 | 3 | +76 |
| | 2687 | 4577.858 | .611 | -131 | - | 2 | - |
| E | 2688 | 4577.895 | .648 | - 30 | 2 | 3 | + 4 |
| | 2689 | 4577.939 | .692 | + 21 | 1 | 1 | -101 |
| | 2690 | 4577.980 | .032 | + 96 | 2 | 1 | -138 |
| | 2694 | 4578.864 | .215 | + 96 | - | 0 | - |
| | 2695 | 4578.900 | .251 | + 34 | - | 1 | - |
| E | 2696 | 4578.943 | .294 | - 43 | - | 0 | - |
| | 2697 | 4578.982 | .333 | -112 | - | 0 | - |
| | 2715 | 4646.738 | .090 | + 96 | - | 0 | - |
| | 2716 | 4646.783 | .135 | + 99 | 3 | 3 | -175 |
| | 2719 | 4647.636 | .287 | + 44 | 2 | 2 | -165 |
| E | 2720 | 4647.683 | .334 | - 65 | 4 | 3 | -95 |
| | 2721 | 4647.731 | .382 | -116 | 4 | 3 | +111 |
| | 2722 | 4647.778 | .430 | -215 | 2 | 1 | +128 |
| | 2725 | 4648.639 | .589 | -146 | 2 | 1 | +53 |
| | 2726 | 4648.699 | .649 | - 72 | 2 | 2 | + 4 |
| E | 2727 | 4648.758 | .007 | + 56 | 2 | 1 | -70 |
| | 2728 | 4648.818 | .067 | + 76 | - | 1 | - |

In six different seasons since 1943, more than one hundred spectrograms of AE Aquarii (Table 1) were obtained on Mount Wilson. The dispersion is about 110 A/mm at $H\gamma$, and the exposure times were usually 1 and 2 hours at the 100-inch and 60-inch telescopes, respectively. The spectrograms all show strong, deep absorption lines corresponding to type dK0. Superposed upon the absorption spectrum are wide emission lines of *H*, *He* I, and *Ca* II, which vary in width and intensity (Fig. 1, *a*, *b*). In the region λλ 3500–3700, many of the plates show an emission continuum (Fig. 1, *d*) whose intensity appears to be correlated with that of the broad emission lines.

Narrow emission lines, 2–5 A in width, are usually present within the broad emission lines H and K (*Ca* II) and are occasionally visible in the hydrogen lines $H\delta$, $H\epsilon$, and $H\zeta$ (Fig. 1, *e*).

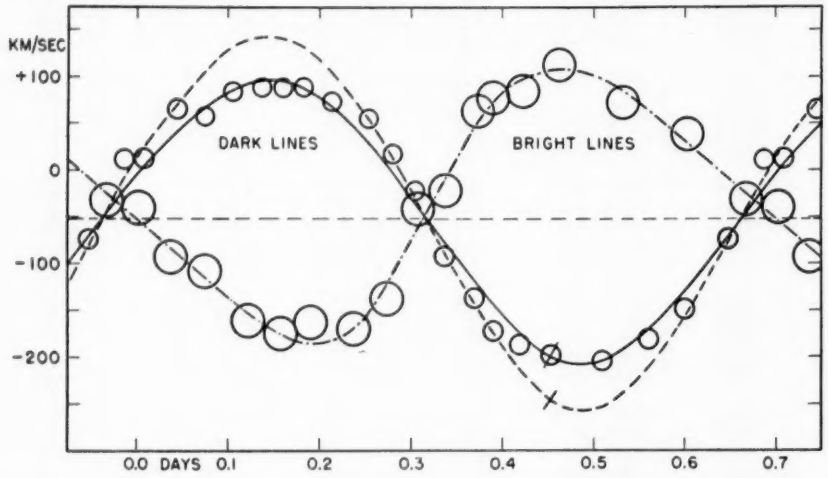


FIG. 2.—Velocity-curves of AE Aquarii. Large circles are means of five observations of the wide bright lines. Small circles are means of five observations of the absorption lines of the K0 star.

By plotting the radial velocities determined from the broad bright lines and the absorption lines (Table 1) against time, a period of 0.701024 day was found to represent the observations reasonably well. Since the observations cover more than 5000 cycles and often were closely spaced throughout single and successive nights, the period must be essentially correct and constant during the time of the observations. Individual cycles may differ somewhat from the mean curve, but the measures are not of sufficient accuracy to decide definitely whether such deviations are real.

In Figure 2 normal places, each representing independent means of the velocities from five plates, are plotted (bright lines, *large circles;* dark lines, *small circles*). The phases are computed from the elements

$$\text{JD } 2431328.7014 + 0^{d}701024E\,,$$

which are based on the velocities from the numerous and well-defined dark lines. The mean values deserve considerable weight in spite of low dispersion. The narrow bright lines of *Ca* II are likewise easily measured and give practically the same velocities as the dark lines. Measures of these bright lines on thirty-seven plates show a mean systematic

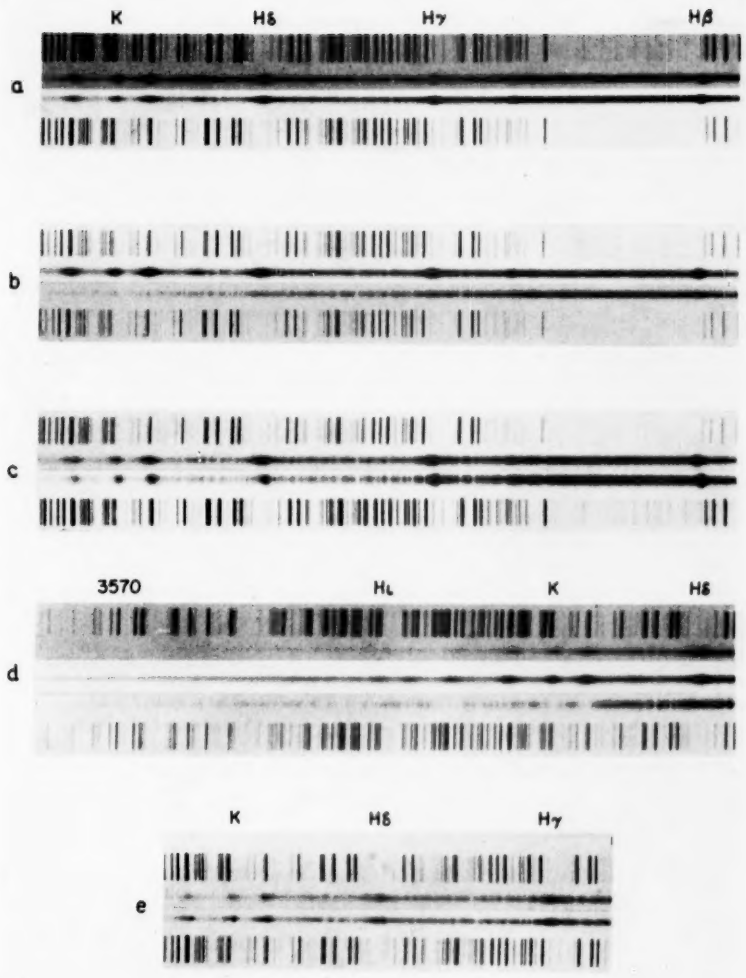


FIG. 1.—Spectra of AE Aquarii. *a*, E 1189 and E 1194, narrow and wide emission of *H* and *Ca* II. *b*, E 1171 and E 1197, strong and weak emission of *H* and *Ca* II. *c*, E 1758 and E 1015, bright lines displaced shortward and to the red. *d*, E 1727, E 1188, and E 1778, faint and strong violet continuum, with spectrum of 20C173 K2 (*below*) for comparison. *e*, E 1505 and E 1199, sharp bright lines *Hδ*, K, and *Hζ* displaced to violet and to red upon the wide bright lines.

deviation of only −0.7 km/sec, as compared with the absorption-line velocities of the same plates.

The broad bright lines of *H* and *Ca* II, on the contrary, are 15–22 A in width and are exceedingly difficult to measure accurately (Fig. 1, *c*). Their symmetry is often poor because of the presence of the narrow emission lines and other unexplained effects. Measures of these lines were made with low magnification, the displacements being determined either by bisecting the lines or by taking the mean of the settings on the edges of the lines. The precision is consequently low.

Curves drawn through the observations resemble those of spectroscopic binaries in which the lines of both components are present. The γ-velocity, determined by equalizing the areas of the curves above and below the γ-line, is −52.6 km/sec for the K0 star. The orbit is nearly circular; $e = 0.031$, $\omega = 160°.6$, and $T$ = phase 0.452 day at periastron.

Attempts to complete the solution of the orbits were futile because gravitational ellipses fail to provide velocity-curves which have steep slopes at conjunctions and flat maxima at elongations, such as seem definitely characteristic of the velocity-curve from the dark lines of AE Aquarii.

The observations near conjunctions at phases 0.223–0.390 and 0.600–0.045 day indicate a large amplitude with $K_1 = 200$ km/sec (solution *I*, *dashed curve*, Fig. 2); but the remaining observations near elongations, phases 0.075–0.185 and 0.450–0.560 day, are well satisfied by $K_1 = 151$ km/sec (solution *II*, *solid line*). The corresponding values of $a_1 \sin i$ are 1,930,000 and 1,460,000 km, respectively.

Whatever the cause of these peculiarities may be, the system is fairly well defined by the velocities deduced from the absorption lines alone, and it seems to resemble a binary rather than a single star disturbed by pulsations or turbulent outbreaks. The absorption spectra show no indications of ionization such as might be expected from periastron effects or of origin in surrounding gaseous shells or envelopes.

The velocity-curve (*dot and dash*) of the bright lines suggests that the source of the broad bright lines is evidently connected with a second component of a binary system. For this source, $K = 146$ km/sec, a value slightly smaller than that found for the K0 star in solution II. The corresponding minimum masses are

Solution I ($K_1 = 200$ km/sec): $m \sin^3 i = 1.70 \odot$,

$$m_1 \sin^3 i = 1.30 \odot ;$$

Solution II ($K_1 = 151$ km/sec): $m \sin^3 i = 0.97 \odot$,

$$m_1 \sin^3 i = 0.94 \odot .$$

The curve of the bright lines shows somewhat larger eccentricity than that of the dark lines, and the γ-velocity is about 10 km/sec more positive. These differences may well be accidental and due to the inaccuracy of the measures, although the displacement of the γ-velocity is about what might be expected from the relativity shift in a small dense body of this kind. The bright lines vary in strength (Table 1, sixth column) and in width; but these changes show no correlation with the orbital period found from the dark lines and may be the result of outbursts in the hot star.

The extreme width of the absorption lines of medium strength, such as λλ 4063, 4260, and 4415 of iron, is 1.5–2.0 A. Widening of this amount may be attributed to change in velocity during the exposure and to rotational broadening, assuming that the period of rotation is nearly the same as that of the orbital period and that the radius of the star is 0.9 ⊙.

Using the formula relating luminosity, temperature, and radius,

$$M_v = \frac{29{,}500}{T} - 5 \log R - 0.08 ,$$

and taking $T = 5000°$ and $R = 0.9 \odot$ for the temperature and radius, respectively, of the dK0 star, we have, for the absolute magnitude, $M_v = +6.0$, which is only slightly below the main sequence at K0. The corresponding parallax is 0".008, using 11.5 for the visual magnitude.

Since the continuous spectrum of the primary star with the bright emission lines is faint as compared with that of the K0 star, its total visual luminosity must be at least 1 mag. fainter than that of the red companion. Its absolute magnitude, then, is about +7.0, and we conclude that it is a faint subdwarf with emission lines. The width of the bright lines indicates a shell or envelope expanding at about 750 km/sec.

Assuming a temperature of 20,000°, which is justified by the ratio of the intensities of the continuous spectrum at λ 3500 A and at λ 4300 A as compared with that of the

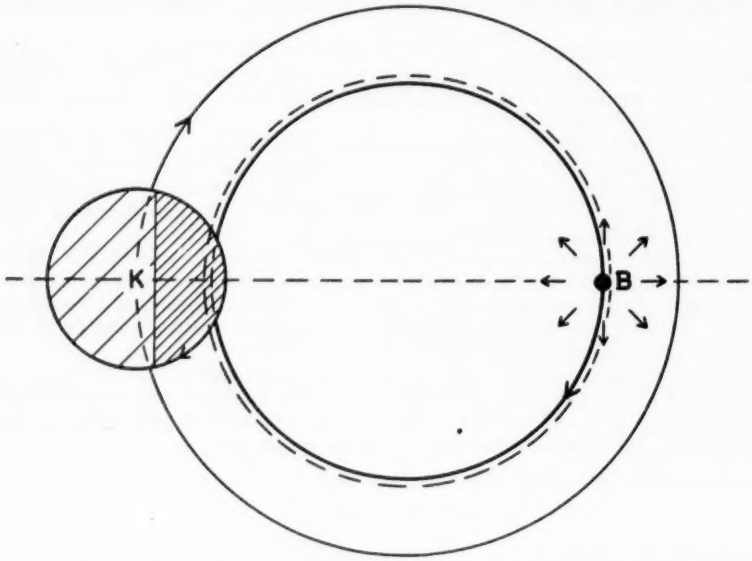


FIG. 3.—Estimated sizes and separation of the two components of AE Aquarii. The shaded portion indicates the area affected by radiation from the small hot star.

B0 stars and taking $M_v = +7.0$ in the same equation used previously, the radius of the hot star is found to be 0.08 ⊙.

No entirely satisfactory explanation for the strange velocity-curve deduced from the absorption lines has been suggested. As indicated in Figure 3, the distance between the two stars is moderately large as compared with their diameters. In stars of small size and high density, large tidal distortion is unlikely. The radiation of the hot star falling upon a hemisphere of the K0 star may be sufficient to displace the maximum illumination toward the substellar point and thus transfer the effective source of light from the center of the disk to a point nearer the center of gravity of the system, where the linear orbital velocity is slower if the star keeps the same face toward its primary. Under these conditions a more rapid rotational velocity would work in the same direction, decreasing the observed radial velocity at elongation. Possibly both these effects may be present. Quantitative analysis of these suggestions is hardly justified until more accurate data can be obtained. If these conditions prevail, solution I would more closely represent the real

orbit of the K0 star, though the greater masses resulting seem less probable. Also, photoelectric observers should be able to detect underlying changes in brightness of the star in the 0.70-day period; for at conjunction the bright side of the K0 star would be in view when it is behind, and the faint side when it is in front. However, no spectroscopic differences have been detected at these phases.

The explanation of the light-changes of AE Aquarii is far from complete. Periodic variation due to possible reflection or heating effects upon one hemisphere of the K0 star has not yet been disentangled from other less regular fluctuations. Three other types of light-variation have been found by the variable-star observers: (1) the occasional outbursts of several magnitudes of the nova or SS Cygni type, which were first noted by Zinner but have not yet been spectroscopically observed; (2) the irregular variation of about ½ mag. in a cycle of several hours (perhaps 1.0 day), as observed by Lenouvel and others; the increases of light due to this type of variation may result in the intensification of the emission continuum and the broad bright lines; (3) the sharp, short flares, which increase the brightness of the star by as much as 1 mag., may occur in either star. Such sudden flares originating in local areas are well known in the late-type dwarfs. In the K0 spectrum they may be manifested by increases in intensity of the sharp *H* and *Ca* II lines. In the hot star such rapid outbreaks may correspond to those found by Merle F. Walker (1954) in several old novae.

The general spectroscopic features of AE Aquarii also are found in the variables SS Cygni and RU Pegasi. The spectral type of SS Cyg from the absorption lines is about dG5, and the shortward continuum is stronger than in AE Aqr. For RU Peg the type is dK0; bright *H* and *Ca* II are weak, and the hot continuum has not been seen. The velocity changes are large and rapid in both stars, but periods have not yet been found.

## REFERENCES

Alden, H. L. 1947, *Pop. Astr.*, **55**, 557.
Chiabetta, R. 1953, *A.A.V.S.O. Abstr.*, p. 3 (fall meeting).
Gaposchkin, S. 1949*a*, *A.J.*, **54**, 128.
———. 1949*b*, *Harvard Bull.*, No. 919, p. 25.
Henize, K. G. 1949, *A.J.*, **54**, 89.
Joy, A. H. 1943, *Pub. A.S.P.*, **55**, 283.
Lenouvel, F. 1952, *C.R. Acad. sci., Paris*, **235**, 1282.
Lenouvel, F., and Golay, M. 1953, *C.R. Acad. sci., Paris*, **237**, 1215.
Mayall, M. 1951, *A.J.*, **56**, 44.
———. 1952, *J.R.A.S. Canad.*, **46**, 247.
———. 1954, *ibid.*, **48**, 22.
Wachmann, A. A. 1931, *A.N.*, **242**, 382.
Walker, Merle. 1954, *Pub. A.S.P.*, **66**, 71.
Zinner, E. 1938, *A.N.*, **265**, 345.

# THE ROTATIONAL VELOCITIES OF A-, F-, AND G-TYPE GIANT STARS

J. B. OKE*
David Dunlap Observatory, University of Toronto

and

JESSE L. GREENSTEIN
Mount Wilson and Palomar Observatories
Carnegie Institution of Washington
California Institute of Technology

*Received June 18, 1954*

## ABSTRACT

Rotational velocities of 34 giant stars of spectral classes A, F, and G have been obtained from high-dispersion spectrograms. Velocities as high as 170 km/sec are found to occur. Comparison of computed and observed broadened profiles indicates that the broadening is probably due to rotation. A study of the positions of the stars in the Hertzsprung-Russell diagram, in conjunction with the evolutionary models of Sandage and Schwarzschild, shows that the rotational velocities observed are consistent with the stars having originally been A- and F-type stars on the main sequence.

## I. INTRODUCTION

Rotational velocities of many stars have been obtained by Struve, Elvey, Westgate, Slettebak, and others, mostly for early-type stars at fairly low dispersion. More recently there has developed an interest in the rotational velocities of later-type stars in which a fairly high dispersion is required to obtain the necessary accuracy. Recent work has been done with a dispersion of about 10 A/mm (Huang 1953; Slettebak 1954). It has already been shown that there is considerable difference between the rotational velocities of main-sequence stars and giant stars of the same spectral class (Herbig and Spalding 1953; Slettebak 1954). Since one of the authors (J. L. G.) had obtained very high-dispersion spectra of many A-, F-, and G-type giant stars, it was decided that a study of the rotational velocities, as measured on these high-dispersion plates, would be valuable, particularly in view of the recent theories of the evolution of such stars.

## II. OBSERVATIONAL MATERIAL

Thirty-four stars for which good spectrograms were available were chosen; their luminosity classes were nearly all from II to IV. All spectrograms, apart from one taken at the McDonald Observatory, were obtained with the coudé spectrograph of the 100-inch telescope. In Table 1 are listed the names of the stars, the spectral and luminosity classes, and the dispersion in A/mm. A step-slit calibration was put on each plate with the standard equipment of the coudé spectrograph. Microphotometer tracings were made between the wave lengths 4460 and 4560 A.

The stars available were observed in the course of a survey by Greenstein of the A and F stars for differences in spectra dependent on space motion. As a consequence, one selection factor is a higher-than-normal fraction of high-velocity stars. But, in addition, unfortunately for statistical completeness, a few well-known giants were not observed because they were known to have excessively large rotation. Of the standard giant stars (Morgan, Keenan, and Kellman 1943), the following were omitted: $\beta$ Tri (A5 III), $\alpha$ Oph (A5 III), $\beta$ Cas (F2 III or IV), $\upsilon$ UMa (F2 III), $\alpha$ Tri (F5 III or IV), and $\beta$ Del (F5 III). A set of visual estimates of line width has been made on available lower-dispersion mate-

* This work was carried out in part at the Princeton University Observatory.

rial for all stars except $\beta$ Tri. These five omitted stars have large rotational velocities, $v \sin i$, in the range of 75–150 km/sec, i.e., line widths comparable to those in $\gamma$ Boo, $\xi$ Gem, and $\gamma$ Her. As a consequence, a more detailed and complete survey of the standard A and F giants would add more high rotational-velocity points to the diagram in Figure 3.

### III. DETERMINATION OF THE ROTATIONAL VELOCITIES

The choice of a line from which to measure the rotational velocity should be based on the following considerations: (1) the unbroadened line should not show much change in shape and intensity over the spectral region being considered; (2) the unbroadened line should be as sharp as possible and preferably symmetrical; (3) the line should be sufficiently isolated so that when it is broadened it remains unblended; (4) the line should be strong enough that it does not disappear when broadened; (5) the line should be in a spectral region where the continuum can be defined fairly accurately. In late-type stars these conditions are satisfied for only a very few lines; the line which was chosen was an *Fe* I line at $\lambda$ 4476.0. This line proved almost ideal, since it satisfied all the foregoing conditions. The only drawback of this line is that it nearly disappears for stars with very

TABLE 1

ROTATIONAL VELOCITIES, LUMINOSITIES, AND RADII

| Star | Spectrum | Dispersion (A/Mm) | $v \sin i$ | $M_b$ | $R/R_\odot$ | $R/R_0$ |
|---|---|---|---|---|---|---|
| $\epsilon$ And | G8 III | 2.9 | 9 | +1.7 | 6.3 | 4.5 |
| $\beta$ Cet | K0 III | 2.9 | 18 | +0.4 | 12.9 | 7.2 |
| $\zeta$ And* | K1 II | 4.5 | 47 | +1.2 | 10.0 | 6.7 |
| $\upsilon$ And | F8 V | 4.5 | 11 | +3.2 | 1.8 | 1.6 |
| $\beta$ Lep | G0 III | 4.1 | 11 | −1.3: | 17.8 | 6.8 |
| $\delta$ Lep | G8 III | 2.9 | 0 | +0.3: | 12.3 | 6.8 |
| $\xi$ Gem | F5 III | 4.5 | 73 | +1.9 | 2.8 | 2.0 |
| $\iota$ Gem | K0 III | 4.5 | 9 | +0.9 | 10.2 | 6.2 |
| $\kappa$ Gem | G8 III | 4.5 | 8 | +0.4: | 11.7 | 6.5 |
| $\rho$ Pup | F6 II | 2.9 | 16 | +0.4: | 6.6 | 3.7 |
| $\epsilon$ Hya† | G0 III | 10.2 | 15 | −1.4: | 18.6 | 6.6 |
| $\theta$ UMa | F6 IV | 4.5 | 8 | +1.9 | 3.0 | 2.1 |
| $\zeta$ Leo | F0 III | 10.2 | 83 | −1.7: | 10.5 | 3.8 |
| 18 Com | F5 III | 4.5 | 98 | ..... | .... | .... |
| 31 Com | G0 III | 4.5 | 78 | +0.0: | 9.8 | 4.9 |
| 53 Vir | F6 III–IV | 10.2 | 19 | +4.0 | 1.2 | 1.1 |
| 20 CVn | F2 III | 10.2 | 16 | +1.0: | 3.5 | 2.1 |
| $\beta$ Com | G0 V | 4.5 | 10 | +4.6 | 0.9 | 1.0 |
| $\eta$ Boo* | G0 IV | 4.5 | 16 | +2.2 | 3.0 | 2.2 |
| $\gamma$ Boo | A7 III | 2.9 | 133 | −1.2: | 7.2 | 2.9 |
| $\beta$ CrB‡ | F0 III | 20.4 | 43 | +1.1 | 2.9 | 1.8 |
| $\gamma$ Her | A9 III | 10.2 | 171 | −0.4: | 5.5 | 2.5 |
| $\eta$ Her | G8 III | 2.9 | 8 | +1.9 | 5.2 | 3.7 |
| 20 Oph | F6 III | 4.5 | 15 | +0.3: | 6.6 | 3.7 |
| $\beta$ Dra | G2 II | 2.9 | 13 | −2.3: | 35 | 11.7 |
| $\pi$ Sgr§ | F2 II | 4.5 | 30 | −0.4: | 6.6 | 3.3 |
| $\gamma$ Equ‡ | F0 IIIp | 2.9 | 0 | +1.3: | 2.6 | 1.6 |
| $\gamma$ Cap | F2 IIIp | 2.9 | 29 | +0.7: | 4.1 | 2.4 |
| $\pi$ Peg‖ | F5 II–III | 4.5 | 147 | −0.2: | .... | .... |
| 37 Peg† | F5 III | 4.5 | 64 | +2.9: | 1.7 | 1.3 |
| $\eta$ Peg | G2 II–III | 2.9 | 9 | −1 : | .... | .... |
| $\xi$ Peg | F7 V | 4.5 | 5 | +2.6 | 2.3 | 2.0 |
| $\mu$ Peg | K0 III | 4.5 | 7 | +0.8 | 10.7 | 6.5 |
| $\gamma$ Psc | G8 III | 4.5 | 7 | +0.5: | 11.2 | 6.2 |

* Spectroscopic binary. Rotation possibly synchronous for $\zeta$ And.

† Brighter component of visual binary.

‡ Magnetic variable.

§ Visual binary, rotational velocity from combined spectrum.

‖ Shell star.

high rotational velocities. To circumvent this difficulty, a strong blended line (*Ti* II and *Fe* II) at λ 4549.6 was also chosen which was used for stars with high rotational velocities. This line is not symmetrical but is still narrow enough that, for high rotational velocities, the profile is not important.

Intensity profiles were obtained for these lines by the usual methods. The continuum was defined by choosing the highest points on the tracing over a region of 100 A, using the sharp-line stars, and the same points were used for all stars. A comparison was also made with the Utrecht atlas of the solar spectrum.

In determining the rotationally broadened profiles, the first step is to obtain the unbroadened profile. It was assumed that the profiles of λ 4476 in the two stars δ Lep (G8 III) and γ Equ (F0 IIIp) were unbroadened by rotation. The second of these stars,

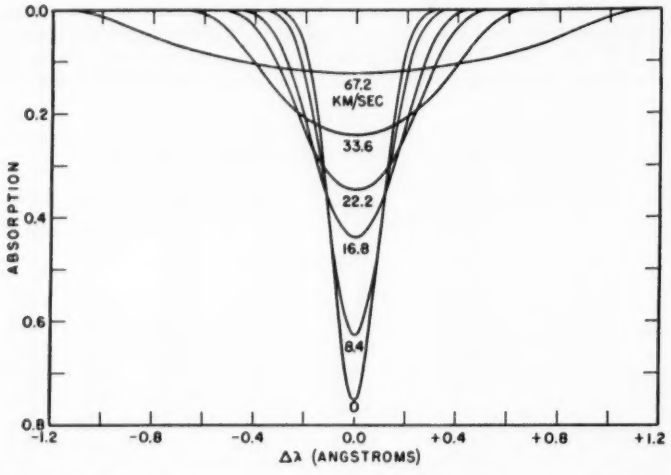


FIG. 1.—Rotationally broadened profiles for the *Fe* I line λ 4476.0 are shown for rotational velocities $v \sin i$ ranging from 0 to 67.2 km/sec. The profiles are calculated, assuming a limb-darkening coefficient of 0.6. All profiles have the same equivalent width.

γ Equ, was used by Deutsch (1952) as a standard narrow-line star. A comparison of λ 4476 in the spectra of the two stars shows that the profiles are almost identical in shape, in spite of the very different spectral classes. It was found also that the profiles could be represented accurately by a Gaussian dispersion curve. This profile was therefore used as the standard unbroadened line profile. It is shown as the zero velocity-curve in Figure 1.

The rotationally broadened profiles were computed by Shajn and Struve's method (1929), in which the star disk is divided up into many narrow strips. A limb-darkening coefficient of 0.6 was used. The resulting profiles are shown in Figure 1 for rotational velocities from 0 to 67.2 km/sec; the curves are all normalized to give the same equivalent width.

The profiles in Figure 1 were used to obtain the relation between the half-width of the line and the rotational velocity $v \sin i$. This is linear for $v \sin i > 20$ km/sec and can be extended to very high velocities, but flattens off as $v \sin i$ approaches zero. For each star the half-width of the line was obtained and $v \sin i$ determined from this relation. For stars with $v \sin i > 90$ km/sec the line λ 4549 was used. Since this line is intrinsically only

about twice as wide as λ 4476, it is safe to use the relation determined above. For stars with $v \sin i$ between 30 and 90 km/sec, both lines were used to obtain $v \sin i$. The agreement was good, the largest difference being for 31 Com, where values of 70 and 85 km/sec were obtained. The final values of $v \sin i$ are given in the fourth column of Table 1. Values below 7 or 8 km/sec are uncertain and mean only that the velocity is small. At these small velocities it is also quite possible that the main broadening agent may be turbulence rather than rotation.

Since only one plate was measured for each star, it is difficult to estimate the accuracy of the rotational velocities. A comparison of the two values of $v \sin i$ for the stars in which

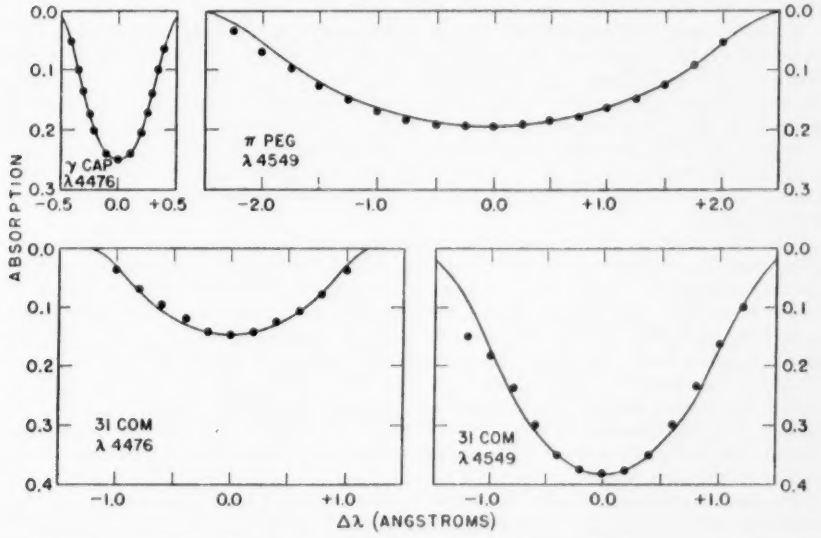


FIG. 2.—Computed rotationally broadened profiles shown by the solid curves are compared with the observed profiles, indicated by dots, for several stars having very broad lines. The profiles have been matched by making the half-widths and central depths of the computed and observed lines agree.

both λ 4476 and λ 4549 were measured gives about 7 per cent for the probable error of a single measure for values of $v \sin i$ in the neighborhood of 50 km/sec. For lower velocities the difference of the profile from the zero-velocity profile is smaller, but the accuracy of the half-width is greater. For very high rotational velocities the half-width is harder to determine and is influenced considerably by the position of the continuum.

With high dispersion it is possible to compare calculated and observed profiles to determine the nature of the broadening. This has been done for several stars having large values of $v \sin i$, with the results shown in Figure 2. The actual fits were made by selecting the proper half-widths and by making the central depths of the lines agree. As can be seen, the comparison indicates that the broadening is compatible with rotation. The profiles do disagree near the extreme limits of the lines, but this may be a result of blending with other lines, of incorrectly chosen limb-darkening or background-continuum level.

## IV. INTERPRETATION

From observational and theoretical work during the last few years we may sketch a possible way by which stars to the right of the main sequence have arrived there. On the

theoretical side, it has been shown that stars having an inhomogeneity of composition in the deep interior will be situated to the right of the main sequence. It has been shown by Sandage and Schwarzschild (1952) that a series of exhausted, contracting-core models predict a color-magnitude array which agrees well with the lower part of the observed globular-cluster array. Using the same series of models, it can be shown that the predicted color-magnitude arrays agree with those for Praesepe (Johnson 1952) and Coma Berenices (Weaver 1952), provided that the age of the clusters (about $10^9$ years) is chosen suitably. The evidence from clusters (Miczaika 1954) favors the view that the stars move off the main sequence to the right, the brightest members always proceeding first. Rather similar conclusions can be reached from a study of visual double stars (Muller 1952; Struve 1954).

A further test of this hypothesis is possible by using the rotational velocities of stars like those chosen for this program. If these stars originated on the main sequence, the relation between the present values of $v \sin i$ and the values of $v \sin i$ they possessed on the main sequence should be predictable. If this relation can be found, then, since previous studies (Westgate 1933) of A stars on the main sequence give us the distribution of $v \sin i$ on the main sequence, we should be able to compare the rotational velocities of giant and main-sequence stars and thus infer where the giant stars originated. We must assume that the form of the distribution of rotational velocities has not changed in the last $10^9$ years.

The way in which $v \sin i$ changes as a star becomes a giant can be determined, provided that the evolutionary models, the existence of differential or rigid-body rotation, and the change, if any, in the total angular momentum are known. In view of the remarks at the beginning of this section, the evolutionary models to choose would appear to be those of Sandage and Schwarzschild (1952). It will be assumed that conservation of angular momentum holds. It is difficult to decide whether to choose differential or rigid rotation. The best that can be done is to take two extreme cases. At the one extreme, case A, we assume that the star rotates at all times as a rigid body. At the other extreme, case B, we assume that each thin shell in the star preserves its own angular momentum. Defining $R/R_0$ to be the ratio of the present radius of the star to its original radius, when it was on the main sequence, then, for case B, $v \sin i/(v \sin i)_0 = R_0/R$, where $(v \sin i)_0$ is the initial rotational velocity. For case A the change in $v \sin i$ from its original value must be further corrected for the change in the distribution of mass within the star. This second factor, which is related to the moment of inertia of the star, has been computed and can be considerably larger than unity. Thus for any given $(v \sin i)_0$ we can obtain the theoretical relation between $v \sin i$ and $R/R_0$ for cases A and B. These are shown by the curves in Figure 3. The curves are completely fixed, apart from the choice of the initial $(v \sin i)_0$, which is a scale factor. The curves shown represent the maximum velocities expected, being based on the maximum value of $(v \sin i)_0 = 225$ km/sec suggested for the A stars by Westgate (1933) or Slettebak (1954).

We also need, for Figure 3, the value of $R/R_0$ for each star. The present radii of the stars are given by their positions in the Hertzsprung-Russell diagram. The effective temperatures were obtained from the temperature scale given by Keenan and Morgan (Hynek 1951) and the spectral classifications in Table 1. Fair trigonometric parallaxes exist for most of these stars; we determine the absolute bolometric magnitudes by using theoretical black-body bolometric corrections, which are small for the stars being considered. The radii can then be obtained from the foregoing data. In the fifth and sixth columns of Table 1 are listed the absolute bolometric magnitudes and the radii, $R$, in terms of the sun, for the stars with trigonometric parallaxes. A colon following the absolute magnitude indicates that the trigonometric parallax is less than $0''.030$. The absolute magnitudes of $\pi$ Peg and $\eta$ Peg are poorly determined.

The original radii, $R_0$, of the stars can be estimated, since, according to the Sandage-Schwarzschild models, a star now well away from the main sequence originated on the

main sequence about 1.1 mag. fainter than its present absolute magnitude. The resulting values of $R/R_0$ are given in the seventh column of Table 1. The original spectral types computed on this basis are between B9 and F8. In Figure 3, $R/R_0$ is plotted against $v \sin i$ for all the stars.

The method of selection and the number of stars are such that no conclusions of a general nature can be inferred from Figure 3. With a very large sample, a comparison of the final velocity distributions with the present velocity distributions of stars like the "parents" would determine the evolutionary tracks of the stars. But certain specific con-

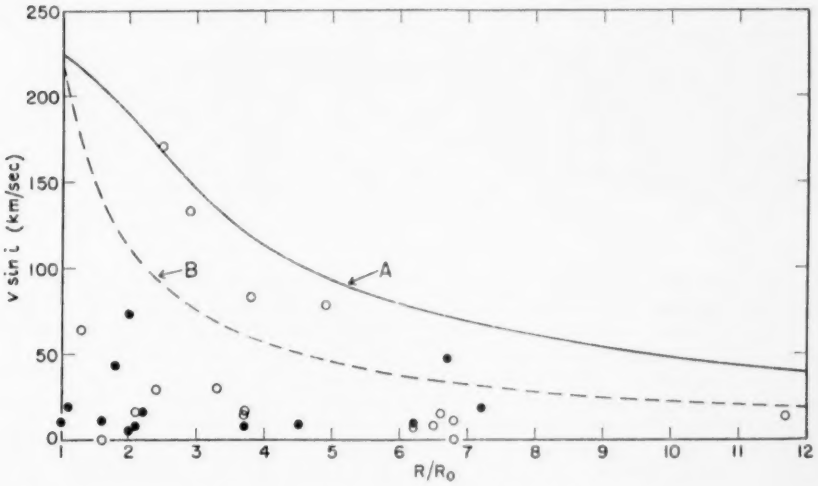


FIG. 3.—The rotational velocity, $v \sin i$, is plotted against $R/R_0$, the ratio of the present radius of the star to its original radius on the main sequence, for all stars. $R_0$ has been obtained by assuming the Sandage-Schwarzschild evolutionary models. The filled circles denote stars with parallaxes greater than 0".030, while the open circles indicate those with smaller parallaxes. The solid curve shows how the rotational velocity of a star which had an initial rotational velocity of 225 km/sec on the main sequence will change with $R/R_0$ according to the Sandage-Schwarzschild models, provided that the star rotates always as a rigid body (case A). The dashed curve gives a similar relation if each thin shell in the star preserves its own angular momentum (case B).

clusions can be made. (1) The observed velocities are completely incompatible with an evolution of these giants from main-sequence stars of types later than F5 but are compatible with evolution from main-sequence stars of earlier types (the deduced original positions of our stars range from B9 to F8). (2) The few stars with large observed rotational velocities (e.g., the eight with $v \sin i > 60$ km/sec) can only have originated from early main-sequence stars, since in no other type of star does such large angular momentum exist. (3) The normal nonrotating giants of types later than G5 could be produced by similar, but more extreme, evolution toward larger values of $R/R_0$; but, since they are so common compared to A and F giants and since none have large rotations, it is probable that they belong to a different family. (4) If all future models of the internal structure demonstrate that giants can exist only if there is a discontinuity of chemical composition, then we can conclude that even the moderately high observed rotational velocities do not produce a complete mixing.

## REFERENCES

Chandrasekhar, S., and Münch, G. 1950, *Ap. J.*, **111**, 142.
Deutsch, A. J. 1952, unpubl. in *Trans. I.A.U.* (in press).
Herbig, G. H., and Spalding, J. F., Jr. 1953, *Pub. A.S.P.*, **65**, 192.
Huang, Su-shu. 1953, *Ap. J.*, **118**, 285.
Hynek, J. A. 1951, *Astrophysics* (1st ed.; New York: McGraw-Hill Book Co., Inc.), p. 20.
Johnson, H. L. 1952, *Ap. J.*, **116**, 640.
———. 1953, *Ap. J.*, **117**, 361.
Miczaika, G. R. 1954, *Les Processus nucléaires dans les astres* (Louvain: Imprimerie Ceuterick), pp. 275–282.
Morgan, W. W., Keenan, P. C., and Kellman, E. 1943, *Atlas of Stellar Spectra* (Chicago: University of Chicago Press).
Muller, P. 1952, *Ann. d'Ap.*, **15**, 79.
Sandage, A. R., and Schwarzschild, M. 1952, *Ap. J.*, **116**, 463.
Shajn, G., and Struve, O. 1929, *M.N.*, **89**, 222.
Slettebak, A. 1953, *A.J.*, **58**, 228.
———. 1954, *Ap. J.*, **119**, 146.
Struve, O. 1954, *Sky and Telescope*, **13**, 256, 295.
Weaver, F. W. 1952, *Ap. J.*, **116**, 612.
Westgate, C. 1933, *Ap. J.*, **78**, 46.

# THE ATMOSPHERE OF THE I COMPONENT OF EPSILON AURIGAE

ROBERT P. KRAFT*
Berkeley Astronomical Department, University of California
*Received May 14, 1954; revised July 13, 1954*

## ABSTRACT

The shell surrounding the I component of $\epsilon$ Aurigae is studied from a coudé spectrogram taken by Adams and Sanford in 1930. Under the assumption that the electron gas of the I star shell is in equilibrium with the radiation of the F2 companion, a curve of growth, based on the measurements of the equivalent widths of 49 lines, is constructed. Departure from thermodynamic equilibrium is considered, and, from this curve of growth, $P_e$ is estimated to lie between $10^{-4}$ and $2.8 \times 10^{-4}$ dynes/cm$^2$, depending on the degree of departure. The explanation is advanced that the anomalous weakness of the *Cr* II lines is a measure of the importance of collisional excitation processes, when the electron temperature is lower than the radiation temperature. The diminution of light during eclipse is found to be consistent with the electron density derived from the curve of growth, if $H^-$ is taken as the source of opacity and the ratio $N_H/N_e$ is of the order of $10^4$.

## I. INTRODUCTION

It is known from the work of Kuiper, Struve, and Strömgren (1937) that the spectrum induced in the I component of $\epsilon$ Aurigae by radiation from the F2 companion not only appears during the time of total eclipse but is also present in great strength near the phases of first and third contact. This effect is particularly well illustrated by a Mount Wilson coudé spectrogram taken by Adams and Sanford (1930) on February 5, 1930, approximately 75 days before the close of egress, according to Miss Güssow's (1936) elements. At this phase the F2 star evidently passes behind the shell-like atmosphere surrounding the I component, which produces about 0.1–0.2 mag. of continuous opacity and considerable line opacity. Owing to the axial rotation of the I star, the I lines are sufficiently well separated from those of the companion that radial-velocity measurements can be made (Adams and Sanford 1930). The present discussion consists of an attempt to obtain some of the physical parameters governing ionization and excitation in the atmosphere of the I component by means of a spectrophotometric analysis of this plate.

## II. SPECTRUM

The Adams-Sanford spectrogram was taken with two 52° prisms, giving a linear dispersion of 4.8 A/mm at $H\gamma$. It is composed of two parts; one section centered on the $H\gamma$ region, and a second centered on the *Na* D lines. The former region, in excellent focus from λ 4150 to λ 4650, was used exclusively in the following discussion.

A portion of the spectrum is reproduced in Figure 1. It is seen that many of the lines, notably those of *Ti* II, *Fe* II, and *Sc* II are distinctly double, with sharp, shortward-displaced components arising from the I star, flanking the broader F2 lines. A similar effect is found in *Ca* I, *Cr* I, and most lines of *Fe* I, with the exception of λ 4260, which shows no line produced in the I component. Since λ 4260 arises from a nonmetastable level, it is a good indicator of dilution effects (Struve 1939), and its absence is understandable in view of the geometry of the eclipse. Since the F2 star, as seen from the I star, subtends an angle of only 1°.8 (Kuiper, Struve, and Strömgren 1937), it is seen that the dilution is of the order of $10^{-4}$.

A curious feature of the spectrum is found in the behavior of the *Cr* II lines, which seem to be either very weak or absent in the I star, while of normal intensity in the F2 component. Since the ionization potentials of *Ti* I, *Sc* I, and *Cr* I are nearly the same

* Predoctoral fellow of the National Science Foundation, 1954–1955.

(6.7–6.8 volts), it is not immediately evident why *Cr* II should be so weak. It will be shown later that the apparently anomalous behavior of *Cr* II gives a means of estimating the importance of collisional excitation processes in the I component.

### III. PLATE CALIBRATION

The spectrogram used in this discussion has no intensity calibration. An attempt to circumvent this difficulty was made by an intensity analysis of the iron-arc comparison lines, plotting their measured intensities against relative *f*-values. In order to obtain a sufficient number of lines of different strengths, it was necessary to employ four iron multiplets, numbers 2, 3, 41, and 42, in the *Revised Multiplet Table* (Moore 1945). In assembling these lines on a single calibration-curve, the assumption was made that the populations of the excited levels from which these lines arise were governed by a Boltzmann distribution. While it is true that one can hardly speak of an iron arc as operating in conditions of thermodynamic equilibrium, it is nevertheless the case that no wide variation existed in the strengths of the lines discussed. It was therefore hoped that even a rough calibration would yield results of the right order of magnitude.[1]

The *f*-values employed were the laboratory absorption values of A. S. King and R. B. King (1938), converted to emission oscillator strengths. It was assumed that the only source of line broadening was instrumental, the line strengths therefore being taken as proportional to the central intensities as read from a microphotometer tracing. The shift in Nf necessary to place the lines of multiplets 41 and 42 on a smooth curve with those of multiplets 2 and 3 gave an arc temperature of 4950° K. This temperature was then used to smooth the positions of lines within each multiplet.

### IV. THE CURVE OF GROWTH IN THERMODYNAMIC EQUILIBRIUM

From an intensity tracing reduced by means of the calibration-curve described earlier, the equivalent widths of 54 neutral and ionized I star lines were measured, in the interval λλ 4200–4600. Since each line was blended, to a certain extent, with the corresponding F2 line, the following method was adopted for drawing the profiles of the I lines. The centers of the F lines were found by applying the constant radial-velocity shift of 30 km/sec (Adams and Sanford 1930) to the positions of the sharp I line centers. The assumption was then made that the longward wing of each F line was free from intensity contribution of the corresponding longward wing of the I line. The shortward wing of each F line was then obtained by reflecting the longward wing about the center of the F line. This shortward wing then constituted the "continuum" seen by the blended I line, and the equivalent width of the latter was correspondingly rectified. The 15 per cent diminution of light of the F star by the I star shell, at this phase, was neglected in making the rectification.

A curve of growth for the I star was constructed by making use of the measured equivalent widths of 49 of these lines. A number of basic assumptions had to be made, owing primarily to the small number of lines used in this study and particularly to the lack of a sufficient number of weak lines. These assumptions were as follows:

1. The curves of growth for all metals, in both neutral and ionized stages, have the same shapes, differing only in zero point. The individual curves of growth were then shifted horizontally and assembled on a single curve of least scatter. *Fe* II was chosen as the "basic" element to which all other elements were referred.

2. The Schuster-Schwarzschild model is applicable, since the atmosphere of the I component produces only a small amount of continuous opacity.

3. The solar log $X_f$-values derived by Wright (1947) were used in the I component, in lieu of the relative oscillator strengths. In the case of a few lines for which Wright has

[1] This method has been used successfully by Keenan (1931) to obtain a calibration for a number of older Yerkes spectrograms.

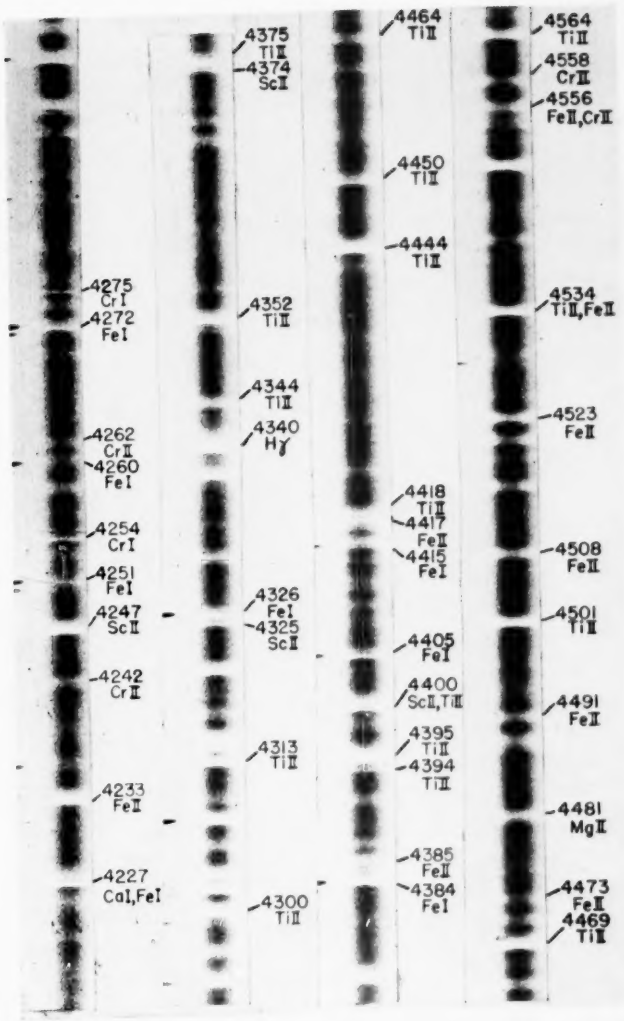


FIG. 1.—A portion of the Adams-Sanford spectrogram of $\epsilon$ Aurigae. The dark streaks at $\lambda$ 4251 and longward of $\lambda$ 4254 are scratches on the original emulsion.

given no $X_f$-values, the solar strengths were obtained from direct measurements in the Utrecht atlas.

4. The I star lines of all elements in all stages of ionization have the same degree of turbulence.

5. The excitation and ionization in the I star are governed by conditions of thermodynamic equilibrium at the radiation temperature $T_r$ of the F2 star.

The appropriate analogue of the solar $X_f$-values for use in the I star is given by the expression

$$\log X_{f*} = \log X_{f\odot} - 5040\chi\left(\frac{1}{T_*} - \frac{1}{T_\odot}\right) + \log \frac{N_{a*}}{B(T_*)} - \log \frac{N_{a\odot}}{B(T_\odot)} + C_* - C_\odot \quad (1)$$

for some element $E$ in stage of ionization $a$, where $B$ is the partition function; $T_*$, the effective temperature of the F2 star; $T_\odot$, the effective temperature of the sun; and $C$ is given by

$$C = \log \frac{\pi e^2}{m c} \frac{1}{\sqrt{\pi}} \frac{1}{v}, \quad (2)$$

$v$ being the effective "thermal" parameter. We also define the quantity

$$\log X'_{f*} = \log X_{f\odot} - 5040\chi\left(\frac{1}{T_*} - \frac{1}{T_\odot}\right). \quad (3)$$

In Table 1 are listed the equivalent widths of the 54 lines measured, together with their $\log X'_{f*}$-values, on the assumption of $T_\odot^{(\mathrm{ion})} = 5300°$ and $T_*^{(\mathrm{ion})} = 6500°$.

The curve of growth based on 49 of these lines is shown in Figure 2. Since *Fe* was the only element for which a sufficient number of both neutral and ionized lines could be measured, an estimate of the electron pressure in the I star was obtained from this curve of growth by means of the following consideration. Let the shift necessary to place the *Fe* I lines on the same curve of growth with the *Fe* II lines be denoted by $\Delta \log X'_{f*}(Fe)$, so that

$$\Delta \log X'_{f*}(Fe) = \log X'_{f*}(Fe\,\mathrm{I}) - \log X'_{f*}(Fe\,\mathrm{II}). \quad (4)$$

If assumptions (1)–(5) are satisfied and the ratio of the partition functions of *Fe* I and *Fe* II is taken as unity, the electron pressure may be obtained from the expression

$$\log \frac{P_{e*}}{W} = -I(\theta_* - \theta_\odot) + \tfrac{5}{2} \log \frac{T_*}{T_\odot} + \log P_{e\odot} - \Delta \log X'_{f*}(Fe), \quad (5)$$

where $I$ is the ionization potential of *Fe* I (7.8 volts) and $W$ is the dilution factor. Adopting $T_\odot$ and $T_*$ as indicated above, $W = 2 \times 10^{-4}$, and $\log P_{e\odot} = 1.20$ (Wright 1947), one obtains for $\Delta \log X'_{f*}(Fe) = 2.53$,

$$P_{e*} = 2.8 \times 10^{-4}\ \mathrm{dynes/cm^2}. \quad (6)$$

## V. DEPARTURE FROM THERMODYNAMIC EQUILIBRIUM

It is clear that the foregoing discussion, based on the Saha equation, is strictly valid only on the assumption that the electron gas is in equilibrium with the radiation temperature. A more general formulation of the problem requires that one consider a steady state, not necessarily in thermodynamic equilibrium, so that the total number of photoionizations per second per cubic centimeter is equal to the total number of radiative recombinations per second per cubic centimeter. If the relaxation time of the electron gas is sufficiently short compared with the characteristic radiative time, the collisions of the electrons will set up a Maxwellian distribution of velocities at a local temperature $T_e$.

TABLE 1

EQUIVALENT WIDTHS OF LINES IN THE I COMPONENT

| No. | λ | Element | Wt. | log $X_{f\odot}$ | log $W/\lambda$ | E.P. (Lower) | log $X'_{f*}$ |
|---|---|---|---|---|---|---|---|
| 1 | 4226.74 | *Ca* I | 1/2 | +2.23 | −4.043 | 0.00 | +2.23 |
| 2 | 4246.84 | *Sc* II | 1 | +0.57 | −3.959 | 0.31 | +0.62 |
| 3 | 4325.00 | | 1/2 | +0.22 | −4.206 | 0.59 | +0.32 |
| 4 | 4354.62 | | 1 | −1.34 | −5.162 | 0.60 | −1.24 |
| 5 | 4305.72 | | 1 | −0.65 | −4.298 | 0.59 | −0.55 |
| 6 | 4374.46 | | 1/2 | +0.10 | −4.365 | 0.62 | +0.20 |
| 7 | 4287.92 | *Ti* II | 1 | −0.58 | −4.349 | 1.08 | −0.38 |
| 8 | 4300.05 | | 1/2 | +0.63 | −3.980 | 1.18 | +0.84 |
| 9 | 4302.04 | | 1/2 | +0.13 | −4.068 | 1.16 | +0.33 |
| 10 | 4312.89 | | 1 | −0.29 | −4.086 | 1.18 | −0.08 |
| 11 | 4344.28 | | 1 | −0.20 | −4.208 | 1.08 | −0.01 |
| 12 | 4394.37 | | 1 | −0.78 | −4.431 | 1.22 | −0.57 |
| 13 | 4395.25 | | 1/2 | +0.32 | −3.808 | 1.08 | +0.51 |
| 14 | 4399.77 | | 1/2 | −0.03 | −4.265 | 1.23 | +0.19 |
| 15 | 4417.71 | | 1/2 | −0.31 | −4.247 | 1.16 | −0.11 |
| 16 | 4443.94 | | 1 | +0.14 | −3.947 | 1.08 | +0.33 |
| 17 | 4450.49 | | 1 | −0.49 | −4.279 | 1.08 | −0.30 |
| 18 | 4464.40 | | 1 | −0.76 | −4.419 | 1.16 | −0.56 |
| 19 | 4468.60 | | 1 | +0.20 | −4.106 | 1.13 | +0.40 |
| 20 | 4470.90 | | 1 | −1.43 | −4.558 | 1.16 | −1.23 |
| 21 | 4501.26 | | 1 | +0.07 | −4.040 | 1.11 | +0.26 |
| 22 | 4529.46 | | 1/2 | −1.44 | −4.595 | 1.56 | −1.17 |
| 23 | 4563.77 | | 1 | +0.04 | −4.061 | 1.22 | +0.25 |
| 24 | 4568.41 | | 1/2 | −2.08 | −5.197 | 1.22 | −1.87 |
| 25 | 4571.97 | | 1 | +0.14 | −3.988 | 1.56 | +0.41 |
| 26 | 4590.02 | | 1/2 | −0.93 | −4.770 | 1.23 | −0.71 |
| 27 | 4322.68 | *V* II | 1/2 | ..... | −5.790 | 1.67 | ..... |
| 28 | 4254.47 | *Cr* I | 1 | +1.22 | −4.333 | 0.00 | +1.22 |
| 29 | 4274.80 | | 1 | +1.03 | −4.238 | 0.00 | +1.03 |
| 30 | 4289.73 | | 1/2 | +0.92 | −4.292 | 0.00 | +0.92 |
| 31 | 4202.17 | *Fe* I | 1 | +1.32 | −4.474 | 1.48 | +1.58 |
| 32 | 4271.70 | | 1/2 | +1.78 | −4.229 | 1.48 | +2.04 |
| 33 | 4325.77 | | 1/2 | +1.69 | −4.210 | 1.60 | +1.97 |
| 34 | 4383.73 | | 1/2 | +2.01 | −4.181 | 1.48 | +2.27 |
| 35 | 4404.78 | | 1 | +1.81 | −4.320 | 1.55 | +2.08 |
| 36 | 4415.13 | | 1/2 | +1.30 | −4.409 | 1.60 | +1.58 |
| 37 | 4528.62 | | 1/2 | +0.99 | −4.967 | 2.17 | +1.37 |
| 38 | 4233.19 | *Fe* II | 1/2 | +0.20 | −3.766 | 2.57 | +0.65 |
| 39 | 4258.17 | | 1/2 | −0.85 | −4.377 | 2.69 | −0.38 |
| 40 | 4296.59 | | 1 | −0.79 | −4.102 | 2.69 | −0.32 |
| 41 | 4351.80 | | 1 | ..... | −4.193 | 2.69 | ..... |
| 42 | 4369.47 | | 1/2 | −1.78 | −4.627 | 2.77 | −1.29 |
| 43 | 4385.39 | | 1/2 | −0.55 | −4.011 | 2.77 | −0.06 |
| 44 | 4472.99 | | 1 | −1.61 | −4.533 | 2.83 | −1.11 |
| 45 | 4491.34 | | 1 | −1.04 | −4.616 | 2.84 | −0.54 |
| 46 | 4508.33 | | 1 | −0.81 | −4.294 | 2.84 | −0.31 |
| 47 | 4515.35 | | 1 | −0.87 | −4.347 | 2.83 | −0.37 |
| 48 | 4520.24 | | 1 | −0.90 | −4.191 | 2.79 | −0.40 |
| 49 | 4522.67 | | 1 | −0.26 | −4.125 | 2.83 | +0.24 |
| 50 | 4541.47 | | 1/2 | −1.58 | −4.873 | 2.84 | −1.08 |
| 51 | 4576.34 | | 1 | −1.46 | −4.438 | 2.83 | −0.96 |
| 52 | 4215.56 | *Sr* II | 1 | +1.08 | −4.145 | 0.00 | +1.08 |
| 53 | 4309.66 | *Y* II | 1 | ..... | −5.130 | 0.18 | ..... |
| 54 | 4554.29 | *Ba* II | 1/2 | +0.55 | −4.498 | 0.00 | +0.55 |

Assuming that the probability of photoionization follows Becker's (1923) $\nu^{-4}$ law, Eddington (1926) has shown that the initial temperature of electrons immediately upon ejection is given, to a first approximation, by an expression of the form

$$T_e = \tfrac{2}{3} T_r \left(1 - \frac{2}{x_0}\right), \tag{7}$$

where $x_0 = h\nu_0/kT_r$. Ordinarily, the initial temperature would be expected to rise to the radiation temperature $T_r$ itself, owing to the fact that the slow electrons are quickly captured. On the other hand, a certain amount of cooling of the electron gas takes place through free-free transitions; moreover, capture processes will tend to be slowed by low

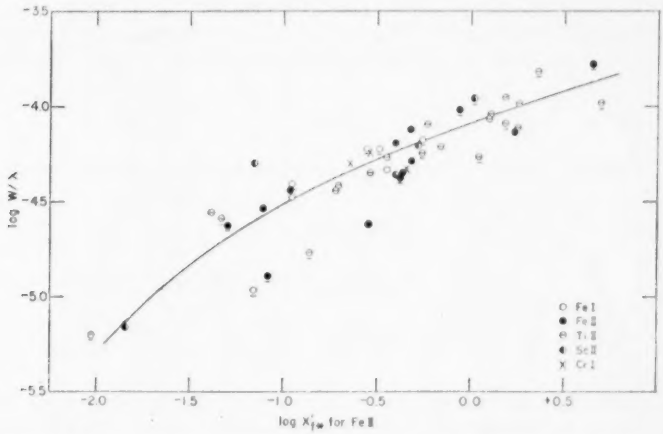


FIG. 2.—Curve of growth for the I component of $\epsilon$ Aurigae. The underscored symbols denote lines of half-weight.

electron pressure. Since $x_0 \sim 10$ for metals, it is not unreasonable to expect $T_e$, for the atmosphere of $\epsilon$ Aurigae I, to lie in the range

$$3250^\circ \text{ K} = 0.50\, T_r \leq T_e \leq T_r = 6500^\circ \text{ K}. \tag{8}$$

For departures from thermodynamic equilibrium of this order, Pannekoek (1926, 1927) has given a corrected formulation of Saha's equation. It is found that equation (4) must be modified so as to involve both the parameters $P_e$ and $T_e$. This correction can be expressed in the form

$$\frac{P_e\,(\text{correct})}{P_{e,\,r}} = \left(\frac{T_e}{T_r}\right)^{3/2}, \tag{9}$$

where $P_{e,\,r}$ is the electron pressure calculated from equation (4) on the basis of thermodynamic equilibrium with the radiation temperature $T_r$. For the range in $T_e$ expressed by equation (8), we find the corresponding range in $P_e$ to be

$$1.0 \times 10^{-4} \leq P_e \leq 2.8 \times 10^{-4} = P_{e,\,r}. \tag{10}$$

If it is now assumed that $T_e$ lies within the range given by equation (8), one may inquire whether there exists any spectroscopic evidence indicating a departure from ther-

modynamic equilibrium of the type described. It has been pointed out earlier in this discussion that the *Cr* II lines in the I component are either weak or absent. Certainly, their equivalent widths cannot be more than one-fifth that of the corresponding *Cr* II lines in the F2 star, whereas the lines of *Ti* II in both components have strengths of the same order of magnitude. It is important to note that each line of *Ti* II, *Fe* II, *Cr* II, and *Sc* II found in the range of spectrum under consideration arises from an excited level that is relatively metastable to the ground state. The argument is therefore advanced that the populations of the excited metastable levels of *Cr* II in the I star are governed by elec-

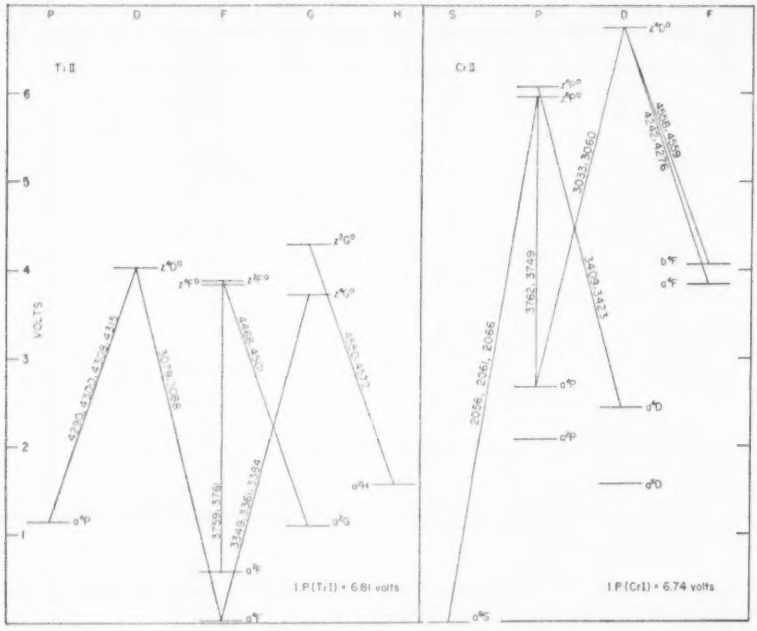


FIG. 3.—Partial term schemes for *Ti* II and *Cr* II. The intersystem transition $a^4P$ to $z^6P^0$ in *Cr* II is quite weak.

tron-collision excitation and de-excitation processes which are of the same order of importance as radiative processes. Since the term schemes of *Ti* II, *Fe* II, and *Sc* II are essentially the same as regards features relevant to the processes described, in opposition to *Cr* II, we shall compare *Cr* II with *Ti* II as a typical case. If collision processes are important in populating the levels of *Cr* II, it follows that $T_e < T_r$ will likely lead to a depopulation of these levels. Furthermore, a depopulation by roughly a single order of magnitude will suffice to give the observed effect.

Partial term schemes of *Cr* II and *Ti* II are shown in Figure 3 and illustrate certain relevant differences (Bacher and Goudsmit 1932). The ground states of *Ti* II and *Cr* II are a $^4F$ and $^6S$, respectively. In the case of *Ti* II, the lowest odd-parity state capable of strong combination with the ground state is a $^4G^0$ at 3.73 volts. The corresponding level in *Cr* II is a $^6P^0$ at 5.97 volts. Below these odd-parity states in both atoms is a number of even-parity levels, relatively metastable to the ground state, from which the lines in the observable region of the spectrum arise. In the case of *Ti* II, observable lines come

from levels only 1–2 volts above the ground state. On the other hand, no line in the observable spectrum of *Cr* II arises from a level below $a^4F$ at 3.85 volts. Moreover, $a^4F$ will be difficult to populate by radiative processes from the $^6S$ ground state, because of intersystem transitions. No such difficulty is encountered with the $a^4P$ level of *Ti* II, for example. Finally, the only possible strong transition out of the ground state of *Cr* II is $a^6S \rightarrow z^6P^0$, whereas a number of strong paths are available in *Ti* II.

The atoms residing in the metastable levels of *Cr* II and *Ti* II are supplied from the ground state by two processes: (1) collisional excitation by electrons; and (2) photo-excitation to states of odd parity, with subsequent cascading. These levels are depopulated by upward collisional excitation, superelastic collisions, and photo-excitation (inverse of process 2).

Suppose we consider, as a limiting case, that collision processes dominate over radiative processes in governing the population of the $b^4F$ level of *Cr* II. Then, if we assume a Boltzmann distribution controlled by the electron temperature $T_e$, we have

$$\frac{N_{^4F}^{(\mathrm{coll})}}{N_g} \sim \exp\left(-\frac{h\nu}{kT_e}\right), \tag{11}$$

whereas under conditions of thermodynamic equilibrium, we would have

$$\frac{N_{^4F}^{(\mathrm{rad})}}{N_g} \sim \exp\left(-\frac{h\nu}{kT_r}\right). \tag{12}$$

Taking $T_e = 4500°$ K, for example, we would have

$$\frac{N_{^4F}^{(\mathrm{coll})}}{N_{^4F}^{(\mathrm{rad})}} = \exp\left[-h\nu\left(\frac{1}{kT_e}-\frac{1}{kT_r}\right)\right] = \exp(-3.15) = 0.04, \tag{13}$$

a quantity representing the depopulation of $b^4F$, if collision processes were in control. On the other hand, the relevant metastable levels of *Ti* II are so low that if $T_e$ and $T_r$ are taken as above, the ratio corresponding to equation (13) for the $a^4P$ level is

$$\frac{N_{^4P}^{(\mathrm{coll})}}{N_{^4P}^{(\mathrm{rad})}} = \exp(-0.90) = 0.41; \tag{14}$$

so that the type of controlling process is relatively unimportant.

We inquire whether collision processes are indeed significant compared with radiative processes. Let us take a simplified model of the term scheme of *Cr* II, consisting only of the ground state (state 1), the lowest odd-parity state $z^6P^0$ (state 3), and the metastable level (say) $b^4F$ (state 2). Let $F^{(\mathrm{coll})}$ be the rate of populating $b^4F$ from the ground state by electron collisions, and let $F^{(\mathrm{rad})}$ be the corresponding radiative rate by way of $z^6P^0$. Making use of the collisional excitation formula given by Hebb and Menzel (1940), one obtains

$$\frac{F^{(\mathrm{coll})}}{F^{(\mathrm{rad})}} = 7.1\times10^{21}\frac{P_e\sigma}{T_e^{1/2}}\,\delta_{13}\,\frac{1}{W}\,\frac{1}{f_{23}}\,\frac{m\,c}{8\pi^2\epsilon^2}\,\lambda_{23}^2\exp\left(\frac{h\nu_{13}}{kT_r}-\frac{h\nu_{12}}{kT_e}\right), \tag{15}$$

where $\sigma$ is the collision cross-section for excitation from the ground state to $b^4F$, $W$ is the dilution factor, $f_{23}$ is the absorption oscillator strength of the transition $2 \rightarrow 3$, and $1/\delta_{13}$ is the fractional depression of the radiation of the F2 star below that of a black body at temperature $T_r$. With $T_r = 6500°$ K, as before, equation (15) simplifies into

$$\frac{F^{(\mathrm{coll})}}{F^{(\mathrm{rad})}} = 7.0\times10^{17}\frac{P_e\sigma\,\delta_{13}}{T_e^{1/2}W\,f_{23}}\exp\left(-\frac{h\nu_{12}}{kT_e}\right). \tag{16}$$

With $W = 2 \times 10^{-4}$ and taking, for example, $T_e = 4500°$ K, then, in view of equation (9), equation (16) becomes

$$\frac{F^{(\text{coll})}}{F^{(\text{rad})}} = 1.1 \times 10^{12} \frac{\delta_{13}}{f_{23}} \sigma . \tag{17}$$

The quantity $\sigma$ for collisional excitation of *Cr* II is unknown. However, Hebb and Menzel (1940) have made quantum-mechanical calculations of the electron-collision cross-sections of *O* III, based on the Born approximation. For intersystem transitions, also having changes in the azimuthal quantum number, these cross-sections are of the order of 10 $\sigma_H$, where $\sigma_H$ is the area of the first Bohr orbit. In a recent article, Seaton (1953) has shown, by more nearly exact calculations, that these cross-sections should be reduced by roughly a factor of 10. If one now makes the assumption that the target areas appropriate for *Cr* II are like those for *O* III, one obtains $\sigma \sim 10^{-16}$ cm$^2$.

Because of the intersystem transitions pointed out earlier, the factor $f_{23}$ is probably of the order of $10^{-2}$ or less, judging by the absolute oscillator strengths of typical weak lines of *Fe* I (R. B. King 1942). There remains the additional uncertain factor $\delta_{13}$, corresponding to a transition with the energy difference of 5.97 volts, a group of lines lying at λλ 2056, 2059, and 2066. In the case of the sun, it is known that the intensity of radiation at λ 2600 is reduced below that corresponding to the black-body temperature by a factor of 10 (Durand, Oberly, and Tousey 1949). Though little quantitative work has so far been published to the shortward of λ 2600, various reproductions of rocket-flight solar spectra below λ 2600 are now available (Kuiper 1953). The wave length λ 2076 corresponds to the head of the ground-state bound-free absorption continuum of *Al* I. It is clear from the reproduction of an Aerobee rocket-flight spectrum of September 2, 1952 (Kuiper 1953) that a considerable depression of the continuum occurs about λ 2080, extending a few hundred angstroms shortward. It may be possible that *Al* I (along with the bound-free head of *Ca* I, which occurs at λ 2030) is responsible for the depression. If one is permitted to extrapolate this depression to the F2 component of ε Aurigae, it is probable that the factor $\delta_{13}$ lies between 10 and 100. In the latter event,

$$\frac{F^{(\text{coll})}}{F^{(\text{rad})}} \sim 1 . \tag{18}$$

In other words, since the wave length of the only upward radiative path arising from the ground state of *Cr* II coincides with the head of the *Al* I bound-free continuum, collision processes may be at least of the same order of importance as radiative processes in populating the b$^4$F state of *Cr* II in the I component. It is reasonable to suppose that, owing to the lower temperature at which the collision processes operate, the level b$^4$F will tend to be depopulated. In this case, in which collisional and radiative processes share about equally, it is difficult to give more than a qualitative indication of the effect.

In summary it must be emphasized that the three factors entering equation (17) are poorly known and that the hypothesis proposed here rather critically depends upon their values. However, in view of the equality of the ionization potentials of *Cr* I and *Ti* I and the differences already cited in the term schemes of *Cr* II and *Ti* II, it seems more reasonable to attribute the weakness of the lines of *Cr* II to some effect related to the excitation rather than to an ionization or abundance anomaly.

## VI. THE CONTINUOUS OPACITY

To account for the observed wave-length independence of the light lost during eclipse, the Yerkes model (Kuiper, Struve, and Strömgren 1937) was based upon electron scattering as the source of continuous opacity. One may now inquire to what extent the electron density of $2 \times 10^8$ cm$^{-3}$, derived from the curve of growth of Section IV, is compatible with the diminution of light required by the eclipse data. If it is assumed that

the I star possesses a definite "edge," then at the phase under consideration the F star is emerging from behind that edge, so that, neglecting limb darkening, about three-eighths of the F star is still obscured by the semitransparent shell. According to the Yerkes model, the obscuration is due to a layer always having the same thickness, so that, whatever the phase under consideration, that part of the light of the F star which passes through the shell is always diminished by about 50 per cent. Moreover, the electron density derived in Section IV will apply at any position on the surface of the shell. The optical depth required by the observations is $\tau = 0.7$. If we now calculate the value of $\tau$ from $N_e \sigma_e s$, where $\sigma_e$ is the Thomson cross-section ($0.66 \times 10^{-24}$ cm$^2$), and use Strömgren's (Kuiper, Struve, and Strömgren 1937) estimate of the path length $s$ ($10^{13}$ cm), we obtain $\tau \sim 10^{-3}$. Thus electron scattering, based on the electron pressure derived in Section IV, is much too small to give the degree of opacity required by the observations.

On the other hand, a satisfactory diminution can be obtained, in accordance with a suggestion by Strömgren,[2] if the $H^-$ ion is taken into account. Assuming that the ionization of $H^-$ is controlled by the F star, the number of $H^-$ ions per unit volume of the shell is given by Saha's equation as

$$N_{H^-} = 0.8 \times 10^{-21} \frac{1}{W} N_H N_e . \tag{19}$$

With $W$ as before and taking for $\lambda$ 5000 A, the absorption coefficient per $H^-$ ion as $3.4 \times 10^{-17}$ (Chandrasekhar 1945), we find

$$\tau = 1.0 \times 10^{-34} N_e N_H s \tag{20}$$

for the optical depth corresponding to the path length $s$. With $N_e$ given by Section IV as $2 \times 10^8$ cm$^{-3}$ and $s = 10^{13}$ cm, we must choose $N_H/N_e$ so that the highly selective effect of Rayleigh scattering by neutral hydrogen atoms remains negligible. For $s = 10^{13}$, Rayleigh scattering can be ignored, provided that $N_H/N_e$ is not larger than $10^4$. In that case, $\tau = 0.4$, in satisfactory agreement with the eclipse data. It should be pointed out that the $H^-$ opacity, together with the rather low electron pressure derived here, permits the ratio $N_H/N_e$ to be chosen roughly compatible with that expected in an F-type star. The earlier difficulty (Kuiper, Struve, and Strömgren 1937) of requiring $N_H/N_e$ to be as small as 10, in order to suppress the effect of Rayleigh scattering, is thereby eased.

The change in the absorption coefficient of $H^-$ from the photographic to the photovisual region amounts to 20 per cent (Chandrasekhar 1945), so that the question remains whether the $H^-$ opacity is sufficiently nonselective. It is hoped that a definitive answer may be given to this and other puzzling features of the system of $\epsilon$ Aurigae during the forthcoming eclipse.

I wish to express my thanks to Dr. Otto Struve for his encouragement and interest in the study of this star, and to Dr. Bengt Strömgren for a valuable suggestion. In addition, the kindness of Dr. I. S. Bowen, director of the Mount Wilson and Palomar Observatories, Dr. W. S. Adams, and Dr. R. F. Sanford for permitting this spectrogram to be studied here is greatly appreciated. I wish also to thank Mr. John Crawford of this department for a valuable discussion.

## REFERENCES

Adams, W. S., and Sanford, R. F. 1930, *Pub. A.S.P.*, **42**, 203.
Bacher, R. F., and Goudsmit, S. 1932, *Atomic Energy States* (New York: McGraw-Hill Book Co.), pp. 161 and 471.
Becker, A. 1923, *Zs. f. Phys.*, **18**, 325.

[2] Private communication. I wish to thank Dr. Strömgren for calling the role of the $H^-$ ion to my attention.

Chandrasekhar, S. 1945, *Ap. J.*, **102**, 395.
Durand, E., Oberly, J. J., and Tousey, R. 1949, *Ap. J.*, **109**, 1.
Eddington, A. S. 1926, *Internal Constitution of the Stars* (Cambridge: At the University Press), pp. 376–377.
Güssow, M. 1936, *Veröff. Berlin-Babelsberg*, Vol. **11**, No. 3.
Hebb, M. S., and Menzel, D. H. 1940, *Ap. J.*, **92**, 408.
Keenan, P. C. 1931, *Ap. J.*, **73**, 118.
King, A. S., and King, R. B. 1938, *Ap. J.*, **87**, 24.
King, R. B. 1942, *Ap. J.*, **95**, 78.
Kuiper, G. P. (ed.). 1953, *The Sun* (Chicago: University of Chicago Press), pp. 670–676.
Kuiper, G. P., Struve, O., and Strömgren, B. 1937, *Ap. J.*, **86**, 570.
Moore, C. E. 1945, *Contr. Princeton U. Obs.*, No. 20.
Pannekoek, A. 1926, *B.A.N.*, No. 110.
———. 1927, *ibid.*, No. 121.
Seaton, M. 1953, *Proc. R. Soc. London, A*, **218**, 400.
Struve, O. 1939, *Proc. Amer. Phil. Soc.*, **8**, 211.
Wright, K. O. 1947, *Pub. Dom. Ap. Obs. Victoria*, **8**, 1.

# THE COMPOSITION OF THE PLANETARY NEBULA NGC 7027

LAWRENCE H. ALLER
University of Michigan Observatory
*Received April 21, 1954*

ABSTRACT

New spectrophotometric data on the bright, high-excitation planetary NGC 7027 are discussed with the aid of improved transition probabilities and Seaton's improved target areas for forbidden-line excitation. The ionic abundances are computed, and the probable filamentary structure of the nebula is discussed. The electron temperature is estimated to be near 15,000° K, and the density to be near $7 \times 10^4$ ions/cm$^3$ in the filaments. The chief difficulty in the chemical analysis lies in allowing for the distribution of atoms of a given element among different stages of ionization. The abundances are comparable with those found in the stars, a result in harmony with the conclusion reached by Bowen and Wyse in 1939.

## I. INTRODUCTION

It has long been recognized that the unusual character of the spectra of the gaseous nebulae arose from the nature of the excitation conditions prevailing in these objects. Hence any attempt to ascertain their quantitative chemical composition requires careful attention to the excitation mechanism responsible for each line utilized. The determination of the composition of a gaseous nebula from the spectral-line intensities involves essentially the following steps:

1. The relative intensities of the relevant nebular lines are measured spectrophotometrically.

2. The transition probabilities and target areas for collisional excitation are utilized to deduce the electron temperature $T_e$ and density $N_e$ of the electron gas from the intensities of the forbidden lines of selected ions. The electron density can also be found from the intensities of the Balmer continuum and the Balmer lines, if the latter can be measured in flux units, i.e., ergs per square centimeter per second, and if the distance of the nebula is known. Some assumption about the uniformity of density within the nebula is necessary.

3. Once values of $N_e$ and $T_e$ are adopted for the emitting regions of the nebula, the relative line intensities may be used to determine the relative abundances of the corresponding ions.

4. The last step is to estimate what fraction of the atoms of a given element exist in the observed stages of ionization. This calculation requires that the ionization equilibrium existing in the nebula be ascertained, and it turns out to be perhaps the most difficult and uncertain step in the whole procedure.

The necessary quantitative data on the line intensities are available for only a very few nebulae. The relative intensities of the stronger lines have been measured in a large number of planetaries, e.g., Berman (1930), Minkowski (1942), and Aller (1941, 1951). The intensities of the weaker lines in a few planetaries were estimated by Bowen and Wyse (1939) and by Wyse (1942). Wyse made eye-estimates with the aid of a scale plate, but his line intensities appear to have been remarkably accurate, considering the roughness of the methods employed. Recently, spectrophotometric measurements have been made for a few bright planetaries, including NGC 7027 (Bowen, Minkowski, and Aller 1955), NGC 7662, and NGC 2392 (Minkowski and Aller 1955); the observational difficulties inherent in the measurement of the intensities of lines embracing more than a thousand fold range in brightness will be discussed in these communications. Fortunately the bright end of the intensity scale, specifically the brightness ratio of the green neb-

ular lines $N_1 + N_2$ to $H\beta$, has been checked photoelectrically (MacRae and Stock 1954; Liller and Aller 1954). The intensities of the weakest lines are inevitably affected by large accidental errors. Accurate Einstein $A$-values for the hydrogen lines are known from the work of Menzel and Pekeris (1935).

In so far as the recombination lines of helium are concerned, the $A$-values are known with probably adequate accuracy (Goldberg 1939; Huang 1948). Sufficiently good $A$-values have also been obtained for the forbidden lines involving equivalent $p$-electrons (Pasternack 1940; Shortley, Aller, Baker, and Menzel 1941; Ufford, Van Vleck, and Aller 1949; Ufford and Gilmour 1950; Garstang 1951, 1952; Naqvi 1951; Osterbrock 1951).

The forbidden lines represent downward transitions from metastable levels belonging to the ground configurations of various ions. Unfortunately, the target areas for the collisional excitation of these metastable levels are difficult to compute. Calculations for *O* I were carried out by Yamanouchi, Inui, and Amemiya (1940); for *O* III by Hebb and Menzel (1940); for *O* II by Aller (1950), and for *N* II by White and Aller (1949). Bates, Fundaminsky, Massey, and Leech (1950) showed that the theory upon which these calculations were based was inexact and that the computed target areas were probably much too high. Layzer (1951) proposed a new approximate method for calculating target areas for collisional excitation, but no numerical computations have been published. Seaton (1953) has also given an improved theory and has carried out actual calculations of target areas for a number of ions of astrophysical interest. It is not certain that even these target areas are sufficiently accurate for a definitive study of nebular composition.

Finally, the state of ionization in the planetary nebulae cannot be represented by the approximation of an assembly of atoms illuminated by dilute, high-temperature, black-body radiation. The apportionment of atoms among various ionization stages must be estimated empirically (Bowen and Wyse 1939; Wyse 1942; Aller and Menzel 1945; Menzel 1951; Aller 1953*a*). This step seems to be particularly uncertain for objects like NGC 7027, which show a huge range of excitation.

Page (1936) discussed the abundances of some of the elements represented by the strongest forbidden lines in the planetaries, specifically, *N*, *O*, *A*, *Ne*, and *S*. He used the ionization formula for a black body of 50,000° K and a dilution factor obtained from an assumed ratio of $O^+$ to $O^{++}$ of $5 \times 10^{-3}$ derived from Berman's data. In view of the approximations involved, little emphasis could be placed on the resulting differences between stellar and nebular abundances. The first definitive attack on the problem was that made by Bowen and Wyse (1939) and Wyse (1942). They utilized their observations of both bright and faint lines and were able to establish the presence of a number of ions that had not been observed previously in the spectra of the planetaries. They concluded that the spectra of the nebulae could be explained on the assumption that these objects had the same composition as the sun. Wyse's observations were re-discussed by Aller and Menzel (1945) from the point of view of the theory developed in the Harvard Observatory series entitled "Physical Processes in Gaseous Nebulae" (1937–1945). The necessary cross-sections for the collisional excitation of the metastable levels were estimated from those obtained for *O* III by Hebb and Menzel (1940). The nebulae were regarded as homogeneous shells or spheres in which the electron temperature and density were constant. Later, Menzel (1951) made an attempt to correct the abundance estimates for the effects of the filamentary structure of the nebulae. He assumed that in all planetaries the ratio of volume occupied by the gaseous filaments to the total volume occupied by the gross structure of the nebula was the same as in the giant planetary in Aquarius, NGC 7293. In this object Menzel estimated that about one three-hundredth of the volume of the nebula was occupied by matter, the rest of the space being essentially empty. An examination of the best direct photographs and slitless spectrograms convinces me that one cannot assume that *all* planetary nebulae possess the same fine structure. For example, NGC 3587, the "Owl Nebula," shows no evidence of any small-

scale structure at all, even though this object is probably comparable in size and density with NGC 7293 (Minkowski and Aller 1954)!

Menzel may have overcorrected for the influence of filamentary structure. Furthermore, the target areas employed in these studies appear to have been much too large. Recently semiempirical target areas were employed in a reanalysis of Wyse's data for NGC 7027 (Aller 1953*a*), but the results still could not be considered satisfactory. The appearance of Seaton's improved cross-sections (1953) and the new photometric data make a re-examination of the problem worth while.

## II. THE OBSERVATIONAL DATA

Of the planetaries observed in our spectrophotometric study, I chose NGC 7027 as the first object for a detailed analysis because of its exceptionally rich bright-line spectrum. The line intensities were measured at two points in NGC 7027, denoted as *a* and *b*. My quantitative discussion is based on point *a*, which is the brightest patch in the nebula.

The observed Balmer decrement in NGC 7027 is very steep, indicating either unusual conditions of excitation or a pronounced space absorption. The latter interpretation seems the more likely. A discussion of the Balmer decrement in a large number of

TABLE 1

BALMER DECREMENT IN NGC 7027 AND ITS CORRECTION FOR SPACE ABSORPTION

| λ (A) | *n* | $I_{th}$ | $I_{obs}$ | $I_c$ | λ (A) | *n* | $I_{th}$ | $I_{obs}$ | $I_c$ |
|---|---|---|---|---|---|---|---|---|---|
| (1) | (2) | (3) | (4) | (5) | (1) | (2) | (3) | (4) | (5) |
| 6563 | 3 | 25.5 | 65 | 25.7 | 3835 | 9 | 0.99 | 0.46 | 0.91 |
| 4861 | 4 | 10.0 | 10 | 10.0 | 3797 | 10 | .74 | .33 | .66 |
| 4340 | 5 | 5.05 | 3.26 | 4.6 | 3770 | 11 | .57 | .33 | .67 |
| 4101 | 6 | 3.05 | 1.63 | 2.70 | 3750 | 12 | .46 | .27 | .56 |
| 3969* | 7 | 1.99 | .... | .... | 3734 | 13 | 0.35 | 0.23 | 0.48 |
| 3889† | 8 | 1.37 | 0.88 | 1.66 | | | | | |

* Blend with [*Ne* III], which is much stronger than *H*7 and not separated from it with our dispersion.

† Blend with *He* I λ 3888.65, which is probably weaker than *H*8.

planetary nebulae (Aller 1951) shows that the observations, after correction for space absorption, agree most closely with Menzel and Baker's (1938) case "B," i.e., an optically thick nebula in which all the Lyman-line quanta are broken down into Lyman-α and the usual Balmer quanta, etc.

Thus, if we compare the observed Balmer decrement with the theoretical Balmer decrement for case B and $T_e = 14{,}000°$ K, and employ the wave-length law of extinction suggested by Whitford (1948), we find the results given in Table 1. Column 3 gives the theoretical Balmer decrement for case B as interpolated from the data of Menzel and Baker (1938). This theoretical decrement is not sensitive to the electron temperature. Column 4 gives the observed Balmer decrement, and column 5 the observed Balmer decrement after correction for space absorption. The required differential correction for space absorption amounts to 2.75 mag. between λ 4220 and λ 10,300! That is, Whitford's $k_\lambda$'s are to be multiplied by 2.75, and the observed relative intensities by antilog 1.10 $k_\lambda$, to correct them for selective space absorption. The amount of the correction can be stated in other terms by noting that the total extinction at $H\beta$ amounts to a factor of 11.

A comparison of the corrected and theoretical values of the Balmer line intensities shows that the higher members ($n \geq 12$) appear to have been measured systematically too strong. Probably the position of the underlying continuum was incorrectly placed. Other lines of the series show deviations of predominantly the opposite sense. Perhaps

I have underestimated the absorption correction. In any event, it appears safe to say that NGC 7027 is about ten times fainter than it would be, could we but observe it without the interference of the intervening interstellar medium.

### III. ESTIMATION OF IONIC ABUNDANCES FROM THEIR FORBIDDEN LINES

Let us consider, first of all, the analysis of the forbidden-line spectrum of NGC 7027. Let the subscript 1 denote the lowest term of the ground $p^n$ configuration of a given ion. The middle term is denoted by 2, and the highest term by 3. For example, in a $p^2$ configuration the $^3P$ term is denoted as "1," the $^1D_2$ term as "2," and the $^1S_0$ term as "3." We denote the statistical weights of the three terms by $\varpi_1$, $\varpi_2$, and $\varpi_3$.

Atoms will enter term 2 from term 1 by inelastic collisions with electrons and from term 3 by superelastic collisions and by auroral transitions. They escape by superelastic collisions and by radiative transitions of the nebular type. Atoms enter term 3 by inelastic collisions from terms 1 and 2 and escape by superelastic collisions and radiative transitions of the auroral and transauroral types. The corresponding equations of statistical equilibrium (see Menzel, Aller, and Hebb 1941, eqs. [7] and [8]) are

$$N_1 \frac{\Omega_{12}}{\varpi_1} C \exp\left(-\frac{\chi_2}{kT_e}\right) + \frac{N_3 C \Omega_{23}}{\varpi_3} + N_3 A_{23} = N_2 \frac{\Omega_{23}}{\varpi_2} C \exp\left(-\frac{\chi_{23}}{kT_e}\right) + \frac{N_2 C \Omega_{21}}{\varpi_2} + N_2 A_{21} \quad (1)$$

and

$$N_1 \frac{\Omega_{13}}{\varpi_1} C \exp\left(-\frac{\chi_3}{kT_e}\right) + N_2 \frac{\Omega_{23}}{\varpi_2} C \exp\left(-\frac{\chi_{23}}{kT_e}\right) = \frac{N_3 C (\Omega_{23} + \Omega_{13})}{\varpi_3} + N_3 (A_{23} + A_{13}) , \quad (2)$$

where $\Omega$ is the target-area parameter employed by Hebb and Menzel (1940) and by Seaton (1953), while.

$$C \equiv \frac{8.54 \times 10^{-6}}{h_e}; \qquad h_e = \frac{\sqrt{T_e}}{N_e}; \quad (3)$$

and

$$\chi_{23} = \chi_3 - \chi_2 \quad (4)$$

denotes the difference in excitation potential between the second and third levels. From equations (1) and (2) we find the relative populations of the second and third levels to be given by:

$$\frac{N_3}{N_2} = \frac{\varpi_3}{\varpi_2} \exp\left[-\frac{\chi_{23}}{kT_e}\right] \left\{1 + \frac{\Omega_{23} \exp(-\chi_{23}/kT_e)}{\Omega_{12}(1 + \Omega_{23}/\Omega_{13})} + \frac{A_{21}\varpi_2}{C\Omega_{12}(1 + \Omega_{23}/\Omega_{13})}\right\} \times \left\{1 + \frac{(A_{32} + A_{31})\varpi_3}{\Omega_{13} C (1 + \Omega_{23}/\Omega_{13})} + \frac{(\Omega_{23} + A_{32}\varpi_3/C) \exp(-\chi_{23}/kT_e)}{\Omega_{12}(1 + \Omega_{23}/\Omega_{13})}\right\}^{-1}, \quad (5)$$

which may be written as

$$\frac{N_3}{N_2} = \frac{b_3}{b_2} \frac{\varpi_3}{\varpi_2} \exp\left(-\frac{\chi_{23}}{kT_e}\right), \quad (6)$$

to exhibit the factor $b_3/b_2$ that measures the deviation from thermodynamic equilibrium. As the density increases, $b_3/b_2 \rightarrow 1$. Similarly, the ratio $N_2/N_1$ may be written as

$$\frac{N_2}{N_1} = \frac{\varpi_2}{\varpi_1} \exp\left(-\frac{\chi_2}{kT_e}\right) \frac{\{\Omega_{12} + \Omega_{13} d \exp(-\chi_{23}/kT_e)\}}{\{\Omega_{12} + A_{21}\varpi_2/C + \Omega_{23}(1 - d)\exp(-\chi_{23}/kT_e)\}}, \quad (7)$$

where

$$d = \frac{\Omega_{23} + A_{23}\varpi_3/C}{\Omega_{13} + \Omega_{23} + (A_{32} + A_{31})\varpi_3/C}. \quad (8)$$

In analogy with equation (6), we may now write

$$\frac{N_2}{N_1} = \frac{b_2}{b_1}\frac{\varpi_2}{\varpi_1}\exp\left(-\frac{\chi_2}{kT_e}\right). \tag{9}$$

Finally,

$$\frac{N_3}{N_1} = \frac{b_3}{b_1}\frac{\varpi_2}{\varpi_1}\exp\left(-\frac{\chi_3}{kT_e}\right). \tag{10}$$

Here

$$\frac{b_3}{b_1} = \frac{\{\Omega_{13}+\Omega_{12}[p+\exp(-\chi_{23}/kT_e)]^{-1}\}}{\{(\Omega_{23}+\Omega_{13})+(A_{32}+A_{31}\varpi_3)/C-(\Omega_{23}+A_{23}\varpi_3/C)[1+p\exp(\chi_{23}/kT_e)]^{-1}\}}, \tag{11}$$

where $p$ is defined by

$$p \equiv \frac{\Omega_{12}}{\Omega_{13}} + \frac{A_{23}\varpi_2}{C\Omega_{23}}. \tag{12}$$

The intensity ratio $I_a/I_n$ of the auroral to nebular lines of [O III] have been employed to estimate $T_e$ (Menzel, Aller, and Hebb 1941). Now

$$\frac{I_a}{I_n} = \frac{N_3 A_{3,2}\nu_{3,2}}{N_2 A_{2,1}\nu_{2,1}} = \frac{b_3}{b_2}\frac{\varpi_3}{\varpi_2}\exp\left(-\frac{\chi_{23}}{kT_e}\right)\frac{A_{3,2}\nu_{3,2}}{A_{2,1}\nu_{2,1}}. \tag{13}$$

Equations (11), (12), and (13) may be combined to yield an expression exhibiting the dependence of $I_a/I_n$ upon $N_e$ and $T_e$ with the $A$'s and $\Omega$'s entering as parameters. At the temperatures and densities prevailing in the gaseous nebulae, an approximate form of equation (13) may be obtained that is sufficiently good for most calculations. Menzel, Aller, and Hebb adopted values of $N_e$ from the surface brightnesses of the nebulae in $H\beta$ or the nebular continuum (Menzel and Aller 1941), Pasternack's $A$-values, the Hebb-Menzel target areas, and computed $T_e$ from the observed $I(4363)/I(N_1 + N_2)$ ratios (Aller 1941).

Some years later the cross-sections for the collisional excitation of the auroral and nebular [N II] lines were determined by the same methods as had been employed for [O III]. If one assumes that the [N II] and [O III] lines arise in the *same* strata, simultaneous transcendental equations of the form (13) involving $N_e$ and $T_e$ must hold (Aller and White 1949). Thus the electron temperature and density in the radiating elements can be found directly. The electron temperatures that were thus obtained did not differ much from those previously found, but the electron densities in the radiating strata turned out to be higher by factors ranging from 1 to 7. The detailed results were not published, since it was shown soon thereafter that the theoretical basis for the target-area calculations was unsound. Very recently, Seaton (1954) has employed similar considerations but with his improved target areas for collisional excitation.

If we employ Seaton's (1953) target areas with $A$-values from the work of Garstang (1951), equation (13) becomes, for [O III],

$$\frac{I(4363)}{I(N_1+N_2)} = 13.1\times 10^{-14,300/T_e}\left\{\frac{1.01+2300h_e}{1.01+270{,}000h_e}\right\} \sim 0.113\times 10^{-14,300/T_e} \tag{14}$$

for low densities, while for the [N II] lines, equation (13) becomes

$$\frac{I(5755)}{I(6560)} = 61.5\times 10^{-10,820/T_e}\left\{\frac{1.01+320h_e}{1+194{,}000h_e}\right\}. \tag{15}$$

The observed intensity ratios on the left-hand side of equations (14) and (15) are 0.0155 and 0.056, respectively. The simultaneous solution of these equations then gives $N_e \sim 7.7\times 10^4$ electrons/cm$^3$ and $T_e \backsim 14{,}500°$ K. On the other hand, if we employ only the

[O III] data together with the photoelectrically measured surface brightness (Liller and Aller 1954) corrected for space absorption and the distance derived by Berman (1937), $N_e$ turns out to be only $1.7 \times 10^4$ electrons/cm$^3$. The electron temperature is then 15,000° K. If the target areas are trustworthy, these results imply that there must be a considerable concentration of the material in filaments, although it is also possible that the [N II] and [O III] radiation originates predominantly in *different* regions within the nebula. In the calculations carried out in the remainder of this paper we have taken $N_e = 7.7 \times 10^4$, $T_e = 14{,}500°$ K, but it must be noted that the adopted temperature is somewhat higher than that implied by the magnitude of the observed Balmer discontinuity, which suggests $T_e \leq 10{,}000°$ K.

The emission per unit volume in nebular or auroral-type transitions by ions of type $i$ will be

$$E_n = N_2 A_{2,1} h\nu_{2,1} = \eta_2 N_i \frac{\varpi_2}{\varpi_1} h\nu_{2,1} A_{2,1} \exp\left(-\frac{\chi_2}{kT_e}\right),$$
$$E_a = N_3 A_{3,1} h\nu_{3,1} = \eta_3 N_i \frac{\varpi_3}{\varpi_1} h\nu_{3,1} A_{3,1} \exp\left(-\frac{\chi_3}{kT_e}\right), \tag{16}$$

where $\eta_2 = b_2/b_1$ and $\eta_3 = b_3/b_1$. The emission in the green nebular lines of [O III] can be written as

$$E_O = N_2^0 A_0 h\nu_0 = \eta_2^0 N_1^0 \frac{\varpi_2}{\varpi_1} h\nu_0 A_0 \exp\left(-\frac{\chi_2^0}{kT_e}\right). \tag{17}$$

If $I_{n,i}$ is the total intensity of the nebular transitions of the ion of type $i$ and $I_0$ is the intensity of the two green nebular lines, the relative numbers of ions of type $i$ and $O^{++}$ ions will be

$$\frac{N_i}{N_0} = \frac{I_{ni}}{I_0}\left\{\frac{5\lambda\varpi_1 A_0 \eta_2^0}{9\lambda_0\varpi_2 A\,\eta_2}\right\} 10^{(\chi - \chi_0)\theta}, \tag{18}$$

where $\theta = 5040/T_e$. The appropriate formulae for the $\eta$'s may be developed from equations (7) and (11). Thus we obtain the following expressions which are valid for nebular temperatures and densities.

Nebular lines of [N II]:

$$\eta_2 = \frac{\{2.39 + 0.217 \times 10^{-2.15\theta}\}}{\{2.39 + 2340 h_e\}} \sim (1 + 960 h_e)^{-1}. \tag{19}$$

Nebular lines of [O III]:

$$\eta_2 = \frac{\{1.73 + 0.171 \times 10^{-2.84\theta}\}}{\{1.73 + 16400 h_e + 0.085 \times 10^{-2.84\theta}\}} \sim [1 + 9380 h_e]^{-1}. \tag{20}$$

Auroral/nebular-line ratio in [O II] requires

$$\frac{\eta_3}{\eta_2} = \frac{\{1 + 0.136 \times 10^{-1.69\theta} + 6.38 h_e\}}{1 + 85200 h_e + [0.136 + 10770 h_e]\, 10^{-1.69\theta}}. \tag{21}$$

Nebular lines of [O II]:

$$\eta_2 = \frac{1.44 + 0.167 \times 10^{-1.69\theta}}{1.44 + 90.2 h_e + 0.444 \times 10^{-1.69\theta}}. \tag{22}$$

The equations for the fluorine and neon ions are relatively simple:

$$\eta_2 = [1 + 35{,}600 h_e]^{-1} \qquad [F\ II], \tag{23}$$

$$\eta_2 = [1 + 200{,}000 h_e]^{-1} \qquad [Ne\ \text{III}], \tag{24}$$

$$\eta_3 = [1 + 363{,}000 h_e]^{-1} \qquad [Ne\ \text{V}]. \tag{25}$$

The large target areas for [S II] result in a relatively complicated expression for $\eta_3$, viz.,

$$\eta_3 = \frac{0.383 + 2.02 a_e \times 10^{1.198}}{13.1 + 656{,}000 h_e - [12.7 + 475{,}000 h_e]\, a_e}, \tag{26}$$

where

$$a_e = [1 + (0.159 + 98.5 h_e)\, 10^{1.198}]^{-1},$$

while for the nebular lines we need the expression

$$\eta_2 = \frac{2.02 + 0.279 \times 10^{-1.198}}{2.02 + 1260 h_e + 3.43 \times 10^{-1.198}}. \tag{27}$$

Equations (14)–(27) embrace the ions for which Seaton has calculated target-area parameters. The spectrum of NGC 7027 includes many lines of ions for which no target areas are available.

Following a suggestion by Seaton, I have estimated Ω's by comparing the Ω-parameters for *S* II and *O* II and assuming that the same ratio holds for the other ions. Thus

$$\frac{\Omega_{1,2}(S\ \text{II})}{\Omega_{1,2}(O\ \text{II})} = 1.40,$$

so we assume

$$\Omega_{1,2}(S\ \text{III}) = 1.40\Omega_{1,2}(O\ \text{III}), \qquad \Omega_{1,2}(Cl\ \text{IV}) = 1.40\Omega_{1,2}(Ne\ \text{IV}), \text{ etc.}$$

Table 2 gives the estimated cross-section parameters for the ions of the $3p^n$ con-

TABLE 2

ASSUMED CROSS-SECTION PARAMETERS $\Omega_{i,j}$ FOR IONS OF $3p^n$ CONFIGURATIONS

| Ion | $\Omega_{1,2}$ | $\Omega_{1,3}$ | $\Omega_{2,3}$ |
|---|---|---|---|
| | | $3p^2$ | |
| *S* III | 2.42 | 0.341 | 4.03 |
| *Cl* IV | 1.69 | .301 | 3.82 |
| *A* V | 1.18 | .275 | 3.5 |
| | | $3p^3$ | |
| *Cl* III | 1.40 | .387 | 20.5 |
| *A* IV | 0.95 | .410 | 23.2 |
| | | $3p^4$ | |
| *A* III | 1.16 | .161 | 1.78 |
| *K* IV | 0.855 | .135 | 1.98 |
| *Ca* V | 0.755 | 0.20 | 1.98 |

figuration. Obviously, abundances computed from these assumed Ω's are subject to large uncertainties.

Expressions similar to equations (19)–(27) may be derived for the forbidden lines of ions in the $3p^n$ configuration. We shall not give the detailed formulae here, as they are based on rather rough cross-sections for collisional excitation.

We calculate the relative concentrations of the various ions on the assumption that all are found in the same layers. In nebulae where stratification exists or where the actual filamentary structure can be seen, this condition is usually not fulfilled. No marked stratification appears in NGC 7027, and such filamentary structure as exists lies below the resolution of the best photographs. It is worth remembering that in

nebulae where the filaments are observed in [*N* II] and [*O* III], for example, the [*O* III] filaments are often much more diffuse and softer in appearance than the [*N* II] filaments.

Since the aforementioned calculations give the concentration of ions in terms of those of $O^{++}$, we must estimate the density of the $O^{++}$ ions. It is assumed that all the material of the nebula is concentrated in filaments with empty space in between. The emission per unit volume per second in $H\beta$ is given, e.g., by (Aller 1953*b*)

$$E(H\beta) = 0.228 \times 10^{-18} N_i N_e b_4 T_e^{-3/2} \exp\left(\frac{hRZ^2}{16kT_e}\right), \tag{28}$$

whereas that in the green nebular lines is given by

$$E(N_1 + N_2) = \tfrac{5}{9} N(O^{++})\, \eta_2 A_0 h\nu 10^{-12,500/T_e}. \tag{29}$$

If we now divide equation (29) by equation (28) and put

$$\frac{E(N_1+N_2)}{E(H\beta)} = \frac{I(N_1+N_2)}{I(H\beta)} = 18.6, \quad N_e = 7.7 \times 10^4, \text{ and } T_e = 14{,}500^\circ K,$$

we find $N(O^{++}) = 14.3$.

Table 3 gives the results obtained from the forbidden-line data. Column 2 gives, for

TABLE 3

ABUNDANCES OF IONS IN NGC 7027 FORBIDDEN-LINE DATA

| Ion (1) | Trans. (2) | λ (3) | $A_n$ (4) | χ (5) | $b_i/b_1$ (6) | $I_c$ (7) | $N_i$ (8) |
|---|---|---|---|---|---|---|---|
| *N* II | N | 6565 | 0.0040 | 1.88 | 0.40 | 124 | 0.900 |
| | A | 5755 | 1.08 | 4.03 | .0020 | 7.1 | 0.935 |
| *O* II | N | 3727 | 0.0577 | 3.31 | .87 | 29 | 2.72 |
| | A | 7325 | 0.200 | 5.00 | .0065 | 22 | 0.97 |
| *O* III | N | 5000 | 0.028 | 2.48 | .064 | 1850 | 14.3 |
| *F* II | N | 4790 | 0.058 | 2.58 | .0176 | 0.7 | 0.010 |
| *Ne* III | N | 3895 | 0.26 | 3.19 | .0032 | 124 | 6.7 |
| *Ne* IV | A | 4724 | 0.534 | 7.38 | .00165 | 9.7 | 6.3 |
| *Ne* V | N | 3400 | 0.52 | 3.70 | .00176 | 236 | 7.3 |
| *S* II | N | 6722 | 0.00107 | 1.84 | .400 | 4.7 | 0.063 |
| *S* II | TA | 4072 | 0.257 | 3.03 | .00132 | 12.0 | 0.53 |
| *S* III | A | 6311 | 3.6 | 3.30 | .00056 | 6.8 | 0.58 |
| *Cl* III | N | 5520 | 0.0042 | 3.69 | .1265 | 2.5 | 0.100 |
| *Cl* IV | N | 7840 | 0.277 | 1.60 | .0066 | 1.26 | 0.017 |
| *Cl* IV | A | 5322 | 4.2 | 3.92 | .00026 | 0.73 | 0.36 |
| *A* III | N | 7360 | 0.404 | 1.68 | .00032 | 22 | 0.043 |
| *A* IV | N | 4720 | 0.0135 | 2.61 | .035 | 17 | 0.27 |
| *A* IV | A | 7250 | 1.75 | 4.31 | .00032 | 2.8 | 0.38 |
| *A* V | N | 6800 | 0.743 | 1.85 | .0017 | 6.5 | 0.134 |
| *K* IV | N | 6101 | 1.037 | 1.95 | .00090 | 1.2 | 0.007 |
| *K* VI | N | 6034 | 1.75 | 2.044 | .00048 | ≦0.2 | 0.001 |
| *Ca* V | N | 5000 | 2.37 | 2.22 | 0.00035 | 1.6 | 0.011 |

each ion, the type of transition observed, nebular (*N*), auroral (*A*), or transauroral (*TA*). Column 3 gives λ, the mean wave length of the forbidden-line multiplet, while column 4 gives the corresponding transition probability. The excitation potential of the upper term of the transition in electron volts is listed in column 5. Column 6 gives the quantity $\eta_2 = b_2/b_1$ (for the nebular transitions) or $\eta_3 = b_3/b_1$ (for auroral and transauroral transitions). In column 7 $I_c$ denotes the intensity of the whole forbidden-line multiplet (corrected for space absorption) and for the contribution of lines that may be masked by blending or otherwise hidden. Column 8 gives $N_i$, the relative number of ions, expressed approximately as numbers of ions per cubic centimeter.

If our assumptions are fulfilled, the concentration of a given ion should be the same

whether it is computed from the auroral, transauroral, or nebular transition. This condition is, of course, fulfilled for the $O^{++}$ and $N^{+}$ ions, as these were employed to fix $N_e$ and $T_e$. It is not fulfilled for the $S^{+}$ or for the $O^{+}$ ions. A comparison of the intensities of the auroral ($\sim\lambda$ 7319) and nebular ($\sim\lambda$ 3727) transitions of $O^{+}$ indicates that the density in the filaments where these radiations are predominantly produced is substantially lower than $7 \times 10^{4}$ ions/cm$^{3}$. On the other hand, the [*S* II] radiations appear to be produced in filaments of much higher density. Hence our results can be understood in terms of a nebula consisting of numerous filaments, knots, and tenuous regions such that the density may range from perhaps less than $10^{4}$ ions/cm$^{3}$ to perhaps something like $2 \times 10^{5}$ ions/cm$^{3}$. It has long been recognized that the [*S* II] lines tend to be strong in objects of high density, particularly in small bright nebulae, whereas the [*O* II] radiation is found to predominate in the outer, less dense regions of many large planetaries. The probable, but not directly observable, filamentary structure of NGC 7027 thus imposes a fundamental limitation on the accuracy with which the abundances of the ions can be found in this object. No credence can be placed in the discrepancies between the abundances derived from the auroral and from the nebular lines of *Cl* IV or *A* IV, since the cross-sections for the collisional excitation of these lines can only be guessed.

## IV. THE RECOMBINATION LINES OF HELIUM

The intensities of the permitted lines of *He* I depend essentially on the concentration of $He^{+}$ ions, while the intensities of $\lambda$ 4686, $\lambda$ 3202, and the Pickering lines of *He* II depend on the concentration of $He^{++}$. Let us consider, first, the line emission from ionized helium.

The total radiation emitted in the $n \rightarrow n'$ transition per cubic centimeter per second by a strictly hydrogen-like ion is (Menzel 1937)

$$E_{nn'} = N_i N_e K Z^4 T_e^{-3/2} b_n(T_e)\, g_{nn'} 2hRZ^2 (n'n)^{-3} \exp(X_n)\,. \tag{30}$$

The emission in $\lambda$ 4686 of $He^{+}$ is found by setting $Z = 2$, $n = 4$, and $n' = 3$. Thus

$$E_{4686} = 3.92 \times 10^{-18} N(He^{++})\, N_e T_e^{-3/2} b_4 \frac{T_e}{4} \exp(X_4)\,, \tag{31}$$

since the solution for the $b_n$'s for hydrogen at a temperature $T_e$ is the same as the solution for ionized helium at the same value of

$$X_n = \frac{hRZ^2}{n^2 kT_e} = \frac{hR}{n^2 k\,(T_e/Z^2)}\,. \tag{32}$$

Thus the values of $b_n$ for ionized helium at a temperature of 16,000° K are the same as those for hydrogen with $T_e = 4000°$ K.

The intensity ratio $I_{4686}/I_{H\beta}$ will be related to the concentration ratio of $He^{++}$ and $H^{+}$ ions by

$$\frac{I_{4686}}{I_{H\beta}} = 17.2\, \frac{N(He^{++})\, b_4(He^{+})}{n(H^{+})\, b_4(H)} \exp\left(\frac{3hRZ^2}{16kT_e}\right). \tag{33}$$

If the observed intensity ratio $I(4686)/I(H\beta) = 0.50$ be employed in this equation with the estimate $b_4(He^{+}) = 0.016$ for $T_e = 14{,}500°$ K, the ratio of doubly ionized helium atoms to ionized hydrogen atoms is found to be 0.066. This figure is sensitive to $T_e$. Similar calculations can be made for the Pickering lines and other lines of the *He* II spectrum, but all involve uncertain $b_n$-factors.

Turning, now, to the lines of neutral helium, we find that the number of helium atoms in level $j$ will be given by the combined Boltzmann and Saha equations as

$$N_j = b_j N(He^{+})\, N_e \left(\frac{h^2}{2\pi m kT_e}\right)^{3/2} \frac{\varpi_j}{4} \exp\left(\frac{I_0 - \chi_j}{kT_e}\right). \tag{34}$$

Here $I_0$ denotes the ionization potential of the *He* I atom, whereas $\chi_j$ and $\varpi_j$ are the excitation potential and statistical weight, respectively, of the upper level of the observed transition. The ratio of the number of atoms in the $j$th level of *He* I to the number in the $n$th level of hydrogen will be

$$\frac{N_j}{N_n} = \frac{\varpi_j b_j N(He^+)}{4n^2 b_n N(H^+)} \exp\left(\frac{I_j}{kT_e} - X_n\right), \tag{35}$$

where

$$I_j = I_0 - \chi_j . \tag{36}$$

If the helium and hydrogen recombination lines originate to the same degree in the same layers,

$$\frac{I_{jj'}}{I_{H\beta}} = \frac{E_{jj'}}{E_{H\beta}}. \tag{37}$$

Hence

$$\frac{N_j}{N_4} = \frac{I_{jj'} A_{H\beta} \lambda_{jj'}}{I_{H\beta} A_{jj'} \lambda_{H\beta}}. \tag{38}$$

Equations (35) and (38) now yield

$$\frac{N(He^+)}{N(H^+)} = \frac{64\, b_4 I_{jj'} A_{H\beta} \lambda_{jj'}}{\varpi_j b_j I_{H\beta} A_{jj'} \lambda_{H\beta}} \exp\left(X_n - \frac{I_j}{kT_e}\right). \tag{39}$$

The necessary $A$-values have been computed by Goldberg (1938), who has also calculated the $b_j$-factors for idealized helium atoms exposed to the dilute temperature-radiation field of a planetary nebula. Since he treated all the high singlet terms as though they constituted a single level, one value of $b_j$ is obtained for all. In reality, $b_j$ must certainly approach 1 as $j$ increases without bound.

Table 4 gives the results obtained from the three best observed lines of the triplet

TABLE 4

ABUNDANCE OF $He^+$ IONS CALCULATED FROM TRIPLET TRANSITIONS

| λ | Transition | $A \times 10^{-8}$ | $I(H\beta = 1)$ | $N(He^+)/N(H^+)$ |
|---|---|---|---|---|
| 5876 | $2\,^3P - 3\,^3D$ | 64.7 | 0.144 | 0.028 |
| 4471 | $2\,^3P - 4\,^3D$ | 25.9 | .050 | .035 |
| 4026 | $2\,^3P - 5\,^3D$ | 12.8 | 0.035 | 0.056 |

series. I have used $b_j(He\ \text{I}) = 0.50$ for all the high triplet levels. The weighted mean value is taken as 0.035. The increase in the computed values with increasing $j$ is to be expected.

The final $H/He$ ratio turns out to be about 10, in probably fortuitous agreement with earlier results for the average of several planetaries (Aller and Menzel 1945). Wurm (1953), however, concludes that the ratio must lie between 6 and 2. If Wurm is right, the $H/He$ ratio may be very different for the planetaries than it is for the stars. He regards the estimation of abundances from the neutral helium lines as unreliable and bases his abundance estimates exclusively on the *He* II λ 4686 line in high-excitation planetaries. The determination of an accurate value of the $H/He$ ratio is complicated by the filamentary structure of most planetary nebulae and by the fact that the temperature may vary from one point in the nebula to another. The ionized helium lines may actually be formed in regions of higher electron temperature than are the hydrogen lines.

## V. DETERMINATION OF THE ABUNDANCES

The determination of the true relative abundances of the elements which are represented by the forbidden lines of ions in one or two stages of ionization is an extremely

difficult task. We must devise some means of guessing the contributions of the unobserved ions. Since the usual ionization formula for dilute temperature radiation cannot represent the observed distribution of the ions in nebulae such as NGC 7027, an empirical approach must be used. We have employed the method used in the Harvard nebular series (Aller and Menzel 1945), which consists in deriving an empirical ionization-curve from the ratios of the numbers of ions of a given element in successive stages of ionization. Such a procedure necessarily introduces a number of serious uncertainties. The ionic abundances themselves are uncertain because of the accidental observational errors, inaccuracies in the target areas, and the complications that may arise from a possible concentration of different ions in different filaments. It is also assumed that the degree of ionization depends only on the ionization potential. The influence of possible strong, bright lines in the far ultraviolet is neglected. In an object like NGC 7027, it is conceivable that such lines might build up to considerable intensity. The factors for reducing the observed number of ions to the total number of atoms of a given element become very large for the metals, whereas they are much smaller for neon. Table 5 compares the abundances (by numbers of atoms) of elements observed in NGC 7027 with the abundances found in a standard star (Aller 1953*a*). In this compilation I have taken the stellar *H*/*He* ratio as about 19, however. The agreement for *H*, *He*, *N*, and *O* is good, considering the uncertainties in the analysis. Fluorine was observed in the nebulae by Wyse (1942) but not by Minkowski and me; I have tentatively adopted the Wyse intensity in my estimates. The stellar data for fluorine are likewise unsatisfactory. Neon would appear to be less plentiful, and sulfur more so, than in the stars. It is probable that the effects of the filamentary structure are operative here. The [*S* II] emission is greatly favored in dense filaments. The data for chlorine, argon, potassium, and calcium are based on extrapolated target areas; the derived abundances must be uncertain not only from this cause but even more so from the insecure allowance for distribution among unobserved ionization stages.

TABLE 5

COMPOSITION OF NGC 7027 COMPARED WITH THAT OF A "NORMAL" STAR

(Logarithm of Relative Numbers of Atoms)

| Element | NGC 7027 | Star | Element | NGC 7027 | Star |
|---|---|---|---|---|---|
| *H* | 13.04 | 13.27 | *S* | 9.21 | 8.52 |
| *He* | 12.0 | 12.0 | *Cl* | 8.39 | 8.3: |
| *N* | 9.56 | 9.49 | *A* | 8.22 | 9.0: |
| *O* | 10.00 | 10.00 | *K* | 6.2: | 6.39 |
| *F* | 7.4: | 7.7: | *Ca* | 6.6: | 7.72 |
| *Ne* | 9.48 | 10.04 | | | |

The chief virtue of NGC 7027 for a composition study comes from the large number of lines observed in its spectrum, so that the estimate of the abundance of any given element is often based on ions of several different ionization stages. The chief disadvantage of this object lies in its possible filamentary structure and the circumstance that the ionization cannot be regarded as a simple phenomenon of dilute temperature radiation. A discussion of other nebulae, such as NGC 7662, NGC 6572, and NGC 1535, is limited by the less complete information on the lines. In a later paper we shall attempt an analysis of NGC 7662, taking the structural features into account.

I am indebted to Dr. R. Minkowski for suggestions and comments, and I should like to express my gratitude to Dr. M. J. Seaton, who communicated his target-area parameters to me in advance of publication.

## REFERENCES


Aller, L. H. 1941, *Ap. J.*, **93**, 236.
———. 1950, *ibid.*, **111**, 609.
———. 1951, *ibid.*, **113**, 125.
———. 1953*a*, *The Atmospheres of the Sun and Stars* (New York: Ronald Press Co.), pp. 327, 329.
———. 1953*b*, *Ap. J.*, **118**, 547.
Aller, L. H., and Menzel, D. H. 1945, *Ap. J.*, **102**, 239.
Aller, L. H., Ufford, C. W., and Van Vleck, J. H. 1949, *Ap. J.*, **109**, 42.
Aller, L. H., and White, M. L. 1949, *A.J.*, **54**, 181.
Bates, D. R., Fundaminsky, A., Leech, J. W., and Massey, H. S. W. 1950, *Phil. Trans. R. Soc. London, A*, **243**, 117.
Berman, L. 1930, *Lick Obs. Bull.*, **15**, 86.
———. 1937, *ibid.*, **18**, 73.
Bowen, I. S., Minkowski, R., and Aller, L. H. 1955 (in press).
Bowen, I. S., and Wyse, A. B. 1939, *Lick Obs. Bull.*, **19**, 1.
Garstang, R. H. 1951, *M.N.*, **111**, 116.
———. 1952, *Ap. J.*, **115**, 506.
Goldberg, L. 1939, *Ap. J.*, **90**, 414.
———. 1941, *ibid.*, **93**, 244.
Huang, Su-shu. 1948, *Ap. J.*, **108**, 354.
Layzer, D. 1951, *Phys. Rev.*, **84**, 1221.
Liller, W., and Aller, L. H. 1954, *Ap. J.*, **120**, 48.
MacRae, D., and Stock, J. 1954, *Nature*, **173**, 589.
Menzel, D. H. 1937, *Ap. J.*, **85**, 330.
———. 1951, *Trans. I.A.U.*, **7**, 471.
Menzel, D. H., and Aller, L. H. 1941, *Ap. J.*, **93**, 145.
Menzel, D. H., Aller, L. H., and Hebb, M. H. 1941, *Ap. J.*, **93**, 230.
Menzel, D. H., and Baker, J. G. 1938, *Ap. J.*, **88**, 52.
Menzel, D. H., and Hebb, M. L. 1940, *Ap. J.*, **92**, 408.
Menzel, D. H., and Pekeris, C. L. 1935, *M.N.*, **96**, 77.
Minkowski, R. 1942, *Ap. J.*, **95**, 243.
Minkowski, R., and Aller, L. H. 1954, *Ap. J.*, **120**, 261.
———. 1955 (in press).
Naqvi, Ali. 1951, Harvard thesis.
Osterbrock, D. 1951, *Ap. J.*, **114**, 469.
Pasternack, S. 1940, *Ap. J.*, **92**, 129.
Seaton, M. J. 1953, *Proc. R. Soc. London, A*, **218**, 400.
———. 1954, *M.N.* (in press). The target area parameters $\Omega_{2,3}$ were communicated to me in advance of publication.
Shortley, G. H., Aller, L. H., Baker, J. G., and Menzel, D. H. 1941, *Ap. J.*, **93**, 178.
Ufford, C. W., and Gilmour, R. M. 1950, *Ap. J.*, **111**, 580.
Wurm, K. 1953, contribution in *Les Processus nucléaires dans les astres* (Liége University, 1954), p. 387.
Wyse, A. B. 1942, *Ap. J.*, **95**, 356.
Yamanouchi, T., Inui, T., and Amemiya, A. 1940, *Proc. Physico-Math. Soc. of Japan*, Ser. 3, **22**, 848.

# MAGNITUDES AND COLOR INDICES OF EXTRAGALACTIC NEBULAE DETERMINED PHOTOELECTRICALLY

EDISON PETTIT
Mount Wilson and Palomar Observatories
Carnegie Institution of Washington
California Institute of Technology

*Received March 12, 1954; revised April 22, and June 15, 1954*

## ABSTRACT

These measures on the International scale are part of the program of detailed investigation of the distance-velocity function of extragalactic systems for which Humason and Mayall have measured the radial velocities. The photometer with 1P21 tube has been tested for light-response, field response, refrigeration phenomena, disturbances, effects of the earth's field, transmissions and color sensibility, and other physical properties. Equivalent photographic magnitude, $m_{pg}$, is made to depend on the free *minus* the yellow response, and color is determined by two methods, the ratios of yellow to free *minus* yellow, and yellow to blue.

Some of the by-products have been a determination of the magnitudes and color indices of the central stars in all the Selected Areas in the 30° zone and of a number of stars in the polar sequence.

All the nebular measures in Tables 5 and 5*a* have been freed from galactic stars. Certain nebulae, like NGC 4569, have a galactic star nearly as bright as the nucleus almost in optical contact with it, but these have been removed. The magnitude of IC 342 and the color and magnitude of IC 1613, two systems of large angular dimensions, have been determined by measurement in sections.

In these tables will be found members of several clusters, more than thirty of the Coma cluster, for example. Several double nebulae are included. Measures with apertures of 0'.7 or less represent essentially measures of the nuclei for 127 nebulae. These nuclei are redder than the nebula as a whole, save in 12 per cent of those measured.

The color indices in Tables 5 and 5*a* are the observed values corrected to the zenith, as are also the magnitudes. These have not been corrected for galactic absorption, which may affect some of low galactic latitude.

The color index as a function of magnitude for the four nebular classes is shown in Figures 2, 3, 4, and 5. The trend of E types is definite and corresponds to the formula C.I. = 0.04 ($m_{pg}$ − 9 mag.) + 0.84 mag. The trend of the S types is assessable and approximates the formula C.I. = 0.08 ($m_{pg}$ − 9 mag.) + 0.50 mag. The E and S types seem to have about the same color at $m_{pg}$ 17, but for brighter nebulae the E nebulae are the redder. The plots of SB type and the irregulars are too scattered to draw conclusions, but no restricted regions of color index were found for the irregulars.

## INTRODUCTION

The determination of magnitudes on the photographic scale and of color indices of extragalactic nebulae was made photoelectrically with a photomultiplier cell attached to the 60- or 100-inch telescope during the years 1947–1954. This forms part of the program for the reinvestigation of the nebular red shift for which Humason at Mount Wilson and Mayall at the Lick Observatory have provided the spectra of an extensive list of systems. The photometry discussed here was done with an instrument constructed along the lines of one used by A. E. Whitford (1947), who, with J. Stebbins, began the investigation and who furnished the author with circuits and other details of his photometer (Stebbins and Whitford 1952).

Essentially, the instrument consists of a 1P21 tube, battery fed, upon the cathode of which an image of the telescope mirror is cast by short-focus fused quartz lenses separated by a thin cellophane partition. A single-stage amplifier was used for objects fainter than 12 or 13 mag., depending on the telescope used. Deflection was observed by galvanometer and scale. It was early found that the coarse zero adjustment by potentiometer across the filament of the amplifier changed the amplification factor, so the potentiometer was provided with a calibrated scale.

The dimensions of the circular apertures in the sliding plate used to isolate the nebulae, and their angular equivalents at the two telescopes are shown in Table 1. The comparison of the areas with sky-deflection measures is shown in the last two columns. The tabular areas are those used in Tables 5 and 5*a*, and, since they are discrete, they indicate which telescope was used. Approximately rectangular apertures were sometimes used to reduce further any unnecessary sky radiation and galactic stars. These were formed by strips of masking tape laid upon the circular aperture listed as the larger dimension in Tables 5 and 5*a*.

Five individual 1P21 cells were used and were tested in the laboratory for response to light-flux over a range equivalent to 5–17 mag. at the 60-inch telescope. No sensible deviation from linearity was found.

The effects of refrigeration on the sensibility of each cell were studied, and about 40

TABLE 1

DIMENSIONS OF THE APERTURE PLATE

| No. | D (Mm) | 60-Inch Min. of Arc | 60-Inch Tabular | 100-Inch Min. of Arc | 100-Inch Tabular | Area Ratios | Sky Deflection |
|---|---|---|---|---|---|---|---|
| 1 | 0.70 | 0.316 | 0.3 | 0.187 | 0.2 | 1 | 0.9 |
| 2 | 1.56 | 0.705 | 0.7 | 0.416 | 0.4 | 5.0 | 5.0 |
| 3 | 2.54 | 1.147 | 1.1 | 0.678 | 0.6 | 13.2 | 13.3 |
| 4 | 5.07 | 2.268 | 2.3 | 1.340 | 1.3 | 51.4 | 49.7 |
| 5 | 9.01 | 4.070 | 4.1 | 2.404 | 2.4 | 166 | 166 |
| 6 | 12.60 | 5.692 | 5.7 | 3.362 | 3.4 | 324 | 323 |
| 7 | 19.05 | 8.605 | 8.6 | 5.082 | 5.1 | 741 | 725 |

minutes' delay was allowed before observing with a freshly filled photometer. The effects of temperature changes on the battery were studied and found to be less than 0.01 mag. in the measures.

TRANSMISSIONS AND COLOR SENSIBILITY

The filters were Schott's BG1, 1 mm thick, and GG7, 2 mm thick. The transmissions *C* and *D*, are shown in Figure 1. The combined transmissions of the two quartz lenses and cellophane pellicle are given in curve *E*. Figure 1 also shows the spectral sensitivity, *A*, of cell No. 6, which is representative of most 1P21 cells, and, *B*, that of cell No. 5, which is exceptional in its red sensitivity. These curves were determined in the laboratory.

Figure 1 shows (*below*) the spectral response of the photometer containing cells Nos. 6 and 5 (*FA*, *FB*) and its spectral response when the filters are in place, *CA*, *CB* (blue) and *DA*, *DB* (yellow). It is seen that the yellow and blue filters cover the ranges of the visual and photographic light which define $m_v$ and $m_{pg}$, respectively. For a solar-type star in the zenith the centers of effective wave length are λλ 4200 and 5300, respectively. While the yellow is confined to the visual region, with maximum near visual maximum, the blue (*CA*, *CB*) reaches into this region somewhat. On this account the free (*FA* or *FB*) *minus* the yellow (*DA* or *DB*) was used for equivalent photographic magnitudes $m_{pg}$ and one system of color index. More exactly, the yellow (according to Fresnel's formula) should be multiplied by the fraction $\frac{13}{12}$ to correct for losses by reflection; but actual test shows that this refinement is indistinguishable, and, since it saved some computing time, the simpler term, free *minus* yellow ($F - Y$), was used.

The effects of the earth's magnetic field upon the sensitivity of the photometer were tested in the laboratory and found to amount to a reduction of 1 per cent between the pole and the equator. No hour-angle effect was observable.

Since the calibrations at the 60-inch telescope are referred to the polar sequence and the celestial pole is about 90° from the magnetic pole, this condition requires a correction of about −0.01 mag. for declinations below +60°, where the magnetic vector at the cell exceeds half the maximum (−0.01 mag.) in the equatorial position. This correction was

therefore applied to all objects below this limit of declination. The magnitudes of the central stars of Selected Areas in the 30° zone given in Table 2 and used for reference standards at the 100-inch telescope have been corrected for the earth's field.

## OBSERVING PROCEDURES

The program of the first two years (1947, 1948) was largely confined to the 60-inch telescope, with two objects in view: (1) to measure the nebulae of larger angular diameter and (2) to provide standards on the International System (Seares 1922) for use at the 100-inch where the polar sequence is unavailable. For this latter purpose the central stars of the Selected Areas in the 30° zone which passes near the zenith were chosen, since they can also be used to measure atmospheric extinction and reddening functions for each night necessary for reduction. This work resulted in photographic magnitudes and color indices measured photoelectrically on the International scale for the 25 stars shown in Table 2, which includes all measures up to December, 1951.

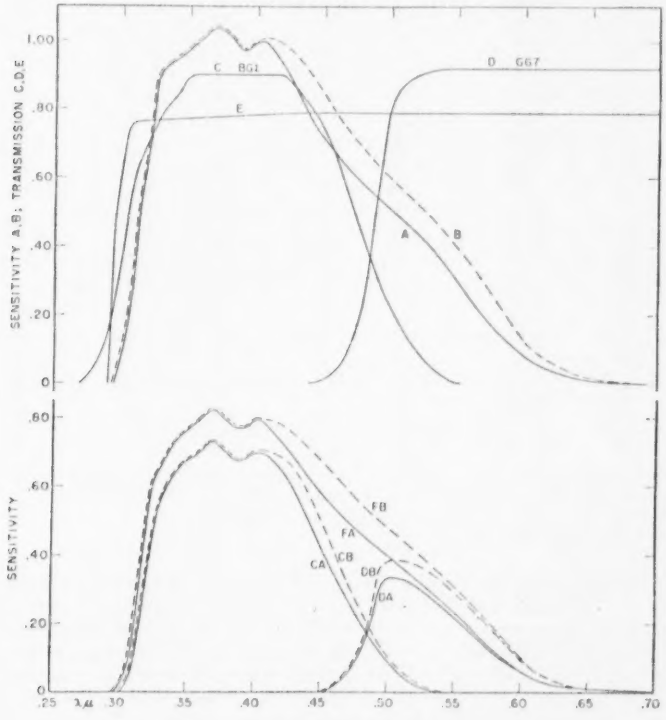


FIG. 1.—Spectral transmission and sensitivity-curves for two 1P21 tubes, solid line *A* for No. 6 and dashed line for *B*, No. 5. *Above: A* and *B* are the cell sensitivity-curves; *C*, *D*, and *E* are the transmissions of the blue (Schott's $BG_1$) filter, yellow (Schott's GG7) filter, and cellophane separator between the two quartz lenses of the photometer.

*Below:* the spectral response of the photometer for each cell *FA* and *FB*, and the same with each filter in place; *CA* and *CB* with the blue filter and *DA* and *DB* with the yellow filter in the beam. All these curves were determined with the aid of a vacuum thermopile and double quartz monochromator.

In Table 2, the first column gives the Selected Area number; the second column, the spectral type so far as it is known; the third column the magnitude measured photoelectrically on the photographic scale; the fourth column, the probable error; the fifth column, the number of measures; the sixth column, the departures from the Mount Wilson *Catalogue* (Seares, Kapteyn, and Van Rhijn 1930). Color indices, probable errors, and number of observations are found in the seventh, eighth, and ninth columns. The data for magnitude are taken from the 60-inch measures only, where the polar sequence was always used to calibrate the instrument.

For the color indices all the 100-inch measures were included, since they depend upon the filters which have been calibrated against the polar-sequence color series. This ac-

TABLE 2

MAGNITUDES AND COLOR INDICES OF CENTRAL STARS OF SELECTED AREAS IN 30° ZONE

| S.A. | Sp. Type* | $m_{pg}$† | P.E. | $N$ | $P-S$ | C.I. | P.E. | $N$ |
|---|---|---|---|---|---|---|---|---|
| 44 | F3 | 9.03 | ±0.012 | 20 | +0.08 | 0.50 | ±0.006 | 31 |
| 45 | gG9 | 8.97 | ± .013 | 27 | − .02 | 1.15 | ± .006 | 45 |
| 46 | sgG4 | 9.26 | ± .008 | 30 | − .24 | 1.17 | ± .007 | 38 |
| 47 | B3 | 7.16 | ± .010 | 29 | − .29 | 0.27 | ± .007 | 29 |
| 48 | dF4 | 6.80 | ± .006 | 31 | − .10 | 0.54 | ± .005 | 39 |
| 49 | K5 | 10.22 | ± .019 | 23 | + .33 | 1.62 | ± .008 | 31 |
| 50 | dF2 | 8.33 | ± .010 | 25 | − .21 | 0.37 | ± .007 | 34 |
| 51 | K0 | 10.63 | ± .08§ | 4 | − .07 | 1.13 | ± .009 | 8 |
| 52 | dF2 | 8.53 | ± .006 | 9 | + .01 | 0.43 | ± .010 | 13 |
| 53 | G0 | 9.43 | ± .009 | 23 | − .09 | 0.42 | ± .006 | 38 |
| 54‡ | F3 | 9.65 | ± .026 | 10 | − .57 | 0.47 | ± .016 | 20 |
| 55 | .... | 9.67 | ± .018 | 11 | − .40 | 0.65 | ± .019 | 15 |
| 56 | gK4 | 9.67 | ± .01§ | 2 | − .45 | 1.62 | ± .05§ | 2 |
| 57 | dG0 | 9.06 | ± .005 | 59 | + .06 | 0.58 | ± .003 | 65 |
| 58 | gM4 | 9.31 | ± .05§ | 3 | − .40 | 1.55 | ± .029 | 9 |
| 59 | gF0 | 9.51 | ± .01§ | 6 | + .09 | 0.50 | ± .014 | 10 |
| 60 | sgG9 | 9.53 | ± .004 | 14 | + .05 | 1.14 | ± .010 | 24 |
| 61 | dF4 | 9.28 | ± .006 | 57 | − .27 | 0.42 | ± .005 | 70 |
| 62 | gG4 | 8.33 | ± .10§ | 4 | − .02 | 1.14 | ± .019 | 9 |
| (62B) | A0 | 8.67 | ± .02§ | 2 | + .15 | 0.23 | ± .02§ | 2 |
| 63 | A2 | 9.17 | ± .021 | 20 | − .45 | 0.08 | ± .008 | 39 |
| 64 | F9 | 8.58 | ± .014 | 10 | + .28 | 0.94 | ± .012 | 23 |
| 65 | F2 | 9.42 | ± .017 | 8 | − .02 | 0.61 | ± .010 | 15 |
| 66 | G4 | 10.13 | ± .016 | 18 | + .04 | 1.15 | ± .008 | 29 |
| 67 | gG7 | 9.06 | ±0.010 | 36 | −0.60 | 1.12 | ±0.006 | 46 |

* For spectral type see Humason (1932), Adams, Joy, Humason, and Brayton (1935), and Wilson (1953).

† All $m_{pg}$ measures were corrected for the earth's magnetic field by applying −0.01 mag. to the measure.

‡ Variable? Range 9.20–9.75 $m_{pg}$.

§ Mean departure from average; no P.E. applicable.

counts for the commonly greater number of color-index measures for a given star. When the number of measures was less than 8, a probable-error solution is not given, but rather the mean departures from the average. The average departure of the Mount Wilson *Catalogue* from this table is −0.12 mag. It will be understood that all measures at the 100-inch are calibrated on three or more stars selected from Table 2, and measures at the 60-inch telescope are calibrated on three or more polar-sequence stars from Table 4. The average number of comparison stars was four.

The observing method was largely to follow that used in previous radiation investigations (Pettit and Nicholson 1928). Briefly, a star is measured from low altitude to meridian on about four occasions during the night, to determine atmospheric extinction and color equation. All nebular measures and measures on comparison stars are then reduced to the zenith before converting them into magnitudes.

Before the program began, Hubble examined the photographs of the nebulae with a

facsimile template of the aperture plate and decided on the apertures to be employed. After the 200-inch plates became available, many of the apertures were increased. In the case of the Lick nebulae, Mayall followed the same procedure. Most of the Lick nebulae and many of the Mount Wilson nebulae were examined by the writer to decide on proper treatment to eliminate galactic stars. Hubble and Mayall also made notes and diagrams to indicate stars to be eliminated.

### REDUCTIONS OF EQUIVALENT PHOTOGRAPHIC MAGNITUDES

Since the magnitudes are made to depend upon the free deflection *minus* the yellow deflection $(F - Y)$, the logarithms of $(F - Y)$ are entered for all objects. To reduce them to the zenith, a plot is made of log $(F - Y)$ against sec $Z$ for the S.A. stars selected from Table 2 for repeated observation from low altitude to meridian passage. From this plot the constant $a$ in the extinction formula,

$$C = a\,(\sec Z - 1)\,, \tag{1}$$

is read. Usually the value of $a$ is about 0.10 but has a range from about 0.07 to 0.16, and this applied to equation (1) furnishes the correction $C$, which, when added to observed log $(F - Y)$, reduces all deflections for the night to the zenith. Since few measures were made when sec $Z$ exceeded 2, the logarithmic correction to the zenith seldom exceeded 0.1000. Here we have neglected a term for the differential color index of the atmospheric stars and object, but this small quantity is practically indeterminate without an expenditure of observing and computing time unavailable in the present program.

The next step in magnitude determination involves calibration of the instrument for the night. Since most objects were fainter than magnitude 9, this was chosen as the basic brightness for calibrations, which means that we determine the log $(F - Y)$ for a ninth-magnitude star at the zenith for the night. If north-polar-sequence stars are used, these must also be reduced to the zenith by equation (1), since their magnitudes are given for the zenith at Mount Wilson. The log $(F - Y)$ for each such star, if it were magnitude 9, is easily obtained by

$$\log (F - Y)_9 = \log (F - Y) + 0.4\,(m_{pg} - 9)\,. \tag{2}$$

It follows that the magnitude of any object for the night is given by

$$m_{pg} = \tfrac{10}{4}\,[\log (F - Y)_9 - \log (F - Y)] + 9\,, \tag{3}$$

where all the variables are zenith values.

### ACCURACY OF THE MAGNITUDES

We may estimate the order of accuracy of the measures of magnitudes of nebulae principally by three methods: (1) the internal agreement of repeated measures, (2) agreement with the measures of others, and (3) the measurement of magnitudes in the polar sequence used for primary calibrations.

For method 1 we have examined all repeated measures of magnitude and color index. These remeasures were made in those cases where some question arose involving the accuracy of the measures, such as disagreement with other catalogues, disagreement between the two determinations of color index, or disagreement between the individual galvanometer deflections. They were therefore a comparison of questionable observations with acceptable ones. The mean departure from the average for the 157 magnitude repetitions was 0.07 mag.

For method 2 three sets of comparative measures are available. The first is the Shapley-Ames (1932) catalogue of magnitudes determined photographically. Available magnitudes from this catalogue appear under "$m_{pg}$ Harv." in Tables 5 and 5*a*. Magnitudes

in parentheses in this column are estimates made by Hubble from plates taken at Mt. Wilson and Palomar Observatories. Since the Shapley-Ames measures are estimates on plates taken with the short-focus lenses of the Harvard Sky Patrol, they approximate the whole light of the nebulae, and their magnitudes appear opposite the largest aperture of the photoelectric measures. The departures O − C between the photoelectric measures and the Shapley-Ames photographic measures listed in Tables 5 and 5*a* are shown for four magnitude ranges in Table 3. There are 21 nebulae not included in Table 3 for which

TABLE 3

COMPARISONS OF NEBULAR MAGNITUDE MEASURES*

| $m_{pg}$ | 8.5–9.5 | 9.5–10.5 | 10.5–11.5 | 11.5–12.5 | 12.5–13.5 | 13.5–14.5 | 14.5–15.5 |
|---|---|---|---|---|---|---|---|
| Mean (O−[S+A]) | ..... | −0.2 | −0.3 | −0.2 | +0.1 | ..... | ..... |
| No. comparisons | ..... | 16 | 73 | 169 | 98 | ..... | ..... |
| Mean (O−Bigay) | ..... | −0.08 | −0.10 | −0.04 | +0.13 | ..... | ..... |
| No. comparisons | ..... | 6 | 30 | 21 | 5 | ..... | ..... |
| Mean (O−[S+W]) | +0.1 | −0.07 | −0.04 | +0.03 | −0.006 | −0.07 | +0.1 |
| No. comparisons | 3 | 6 | 16 | 26 | 17 | 3 | 5 |

* Departures in $m_{pg}$, observed *minus* measures of others.

O − (*S* + *A*) exceeded 0.8 mag. These have been remeasured, and the large departures have been verified.

The work of Bigay (1951), in which the optical system was of the same fundamental design as that used here, depended on surface photometry on photographs of the objective illuminated by nebular light. There are 67 coincidences where nearly the same aperture was used or where interpolation was possible. The average departure, O − Bigay, is −0.06 mag. While the amount of data is too small to analyze in magnitude classes with significant result, Table 3 shows the observed differentials. About 25 departures exceed 0.2 mag. regardless of sign, and 5 exceed ½ mag. The distribution of residuals suggests that the departures are accidental.

The photoelectric measures of Stebbins and Whitford furnish 76 coincidences of the same aperture in magnitude and 36 in color. The mean departure O − (*S* + *W*) is +0.005 mag. Only 4 residuals reach 0.4 mag. The mean departures in the magnitude classes are listed in Table 3.

For method 3 we have determined, in the routine reduction, the magnitudes of the stars in the polar sequence which were used at the 60-inch telescope each night to calibrate the instrument. These depend on an average of 4 polar-sequence stars, of which they are a member, used to determined the log deflections of a ninth-magnitude star at the zenith.

Table 4 lists 51 stars of the polar sequence, of which 35 have been observed on two or more nights. The same group of stars was not always observed together for calibration purposes. Thus for NPS 8, observed on 4 nights, 5 stars were used; for NPS 9, observed on 8 nights, 11 stars were used; and for NPS 10, observed on 15 nights, 31 stars were used.

## CERTAIN COMPUTATIONAL CHECKS

Of all the observational errors, an improper record of the Ayrton shunt box is the most serious. A check on this, when doubt occurs, is the sky deflection for a given aperture. Occasionally a night of rapidly variable transmission occurs which is difficult to recognize. However, there is a relation between the color deflections and the free deflection which depends mostly on the sensibility-curve of the cell. This has the form

$$1.2\,(V+B) = F\,. \tag{4}$$

The coefficient of (*V* + *B*) has a variation of ±2 per cent, depending on the spectral type, but 1.2 is sufficient for check purposes. An application of equation (4) to the first

observations of each night will avoid a record which has finally to be rejected. It also happens that the galvanometer reader may make an erroneous record of a deflection or may improperly state the zeros, and this can be detected by equation (4).

Gross errors may be detected by comparing sequences of magnitudes observed with the photoelectric photometer with those apparent on photographic plates when two or more nebulae are recorded there. A negative lens can be used to bring the nebulae to a

TABLE 4

MAGNITUDES AND COLOR INDICES OF STARS IN NORTH POLAR SEQUENCE

| | $m_{pg}$ | | | | C.I. | | | |
|---|---|---|---|---|---|---|---|---|
| NPS | Cat. | Photoelec. | O−C | No. Obs. | Cat. | Photoelec. | O−C | No. Obs. |
| 8 | 8.32 | 8.37 | +0.05 | 4 | +0.19 | +0.36 | +0.17 | 4 |
| 9 | 8.93 | 9.01 | + .08 | 8 | +0.10 | +0.29 | + .19 | 8 |
| 10 | 9.11 | 9.17 | + .06 | 15 | +0.05 | +0.25 | + .20 | 15 |
| 1r | 6.69 | 6.59 | − .10 | 3 | +1.60 | +1.61 | + .01 | 3 |
| 6r | 10.53 | 10.49 | − .04 | 20 | +1.29 | +1.31 | + .02 | 21 |
| 6 | 7.12 | 7.18 | + .06 | 13 | +0.06 | +0.21 | + .15 | 13 |
| 338 | 14.72 | 14.89 | + .17 | 2 | +0.88 | +0.81 | − .07 | 2 |
| 4s | 10.31 | 10.27 | − .04 | 9 | +0.48 | +0.50 | + .02 | 9 |
| 329 | 14.32 | 14.30 | − .02 | 1 | +0.81 | +0.71 | − .10 | 1 |
| 341 | 15.16 | 15.09 | − .07 | 1 | +1.14 | +0.84 | − .30 | 1 |
| 319 | 14.44 | 14.59 | + .15 | 1 | +0.83 | +0.50 | − .33 | 1 |
| 15 | 11.27 | 11.25 | − .02 | 13 | +0.39 | +0.44 | + .05 | 13 |
| 172 | 13.75 | 13.78 | + .03 | 7 | +1.51 | +1.51 | .00 | 7 |
| 403 | 14.51 | 14.66 | + .15 | 1 | +0.68 | +0.61 | − .07 | 1 |
| 256 | 14.65 | 14.59 | − .06 | 1 | +0.81 | +0.53 | − .28 | 1 |
| 7 | 7.38 | 7.22 | − .16 | 6 | −0.17 | +0.03 | + .20 | 6 |
| 14 | 10.92 | 10.89 | − .03 | 16 | +0.36 | +0.47 | + .11 | 15 |
| 11 | 9.77 | 9.75 | − .02 | 12 | +0.21 | +0.29 | + .08 | 12 |
| 151 | 13.71 | 13.80 | + .09 | 3 | +1.05 | +0.98 | − .07 | 3 |
| 23 | 13.59 | 13.56 | − .03 | 3 | +0.59 | +0.59 | .00 | 3 |
| 12s | 15.35 | 15.38 | + .03 | 1 | +0.68 | +0.40 | − .28 | 1 |
| 6s | 11.36 | 11.38 | + .02 | 12 | +0.64 | +0.72 | + .08 | 12 |
| 10r | 12.61 | 12.60 | − .01 | 10 | +0.58 | +0.53 | − .05 | 10 |
| 176 | 14.35 | 14.40 | + .05 | 1 | +0.57 | +0.66 | + .09 | 1 |
| 5r | 10.16 | 10.20 | + .04 | 1 | +1.53 | +1.53 | .00 | 1 |
| 11r | 13.22 | 13.23 | + .01 | 1 | +1.15 | +1.17 | + .02 | 1 |
| 5s | 11.07 | 11.04 | − .03 | 7 | +1.01 | +1.21 | + .20 | 6 |
| 20 | 12.98 | 12.93 | − .05 | 1 | +0.46 | +0.39 | − .07 | 1 |
| 12 | 10.08 | 10.07 | − .01 | 3 | +0.31 | +0.27 | − .04 | 2 |
| 19 | 12.68 | 12.65 | − .03 | 1 | +0.44 | +0.37 | − .07 | 1 |
| 25 | 14.10 | 14.21 | + .11 | 1 | +0.52 | +0.47 | − .05 | 1 |
| 9r | 11.95 | 12.01 | + .06 | 8 | +1.00 | +1.12 | + .12 | 8 |
| 7r | 10.96 | 10.94 | − .02 | 12 | +1.09 | +1.19 | + .10 | 12 |
| 13 | 10.52 | 10.57 | + .05 | 6 | +0.15 | +0.37 | + .22 | 6 |
| 12r | 13.78 | 13.84 | + .06 | 1 | +1.31 | +1.27 | − .04 | 1 |
| 277 | 15.34 | 15.38 | + .04 | 1 | +0.78 | +0.48 | − .30 | 1 |
| 24 | 13.92 | 13.93 | + .01 | 1 | +0.61 | +0.74 | + .13 | 1 |
| 8r | 11.44 | 11.41 | − .03 | 21 | +0.98 | +1.09 | + .11 | 21 |
| 22 | 13.46 | 13.49 | + .03 | 5 | +0.62 | +0.57 | − .05 | 5 |
| 345 | 13.78 | 13.75 | − .03 | 3 | +1.73 | +1.58 | − .15 | 3 |
| 350 | 11.00 | 10.97 | − .03 | 16 | +0.29 | +0.35 | + .06 | 16 |
| 297 | 15.84 | 15.96 | + .12 | 2 | +1.05 | +0.86 | − .19 | 1 |
| 18 | 12.28 | 12.31 | + .03 | 12 | +0.38 | +0.49 | + .11 | 14 |
| 17 | 11.88 | 11.88 | .00 | 15 | +0.58 | +0.70 | + .12 | 15 |
| 342 | 14.87 | 14.92 | + .05 | 5 | +0.78 | +0.68 | − .10 | 5 |
| 427 | 13.21 | 13.20 | − .01 | 8 | +1.16 | +1.12 | − .04 | 8 |
| 16 | 11.58 | 11.62 | + .04 | 11 | +0.36 | +0.45 | + .09 | 11 |
| 426 | 13.83 | 13.82 | − .01 | 3 | +0.45 | +0.44 | − .01 | 3 |
| 2r | 7.93 | 7.80 | − .13 | 10 | +1.61 | +1.51 | − .10 | 10 |
| 4r | 9.18 | 9.21 | + .03 | 12 | +0.91 | +1.05 | + .14 | 12 |
| 21 | 13.34 | 13.44 | +0.10 | 1 | +0.85 | +0.55 | −0.30 | 1 |

more starlike appearance. This check is particularly adapted to clusters of nebulae and has been applied wherever possible to the measures recorded in Tables 5 and 5*a*.

### REDUCTION OF COLOR INDEX

Like the magnitude system, the color indices are made to depend on the polar sequence. A sequence of colors from C.I. $= -0.17$ to C.I. $= +1.61$ can be observed without using stars fainter than 13.5 $m_{pg}$. The dispersion among the color indices between $C_m$ (from $m_{pg} - m_{pv}$) and $C_e$ (from exposure ratios) for stars brighter than 13.5 $m_{pg}$ in the polar sequence (Seares 1922) averages 0.06 mag., regardless of sign. Color calibrations cannot be expected to show better agreement in either system.

From Figure 1 it will be seen that the yellow and the blue, or free *minus* yellow, cover essentially the spectral ranges of the visual and photographic light. It follows that the color index will be expressed by

$$\text{C.I.} = \tfrac{10}{4} \log \frac{V}{B} + C = \tfrac{10}{4} \log \frac{V}{F - V} + C^1 .$$

For computational simplification it is found convenient to multiply $V$ by 10, to reduce the magnitudes of $C$ and $C^1$, which leads to

$$\text{C.I.} = \tfrac{10}{4} \log \frac{10V}{B} + C = \tfrac{10}{4} \log \frac{10V}{F - V} + C^1 . \tag{5}$$

The values of $C$ and $C^1$ obtained from the polar sequence must be corrected for atmospheric reddening, since the polar sequence refers to the zenith. The reduction of color index in general involves the following procedures. (1) The quantity $\log 10V/B$ for the atmospheric extinction star is plotted against sec $Z$, and $\Delta \log 10V/B$ for sec $Z = 1$ *minus* that for sec $Z = 2$ is read off. This is a negative quantity, since $\log 10V/B$ increases with sec $Z$. Expressed in magnitudes by multiplying by 2.5, it forms the reddening coefficient $ZR$, which amounts on the best nights to about $-\frac{1}{16}$ mag. but often reaches $-\frac{1}{8}$ mag. (2) The color index is computed by equation (5) with both equations, and the average of the two is taken for the final color index. (3) The correction to the zenith $CZ$ is given by

$$CZ = ZR\,(\sec Z - 1) , \tag{6}$$

and equation (6) must be added to equation (5) to get the final color index of the object at the zenith.

To illustrate the color calibration of a photometer, cell No. 5 was tested on 21 stars of the polar sequence in January, 1949. Their zenith colors ranged from $-0.17$ to $+1.73$ mag. The average correction to the pole at sec $Z = 1.79$ for the nights in question was $+0.11$ mag. The values of the resulting constants were $C = -1.71$, $C^1 = -1.32$. A reinvestigation, using all the polar-sequence measures of color with this cell to 1951, showed that the constants should be corrected by $-0.05$ mag. This made their effective values $C = -1.76$, $C^1 = -1.37$.

Some idea of the reliability of the color indices can be obtained from the polar-sequence stars in Table 4, where the sum of the residuals of color index in the eighth column is $-0.27$ mag., which is an average residual of $-0.005$ mag. Besides the International color indices in Table 4, we have available the color indices from spectral type in the central stars of selected areas in Table 2 and additional stars measured for the purpose, which furnish a total of 107 stars of known spectral class for which the color index was computed (Russell *et al.* 1927). In general, if the color test in equation (4) does not apply, the color indices in the two systems of equation (5) will not agree. The repeated measures of nebulae also furnish evidence of reliability. From 157 color-index residuals in the repeated measures of nebulae, we find that the average residual, observed *minus* mean, is 0.07 mag., regardless of sign.

## TABLE 5

### Magnitude and Color Indices of Extragalactic Nebulae Determined Photoelectrically

| NGC IC* | Type | R.A. l | Dec. b | Mpg Harv. | PHOTOELECTRIC Mpg | C.I. | Ap. |
|---|---|---|---|---|---|---|---|
| 16 | SB0 | $0^h\ 6^m.5$ 80° | +27°27' -34° | 13.0 | 13.26 | 1.00 | 1.1 |
| | | | | | 13.20 | 0.97 | 2.3 |
| 23 | Sb | 0 7.3 80° | +25 39 -36° | 12.7 | 13.73 | 0.84 | 0.4 |
| | | | | | 12.92 | 0.83 | 2.3 |
| 68 | S0 | 0 15.8 83° | +29 48 -32° | (14) | 14.68 | 0.91 | 0.7 |
| 69 | SB0 | 0 15.8 83° | +29 46 -32° | (15.5) | 15.89 | 1.05 | 0.6 |
| 71 | E2 | 0 15.8 83° | +29 47 -32° | (14.5) | 14.99 | 1.22 | 0.4 |
| | | | | | 14.92 | 1.06 | 0.6 |
| 72 | SBa | 0 15.9 83° | +29 46 -32° | (15) | 15.21 | 1.23 | 0.6 |
| | | | | | 14.75 | 1.07 | 1.3 |
| Anon | E4 | 0 16.0 83° | +29 46 -32° | (15.5) | 15.87 | 1.03 | 0.6 |
| 10* | Sc | 0 17.8 87° | +59 2 - 3° | - | 13.68 | 0.91 | 2.3 |
| 80 | S0 | 0 18.6 83° | +22 5 -40° | (15) | 14.05 | 1.07 | 0.7 |
| 83 | E0 | 0 18.8 83° | +22 9 -40° | (15.5) | 14.48 | 1.15 | 0.6 |
| 105 | Sa | 0 22.7 82° | +12 37 -49° | - | 13.89 | 0.67 | 2.3 |
| 124 | E1 | 0 36.8 87° | + 2 46 -58° | (13) | 13.65 | 1.04 | 1.3 |
| | | | | | 13.35 | 0.99 | 2.4 |
| 128 | S0 | 0 26.7 82° | + 2 33 -60° | 12.9 | 12.84 | 1.07 | 2.3 |
| | | | | | 12.76 | 1.04 | 2.4 |
| 147 | Epec | 0 30.4 87° | +48 14 -14° | 12.1 | 12.60 | 0.63 | 2.3 |
| | | | | | 11.64 | 0.88 | 4.1 |
| 151 | SBb | 0 31.6 80° | - 9 58 -72° | 12.9 | 14.32 | 1.17 | 0.4 |
| | | | | | 12.40 | 0.85 | 3.4 |
| 157 | Sc | 0 32.3 82° | - 8 40 -71° | | 14.43 | 0.88 | 0.3 |
| | | | | | 11.19 | 0.46 | 2.3 |
| | | | | | 11.01 | 0.51 | 4.1 |
| | | | | 11.1 | 10.98 | 0.50 | 5.7 |
| 160 | Sa | 0 33.4 87° | +23 41 -38° | (13.5) | 14.76 | 1.14 | 0.4 |
| | | | | | 13.73 | 1.01 | 2.4 |
| 178 | SBb | 0 36.6 83° | -14 27 -77° | 12.9 | 13.03 | 0.49 | 2.4 |
| 182 | Sa | 0 35.7 87° | + 2 28 -60° | (14) | 13.51 | 0.85 | 2.3 |
| 185 | Epec | 0 36.1 89° | +48 6 -14° | 11.8 | 10.98 | 0.86 | 4.1 |
| 194 | E1 | 0 36.8 87° | + 2 46 -60° | (13) | 13.56 | 1.05 | 1.1 |
| | | | | | 13.19 | 0.89 | 2.3 |
| 205 | SB0 | 0 37.6 89° | +41 25 -21° | | 10.73 | 0.71 | 2.3 |
| | | | | | 10.05 | 0.73 | 4.1 |
| | | | | 10.8 | 9.84 | 0.77 | 5.7 |
| 210 | Sb | 0 38.0 85° | -14 9 -76° | | 13.73 | 0.99 | 0.3 |
| | | | | | 12.46 | 0.82 | 2.3 |
| | | | | 12.5 | 11.77 | 0.72 | 2.2 |
| | | | | | | | X5.7 |
| 214 | Sc | $0^h\ 38^m.7$ 80° | +25°14' -37° | 12.8 | 14.63 | 0.85 | 0.3 |
| | | | | | 12.94 | 0.67 | 2.3 |
| 221 | E2 | 0 40.0 89° | +40 36 -22° | 9.5 | 10.35 | 0.93 | 0.7 |
| | | | | | 9.46 | 0.91 | 4.1 |
| 227 | E4 | 0 40.1 89° | - 1 48 -64° | 13.1 | 13.53 | 0.94 | 1.1 |
| 247 | Sc | 0 44.6 94° | -21 1 -83° | 10.7 | 10.38 | 0.67 | 8.8 |
| 255 | SBbc | 0 45.2 92° | -11 45 -74° | 12.8 | 14.55 | 0.63 | 0.4 |
| | | | | | 12.32 | 0.53 | 5.1 |
| 278 | Scp | 0 49.2 91° | +47 18 -15° | 11.6 | 13.18 | 0.66 | 0.3 |
| | | | | | 11.53 | 0.58 | 2.3 |
| 1613* | Irr | 1 2.5 99° | + 1 51 -60° | 11.2 | 10.86 | 0.59 | 14 |
| 357 | SBa | 1 0.8 103° | - 6 37 -69° | 13.0 | 13.45 | 1.13 | 1.1 |
| | | | | | (13.48) | 1.15 | 1.3 |
| 375 | E5 | 1 4.3 95° | +32 5 -30° | (15) | 15.85 | 1.08 | 0.7 |
| 379 | S0 | 1 4.5 95° | +32 15 -30° | | 14.21 | 1.10 | 0.7 |
| | | | | | 14.15 | 1.10 | 1.1 |
| | | | | (14) | 14.05 | 1.09 | 1.3 |
| 380 | E2 | 1 4.5 95° | +32 13 -30° | | 14.24 | 1.07 | 0.7 |
| | | | | | 14.09 | 1.09 | 1.1 |
| | | | | (14) | 13.93 | 1.13 | 1.3 |
| 383 | S0 | 1 4.6 95° | +32 9 -30° | (13.5) | 13.61 | 1.08 | 1.1 |
| 384 | S0 | 1 4.6 95° | +32 2 -30° | (14.5) | 14.47 | 0.91 | 1.1 |
| 385 | E3 | 1 4.7 95° | +32 3 -30° | | 14.44 | 0.95 | 1.1 |
| | | | | (14.5) | 14.25 | 1.10 | 1.3 |
| 386 | E4 | 1 4.7 95° | +32 5 -30° | (16) | 15.65 | 1.11 | 0.7 |
| 388 | E3 | 1 5.0 95° | +32 2 -30° | | 15.83 | 1.12 | 0.7 |
| | | | | | 15.77 | 0.85 | 1.1 |
| | | | | (15) | 15.51 | (0.95) | 1.3 |
| 404 | S0 | 1 6.6 95° | +35 27 -26° | 11.9 | 11.55 | 0.89 | 2.3 |
| 428 | Sc | 1 10.4 105° | + 0 43 -61° | 11.9 | 11.97 | 0.38 | 5.1 |
| | | | | | 11.85 | 0.40 | 5.7 |
| 474 | E0 | 1 17.5 107° | + 3 10 -58° | 12.6 | 13.67 | 0.93 | 0.7 |
| | | | | | 13.29 | 0.89 | 1.1 |
| 488 | Sb | 1 19.1 106° | + 5 0 -56° | | 13.85 | 1.03 | 0.3 |
| | | | | | 13.56 | 1.01 | 0.4 |
| | | | | 11.8 | 11.69 | 0.87 | 2.3 |
| 514 | Sc | 1 21.3 105° | +12 39 -50° | 12.4 | 12.25 | 0.61 | 5.7 |
| 520 | Irr | 1 22.0 109° | + 3 32 -58° | | 14.70 | 0.57 | 0.3 |
| | | | | | 12.16 | 0.76 | 4.1 |
| | | | | 12.4 | 12.16 | 0.75 | 2.7 |
| | | | | | | | X5.7 |
| 524 | S0 | 1 22.1 106° | + 9 16 -52° | | 13.21 | 1.15 | 0.4 |
| | | | | | 12.45 | 1.05 | 1.1 |
| | | | | 12.0 | 11.85 | 0.95 | 2.3 |

TABLE 5—*Continued*

| NGC IC* | Type | R.A. l | Dec. b | Mpg Harv. | PHOTOELECTRIC Mpg | C.I. | Ap. |
|---|---|---|---|---|---|---|---|
| 560 | S0 | 1h 24m.9<br>113° | - 2°11'<br>-62° | | 14.01 | (1.05) | 0.5<br>X2.3 |
| | | | | (14) | 14.01 | 0.99 | 2.4 |
| 564 | E3 | 1 25.2<br>113° | - 2 9<br>-62° | (14) | 14.22 | 1.01 | 0.6 |
| 578 | Sc | 1 28.0<br>157° | -22 56<br>-79° | | 13.59 | 0.61 | 0.7 |
| | | | | | 11.65 | 0.59 | 4.1 |
| | | | | 11.7 | (11.69) | 0.52 | 5.7 |
| 584 | E3 | 1 28.8<br>120° | - 7 7<br>-67° | 11.6 | 12.00 | 0.87 | 1.1 |
| 596 | E0 | 1 30.3<br>121° | - 7 17<br>-67° | 12.2 | 12.51 | 0.86 | 1.1 |
| 604 | Emis Patch | 1 31.7<br>102° | +30 32<br>-31° | (11.7) | 12.04 | -0.01 | 1.1 |
| 613 | Sb | 1 32.0<br>194° | -29 40<br>-78° | 11.1 | 10.77 | 0.74 | 2.3<br>X8.6 |
| 628 | Sc | 1 34.0<br>108° | +15 32<br>-45° | | 14.35 | 0.87 | 0.3 |
| | | | | | 10.42 | 0.56 | 5.7 |
| | | | | 11.2 | 10.10 | 0.55 | 8.6 |
| 1727* | SBc | 1 44.7<br>106° | +27 5<br>-34° | 13.0 | 12.70 | 0.60 | 3.4 |
| 636 | E1 | 1 36.6<br>125° | - 7 45<br>-66° | 12.6 | 12.44 | 0.97 | 2.3 |
| 672 | SBc | 1 45.0<br>106° | +27 11<br>-34° | 11.9 | 11.61 | 0.51 | 1.8<br>X5.7 |
| 681 | Sb | 1 46.7<br>135° | -10 40<br>-67° | | 14.88 | 0.93 | 0.3 |
| | | | | 12.9 | 12.88 | 0.90 | 2.3 |
| 718 | Sa | 1 50.7<br>118° | + 3 57<br>-55° | | 13.96 | 0.87 | 0.3 |
| | | | | 12.7 | 12.54 | 0.83 | 2.3 |
| 720 | E5 | 1 50.6<br>142° | -13 59<br>-69° | 11.7 | 11.55 | 0.93 | 2.3 |
| 721 | SBb | 1 51.9<br>104° | +39 8<br>-21° | - | 14.23 | 0.65 | 1.3 |
| 736 | E1 | 1 53.8<br>107° | +32 48<br>-27° | | 14.08 | 1.01 | 0.7 |
| | | | | (14) | 13.63 | 0.95 | 1.1 |
| 741 | E0 | 1 53.8<br>120° | + 5 23<br>-53° | | 13.41 | 1.11 | 1.1 |
| | | | | 13.0 | 13.18 | 1.07 | 1.3 |
| 750 | E0 | 1 54.6<br>106° | +32 58<br>-27° | - | 13.91 | 1.11 | 0.7 |
| 751 | E0 | 1 54.6<br>107° | +32 58<br>-27° | - | 14.21 | 0.95 | 0.7 |
| 750 +751 | E0 | 1 54.6<br>107° | +32 58<br>-27° | | 13.30 | 0.97 | 1.1 |
| | | | | 12.9 | 13.17 | 1.17 | 2.3 |
| 753 | Sc | 1 54.6<br>105° | +35 41<br>-25° | 13.0 | 12.91 | (0.61) | 2.4 |
| 770 | SBa | 1 56.5<br>113° | +18 43<br>-40° | (13.5) | 14.76 | 1.26 | 0.4 |
| 772 | Sb | 1 56.6<br>113° | +18 46<br>-40° | 12.0 | 11.43 | 0.77 | 4.1 |
| 779 | Sb | 1h 57m.2<br>132° | - 6°12'<br>-62° | | 12.92 | 0.94 | 0.7 |
| | | | | 11.8 | 11.90 | 0.84 | 4.1 |
| 788 | Sa | 1 58.6<br>134° | - 7 3<br>-62° | 13.1 | 13.20 | (0.70) | 1.1 |
| 821 | E6 | 2 5.6<br>120° | +10 46<br>-47° | | 13.66 | 1.19 | 0.4 |
| | | | | | 12.80 | 1.00 | 1.1 |
| | | | | | 12.12 | 1.00 | 2.3 |
| | | | | | (12.38) | (1.07) | 2.4 |
| | | | | 12.7 | 11.91 | 0.97 | 4.1 |
| 864 | Sbc | 2 12.8<br>126° | + 5 45<br>-51° | | 14.98 | 0.64 | 0.3 |
| | | | | | 13.49 | 0.64 | 1.1 |
| | | | | 12.3 | 11.75 | 0.53 | 4.1 |
| 871 | Sc | 2 14.5<br>121° | +14 19<br>-43° | - | 14.13 | 0.56 | 1.3 |
| 877 | Sc | 2 15.3<br>121° | +14 19<br>-43° | 12.4 | 12.59 | 0.63 | 2.3 |
| 890 | S0 | 2 19.1<br>112° | +33 2<br>-25° | 12.7 | 12.95 | 1.00 | 1.1 |
| 891 | Sb | 2 19.3<br>108° | +42 7<br>-17° | 12.2 | 11.23 | 0.95 | 1.4<br>X8.6 |
| 908 | Sc | 2 20.8<br>170° | -21 27<br>-67° | | 13.30 | 0.75 | 0.7 |
| | | | | 11.1 | 10.95 | 0.63 | 2.7<br>X5.7 |
| 922 | Sc | 2 22.9<br>178° | -25 1<br>-67° | 12.3 | 12.40 | 0.65 | 2.3 |
| 925 | Sc | 2 24.3<br>113° | +33 22<br>-24° | | 13.75 | 0.49 | 0.7 |
| | | | | | 11.52 | 0.53 | 4.1 |
| | | | | 12.6 | 10.64 | 0.55 | 8.6 |
| 936 | SBa | 2 25.1<br>137° | - 1 22<br>-54° | 11.5 | 11.33 | 0.95 | 4.1 |
| 972 | Sb | 2 31.3<br>117° | +29 6<br>-27° | 12.6 | 12.33 | 0.85 | 2.3 |
| Anon | SBa | 2 34.6<br>115° | +34 12<br>-23° | - | 14.54 | 0.70 | 0.7 |
| 1003 | Sc | 2 36.1<br>112° | +40 40<br>-17° | (13.4) | 12.34 | 0.46 | 1.1<br>X4.1 |
| 1023 | SB0 | 2 37.2<br>113° | +38 51<br>-18° | 11.2 | 10.59 | 0.97 | 1.8<br>X4.1 |
| 1042 | Sc | 2 38.0<br>152° | - 8 40<br>-56° | - | 15.70 | 0.79 | 0.3 |
| 1048 | Sa | 2 38.2<br>152° | - 8 46<br>-56° | (15) | 15.62<br>15.55 | 1.03<br>- | 0.4<br>4.1 |
| 1049 | GC1 | 2 37.7<br>202° | -34 29<br>-64° | (14.2) | 13.59 | 0.62 | 0.6 |
| 1052 | E3 | 2 38.6<br>150° | - 8 28<br>-56° | 11.6 | 11.71 | 0.96 | 2.3 |
| 1058 | Sc | 2 40.2<br>115° | +37 08<br>-20° | 12.7 | 12.21 | 0.44 | 2.3 |
| 1068 | Sb | 2 40.1<br>141° | - 0 14<br>-51° | | 11.36 | 0.89 | 0.4 |
| | | | | | 10.15 | 0.63 | 2.3 |
| | | | | 10.0 | 10.01 | 0.67 | 4.1 |

TABLE 5—*Continued*

| NGC IC* | Type | R.A. l | Dec. b | Mpg Harv. | PHOTOELECTRIC Mpg | C.I. | Ap. |
|---|---|---|---|---|---|---|---|
| 1073 | SBc | $2^h\ 42^m.2$ 139° | + 1°10' -50° | 12.0 | 11.95 | 0.44 | 3.4 |
| 1084 | Sc | 2 43.5 151° | - 7 47 -55° | 11.2 | 13.58<br>11.20<br>11.17 | 0.81<br>-<br>0.58 | 0.4<br>2.3<br>4.1 |
| 1087 | Sc | 2 43.9 142° | - 0 42 -51° | 11.2 | 14.27<br>11.44 | 0.51<br>0.52 | 0.4<br>4.1 |
| 1097 | SBb | 2 44.3 193° | -30 29 -63° | 10.6 | 10.98<br>10.50 | 1.04<br>0.58 | 3.4<br>2.1<br>X5.1 |
| 1140 | Irr | 2 52.2 156° | -10 14 -55° | 13.0 | 12.72 | 0.29 | 2.3 |
| 1156 | Irr | 2 56.7 128° | +25 3 -28° | 12.9 | 12.71<br>12.22 | 0.37<br>0.51 | 2.3<br>4.1 |
| 1201 | S0 | 3 2.0 185° | -26 15 -59° | 12.0 | 11.95 | 0.91 | 2.3 |
| 1209 | E6 | 3 3.8 167° | -15 48 -55° | 12.5 | 12.92<br>12.69<br>12.48 | 0.95<br>1.05<br>1.01 | 1.1<br>2.3<br>4.1 |
| 1232 | Sc | 3 07.5 176° | -20 46 -57° | 11.1 | 13.71<br>10.83 | 1.19<br>0.73 | 0.7<br>5.7 |
| 1270 | E3 | 3 15.6 118° | +41 14 -12° | - | 14.65 | 1.23 | 0.7 |
| 1273 | E1 | 3 16.1 118° | +41 19 -12° | (13.5) | 14.88 | 1.21 | 0.7 |
| 1275 | Sp | 3 16.5 118° | +41 17 -12° | 12.7 | 13.27 | 0.78 | 1.1 |
| 1277 | E4 | 3 16.5 119° | +41 22 -12° | - | 14.89 | 1.16 | 0.7 |
| 1278 | E1 | 3 16.6 119° | +41 21 -12° | - | 14.47 | 1.14 | 0.7 |
| 1300 | SBb | 3 17.5 176° | -19 35 -54° | 11.8 | 14.72<br>11.30 | 0.85<br>0.67 | 0.3<br>5.7 |
| 1302 | Sa | 3 17.7 187° | -26 14 -55° | 11.9 | 12.09 | 0.65 | 1.3 |
| 1316 | Irr | 3 20.7 206° | -37 25 -55° | 10.1 | 9.95 | 0.81 | 3.4 |
| 1317 | Sa | 3 20.8 206° | -37 17 -56° | 12.2 | 13.02<br>12.14 | 0.73<br>0.61 | 0.4<br>1.3 |
| 1331 | E2 | 3 24.2 179° | -21 29 -53° | - | 15.01 | 0.74 | 0.6 |
| 1332 | S0 | 3 24.1 179° | -21 28 -53° | 11.4 | 12.84<br>11.36 | 1.13<br>0.92 | 0.4<br>1.1<br>X3.4 |
| 1359 | SBc | 3 31.5 176° | -19 41 -51° | 12.8 | 12.45 | 0.23 | 4.1 |
| 1380 | Sa | 3 34.6 202° | -35 9 -53° | 11.4 | 11.56 | 0.77 | 1.3 |
| 1385 | Sc | $3^h\ 35^m.2$ 186° | -24°40' -51° | 11.8 | 11.72 | 0.59 | 2.4 |
| 1395 | E2 | 3 36.3 183° | -23 11 -51° | 11.2 | 11.93 | 0.94 | 1.1 |
| 1398 | SBb | 3 36.8 189° | -26 30 -52° | 11.03 | 12.87<br>10.92 | 0.97<br>1.01 | 0.3<br>4.1 |
| 1399 | E2 | 3 36.6 203° | -35 37 -52° | 10.9 | 12.27<br>11.38 | 0.90<br>0.73 | 0.4<br>1.3 |
| 1400 | E1 | 3 37.2 177° | -18 51 -49° | 12.5 | 12.60<br>12.30<br>12.18 | 0.96<br>0.99<br>0.96 | 1.1<br>2.3<br>4.1 |
| 1404 | E1 | 3 37.0 204° | -35 45 -52° | 11.5 | 12.12<br>11.38 | 0.93<br>0.85 | 0.4<br>1.3 |
| 1407 | E0 | 3 37.9 177° | -18 44 -49° | 11.5 | 13.39<br>11.25 | 1.15<br>1.00 | 0.4<br>2.3 |
| 1426 | E4 | 3 40.6 182° | -22 16 -50° | 12.8 | 13.88<br>12.75<br>12.58<br>12.41 | 0.92<br>0.79<br>0.93<br>0.87 | 0.3<br>1.1<br>2.3<br>4.1 |
| 342* | Sc | 3 41.9 106° | +67 57 +11° | - | 12.56<br>10.73 | 0.97<br>- | 2.3<br>18.1 |
| 1439 | E0 | 3 42.6 182° | -22 5 -49° | 12.9 | 13.01 | 0.89 | 1.1 |
| 1441 | Sa | 3 43.2 160° | - 4 15 -41° | - | 14.07 | 1.06 | 1.1 |
| 1449 | S0 | 3 43.6 160° | - 4 18 -41° | - | 14.65 | 0.91 | 0.7 |
| 1451 | E3 | 3 43.6 160° | - 4 13 -41° | - | 14.55 | 1.13 | 0.7 |
| 1453 | E1 | 3 44.0 160° | - 4 8 -41° | 12.8 | 13.10 | 1.11 | 1.1 |
| 1518 | Irr | 4 04.7 197° | -21 18 -47° | 12.1 | 12.30 | 0.54 | 4.1 |
| 1569 | Irr | 4 26.0 111° | +64 45 +12° | 12.4 | 11.90 | 0.80 | 0.9<br>X2.3 |
| 1587 | E1 | 4 28.1 162° | + 0 33 -29° | - | 13.63 | 1.00 | 0.7 |
| 1600 | E5 | 4 29.2 168° | - 5 10 -32° | 12.7 | 13.00<br>12.35<br>12.22 | 1.01<br>0.99<br>1.00 | 1.1<br>2.4<br>3.4 |
| 1601 | S0 | 4 29.2 168° | - 5 10 -32° | - | 15.11 | 0.99 | 0.7 |
| Anon | S0 | 4 38.1 160° | + 4 10 -25° | - | 15.12 | (0.90) | 0.7 |
| 1637 | Sc | 4 38.9 167° | - 2 56 -29° | 11.6 | 11.99<br>11.70 | 0.49<br>0.60 | 2.3<br>4.1 |
| 1640 | SBb | 4 40.1 187° | -20 32 -36° | 12.6 | 14.47<br>12.55 | 0.91<br>0.71 | 0.3<br>2.3 |

## TABLE 5—*Continued*

| NGC IC* | Type | R.A. l | Dec. b | Mpg Harv. | PHOTOELECTRIC Mpg | C.I. | Ap. |
|---|---|---|---|---|---|---|---|
| 391* | Sb | $4^h\ 49^m.7$ 101° | +78° 6' +22° | 13.5 | 12.85 | 0.15 | 2.3 |
| 1659 | Sc | 4 44.0 170° | - 4 53 -28° | 12.9 | 13.19 | 0.60 | 2.4 |
| 1700 | E3 | 4 54.4 171° | - 4 56 -26° | 12.4 | 12.70<br>12.05<br>12.02 | 0.79<br>0.89<br>1.01 | 1.1<br>2.4<br>3.4 |
| 1744 | Sc | 4 57.9 194° | -26 6 -33° | 12.5 | 12.20 | 0.39 | 4.1 |
| 1832 | Sb | 5 10.0 184° | -15 47 -27° | 12.6 | 14.20<br>12.18 | 0.90<br>0.80 | 0.3<br>2.3 |
| 1888 +1889 | Sb | 5 20.3 181° | -11 32 -23° | (13.5) | 12.86<br>12.69 | 0.89<br>0.95 | 2.3<br>4.1 |
| 1889 | E0 | 5 20.3 181° | -11 32 -23° | (14) | 14.55 | 0.94 | 0.3 |
| 1961 | Sb | 5 36.8 110° | +69 24 +21° | 11.6 | 12.52<br>12.09 | 0.76<br>0.71 | 2.3<br>4.1 |
| 1964 | Sb | 5 31.2 193° | -21 59 -25° | 12.0 | 11.56 | 0.76 | 1.8<br>X5.7 |
| 2139 | SBc | 5 58.6 198° | -23 49 -20° | 12.5 | 12.01 | 0.09 | 2.4 |
| 2146 | Sap | 6 10.7 103° | +78 23 +26° | 11.6 | 11.44 | 0.79 | 5.7 |
| 2207 | Sc | 6 18.2 196° | -21 21 -16 | 12.3 | 14.27<br>11.42 | 0.96<br>0.66 | 0.3<br>4.1 |
| 2217 | SBa | 6 18.7 202° | -27 14 -17° | 12.6 | 11.96 | 0.89 | 2.4 |
| 2268 | Sc | 7 01.3 96° | 84 30 +28° | 12.2 | 14.50<br>12.22 | 1.05<br>0.69 | 0.3<br>4.1 |
| Anon | Sa | 7 4.4 150° | +35 4 +20° | (16.6) | 17.24 | 1.11 | 0.3 |
| 2276 | Sc | 7 11.0 95° | +85 52 +28° | 12.4 | 11.90 | 0.62 | 2.7<br>X5.7 |
| 2300 | E1 | 7 16.5 95° | +85 50 +28° | 12.2 | 12.37 | 1.00 | 2.3 |
| 2314 | E3 | 7 3.8 107° | +75 19 +28° | 12.9 | 13.33 | 0.98 | 1.1 |
| 2336 | Sb | 7 16.2 102° | +80 20 +29° | 12.4 | 14.60<br>11.37 | 0.88<br>0.68 | 0.3<br>3.2<br>X5.7 |
| 2339 | Sb | 7 5.4 165° | +18 52 +14 | 12.7 | 13.66<br>(13.33)<br>12.53 | 0.95<br>0.85<br>0.69 | 0.3<br>1.1<br>2.3 |
| 2347 | Sb | 7 11.6 118° | +64 54 +28° | 12.7 | 14.48<br>13.23 | 0.93<br>0.77 | 0.3<br>1.1 |
| 2366 | Irr | 7 23.6 114° | +69 08 +29° | 12.6 | 13.87<br>11.61 | 0.85<br>0.55 | 0.3<br>2.7<br>X5.7 |
| 2379 | S1 | 7 24.2 152° | +33 55 +23° | (14) | 14.80<br>14.70 | 0.91<br>1.07 | 0.7<br>1.1 |
| 2389 | Sc | $7^h\ 25^m.9$ 152° | +33°58' +23° | - | 13.62<br>13.28 | 0.40<br>0.48 | 1.3<br>2.3 |
| 2403 | Sc | 7 32.0 118° | +65 43 +30° | 10.2 | 12.72<br>9.20 | 0.61<br>0.47 | 0.7<br>8.6 |
| 2441 | Sc | 7 47.1 109° | +73 6 +36° | 12.7 | 13.08 | 0.81 | 2.3 |
| 2460 | Sb | 7 52.7 124° | +60 31 +32° | 12.7 | 14.24<br>12.82 | 0.97<br>0.89 | 0.3<br>2.3 |
| 2500 | Sc | 7 58.2 136° | +50 54 +33° | 12.6 | 12.35 | 0.52 | 2.3 |
| 2525 | SBb | 8 03.3 200° | -11 17 +12° | 12.2 | 12.21 | 0.52 | 2.4 |
| 2523 | S | 8 9.2 107° | +70 45 +33° | 12.7 | 14.19<br>12.64 | 1.01<br>0.64 | 0.7<br>4.1 |
| 2532 | Sc | 8 7.0 155° | +34 6 +32° | (13.0) | 13.05 | 0.57 | 2.3 |
| 2535 | Sc | 8 8.2 165° | +25 22 +29° | (13.7) | 13.24<br>13.21 | 0.37<br>0.51 | 2.3<br>2.4 |
| 2536 | Sb | 8 8.2 165° | +25 21 +29° | (14) | 14.69 | 0.51 | 1.1 |
| 2537 | Sc | 8 9.7 141° | +46 9 +34° | 12.2 | 12.43<br>12.33 | 0.56<br>0.59 | 1.1<br>2.3 |
| 2545 | Sb | 8 11.3 169° | +21 30 +28° | 13.0 | 15.10<br>14.01<br>13.24 | 0.90<br>0.94<br>0.78 | 0.4<br>0.6<br>2.4 |
| 2549 | S0 | 8 14.9 127° | +57 58 +35° | 12.5 | 12.22<br>12.20 | 0.95<br>0.97 | 2.3<br>4.1 |
| 2551 | Sab | 8 18.8 107° | +73 35 +33° | 13.1 | 13.58<br>13.22 | 1.03<br>1.09 | 0.7<br>2.3 |
| 2562 | Sa | 8 17.5 170° | +21 18 +30° | (13.5) | 14.11<br>14.02 | 1.15<br>1.07 | 1.1<br>1.3 |
| 2563 | S0 | 8 17.7 170° | +21 14 +30° | (13.5) | 13.79 | 1.01 | 1.1 |
| 2608 | Sc | 8 32.2 163° | +28 38 +35° | (12.9) | 12.83 | 0.72 | 2.3 |
| 2613 | Sb | 8 31.1 212° | -22 48 +12° | 11.3 | 14.14<br>11.05 | 1.01<br>0.41 | 0.4<br>5.7 |
| 2633 | SBc | 8 42.7 106° | +74 18 +35° | 12.6 | 14.03<br>13.45<br>13.00 | 0.52<br>0.79<br>1.01 | 0.3<br>0.7<br>2.3 |
| 2639 | Sa | 8 40.1 136° | +50 24 +39° | 12.4 | 12.56 | 0.89 | 2.3 |
| 2642 Nuc. | SBb | 8 38.3 198° | - 3 57 +23° | 12.7 | 15.10 | 1.12 | 0.4 |
| 2389* | SB0 | 8 42.6 106° | +73 43 +35° | - | 14.02 | 0.61 | 1.1 |
| 2646 | SB0 | 8 48.6 106° | +73 42 +35° | 12.8 | 14.41<br>13.32 | 1.11<br>1.06 | 0.3<br>1.1 |
| 2654 | Sa | 8 44.3 123° | +60 28 +39° | 12.9 | 12.86 | 0.93 | 4.1 |

## TABLE 5—*Continued*

| NGC IC* | Type | R.A. l | Dec. b | Mpg Harv. | PHOTOELECTRIC Mpg | C.I. | Ap. |
|---|---|---|---|---|---|---|---|
| 2655 | S0 | 8h 49.4 102° | +78°25' +33° | 11.6 | 12.94<br>11.11 | 0.93<br>0.87 | 0.3<br>4.1 |
| 2672 | E1 | 8 46.6 175° | +19 16 +36° | 12.6 | 14.25<br>13.58 | 1.05<br>1.11 | 0.3<br>0.7 |
| 2673 | E0 | 8 46.6 175° | +19 16 +36° | (14.0) | 14.45 | 0.76 | 0.7 |
| 2681 | Sa | 8 50.0 134° | +51 31 +41° | (11.3) | 11.38<br>11.17 | 0.81<br>0.81 | 2.3<br>4.1 |
| 2683 | Sb | 8 49.6 158° | +33 38 +40° | 10.8 | 10.99<br>10.65 | (1.81)<br>0.88 | 2.3<br>1.4<br>X8.6 |
| 2685 | S0p | 8 52.2 125° | +58 59 +40° | 12.5 | 13.99<br>12.33<br>12.27 | 1.15<br>0.83<br>0.85 | 0.3<br>2.3<br>4.1 |
| 2693 | E2 | 8 53.5 134° | +51 33 +42° | 12.9 | 14.58<br>13.48 | 1.30<br>1.05 | 0.3<br>1.1 |
| 2694 | E0 | 8 53.5 134° | +51 32 +42° | (14.5) | 15.46 | 1.09 | 0.7 |
| 2712 | SBb | 8 56.2 143° | +45 7 +42° | 12.7 | 12.84 | 0.67 | 2.3 |
| 2715 | Sc | 9 02.0 102° | +78 16 +34° | 12.1 | 12.08 | 0.61 | 4.1 |
| 2716 | Sa | 8 55.0 194° | + 3 17 +31° | (13.3) | 13.55<br>13.08 | 0.86<br>0.85 | 1.1<br>2.3 |
| 2732 | S0 | 9 07.3 100° | +79 24 +33 | 13.0 | 14.01<br>13.17 | 1.01<br>1.05 | 0.3<br>1.1 |
| 2744 | Sb | 9 1.8 178° | +18 40 +39° | (13.5) | 13.75 | 0.31 | 2.3 |
| 2748 | Sb | 9 08.2 104° | +76 41 +35° | 12.4 | 12.54 | 0.73 | 2.3 |
| 2749 | E2 | 9 2.5 178° | +18 31 +39° | 13.1 | 13.65 | 1.05 | 1.1 |
| 2768 | S0 | 9 7.8 122° | +60 16 +42° | 12.0 | 13.54<br>11.26 | 1.51<br>0.97 | 0.3<br>3.2<br>X4.1 |
| 2775 | Sa | 9 7.7 191° | + 7 15 +35° | 11.5 | 11.76<br>11.38 | 0.91<br>0.85 | 2.3<br>4.1 |
| 2776 | Sc | 9 08.9 144° | +45 11 +44° | 12.2 | 12.24 | 0.57 | 2.3 |
| 2782 | Sa | 9 10.9 149° | +40 19 +45° | 12.4 | 12.74 | 0.65 | 2.3 |
| 2787 | SBa | 9 14.9 111° | +69 25 +39° | 12.1 | 13.50<br>12.34<br>12.01 | 1.08<br>1.08<br>1.06 | 0.3<br>1.1<br>2.3 |
| 2798 | SBa | 9 14.4 147° | +42 10 +46° | 12.9 | 14.03<br>12.97 | 0.65<br>0.71 | 0.3<br>2.3 |
| 2811 | Sa | 9 13.9 214° | -16 6 +23° | 12.5 | 12.50 | 0.69 | 2.3 |
| 2831 | E1 | 9 16.7 159° | +33 59 +46° | (14.5) | 15.13<br>14.71 | 1.05<br>1.12 | 0.4<br>0.6 |
| 2832 | E3 | 9h 16.8 159° | +33°59' +46° | 12.9 | 13.81 | 1.03 | 0.6 |
| 2841 | Sb | 9 18.6 134° | +51 12 +45° | 10.5 | 10.42<br>10.02 | 0.91<br>0.82 | 5.7<br>8.6 |
| 2855 | S0 | 9 19.1 212° | -11 41 +27° | 12.4 | 12.68 | 0.89 | 2.3 |
| 2859 | SB0 | 9 21.3 158° | +34 44 +47° | 12.2 | 12.11<br>11.91 | 0.93<br>1.00 | 2.3<br>4.1 |
| 2865 | E3 | 9 21.2 221° | -22 58 +20° | 12.6 | 12.48<br>12.37 | 0.61<br>0.83 | 2.3<br>2.4 |
| 2880 | SB0 | 9 25.7 118° | +62 44 +43° | 12.9 | 12.66 | 0.89 | 2.3 |
| 2903 | Sc | 9 29.3 177° | +21 44 +46° | 10.3 | 12.00<br>9.93<br>9.86 | 0.79<br>0.69<br>0.64 | 0.7<br>5.7<br>8.6 |
| 2911 | S0p | 9 31.0 191° | +10 22 +42° | 13.1 | 13.70 | 1.11 | 1.1 |
| 2914 | Sa | 9 31.4 192° | +10 20 +42° | (13.0) | 14.17 | 0.96 | 1.1 |
| 2950 | SB0 | 9 39.1 122° | +59 5 +46° | 12.1 | 12.96<br>12.16<br>11.96 | 0.99<br>0.91<br>0.94 | 0.3<br>1.1<br>2.3 |
| 2964 | Sc | 9 40.0 162° | +32 5 +50° | 11.9 | 12.11<br>12.07 | 0.61<br>0.79 | 2.3<br>4.1 |
| 2974 | E4 | 9 40.0 208° | - 3 29 +36° | 12.7 | 12.54<br>12.14<br>11.85 | 0.94<br>1.01<br>1.07 | 1.1<br>2.3<br>4.1 |
| 2976 | Sc | 9 43.2 110° | +68 8 +42° | 11.2 | 11.01 | 0.60 | 5.7 |
| 2983 | SBa | 9 41.3 223° | -20 15 +25° | 12.8 | 13.07<br>12.85 | 0.97<br>0.96 | 1.1<br>2.3 |
| 2985 | Sb | 9 46.0 106° | +72 31 +39° | 11.8 | 11.36 | 0.73 | 4.1 |
| 2986 | E2 | 9 42.0 223° | -21 3 +25° | 12.2 | 12.87<br>12.30 | 0.93<br>0.95 | 1.1<br>2.3 |
| 3003 | Sc | 9 45.6 160° | +33 39 +52° | 12.5 | 12.27 | 0.42 | 1.4<br>X5.7 |
| 3031 | Sb | 9 51.5 109° | +69 18 +69° | 8.9 | 11.65<br>8.43 | 1.05<br>0.98 | 0.3<br>8.6 |
| 3032 | S0 | 9 49.2 167° | +29 28 +52° | 12.8 | 12.89 | 0.70 | 1.1 |
| 3034 | Irr | 9 51.9 108° | +69 56 +41° | 9.4 | 9.45 | 0.85 | 8.6 |
| 3055 | Sc | 9 52.7 203° | + 4 31 +44° | 12.5 | 12.72 | 0.56 | 2.4 |
| 3065 | S0 | 9 57.7 105° | +72 25 +40° | 12.9 | 13.52 | 0.99 | 0.7 |
| 3066 | Sb | 9 57.7 105° | +72 22 +40° | (13.0) | 13.58 | 0.74 | 1.1 |

## TABLE 5—*Continued*

| NGC IC* | Type | R.A. l | Dec. b | Mpg Harv. | PHOTOELECTRIC Mpg | C.I. | Ap. |
|---|---|---|---|---|---|---|---|
| 3067 | Sbp | $9^h\ 55^m.4$ 162° | +32°37' +54° | 12.8 | 12.68<br>12.51 | 0.60<br>0.49 | 2.3<br>4.1 |
| 3077 | Irr | 9 59.4 109° | +68 58 +42° | 11.4 | 11.28 | 0.78 | 2.3 |
| 3078 | E2 | 9 56.2 230° | -26 41 +22° | 12.4 | 12.46<br>12.18 | 0.87<br>0.78 | 1.1<br>2.3 |
| Wilson Dwarf | Irr | 9 57.3 201° | + 5 24 +44° | - | 12.96 | 0.42 | 2.4 |
| 3115 | E7 | 10 2.8 216° | - 7 28 +38° | 9.8 | 11.28<br>10.35<br>10.27 | 1.08<br>1.06<br>0.97 | 0.6<br>3.4<br>2.7<br>X8.6 |
| 3147 | Sb | 10 12.8 103° | +73 39 +40° | 11.9 | 13.62<br>11.76<br>11.58 | 0.95<br>0.81<br>0.81 | 0.3<br>2.3<br>4.1 |
| 3158 | E3 | 10 10.9 150° | +39 0 +57° | 12.7 | 13.61<br>13.11 | 1.06<br>1.05 | 1.1<br>2.3 |
| 3166 | Sa | 10 11.2 207° | + 3 40 +47° | 11.6 | 13.27<br>11.38 | 1.11<br>0.94 | 0.3<br>4.1 |
| 3169 | Sa | 10 11.7 207° | + 3 43 +47° | 11.9 | 11.30 | 0.79 | 4.1 |
| 3184 | Sc | 10 15.2 145° | +41 40 +57° | 11.8 | (13.80)<br>10.66 | 0.83<br>0.66 | 0.3<br>5.7 |
| 3185 | SBa | 10 14.9 182° | +21 56 +56° | 12.7 | 13.10 | 0.79 | 2.3 |
| 3190 | Sb | 10 15.4 180° | +22 5 +56° | 12.1 | 12.16 | 1.01 | 1.4<br>X5.7 |
| 3193 | E2 | 10 15.7 181° | +22 9 +56° | 12.6 | 12.20 | 0.95 | 2.3 |
| Sextans Sys. | Irr | 10 18.6 215° | - 4 23 +40° | (12.7) | 13.16 | 0.45 | 8.6 |
| 3222 | SB0 | 10 19.7 185° | +20 8 +57° | (14) | 13.87 | 0.97 | 1.1 |
| 3226 | E1 | 10 20.7 185° | +20 9 +57° | 12.8 | 12.97 | 0.93 | 1.1 |
| 3227 | Sb | 10 20.7 185° | +20 7 +57° | 12.2 | 11.71 | 0.79 | 1.8<br>X3.6 |
| 3239 | Irr | 10 22.4 191° | +17 24 +56° | (14) | 12.86 | 0.32 | 1.3 |
| Anon | E0 | 10 24.4 201° | +10 39 +54° | - | 16.19 | 1.17 | 0.6 |
| 3245 | S0 | 10 24.5 170° | +28 46 +60° | 12.0 | 11.90<br>11.75 | 0.92<br>0.88 | 2.3<br>4.1 |
| 3254 | Sc | 10 26.5 168° | +29 45 +60° | 12.6 | 12.26 | 0.64 | 4.1 |
| 3277 | Sa | 10 30.2 170° | +28 46 +61° | 12.6 | 12.53<br>12.28 | .85<br>.85 | 2.3<br>2.4 |
| 3301 | Sa | 10 34.3 184° | +22 8 +61° | 12.4 | 12.38 | 0.91 | 2.4 |
| 3310 | Sb | $10^h\ 35^m.7$ 123° | +53°46' +55° | 10.9 | 11.58<br>11.22 | 0.31<br>0.26 | 0.7<br>2.3 |
| 3344 | Sc | 10 40.7 178° | +25 11 +63° | 11.9 | 14.92<br>10.66 | (1.30)<br>0.65 | 0.3<br>5.7 |
| 3351 | SBb | 10 41.3 203° | +11 58 +58° | 11.5 | 10.81 | 0.77 | 5.7 |
| 3359 | SBb | 10 43.4 110° | +63 30 +52° | 12.2 | 12.68<br>11.05 | 0.87<br>0.51 | 0.7<br>3.2<br>X8.6 |
| 3367 | SBc | 10 44.0 200° | +14 1 +59° | 12.3 | 12.11<br>11.97 | 0.55<br>0.45 | 2.3<br>4.1 |
| 3368 | Sa | 10 44.2 204° | +12 5 +59° | 10.4 | 10.18 | 0.91 | 5.7 |
| 3377 | E6 | 10 45.1 200° | +14 15 +60° | 11.6 | 11.48<br>11.29 | 0.76<br>0.87 | 2.3<br>4.1 |
| 3379 | E0 | 10 45.2 203° | +12 51 +59° | 10.8 | 10.81<br>10.57 | (0.81)<br>(0.95) | 2.3<br>4.1 |
| 3384 | SB0 | 10 45.7 203° | +12 54 +59° | 11.3 | 11.02 | 0.87 | 4.1 |
| 3389 | Sc | 10 45.8 203° | +12 48 +59° | 12.6 | 12.24 | 0.43 | 2.3 |
| 3412 | SB0 | 10 48.3 202° | +13 41 +60° | 11.6 | 13.03<br>11.58 | 0.96<br>0.91 | 0.3<br>4.1 |
| 3414 | SBa | 10 48.6 172° | +28 15 +65° | 12.2 | 12.11 | 0.94 | 2.3 |
| 3430 | Sc | 10 49.5 162° | +33 14 +65° | 12.4 | 12.20 | 0.67 | 2.3<br>X4.1 |
| Anon N1+N1a | E | 10 55.4 115° | +57 3 +55° | (16.8) | 17.62 | 1.25 | 0.4 |
| Anon | S0 | 10 55.7 115° | +57 1 +55° | (17.0) | 19.11 | 1.41 | 0.4 |
| 3486 | Sc | 10 57.8 170° | +29 15 +67° | 11.4 | 11.15<br>10.95 | 0.51<br>0.35 | 4.1<br>5.7 |
| 3489 | Sap | 10 57.7 203° | +14 10 +62° | 11.3 | 11.01<br>11.01 | 0.54<br>0.47 | 2.4<br>3.4 |
| 3504 | SBb | 11 0.5 173° | +28 15 +67° | 11.7 | 11.74<br>11.58 | 0.53<br>0.79 | 4.1<br>5.1 |
| 3516 | SB0 | 11 3.4 100° | +72 50 +43° | 12.2 | 13.22<br>12.73 | 1.15<br>.83 | 0.3<br>2.3 |
| 3521 | Sb | 11 3.2 225° | + 0 14 +54° | 10.3 | 12.45<br>9.84<br>9.76 | 0.97<br>0.83<br>0.83 | 0.3<br>5.7<br>8.6 |
| 3556 | Sc | 11 8.7 114° | +55 57 +57° | 11.0 | 10.63 | 0.56 | 2.7<br>X8.6 |
| 3585 | E6 | 11 10.9 246° | -26 29 +31° | 11.5 | 11.16<br>11.10 | 1.01<br>0.98 | 2.3<br>4.1 |
| 3593 | S0p | 11 12.0 210° | +13 6 +64° | 12.4 | 11.84 | 0.73 | 3.4 |
| 3605 | E4 | 11 14.2 200° | +18 18 +68° | 13.1 | 14.43<br>13.95 | 0.93<br>1.01 | 0.3<br>2.3 |

TABLE 5—*Continued*

| NGC IC* | Type | R.A. l | Dec. b | Mpg Harv. | PHOTOELECTRIC Mpg | C.I. | Ap. | NGC IC* | Type | R.A. l | Dec. b | Mpg Harv. | PHOTOELECTRIC Mpg | C.I. | Ap. |
|---|---|---|---|---|---|---|---|---|---|---|---|---|---|---|---|
| 3607 | S0 | 11h 14m.3<br>200° | +18°20'<br>+68° | 11.4 | 10.97 | 0.95 | 4.1 | 4116 | SBc | 12h 05m.1<br>248° | + 2°58'<br>+64° | 12.4 | 12.57 | 0.55 | 4.1 |
| 3608 | E1 | 11 14.4<br>200° | +18 26<br>+68° | 12.5 | 12.18 | 0.90 | 2.3 | 4150 | S0 | 12 8.0<br>156° | +30 41<br>+82° | 12.6 | 12.63 | 0.77 | 2.3 |
| 3610 | E5 | 11 15.6<br>109° | +59 4<br>+55° | 11.7 | 13.21<br>11.95 | 0.96<br>0.85 | 0.3<br>2.3 | 4179 | E7 | 12 10.3<br>252° | + 1 35<br>+63° | 11.8 | 11.94<br>(12.00) | 0.92<br>0.95 | 2.3<br>4.1 |
| 3611 | Sa | 11 14.9<br>225° | + 4 50<br>+59° | 12.5 | 12.78 | 0.47 | 2.4 | 4192 | Sb | 12 11.3<br>238° | +15 11<br>+75° | 11.4 | 10.89 | 0.73 | 2.7<br>X8.6 |
| 3623 | Sa | 11 16.3<br>211° | +13 23<br>+65° | 10.5 | 10.10 | 0.71 | 2.3<br>X8.6 | 4203 | SB0 | 12 12.6<br>136° | +33 29<br>+81° | 12.0 | 12.27<br>11.78 | 0.93<br>0.88 | 1.1<br>2.3 |
| 3626 | Sa | 11 17.4<br>200° | +18 38<br>+68° | 11.8 | 11.23 | 0.60 | 2.4 | 4244 | Sc | 12 15.0<br>118° | +38 5<br>+78° | 11.0 | 10.81 | 0.37 | 2.7<br>X8.6 |
| 3627 | Sb | 11 17.6<br>212° | +13 17<br>+66° | 9.9 | 9.83<br>9.67 | 0.60<br>0.59 | 5.7<br>8.6 | 4258 | Sb | 12 16.5<br>102° | +47 35<br>+69° | 10.2 | 9.39 | 0.75 | 4.1<br>X8.6 |
| 3640 | E2 | 11 18.5<br>227° | + 3 31<br>+58° | 11.6 | 11.69 | 0.95 | 2.4 | 4273 | Sc | 12 17.4<br>254° | + 5 37<br>+67° | 12.2 | 12.26<br>12.14 | 0.29<br>0.35 | 2.3<br>4.1 |
| 3646L | Sc | 11 19.2<br>197° | +20 27<br>+69° | 11.8 | 11.84 | 0.62 | 3.2<br>X5.7 | 4274 | Sa | 12 17.4<br>160° | +29 53<br>+84° | 11.7 | 11.27 | 0.87 | 4.1 |
| 3665 | S0 | 11 22.1<br>141° | +39 2<br>+70° | 12.3 | 11.94 | 0.99 | 2.4 | 4281 | S0 | 12 17.8<br>254° | + 5 40<br>+67° | 12.2 | 12.33 | 0.88 | 2.3 |
| 3681 | Sb | 11 23.9<br>206° | +17 9<br>+69° | 12.8 | 12.51<br>12.44 | 0.55<br>0.76 | 2.3<br>3.4 | 4303 | Sc | 12 19.4<br>256° | + 4 45<br>+66° | 10.4 | 10.16<br>(10.18) | 0.37<br>0.57 | 5.7<br>8.6 |
| 3684 | Sc | 11 24.5<br>206° | +17 18<br>+69° | 12.6 | 12.33 | 0.60 | 4.1 | 4314 | SBa | 12 20.0<br>152° | +30 10<br>+84° | 11.7 | 11.55<br>11.45 | 0.83<br>0.88 | 4.1<br>5.7 |
| 3686 | Sb | 11 25.1<br>206° | +17 30<br>+69° | 12.3 | 11.99 | 0.51 | 4.1 | 4350 | E7 | 12 21.4<br>245° | +16 58<br>+78° | 12.0 | 12.03 | 0.85 | 2.3 |
| 3810 | Sc | 11 38.4<br>223° | +11 45<br>+68° | 11.8 | 11.22<br>11.20 | 0.37<br>0.43 | 4.1<br>5.7 | 4374 | E1p | 12 22.6<br>251° | +13 10<br>+75° | 10.9 | 10.65<br>10.49 | 1.03<br>1.00 | 4.1<br>5.7 |
| 3818 | E5 | 11 39.4<br>243° | - 5 53<br>+53° | 12.7 | 12.86 | 0.91 | 2.3 | 4394 | SBb | 12 23.4<br>244° | +18 29<br>+80° | 12.2 | 11.91<br>11.60 | 0.84<br>0.69 | 4.1<br>5.7 |
| U.Mj.1<br>No.24 | E3 | 11 44.5<br>106° | +56 1<br>+60° | - | 15.98 | 1.04 | 0.6 | 4414 | Sc | 12 24.0<br>136° | +31 30<br>+85° | 11.1 | 10.94<br>10.96 | 0.65<br>0.65 | 4.1<br>5.7 |
| 3872 | E3 | 11 43.2<br>222° | +14 3<br>+70° | 12.8 | 12.91 | 0.99 | 2.3 | 4421 | SBa | 12 24.5<br>250° | +15 44<br>+77° | - | 12.42<br>11.87 | 0.81<br>(0.85) | 1.3<br>2.4 |
| 3900 | Sa | 11 46.6<br>179° | +27 17<br>+78° | 12.7 | 12.47<br>12.33 | 0.80<br>0.84 | 2.3<br>4.1 | 4425 | Sa | 12 24.7<br>253° | +13 1<br>+75° | 13.1 | 13.29 | 1.02 | 2.3 |
| 3904 | E2 | 11 46.7<br>256° | -29 2<br>+32° | 11.9 | 12.20 | 1.07 | 2.3 | 4429 | Sa | 12 24.9<br>255° | +11 23<br>+73° | 11.7 | 10.99 | 0.95 | 4.1 |
| 3923 | E4 | 11 48.5<br>256° | -28 33<br>+32° | 11.1 | 11.41 | 1.05 | 2.3 | 4435 | SB0 | 12 25.2<br>254° | +13 21<br>+75° | 11.8 | 11.80 | 0.94 | 2.3 |
| 3953 | Sb | 11 51.2<br>107° | +52 37<br>+63° | 11.5 | 13.78<br>10.87 | -<br>0.70 | 0.3<br>5.7 | 4438 | Sap | 12 25.2<br>254° | +13 17<br>+75° | 11.9 | 11.42<br>11.14 | 0.85<br>0.87 | 4.1<br>5.7 |
| 3962 | E1 | 11 52.2<br>252° | -13 42<br>+47° | 12.2 | 11.96 | 1.01 | 2.3 | 4442 | SB0 | 12 25.6<br>256° | +10 5<br>+72° | 11.4 | 11.35 | 0.93 | 4.1 |
| 4105 | E2 | 12 4.1<br>260° | -29 30<br>+32° | 12.0 | 12.22 | 1.03 | 1.1 | 4448 | Sa | 12 25.8<br>161° | +28 54<br>+86° | 11.9 | 12.08 | 0.96 | 4.1 |
| 4106 | SB0 | 12 4.2<br>260° | -29 31<br>+32° | 12.5 | 12.61 | 1.02 | 1.1 | 4459 | S0 | 12 26.5<br>254° | +14 15<br>+76° | 11.9 | 11.61 | 0.87 | 2.3 |

TABLE 5—*Continued*

| NGC IC* | Type | R.A. l | Dec. b | Mpg Harv. | PHOTOELECTRIC Mpg | C.I. | Ap. |
|---|---|---|---|---|---|---|---|
| 4461 | SO | 12h 26.6 | +13°28' | 12.4 | 12.02 | 0.77 | 4.1 |
| | | 254° | +75° | | | | |
| 4473 | E5 | 12 27.3 | +13 42 | | 11.54 | 0.85 | 2.3 |
| | | 255° | +76° | 11.7 | 11.30 | 0.83 | 4.1 |
| 4474 | S0 | 12 27.4 | +14 21 | 12.9 | 12.68 | 0.99 | 2.4 |
| | | 255° | +76° | | | | |
| 4477 | SB0 | 12 27.6 | +13 55 | 11.8 | 11.80 | 0.85 | 2.3 |
| | | 255° | +76° | | | | |
| 4478 | E2 | 12 27.8 | +12 36 | 12.5 | 12.27 | 0.89 | 2.4 |
| | | 257° | +75° | | | | |
| 4479 | S0 | 12 27.8 | +13 51 | (13.5) | 13.57 | 0.97 | 2.4 |
| | | 255° | +76° | | | | |
| Anon | E0 | 12 27.9 | +12 47 | (15) | 15.32 | (1.11) | 0.6 |
| | | 256° | +75° | | | | |
| 4482 | Sa | 12 28.5 | + 8 21 | (14.0) | 13.45 | 0.59 | 1.1 |
| | | 260° | +70° | | | | |
| 4526 | S0 | 12 31.6 | + 7 58 | | 10.70 | 0.96 | 3.2 |
| | | 262° | +70° | | | | X5.7 |
| | | | | 10.7 | 10.71 | 0.99 | 3.2 |
| | | | | | | | X8.6 |
| 4527 | Sb | 12 31.6 | + 2 56 | 11.3 | 11.55 | 0.71 | 3.2 |
| | | 263° | +65° | | | | X8.6 |
| 4546 | SB0 | 12 32.9 | - 3 31 | 11.4 | 11.54 | 1.03 | 2.3 |
| | | 266° | +59° | | | | |
| 4548 | SBb | 12 32.9 | +14 46 | 11.9 | 11.04 | 0.94 | 5.7 |
| | | 260° | +77° | | | | |
| 4550 | E7 | 12 32.9 | +12 30 | 12.7 | 12.58 | 0.97 | 4.1 |
| | | 261° | +75° | | | | |
| 4552 | E0 | 12 33.1 | +12 50 | | 11.19 | 0.79 | 2.4 |
| | | 260° | +75° | 11.3 | 11.12 | 0.81 | 3.4 |
| 4569 | Sb | 12 34.3 | +13 26 | 11.2 | 10.40 | 0.87 | 8.6 |
| | | 262° | +76° | | | | |
| 4570 | E7 | 12 34.4 | + 7 31 | 12.0 | 11.81 | 0.99 | 2.7 |
| | | 264° | +70° | | | | X5.7 |
| Anon Virgo No.4 | E2 2 | 12 38.0 | +18 52 | - | 15.31 | 1.31 | 1.3 |
| | | 265° | +81° | | | | |
| 4621 | E5 | 12 39.5 | +11 55 | 11.4 | 10.95 | 0.98 | 4.1 |
| | | 267° | +74° | | | | |
| 4631 | Se | 12 39.8 | +32 49 | 9.6 | 9.91 | 0.42 | 8.6 |
| | | 96° | +85° | | | | |
| 4631B | Ep | 12 39.8 | +32 50 | - | 13.28 | 0.78 | 2.3 |
| | | 98° | +84° | | | | |
| 4638 | E6 | 12 40.2 | +11 43 | 12.2 | 12.16 | 0.75 | 2.3 |
| | | 268° | +74° | | | | |
| 4647 | Sc | 12 41.0 | +11 51 | 12.0 | 12.39 | 0.69 | 2.3 |
| | | 268° | +74° | | | | |
| 4649 | E2 | 12 41.1 | +11 49 | 10.6 | 10.11 | 0.97 | 4.1 |
| | | 269° | +74° | | | | |
| 4660 | E5 | 12 42.0 | +11 26 | 12.3 | 12.06 | 0.97 | 2.3 |
| | | 270° | +74° | | | | |

| NGC IC* | Type | R.A. l | Dec. b | Mpg Harv. | PHOTOELECTRIC Mpg | C.I. | Ap. |
|---|---|---|---|---|---|---|---|
| 4666 | Sc | 12h 42.6 | - 0°12' | | 13.70 | 1.01 | 0.7 |
| | | 270° | +62° | 11.3 | 11.58 | 0.84 | 5.1 |
| 4697 | E5 | 12 46.0 | - 5 32 | 10.6 | 10.47 | 0.91 | 4.1 |
| | | 272° | +57° | | | | |
| 4698 | Sa | 12 45.8 | + 8 45 | 12.2 | 11.65 | 0.76 | 3.4 |
| | | 273° | +71° | | | | |
| 4699 | Sb | 12 46.5 | - 8 24 | | 11.75 | 0.95 | 0.4 |
| | | 272° | +54° | 10.5 | 10.68 | 0.96 | 2.4 |
| 4710 | S0 | 12 47.1 | +15 26 | 12.0 | 11.91 | 0.84 | 1.8 |
| | | 275° | +78° | | | | X4.1 |
| 4742 | E4 | 12 49.2 | -10 12 | 11.9 | 12.50 | 1.07 | 2.4 |
| | | 273° | +52° | | | | |
| 4753 | S0p | 12 49.8 | - 0 55 | | 12.85 | 1.11 | 0.4 |
| | | 277° | +61° | 10.5 | 10.98 | 0.96 | 3.4 |
| 4754 | SB0 | 12 49.7 | +11 35 | 12.0 | 11.59 | 0.99 | 4.1 |
| | | 276° | +74° | | | | |
| 4762 | Sa | 12 50.4 | +11 31 | 11.8 | 11.17 | 0.69 | 1.8 |
| | | 277° | +74° | | | | X5.7 |
| Anon | Pec | 12 54.2 | +32 46 | (14) | 15.07 | 0.09 | 1.3 |
| | | 63° | +84° | | | | |
| 4850 | S0 | 12 55.8 | +28 14 | (16) | 15.35 | 1.13 | 0.6 |
| | | 10° | +86° | | 15.37 | 1.02 | 1.3 |
| 3946* | S0 | 12 56.4 | +28 5 | (16) | 15.36 | 1.25 | 0.6 |
| | | 7° | +87° | | 15.20 | 1.05 | 1.3 |
| 4853 | E1 | 12 56.2 | +27 52 | | 14.49 | 0.93 | 0.6 |
| | | 4° | +87° | (15) | 14.43 | 0.91 | 1.3 |
| 4856 | SBa | 12 56.7 | -14 46 | | 11.65 | 1.01 | 2.4 |
| | | 275° | +47° | 11.4 | 11.66 | 1.03 | 3.4 |
| 4860 | E2 | 12 56.5 | +28 24 | | 15.30 | 0.95 | 0.4 |
| | | 13° | +87° | (15.5) | 14.93 | 1.22 | 0.6 |
| 4861 | Irr | 12 56.7 | +35 8 | | 13.82 | 0.37 | 0.4 |
| | | 70° | +83° | 12.7 | 13.10 | 0.47 | 2.4 |
| 4864 | E1 | 12 56.8 | +28 15 | (16) | 14.81 | 0.97 | 0.6 |
| | | 10° | +87° | | | | |
| 4865 | E6 | 12 56.8 | +28 21 | | 14.97 | 1.09 | 1.1 |
| | | 13° | +87° | (15.3) | 14.44 | 0.82 | 1.3 |
| 4866 | Sa | 12 57.0 | +14 27 | 12.1 | 12.14 | 0.86 | 4.1 |
| | | 284° | +76° | | | | |
| 4867 | E3 | 12 56.9 | +28 16 | (16) | 15.61 | 0.99 | 0.6 |
| | | 10° | +87° | | | | |
| 4869 | E3 | 12 57.0 | +28 11 | | 14.97 | 1.07 | 0.6 |
| | | 10° | +87° | (16) | 14.92 | 1.11 | 1.3 |
| 4872 | E0 | 12 57.2 | +28 43 | | 15.53 | 1.03 | 0.4 |
| | | 5° | +86° | (15) | 15.38 | 1.10 | 0.6 |
| 4874 | S0 | 12 57.2 | +28 14 | | 14.42 | 1.13 | 0.6 |
| | | 10° | +87° | (14.5) | 13.78 | 1.22 | 1.1 |
| 4881 | E1 | 12 57.5 | +28 31 | (16) | 14.75 | 1.13 | 1.3 |
| | | 14° | +87° | | | | |

TABLE 5—*Continued*

| NGC IC* | Type | R.A. l | Dec. b | Mpg Harv. | PHOTOELECTRIC Mpg | C.I. | Ap. |
|---|---|---|---|---|---|---|---|
| 4889 | E4 | $12^h\ 57^m.7$ 9° | +28°15' +86° | 12.6 | 13.92<br>13.24<br>12.83 | 1.25<br>1.23<br>1.21 | 0.6<br>1.1<br>2.3 |
| 4886 | S0 | 12 57.6 9° | +28 20 +86° | (16) | 15.18 | 0.99 | 0.6 |
| 4021* | E0 | 12 57.8 11° | +28 19 +86° | (16.5) | 15.96<br>15.52 | 0.80<br>0.74 | 0.6<br>1.3 |
| 4895 | S0 | 12 57.9 14° | +28 28 +86° | (15) | 14.65<br>14.35 | 1.11<br>1.07 | 0.6<br>1.3 |
| 4896 | S0 | 12 57.9 15° | +28 35 +86° | (16) | 15.16 | 1.02 | 0.6 |
| 4898 a+b | S0 | 12 57.9 9° | +28 13 +86° | (16) | 14.67 | 1.08 | 0.6 |
| 4900 | Sc | 12 58.2 279° | + 2 46 +64° | 11.8 | 12.07 | 0.60 | 2.4 |
| 4902 | SBb | 12 58.3 276° | -14 15 +47° | 11.6 | 13.99<br>11.90 | 1.15<br>0.70 | 0.4<br>2.4 |
| 4908 | E4 | 12 58.4 10° | +28 18 +86° | (16) | 15.07 | 1.11 | 0.6 |
| 4045* | E2 | 12 58.4 10° | +28 22 +86° | (16) | 15.33 | 1.08 | 0.6 |
| 4051* | E1 | 12 58.5 9° | +28 17 +86° | (16) | 14.96 | 1.06 | 0.6 |
| 4911 | Sb | 12 58.2 6° | +28 3 +86° | - | 13.93<br>13.50 | 1.14<br>0.80 | 1.3<br>3.4 |
| 4926 | E2 | 12 59.5 6° | +27 54 +86° | - | 14.36<br>14.13 | 1.21<br>1.15 | 1.3<br>2.4 |
| 4907 | SBb | 12 58.4 10° | +28 26 +86° | - | 14.74 | 1.35 | 1.3 |
| 4915 | E0 | 12 58.8 278° | - 4 16 +58° | 12.9 | 13.19<br>13.00 | 0.91<br>0.91 | 1.1<br>2.3 |
| 4941 | Sa | 13 1.6 279° | - 5 17 +57° | 12.4 | 11.97 | 0.87 | 4.1 |
| 4958 | E7 | 13 3.1 279° | - 7 45 +54° | 11.6 | 11.58<br>11.54 | 0.85<br>0.91 | 2.3<br>2.7<br>X4.1 |
| 4995 | Sb | 13 07.0 281° | - 7 34 +55° | 11.7 | 13.74<br>12.02 | 0.91<br>0.89 | 0.4<br>2.4 |
| 5005 | Sb | 13 8.5 62° | +37 19 +79° | 11.3 | 12.59<br>10.71 | 1.09<br>0.98 | 0.4<br>5.1 |
| 5018 | E4 | 13 10.3 279° | -19 15 +43° | 11.6 | 12.26 | 1.12 | 2.4 |
| 5033 | Sc | 13 11.2 58° | +36 51 +79° | 11.6 | (10.78) | (0.46) | 8.6 |
| 5049 | S0 | 13 13.3 281° | -16 8 +45° | - | 13.70<br>(13.81) | 0.65<br>0.63 | 1.3<br>2.4 |
| 5077 | E3 | 13 16.9 283° | -12 24 +49° | 12.2 | 12.58 | 1.25 | 1.3 |
| 5087 | S0 | 13 17.7 281° | -20 21 +41° | 12.4 | 12.21 | 1.09 | 2.4 |

| NGC IC* | Type | R.A. l | Dec. b | Mpg Harv. | PHOTOELECTRIC Mpg | C.I. | Ap. |
|---|---|---|---|---|---|---|---|
| 5194 | Sc | $13^h\ 27^m.8$ 69° | +47°27' +68° | 10.1 | 12.79<br>8.89 | 0.47<br>0.38 | 0.3<br>8.6 |
| 5195 | Irr | 13 27.9 69° | +47 31 +68° | 11.1 | 12.51<br>10.71 | 1.03<br>0.77 | 0.3<br>4.1 |
| 5204 | Scp | 13 28.3 80° | +58 40 +58° | 12.2 | 11.90 | 0.41 | 4.1 |
| 5236 | Sc | 13 34.3 283° | -29 37 +31° | 8.0 | 10.89<br>8.36 | 0.59<br>0.67 | 0.7<br>8.6 |
| 5248 | Sc | 13 35.1 306° | + 9 8 +67° | 11.0 | 10.98<br>10.98 | 0.63<br>0.53 | 5.7<br>8.6 |
| 5308 | S0 | 13 45.4 77° | +61 14 +55° | 12.8 | 12.35<br>12.33 | 0.81<br>0.95 | 2.3<br>2.3<br>X4.1 |
| 5322 | E4 | 13 47.6 76° | +60 26 +55° | 11.6 | 11.05<br>11.01 | 0.93<br>0.86 | 2.3<br>4.1 |
| 5328 | E1 | 13 50.0 288° | -28 14 +32° | 12.9 | 13.12 | 0.87 | 1.1 |
| 5353 | S0 | 13 51.3 46° | +40 32 +71° | 12.4 | 12.14 | 1.06 | 2.3 |
| 5354 | S0 | 13 51.3 46° | +40 33 +71° | - | 12.48 | 0.94 | 2.3 |
| 5364 | Sc | 13 53.7 310° | + 5 15 +62° | 11.8 | 11.18 | 0.59 | 5.7 |
| 5371 | Sb | 13 53.6 46° | +40 43 +70° | 11.7 | 11.59 | 0.61 | 4.1 |
| 5377 | Sa | 13 54.3 60° | +47 27 +66° | 12.8 | 12.43<br>12.05 | 0.94<br>0.72 | 1.8<br>X4.1<br>1.8<br>X5.7 |
| 5394 | Sb | 13 56.5 37° | +37 41 +71° | (13) | 13.51 | 0.62 | 2.3 |
| 5395 | Sb | 13 56.5 40° | +37 39 +72° | 13.0 | 12.44 | 0.76 | 2.3 |
| 5457 | Sc | 14 1.4 67° | +54 35 +60° | 9.0 | 9.17 | 0.50 | 8.6 |
| 5473 | SB0 | 14 3.0 68° | +55 8 +59° | 12.8 | 12.74<br>12.39 | 0.83<br>0.85 | 1.1<br>2.3 |
| 5485 | S0 | 14 5.5 67° | +55 14 +59° | 12.9 | 12.58 | 0.93 | 2.3 |
| 5493 | Sa | 14 8.9 306° | - 4 49 +51° | 12.4 | 12.59<br>12.38 | 0.87<br>0.96 | 1.1<br>2.3 |
| 5566 | Sa | 14 17.8 318° | + 4 11 +57° | 11.9 | 11.50 | 0.78 | 5.7 |
| 5574 | SB0 | 14 18.4 317° | + 3 28 +57° | 13.1 | 13.35 | 0.83 | 2.3 |
| 5576 | E4 | 14 18.5 318° | + 3 30 +57° | 11.9 | 12.01 | 0.80 | 2.3 |
| 5633 | Sb | 14 25.6 49° | +46 22 +63° | 12.8 | 14.69<br>13.06 | 0.89<br>0.46 | 0.3<br>1.1 |
| 5638 | E1 | 14 27.1 320° | + 3 27 +55° | 12.6 | 12.45 | 0.87 | 2.3 |

TABLE 5—*Continued*

| NGC IC* | Type | R.A. l | Dec. b | Mpg. Harv. | PHOTOELECTRIC Mpg | C.I. | Ap. |
|---|---|---|---|---|---|---|---|
| 5668 | Sc | 14h 30m.9 323° | + 4°40' +55° | 12.4 | 14.45<br>12.24 | 0.71<br>0.62 | 0.4<br>3.4 |
| 5672 | Sb | 14 30.5 16° | +31 53 +66° | (14) | 14.75<br>14.04 | 0.67<br>0.66 | 0.4<br>1.3 |
| 5676 | Sc | 14 31.0 55° | +49 41 +60° | 11.9 | 14.62<br>11.85<br>(11.93) | 1.19<br>0.71<br>0.61 | 0.3<br>2.3<br>1.4<br>X4.1 |
| 5687 | E3 | 14 33.3 61° | +54 42 +56° | 12.7 | 12.63 | 0.85 | 1.8<br>X5.1 |
| 5689 | S0 | 14 33.7 52° | +48 47 +60° | 12.6 | 12.84 | 0.97 | 1.8<br>X4.1 |
| 5713 | Sb | 14 37.6 320° | - 0 5 +51° | 11.8 | 11.98 | 0.63 | 2.3 |
| 5746 | Sb | 14 42.3 324° | + 2 10 +52° | 11.8 | 13.01<br>11.47 | 1.13<br>0.93 | 0.7<br>2.3<br>X8.6 |
| 5806 | Sb | 14 57.5 327° | + 2 5 +49° | 12.5 | 12.34 | 0.67 | 4.1 |
| 5812 | E1 | 14 58.2 318° | - 7 16 +42° | 12.5 | 12.56 | 1.03 | 2.3 |
| 5813 | E1 | 14 58.7 327° | + 1 54 +48° | 12.2 | 13.46<br>11.98<br>(12.08) | 1.07<br>1.04<br>1.03 | 0.4<br>2.3<br>2.4 |
| 5820 | S0 | 14 57.2 56° | +54 2 +54° | 12.8 | 13.03 | 0.97 | 2.3 |
| 5831 | E3 | 15 1.6 328° | + 1 24 +48° | 12.7 | 12.55 | 0.80 | 2.3 |
| 5838 | S0 | 15 2.9 329° | + 2 18 +48° | 12.1 | 11.88 | 0.99 | 4.1 |
| 5846 +Anon | E0 E3 | 15 4.0 329° | + 1 48 +47° | 11.6 | 11.26 | 0.93 | 4.1 |
| Anon | E3 | 15 4.0 329° | + 1 47 +47° | - | 14.61<br>14.03 | 1.04<br>1.04 | 0.3<br>0.7 |
| 5850 | SBb | 15 4.6 329° | + 1 44 +47° | 12.9 | 12.20<br>11.80 | 0.83<br>0.86 | 4.1<br>5.7 |
| 5854 | Sba | 15 5.3 330° | + 2 46 +48° | 12.7 | 12.69 | 0.85 | 2.3 |
| 5857 | Sb | 15 5.2 354° | +19 47 +57° | - | 13.83 | 0.66 | 2.3 |
| 5859 | Sb | 15 5.3 354° | +19 46 +57° | - | 13.33<br>13.28 | 0.90<br>(0.81) | 1.4<br>X3.6<br>4.1 |
| 5857 +5859 | | 15 5.3 354° | +19 46 +57° | - | 12.90 | 0.79 | 2.7<br>X5.7 |
| 5866 | S0 | 15 5.1 58° | +55 57 +52° | 11.5 | 10.89 | 0.82 | 4.1 |
| 5878 | Sb | 15 11.0 315° | -14 5 +35° | 12.9 | 12.37 | 0.81 | 4.1 |
| 5879 | Sb | 15 8.4 59° | +57 12 +51° | 12.1 | 11.97<br>11.98 | 0.53<br>0.53 | 4.1<br>3.6<br>X5.7 |
| 5898 | E0 | 15 15.2 309° | -23 55 +27° | 12.6 | 12.51 | 0.69 | 2.3 |
| 5899 | Sb | 15h 13m.2 35° | +42°14' +56° | 12.4 | 12.48 | 0.75 | 4.1 |
| 5903 | E2 | 15 15.6 309° | -23 51 +27° | 12.9 | 12.59 | 0.81 | 2.3 |
| 5907 | Sb | 15 14.6 58° | +56 31 +51° | 11.8 | 11.19 | 0.82 | 8.6 |
| 5921 | SBb | 15 19.5 336° | + 5 15 +46° | 12.5 | 11.91<br>11.59 | 0.93<br>0.61 | 2.4<br>4.1 |
| 5962 | Sc | 15 34.2 354° | +16 46 +49° | 12.5 | 12.15 | 0.59 | 4.1 |
| 5970 | SBb | 15 36.1 348° | +12 20 +47° | 12.4 | 12.23 | 0.70 | 5.1 |
| 5976 | S0 | 15 35.8 59° | +59 36 +47° | (15) | 15.95 | (1.09) | 1.1 |
| 5981 | Sab | 15 36.9 59° | +59 33 +47° | (13.5) | 14.20 | 0.93 | 1.1 |
| 5982 | E4 | 15 37.6 59° | +59 32 +47° | 12.5 | 12.33 | 0.94 | 2.3 |
| 6015 | Sc | 15 50.7 63° | +62 28 +43° | 12.1 | 11.65 | 0.54 | 4.1 |
| 6027b | Sa | 15 57.0 2° | +20 55 +45° | (15.5) | 15.73 | 0.79 | 0.4 |
| 6027d | Sa | 15 57.0 2° | +20 55 +45° | (15) | 14.94<br>14.77 | 1.03<br>0.92 | 0.4<br>0.6 |
| 1183* | E1 | 16 359° | +17 54 +43° | - | 15.75 | 1.22 | 0.6 |
| 1185* | Sa | 16 359° | +17 51 +43° | - | 14.91<br>14.77 | 0.91<br>0.94 | 0.7<br>1.1 |
| 1194* | E1 | 16 359° | +17 55 +43° | - | 15.51<br>15.34 | 0.95<br>1.12 | 0.7<br>1.1 |
| 6070 | Sc | 16 340° | + 0 50 +34° | 12.7 | 12.44 | 0.62 | 3.4 |
| 6181 | Sc | 16 4° | +19 56 +38° | 12.6 | 12.48<br>12.45 | 0.53<br>0.57 | 2.4<br>2.4<br>X3.4 |
| 6207 | Sc | 16 41.3 26° | +36 56 +39° | 12.3 | (12.13) | 0.45 | 2.4 |
| 6217 | Sc | 16 34.8 78° | +78 18 +33° | 12.6 | 11.83 | 0.58 | 4.1 |
| 6239 | SBb | 16 48.5 35° | +42 50 +39° | 13.1 | 13.00<br>12.70 | 0.46<br>0.61 | 1.4<br>X4.1<br>5.1 |
| 6314 | Sa | 17 10.1 12° | +23 20 +30° | - | 15.14<br>14.10 | 0.85<br>0.78 | 0.3<br>1.1 |
| 6340 | Sa | 17 11.1 71° | +72 22 +33° | 12.8 | 12.30<br>12.02 | 0.87<br>0.86 | 2.3<br>4.1 |
| 6359 | E1 | 17 17.4 58° | +61 50 +34° | - | 13.76 | 0.91 | 1.1 |
| 6384 | SBb | 17 29.9 358° | + 7 6 +19° | 12.7 | 11.87<br>11.46 | 0.63<br>0.67 | 3.4<br>4.5<br>X5.7 |
| 6412 | Sc | 17 30.8 74° | +75 45 +31° | 12.8 | 12.36 | 0.45 | 4.1 |

TABLE 5—*Continued*

| NGC IC* | Type | R.A. l | Dec. b | Mpg Harv. | PHOTOELECTRIC Mpg | C.I. | Ap. |
|---|---|---|---|---|---|---|---|
| 6482 | E3 | 17h 49m8 +23° 5' 16° +22° | | 12.2 | 13.20 | 1.07 | 1.3 |
| 6503 | Sc | 17 49.9 +70 10 66° +31° | | 11.4 | 10.87 | 0.63 | 4.1 |
| 6574 | Sb | 18 9.5 +14 58 10° +14° | | 12.7 | 12.99<br>12.88 | 0.82<br>0.82 | 1.1<br>2.3 |
| 6627 | SBb | 18 20.4 +15 39 12° +12° | | - | 14.48 | 1.07 | 1.3 |
| 6635 | E | 18 25.3 +14 45 11° +10° | | (14.9) | 14.98 | 1.08 | 0.4 |
| 6643 | Sc | 18 21.2 +74 33 72° +28° | | 12.7 | 15.01<br>11.88 | 0.74<br>0.69 | 0.3<br>1.4<br>X4.1 |
| 6654 | SBa | 18 25.2 +73 9 71° +28° | | - | 15.55<br>12.80 | 0.93<br>0.95 | 0.3<br>2.3 |
| 6658 | S0 | 18 31.9 +22 50 19° +12° | | (14.2) | 14.73<br>14.42<br>14.13 | 1.15<br>1.25<br>1.09 | 0.4<br>1.1<br>1.3 |
| 6661 | S0 | 18 32.5 +22 52 19° +12° | | - | 14.23<br>13.11<br>(13.19) | 1.15<br>1.11<br>1.07 | 0.4<br>2.3<br>2.4 |
| 6674 | SBb | 18 36.5 +25 20 22° +13° | | (13.3) | 14.68<br>12.96 | 1.19<br>0.81 | 0.4<br>4.1 |
| 6702 | E2 | 18 45.5 +45 39 42° +19° | | (14) | 14.35<br>13.95 | 1.09<br>1.04 | 0.7<br>1.1 |
| 6703 | S0 | 18 46.2 +45 30 42° +19° | | (13.7) | 13.02 | 0.95 | 1.1 |
| 6710 | Sa | 18 48.6 +26 47 25° +11° | | (14.5) | 14.57<br>14.19 | 1.05<br>1.11 | 1.1<br>1.3 |
| 1302* | Sb | 19 29.0 +35 39 36° + 7° | | (14) | 14.23 | 0.74 | 0.7 |
| 6814 | Sb | 19 39.9 -10 25 357° -17° | | 12.2 | 14.21<br>12.39<br>12.17 | 1.17<br>0.88<br>0.89 | 0.4<br>2.3<br>4.1 |
| 1308* | Em.N | 19 42.3 -14 51 353° -20° | | - | 14.10 | 0.71 | 1.1 |
| Anon a | | 19 55.1 +40 17 43° + 5° | | - | 15.13 | 1.35 | 0.4 |
| Anon b | | 19 55.1 +40 17 43° + 5° | | - | 16.44 | 1.01 | 0.4 |
| 6824 | Sb | 19 42.6 +55 59 56° +15° | | (14) | 13.06 | 0.83 | 1.1 |
| 1317* | SB0 | 20 20.7 + 0 30 12° +21° | | - | 14.70<br>14.68 | 0.74<br>0.92 | 0.3<br>0.7 |
| 6921 | Sa | 20 26.4 +25 33 35° - 8° | | (13.5) | 14.63 | 1.20 | 1.3 |
| 6927 | S0 | 20 30.2 + 9 43 22° -18° | | (15) | 15.56 | 1.04 | 0.7 |
| 6928 | Sa | 20 30.4 + 9 45 22° -18° | | (13.5) | 14.44<br>13.83<br>13.72 | 1.16<br>1.12<br>1.03 | 0.4<br>2.3<br>1.4<br>X2.4 |
| 6930 | Sb | 20 30.6 + 9 41 22° -18° | | (14) | 14.14 | 0.91 | 1.1 |

| NGC | Type | R.A. l | Dec. b | Mpg Harv. | PHOTOELECTRIC Mpg | C.I. | Ap. |
|---|---|---|---|---|---|---|---|
| 6944 | E1 | 20h 35m9 + 6°49' 20° -21° | | (14.5) | 14.81 | 1.18 | 0.7 |
| 6946 | Sc | 20 33.9 +59 58 63° +11° | | 11.1 | 10.34 | 0.79 | 5.7 |
| 6951 | SBb | 20 36.5 +65 56 67° +17° | | 12.4 | 14.74<br>12.88 | 1.22<br>1.11 | 0.3<br>2.3 |
| 6954 | Sa | 20 41.5 + 3 1 18° -24° | | (14) | 14.14 | 0.90 | 1.1 |
| 6962 | Sb | 20 44.7 + 0 8 15° -27° | | (14) | 14.35<br>13.12 | 1.21<br>0.88 | 0.4<br>2.3 |
| 6963 | E0 | 20 44.8 + 0 20 15° -27° | | (15.5) | (15.88)<br>(15.11) | 1.02<br>0.89 | 0.3<br>0.7 |
| 6964 | E4 | 20 44.8 + 0 7 15° -27° | | (14) | 14.20<br>14.35<br>14.06 | 1.09<br>1.13<br>1.05 | 0.4<br>1.1<br>1.3 |
| 7137 | Sc | 21 45.9 +21 56 45° -24° | | 13.1 | 13.21<br>13.00<br>(13.17) | 0.59<br>0.65<br>0.75 | 2.4<br>3.4<br>4.1 |
| Anon | E1 | 20 58.5 +16 7 32° -20° | | (14.5) | 15.34 | 1.16 | 0.7 |
| Anon | Sa | 20 58.8 +15 56 32° -20° | | (15.5) | 16.12 | 0.64 | 0.7 |
| Anon | S0 | 20 59.6 +15 56 32° -20° | | (15.5) | 16.46 | 0.59 | 0.7 |
| 7171 | Sb | 21 58.3 -13 31 12° -49° | | 12.8 | 15.09<br>13.20 | 0.95<br>0.69 | 0.4<br>2.3 |
| 7177 | Sb | 21 58.3 +17 29 44° -30° | | 12.1 | 13.20<br>12.03<br>(12.11) | 1.03<br>0.83<br>(0.89) | 0.4<br>2.3<br>3.4 |
| 7217 | Sb | 22 5.6 +31 7 55° -20° | | 11.6 | 11.87<br>11.09 | 1.00<br>0.97 | 1.1<br>4.1 |
| 7240 | S0 | 22 13.4 +37 2 60° -16° | | (14.5) | 15.71<br>15.49 | 1.18<br>1.15 | 0.3<br>0.4 |
| 7242 | E3 | 22 13.5 +37 3 60° -16° | | (14.5) | 14.67 | 1.06 | 0.7 |
| 7252 | S0 | 22 18.0 -24 56 356° -58° | | 13.0 | 13.23 | 0.76 | 1.1 |
| 7302 | S0 | 22 29.7 -14 23 16° -56° | | 13.1 | 13.91<br>13.13 | 1.00<br>0.85 | 0.4<br>2.3 |
| 7314 | Sc | 22 33.0 -26 18 354° -62° | | 11.9 | 11.66<br>11.63 | 0.65<br>0.69 | 1.8<br>X4.1<br>1.8<br>X5.7 |
| 7317 | E4 | 22 33.6 +33 41 62° -21° | | - | 15.62<br>15.21 | 0.98<br>(0.92) | 0.3<br>0.7 |
| 7318 (a) | E2 | 22 33.7 +33 42 62° -21° | | - | 15.45<br>15.20<br>14.75 | 1.15<br>1.12<br>1.05 | 0.3<br>0.4<br>0.6 |
| 7318 (b) | SBb | 22 33.7 +33 42 62° -21° | | - | 15.40<br>15.01 | 1.20<br>1.07 | 0.3<br>0.7 |
| 7318 (a+b) | - | 22 33.7 +33 42 62° -21° | | - | 13.95<br>13.88 | 1.01<br>0.94 | 1.1<br>1.3 |
| 7319 | SBb | 22 33.8 +33 43 62° -21° | | - | 13.65 | 0.69 | 1.3 |

TABLE 5—*Continued*

| NGC IC* | Type | R.A. l | Dec. b | Mpg Harv. | PHOTOELECTRIC Mpg | C.I. | Ap. |
|---|---|---|---|---|---|---|---|
| 7331 | Sb | $22^h\ 34^m.8$ $62°$ | $+34°10'$ $-21°$ | 11.2 | 13.51<br>12.58<br>10.56 | 1.18<br>1.15<br>0.91 | 0.2<br>0.4<br>4.1<br>X8.6 |
| 7332 | S0 | 22 $35.0$ $56°$ | $+23\ 32$ $-30°$ | 12.6 | 13.08<br>12.07 | 0.93<br>0.87 | 0.3<br>0.9<br>X2.3 |
| 7339 | Sc | 22 $35.4$ $56°$ | $+23\ 31$ $+30°$ | (13.3) | 13.24 | 0.85 | 0.7<br>X2.3 |
| 7343 | E3 | 22 $36.3$ $41°$ | $+33\ 45$ $-47°$ | (14) | 14.42 | 0.91 | 1.3 |
| 7377 | Sap | 22 $45.1$ $4°$ | $-22\ 35$ $-62°$ | 12.7 | 13.92<br>12.32 | 1.13<br>0.81 | 0.3<br>2.3 |
| 7385 | E0 | 22 $47.4$ $51°$ | $+11\ 21$ $-42°$ | (14) | 14.32 | 1.09 | 0.7 |
| 7386 | S0 | 22 $47.6$ $51°$ | $+11\ 26$ $-42°$ | (14) | 14.66 | 1.13 | 0.7 |
| 7392 | Sa | 22 $49.2$ $10°$ | $-20\ 53$ $-63°$ | 12.6 | 12.69 | 0.99 | 2.3 |
| 1460* | S0 | 22 $54.5$ $47°$ | $+4\ 25$ $-49°$ | (15) | 15.22<br>15.13 | 0.61<br>0.87 | 0.7<br>1.1 |
| 7448 | Sc | 22 $57.6$ $56°$ | $+15\ 43$ $-40°$ | 11.8 | 12.11<br>11.99 | 0.39<br>0.41 | 2.3<br>4.1 |
| 7457 | S0 | 22 $56.6$ $65°$ | $+29\ 53$ $-27°$ | 12.3 | 12.78 | 0.95 | 1.1 |
| 7469 | Sa | 23 $0.7$ $52°$ | $+8\ 36$ $-46°$ | 13.0 | 12.84 | 0.61 | 2.3 |
| 7479 | SBc | 23 $2.4$ $55°$ | $+12\ 3$ $-43°$ | 11.9 | 16.86<br>11.72 | 1.13<br>0.63 | 0.3<br>4.1 |
| 7503 | E1 | 23 $8.0$ $54°$ | $+7\ 15$ $-48°$ | - | 15.04<br>14.64 | 1.11<br>1.20 | 1.1<br>1.3 |
| 7507 | E0 | 23 $9.5$ $352°$ | $-28\ 49$ $-70°$ | 12.0 | 11.92<br>11.59 | 0.91<br>0.89 | 1.1<br>2.3 |
| 7537 | Sbc | 23 $12.0$ $52°$ | $+4\ 13$ $-51°$ | (13.3) | 13.86 | 0.55 | 2.3 |
| 7541 | Sc | 23 $12.2$ $52°$ | $+4\ 16$ $-51°$ | 12.8 | 12.58 | 0.73 | 4.1 |
| 7562 | E2 | 23 $13.5$ $54°$ | $+6\ 25$ $-50°$ | -<br>- | 13.88<br>13.42<br>13.34<br>12.87 | 1.19<br>1.11<br>1.19<br>1.14 | 0.4<br>0.6<br>1.3<br>2.4 |
| 7576 | Sa | 23 $14.8$ $43°$ | $-5\ 0$ $-59°$ | (13.0) | 13.91 | 0.81 | 1.1 |
| 7585 | Sap | 23 $15.4$ $44°$ | $-4\ 56$ $-59°$ | 12.8 | 12.94 | 0.95 | 1.1 |
| 7600 | E5 | 23 $16.3$ $40°$ | $-7\ 52$ $-62°$ | 13.1 | 12.90 | 0.94 | 2.4 |
| 7606 | Sc | 23 $16.5$ $39°$ | $-8\ 46$ $-62°$ | 11.9 | 12.06<br>11.76 | 1.00<br>0.73 | 0.4<br>4.1 |
| 7611 | S0 | 23 $17.1$ $57°$ | $+7\ 46$ $-49°$ | (13.5) | 13.93<br>13.65 | 0.96<br>1.01 | 1.1<br>1.3 |
| 7617 | S0 | 23 $17.6$ $59°$ | $+7\ 53$ $-51°$ | (14) | 14.97 | 0.95 | 1.3 |
| 7619 | E3 | $23^h\ 17^m.8$ $57°$ | $+7°55'$ $-49°$ | 12.8 | 13.12<br>12.79<br>12.42<br>12.40 | 1.17<br>1.07<br>1.05<br>1.11 | 1.1<br>1.3<br>2.3<br>3.4 |
| 7623 | E4 | 23 $18.0$ $57°$ | $+8\ 7$ $-49°$ | (14) | 14.36<br>13.91 | 1.06<br>1.09 | 0.4<br>1.3 |
| 7625 | S0p | 23 $18.0$ $63°$ | $+16\ 57$ $-41°$ | 12.9 | 13.15 | 0.69 | 2.3 |
| 7626 | E1 | 23 $18.2$ $57°$ | $+7\ 56$ $-49°$ | 12.8 | 13.06<br>12.97<br>12.68<br>12.66 | 1.08<br>0.95<br>1.07<br>1.09 | 1.1<br>1.3<br>2.3<br>2.4 |
| 7640 | SBc | 23 $19.7$ $73°$ | $+40\ 35$ $-19°$ | 12.5 | 11.85 | 0.61 | 5.7 |
| 7671 | S0 | 23 $24.8$ $62°$ | $+12\ 12$ $-46°$ | - | 14.04 | 0.95 | 0.7 |
| 7678 | Sc | 23 $26.1$ $68°$ | $+22\ 9$ $-37°$ | 12.9 | 15.23<br>12.54 | 0.87<br>0.63 | 0.3<br>2.3 |
| 7679 | S0 | 23 $26.2$ $56°$ | $+3\ 15$ $-54°$ | 13.1 | 13.23 | 0.47 | 1.1 |
| 7682 | SBa | 23 $26.5$ $56°$ | $+3\ 15$ $-54°$ | (14) | 14.45<br>14.00 | 0.97<br>1.05 | 1.1<br>2.3 |
| 7716 | Sb | 23 $33.9$ $56°$ | $0\ 1$ $-58°$ | 13.0 | 14.17<br>12.92 | 0.56<br>0.69 | 0.4<br>2.3 |
| 7723 | SBb | 23 $36.4$ $40°$ | $-13\ 14$ $-69°$ | 12.1 | 14.23<br>12.04<br>11.97 | 0.71<br>0.59<br>0.66 | 0.4<br>2.3<br>4.1 |
| 7727 | Sa | 23 $37.3$ $41°$ | $-12\ 34$ $-69°$ | 12.0 | 13.22<br>11.92<br>11.66 | 0.67<br>0.87<br>0.85 | 0.4<br>2.3<br>4.1 |
| 7741 | SBb | 23 $41.4$ $73°$ | $+25\ 48$ $-34°$ | 12.6 | 14.61<br>12.47 | 0.47<br>0.59 | 0.4<br>1.6<br>X3.4 |
| 7742 | Sb | 23 $41.8$ $67°$ | $+10\ 29$ $-49°$ | 12.7 | 12.40<br>12.29 | 0.67<br>0.69 | 1.1<br>2.3 |
| 7743 | SBa | 23 $41.8$ $67°$ | $+9\ 39$ $-50°$ | 12.8 | 12.49 | 1.04 | 2.3 |
| 7769 | Sc | 23 $48.5$ $74°$ | $+19\ 52$ $-40°$ | 12.9 | 15.24<br>12.88 | 0.93<br>0.52 | 0.4<br>1.1 |
| 7770 | SBb | 23 $48.9$ $74°$ | $+19\ 49$ $-40°$ | - | 14.52 | 1.51 | 0.7 |
| 7771 | Sb | 23 $48.9$ $74°$ | $+19\ 50$ $-40°$ | - | 13.15 | 0.85 | 0.7<br>X2.3 |
| 7785 | E5 | 23 $52.8$ $68°$ | $+5\ 38$ $-55°$ | 12.9 | 13.27 | 1.11 | 1.3 |
| Lundmark Nallotte | Irr | 23 $59.4$ $48°$ | $-15\ 44$ $-74°$ | (11.7) | 11.93<br>11.48 | 0.29<br>0.17 | 5.1<br>8.6 |
| 7814 | Sa | 0 $0.7$ $76°$ | $+15\ 51$ $-45°$ | 12.4 | 14.08<br>11.76 | 1.03<br>1.02 | 0.4<br>4.1 |

## TABLE 5a

### Magnitude and Color Indices of Extragalactic Nebulae Determined Photoelectrically

| NGC IC* | Type | R.A. l | Dec. b | Mpg Harv. | PHOTOELECTRIC Mpg | C.I. | Ap. |
|---|---|---|---|---|---|---|---|
| 23 | S | $0^h07^m18^s$ 82° | +25°39' -36° | - | 12.85 | 0.79 | 2.4 |
| Haufen C1A.No.1 | E1 | 1 06 27 116° | -15 40 -77° | - | 16.34 | 1.20 | 0.4 |
| " No.2 | So | 1 06 27 116° | -15 40 -77° | - | 17.02 | 1.09 | 0.4 |
| " No.3+ 3a | E1, E2 | 1 06 27 116° | -15 40 -77° | - | 15.03 | 1.29 | 0.6 |
| " No.4 | So | 1 06 27 116° | -15 40 -77° | - | 15.95 | 0.79 | 0.4 |
| 628 | Sc | 1 34 00 108° | +15 32 -45° | 11.2 | 10.47 | 0.68 | 5.1 |
| 779 | Sb | 1 57 12 132° | - 6 12 -62° | 11.8 | 11.90 | 0.87 | 1.9 X5.1 |
| 925 | Sc | 2 24 18 113° | +33 22 -24° | 12.6 | 11.54 | 0.52 | 5.1 |
| 1087 | Sc | 2 43 54 142° | - 0 42 -51° | 11.2 | 11.55 | 0.58 | 3.4 |
| 1079 | SBa | 2 41 36 189° | -29 13 -63° | 12.6 | 12.51 | 0.99 | 2.4 |
| Comp.to 1097 | E5 | 2 44 18 193° | -30 29 -63° | - | 14.21 | 1.00 | 0.6 |
| 1272 | So | 3 15 43 118° | +41 16 -12° | - | 14.52 | 1.27 | 0.6 |
| 1282 | E3 | 3 16 35 118° | +41 8 -12° | - | 14.69 | 1.25 | 0.6 |
| 1293 | E3 | 3 17 57 118° | +41 10 -12° | - | 14.80 | 1.11 | 0.6 |
| 1294 | E | 3 18 00 118° | +41 8 -12° | - | 14.77 | 1.19 | 0.6 |
| 2713 | SBb | 8 55 00 194° | + 3 11 +31° | - 12.7 | 14.03 12.90 | 1.13 1.01 | 0.4 2.1 X5.1 |
| 3115 | E7 | 10 02 48 216° | - 7 28 +38° | 9.8 | 10.38 | 1.01 | 1.6 X5.1 |
| 3338 | Sbc | 10 39 30 199° | +14 0 +58° | 12.2 | 13.68 | 0.95 | 0.6 |
| 3512 | Sc | 11 01 18 172° | +28 18 +68° | 12.8 | 13.00 | 0.59 | 2.4 |
| U.Mj 1 No.7 | E3 | 11 45 28 108° | +56 2 +60° | - | 15.98 | 1.07 | 0.6 |
| U.Mj 1 No.24 | E3 | 11 44 40 106° | +56 0.5 +60° | - | 16.00 | 1.11 | 0.6 |
| U.Mj 1 No.25 | So | $11^h44^m41^s$ 106° | +55°57'6 +60° | — | 16.87 | 1.11 | 0.6 |
| 4237 | Sb | 12 14 42 241° | +15 36 +76° | 12.6 | 12.61 12.58 | 0.92 0.83 | 2.4 5.1 |
| 4262 | SB0 | 12 17 00 244° | +15 9 +76° | 12.6 | 12.88 12.52 | 1.11 1.10 | 0.6 2.4 |
| 4379 | SB0 | 12 22 48 248° | +15 53 +77° | 13.0 | 12.79 | 1.03 | 1.3 |
| 4419 | SBa | 12 24 24 250° | +15 19 +77° | 12.1 | 12.90 12.08 | 1.10 1.07 | 0.6 3.4 |
| 4440 | SBab | 12 25 18 254° | +12 30 +74° | 13.1 | 13.38 (12.87) | 1.03 (1.08) | 0.6 2.4 |
| 4451 | Sb | 12 26 02 257° | + 9 31 +71° | 13.4 | 13.41 | 0.79 | 1.3 |
| 4452 | Sa | 12 26 12 255° | +12 2 +74° | 13.2 | 12.98 | 1.19 | 3.4 |
| 4491 | SBa | 12 28 22 258° | +11 45 +74° | 13.5 | 13.53 | 0.94 | 2.4 |
| 4528 | So | 12 31 31 260° | +11 35 +74° | 13.2 | 12.98 | 1.06 | 1.3 |
| 4564 | E7 | 12 34 0 262° | +11 43 +74° | 12.1 | 12.69 12.06 | 1.09 1.05 | 0.6 2.4 |
| 4578 | So | 12 35 0 264° | + 9 50 +72° | 12.4 | 13.23 12.42 | 1.04 1.07 | 0.6 3.4 |
| Virgo2 No.1 | E1 | 12 37 40 265° | +18 50.5 +81° | - | 16.15 16.08 | 1.18 1.21 | 0.4 0.6 |
| Virgo2 No.2 | E1 | 12 37 49 265° | +18 47.4 +81° | - | 15.67 | 0.59 | 0.6 |
| Virgo2 No.3 | E3 | 12 37 54 265° | +18 48.3 +81° | - | 16.60 | 1.28 | 0.6 |
| Virgo2 No.4 | So | 12 37 58 265° | +18 51.6 +81° | - | 15.31 | 1.31 | 1.3 |
| Virgo2 No.5 | Eo | 12 39 30 265° | +18 52.3 +81° | - | 16.77 | 1.17 | 0.6 |
| Virgo2 No.6 | E1 | 12 39 32 265° | +18 52.7 +81° | - | 16.25 | 0.93 | 0.4 |
| 4789 | E | 12 51 54 351° | +27 21 +88° | (14) | 13.20 | 1.15 | 3.4 |
| 4793 | Sb | 12 52 12 30° | +29 13 +87° | - | 13.90 12.26 | 0.72 0.61 | 0.6 5.1 |
| 4798 | E2 | 12 52 24 0° | +27 42 +88° | - | 14.31 | 1.14 | 2.4 |

TABLE 5a—*Continued*

| NGC IC* | Type | R.A. l | Dec. b | Mpg Harv. | PHOTOELECTRIC Mpg | C.I. | Ap. | NGC IC* | Type | R.A. l | Dec. b | Mpg Harv. | PHOTOELECTRIC Mpg | C.I. | Ap. |
|---|---|---|---|---|---|---|---|---|---|---|---|---|---|---|---|
| 4827 | E | $12^h54^m48^s$ 355° | +27°27' +87° | - | 13.95 | 0.98 | 3.4 | CorBor No. 2 | E1 | $15^h20^m10^s$ 10° | +27°54' +55° | - | 16.71 | 1.15 | 0.6 |
| 4841 D.Neb | $E_1$,Eo | 12 55 12 21° | +28 45 +87° | - | 13.65 | 1.11 | 3.4 | CorBor No.3 | E1 | 15 20 10 10° | +27 54 +55° | - | 16.42 | 0.91 | 0.6 |
| 4874 | So | 12 57 12 10° | +28 14 +87° | - | 13.83 | 1.15 | 1.3 | CorBor No. 4 | E2 | 15 20 10 10° | +27 54 +55° | - | 16.84 | 1.13 | 0.4 |
| 4012* | Eo | 12 57 48 10° | +28 19 +87° | - | 16.21 | 1.25 | 1.3 | Zwicky Dwarf | Irr | 21 43 54 | -21 28 | - | 12.63 | 0.93 | 3.4 |
| 4921 | Sa | 12 59 18 7° | +28 9 +86° | - | 13.64 | 1.05 | 3.4 | Anon | So | 23 6 54° | 38.2 +7 14.5 -48° | - | 16.01 | 1.31 | 0.6 |
| 4931 | E4 | 13 00 36 4° | +28 18 +86° | - | 14.60 | 1.11 | 2.4 | Anon | Eo | 23 7 54° | 27.2 +7 4.3 -58° | - | 16.46 | 1.11 | 0.6 |
| 4957 | E2 | 13 02 48 2° | +27 50 +85° | - | 14.19 | 1.13 | 2.4 | Anon | Eo | 23 7 54° | 48.6 +7 5.8 -48° | - | 16.05 | 1.13 | 0.6 |
| 4961 | Irr | 13 03 36 5° | +28 0 +85° | - | 13.84 | 0.32 | 3.4 | 7499 | So | 23 7 54° | 51.4 +7 18.5 -48° | - | 15.18 | 1.14 | 0.6 |
| 5363 | Irr | 13 53 36 310° | + 5 29 +62° | 11.0 | 12.69<br>11.35 | 1.13<br>1.05 | 0.6<br>2.4 | 7501 | E3 | 23 7 54° | 59.4 +7 19.1 -48° | - | 15.37 | 1.25 | 0.6 |
| 5426 | So | 14 00 48 302° | - 5 49 +51° | 12.8 | 14.25<br>13.10 | 0.68<br>0.64 | 0.6<br>1.3 | Anon | Eo | 23 8 54° | 28.5 +7 23.4 -48° | - | 16.33 | 1.18 | 0.6 |
| 5427 | Sa | 14 00 48 302° | - 5 47 +52° | 12.0 | 14.39<br>11.91 | 0.81<br>0.56 | 0.6<br>2.4 | Anon | Eo | 23 9 54° | 6.2 +7 28.0 -48° | - | 15.80 | 1.23 | 0.6 |
| 5474 | Sc | 14 03 12 65° | +53 54 +60° | 11.7 | 12.56 | 0.61 | 2.4 | 7611 | So | 23 17 56° | 6 +7 46 -49° | - | 14.19 | 0.95 | 0.4 |
| 5533 | Sb | 14 14 06 28° | +35 35 +69° | 12.8 | 12.82 | 0.91 | 3.4 | 7619 | E3 | 23 17 56° | 48 +7 55 -49° | - | 13.64 | 1.10 | 0.4 |
| 5548 | Sa | 14 15 42 359° | +25 22 +69° | 12.8 | 12.92 | 0.51 | 2.4 | 7626 | E1 | 23 18 56° | 02 +7 56 -49° | - | 13.68<br>12.35 | 1.08<br>1.07 | 0.4<br>3.4 |
| 5557 | E1 | 14 16 24 30° | +36 43 +68° | 12.5 | 12.33 | 0.99 | 2.4 | 7741 | SBb | 23 41 71° | 24 +25 48 -34° | - | 12.60 | 0.59 | 1.3<br>X2.3 |
| 5585 | Sc | 14 18 00 65° | +56 57 +57° | 12.0 | 11.54 | 0.41 | 5.1 | 7793 | Sc | 23 55 230° | 18 -32 51 -79° | 9.7 | 11.37 | 0.59 | 2.4 |
| 5740 | Sb | 14 41 54 323° | + 1 54 +52° | 12.8 | 12.48 | 0.53 | 5.1 | | | | | | | | |
| 5850 | SBb | 15 04 36 329° | + 1 44 +46° | 12.9 | 11.93 | 0.86 | 4.3<br>X5.1 | | | | | | | | |
| CorBor No. 1 | E1 | 15 20 10 10° | +27 54 +55° | (16.5) | 16.52 | 1.29 | 0.6 | | | | | | | | |

### THE NEBULAR MEASURES

In Tables 5 and 5*a* are listed the measures of 558 individual nebulae and 3 double systems. The first column gives the *New General Catalogue* number unless starred, which latter indicates the *Index Catalogue* number. Types estimated by Hubble appear in the second column and 1950 positions in the third and fourth columns. Below the right ascension is the galactic longitude, and below the declination is the galactic latitude. The fifth column ("Harv.") shows the photographic magnitude given by Shapley and Ames (1932). Magnitudes in parentheses are estimates by Hubble from Mount Wilson plates. In the next two columns are the equivalent photographic magnitude and color index determined photoelectrically as described here. The last column shows the aperture in minutes of arc used in the measures.

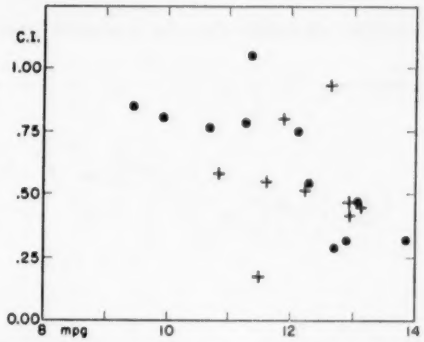


FIG. 2.—Plot of color index against magnitude for the irregular nebulae. The crosses indicate dwarf systems, and the dots indicate giants.

Where there appear more than one measure of magnitude in the sixth column, the value should decrease with increasing aperture. Sometimes the decrease is very small, as in NGC 16, indicating that the smaller aperture has already transmitted nearly the whole nebula. When this is the case, accidental errors may make the magnitude determined with the larger aperture the larger, as in NGC 578, where the magnitude so affected appears in parentheses. Where three or more measures of color index have been made, they may increase or decrease with aperture. If one is noted which does not follow the trend of the others, it also appears in parentheses, as in NGC 821.

### COLOR INDEX AS A FUNCTION OF MAGNITUDE

The magnitudes, $m_{pg}$, and color indices in Tables 5 and 5*a* corresponding to the largest apertures in every case have been segregated according to the classes Irr., E, S, and SB. For each class the color index has been plotted against $m_{pg}$. Only 20 examples of the irregular type were observed. All these lie between magnitudes 9.4 and 13.9. The giant systems are shown by dots and the dwarfs by crosses in Figure 2. No difference in the trend is observable. Holmberg (1950) and Stebbins and Whitford (1952*b*) considered these nebulae to be restricted in color index, and their measures were verified here. However, the evidence of clustering of measures at two color levels in the plot of color index against $m_{pg}$ shown in Figure 2 has disappeared with the added material; and, while the plot seems to show that the fainter nebulae are the bluer, we still have insufficient material to justify so important a conclusion.

A total of 150 nebulae of type E have been measured between magnitudes 9 and 18.

The plot of color index against $m_{pg}$ is shown in Figure 3. Here it is noted that the color index definitely rises from about 0.87 at $m_{pg}$ 10 to 1.12 at $m_{pg}$ 16. This increase is expressed in magnitudes by

$$\text{C.I.} = 0.04\ (m_{pg} - 9\ \text{mag.}) + 0.84\ \text{mag.}, \tag{7}$$

which amounts to saying that the color index increases 0.04 mag. per magnitude decrease in light.

The color indices of the S-type nebulae are plotted in Figure 4. Here the plot is much more scattered than in Figure 3, but a definite inclination of the mean line is observable, which rises from about color index 0.58 at $m_{pg}$ 10 to 1.08 at $m_{pg}$ 16. This leads to the relation

$$\text{C.I.} = 0.08\ (m_{pg} - 9\ \text{mag.}) + 0.50\ \text{mag.} \tag{8}$$

This means that the E nebulae are redder than the S nebulae brighter than $m_{pg}$ 17. The

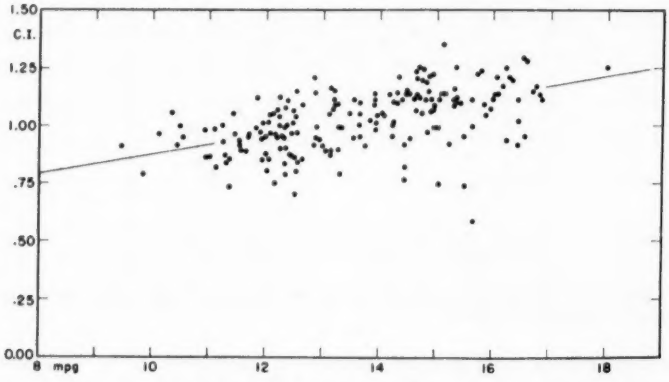


FIG. 3.—Plot of color index against magnitude for the E-type nebulae. The mean line corresponds to the formula C.I. = 0.04 ($m_{pg}$ − 9 mag.) + 0.84 mag.

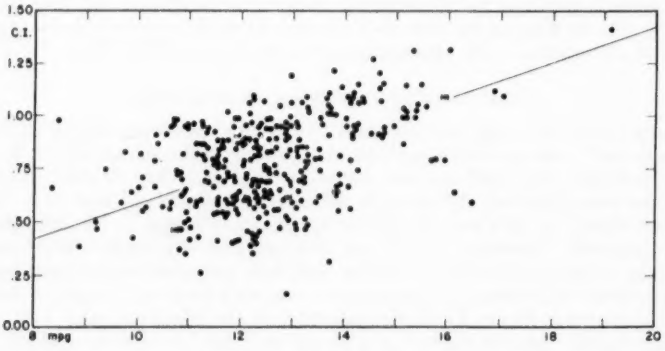


FIG. 4.—Plot of color index against magnitude for the S-type nebulae. The mean line corresponds to the formula C.I. = 0.08 ($m_{pg}$ − 9 mag.) + 0.50 mag.

scattering of the plot of color index against magnitude is too great in the type SB (Fig. 5) to indicate any definite trend.

### COLOR OF THE NUCLEUS

The color index of the nucleus was measured in 127 nebulae in which the nucleus was a well-marked feature. This was measured with aperture of 0.″7 or 0.″3 at the 60-inch and 0.″6, 0.″4, or 0.″2 at the 100-inch telescope. Usually the nucleus was not more than 0.″1, but it was difficult to adjust the telescope drive to hold the image central within a smaller aperture than 0.″3.

The color indices range from 0.31 to 1.51 mag. Of the 127 nuclei, 58, or 46 per cent,

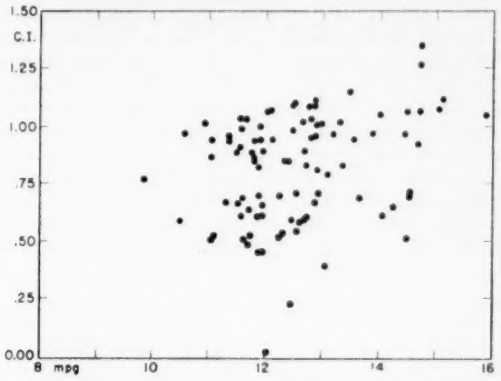


FIG. 5.—Plot of color index against magnitude for the SB-type nebulae

TABLE 6

FREQUENCY OF REDDENING TOWARD CENTERS OF NEBULAE

| Type | Per Cent Redder | Per Cent Neutral | No. Nebulae |
|---|---|---|---|
| S | 75 | 5 | 130 |
| SB | 67 | 0 | 38 |
| E | 52 | 16 | 58 |

exceed color index 1 mag. Generally they are redder than the whole nebula. Only 15, or 12 per cent, are bluer.

If we examine those nebulae in Tables 5 and 5*a* in which two or more apertures have been used, we find Table 6, which shows the predominance of reddening toward the center in the S, SB, and E types, also the per cent neutral.

The writer is indebted to Mrs. Pettit for the extensive reductions of all the nebular measures in this paper, thanks to her computing skill developed in the early days of photographic parallax and proper motion. He is also indebted to the night assistants, R. Bennewitz, E. Hancock, A. Olmstead, and A. Ratzlaff, for galvanometer manipulation; to E. P. Hubble, M. L. Humason, and N. U. Mayall, who prepared the observing program with plates, prints, and sketches for identification; to M. L. Humason and A. R. Sandage for reading the manuscript; and to A. E. Whitford for circuits from which the photometer was built.

## REFERENCES

Adams, W. S., Joy, A. H., Humason, M. L., and Brayton, A. M. 1935, *Ap. J.*, **81**, 187; *Mt. W. Contr.*, No. 511
Bigay, J.-H. 1951, "Photométrie photographique des nébuleuses extragalactiques," *Ann. d'ap.*, **14**, 21.
Holmberg, E. 1950, *Lund Medd.*, Ser. II, No. 128.
Humason, M. L. 1932, *Ap. J.*, **76**, 224; *Mt. W. Contr.*, No. 458.
Pettit, E., and Nicholson, S. B. 1928, *Ap. J.*, **68**, 279; *Mt. W. Contr.*, No. 369.
Seares, F. H. 1922, "Report of Commission 25," *Trans. I.A.U.*, **1**, 69.
Seares, F. H., Kapteyn, J. C., and Van Rhijn, P. J. 1930, *Mount Wilson Catalogue of Photographic Magnitudes in Selected Areas 1–139* ("Carnegie Institution of Washington Publications," No. 402).
Shapley, H., and Ames, A. 1932, *Ann. Harvard College Obs.*, Vol. **88**, No. 2.
Stebbins, J., and Whitford, A. E. 1952*a*, *Ap. J.*, **115**, 284; *Mt. W. and Palomar Reprint*, No. 64.
———. 1952*b*, *Ap. J.*, **115**, 242; *Mt. W. and Palomar Reprint*, No. 64.
Russell, H. N., Dugan, R. S., and Stewart, J. Q. 1927, *Astronomy* (New York: Ginn & Co.), p. 734.
Wilson, R. E. 1953, *General Catalogue of Stellar Radial Velocities* ("Carnegie Institution of Washington Publications," No. 601).

# PHOTOELECTRIC MEASUREMENTS OF EXTRAGALACTIC NEBULAE*

C. J. VAN HOUTEN, J. H. OORT, AND W. A. HILTNER
Yerkes, McDonald, and Leiden Observatories

*Received June 8, 1954*

ABSTRACT

This article gives the intensity distribution in nine extragalactic nebulae, measured photoelectrically with the 82-inch reflector of the McDonald Observatory. The observations were made with three different color filters and with diaphragms of various sizes.

Studies of the distribution of brightness in extragalactic nebulae have been made by Hubble (1930), Redman and Shirley (1938), Evans (1951, 1952), and De Vaucouleurs (1948), while measurements of individual objects have been made by Carpenter, Reynolds, Seyfert, Lindblad, Holmberg, Oort, and others. They were all done photographically; and, as the difference in brightness between the nucleus and the outer parts of an extragalactic nebula is considerable, a very precise determination of the gradation curves of the photographic plates was necessary. To avoid this difficulty, it was planned to measure photoelectrically the intensity distribution in a number of extragalactic nebulae. The measurements were made in January, 1948, with the 82-inch reflector of the McDonald Observatory by Hiltner, Oort, and Heyduck and are discussed in this paper. We are indebted to Dr. Strömgren for assistance with part of the measurements.

TABLE 1

A COMPARISON OF THE VARIOUS SENSITIVITY RATIOS

| log | From Tracings | Mean Error | From Star | Laboratory 1948 | Laboratory 1951 | Hiltner Mean |
|---|---|---|---|---|---|---|
| L1/L2 | 0.658 | ±0.012 | 0.662 | 0.669 | 0.640 | 0.657 |
| L2/L3 | .759 | ± .029 | .753 | .751 | .740 | .749 |
| L3/L4 | 0.754 | ±0.027 | 0.779 | 0.715 | 0.712 | 0.735 |

The observations were made with a refrigerated RCA 1P21 photomultiplier; the output of the cell was fed into a d.c. amplifier, and the amplified current was recorded by a Brown recorder. A diaphragm could be moved by a synchronous motor in the Cassegrain focal plane of the reflector in any arbitrary direction; three velocities were possible, 11".3, 28".1, and 70".4 per minute. Tracings were made along the major or minor axes of the nebulae, and in some cases also outside the nucleus. Most tracings were made with a color filter behind the diaphragm; the filters used were Schott Ug-2, and Corning 5850 and 3385, with effective wave lengths about 3650, 3900, and 5300 A. They will be denoted as F1, F2, and F3.

The sensitivity of the amplifier could be varied by the use of different grid leaks; the leaks used were 0.8, 4, 20, and 100 megohms, respectively. They will be denoted as L1, L2, L3, and L4. In order to insure reasonable accuracy for nucleus as well as outer parts of the nebulae, the grid leaks were changed repeatedly during a tracing. It was thought that a determination of the relative sensitivities of the grid leaks after the conclusion of the observations would be sufficient, but during the reductions it appeared that these ratios were not constant. The explanation must probably be found in changing temperature and humidity during the observations. The sensitivity ratios of the grid leaks were determined by Hiltner at the telescope from measures of stars and also in the laboratory (in 1948 and 1951). In addition, it appeared possible to determine these ratios from some tracings, where the light-variation was very regular, by extrapolating the measures on

* *Contributions from the McDonald Observatory, University of Texas*, No. 247.

both sides of the switch-over point. A comparison between the various results is shown in Table 1.

When the sensitivity ratio was determined from the tracing itself, this value was used in the reduction of the tracing. This was possible only with tracings of the nebulae NGC 221, 3115, and 4594. In all other cases the mean values were used, as found from the tracings. The values determined from stellar observations and in the laboratory were not used. This introduces some uncertainties, as these values are systematically lower. However, the differences are smaller than the deviations of the ratios from their mean value.

The sensitivity could be changed by a variation of grid leaks and also by the feedback loop. Various diaphragms were used: four were circular, with diameters of about 20″, 9″, 3.″6, and 1.″7, while rectangular diaphragms could be formed from a number of strips, five in the long and four in the short directions. No absolute determination of the areas was made, but they were measured on a moonlit sky, so that the relative transmission could be ascertained. These values are collected in Table 2 in the columns marked "Size"; the length indicated as 100″ and the width indicated as 8″ were arbitrarily assumed to be accurately 100″ and 8″. The dark deflection was determined before and after each tracing; measures of the night sky were made only once a night for each nebula. However, the sky appeared not to be constant during this time. This caused serious errors in the reduction of the faintest parts of the nebulae; sometimes the resulting intensities of the outermost parts were negative. In these cases the sky intensity was altered until the marginal values corresponded to those of other tracings. The effects of wrong sky cor-

TABLE 2

AREAS OF DIAPHRAGMS

| Length | | Width | | Area of Circular Diaphragm | |
|---|---|---|---|---|---|
| Called | Size | Called | Size | Called | Size |
| 100″ | 100″ | 8″ | 8″ | 8″ | 300(″)² |
| 50 | 51.2 | 4 | 3.31 | 4 | 64.2 |
| 25 | 27.5 | 2 | 1.54 | 2 | 10.2 |
| 12 | 13.1 | 1 | 1.06 | 1 | 2.2 |
| 6 | 6.38 | | | | |

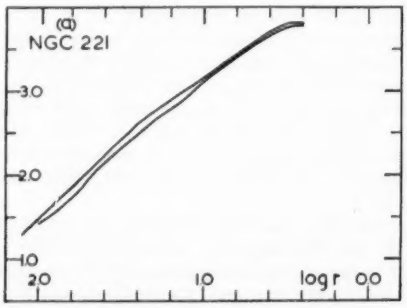


FIG. 1.—Position angles (p.a.) are counted from north through east, as usual. In each graph the abscissa, $x$ or $y$, increases in the direction p.a. $+180°$. The letter $x$ is used for the co-ordinates parallel to the major axis, while $y$ indicates the co-ordinates parallel to the minor axis. Both are expressed in seconds of arc. Ordinates are logarithms of intensities. In several cases where the nebulae appeared to be symmetrical, the two halves of the intensity-curves were averaged. Log $I$ was then plotted against log $x$ or log $y$. When a rectangular diaphragm was used, it was always placed in such a way that the short axis was in the direction in which the tracing was done. *a*, NGC 221, major and minor axes, no filter. P.a. 90° and 0°, respectively; D4″.

rections are clearly seen in some of the tracings of Figures 1–5. The sky has only a very small influence on the brightness of the inner parts of the nebulae; accordingly, these values are much more reliable than the parts of low intensity.

The unit of intensity used in this article is a hundredth part of the vertical scale of the recorder paper when the instrument was used with the largest grid leak and the greatest

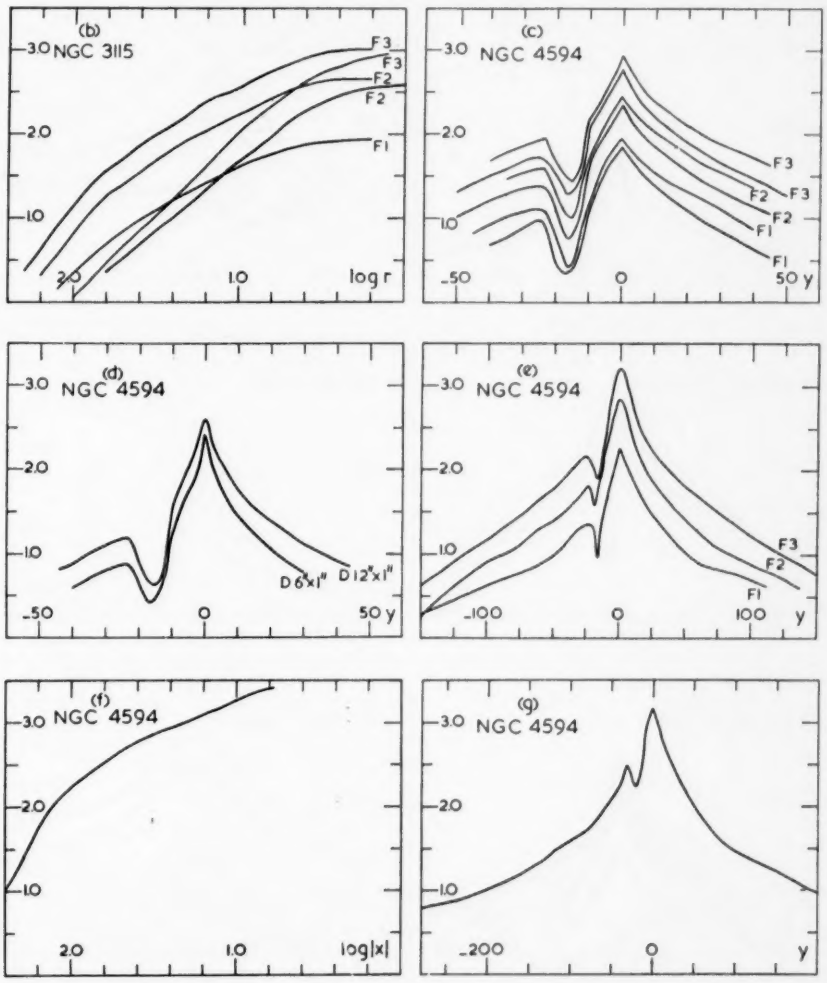


FIG. 2.—*b*, NGC 3115, major and minor axes. P.a. 44°.1 with D4″ and 314°.1 with D12″ × 4″, respectively. *c*, NGC 4594, minor axis. P.a. 0°; D50″ × 1″ and D100″ × 1″. *d*, NGC 4594, minor axis. P.a. 0°; F3. End of measures in twilight. *e*, NGC 4594, minor axis. P.a. 0°; D50″ × 4″. Sky corrections uncertain. *f*, NGC 4594, major axis. P.a. 90°; F3. D8″. *g*, NGC 4594, minor axis. P.a. 0°; F3. D100″ × 4″. Measures of dark current incomplete. Otherwise the arrangement is the same as in Fig. 1.

sensitivity. This unit is, of course, intrinsically variable, but no better method was possible, because the sensitivity variations were not known. On some nights comparison stars near the nebulae were measured and compared with stars in the polar cap. Since, however, no extinction measures were made, an accurate determination of the zero point of brightness was not possible. All measures were corrected for extinction by means

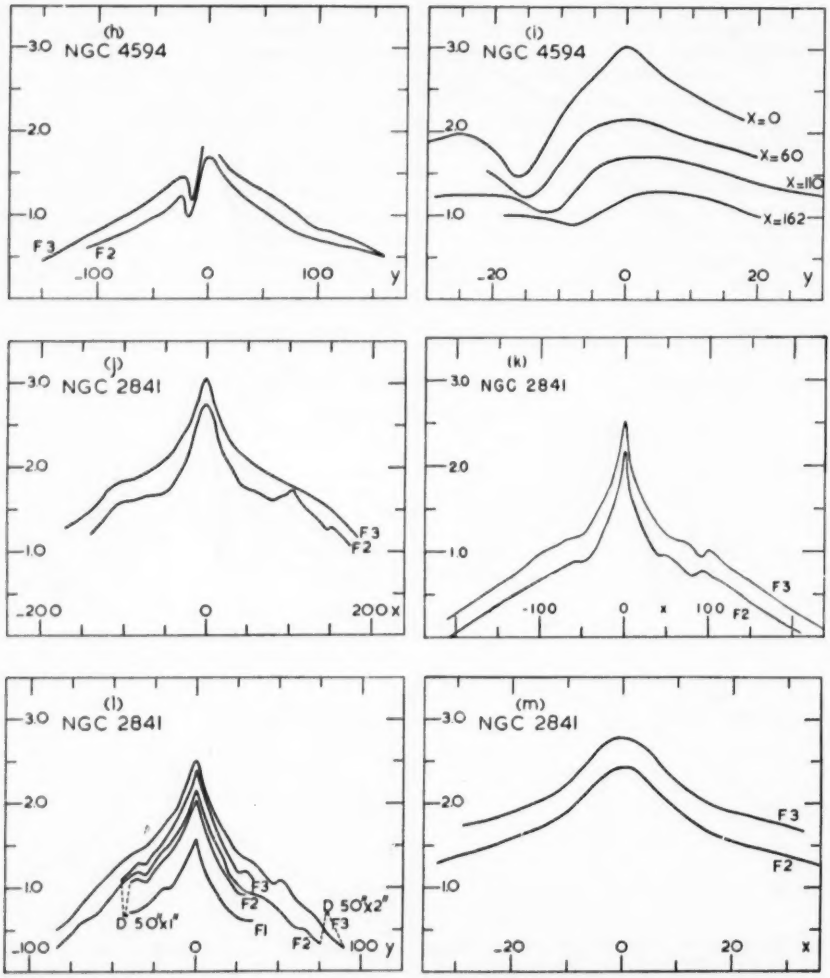


FIG. 3.—*h*, NGC 4594. Tracings across shadow band 1′ outside nucleus. P.a. 0°; D50″ × 2″. *i*, NGC 4594. Tracings across shadow band. P.a. 0°; F3; D25″ × 4″. Measures of dark current incomplete. *j*, NGC 2841, major axis. P.a. 330°; D8″. *k*, NGC 2841, major axis. P.a. 330°; D12″ × 4″. *l*, NGC 2841, minor axis. P.a. 60°; D50″ × 2″ and D50″ × 1″. *m*, NGC 2841, major axis. P.a. 330°; D4″. Otherwise the arrangement is the same as in Fig. 1.

of the well-known formula

$$m = m_0 + K \sec z .$$

The values used for $K$ were 0.55, 0.24, and 0.15 mag. for filters F1, F2, and F3, respectively. All magnitudes were reduced to the zenith, i.e., they were diminished by $K$ (sec

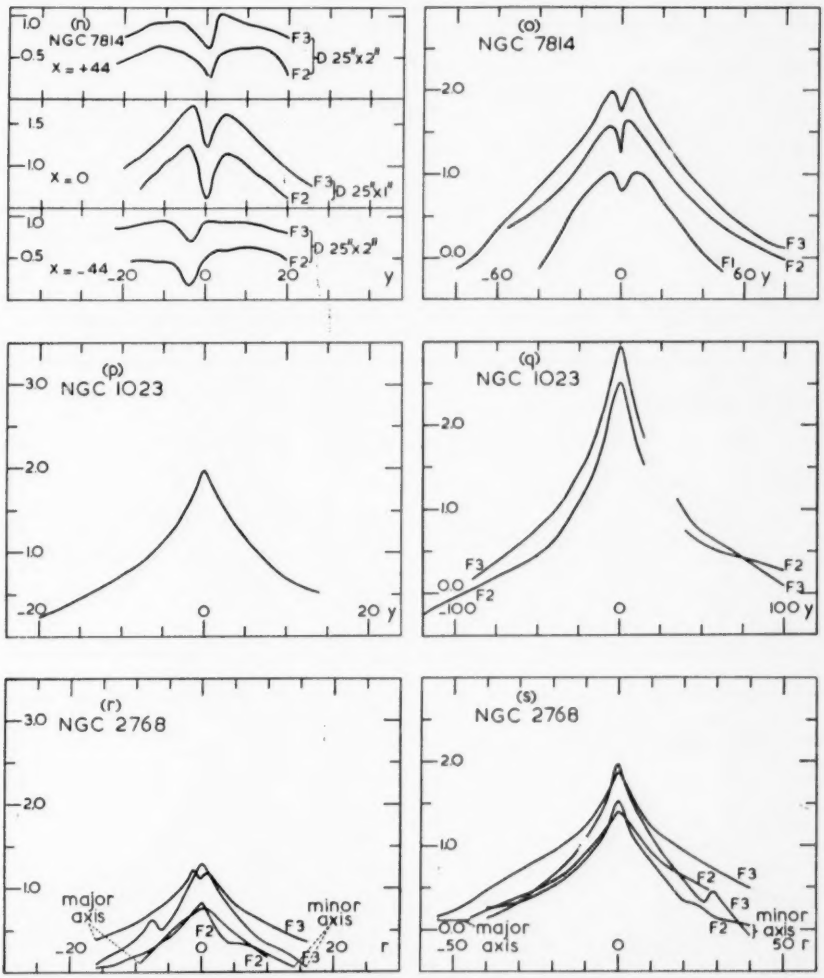


FIG. 4.—*n*, NGC 7814. Tracings across shadow band. P.a. 45″. For $x = 0$, D25″ × 1″; for $x = \pm 44$″, D25″ × 2″. *o*, NGC 7814, minor axis. P.a. 45°; D25″ × 4″. *p*, NGC 1023, minor axis. P.a. 353°.5; F3; D1″. *q*, NGC 1023, minor axis. P.a. 353°.5; D4″. Corrections for sky and dark current uncertain. Star in slit at about $y = 25$″. *r*, NGC 2768, major and minor axes. P.a. 10° and 100°, respectively; D1″. *s*, NGC 2768, major and minor axes. P.a. 10° and 100°, respectively; D2″. Otherwise the arrangement is the same as in Fig. 1.

$z - 1$). The brightness found in this way is not independent of the value of the absorption coefficient, but only a mean extinction coefficient was used; in this way the corrections, and also the errors in the corrections, are smaller.

The results of the color measures of the standard stars and the nuclei of the nebulae are shown in Table 3. It follows from Table 3 that the colors of the nuclei of the nebulae

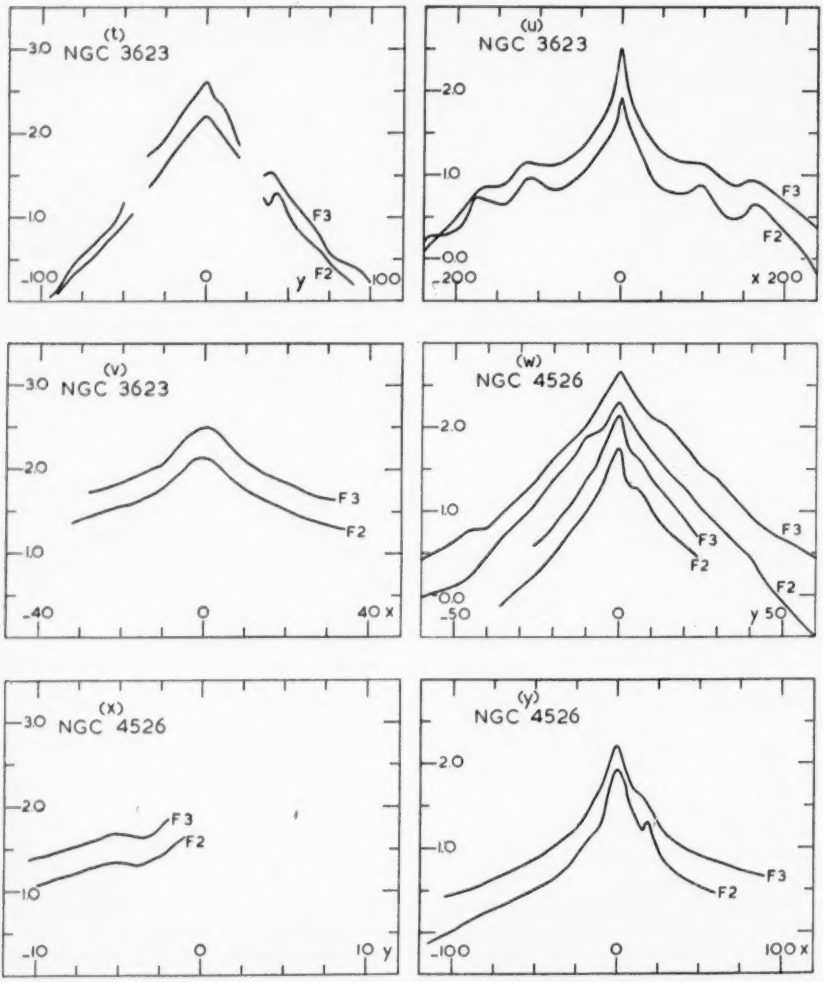


FIG. 5.—*t*, NGC 3623, minor axis. P.a. 82°; D50″ × 4″. Star in slit at approximately $y = -40''$ and $y = +25''$. *u*, NGC 3623, major axis. P.a. 352°; D12″ × 4″. *v*, NGC 3623, major axis. P.a. 352°; D4″. *w*, NGC 4526, minor axis. P.a. 20°.5; D25″ × 4″ and D12″ × 1″. *x*, NGC 4526, minor axis. Tracings across shadow band. P.a. 20°.5; D12″ × 1″. *y*, NGC 4526, major axis. P.a. 290°.5; D6″ × 4″. Otherwise the arrangement is the same as in Fig. 1.

NGC 2841

NGC 3623

NGC 4526

NGC 4594

NGC 7814

FIG. 6.—Extragalactic nebulae

correspond to a spectral type of about G6 or G7. The brightness of the standard stars as measured with F2 was compared with the HD photographic magnitudes. The result is shown in Table 4. The last two columns of Table 4 show systematic differences, depending on the spectral type. This makes possible the reduction of the F2 intensities to the photographic system. The result is that a star of spectral type G6 and photographic magnitude 10.0 would have a brightness of log $I = 4.00$ with F3 in our system.

The nebulae studied in this investigation are NGC 221, 3115, 4594, 2841, 1023, 2768, 3623, 4526, and 7814. Types, magnitudes, and dimensions are given in Table 5. These

TABLE 3

COLORS OF STANDARD STARS AND NUCLEI OF NEBULAE

| Standard Star | Sp. | log F3/F2 | log F1/F2 | NGC | log F3/F2 | log F1/F2 |
|---|---|---|---|---|---|---|
| BD+80°80 | K5 | +0.87 | −0.83 | 221 | +0.36 | −0.53 |
| BD+80°121 | K0 | + .55 | − .60 | 3115 | + .40 | − .52 |
| BD+80°159 | F0 | + .02 | − .37 | 4594 | + .43 | −0.53 |
| BD+80°233 | F8 | + .11 | − .41 | 2841 | + .39 | ..... |
| BD+80°338 | K0 | +0.60 | −0.68 | 1023 | + .47 | ..... |
| | | | | 2768 | + .45 | ..... |
| | | | | 3623 | +0.41 | ..... |

TABLE 4

GENERAL INFORMATION ABOUT THE STANDARD STARS

| Standard Star | Sp. | log $I$ (F3) | $\Delta m$, HD | $\Delta m$, F2 |
|---|---|---|---|---|
| BD+80°80 | K5 | 4.51 | 0.00 | 0.00 |
| BD+80°121 | K0 | 4.63 | −1.09 | −1.12 |
| BD+80°159 | F0 | 4.28 | −1.04 | −1.56 |
| BD+80°233 | F8 | 4.24 | −0.82 | −1.24 |
| BD+80°338 | K0 | 4.64 | −0.93 | −1.03 |

TABLE 5

GENERAL INFORMATION ABOUT THE NEBULAE

| Nebula | Type | $m_{pg}$ | Diameters |
|---|---|---|---|
| NGC 221 | E | 9.5 | 2'.6 × 2'.1 |
| NGC 1023 | SBa | 11.2 | 6.9 × 1.3 |
| NGC 2768 | E5 | 12.0 | 1.5 × 0.7 |
| NGC 2841 | Sb | 10.5 | 6.0 × 1.6 |
| NGC 3115 | E7 | 9.8 | 4.0 × 1.0 |
| NGC 3623 | Sb | 10.5 | 8.0 × 2.0 |
| NGC 4526 | Sa | 10.7 | 6.0 × 1.2 |
| NGC 4594 | Sa | 8.1 | 7.0 × 1.5 |
| NGC 7814 | Sa | 12.4 | 3.0 × 0.8 |

were taken from Shapley and Miss Ames's catalogue (1932). Reproductions of NGC 2841, 3623, 4526, 4594, and 7814 are shown in Figure 6. The other nebulae have an entirely smooth structure.

The results of the tracings are collected in Table 6 and in Figures 1–5. As a rule the logarithm of the brightness ($I$) was tabulated as a function of the distance to the nucleus. Co-ordinates parallel to the major axis are denoted by $x$, those parallel to the minor axis by $y$. Both are expressed in seconds of arc and are counted from the nucleus as zero point. Only when the intensity distribution in the tracing was very regular, was log $I$ compared with log $x$ or log $y$. This has been done with NGC 221, NGC 3115, and the major axis of NGC 4594. Here, symmetry relative to the nucleus was assumed, and, accordingly, the two sides were combined in one figure (Figs. 1, *b*, and 2, *f*). The values in Table 6 were obtained by drawing a smooth line through the tracing on the recorder

TABLE 6

Photometry of Extragalactic Nebulae

| (a) | NGC 221*, No Filter | | | |
|---|---|---|---|---|
| | Minor Axis | | Major Axis | |
| log r | D 2" | D 4" | D 2" | D 4" |
| - ∞ | 3.50 | | 3.40 | 3.83 |
| 0.4 | 2.89 | 3.81 | 3.14 | 3.79 |
| 0.5 | 2.77 | 3.79 | 3.05 | 3.75 |
| 0.6 | 2.64 | 3.70 | 2.89 | 3.66 |
| 0.7 | 2.50 | 3.57 | 2.74 | 3.54 |
| 0.8 | 2.35 | 3.43 | 2.58 | 3.41 |
| 0.9 | 2.20 | 3.29 | 2.42 | 3.26 |
| 1.0 | 2.06 | 3.16 | 2.30 | 3.11 |
| 1.1 | 1.88 | 3.03 | 2.15 | 2.93 |
| 1.2 | 1.71 | 2.89 | 1.99 | 2.78 |
| 1.3 | 1.51 | 2.75 | 1.85 | 2.64 |
| 1.4 | 1.33 | 2.59 | 1.71 | 2.48 |
| 1.5 | | 2.42 | 1.54 | 2.32 |
| 1.6 | | 2.23 | 1.34 | 2.15 |
| 1.7 | | 2.04 | 1.11 | 1.94 |
| 1.8 | | 1.85 | 0.86 | 1.73 |
| 1.9 | | 1.68 | | 1.55 |
| 2.0 | | 1.48 | | 1.42 |
| 2.1 | | 1.29 | | |

*Since the sensitivity of the amplifier was not recorded the zero point is not known.

| (b) | NGC 3115 | | | | |
|---|---|---|---|---|---|
| | Minor Axis D 12"x4" | | Major Axis ; D 4" | | |
| log r | F2 | F3 | F1 | F2 | F3 |
| - ∞ | 2.62 | 3.02 | 1.98 | 2.71 | 3.05 |
| 0.2 | 2.55 | 2.92 | 1.94 | 2.67 | 3.02 |
| 0.4 | 2.45 | 2.80 | 1.92 | 2.65 | 2.99 |
| 0.5 | 2.37 | 2.73 | 1.90 | 2.63 | 2.96 |
| 0.6 | 2.27 | 2.62 | 1.87 | 2.59 | 2.91 |
| 0.7 | 2.13 | 2.48 | 1.83 | 2.52 | 2.84 |
| 0.8 | 1.97 | 2.34 | 1.76 | 2.43 | 2.75 |
| 0.9 | 1.82 | 2.19 | 1.69 | 2.33 | 2.66 |
| 1.0 | 1.68 | 2.02 | 1.62 | 2.23 | 2.55 |
| 1.1 | 1.53 | 1.83 | 1.53 | 2.14 | 2.47 |
| 1.2 | 1.35 | 1.63 | 1.43 | 2.04 | 2.39 |
| 1.3 | 1.17 | 1.42 | 1.32 | 1.94 | 2.25 |
| 1.4 | 1.01 | 1.22 | 1.22 | 1.82 | 2.11 |
| 1.5 | 0.86 | 1.04 | 1.10 | 1.69 | 1.99 |
| 1.6 | 0.69 | 0.87 | 0.97 | 1.54 | 1.86 |
| 1.7 | 0.53 | 0.68 | 0.84 | 1.40 | 1.71 |
| 1.8 | 0.36 | 0.48 | 0.70 | 1.26 | 1.57 |
| 1.9 | | 0.26 | 0.54 | 1.08 | 1.39 |
| 2.0 | | 0.05 | 0.35 | 0.82 | 1.15 |
| 2.1 | | | 0.16 | 0.56 | 0.91 |
| 2.2 | | | | 0.32 | 0.64 |
| 2.3 | | | | | 0.37 |

| (c) and (d) | NGC 4594, Minor Axis | | | | | | | |
|---|---|---|---|---|---|---|---|---|
| | D 100"x1" | | | D 50"x1" | | | D 12"x1" | D 6"x1" |
| y | F1 | F2 | F3 | F1 | F2 | F3 | F3 | F3 |
| -50 | | | | | 1.01 | 1.31 | | |
| -45 | 0.82 | | | | 1.11 | 1.41 | | |
| -40 | 0.92 | | 1.68 | 0.68 | 1.21 | 1.50 | 0.89 | 0.58 |
| -35 | 1.02 | 1.46 | 1.78 | 0.76 | 1.27 | 1.57 | 1.01 | 0.71 |
| -30 | 1.06 | 1.53 | 1.85 | 0.88 | 1.35 | 1.68 | 1.10 | 0.80 |
| -25 | 1.10 | 1.58 | 1.92 | 0.98 | 1.37 | 1.72 | 1.17 | 0.87 |
| -23 | 1.08 | 1.58 | 1.94 | 0.90 | 1.36 | 1.70 | 1.19 | 0.87 |
| -20 | 0.78 | 1.30 | 1.67 | 0.47 | 1.09 | 1.52 | 0.90 | 0.66 |
| -17 | 0.45 | 1.06 | 1.51 | 0.35 | 0.78 | 1.29 | 0.67 | 0.42 |
| -16 | 0.42 | 1.03 | 1.47 | 0.37 | 0.76 | 1.29 | 0.65 | 0.45 |
| -15 | 0.46 | 1.01 | 1.44 | 0.39 | 0.80 | 1.31 | 0.63 | 0.46 |
| -13 | 0.77 | 1.23 | 1.57 | 0.55 | 1.00 | 1.44 | 0.72 | 0.63 |
| -10 | 1.17 | 1.75 | 2.16 | 1.13 | 1.65 | 2.08 | 1.52 | 1.23 |
| - 5 | 1.69 | 2.14 | 2.52 | 1.58 | 2.06 | 2.42 | 2.03 | 1.73 |
| 0 | 1.95 | 2.45 | 2.93 | 1.85 | 2.35 | 2.79 | 2.60 | 2.42 |
| 5 | 1.70 | 2.20 | 2.60 | 1.59 | 2.04 | 2.42 | 2.07 | 1.77 |
| 10 | 1.54 | 2.02 | 2.39 | 1.39 | 1.86 | 2.20 | 1.76 | 1.45 |
| 15 | 1.41 | 1.89 | 2.24 | 1.23 | 1.70 | 2.04 | 1.54 | 1.25 |
| 20 | 1.31 | 1.76 | 2.10 | 1.09 | 1.56 | 1.90 | 1.39 | 1.07 |
| 25 | 1.21 | 1.63 | 1.99 | 0.95 | 1.42 | 1.77 | 1.25 | 0.90 |
| 30 | 1.11 | 1.55 | 1.88 | 0.84 | 1.32 | 1.65 | 1.12 | 0.77 |
| 35 | 0.97 | 1.45 | 1.80 | 0.74 | 1.23 | 1.56 | 1.02 | |
| 40 | 0.87 | 1.36 | 1.72 | 0.63 | 1.13 | 1.47 | 0.92 | |
| 45 | | | 1.63 | 0.54 | 1.05 | 1.38 | | |
| 50 | | | | | | 1.27 | | |

TABLE 6 (Cont'd)

(e) NGC 4594, Minor Axis

D 50"x4"

| y | F1 | F2 | F3 | y | F1 | F2 | F3 |
|---|---|---|---|---|---|---|---|
| -170 | 0.19 | | | 10 | 1.89 | 2.38 | 2.73 |
| -160 | 0.23 | 0.09 | | 20 | 1.61 | 2.02 | 2.39 |
| -150 | 0.28 | 0.25 | | 30 | 1.36 | 1.76 | 2.12 |
| -140 | 0.35 | 0.40 | 0.73 | 40 | 1.20 | 1.58 | 1.96 |
| -130 | 0.42 | 0.54 | 0.85 | 50 | 1.05 | 1.43 | 1.80 |
| -120 | 0.49 | 0.68 | 0.97 | 60 | 0.92 | 1.31 | 1.68 |
| -110 | 0.56 | 0.80 | 1.06 | 70 | 0.84 | 1.14 | 1.55 |
| -100 | 0.62 | 0.91 | 1.17 | 80 | 0.80 | 1.05 | 1.45 |
| - 90 | 0.69 | 0.97 | 1.28 | 90 | 0.75 | 0.98 | 1.33 |
| - 80 | 0.75 | 1.05 | 1.39 | 100 | 0.70 | 0.89 | 1.23 |
| - 70 | 0.80 | 1.19 | 1.52 | 110 | 0.64 | 0.83 | 1.14 |
| - 60 | 0.89 | 1.30 | 1.65 | 120 | 0.59 | 0.75 | 1.04 |
| - 50 | 0.99 | 1.39 | 1.76 | 130 | | 0.67 | 0.95 |
| - 40 | 1.15 | 1.52 | 1.93 | 140 | | 0.59 | 0.85 |
| - 30 | 1.31 | 1.68 | 2.10 | 150 | | 0.52 | 0.76 |
| - 20 | 1.33 | 1.66 | 2.05 | 160 | | 0.47 | 0.66 |
| - 15 | 1.16 | 1.87 | 1.93 | 170 | | 0.41 | 0.56 |
| - 10 | 1.62 | 2.29 | 2.37 | 180 | | | 0.46 |
| 0 | 2.24 | 2.85 | 3.21 | | | | |

(f) NGC 4594 Major Axis

D 8"

| Log \|x\| | F3 |
|---|---|
| - ∞ | 3.47 |
| 0.8 | 3.41 |
| 0.9 | 3.35 |
| 1.0 | 3.28 |
| 1.1 | 3.19 |
| 1.2 | 3.11 |
| 1.3 | 3.03 |
| 1.4 | 2.93 |
| 1.5 | 2.86 |
| 1.6 | 2.77 |
| 1.7 | 2.67 |
| 1.8 | 2.53 |
| 1.9 | 2.38 |
| 2.0 | 2.23 |
| 2.1 | 2.04 |
| 2.2 | 1.75 |
| 2.3 | 1.34 |
| 2.4 | 1.02 |
| 2.5 | 0.69 |

(g) NGC 4594, Minor Axis

D 100"x4"

| y | F3 | y | F3 |
|---|---|---|---|
| -290 | 0.76 | -40 | 2.23 |
| -280 | 0.79 | -30 | 2.49 |
| -270 | 0.81 | -20 | 2.24 |
| -260 | 0.83 | -10 | 2.79 |
| -250 | 0.85 | 0 | 3.17 |
| -240 | 0.87 | 10 | 2.87 |
| -230 | 0.91 | 20 | 2.59 |
| -220 | 0.94 | 30 | 2.37 |
| -210 | 0.98 | 40 | 2.20 |
| -200 | 1.01 | 50 | 2.02 |
| -190 | 1.05 | 60 | 1.85 |
| -180 | 1.09 | 70 | 1.72 |
| -170 | 1.14 | 80 | 1.63 |
| -160 | 1.19 | 90 | 1.55 |
| -150 | 1.25 | 100 | 1.47 |
| -140 | 1.31 | 110 | 1.41 |
| -130 | 1.39 | 120 | 1.36 |
| -120 | 1.46 | 130 | 1.31 |
| -110 | 1.52 | 140 | 1.27 |
| -100 | 1.59 | 150 | 1.23 |
| - 90 | 1.65 | 160 | 1.18 |
| - 80 | 1.72 | 170 | 1.12 |
| - 70 | 1.81 | 180 | 1.06 |
| - 60 | 1.95 | 190 | 1.01 |
| - 50 | 2.09 | 200 | 0.98 |

(h) NGC 4594, Tracings Across Shadow Band

D 50"x2" |x|=60

| y | F2 | F3 | y | F2 | F3 |
|---|---|---|---|---|---|
| -150 | | 0.45 | - 5 | 1.62 | 1.81 |
| -140 | | 0.51 | 0 | 1.69 | |
| -130 | | 0.59 | 10 | 1.54 | 1.72 |
| -120 | | 0.66 | 20 | 1.38 | 1.55 |
| -110 | 0.60 | 0.74 | 30 | 1.24 | 1.45 |
| -100 | 0.64 | 0.81 | 40 | 1.14 | 1.36 |
| - 90 | 0.70 | 0.88 | 50 | 1.05 | 1.29 |
| - 80 | 0.76 | 0.96 | 60 | 0.96 | 1.21 |
| - 70 | 0.82 | 1.03 | 70 | 0.87 | 1.13 |
| - 60 | 0.90 | 1.11 | 80 | 0.80 | 1.04 |
| - 50 | 0.97 | 1.20 | 90 | 0.74 | 0.91 |
| - 40 | 1.04 | 1.31 | 100 | 0.70 | 0.83 |
| - 30 | 1.16 | 1.41 | 110 | 0.67 | 0.81 |
| - 25 | 1.23 | 1.45 | 120 | 0.63 | 0.76 |
| - 20 | 1.02 | 1.45 | 130 | 0.61 | 0.72 |
| - 18 | 0.99 | 1.37 | 140 | 0.57 | 0.66 |
| - 15 | 1.07 | 1.19 | 150 | 0.54 | 0.59 |
| - 10 | 1.39 | 1.43 | 160 | 0.51 | 0.52 |

TABLE 6 (Cont'd)

| (1) | NGC 4594; Tracings Across Shadow Band | | | | | | | | |
|---|---|---|---|---|---|---|---|---|---|
| | D 25"x14" ; F3 | | | | | | | | |
| y | x=0 | \|x\|=60 | \|x\|=110 | \|x\|=162 | y | x=0 | \|x\|=60 | \|x\|=110 | \|x\|=162 |
| -32 | 1.84 | | | | 0 | 3.02 | 2.15 | 1.69 | 1.22 |
| -30 | 1.88 | | | | 2 | 2.94 | 2.14 | 1.71 | 1.27 |
| -28 | 1.92 | | 1.23 | | 4 | 2.78 | 2.11 | 1.72 | 1.30 |
| -26 | 1.96 | | 1.24 | | 6 | 2.66 | 2.04 | 1.70 | 1.30 |
| -24 | 1.95 | | 1.24 | | 8 | 2.56 | 2.00 | 1.67 | 1.29 |
| -22 | 1.90 | | 1.24 | | 10 | 2.46 | 1.94 | 1.64 | 1.26 |
| -20 | 1.79 | 1.47 | 1.24 | | 12 | 2.36 | 1.90 | 1.60 | 1.23 |
| -18 | 1.56 | 1.35 | 1.22 | 1.00 | 14 | 2.29 | 1.85 | 1.55 | 1.18 |
| -16 | 1.48 | 1.24 | 1.17 | 0.99 | 16 | 2.22 | 1.81 | 1.50 | 1.12 |
| -14 | 1.59 | 1.24 | 1.08 | 0.98 | 18 | 2.15 | 1.76 | 1.44 | 1.06 |
| -12 | 1.90 | 1.39 | 1.05 | 0.96 | 20 | | 1.71 | 1.39 | 1.01 |
| -10 | 2.18 | 1.64 | 1.10 | 0.93 | 22 | | | 1.36 | |
| - 8 | 2.40 | 1.84 | 1.27 | 0.91 | 24 | | | 1.33 | |
| - 6 | 2.57 | 1.99 | 1.45 | 0.95 | 26 | | | 1.30 | |
| - 4 | 2.75 | 2.08 | 1.60 | 1.03 | 28 | | | 1.27 | |
| - 2 | 2.92 | 2.12 | 1.65 | 1.13 | 30 | | | 1.25 | |

| (j) and (k) | NGC 2841; Major Axis | | | | | | | | |
|---|---|---|---|---|---|---|---|---|---|
| | D 8" | | D 12"x14" | | | D 8" | | D 12"x14" | |
| x | F2 | F3 | F2 | F3 | x | F2 | F3 | F2 | F3 |
| -230 | | | -0.17 | | 10 | 2.52 | 2.75 | 1.59 | 1.90 |
| -220 | | | -0.08 | | 20 | 2.20 | 2.47 | 1.32 | 1.66 |
| -210 | | | -0.01 | 0.22 | 30 | 2.00 | 2.30 | 1.11 | 1.46 |
| -200 | | | 0.06 | 0.29 | 40 | 1.83 | 2.19 | 0.96 | 1.31 |
| -190 | | | 0.13 | 0.35 | 50 | 1.76 | 2.10 | 0.95 | 1.21 |
| -180 | | | 0.20 | 0.42 | 60 | 1.72 | 2.03 | 0.89 | 1.14 |
| -170 | | 1.28 | 0.26 | 0.50 | 70 | 1.67 | 1.95 | 0.79 | 1.12 |
| -160 | | 1.33 | 0.32 | 0.55 | 80 | 1.61 | 1.89 | 0.72 | 1.06 |
| -150 | | 1.40 | 0.39 | 0.61 | 90 | 1.66 | 1.84 | 0.77 | 0.94 |
| -140 | 1.20 | 1.47 | 0.44 | 0.65 | 100 | 1.70 | 1.80 | 0.75 | 1.02 |
| -130 | 1.29 | 1.56 | 0.50 | 0.72 | 110 | 1.65 | 1.76 | 0.68 | 0.96 |
| -120 | 1.42 | 1.71 | 0.56 | 0.82 | 120 | 1.52 | 1.70 | 0.62 | 0.87 |
| -110 | 1.53 | 1.78 | 0.62 | 0.91 | 130 | 1.45 | 1.63 | 0.56 | 0.77 |
| -100 | 1.59 | 1.83 | 0.68 | 0.99 | 140 | 1.33 | 1.57 | 0.50 | 0.70 |
| - 90 | 1.60 | 1.85 | 0.73 | 1.01 | 150 | 1.29 | 1.51 | 0.41 | 0.64 |
| - 80 | 1.63 | 1.88 | 0.77 | 1.07 | 160 | 1.22 | 1.41 | 0.34 | 0.59 |
| - 70 | 1.67 | 1.94 | 0.84 | 1.12 | 170 | 1.13 | 1.32 | 0.28 | 0.52 |
| - 60 | 1.67 | 2.00 | 0.88 | 1.14 | 180 | | 1.21 | 0.22 | 0.45 |
| - 50 | 1.70 | 2.09 | 0.88 | 1.20 | 190 | | | 0.16 | 0.38 |
| - 40 | 1.80 | 2.19 | 0.95 | 1.34 | 200 | | | 0.10 | 0.31 |
| - 30 | 1.97 | 2.36 | 1.12 | 1.52 | 210 | | | 0.05 | 0.26 |
| - 20 | 2.21 | 2.52 | 1.35 | 1.70 | 220 | | | 0.00 | 0.19 |
| - 10 | 2.55 | 2.79 | 1.63 | 2.02 | 230 | | | | 0.14 |
| 0 | 2.75 | 3.05 | 2.17 | 2.52 | 240 | | | | 0.07 |

TABLE 6 (Cont'd)

(l) NGC 2841; Minor Axis

D 50"x1"

| y | F1 | F2 | F3 |
|---|---|---|---|
| -45 | | | 1.10 |
| -40 | 0.71 | 1.07 | 1.18 |
| -35 | 0.72 | 1.10 | 1.29 |
| -30 | 0.78 | 1.07 | 1.28 |
| -25 | 0.88 | 1.21 | 1.43 |
| -20 | 0.99 | 1.33 | 1.54 |
| -15 | 0.99 | 1.42 | 1.70 |
| -10 | 1.17 | 1.58 | 1.87 |
| - 5 | 1.36 | 1.82 | 2.08 |
| 0 | 1.57 | 2.04 | 2.39 |
| 5 | 1.22 | 1.70 | 2.10 |
| 10 | 1.03 | 1.46 | 1.81 |
| 15 | 0.86 | 1.24 | 1.59 |
| 20 | 0.73 | 1.09 | 1.37 |
| 25 | 0.65 | 0.94 | 1.19 |
| 30 | 0.61 | 0.92 | 1.20 |
| 35 | 0.61 | | 1.09 |

(l) NGC 2841; Minor Axis

D 50"x2"

| y | F2 | F3 |
|---|---|---|
| -80 | 0.36 | 0.56 |
| -70 | 0.57 | 0.78 |
| -60 | 0.68 | 1.00 |
| -50 | 0.92 | 1.22 |
| -40 | 1.14 | 1.39 |
| -30 | 1.16 | 1.49 |
| -20 | 1.44 | 1.73 |
| -10 | 1.68 | 2.02 |
| 0 | 2.16 | 2.51 |
| 10 | 1.60 | 1.94 |
| 20 | 1.16 | 1.57 |
| 30 | 0.95 | 1.34 |
| 40 | 0.89 | 1.18 |
| 50 | 0.73 | 1.08 |
| 60 | 0.52 | 0.86 |
| 70 | 0.42 | 0.70 |
| 80 | | 0.44 |
| 90 | | 0.28 |

(m) NGC 2841;Major Axis

D 4"

| Log \|x\| | F2 | F3 |
|---|---|---|
| - ∞ | | 2.78 |
| 0.4 | 2.37 | 2.75 |
| 0.5 | 2.35 | 2.73 |
| 0.6 | 2.31 | 2.69 |
| 0.7 | 2.23 | 2.60 |
| 0.8 | 2.15 | 2.50 |
| 0.9 | 2.04 | 2.38 |
| 1.0 | 1.92 | 2.26 |
| 1.1 | 1.80 | 2.12 |
| 1.2 | 1.69 | 2.02 |
| 1.3 | 1.58 | 1.92 |
| 1.4 | 1.47 | 1.82 |
| 1.5 | 1.35 | 1.71 |
| 1.6 | 1.23 | |

(n) NGC 7814; Minor Axis

D 25"x1"

| y | F2 | F3 |
|---|---|---|
| -20 | | 0.97 |
| -18 | | 1.04 |
| -16 | 0.72 | 1.10 |
| -14 | 0.85 | 1.19 |
| -12 | 0.92 | 1.28 |
| -10 | 1.04 | 1.38 |
| - 8 | 1.09 | 1.50 |
| - 6 | 1.19 | 1.60 |
| - 4 | 1.24 | 1.70 |
| - 3 | 1.15 | 1.72 |
| - 2 | 1.02 | 1.63 |
| - 1 | 0.77 | 1.48 |
| 0 | 0.62 | 1.25 |
| 0.5 | 0.63 | 1.23 |
| 1 | 0.69 | 1.29 |
| 2 | 0.92 | 1.44 |
| 3 | 1.03 | 1.53 |
| 4 | 1.11 | 1.59 |
| 5 | 1.15 | 1.62 |
| 6 | 1.14 | 1.60 |
| 8 | 1.10 | 1.53 |
| 10 | 1.01 | 1.43 |
| 12 | 0.92 | 1.33 |
| 14 | 0.86 | 1.24 |
| 16 | 0.78 | 1.14 |
| 18 | 0.70 | 1.05 |
| 20 | 0.62 | 0.96 |
| 22 | | 0.89 |
| 24 | | 0.82 |
| 26 | | 0.77 |

(n) NGC 7814; Tracings Across Shadow Band

D 25"x2"

| | x=+14 | | x=-14 | |
|---|---|---|---|---|
| y | F2 | F3 | F2 | F3 |
| -22 | 0.43 | | | 0.86 |
| -20 | 0.47 | 0.75 | | 0.86 |
| -18 | 0.51 | 0.79 | 0.47 | 0.88 |
| -16 | 0.55 | 0.84 | 0.48 | 0.90 |
| -14 | 0.60 | 0.89 | 0.48 | 0.92 |
| -12 | 0.63 | 0.91 | 0.47 | 0.94 |
| -10 | 0.62 | 0.92 | 0.47 | 0.95 |
| - 8 | 0.60 | 0.93 | 0.44 | 0.92 |
| - 7 | 0.58 | 0.93 | 0.39 | 0.87 |
| - 6 | 0.57 | 0.92 | 0.32 | 0.82 |
| - 5 | 0.54 | 0.89 | 0.23 | 0.76 |
| - 4 | 0.51 | 0.84 | 0.18 | 0.71 |
| - 3 | 0.48 | 0.79 | 0.21 | 0.72 |
| - 2 | 0.44 | 0.74 | 0.32 | 0.80 |
| - 1 | 0.39 | 0.69 | 0.44 | 0.91 |
| 0 | 0.31 | 0.63 | 0.50 | 0.93 |
| 1 | 0.26 | 0.63 | 0.54 | 0.94 |
| 2 | 0.43 | 0.85 | 0.57 | 0.94 |
| 3 | 0.53 | 1.01 | 0.59 | 0.93 |
| 4 | 0.55 | 1.02 | 0.59 | 0.93 |
| 6 | 0.59 | 0.98 | 0.60 | 0.93 |
| 8 | 0.61 | 0.95 | 0.62 | 0.93 |
| 10 | 0.61 | 0.91 | 0.63 | 0.92 |
| 12 | 0.62 | 0.88 | 0.62 | 0.91 |
| 14 | 0.61 | 0.86 | 0.61 | 0.89 |
| 16 | 0.56 | 0.83 | 0.59 | 0.85 |
| 18 | 0.45 | 0.79 | 0.55 | 0.83 |
| 20 | 0.29 | 0.73 | 0.48 | 0.80 |

TABLE 6 (Cont'd)

(o) NGC 7814; Minor Axis

D 25"x14"

| y | F1 | F2 | F3 |
|---|---|---|---|
| -110 | | | -0.40 |
| -100 | | | -0.32 |
| - 90 | | | -0.23 |
| - 80 | | 0.08 | -0.13 |
| - 70 | | 0.19 | 0.03 |
| - 60 | | 0.30 | 0.32 |
| - 50 | | 0.43 | 0.58 |
| - 40 | -0.14 | 0.60 | 0.84 |
| - 30 | 0.27 | 0.81 | 1.10 |
| - 20 | 0.69 | 1.11 | 1.38 |
| - 10 | 0.95 | 1.46 | 1.77 |
| - 5 | 1.02 | 1.56 | 1.98 |
| 0 | 0.80 | 1.25 | 1.74 |
| 5 | 1.00 | 1.61 | 2.02 |
| 10 | 1.00 | 1.45 | 1.84 |
| 20 | 0.67 | 1.12 | 1.43 |
| 30 | 0.36 | 0.80 | 1.09 |
| 40 | 0.05 | 0.56 | 0.81 |
| 50 | -0.18 | 0.35 | 0.56 |
| 60 | | 0.21 | 0.36 |
| 70 | | 0.08 | 0.21 |
| 80 | | -0.02 | 0.12 |
| 90 | | | 0.05 |
| 100 | | | -0.01 |
| 110 | | | -0.07 |
| 120 | | | -0.13 |
| 130 | | | -0.20 |
| 140 | | | -0.28 |
| 150 | | | -0.35 |

(p) NGC 1023

D 1"; Minor Axis

| y | F3 |
|---|---|
| -20 | 0.23 |
| -18 | 0.31 |
| -16 | 0.40 |
| -14 | 0.50 |
| -12 | 0.60 |
| -10 | 0.72 |
| - 8 | 0.85 |
| - 6 | 1.02 |
| - 4 | 1.24 |
| - 2 | 1.54 |
| 0 | 1.97 |
| 2 | 1.62 |
| 4 | 1.31 |
| 6 | 1.07 |
| 8 | 0.85 |
| 10 | 0.69 |
| 12 | 0.59 |
| 14 | 0.52 |

(q) NGC 1023

D 4"; Minor Axis

| y | F2 | F3 |
|---|---|---|
| -120 | -0.25 | -0.16 |
| -110 | -0.16 | -0.06 |
| -100 | -0.06 | 0.05 |
| - 90 | 0.03 | 0.16 |
| - 80 | 0.14 | 0.30 |
| - 70 | 0.23 | 0.44 |
| - 60 | 0.33 | 0.60 |
| - 50 | 0.44 | 0.77 |
| - 40 | 0.62 | 0.98 |
| - 30 | 0.92 | 1.25 |
| - 20 | 1.25 | 1.61 |
| - 10 | 1.81 | 2.19 |
| 0 | 2.51 | 2.94 |
| 10 | 1.84 | 2.19 |
| 20 | 1.34 | |
| 30 | | |
| 40 | 0.76 | 0.99 |
| 50 | 0.60 | 0.73 |
| 60 | 0.50 | 0.60 |
| 70 | 0.44 | 0.49 |
| 80 | 0.39 | 0.35 |
| 90 | 0.32 | 0.22 |
| 100 | 0.27 | 0.06 |
| 110 | 0.21 | 0.01 |

(r) NGC 2768

| | D 1", Minor Axis | | D 1", Major Axis | |
|---|---|---|---|---|
| r | F2 | F3 | F2 | F3 |
| -16 | 0.05 | 0.10 | | 0.39 |
| -14 | 0.07 | 0.19 | | 0.45 |
| -12 | 0.13 | 0.27 | | 0.51 |
| -10 | 0.19 | 0.39 | | 0.59 |
| - 8 | 0.25 | 0.59 | 0.21 | 0.69 |
| - 6 | 0.37 | 0.51 | 0.38 | 0.80 |
| - 4 | 0.47 | 0.71 | 0.53 | 0.92 |
| - 2 | 0.66 | 1.04 | 0.66 | 1.11 |
| 0 | 0.82 | 1.29 | 0.76 | 1.13 |
| 2 | 0.56 | 1.04 | 0.68 | 1.10 |
| 4 | 0.35 | 0.81 | 0.54 | 0.89 |
| 6 | 0.34 | 0.62 | 0.40 | 0.75 |
| 8 | 0.30 | 0.45 | 0.30 | 0.67 |
| 10 | 0.21 | 0.34 | 0.19 | 0.58 |
| 12 | 0.13 | 0.27 | | 0.51 |
| 14 | 0.06 | 0.18 | | 0.43 |
| 16 | | 0.06 | | 0.37 |

(s) NGC 2768

| | D 2", Minor Axis | | D 2", Major Axis | |
|---|---|---|---|---|
| r | F2 | F3 | F2 | F3 |
| -55 | | | | 0.16 |
| -50 | | | | 0.22 |
| -45 | | 0.04 | 0.14 | 0.32 |
| -40 | 0.25 | 0.14 | 0.23 | 0.47 |
| -35 | 0.26 | 0.22 | 0.29 | 0.59 |
| -30 | 0.31 | 0.34 | 0.38 | 0.70 |
| -25 | 0.40 | 0.49 | 0.47 | 0.81 |
| -20 | 0.50 | 0.64 | 0.57 | 0.92 |
| -15 | 0.64 | 0.81 | 0.70 | 1.07 |
| -10 | 0.84 | 1.09 | 0.90 | 1.23 |
| - 5 | 1.08 | 1.42 | 1.11 | 1.51 |
| 0 | 1.52 | 1.97 | 1.41 | 1.87 |
| 5 | 1.06 | 1.45 | 1.18 | 1.49 |
| 10 | 0.79 | 1.12 | 0.90 | 1.22 |
| 15 | 0.55 | 0.79 | 0.75 | 1.07 |
| 20 | 0.32 | 0.57 | 0.62 | 0.93 |
| 25 | 0.26 | 0.34 | 0.52 | 0.81 |
| 30 | 0.12 | 0.40 | 0.40 | 0.70 |
| 35 | 0.08 | 0.15 | | 0.59 |
| 40 | 0.04 | -0.08 | | 0.49 |
| 45 | | -0.28 | | |

TABLE 6 (Cont'd)

(t) NGC 3623; Minor Axis

D 50"x4"

| y | F2 | F3 | y | F2 | F3 |
|---|---|---|---|---|---|
| -95 | -0.02 | 0.05 | 5 | 2.09 | 2.41 |
| -90 | 0.09 | 0.15 | 10 | 1.97 | 2.32 |
| -85 | 0.21 | 0.30 | 15 | 1.83 | 2.13 |
| -80 | 0.33 | 0.46 | 20 | 1.71 | 1.85 |
| -75 | 0.41 | 0.55 | 25 | | |
| -70 | 0.50 | 0.64 | 30 | | |
| -65 | 0.59 | 0.74 | 35 | 1.23 | 1.50 |
| -60 | 0.72 | 0.84 | 40 | 1.23 | 1.54 |
| -55 | 0.81 | 0.95 | 45 | 1.24 | 1.41 |
| -50 | 0.92 | 1.18 | 50 | 1.06 | 1.25 |
| -45 | 1.04 | | 55 | 0.87 | 1.14 |
| -40 | | 1.62 | 60 | 0.77 | 1.03 |
| -35 | 1.36 | 1.75 | 65 | 0.67 | 0.90 |
| -30 | 1.48 | 1.82 | 70 | 0.59 | 0.74 |
| -25 | 1.63 | 1.94 | 75 | 0.45 | 0.57 |
| -20 | 1.76 | 2.09 | 80 | 0.35 | 0.49 |
| -15 | 1.89 | 2.24 | 85 | 0.28 | 0.45 |
| -10 | 2.01 | 2.36 | 90 | 0.19 | 0.41 |
| - 5 | 2.11 | 2.49 | 95 | | 0.35 |
| 0 | 2.20 | 2.61 | 100 | | 0.21 |

(u) NGC 3623; Major Axis

D 12"x4"

| x | F2 | F3 | x | F2 | F3 |
|---|---|---|---|---|---|
| -260 | -0.12 | -0.15 | 10 | 1.60 | 1.94 |
| -250 | 0.00 | -0.04 | 20 | 1.36 | 1.70 |
| -240 | 0.20 | 0.07 | 30 | 1.14 | 1.53 |
| -230 | 0.28 | 0.19 | 40 | 0.93 | 1.39 |
| -220 | 0.28 | 0.29 | 50 | 0.84 | 1.27 |
| -210 | 0.30 | 0.39 | 60 | 0.80 | 1.21 |
| -200 | 0.35 | 0.49 | 70 | 0.79 | 1.17 |
| -190 | 0.46 | 0.61 | 80 | 0.80 | 1.16 |
| -180 | 0.72 | 0.75 | 90 | 0.86 | 1.15 |
| -170 | 0.72 | 0.84 | 100 | 0.88 | 1.14 |
| -160 | 0.69 | 0.86 | 110 | 0.74 | 1.09 |
| -150 | 0.65 | 0.88 | 120 | 0.60 | 1.01 |
| -140 | 0.64 | 0.90 | 130 | 0.50 | 0.93 |
| -130 | 0.75 | 1.00 | 140 | 0.47 | 0.89 |
| -120 | 0.91 | 1.12 | 150 | 0.52 | 0.92 |
| -110 | 0.97 | 1.14 | 160 | 0.64 | 0.94 |
| -100 | 0.91 | 1.12 | 170 | 0.64 | 0.92 |
| - 90 | 0.85 | 1.12 | 180 | 0.54 | 0.85 |
| - 80 | 0.83 | 1.14 | 190 | 0.44 | 0.77 |
| - 70 | 0.85 | 1.16 | 200 | 0.33 | 0.69 |
| - 60 | 0.92 | 1.22 | 210 | 0.23 | 0.61 |
| - 50 | 1.00 | 1.30 | 220 | 0.13 | 0.53 |
| - 40 | 1.10 | 1.42 | 230 | -0.01 | 0.45 |
| - 30 | 1.24 | 1.56 | 240 | -0.18 | 0.37 |
| - 20 | 1.37 | 1.72 | 250 | -0.32 | 0.25 |
| - 10 | 1.53 | 1.94 | 260 | -0.43 | 0.08 |
| 0 | 1.92 | 2.51 | 270 | | -0.11 |

(v) NGC 3623; Major Axis

D 4"

| x | F2 | F3 | x | F2 | F3 |
|---|---|---|---|---|---|
| -32 | 1.36 | | 2 | 2.10 | 2.48 |
| -30 | 1.40 | | 4 | 2.02 | 2.41 |
| -28 | 1.43 | 1.72 | 6 | 1.92 | 2.29 |
| -26 | 1.46 | 1.74 | 8 | 1.84 | 2.20 |
| -24 | 1.50 | 1.77 | 10 | 1.76 | 2.10 |
| -22 | 1.53 | 1.80 | 12 | 1.71 | 2.04 |
| -20 | 1.56 | 1.84 | 14 | 1.66 | 1.96 |
| -18 | 1.58 | 1.89 | 16 | 1.61 | 1.93 |
| -16 | 1.62 | 1.93 | 18 | 1.56 | 1.38 |
| -14 | 1.67 | 1.97 | 20 | 1.52 | 1.84 |
| -12 | 1.71 | 2.02 | 22 | 1.48 | 1.80 |
| -10 | 1.77 | 2.06 | 24 | 1.43 | 1.75 |
| - 8 | 1.87 | 2.17 | 26 | 1.40 | 1.71 |
| - 6 | 1.95 | 2.29 | 28 | 1.37 | 1.67 |
| - 4 | 2.07 | 2.40 | 30 | 1.34 | 1.65 |
| - 2 | 2.12 | 2.46 | 32 | 1.31 | 1.64 |
| 0 | 2.13 | 2.50 | 34 | 1.29 | |

(w) NGC 4526; Minor Axis

D 12"x1"

| y | F2 | F3 | y | F2 | F3 |
|---|---|---|---|---|---|
| - 36 | -0.13 | | - 4 | 1.42 | 1.84 |
| - 34 | -0.06 | | - 2 | 1.62 | 2.00 |
| - 32 | 0.01 | | 0 | 1.74 | 2.14 |
| - 30 | 0.08 | | 2 | 1.40 | 1.88 |
| - 28 | 0.15 | | 4 | 1.28 | 1.69 |
| - 26 | 0.21 | 0.59 | 5 | 1.28 | 1.67 |
| - 24 | 0.29 | 0.64 | 6 | 1.27 | 1.63 |
| - 22 | 0.39 | 0.72 | 8 | 1.17 | 1.51 |
| - 20 | 0.47 | 0.81 | 10 | 1.04 | 1.38 |
| - 18 | 0.59 | 0.93 | 12 | 0.91 | 1.29 |
| - 16 | 0.69 | 1.02 | 14 | 0.81 | 1.20 |
| - 14 | 0.80 | 1.12 | 16 | 0.72 | 1.11 |
| - 12 | 0.89 | 1.23 | 18 | 0.66 | 1.00 |
| - 10 | 0.99 | 1.37 | 20 | 0.60 | 0.91 |
| - 8 | 1.12 | 1.47 | 22 | 0.53 | 0.81 |
| - 6 | 1.24 | 1.61 | 24 | 0.46 | 0.70 |

TABLE 6 (Cont'd)

(w) NGC 4526; Minor Axis

D 25"x4"

| y | F2 | F3 | y | F2 | F3 |
|---|---|---|---|---|---|
| -80 | | 0.09 | - 5 | 1.97 | 2.35 |
| -75 | | 0.18 | 0 | 2.29 | 2.66 |
| -70 | | 0.26 | 5 | 1.98 | 2.35 |
| -65 | -0.07 | 0.34 | 10 | 1.70 | 2.11 |
| -60 | -0.02 | 0.44 | 15 | 1.47 | 2.00 |
| -55 | 0.04 | 0.53 | 20 | 1.28 | 1.78 |
| -50 | 0.11 | 0.64 | 25 | 1.04 | 1.53 |
| -45 | 0.23 | 0.78 | 30 | 0.85 | 1.39 |
| -40 | 0.46 | 0.79 | 35 | 0.64 | 1.18 |
| -35 | 0.71 | 0.99 | 40 | 0.45 | 0.96 |
| -30 | 0.90 | 1.18 | 45 | 0.14 | 0.77 |
| -25 | 1.10 | 1.37 | 50 | -0.09 | 0.66 |
| -20 | 1.37 | 1.62 | 55 | -0.29 | 0.56 |
| -15 | 1.59 | 1.82 | 60 | -0.50 | 0.44 |
| -10 | 1.88 | 2.02 | 65 | | 0.36 |

(x) NGC 4526; Tracings Across Shadow Band

D 12"x1"

| y | F2 | F3 | y | F2 | F3 |
|---|---|---|---|---|---|
| -1 | 1.65 | | - 6 | 1.32 | 1.64 |
| -1.5 | 1.57 | | - 6.5 | 1.28 | 1.60 |
| -2 | 1.50 | 1.86 | - 7 | 1.26 | 1.58 |
| -2.5 | 1.42 | 1.76 | - 7.5 | 1.22 | 1.54 |
| -3 | 1.39 | 1.67 | - 8 | 1.19 | 1.51 |
| -3.5 | 1.33 | 1.64 | - 8.5 | 1.16 | 1.48 |
| -4 | 1.31 | 1.65 | - 9 | 1.14 | 1.45 |
| -4.5 | 1.33 | 1.67 | - 9.5 | 1.10 | 1.42 |
| -5 | 1.34 | 1.68 | -10 | 1.07 | 1.40 |
| -5.5 | 1.33 | 1.68 | -10.5 | | 1.37 |

(y) NGC 4526; Major Axis

D 6"x4"

| x | F2 | F3 | x | F2 | F3 |
|---|---|---|---|---|---|
| -115 | -0.13 | | -10 | 1.27 | 1.71 |
| -110 | -0.08 | | - 5 | 1.67 | 1.97 |
| -105 | -0.03 | 0.43 | 0 | 1.93 | 2.21 |
| -100 | 0.01 | 0.44 | 5 | 1.71 | 1.92 |
| - 95 | 0.08 | 0.46 | 10 | 1.38 | 1.69 |
| - 90 | 0.13 | 0.49 | 15 | 1.22 | 1.61 |
| - 85 | 0.18 | 0.54 | 20 | 1.24 | 1.47 |
| - 80 | 0.23 | 0.59 | 25 | 0.99 | 1.29 |
| - 75 | 0.27 | 0.62 | 30 | 0.80 | 1.15 |
| - 70 | 0.30 | 0.66 | 35 | 0.70 | 1.07 |
| - 65 | 0.36 | 0.71 | 40 | 0.64 | 1.00 |
| - 60 | 0.41 | 0.76 | 45 | 0.59 | 0.95 |
| - 55 | 0.46 | 0.82 | 50 | 0.54 | 0.91 |
| - 50 | 0.50 | 0.86 | 55 | 0.50 | 0.87 |
| - 45 | 0.56 | 0.94 | 60 | 0.45 | 0.83 |
| - 40 | 0.62 | 1.00 | 65 | | 0.80 |
| - 35 | 0.71 | 1.08 | 70 | | 0.76 |
| - 30 | 0.78 | 1.14 | 75 | | 0.72 |
| - 25 | 0.90 | 1.22 | 80 | | 0.70 |
| - 20 | 1.04 | 1.37 | 85 | | 0.67 |
| - 15 | 1.16 | 1.55 | | | |

paper and reading from this line the intensities at given points. It must be kept in mind that small irregularities are smoothed out in this way, even when they are real. The letters *a*, *b*, etc., in Table 6 serve as references to Figures 1–5, which are marked with the same letters.

For some nebulae, color measures were also made with a fixed diaphragm at various points of the nebula. As a rule, these measures yielded poor results because the telescope could not be guided during the measures. It is reasonable to suppose that the tracings were also influenced by the lack of guiding. To minimize this effect as much as possible, very long diaphragms were used for the tracings of some large nebulae; in this way the nucleus was always caught, even if not in the center of the diaphragm. When the size of the nebula was too small, this could not be done, and in these cases the nucleus was sometimes missed. These tracings were omitted from the discussion.

When the central intensities of the nebular tracings are compared with intensity measures of the nucleus made with fixed diaphragm in the same night, it appears that the latter values are always smaller than the former. This may have been caused by irregular guiding. Another explanation may be found in a too large scanning speed near the nucleus, where the intensity gradient is often very great. The differences between the nuclear values with fixed and with moving diaphragms vary between 0.04 and 0.20 mag. and are generally larger for F2 than for F3. It seems difficult to explain this latter difference.

The general conclusion of this paper is that the attempt to measure the intensity distribution of the nebulae photoelectrically has succeeded, although for a variety of reasons the accuracy of the measures is less than that anticipated from photoelectric observations. The authors regret that, because of unforeseen circumstances, publication was delayed until now.

In a forthcoming publication a discussion of these measures will be given, in combination with intensity distributions derived photographically.

## REFERENCES

Evans, David S. 1951, *M.N.*, **111**, 526–536.
———. 1952, *ibid.*, **112**, 606–613.
Hubble, Edwin. 1930, *Ap. J.*, **71**, 231–276.
Redman, R. O., and Shirley, E. G. 1938, *M.N.*, **98**, 613–623.
Shapley, Harlow, and Ames, Adelaide. 1932, *Harvard Ann.*, **88**, No. 2, 41–75.
Vaucouleurs, Gérard de. 1948, *Ann. d'ap.*, **11**, 247–287.

# INTERSTELLAR POLARIZATION OF 405 STARS*

W. A. HILTNER
Yerkes and McDonald Observatories

*Received May 26, 1954*

ABSTRACT

The interstellar polarization of 405 stars is given in Table 1. The stars are primarily early-type stars of high luminosity.

In addition to the observation of stars for interstellar polarization especially selected for particular problems relating to the galactic magnetic fields, many faint and a few brighter stars, primarily of high luminosity, have been observed and are herewith published. The stars were selected from published lists of early-type stars. Lists published by González and González (1952, 1953), Münch (1953), Iriarte and Chavira (1954), and Nassau and Harris (1952) have received special attention. Also a few stars from miscellaneous lists were included.

The observational procedure did not differ significantly from that employed previously (Hiltner 1951). The only instrumental change was the replacement of the RCA 1P21 photomultiplier by an EMI 5659 cell. This cell has a semitransparent photocathode, and the plane of this photocathode is placed perpendicular to the optical axis.

The reduction method of the observations was altered. Instead of a graphical solution for the amount of polarization and the plane of vibration, the observations at different position angles of an individual star, properly weighted, were solved by least squares. The resulting accuracy in the reductions is not significantly altered, however.

All the observations are collected in Table 1. The first and second columns give the *Henry Draper* and the *Bonner Durchmusterung* catalogue numbers, if any, respectively. The third column primarily identifies stars without either a *Henry Draper* or a *Bonner Durchmusterung* catalogue number. In this column the number of a star in a particular catalogue is followed by a reference number of that catalogue. The list of references is as follows: (1) González and González (1952); (2) González and González (1953); (3) Nassau and Harris (1952), Table 1; (4) Münch (1953). The fourth and fifth columns give the 1900 right ascension and declination, respectively. The next three columns give the galactic longitude, latitude, and the galactic parallactic angle, respectively, obtained from the Lund tables (Ohlsson 1932). The ninth and tenth columns contain the observed polarization in magnitudes and the observed position angle of the plane of vibration. The last column gives the position angle of the plane of vibration in galactic co-ordinates.

It will be noted that magnitudes and spectral types of the stars are not given. This deficiency will be corrected in a future publication, when the classification of slit spectra and photoelectric colors and magnitudes of most stars in this catalogue will be published. It suffices here to say that, on the whole, the stars are early-type O and B stars with photographic magnitudes not fainter than 12.0. One exception is TV Aur, which is an S star.

The largest interstellar polarization reported here is 0.168, star No. 4, ref. 2. Larger polarization has been observed (0.183 mag.) in a thirteenth-magnitude star in Cassiopeia. It is not recorded in Table 1 because of the absence of a published identification chart and catalogue number.

* *Contributions from the McDonald Observatory, University of Texas*, No. 241.

TABLE 1

| Star | | | 1900 | | l | b | $\phi$ | p | $\theta$ | $\theta$ |
|---|---|---|---|---|---|---|---|---|---|---|
| HD | BD | Other Designation | $\alpha$ | $\delta$ | | | | | | |
| | | No. 40, Ref. 1 | $0^h\ 1^m1$ | +61°58' | 85.4 | + 0.3 | 8.6 | 0.053 | 59° | 68° |
| | | No. 41, Ref. 1 | 0 1.3 | +59 45 | 85.1 | - 1.9 | 8.5 | 0.015 | 129 | 29 |
| | +62° 1 | | 0 2.4 | +62 31 | 85.7 | + 0.8 | 8.3 | 0.076 | 71 | 79 |
| 1337 | +50 46 | AO Cas | 0 12.5 | +50 53 | 85.6 | -10.9 | 6.2 | 0.015 | 40 | 46 |
| | +61 40 | | 0 15.0 | +61 50 | 87.0 | 0.0 | 5.5 | 0.068 | 58 | 64 |
| | +61 77 | | 0 20.8 | +62 13 | 87.8 | + 0.3 | 4.2 | 0.039 | 90 | 94 |
| | +61 122 | | 0 29.2 | +61 53 | 88.7 | - 0.1 | 2.4 | 0.060 | 85 | 87 |
| | | No. 1, Ref. 2 | 0 53.1 | +62 31 | 91.5 | + 0.6 | 357.1 | 0.109 | 95 | 92 |
| | +62 186 | | 0 56.2 | +62 27 | 91.9 | + 0.5 | 356.4 | 0.105 | 93 | 89 |
| | | No. 2, Ref. 2 | 0 57.6 | +63 13 | 92.0 | + 1.3 | 356.1 | 0.096 | 98 | 94 |
| | +60 169 | | 1 02.7 | +60 56 | 92.8 | - 1.0 | 355.0 | 0.082 | 86 | 81 |
| | +62 212 | | 1 02.8 | +63 09 | 92.6 | + 1.3 | 355.0 | 0.100 | 96 | 91 |
| E236633 | +59 191 | | 1 02.9 | +60 06 | 92.7 | - 1.8 | 354.9 | 0.123 | 86 | 81 |
| | +61 220 | | 1 05.1 | +62 12 | 92.9 | + 0.3 | 354.5 | 0.098 | 100 | 94 |
| | +60 191 | | 1 08.1 | +60 48 | 93.4 | - 1.0 | 353.8 | 0.076 | 89 | 83 |
| | +63 167 | | 1 11.6 | +63 47 | 93.5 | + 2.0 | 353.0 | 0.106 | 85 | 78 |
| 7720 | +61 240 | | 1 11.9 | +61 22 | 93.8 | - 0.4 | 353.0 | 0.071 | 107 | 100 |
| | +62 245 | | 1 17.7 | +62 18 | 94.4 | + 0.6 | 351.7 | 0.076 | 107 | 99 |
| | +62 249 | | 1 19.5 | +62 31 | 94.5 | + 0.9 | 351.3 | 0.120 | 104 | 95 |
| | +58 241 | | 1 21.4 | +58 43 | 95.4 | - 2.8 | 350.9 | 0.081 | 101 | 92 |
| | +62 258 | | 1 23.3 | +63 04 | 94.9 | + 1.5 | 350.4 | 0.111 | 103 | 93 |
| | +61 285 | | 1 25.9 | +61 27 | 95.5 | - 0.1 | 349.9 | 0.091 | 111 | 101 |
| | +62 275 | | 1 29.1 | +63 08 | 95.5 | + 1.6 | 349.2 | 0.091 | 102 | 91 |
| | +60 322 | | 1 38.2 | +60 18 | 97.2 | - 0.9 | 347.2 | 0.066 | 108 | 95 |
| | +58 310 | | 1 43.7 | +58 45 | 98.2 | - 2.2 | 346.0 | 0.092 | 99 | 85 |
| | +60 362 | | 1 44.0 | +60 51 | 97.7 | - 0.2 | 345.9 | 0.109 | 106 | 92 |
| | +61 342 | | 1 46.1 | +62 03 | 97.7 | + 1.0 | 345.4 | 0.074 | 104 | 89 |
| | +59 357 | | 1 49.4 | +60 05 | 98.6 | - 0.8 | 344.7 | 0.084 | 99 | 84 |
| | +60 389 | | 1 50.3 | +60 38 | 98.6 | - 0.4 | 344.5 | 0.084 | 103 | 87 |
| | | No. 3, Ref. 2 | 1 50.8 | +59 30 | 98.9 | - 1.3 | 344.4 | 0.116 | 95 | 79 |
| | | No. 4, Ref. 2 | 1 51.1 | +61 29 | 98.3 | + 0.8 | 344.4 | 0.168 | 102 | 86 |
| | | No. 5, Ref. 2 | 1 51.7 | +60 08 | 98.8 | - 0.6 | 344.2 | 0.092 | 99 | 83 |
| | +60 416 | | 1 54.6 | +60 34 | 99.0 | - 0.1 | 343.6 | 0.115 | 99 | 83 |
| | +59 388 | | 1 55.6 | +59 30 | 99.5 | - 1.1 | 343.4 | 0.096 | 101 | 84 |
| | +61 370 | | 1 56.4 | +61 34 | 99.0 | + 0.7 | 343.2 | 0.165 | 104 | 87 |
| | +61 375 | | 1 57.8 | +61 36 | 99.1 | + 1.0 | 342.9 | 0.062 | 105 | 88 |
| | | No. 6, Ref. 2 | 1 58.6 | +62 53 | 98.8 | + 2.2 | 342.7 | 0.129 | 108 | 91 |
| | +60 435 | | 2 00.9 | +60 55 | 99.7 | + 0.4 | 342.2 | 0.084 | 114 | 96 |
| 13036 | +58 384 | | 2 02.5 | +59 09 | 100.4 | - 1.3 | 341.9 | 0.078 | 114 | 96 |
| 13256 | +60 447 | | 2 04.5 | +60 14 | 100.3 | - 0.1 | 341.4 | 0.138 | 100 | 81 |
| | | No. 7, Ref. 2 | 2 05.4 | +59 26 | 100.7 | - 0.8 | 341.2 | 0.105 | 94 | 75 |
| | +57 520 | | 2 06.7 | +57 58 | 101.3 | - 2.1 | 341.0 | 0.102 | 105 | 86 |
| | +59 451 | | 2 09.0 | +59 13 | 101.2 | - 0.9 | 340.5 | 0.097 | 101 | 81 |
| | | No. 8, Ref. 2 | 2 09.7 | +57 50 | 101.7 | - 2.1 | 340.3 | 0.084 | 117 | 97 |
| | +59 456 | | 2 11.0 | +59 20 | 101.4 | - 0.7 | 340.0 | 0.107 | 107 | 87 |
| | +60 470 | | 2 15.8 | +60 22 | 101.6 | + 0.5 | 339.0 | 0.068 | 116 | 95 |
| | +58 458 | | 2 16.3 | +58 30 | 102.3 | - 1.2 | 338.9 | 0.102 | 115 | 94 |
| | +57 558 | | 2 17.3 | +57 52 | 102.7 | - 1.7 | 338.7 | 0.076 | 115 | 94 |
| | | No. 9, Ref. 2 | 2 18.6 | +59 32 | 102.2 | - 0.1 | 338.4 | 0.097 | 115 | 93 |
| | | No. 10, Ref. 2 | 2 19.6 | +57 24 | 103.1 | - 2.1 | 338.2 | 0.073 | 118 | 96 |
| | | No. 11, Ref. 2 | 2 22.2 | +57 46 | 103.3 | - 1.6 | 337.6 | 0.089 | 113 | 91 |
| | +57 579 | | 2 23.0 | +57 13 | 103.6 | - 2.1 | 337.4 | 0.083 | 108 | 85 |
| | +60 493 | | 2 23.3 | +60 44 | 102.3 | + 1.2 | 337.4 | 0.091 | 111 | 88 |
| | | No. 12, Ref. 2 | 2 24.8 | +59 36 | 102.9 | + 0.2 | 337.1 | 0.104 | 107 | 84 |
| | +57 586 | | 2 26.1 | +58 09 | 103.6 | - 1.0 | 336.8 | 0.110 | 122 | 99 |

TABLE 1 (Cont'd)

| Star | | | 1900 | | l | b | $\phi$ | p | $\theta$ | $\theta'$ |
|---|---|---|---|---|---|---|---|---|---|---|
| HD | BD | Other Designation | $\alpha$ | $\delta$ | | | | | | |
| | +59° 510 | | $2^h26.^m7$ | +59°34' | 103.1 | + 0.3 | 336.6 | 0.097 | 117° | 94° |
| | +58 488 | | 2 27.2 | +59 06 | 103.4 | - 0.2 | 336.5 | 0.131 | 107 | 83 |
| E236971 | +56 660 | | 2 28.3 | +57 03 | 104.3 | - 1.9 | 336.3 | 0.096 | 119 | 95 |
| | +57 593 | | 2 28.6 | +57 22 | 104.2 | - 1.6 | 336.2 | 0.093 | 118 | 94 |
| 16264 | +56 676 | | 2 31.5 | +57 10 | 104.7 | - 1.6 | 335.6 | 0.063 | 121 | 97 |
| | +56 739 | | 2 47.4 | +57 02 | 106.7 | - 0.8 | 332.2 | 0.100 | 115 | 87 |
| | | No. 13, Ref. 2 | 2 51.1 | +57 42 | 106.8 | 0.0 | 331.4 | 0.121 | 116 | 87 |
| | +59 584 | | 2 54.5 | +59 15 | 106.4 | + 1.6 | 330.8 | 0.048 | 119 | 90 |
| | +58 554 | | 2 56.7 | +59 04 | 106.8 | + 1.6 | 330.2 | 0.076 | 114 | 84 |
| 18877 | +59 589 | | 2 57.1 | +59 39 | 106.5 | + 2.1 | 330.2 | 0.046 | 126 | 96 |
| | +57 687 | | 2 58.7 | +57 27 | 107.8 | + 0.3 | 329.8 | 0.116 | 118 | 88 |
| | | BSD9-419 | 2 59.1 | +59 01 | 107.1 | + 1.7 | 329.8 | 0.034 | 123 | 93 |
| | | BSD9-69 | 3 01.3 | +58 31 | 107.6 | + 1.4 | 329.3 | 0.105 | 108 | 77 |
| | +59 597 | | 3 01.4 | +60 04 | 106.8 | + 2.7 | 329.2 | 0.058 | 119 | 88 |
| 19536 | +60 636 | | 3 03.5 | +60 15 | 106.9 | + 3.0 | 328.8 | 0.018 | 131 | 100 |
| 19653 | +60 640 | | 3 04.8 | +60 26 | 107.0 | + 3.2 | 328.5 | 0.048 | 124 | 92 |
| | | BSD9-532 | 3 05.1 | +59 23 | 107.6 | + 2.4 | 328.5 | 0.126 | 104 | 72 |
| | +60 644 | | 3 06.0 | +60 30 | 107.1 | + 3.4 | 328.3 | 0.037 | 126 | 94 |
| | | BSD9-1161 | 3 06.7 | +60 21 | 107.2 | + 3.3 | 328.1 | 0.038 | 126 | 94 |
| 19968 | +60 651 | | 3 07.5 | +60 45 | 107.1 | + 3.7 | 327.9 | 0.039 | 31 | 179 |
| 20040 | +59 616 | | 3 08.2 | +59 44 | 107.7 | + 2.9 | 327.8 | 0.025 | 119 | 87 |
| 20095 | +59 621 | | 3 08.7 | +59 37 | 107.8 | + 2.8 | 327.7 | 0.019 | 130 | 98 |
| | | BSD9-161 | 3 10.9 | +58 46 | 108.5 | + 2.3 | 327.3 | 0.085 | 112 | 79 |
| 21803 | +44 734 | | 3 25.8 | +44 31 | 118.3 | - 8.2 | 323.8 | 0.034 | 132 | 96 |
| E237153 | +58 622 | | 3 26.6 | +58 19 | 110.5 | + 3.0 | 324.0 | 0.119 | 115 | 79 |
| 22298 | +54 698 | | 3 30.3 | +54 50 | 112.9 | + 0.5 | 323.3 | 0.055 | 119 | 82 |
| | +61 623 | | 3 31.5 | +61 31 | 109.0 | + 6.0 | 322.8 | 0.117 | 130 | 93 |
| 22951 | +33 698 | | 3 36.0 | +33 39 | 126.9 | -15.6 | 320.4 | 0.021 | 78 | 38 |
| | +31 643 | | 3 38.3 | +31 51 | 128.5 | -16.6 | 319.7 | 0.024 | 150 | 110 |
| 23478 | +31 649 | | 3 40.4 | +32 00 | 128.7 | -16.2 | 319.4 | 0.035 | 31 | 170 |
| 23475 | +65 369 | | 3 40.4 | +65 13 | 107.5 | + 9.5 | 320.6 | 0.066 | 111 | 72 |
| 24131 | +33 728 | | 3 45.5 | +34 03 | 128.2 | -14.0 | 318.8 | 0.022 | 88 | 47 |
| | | No. 14, Ref. 2 | 3 46.1 | +52 56 | 115.9 | + 0.5 | 320.2 | 0.030 | 124 | 84 |
| 24398 | | $\zeta$ Per | 3 47.8 | +31 35 | 130.2 | -15.5 | 318.0 | 0.029 | 62 | 20 |
| 24534 | +30 591 | | 3 49.1 | +30 45 | 131.0 | -15.9 | 317.6 | 0.025 | 49 | 7 |
| 24640 | +34 768 | | 3 50.0 | +34 47 | 128.4 | -12.8 | 318.1 | 0.020 | 99 | 57 |
| | +52 729 | | 3 50.1 | +52 25 | 116.7 | + 0.5 | 319.4 | 0.085 | 125 | 84 |
| 24912 | +35 775 | | 3 52.5 | +35 30 | 128.3 | -12.0 | 317.8 | 0.027 | 102 | 60 |
| | | No. 15, Ref. 2 | 3 54.7 | +52 33 | 117.2 | + 1.0 | 318.4 | 0.057 | 128 | 86 |
| 25833 | +33 785 | | 4 00.6 | +33 11 | 131.2 | -12.5 | 316.0 | 0.025 | 87 | 43 |
| | | RW Per | 4 13.3 | +42 04 | 126.7 | - 4.4 | 314.7 | 0.048 | 112 | 67 |
| | | TV Aur | 4 50.6 | +48 24 | 126.3 | + 4.7 | 308.1 | 0.038 | 148 | 96 |
| | +36 986 | | 4 56.4 | +36 16 | 136.5 | - 1.9 | 307.4 | 0.030 | 151 | 98 |
| 32672 | +38 1020 | | 4 59.8 | +38 23 | 135.3 | - 0.1 | 306.9 | 0.073 | 167 | 114 |
| 33152 | +36 1021 | | 5 03.2 | +36 53 | 136.8 | - 0.4 | 306.4 | 0.030 | 5 | 131 |
| | +39 1204 | | 5 05.3 | +39 26 | 135.0 | + 1.4 | 306.0 | 0.054 | 153 | 99 |
| | | No. 16, Ref. 2 | 5 08.2 | +36 36 | 137.7 | + 0.2 | 305.6 | 0.063 | 137 | 83 |
| 34333 | +36 1073 | EO Aur | 5 11.6 | +36 31 | 138.2 | + 0.7 | 305.1 | 0.030 | 157 | 102 |
| | | No. 17, Ref. 2 | 5 16.7 | +33 29 | 141.2 | - 0.2 | 304.4 | 0.062 | 154 | 98 |
| | +33 1056 | | 5 21.6 | +33 14 | 142.0 | + 0.6 | 303.7 | 0.093 | 161 | 105 |
| | +34 1059 | | 5 22.0 | +34 56 | 140.7 | + 1.6 | 303.6 | 0.055 | 153 | 97 |
| E244894 | +27 797 | | 5 28.3 | +27 31 | 147.6 | - 1.4 | 302.8 | 0.035 | 18 | 141 |
| E245770 | +26 883 | | 5 32.7 | +26 16 | 149.2 | - 1.2 | 302.3 | 0.016 | 0 | 122 |
| E246878 | +27 850 | | 5 38.2 | +27 12 | 149.0 | + 0.3 | 301.7 | 0.012 | 133 | 75 |
| E247176 | +26 943 | | 5 39.5 | +26 32 | 149.7 | + 0.2 | 301.5 | 0.020 | 131 | 73 |

TABLE 1 (Cont'd)

| Star | | | 1900 | | l | b | $\phi$ | p | $\theta$ | $\theta'$ |
|---|---|---|---|---|---|---|---|---|---|---|
| HD | BD | Other Designation | $\alpha$ | $\delta$ | | | | | | |
| E247754 | +25° 989 | | $5^h42^m4$ | +25°04' | 151.2 | 0.0 | 301.2 | 0.053 | 150° | 91° |
| E249071 | +27 909 | | 5 49.0 | +27 54 | 149.6 | + 2.7 | 300.4 | 0.070 | 168 | 108 |
| | | No. 18, Ref. 2 | 5 49.9 | +25 23 | 151.9 | + 1.6 | 300.4 | 0.070 | 162 | 102 |
| | | No. 19, Ref. 2 | 5 49.8 | +20 04 | 156.5 | - 1.1 | 300.4 | 0.049 | 152 | 92 |
| | | No. 20, Ref. 2 | 5 56.0 | +20 12 | 157.1 | + 0.2 | 299.9 | 0.044 | 170 | 110 |
| 40893 | +31 1174 | | 5 56.7 | +31 02 | 147.8 | + 5.7 | 299.4 | 0.030 | 140 | 79 |
| E251204 | +23 1179 | | 5 59.0 | +23 24 | 154.7 | + 2.4 | 299.6 | 0.101 | 155 | 95 |
| E252325 | +20 1278 | | 6 03.1 | +20 39 | 157.5 | + 1.9 | 299.3 | 0.104 | 164 | 103 |
| | | No. 21, Ref. 2 | 6 04.3 | +13 08 | 164.2 | - 1.5 | 299.2 | 0.079 | 167 | 106 |
| | | No. 22, Ref. 2 | 6 05.1 | +13 12 | 164.3 | - 1.3 | 299.2 | 0.087 | 161 | 100 |
| E252956 | +13 1148 | | 6 05.4 | +13 09 | 164.4 | - 1.3 | 299.2 | 0.080 | 160 | 99 |
| E254647 | +11 1100 | | 6 12.0 | +11 14 | 166.8 | - 0.8 | 298.8 | 0.024 | 11 | 130 |
| | | No. 23, Ref. 2 | 6 13.1 | +14 33 | 164.0 | + 1.0 | 298.7 | 0.056 | 159 | 98 |
| | | No. 24, Ref. 2 | 6 17.1 | +16 00 | 163.2 | + 2.6 | 298.4 | 0.050 | 8 | 126 |
| 45910 | + 5 1267 | | 6 25.2 | + 5 57 | 173.0 | - 0.5 | 298.2 | 0.017 | 2 | 120 |
| | | No. 25, Ref. 2 | 6 27.0 | + 3 38 | 175.3 | - 1.2 | 298.2 | 0.053 | 18 | 136 |
| E259597 | + 8 1388 | | 6 28.1 | + 8 24 | 171.2 | + 1.3 | 298.1 | 0.030 | 75 | 13 |
| | | No. 26, Ref. 2 | 6 28.9 | +11 14 | 168.8 | + 2.8 | 298.0 | 0.050 | 161 | 99 |
| 46711 | + 2 1299 | | 6 29.8 | + 2 51 | 176.2 | - 0.9 | 298.1 | 0.064 | 37 | 155 |
| 46847 | + 2 1302 | | 6 30.5 | + 2 47 | 176.4 | - 0.8 | 298.1 | 0.042 | 22 | 140 |
| 46867 | + 5 1315 | | 6 30.6 | + 5 24 | 174.1 | + 0.5 | 298.1 | 0.044 | 156 | 94 |
| 47032 | + 4 1341 | | 6 31.5 | + 4 46 | 174.9 | + 0.4 | 298.1 | 0.038 | 161 | 99 |
| | | No. 27, Ref. 2 | 6 32.9 | + 2 28 | 177.0 | - 0.4 | 298.0 | 0.038 | 13 | 131 |
| | | No. 28, Ref. 2 | 6 33.9 | + 3 44 | 176.0 | + 0.4 | 298.0 | 0.044 | 17 | 135 |
| | | No. 29, Ref. 2 | 6 40.0 | + 2 12 | 178.0 | + 1.0 | 298.0 | 0.032 | 164 | 102 |
| 54439 | -11 1812 | | 7 03.7 | -11 42 | 193.1 | - 0.3 | 298.6 | 0.018 | 136 | 75 |
| 54464 | - 3 1762 | | 7 03.8 | - 3 54 | 186.2 | + 3.4 | 298.4 | < 003 | .... | .... |
| | - 0 1618 | | 7 03.9 | - 0 52 | 183.6 | + 4.9 | 298.2 | < 002 | .... | .... |
| 54786 | -15 1672 | | 7 05.1 | -15 56 | 197.0 | - 2.1 | 298.6 | 0.017 | 116 | 55 |
| 59075 | -18 1847 | | 7 23.3 | -18 17 | 201.1 | + 0.6 | 299.8 | 0.024 | 3 | 123 |
| 59094 | -15 1837 | | 7 23.3 | -15 53 | 199.1 | + 1.8 | 299.8 | 0.011 | 118 | 58 |
| 59114 | -15 1839 | | 7 23.4 | -15 11 | 198.5 | + 2.1 | 299.8 | 0.059 | 159 | 99 |
| | -22 4543 | | 17 58.2 | -22 29 | 335.4 | - 1.8 | 60.3 | 0.006 | 130 | 10 |
| | -17 5020 | | 18 00.7 | -17 12 | 340.3 | + 0.3 | 60.5 | 0.027 | 156 | 36 |
| | -15 4854 | | 18 06.0 | -15 37 | 342.3 | 0.0 | 60.8 | 0.028 | 32 | 93 |
| | -15 4861 | | 18 06.6 | -15 36 | 342.4 | - 0.2 | 60.9 | 0.024 | 50 | 111 |
| | -12 4949 | | 18 08.0 | -12 55 | 344.9 | + 0.8 | 61.0 | 0.027 | 58 | 119 |
| | -20 5043 | | 18 08.1 | -20 20 | 338.4 | - 2.8 | 61.1 | 0.075 | 62 | 123 |
| | -20 5060 | | 18 09.7 | -20 23 | 338.5 | - 3.1 | 61.2 | 0.019 | 153 | 34 |
| | -14 4957 | | 18 10.4 | -14 39 | 343.6 | - 0.5 | 61.1 | 0.054 | 126 | 7 |
| | -12 4964 | | 18 11.8 | -12 20 | 345.8 | + 0.3 | 61.2 | 0.066 | 96 | 157 |
| | -12 4970 | | 18 12.1 | -12 32 | 345.7 | + 0.2 | 61.2 | 0.054 | 88 | 149 |
| | -19 4955 | | 18 12.2 | -19 09 | 339.9 | - 3.0 | 61.3 | 0.061 | 179 | 60 |
| | -12 4979 | | 18 12.4 | -12 17 | 345.9 | + 0.2 | 61.2 | 0.021 | 118 | 179 |
| | -11 4586 | | 18 12.5 | -11 20 | 346.8 | + 0.8 | 61.2 | 0.062 | 92 | 153 |
| | -12 4982 | | 18 12.6 | -12 13 | 346.0 | + 0.2 | 61.2 | 0.024 | 94 | 155 |
| | -12 4984 | | 18 12.7 | -12 00 | 346.2 | + 0.3 | 61.2 | 0.050 | 103 | 164 |
| | -13 4928 | | 18 13.0 | -13 49 | 344.7 | - 0.6 | 61.3 | 0.060 | 72 | 133 |
| | -13 4929 | | 18 13.0 | -13 48 | 344.7 | - 0.6 | 61.3 | 0.061 | 78 | 139 |
| | -13 4930 | | 18 13.2 | -13 52 | 344.6 | - 0.7 | 61.3 | 0.045 | 77 | 138 |
| | -13 4936 | | 18 13.4 | -13 59 | 344.6 | - 0.8 | 61.3 | 0.035 | 101 | 162 |
| | -12 4994 | | 18 13.4 | -12 09 | 346.2 | + 0.1 | 61.3 | 0.034 | 156 | 37 |
| | -13 4941 | | 18 14.4 | -13 05 | 345.4 | - 0.4 | 61.3 | 0.040 | 29 | 90 |
| | -12 5008 | | 18 14.5 | -12 41 | 345.8 | - 0.4 | 61.4 | 0.048 | 149 | 30 |
| | -12 5009 | | 18 14.7 | -12 13 | 346.3 | - 0.2 | 61.4 | 0.015 | 3 | 64 |

TABLE 1 (Cont'd)

| Star | | | 1900 | | l | b | $\phi$ | p | $\theta$ | $\theta'$ |
|---|---|---|---|---|---|---|---|---|---|---|
| HD | BD | Other Designation | $\alpha$ | $\delta$ | | | | | | |
| | -20°5108 | | 18h16m4 | -20°07' | 339.5 | - 4.4 | 61.7 | 0.032 | 39° | 101° |
| | -14 5016 | | 18 17.0 | -14 42 | 344.4 | - 1.9 | 61.5 | 0.011 | 85 | 147 |
| | -14 5029 | | 18 18.1 | -14 12 | 344.9 | - 1.9 | 61.6 | 0.029 | 70 | 132 |
| | - 9 4713 | | 18 18.4 | - 9 57 | 348.7 | 0.0 | 61.5 | 0.012 | 46 | 108 |
| | -14 5030 | | 18 18.6 | -14 13 | 345.0 | - 2.0 | 61.6 | 0.029 | 3 | 65 |
| | -14 5037 | | 18 19.4 | -14 42 | 344.6 | - 2.4 | 61.7 | 0.065 | 177 | 59 |
| | -13 4979 | | 18 21.0 | -13 43 | 345.7 | - 2.3 | 61.7 | 0.033 | 48 | 110 |
| | -14 5062 | | 18 22.2 | -14 46 | 344.9 | - 3.1 | 61.8 | 0.027 | 75 | 137 |
| | - 8 4617 | | 18 23.8 | - 8 38 | 350.5 | - 0.5 | 61.7 | 0.042 | 138 | 20 |
| | -12 5083 | | 18 25.8 | -12 25 | 347.4 | - 2.7 | 61.9 | 0.017 | 169 | 51 |
| | -11 4667 | | 18 26.8 | -11 22 | 348.4 | - 2.4 | 61.9 | 0.050 | 145 | 27 |
| | -14 5102 | | 18 27.4 | -13 58 | 346.2 | - 3.8 | 62.1 | <002 | .... | .... |
| | -12 5104 | | 18 28.3 | -12 20 | 347.7 | - 3.2 | 62.0 | 0.046 | 148 | 30 |
| | -12 5133 | | 18 34.4 | -12 31 | 348.3 | - 4.6 | 62.3 | 0.094 | 148 | 30 |
| | -13 5065 | | 18 34.7 | -13 30 | 347.4 | - 5.2 | 62.4 | 0.106 | 150 | 32 |
| | -13 5073 | | 18 35.7 | -13 57 | 347.2 | - 5.6 | 62.5 | 0.100 | 151 | 33 |
| | -12 5163 | | 18 41.3 | -12 24 | 349.2 | - 6.1 | 62.6 | 0.032 | 105 | 168 |
| | -12 5166 | | 18 41.5 | -12 14 | 349.3 | - 6.0 | 62.6 | 0.027 | 129 | 12 |
| | - 0 3584 | | 18 48.4 | - 0 41 | 0.4 | - 2.2 | 62.0 | 0.011 | 42 | 104 |
| | + 2 3771 | | 18 59.2 | + 2 58 | 4.8 | - 2.9 | 61.8 | 0.013 | 96 | 158 |
| | +14 3887 | | 19 17.0 | +14 42 | 17.3 | - 1.0 | 60.6 | 0.056 | 3 | 64 |
| E231285 | +14 3898 | | 19 18.9 | +15 01 | 17.8 | - 1.3 | 60.5 | 0.015 | 53 | 113 |
| | +22 3687 | | 19 20.5 | +22 34 | 24.5 | + 2.1 | 60.4 | 0.048 | 0 | 60 |
| E231564 | +12 3927 | | 19 24.8 | +12 22 | 16.2 | - 3.8 | 60.2 | 0.059 | 35 | 95 |
| | +23 3730 | | 19 36.0 | +23 47 | 27.4 | - 0.4 | 59.0 | 0.076 | 21 | 80 |
| | +28 3434 | | 19 37.3 | +28 55 | 31.9 | + 2.0 | 58.9 | 0.018 | 46 | 105 |
| | +28 3438 | | 19 38.1 | +28 46 | 31.9 | + 1.8 | 58.8 | 0.009 | 96 | 155 |
| | +23 3745 | | 19 38.6 | +23 13 | 27.2 | - 1.2 | 58.7 | 0.132 | 26 | 85 |
| | +23 3747 | | 19 38.9 | +23 12 | 27.2 | - 1.2 | 58.7 | 0.066 | 14 | 73 |
| | +22 3782 | | 19 39.0 | +23 03 | 27.1 | - 1.3 | 58.7 | 0.089 | 8 | 67 |
| | +23 3759 | | 19 41.0 | +23 48 | 28.0 | - 1.3 | 58.4 | 0.062 | 11 | 69 |
| | +23 3761 | | 19 41.2 | +24 04 | 28.1 | - 1.3 | 58.4 | 0.042 | 28 | 86 |
| | +23 3762 | | 19 41.4 | +23 44 | 28.0 | - 1.4 | 58.4 | 0.043 | 27 | 85 |
| | +22 3800 | | 19 41.5 | +22 57 | 27.3 | - 1.9 | 58.4 | 0.012 | 19 | 77 |
| | +25 3952 | | 19 41.5 | +25 07 | 29.2 | - 0.7 | 58.4 | 0.025 | 38 | 96 |
| | +27 3512 | | 19 42.6 | +28 00 | 31.8 | + 0.6 | 58.2 | 0.008 | 17 | 75 |
| | +24 3881 | | 19 42.8 | +24 36 | 28.9 | - 1.2 | 58.2 | 0.021 | 37 | 95 |
| | +34 3707 | | 19 42.9 | +34 24 | 37.2 | + 3.9 | 58.4 | 0.023 | 67 | 125 |
| | +27 3513 | | 19 42.9 | +27 48 | 31.7 | + 0.3 | 58.2 | 0.023 | 40 | 98 |
| | +28 3485 | | 19 44.3 | +28 33 | 32.5 | + 0.5 | 58.0 | 0.027 | 57 | 115 |
| E225985 | +32 3583 | | 19 45.7 | +32 43 | 36.1 | + 2.5 | 57.9 | 0.011 | 149 | 27 |
| | +22 3836 | | 19 46.8 | +22 35 | 27.7 | - 3.0 | 57.9 | 0.046 | 35 | 93 |
| | +33 3618 | | 19 47.0 | +33 24 | 36.8 | + 2.6 | 57.8 | 0.071 | 41 | 99 |
| | +27 3550 | | 19 50.1 | +28 04 | 32.7 | - 0.7 | 57.4 | 0.035 | 64 | 121 |
| E226868 | | | 19 54.6 | +34 56 | 39.0 | + 2.1 | 56.8 | 0.108 | 135 | 12 |
| E227018 | +34 3828 | | 19 56.1 | +35 02 | 39.2 | + 1.9 | 56.6 | 0.048 | 120 | 177 |
| | +29 3842 | | 19 56.6 | +30 06 | 35.2 | - 0.9 | 56.5 | 0.034 | 85 | 141 |
| E227245 | +35 3924 | | 19 58.6 | +35 24 | 39.8 | + 1.7 | 56.3 | 0.049 | 135 | 11 |
| | +36 3827 | | 19 58.6 | +36 49 | 41.0 | + 2.5 | 56.3 | 0.013 | 78 | 134 |
| | +28 3598 | | 19 59.1 | +28 25 | 34.1 | - 2.2 | 56.3 | 0.076 | 39 | 95 |
| | +25 4083 | | 19 59.9 | +25 59 | 32.2 | - 3.7 | 56.2 | 0.042 | 160 | 36 |
| | +31 3921 | | 20 00.3 | +31 52 | 37.1 | - 0.5 | 56.0 | 0.015 | 40 | 96 |
| | +33.3717 | | 20 00.6 | +33 25 | 38.4 | + 0.3 | 56.0 | 0.034 | 75 | 131 |
| E227611 | | | 20 02.0 | +35 37 | 40.4 | + 1.3 | 55.7 | 0.035 | 14 | 70 |
| | +35 3956 | | 20 02.2 | +35 28 | 40.3 | + 1.2 | 55.8 | 0.008 | 27 | 83 |

TABLE 1 (Cont'd)

| Star | | | 1900 | | l | b | $\phi$ | p | $\theta$ | $\theta'$ |
|---|---|---|---|---|---|---|---|---|---|---|
| HD | BD | Other Designation | $\alpha$ | $\delta$ | | | | | | |
| E227634 | +35°3957 | | $20^h02^m.3$ | +35°29' | 40.3 | + 1.1 | 55.8 | 0.020 | 4° | 60° |
| 190991 | +39 4033 | | 20 02.5 | +39 47 | 43.9 | + 3.5 | 55.9 | 0.027 | 100 | 156 |
| E227704 | +34 3874 | | 20 02.9 | +34 38 | 39.7 | + 0.6 | 55.7 | 0.032 | 136 | 12 |
| E227757 | +35 3983 | | 20 03.5 | +36 04 | 40.9 | + 1.2 | 55.6 | 0.025 | 101 | 157 |
| | +36 3882 | | 20 03.7 | +36 16 | 41.1 | + 1.3 | 55.6 | 0.046 | 130 | 6 |
| 191396 | +37 3783 | | 20 04.6 | +37 50 | 42.5 | + 2.1 | 55.5 | 0.028 | 42 | 97 |
| 191423 | +42 3599 | | 20 04.7 | +42 19 | 46.2 | + 4.6 | 55.7 | 0.018 | 106 | 162 |
| E227902 | +37 3785 | | 20 04.9 | +37 13 | 42.0 | + 1.7 | 55.4 | 0.033 | 3 | 58 |
| | +40 4032 | | 20 04.9 | +40 57 | 45.1 | + 3.8 | 55.6 | 0.025 | 79 | 135 |
| E228041 | +35 3998 | | 20 06.2 | +35 12 | 40.5 | + 0.3 | 55.2 | 0.041 | 130 | 5 |
| E228053 | +36 3914 | | 20 06.3 | +36 24 | 41.5 | + 1.0 | 55.2 | 0.011 | 115 | 170 |
| E228101 | +37 3804 | | 20 06.9 | +37 10 | 42.2 | + 1.3 | 55.1 | 0.015 | 163 | 38 |
| E228104 | +35 4004 | | 20 06.9 | +35 35 | 40.9 | + 0.5 | 55.1 | 0.012 | 75 | 130 |
| | +35 4006 | | 20 07.2 | +35 39 | 41.0 | + 0.4 | 55.1 | 0.014 | 77 | 132 |
| 191978 | +40 4050 | | 20 07.5 | +41 04 | 45.5 | + 3.8 | 55.2 | <002 | .... | .... |
| E228263 | +37 3819 | | 20 08.4 | +37 21 | 42.6 | + 1.2 | 54.9 | 0.012 | 141 | 16 |
| | +39 4076 | | 20 08.4 | +39 42 | 44.5 | + 2.5 | 55.0 | 0.029 | 59 | 114 |
| E228368 | +34 3920 | | 20 09.5 | +34 43 | 40.5 | - 0.5 | 54.7 | 0.046 | 174 | 49 |
| | +40 4061 | | 20 09.5 | +40 43 | 45.4 | + 3.0 | 54.8 | 0.005 | 147 | 22 |
| | +32 3749 | | 20 09.7 | +32 15 | 38.5 | - 2.0 | 54.8 | 0.080 | 19 | 74 |
| E228452 | +34 3929 | | 20 10.2 | +35 06 | 40.9 | - 0.4 | 54.6 | 0.075 | 1 | 56 |
| E228456 | +36 3948 | | 20 10.3 | +36 30 | 42.1 | + 0.4 | 54.6 | 0.025 | 139 | 14 |
| | +37 3837 | | 20 10.3 | +37 56 | 43.1 | + 1.2 | 54.6 | 0.014 | 159 | 34 |
| | +32 3752 | | 20 10.4 | +33 08 | 39.3 | - 1.6 | 54.6 | 0.076 | 76 | 131 |
| | +41 3670 | | 20 11.2 | +41 32 | 46.3 | + 3.2 | 54.6 | 0.038 | 33 | 88 |
| | +37 3844 | | 20 11.3 | +37 50 | 43.3 | + 1.0 | 54.5 | 0.024 | 32 | 86 |
| E228548 | +39 4098 | | 20 11.4 | +39 40 | 44.8 | + 2.0 | 54.5 | 0.018 | 105 | 159 |
| E228587 | +36 3966 | | 20 11.7 | +36 19 | 42.1 | 0.0 | 54.4 | 0.026 | 131 | 5 |
| E228602 | +36 3968 | | 20 11.8 | +36 32 | 42.3 | + 0.2 | 54.4 | 0.010 | 143 | 17 |
| | +34 3952 | | 20 12.7 | +34 48 | 41.0 | - 1.0 | 54.3 | 0.023 | 1 | 55 |
| E228690 | +37 3861 | | 20 12.8 | +37 37 | 43.3 | + 0.6 | 54.3 | 0.015 | 59 | 113 |
| | +37 3862 | | 20 12.8 | +37 20 | 43.3 | + 0.4 | 54.2 | 0.005 | 128 | 2 |
| E228712 | +40 4087 | | 20 13.1 | +40 34 | 45.7 | + 2.3 | 54.3 | 0.034 | 7 | 61 |
| E228779 | +34 3961 | | 20 14.0 | +34 30 | 40.9 | - 1.4 | 54.1 | 0.045 | 0 | 54 |
| | +39 4117 | | 20 14.2 | +39 43 | 45.1 | + 1.6 | 54.1 | 0.017 | 156 | 30 |
| | +30 3980 | | 20 14.4 | +30 30 | 37.7 | - 3.8 | 54.2 | 0.099 | 13 | 67 |
| E228854 | +35 4062 | | 20 15.0 | +36 02 | 42.2 | - 0.7 | 53.9 | 0.032 | 42 | 96 |
| | +36 4000 | | 20 15.1 | +36 56 | 42.9 | - 0.2 | 53.9 | 0.054 | 81 | 135 |
| E228860 | +36 4001 | | 20 15.1 | +36 39 | 42.8 | - 0.3 | 53.9 | 0.030 | 102 | 156 |
| | +38 4002 | | 20 15.1 | +39 06 | 44.7 | + 1.2 | 53.9 | 0.033 | 172 | 46 |
| | +36 4004 | | 20 15.4 | +37 05 | 43.2 | - 0.1 | 53.9 | 0.035 | 73 | 127 |
| E228882 | +40 4113 | | 20 15.4 | +40 23 | 45.8 | + 1.8 | 53.9 | 0.039 | 136 | 10 |
| E228913 | +35 4067 | | 20 15.8 | +35 54 | 42.2 | - 0.9 | 53.8 | 0.041 | 51 | 105 |
| E228919 | +39 4135 | | 20 15.9 | +40 08 | 45.7 | + 1.6 | 53.8 | 0.017 | 89 | 143 |
| E228928 | +40 4117 | | 20 16.0 | +40 20 | 45.8 | + 1.7 | 53.8 | <003 | .... | .... |
| E228929 | +39 4136 | | 20 16.0 | +39 36 | 45.2 | + 1.3 | 53.8 | 0.058 | 51 | 105 |
| | +38 4017 | | 20 16.4 | +38 39 | 44.5 | + 0.7 | 53.7 | 0.015 | 172 | 46 |
| E228969 | +38 4018 | | 20 16.5 | +38 21 | 44.3 | + 0.5 | 53.7 | 0.026 | 174 | 48 |
| E228989 | +38 4025 | | 20 16.7 | +38 23 | 44.4 | + 0.5 | 53.7 | 0.031 | 170 | 44 |
| E229033 | +37 3898 | | 20 17.2 | +37 25 | 43.6 | - 0.2 | 53.6 | 0.019 | 82 | 136 |
| | +36 4022 | | 20 17.3 | +36 29 | 42.9 | - 0.7 | 53.6 | 0.057 | 65 | 119 |
| E229049 | +38 4031 | | 20 17.4 | +38 42 | 44.7 | + 0.6 | 53.6 | 0.033 | 14 | 68 |
| E229059 | +36 4024 | | 20 17.5 | +37 05 | 43.4 | - 0.4 | 53.5 | 0.045 | 59 | 113 |
| | +37 3901 | | 20 17.7 | +37 32 | 43.8 | - 0.2 | 53.5 | 0.015 | 69 | 123 |
| | +45 3149 | | 20 17.9 | +45 44 | 50.4 | + 4.6 | 53.7 | 0.032 | 163 | 37 |

TABLE 1 (Cont'd)

| Star | | | 1900 | | l | b | $\phi$ | p | $\theta$ | $\theta'$ |
|---|---|---|---|---|---|---|---|---|---|---|
| HD | BD | Other Designation | $\alpha$ | $\delta$ | | | | | | |
| | +38°4036 | | 20h18m.2 | +38°18' | 44.4 | + 0.2 | 53.4 | 0.032 | 23° | 76° |
| E229108 | +38 4038 | | 20 18.3 | +39 08 | 45.1 | + 0.7 | 53.4 | 0.093 | 51 | 104 |
| E229115 | +34 3992 | | 20 18.4 | +34 55 | 41.8 | - 1.9 | 53.4 | 0.065 | 24 | 77 |
| | +38 4043 | | 20 18.7 | +38 24 | 44.6 | + 0.2 | 53.4 | 0.030 | 50 | 103 |
| | +38 4044 | | 20 18.7 | +38 35 | 44.7 | + 0.3 | 53.4 | 0.049 | 43 | 96 |
| | | No. 14, Ref. 3 | 20 19.2 | +39 10 | 45.3 | + 0.5 | 53.3 | 0.022 | 115 | 168 |
| 194205 | +38 4053 | | 20 19.3 | +39 02 | 45.2 | + 0.4 | 53.3 | 0.075 | 61 | 114 |
| | +38 4054 | | 20 19.5 | +38 50 | 45.0 | + 0.3 | 53.2 | 0.069 | 73 | 126 |
| 194280 | +38 4057 | | 20 19.7 | +38 37 | 44.9 | + 0.1 | 53.2 | 0.094 | 65 | 118 |
| E229196 | +40 4147 | | 20 19.7 | +40 34 | 46.4 | + 1.3 | 53.2 | 0.043 | 156 | 29 |
| | +36 4049 | | 20 19.8 | +36 36 | 43.3 | - 1.1 | 53.2 | 0.008 | 81 | 134 |
| | | No. 16, Ref. 3 | 20 19.8 | +39 02 | 45.2 | + 0.4 | 53.2 | 0.121 | 56 | 109 |
| E229202 | +39 4162 | | 20 19.8 | +39 50 | 45.9 | + 0.8 | 53.2 | 0.011 | 109 | 162 |
| E229214 | +36 4050 | | 20 20.0 | +36 12 | 43.0 | - 1.4 | 53.2 | 0.037 | 38 | 91 |
| | | No. 17, Ref 3 | 20 20.5 | +39 20 | 45.6 | + 0.4 | 53.1 | 0.059 | 27 | 80 |
| | +39 4168 | | 20 20.7 | +39 26 | 45.6 | + 0.5 | 53.0 | 0.043 | 4 | 57 |
| | +37 3927 | | 20 21.3 | +37 09 | 43.9 | - 1.0 | 53.0 | 0.029 | 61 | 114 |
| | | No. 19, Ref. 3 | 20 21.3 | +39 08 | 45.5 | + 0.2 | 53.0 | 0.089 | 55 | 108 |
| 194649 | +39 4177 | | 20 21.7 | +39 54 | 46.1 | + 0.6 | 52.9 | 0.014 | 22 | 75 |
| | +36 4063 | | 20 21.9 | +37 03 | 43.9 | - 1.2 | 52.9 | 0.099 | 49 | 102 |
| | +40 4179 | | 20 24.1 | +40 16 | 46.7 | + 0.4 | 52.5 | 0.020 | 20 | 72 |
| 195213 | +40 4187 | | 20 24.9 | +40 28 | 47.0 | + 0.4 | 52.4 | 0.019 | 68 | 120 |
| 195229 | +41 3765 | | 20 25.0 | +41 40 | 47.9 | + 1.2 | 52.4 | 0.032 | 52 | 104 |
| | +46 2948 | | 20 26.1 | +46 19 | 51.7 | + 3.8 | 52.4 | 0.046 | 6 | 58 |
| | +40 4212 | | 20 28.0 | +40 52 | 47.6 | + 0.2 | 51.9 | 0.130 | 106 | 158 |
| | +40 4219 | | 20 28.6 | +41 06 | 47.9 | + 0.3 | 51.8 | 0.051 | 78 | 130 |
| | +40 4220 | | 20 28.8 | +40 58 | 47.8 | + 0.2 | 51.8 | 0.083 | 80 | 132 |
| | +40 4227 | | 20 29.6 | +40 58 | 47.9 | 0.0 | 51.6 | 0.023 | 86 | 138 |
| | +41 3804 | | 20 30.2 | +41 12 | 48.2 | + 0.1 | 51.5 | 0.008 | 51 | 103 |
| | +45 3216 | | 20 30.5 | +45 19 | 51.4 | + 2.6 | 51.6 | 0.021 | 17 | 69 |
| | +41 3807 | | 20 30.6 | +41 16 | 48.3 | + 0.1 | 51.4 | 0.075 | 159 | 30 |
| | +45 3230 | | 20 33.9 | +45 47 | 52.2 | + 2.5 | 51.0 | 0.072 | 177 | 48 |
| | +47 3162 | | 20 36.8 | +47 44 | 54.0 | + 3.3 | 50.5 | 0.042 | 75 | 125 |
| | +45 3246 | | 20 39.1 | +45 32 | 52.4 | + 1.7 | 50.2 | <003 | .... | .... |
| | +45 3260 | | 20 42.2 | +45 58 | 53.2 | + 1.5 | 49.5 | 0.035 | 21 | 71 |
| | | No. 44, Ref. 1 | 20 48.2 | +45 39 | 53.7 | + 0.5 | 48.4 | 0.050 | 9 | 57 |
| | +47 3211 | | 20 49.7 | +47 33 | 55.2 | + 1.5 | 48.2 | 0.068 | 10 | 58 |
| | +44 3627 | | 20 51.3 | +44 28 | 53.2 | - 0.7 | 47.9 | 0.017 | 46 | 94 |
| | +45 3339 | | 20 53.2 | +45 58 | 54.5 | 0.0 | 47.6 | 0.053 | 29 | 77 |
| | | No. 4, Ref. 1 | 21 01.4 | +47 33 | 56.6 | + 0.1 | 46.1 | 0.039 | 33 | 79 |
| | +45 3406 | | 21 03.0 | +45 27 | 55.3 | - 1.4 | 45.8 | 0.048 | 48 | 94 |
| | +47 3302 | | 21 05.0 | +47 16 | 56.8 | - 0.5 | 45.4 | 0.026 | 0 | 45 |
| | +44 3731 | | 21 07.8 | +45 05 | 55.7 | - 2.4 | 44.8 | 0.036 | 26 | 71 |
| | | No. 7, Ref. 1 | 21 10.1 | +48 00 | 58.0 | - 0.6 | 44.4 | 0.044 | 10 | 54 |
| | +47 3421 | | 21 25.0 | +47 37 | 59.5 | - 2.6 | 41.6 | <005 | .... | .... |
| | | No. 1, Ref. 4 | 21 32.2 | +54 48 | 65.1 | + 2.1 | 40.2 | 0.079 | 26 | 66 |
| | | No. 9, Ref. 1 | 21 36.5 | +49 56 | 62.6 | - 2.1 | 39.4 | 0.044 | 52 | 91 |
| | +56 2626 | | 21 38.4 | +56 15 | 66.7 | + 2.6 | 39.0 | 0.048 | 20 | 59 |
| | +56 2640 | | 21 43.1 | +56 27 | 67.3 | + 2.4 | 38.0 | 0.034 | 23 | 61 |
| | +54 2623 | | 21 43.5 | +54 52 | 66.4 | + 1.1 | 37.9 | 0.059 | 23 | 61 |
| | +54 2629 | | 21 44.2 | +54 52 | 66.4 | + 1.0 | 37.8 | 0.048 | 22 | 60 |
| | | No. 6, Ref. 4 | 21 45.0 | +55 43 | 67.1 | + 1.6 | 37.6 | 0.043 | 19 | 57 |
| | | No. 47, Ref. 1 | 21 50.2 | +53 45 | 66.5 | - 0.4 | 36.6 | 0.054 | 72 | 109 |
| | +58 2373 | | 21 58.1 | +59 01 | 70.4 | + 3.2 | 35.0 | 0.075 | 41 | 76 |
| | +54 2676 | | 21 59.7 | +54 37 | 67.1 | - 0.5 | 34.6 | 0.060 | 65 | 100 |

TABLE 1 (Cont'd)

| Star | | | 1900 | | l | b | $\phi$ | p | $\theta$ | $\theta'$ |
|---|---|---|---|---|---|---|---|---|---|---|
| HD | BD | Other Designation | $\alpha$ | $\delta$ | | | | | | |
| | +53°2790 | | $22^h04^m3$ | +54°02' | 66.3 | - 1.3 | 33.7 | 0.070 | 40° | 74° |
| | | No. 12, Ref. 4 | 22 04.3 | +57 25 | 70.2 | + 1.5 | 33.7 | 0.088 | 38 | 72 |
| | +57 2465 | | 22 05.9 | +57 22 | 70.4 | + 1.3 | 33.4 | 0.097 | 41 | 74 |
| | | No. 49, Ref. 1 | 22 09.4 | +57 10 | 70.7 | + 0.9 | 32.6 | 0.079 | 45 | 78 |
| | +53 2820 | | 22 10.1 | +53 55 | 69.0 | - 1.9 | 32.5 | 0.049 | 49 | 81 |
| | | No. 50, Ref. 1 | 22 10.7 | +53 47 | 69.0 | - 2.1 | 32.4 | 0.028 | 68 | 100 |
| | +54 2718 | | 22 11.3 | +54 58 | 68.9 | - 1.1 | 32.2 | 0.060 | 56 | 88 |
| | | No. 17, Ref. 1 | 22 11.7 | +60 35 | 72.7 | + 3.6 | 32.2 | 0.006 | 100 | 132 |
| | | No. 52, Ref. 1 | 22 14.4 | +55 25 | 70.3 | - 1.0 | 31.6 | 0.102 | 45 | 77 |
| | +60 2380 | | 22 15.6 | +60 16 | 73.0 | + 3.1 | 31.4 | 0.008 | 168 | 19 |
| E239923 | +58 2421 | | 22 15.8 | +58 27 | 72.1 | + 1.5 | 31.3 | 0.069 | 54 | 85 |
| | | No. 18, Ref. 1 | 22 16.5 | +55 53 | 70.8 | - 0.7 | 31.2 | 0.094 | 58 | 89 |
| | +54 2745 | | 22 17.4 | +55 03 | 70.5 | - 1.5 | 31.0 | 0.069 | 53 | 84 |
| | | No. 20, Ref. 1 | 22 18.2 | +59 47 | 73.0 | + 2.5 | 30.8 | 0.060 | 114 | 145 |
| | | No. 21, Ref. 1 | 22 18.5 | +55 08 | 70.4 | - 1.5 | 30.8 | 0.073 | 48 | 79 |
| | +54 2761 | | 22 19.9 | +55 11 | 70.9 | - 1.6 | 30.5 | 0.065 | 48 | 78 |
| | | No. 55, Ref. 1 | 22 21.0 | +61 03 | 74.0 | + 3.4 | 30.3 | 0.033 | 94 | 124 |
| | +57 2525 | | 22 21.3 | +57 20 | 72.1 | + 0.2 | 30.2 | 0.046 | 43 | 73 |
| | +55 2748 | | 22 21.5 | +55 47 | 71.4 | - 1.2 | 30.1 | 0.073 | 53 | 83 |
| | +62 2078 | | 22 22.2 | +62 54 | 75.0 | + 4.9 | 30.1 | 0.152 | 74 | 104 |
| | | No. 21, Ref. 4 | 22 23.7 | +55 37 | 71.6 | - 1.5 | 29.7 | 0.064 | 52 | 82 |
| | +57 2536 | | 22 23.7 | +57 52 | 72.7 | + 0.5 | 29.6 | 0.064 | 37 | 67 |
| | | No. 25, Ref. 1 | 22 23.9 | +56 59 | 72.2 | - 0.3 | 29.6 | 0.078 | 37 | 67 |
| | | No. 22, Ref. 4 | 22 25.8 | +54 55 | 71.5 | - 2.2 | 29.2 | 0.061 | 59 | 88 |
| | | No. 23, Ref. 4 | 22 26.1 | +55 02 | 71.6 | - 2.1 | 29.2 | 0.085 | 61 | 90 |
| | | No. 58, Ref. 1 | 22 26.2 | +56 30 | 72.3 | - 0.9 | 29.1 | 0.048 | 59 | 88 |
| | | No. 24, Ref. 4 | 22 26.6 | +54 28 | 71.4 | - 2.7 | 29.1 | 0.058 | 61 | 90 |
| | | No. 59, Ref. 1 | 22 26.7 | +56 07 | 72.2 | - 1.2 | 29.0 | 0.034 | 62 | 91 |
| | | No. 25, Ref. 4 | 22 27.2 | +56 46 | 72.5 | - 0.7 | 28.9 | 0.086 | 49 | 78 |
| | +60 2405 | | 22 27.5 | +61 06 | 74.7 | + 3.1 | 28.9 | 0.055 | 88 | 117 |
| | | No. 26, Ref. 4 | 22 29.6 | +57 56 | 73.4 | + 0.2 | 28.4 | 0.095 | 50 | 78 |
| | +55 2770 | (Preceding) | 22 29.9 | +56 01 | 72.5 | - 1.5 | 28.4 | 0.070 | 60 | 88 |
| | +55 2770 | (Following) | 22 29.9 | +56 01 | 72.5 | - 1.5 | 28.4 | 0.070 | 60 | 88 |
| | +55 2771 | | 22 30.4 | +56 11 | 72.6 | - 1.4 | 28.2 | 0.075 | 62 | 90 |
| | | No. 62, Ref. 1 | 22 30.4 | +57 50 | 73.4 | 0.0 | 28.2 | 0.056 | 44 | 72 |
| | | No. 29, Ref. 4 | 22 33.8 | +57 50 | 73.8 | - 0.2 | 27.5 | 0.115 | 55 | 83 |
| | | No. 30, Ref. 4 | 22 33.9 | +57 37 | 73.7 | - 0.4 | 27.5 | 0.048 | 53 | 81 |
| | +57 2581 | | 22 36.1 | +57 54 | 74.1 | - 0.3 | 27.0 | 0.063 | 72 | 99 |
| | | No. 31, Ref. 4 | 22 36.5 | +58 25 | 74.4 | + 0.2 | 27.0 | 0.073 | 36 | 63 |
| | | No. 33, Ref. 4 | 22 39.2 | +58 01 | 74.6 | - 0.3 | 26.4 | 0.040 | 45 | 71 |
| | | No. 35, Ref. 4 | 22 39.7 | +57 31 | 74.4 | - 0.8 | 26.3 | 0.065 | 51 | 77 |
| | | No. 36, Ref. 4 | 22 40.3 | +56 03 | 73.8 | - 2.2 | 26.2 | 0.086 | 54 | 80 |
| | +57 2611 | | 22 43.4 | +57 58 | 75.0 | - 0.8 | 25.5 | 0.041 | 72 | 98 |
| | | No. 65, Ref. 1 | 22 43.8 | +56 45 | 74.6 | - 1.8 | 25.4 | 0.062 | 53 | 78 |
| | | No. 43, Ref. 4 | 22 44.3 | +57 00 | 74.7 | - 1.6 | 25.3 | 0.042 | 63 | 88 |
| | | No. 44, Ref. 4 | 22 44.4 | +57 58 | 75.2 | - 0.6 | 25.3 | 0.052 | 65 | 90 |
| | | No. 45, Ref. 4 | 22 46.2 | +56 36 | 74.8 | - 2.0 | 24.9 | 0.049 | 59 | 84 |
| | +58 2520 | | 22 55.9 | +58 45 | 76.8 | - 0.6 | 22.8 | 0.050 | 69 | 92 |
| | +57 2678 | | 22 59.4 | +57 46 | 76.9 | - 1.7 | 22.0 | 0.063 | 64 | 86 |
| | +58 2549 | | 23 04.5 | +58 35 | 77.8 | - 1.2 | 20.9 | 0.097 | 75 | 96 |
| | +60 2493 | | 23 05.4 | +60 56 | 78.8 | + 1.0 | 20.8 | 0.070 | 106 | 127 |
| | +57 2700 | | 23 05.7 | +57 36 | 77.6 | - 2.1 | 20.7 | 0.047 | 66 | 87 |
| | | No. 53, Ref. 4 | 23 06.2 | +56 45 | 77.4 | - 3.0 | 20.6 | 0.037 | 57 | 78 |
| | | No. 67, Ref. 1 | 23 07.0 | +59 13 | 78.4 | - 0.7 | 20.4 | 0.018 | 63 | 83 |
| | +59 2664 | | 23 07.0 | +60 03 | 78.6 | + 0.1 | 20.4 | 0.066 | 67 | 87 |

TABLE 1 (Cont'd)

| Star | | | 1900 | | l | b | $\phi$ | p | $\theta$ | $\theta'$ |
|---|---|---|---|---|---|---|---|---|---|---|
| HD | BD | Other Designation | $\alpha$ | $\delta$ | | | | | | |
| | | No. 30, Ref. 1 | $23^h10^m5$ | +59°01' | 78.7 | - 1.0 | 19.6 | 0.047 | 84° | 104° |
| | | No. 54, Ref. 4 | 23 10.5 | +59 24 | 78.8 | - 0.6 | 19.6 | 0.046 | 73 | 93 |
| | +61°2408 | | 23 11.1 | +61 32 | 79.6 | + 1.3 | 19.5 | 0.072 | 93 | 113 |
| | | No. 55, Ref. 4 | 23 12.0 | +59 55 | 79.2 | - 0.2 | 19.3 | 0.048 | 82 | 101 |
| | | No. 32, Ref. 1 | 23 12.8 | +61 20 | 79.7 | + 1.1 | 19.2 | 0.051 | 105 | 124 |
| | | No. 68, Ref. 1 | 23 13.0 | +59 29 | 79.2 | - 0.7 | 19.1 | 0.008 | 39 | 58 |
| | +58 2580 | | 23 16.7 | +58 25 | 79.3 | - 1.8 | 18.3 | 0.094 | 75 | 93 |
| | +59 2707 | | 23 17.7 | +59 49 | 79.8 | - 0.6 | 18.1 | 0.028 | 76 | 94 |
| | +60 2527 | | 23 17.9 | +60 29 | 80.0 | + 0.1 | 18.0 | 0.019 | 27 | 45 |
| | | No. 70, Ref. 1 | 23 18.4 | +61 35 | 80.5 | + 1.1 | 17.9 | 0.065 | 86 | 104 |
| | | No. 60, Ref. 4 | 23 19.8 | +59 03 | 79.8 | - 1.4 | 17.6 | 0.056 | 116 | 134 |
| | | No. 61, Ref. 4 | 23 20.1 | +59 23 | 80.0 | - 1.1 | 17.6 | 0.056 | 98 | 116 |
| | +59 2719 | | 23 20.9 | +60 06 | 80.2 | - 0.4 | 17.4 | 0.037 | 136 | 153 |
| | +60 2553 | | 23 24.1 | +60 45 | 80.9 | + 0.1 | 16.7 | 0.028 | 72 | 89 |
| | +59 2735 | | 23 25.5 | +59 18 | 80.6 | - 1.3 | 16.4 | 0.100 | 63 | 79 |
| | +60 2584 | | 23 31.0 | +60 38 | 81.6 | - 0.2 | 15.2 | 0.049 | 59 | 74 |
| | | No. 36, Ref. 1 | 23 38.6 | +60 57 | 82.6 | - 0.2 | 13.5 | 0.062 | 62 | 76 |
| | +61 2515 | | 23 40.9 | +61 43 | 83.0 | + 0.5 | 13.0 | 0.061 | 84 | 97 |
| | | No. 38, Ref. 1 | 23 51.7 | +60 40 | 84.1 | - 0.8 | 10.6 | 0.054 | 89 | 100 |
| | | No. 39, Ref. 1 | 23 53.7 | +60 36 | 84.4 | - 0.9 | 10.2 | 0.046 | 85 | 95 |

It is a pleasure to thank Srtas. González and Srs. Iriarte and Chavira for their lists and identification charts of early-type stars in advance of publication; Miss Barbara Perkins for much of the computations in the reductions of the observations; and the National Science Foundation for financial support.

## REFERENCES

González, G., and González, G. 1952, *Bol. Obs. Ton. y Tac.*, No. 5, pp. 1–7.
———. 1953, *ibid.*, No. 7, pp. 3–10.
Hiltner, W. A. 1951, *Ap. J.*, **114**, 241–271.
Iriarte, Braulio, and Chavira, Enrique. 1954, *Bol. Obs. Ton. y Tac.*, No. 9, pp. 41–45.
Münch, Luis. 1953, *Bol. Obs. Ton. y Tac.*, No. 7, pp. 23–32.
Nassau, J. J., and Harris, Daniel III, 1952, *Ap. J.* **115**, 459–474.
Ohlsson, John. 1932, *Ann. Obs. Lund*, No. 3, pp. 1–147.

# A STUDY OF THE DISTRIBUTION OF RELATIVELY COOL STARS IN THE MILKY WAY

J. J. NASSAU AND V. M. BLANCO
Warner and Swasey Observatory, Case Institute of Technology, Cleveland, Ohio
*Received July 12, 1954*

ABSTRACT

Infrared objective-prism plates have been employed in the study of the distribution of relatively cool stars within a 4°-wide zone centered at the galactic equator and extending from $l = 333°$ to $l = 201°$. A similar study was carried out in regions at right angles to the galactic equator to $\pm 18°$ latitude at intervals of 21° in longitude. The survey includes stars of spectral classes M5 or later, N, R, and S, as well as highly reddened M0–M4 stars. The limiting infrared magnitude of the survey is about 10. The number of late M stars shows a uniform decrease without clusterings from the galactic center to the anti-center, except in regions of heavy obscurations. These stars also show a marked latitude effect. Their distribution suggests that the majority of these stars are components of the galactic disk. The carbon stars show clusterings, and they appear less numerous in the direction of the galactic center, while their galactic concentration is higher. The N stars appear to be spiral-arm objects. The S stars as well as the reddened early M stars appear in groups which in some cases agree in position with previously known concentrations of OB stars.

## I. INTRODUCTION

The present investigation deals with the study of the distribution of relatively cool stars in a belt 4° wide along the galactic equator from longitude 333° through zero to 201°. A similar study has been carried out in regions at right angles to the galactic equator to $\pm 18°$ latitude at intervals of 21° in longitude from $l = 342°$ to $l = 171°$.

The two surveys are limited to the late M-type stars beginning with M5. This spectral class forms a convenient division, inasmuch as it is fairly easy to identify. Among these stars, however, a significant number show *VO* bands in their spectra (Nassau and Cameron 1954), and, since they prove to be variable, they are included in a brief separate discussion. Similarly N, R, and S stars and highly reddened early M stars are considered separately. The complete data for these stars which are in the galactic zone have been published elsewhere (Nassau and Blanco 1954*a*, *b*; Nassau, Blanco, and Morgan 1954). Table 1 gives the number of stars of each type on which the present discussion is based.

TABLE 1

NUMBER OF STARS IN THE TWO SURVEYS

| | | | |
|---|---|---|---|
| Late M stars | 6637 | Reddened early M stars | 120 |
| Carbon stars | 422 | S stars | 31 |

## II. THE SPECTRAL PLATES COVERING THE REGION OF THE SURVEY

To cover the equatorial galactic zone, 65 plates were taken with distance between the centers of 3°.5. The plates are circular, with a diameter of 5°.2. The distance between plate centers for the zones to latitudes $\pm 18°$ was 4°. Eight plates were needed to cover each latitude zone. The Lund pole (Ohlsson 1932) was used in defining the galactic equator. Nearly all plates were taken within 1 hour of the meridian with the telescope unguided. This method yielded the desirable narrow spectra. With the exception of regions of declination $-10°$ or less, all exposures were of 5 minutes' duration.

## III. SPECTRA

The surveys were carried out with the 2° objective prism of the Burrell telescope with Kodak 1-N emulsion and No. 89 Wratten filter. Thus the spectral region is limited from

about λ 6800 to λ 8800. The dispersion at the telluric A band, which divides the spectrum into two nearly equal parts, is 3400 A/mm. The recognition of a spectrum belonging to the late M group and its classification presents, in general, no serious difficulties and follows our previously established system (Nassau and van Albada 1949). At M5 the *TiO* band heads at λ 7054 and λ 7589 are strong, with λ 8432 just beginning to appear. Dense spectra, for which the bands are not clearly visible, are classified by comparing their appearance with overexposed spectra of known late M-type stars. For faint spectral images the selection was limited to stars within 0.5 mag. of the faintest image just visible. The survey, however, cannot be said to be complete, particularly on account of the presence of variables which at the time of the exposure may have been earlier than M5 or fainter than the limit of the plate.

## IV. MAGNITUDES

With the exception of the brightest stars, no attempt was made to determine the magnitudes of the stars in the survey. It is estimated that the limiting infrared magnitude of the survey is 10.2. For the bright stars the magnitudes were estimated from the density of the spectra as described in a previous paper (Nassau and Blanco 1954*a*). All plates were taken and treated with the usual precautions, in order to achieve uniformity. Checks on the uniformity of the plates were made with the following methods: (*a*) the generous overlaps between plates; (*b*) the spectral and magnitude data of the LF regions (McCuskey and Seyfert 1947), which are located at approximately regular intervals in the Milky Way; and (*c*) the magnitude of the BD stars. It is estimated that the limiting magnitude of the plates is not uncertain by more than 0.4 mag. Plates deviating by more than this amount were repeated. The quality of the plates was uniformly good except for those taken south of declination −10°.

The latitude zones were treated as far as possible in the same manner, although the spectral and magnitude data of the LF regions were not available for these zones. The symmetry obtained in the number of stars counted at corresponding latitudes north and south of the galactic equator may be considered an index of uniformity.

## V. THE SURVEY OF THE GALACTIC BELT

The selection of late M stars in the central zone was made independently by the two authors. Disagreements were accidental and of the order of 5–20 per cent, depending on the plate quality. In the higher-latitude belts, where this precaution was not taken, alternate plates were examined by the same person, and the overlap areas provided sufficient controls. The counts of the stars in the central zones are given in Table 2. The first column gives the galactic longitude of the center of each square of 4° × 4°. The second column gives the number of late M stars in each square.

A study of the surface distribution of these stars indicates a marked absence of clustering. In general, a uniform and gradual change in the number of stars is present, affected only by the Milky Way obscurations. This is well illustrated in Figures 1 and 2, where the background material was copied from Becvar's *Atlas of the Heavens*. The boundaries of the diffuse nebulae are presented by heavy dashes and those of dark nebulae by continuous fine lines. The boundaries of the Milky Way are indicated by continuous heavy lines. These features might be in error by 0°.3, owing to the method of copying. The obscuration between $l = 44°$ and $l = 52°$ produces a marked discontinuity, while in the region between $l = 60°$ and $l = 80°$ the stars appear more uniform. In these regions a gradual diminution of stars may be noticed with increasing longitude. This gradual longitude effect in the number of M stars stands out clearly from longitude 335° to the galactic anticenter if the star counts are made only in relatively clear regions. The presence of the Great Rift between $l = 345°$ and $l = 30°$, however, affects greatly the numbers presented in Table 2. If the star counts are limited to the clearest regions, five times as many stars are observed toward the galactic center as toward the anticenter. The

TABLE 2

DISTRIBUTION OF RELATIVELY COOL STARS ALONG GALACTIC EQUATOR

| Long. | Late M's | N | R | C | Reddened Early M's | S Stars |
|---|---|---|---|---|---|---|
| 335° | 118 | 2 | 0 | 0 | 0 | 0 |
| 339 | 110 | 1 | 1 | 0 | 0 | 1 |
| 343 | 97 | 4 | 2 | 0 | 5 | 2 |
| 347 | 90 | 1 | 0 | 0 | 3 | 0 |
| 351 | 111 | 5 | 1 | 1 | 1 | 1 |
| 355 | 114 | 2 | 0 | 0 | 0 | 4 |
| 359 | 58 | 1 | 0 | 3 | 1 | 0 |
| 3 | 37 | 1 | 1 | 0 | 2 | 0 |
| 7 | 46 | 1 | 1 | 0 | 3 | 1 |
| 11 | 87 | 1 | 0 | 0 | 2 | 2 |
| 15 | 85 | 3 | 0 | 0 | 1 | 0 |
| 19 | 63 | 2 | 0 | 1 | 1 | 0 |
| 23 | 58 | 0 | 1 | 0 | 1 | 1 |
| 27 | 73 | 0 | 0 | 0 | 0 | 1 |
| 31 | 101 | 4 | 1 | 0 | 1 | 3 |
| 35 | 118 | 4 | 0 | 2 | 4 | 0 |
| 39 | 96 | 6 | 0 | 0 | 1 | 0 |
| 43 | 59 | 2 | 4 | 0 | 5 | 1 |
| 47 | 18 | 1 | 0 | 0 | 4 | 1 |
| 51 | 15 | 2 | 1 | 1 | 1 | 0 |
| 55 | 123 | 5 | 5 | 0 | 1 | 3 |
| 59 | 96 | 4 | 0 | 0 | 0 | 1 |
| 63 | 75 | 4 | 0 | 0 | 0 | 1 |
| 67 | 95 | 12 | 1 | 1 | 0 | 0 |
| 71 | 103 | 6 | 1 | 0 | 1 | 0 |
| 75 | 50 | 11 | 1 | 1 | 7 | 0 |
| 79 | 45 | 1 | 0 | 0 | 9 | 2 |
| 83 | 58 | 7 | 0 | 0 | 2 | 2 |
| 87 | 45 | 4 | 2 | 0 | 0 | 0 |
| 91 | 53 | 5 | 2 | 1 | 2 | 2 |
| 95 | 36 | 6 | 3 | 0 | 1 | 2 |
| 99 | 28 | 2 | 0 | 2 | 3 | 0 |
| 103 | 30 | 0 | 0 | 2 | 3 | 0 |
| 107 | 28 | 3 | 3 | 0 | 4 | 0 |
| 111 | 11 | 0 | 0 | 1 | 5 | 0 |
| 115 | 13 | 2 | 2 | 0 | 1 | 0 |
| 119 | 15 | 4 | 1 | 0 | 0 | 0 |
| 123 | 28 | 3 | 2 | 2 | 0 | 0 |
| 127 | 20 | 3 | 1 | 0 | 3 | 0 |
| 131 | 33 | 13 | 0 | 2 | 3 | 0 |
| 135 | 22 | 5 | 1 | 1 | 0 | 0 |
| 139 | 23 | 2 | 1 | 1 | 0 | 0 |
| 143 | 23 | 9 | 1 | 0 | 0 | 0 |
| 147 | 14 | 4 | 1 | 1 | 1 | 0 |
| 151 | 23 | 3 | 0 | 1 | 1 | 0 |
| 155 | 42 | 3 | 2 | 0 | 0 | 0 |
| 159 | 35 | 1 | 0 | 0 | 1 | 0 |
| 163 | 26 | 1 | 0 | 1 | 2 | 0 |
| 167 | 28 | 0 | 0 | 2 | 1 | 0 |
| 171 | 25 | 6 | 0 | 0 | 0 | 0 |
| 175 | 15 | 0 | 0 | 1 | 0 | 0 |
| 179 | 21 | 5 | 0 | 0 | 0 | 0 |
| 183 | 23 | 1 | 1 | 0 | 0 | 0 |
| 187 | 47 | 3 | 1 | 1 | 0 | 0 |
| 191 | 39 | 3 | 0 | 3 | 1 | 0 |
| 195 | 28 | 4 | 0 | 0 | 0 | 0 |
| 199 | 37 | 6 | 0 | 0 | 0 | 0 |

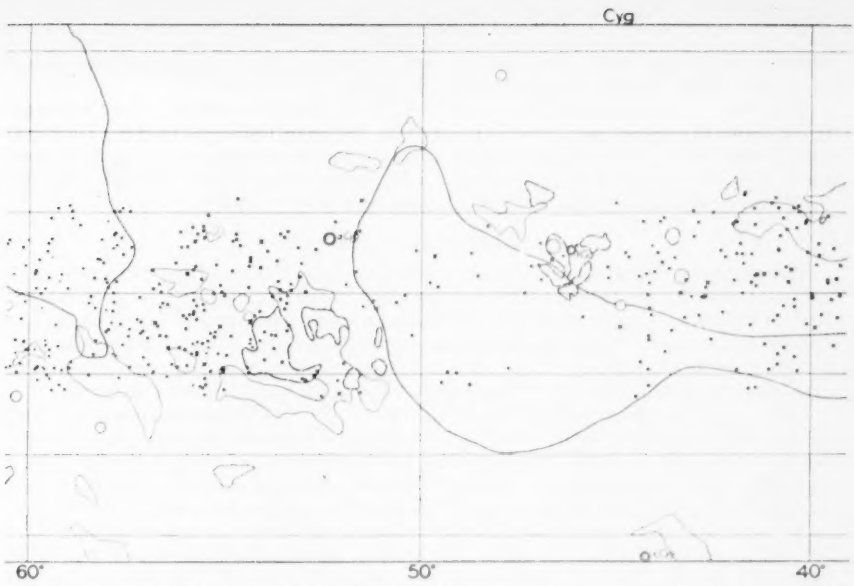


FIG. 1.—Plot of late M stars (*dots*) from longitude 40° to 60° and between ± 2° of the galactic equator

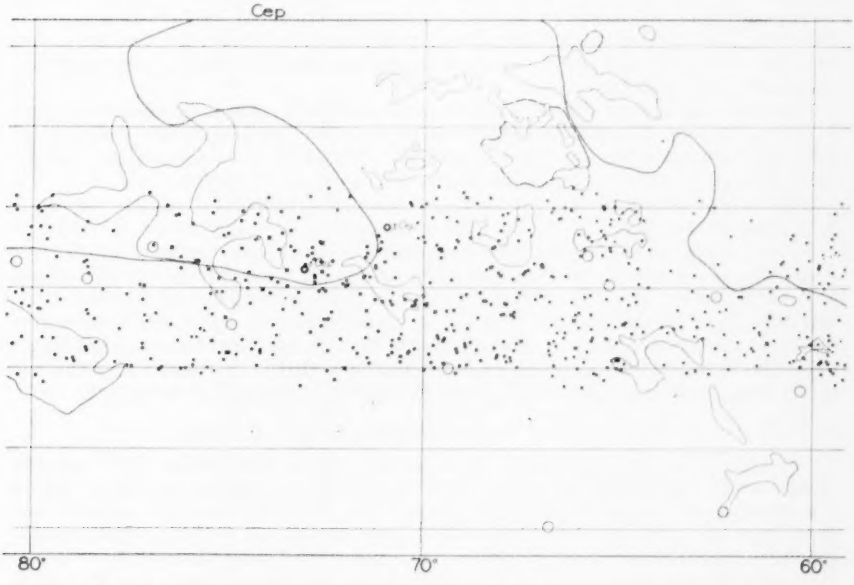


FIG. 2.—Plot of late M stars (*dots*) from longitude 60° to 80° and between ± 2° of the galactic equator

high-latitude plates, which are to be discussed later, also show the gradual diminution of M stars as the longitudes approach the anticenter.

The total number of stars in the zone is 3010. Approximate infrared magnitudes up to 8.2 were determined for the brighter stars in the group. Among the 384 such stars, about one-third are in the BD catalogue, while the rest are fainter. A catalogue of these stars, with their approximate magnitudes and spectral classes with sufficient data for their identification has been published (Nassau and Blanco 1954*a*).

## VI. GALACTIC-LATITUDE REGIONS

The positions of the higher-latitude regions as well as the method of securing the necessary data for the late M stars were described earlier. The limiting infrared magnitude of this survey is also about 10.2 The data for these stars are given in Table 3. The first column gives the longitude, the second the latitude of the center of each plate, and the third the number of late M stars within the area of each plate. For completeness the counts of the plate of the central zone nearest the given longitude are also given.

Here again the effect of obscuration is apparent. When interstellar absorption does not seriously affect the counts, a fairly good symmetry with respect to the galactic equator is shown by the uniform decrease in the number of stars per plate as the latitude of its center increases (see Fig. 3, *a*). At high latitudes, where the effect of absorption is not serious, the decrease in the number of M's toward the anticenter is clearly shown.

A grouping of the data of Table 3 for all latitudes and for the various longitudes (first column) is given in Table 4. A reasonably smooth distribution gradually decreasing in numbers from $l = 3°$ to the anticenter of the galaxy is apparent. The deficiency in the number of late M's at $l = 108°$ is believed to be due partly to obscuration at this longitude. A more serious deficiency exists at $l = 342°$, which may be attributed to obscuration as well as to poorer-quality plates for this low-declination region.

The regrouping of the same material for all longitudes and at the various latitudes is shown in Table 5. The first column gives the latitude; the second, the number of late M's; and the third, their percentage at different latitudes. The effect of obscuration at the central zone is clearly shown.

The relatively smooth surface distribution of the late M stars is illustrated in Figure 4. Here a number of overlapping plates are shown, covering an area of approximately 400 square degrees in the vicinity of longitude 7°. The effect of the obscuration near the galactic equator, as well as the latitude effect, is shown clearly in this figure.

As has been stated, the surveys were carried out with plates of 5 minutes' exposure. A hypersensitized plate with an exposure of 30 minutes was taken at $l = 66°$ and $b = -16°$ with an estimated limiting infrared magnitude of 13.5. The number of late M stars found was 42, while the short-exposure plate yielded 33. A similar test was carried out at $l = 6°.5$ and $b = -16°$. Here the long-exposure plate yielded 184, and the short-exposure only 30. At the galactic pole, within an area of 50 square degrees, 5 late M stars were found, on short as well as long exposures. No additional stars were found with still longer exposures of 60 minutes' duration on hypersensitized plates. This is also an indication of the small number of dwarfs which may be present to the limit of the survey.

## VII. THE GALACTIC DISTRIBUTION OF LATE M STARS

The data presented may be used to deduce the galactic distribution of the majority of M stars studied in this survey. It should be pointed out that on the clearer regions the extent of the survey in distance is about 4 kpc. The longitude effect suggests that these stars are very numerous toward the galactic center and that their space density gradually diminishes with distance from the center of the Galaxy. In a study of late M stars with long-exposure plates in the large Sagittarius Cloud, Nassau and McCuskey (1954) have verified the continued increase in the number of these stars to a distance reaching the center of the Galaxy.

TABLE 3

NUMBER OF STARS IN ZONES 5° WIDE AND PERPENDICULAR TO GALACTIC EQUATOR

| Long. | Lat. | Late M's | M's with *VO* | Carbons N | Carbons R | Carbons C | Reddened Early M's |
|---|---|---|---|---|---|---|---|
| 342° | +16° | 8 | 1 | 0 | 0 | 0 | 0 |
| | +12 | 15 | 0 | 0 | 0 | 0 | 0 |
| | + 8 | 26 | 2 | 0 | 0 | 0 | 0 |
| | + 4 | 42 | 1 | 2 | 0 | 0 | 1 |
| | 0 | 168 | 13 | 5 | 1 | 0 | 5 |
| | − 4 | 122 | 10 | 1 | 2 | 0 | 2 |
| | − 8 | 55 | 4 | 0 | 0 | 0 | 1 |
| | −12 | 15 | 0 | 1 | 0 | 0 | 0 |
| | −16 | 12 | 0 | 0 | 0 | 0 | 0 |
| 3° | +16 | 46 | 2 | 0 | 0 | 0 | 0 |
| | +12 | 80 | 5 | 0 | 1 | 0 | 0 |
| | + 8 | 82 | 1 | 0 | 0 | 0 | 0 |
| | + 4 | 240 | 9 | 1 | 1 | 0 | 0 |
| | 0 | 41 | 7 | 2 | 1 | 0 | 3 |
| | − 4 | 188 | 7 | 0 | 0 | 0 | 3 |
| | − 8 | 90 | 3 | 0 | 1 | 0 | 2 |
| | −12 | 72 | 5 | 1 | 0 | 0 | 0 |
| | −16 | 61 | 4 | 0 | 0 | 0 | 0 |
| 24° | +16 | 19 | 3 | 1 | 0 | 0 | 0 |
| | +12 | 42 | 4 | 0 | 0 | 0 | 0 |
| | + 8 | 71 | 5 | 1 | 0 | 0 | 0 |
| | + 4 | 92 | 3 | 1 | 2 | 0 | 1 |
| | 0 | 75 | 9 | 0 | 1 | 0 | 1 |
| | − 4 | 79 | 1 | 3 | 0 | 0 | 1 |
| | − 8 | 112 | 5 | 0 | 0 | 0 | 0 |
| | −12 | 79 | 5 | 0 | 0 | 0 | 0 |
| | −16 | 37 | 5 | 0 | 0 | 0 | 0 |
| 45° | +16 | 22 | 1 | 0 | 0 | 0 | 0 |
| | +12 | 38 | 3 | 2 | 0 | 0 | 0 |
| | + 8 | 57 | 3 | 3 | 0 | 0 | 0 |
| | + 4 | 78 | 8 | 2 | 2 | 1 | 0 |
| | 0 | 54 | 9 | 3 | 2 | 0 | 8 |
| | − 4 | 32 | 2 | 1 | 1 | 0 | 3 |
| | − 8 | 98 | 12 | 2 | 0 | 0 | 0 |
| | −12 | 63 | 3 | 1 | 0 | 0 | 0 |
| | −16 | 35 | 3 | 0 | 0 | 0 | 0 |
| 66° | +16 | 27 | 3 | 0 | 0 | 0 | 1 |
| | +12 | 21 | 1 | 0 | 0 | 0 | 0 |
| | + 8 | 44 | 4 | 1 | 1 | 0 | 0 |
| | + 4 | 35 | 1 | 8 | 0 | 1 | 0 |
| | 0 | 128 | 14 | 13 | 1 | 1 | 0 |
| | − 4 | 73 | 7 | 2 | 2 | 1 | 0 |
| | − 8 | 61 | 6 | 2 | 0 | 0 | 0 |
| | −12 | 49 | 3 | 1 | 0 | 0 | 0 |
| | −16 | 33 | 4 | 0 | 0 | 0 | 0 |
| 87° | +16 | 14 | 1 | 0 | 0 | 0 | 0 |
| | +12 | 33 | 2 | 0 | 0 | 0 | 0 |
| | + 8 | 36 | 4 | 1 | 2 | 0 | 0 |
| | + 4 | 54 | 3 | 6 | 2 | 1 | 3 |
| | 0 | 58 | 6 | 7 | 3 | 0 | 0 |
| | − 4 | 103 | 6 | 6 | 1 | 0 | 2 |
| | − 8 | 35 | 2 | 1 | 1 | 0 | 0 |
| | −12 | 26 | 0 | 1 | 0 | 0 | 0 |
| | −16 | 13 | 2 | 1 | 0 | 0 | 0 |

TABLE 3—*Continued*

| Long. | Lat. | Late M's | M's with *VO* | Carbons N | R | C | Reddened Early M's |
|---|---|---|---|---|---|---|---|
| 108° | +16 | 13 | 3 | 1 | 0 | 0 | 0 |
| | +12 | 17 | 4 | 0 | 0 | 0 | 0 |
| | + 8 | 23 | 1 | 1 | 1 | 0 | 0 |
| | + 4 | 41 | 7 | 1 | 1 | 2 | 4 |
| | 0 | 11 | 2 | 1 | 3 | 0 | 5 |
| | − 4 | 55 | 3 | 1 | 1 | 0 | 0 |
| | − 8 | 31 | 4 | 0 | 3 | 0 | 0 |
| | −12 | 13 | 2 | 2 | 0 | 0 | 0 |
| | −16 | 11 | 0 | 0 | 0 | 0 | 0 |
| 129° | +16 | 28 | 1 | 0 | 1 | 0 | 0 |
| | +12 | 32 | 7 | 2 | 0 | 0 | 0 |
| | + 8 | 55 | 11 | 2 | 1 | 0 | 0 |
| | + 4 | 38 | 0 | 5 | 0 | 0 | 0 |
| | 0 | 31 | 5 | 10 | 0 | 2 | 4 |
| | − 4 | 38 | 4 | 5 | 3 | 1 | 2 |
| | − 8 | 61 | 4 | 3 | 0 | 0 | 1 |
| | −12 | 23 | 2 | 0 | 0 | 0 | 0 |
| | −16 | 22 | 5 | 0 | 0 | 0 | 0 |
| 150° | +16 | 10 | 0 | 1 | 0 | 0 | 0 |
| | +12 | 22 | 9 | 1 | 0 | 0 | 0 |
| | + 8 | 29 | 6 | 2 | 1 | 1 | 0 |
| | + 4 | 40 | 2 | 5 | 1 | 1 | 1 |
| | 0 | 16 | 3 | 3 | 0 | 2 | 1 |
| | − 4 | 14 | 1 | 3 | 2 | 1 | 0 |
| | − 8 | 29 | 3 | 0 | 0 | 0 | 0 |
| | −12 | 6 | 1 | 0 | 0 | 0 | 0 |
| | −16 | 11 | 3 | 1 | 0 | 0 | 0 |
| 171° | +16 | 17 | 3 | 0 | 0 | 0 | 0 |
| | +12 | 35 | 2 | 1 | 0 | 0 | 0 |
| | + 8 | 24 | 4 | 0 | 4 | 1 | 0 |
| | + 4 | 51 | 9 | 2 | 1 | 1 | 0 |
| | 0 | 26 | 3 | 6 | 0 | 0 | 0 |
| | − 4 | 33 | 6 | 2 | 1 | 2 | 1 |
| | − 8 | 17 | 2 | 2 | 0 | 0 | 0 |
| | −12 | 12 | 2 | 1 | 0 | 0 | 0 |
| | −16 | 11 | 4 | 0 | 0 | 0 | 0 |

The galactic-latitude distributions presented earlier, as well as the number of M stars found for short and long exposures at latitude −16° and longitude 3° and 66° and toward the galactic pole, show that these stars are generally found close to the galactic plane in a layer that is thicker toward the galactic center.

The lack of clustering shown everywhere by these stars, especially in the directions of the known local galactic spiral arm, plus the effects outlined earlier, all support the conclusion that the majority of late M stars are not associated with the galactic spiral arms. A comparison of their distribution with the one observed for the carbon stars, which will be presented later, also supports this conclusion. Thus the majority of the late M stars appear to form part of the disk population of our Galaxy.

## VIII. LATE M STARS WITH *VO* BANDS

A number of spectra in the survey show peculiarities which proved to be of considerable interest. In this section the discussion is limited to the late M stars which show the *VO* bands at λ 7400 and λ 7900 (Nassau, van Albada, and Keenan 1949). The spectra of these stars exhibit a unique appearance, particularly when the 2° objective prism is used. In a hundred or more cases examined, the presence of the *VO* bands indicates

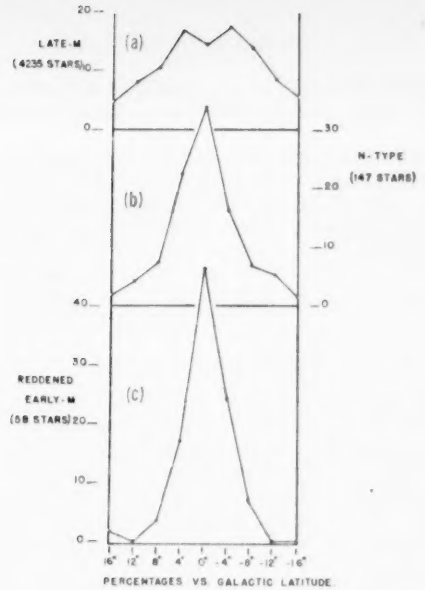


FIG. 3.—The distribution of relatively cool stars for all longitudes at the given latitudes. *a*, Late M stars; *b*, N stars; *c*, reddened early M stars.

TABLE 4

GROUPING OF DATA OF TABLE 3 FOR ALL LATITUDES AT VARIOUS LONGITUDES

| Long. | Late M's | M's with *VO* | N | R | C | Reddened Early M's |
|---|---|---|---|---|---|---|
| 342° | 463 | 31 | 9 | 3 | 0 | 9 |
| 3 | 900 | 43 | 4 | 4 | 0 | 8 |
| 24 | 606 | 40 | 6 | 3 | 0 | 3 |
| 45 | 477 | 44 | 14 | 5 | 1 | 13 |
| 66 | 471 | 43 | 27 | 4 | 3 | 1 |
| 87 | 367 | 26 | 23 | 9 | 1 | 5 |
| 108 | 215 | 26 | 7 | 9 | 2 | 9 |
| 129 | 328 | 39 | 27 | 5 | 3 | 7 |
| 150 | 177 | 28 | 16 | 4 | 5 | 2 |
| 171 | 226 | 35 | 14 | 6 | 4 | 1 |

TABLE 5

REGROUPING OF DATA OF TABLE 3 FOR ALL LONGITUDES AT VARIOUS LATITUDES

| | Late M's | | M's with *VO* | | N | | R | | C | Reddened Early M's | |
|---|---|---|---|---|---|---|---|---|---|---|---|
| | | Per | | Per | | Per | | Per | | | Per |
| Lat. | No. | Cent | No. | Cent | No. | Cent | No. | Cent | No. | No. | Cent |
| +16° | 204 | 5 | 18 | 5 | 3 | 2 | 1 | 2 | 0 | 1 | 2 |
| +12 | 335 | 8 | 37 | 10 | 6 | 4 | 1 | 2 | 0 | 0 | 0 |
| + 8 | 447 | 11 | 41 | 12 | 11 | 7 | 10 | 19 | 2 | 2 | 3 |
| + 4 | 711 | 17 | 43 | 12 | 33 | 22 | 10 | 19 | 7 | 10 | 17 |
| 0 | 608 | 14 | 71 | 20 | 50 | 34 | 12 | 23 | 5 | 27 | 47 |
| − 4 | 737 | 17 | 47 | 13 | 24 | 16 | 13 | 25 | 5 | 14 | 24 |
| − 8 | 589 | 14 | 45 | 13 | 10 | 7 | 5 | 10 | 0 | 4 | 7 |
| −12 | 358 | 8 | 23 | 6 | 8 | 5 | 0 | 0 | 0 | 0 | 0 |
| −16 | 246 | 6 | 30 | 8 | 2 | 1 | 0 | 0 | 0 | 0 | 0 |

variability, usually of the Mira type or long-period variable. This is in agreement with the studies of Keenan and Schroeder (1952), who observed the presence of *VO* bands in long-period variables.

Usually the spectrum of the variable is that of a normal late M at maximum, and as the star diminishes in brightness, the *VO* bands increase in strength. In other cases the spectrum at maximum light shows weak *VO* bands increasing in strength as the star approaches minimum (Nassau and Cameron 1954). The number of stars in the two sur-

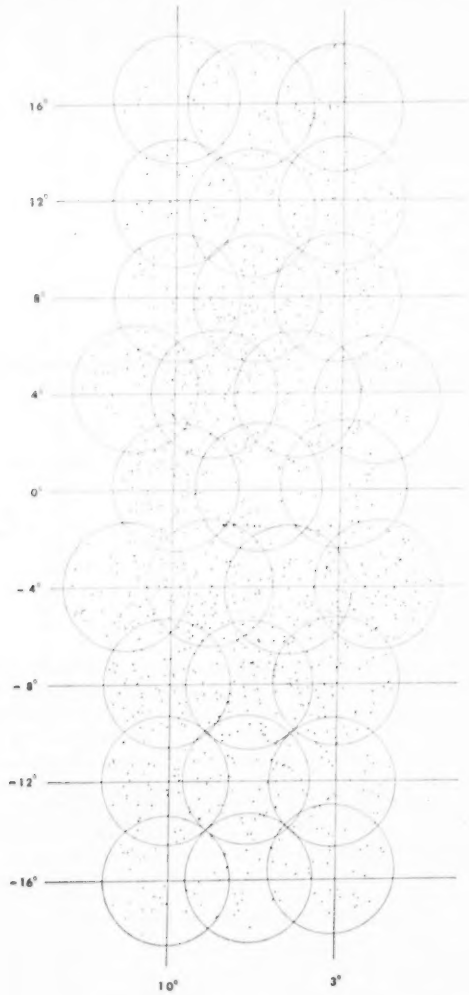


FIG. 4.—The dots represent late M stars. The circles show the overlapping photographic plates. Galactic longitudes are indicated on the bottom, while the vertical scale gives the galactic latitudes.

veys showing the *VO* bands in their spectra is given in the following tables: 3, fourth column; 4, third column; and 5, fourth column. In each case they are included in the counts of late M's.

The percentages of late M and *VO* stars for different latitudes are given, respectively, in the third and fifth columns of Table 5. The two groups of stars do not show marked differences in their latitude distribution. The more detailed data of Table 3 support this conclusion. A marked difference in the ratio of the number of late M stars to the *VO* stars is apparent in the different longitude groups, as a comparison of the second and third columns of Table 4 shows. Although the facts suggest a possible lower luminosity for these stars, there are many uncertainties. The bands are often weak, and a slight difference in plate quality may affect their detection.

## IX. N- AND R-TYPE STARS

In the infrared spectral region under discussion carbon stars, as defined by Keenan and Morgan (1941), are recognized by the presence of cyanogen bands. The strength of these bands has been found to be a reasonably good criterion for separating the class-N and the class-R stars. Since the major portion of our surveys is carried out with the 2° objective prism, the estimate of the band strength was made from spectra of this dispersion. A discussion of the segregation of these stars has been published (Nassau and Blanco 1954*b*). It should be stated that among the N stars in the present discussion some

TABLE 6

DISTRIBUTION OF M AND N STARS IN THE GALACTIC ZONE

| Long. | No. of Late M's | No. of N Stars |
|---|---|---|
| 333°–37° | 1366 | 32 |
| 73°–137° | 515 | 69 |
| 137°–201° | 449 | 51 |

TABLE 7

DISTRIBUTION OF M AND N STARS IN LATITUDE ZONES

| Long. | No. of Late M's | No. of N Stars |
|---|---|---|
| 342°, 3°, 24° | 1969 | 19 |
| 66°, 87°, 108° | 1058 | 57 |
| 129°, 150°, 171° | 731 | 57 |

few R stars might have been included; however, they are not sufficient in number to affect the conclusions made.

The number of N stars in the equatorial zone is given in Table 2, third column. The R stars are given in the fourth column; and the stars too faint to be classified as N or R are designated C and given in the fifth column. Although the number of N stars is small, it appears that their distribution does not follow the pattern of the M stars, and clusterings appear to be present. Some evidence of this will be presented later. Table 5, sixth column, gives the number of N stars, and the seventh column gives their percentage at the various latitude zones for all longitudes combined. The symmetry with respect to the galactic equator is striking (Fig. 3, *b*). Their concentration in the galactic plane is much greater than that of the late M stars. Within the galactic zone of $\pm 6°$ the percentage of M stars is 48, while that of the N stars is 72.

The zero-degree latitude zone contains 34 per cent of the N stars. This is greater than the percentage found in either of the adjacent zones of $+4°$ and $-4°$, in spite of the obscuration in the central zone, which is evident from the deficiency of the M's in this zone. Part of this may be due to a difference in the absolute magnitude of the two types of stars, but the fact remains that the distribution of the N stars does not follow the pattern of the M stars with respect to longitude. Nearly all the late M and N stars in the central zone given in Table 2 are subdivided into three equal areas, as shown in Table 6. Only the region at longitude 45° is omitted. The first area from $l = 333°$ to $l = 37°$ (Table 6) covers the region between the central of the Galaxy and the direction of the local spiral arm. The two other areas are in directions outside the arm. The late M stars

follow the expected distribution, as stated before, while the N stars are, on the contrary, more numerous in directions outside the local arm.

Similar results were obtained when the stars in the different latitude zones were employed. Table 7 gives the three longitudes included in each case. As before, the first group is in the direction between the galactic center and the direction of the local spiral arm, while the other two groups are in directions outside the arm. The number of M and N stars included in each group again shows the dissimilarity in the distribution of the two classes of stars.

The fact that late M and N stars do not have the same distribution is further supported from data secured by means of long-exposure plates. In the direction of the Large Sagittarius Cloud ($l = 329°$, $b = -8°$) Nassau and McCuskey (1954) find in an area of 11 square degrees over 300 late M stars per square degree and only 4 carbon stars throughout the region. Similar results were obtained in the direction of the Scutum Cloud. Within a region of 21 square degrees the number of late M stars per square degree on long-exposure plates was 140, while the total number of N stars was 3.

The fact that the N stars do not follow the same distribution as the late M stars, that they show higher galactic concentration, and that they appear in groups suggests that they may be within regions of spiral arms. Sanford (1944) finds that these stars do not belong to the high-velocity group, which gives additional strength to the assumption. Evidence in the same sense is provided by the distribution of N stars observed at Dearborn (Lee *et al.* 1947). The Dearborn observers call attention to a "nest" of N stars at about $l = 170°$. This is now known to coincide with the direction of the local spiral arm toward Monoceros. A second, but less obvious, concentration is shown in Cygnus, coinciding approximately with the other direction of the arm.

The identification of N stars as spiral-arm objects makes them very important in tracing the spiral arms of our Galaxy, as they can be detected by means of their infrared spectra at great distances. By way of illustration the following provisional results are presented. A region in the form of a square of $16° \times 16°$ with center at $l = 66°$ and $b = 0°$ was examined on plates with limiting infrared magnitude of 11. Of the 40 N-type stars found, 4 had an approximate magnitude of 6.0, and the rest 9.5. The suggestion is made that the small group of bright stars are in the spiral arm in which the sun is located and the faint group in the outer arm. However, for definite results the following must be considered: (*a*) variables in the group, (*b*) the determination of absolute magnitudes, and (*c*) the determination of interstellar absorption in this direction.

The number of R stars which are located within the central zone are given in Table 2, fourth column. Their identification is given in a previous publication (Nassau and Blanco 1954*b*). The number of R stars at the different latitude zones is given in Table 3, sixth column. In all, there are 85 stars in the two surveys, altogether too few for a detailed distribution study. When grouped at the different longitudes, as shown in the fifth column of Table 4, they appear to be distributed much like the N stars. Their grouping in latitude, which is given in Table 5, eighth and ninth columns, shows a somewhat smaller degree of galactic concentration when compared with N stars, in agreement with previous studies (Sanford 1944).

The distribution of the carbon stars exhibits definite clustering tendencies, with the R stars showing this effect more than the N stars. The total area of the central zone which was examined for carbon stars is 1081 square degrees and includes 195 N stars and 44 R stars, as well as 32 carbon stars that were too faint to classify into the N or R groups. Among the N stars there are four main groups centered approximately in longitudes 67°, 75°, 130°, and 142°. The principal groups of the R stars appear at longitudes 43°, 54°, 92°, and 120°. The clusterings of the N and R stars are, in general, independent of each other. The clustering tendency of the carbon stars stands out when they are compared in number with the M stars listed in Table 2. In such a comparison the effects of the regions of obscuration are roughly eliminated. In direct photographs the groups mentioned appear

to occur in moderately rich areas of the Milky Way, as well as in regions of obvious obscuration. There is a tendency for the groups, as well as for the individual stars, to avoid the brightest areas. For example, the group at longitude 67° is of interest in this respect, because the stars appear to avoid the clearest regions, being concentrated in areas of evidently distant obscuration, as indicated by the number of foreground stars.

Tentative distance determinations of the N-star groups place them at 2.0–3.0 kpc. For the group at 67° longitude, this is in agreement with the distance of the outer spiral arm. If this result is accepted, the diameter of a group is of the order of 200 psc. Similar but close groups would, in general, be too spread out to be conspicuous. R-star groups appear to be within 1.0 kpc. The lack of distant groups may be attributed to the fact that it is difficult to segregate the R stars from faint carbon-star spectra. The provisional character of the foregoing conclusions is obvious. It is also important to emphasize that the present discussion does not include carbon stars with very weak *CN* bands (Nassau and Blanco 1954*b*). The extension of the survey with long exposures is in progress.

### X. REDDENED EARLY M- AND S-TYPE STARS

In unwidened spectra some stars of class M0–M4 show images that are wedge-shaped, with the tapering toward the shorter wave lengths. The spectra of the supergiant early M stars in h and $\chi$ Persei show this unique appearance and have been used as standards in segregating the stars in the present surveys, many of which are likewise presumed to be supergiants (Nassau, Blanco, and Morgan 1954). The sixth column of Table 2 gives the number of these stars in the central zone; their identification is published in the paper cited. The number of stars in the different latitude zones is given in the eighth column of Table 3. Table 4, seventh column, gives their distribution in longitude and shows relatively few stars in the direction of the anticenter. The very marked galactic concentration is shown by the last two columns in Table 5 and in Figure 3, *c*. In interpreting the surface distribution of these objects, it should be pointed out that the wedge-shaped spectra according to which they were selected is primarily due to interstellar reddening (Blanco 1954).

The reddened early M stars often form small groups of 3–5 stars, each within areas less than 1° in radius. Due consideration was given to effects of obscuration producing apparent clusterings. Such groups are at the following longitudes: 342°, 354°, 35°, 47°, 73°, 79°, and 81°. In other regions where the areas are most extensive but still less than 2° in radius, they are more numerous, and some S-type stars are among them.

The surface distribution of the reddened early M stars shows a close resemblance to that of the emission nebulae listed by Sharpless (1953). This is particularly true of the stars previously designated as most likely to be supergiants (Nassau, Blanco, and Morgan 1954). In addition, Sharpless found no nebulae in a relatively clear region between longitude 62° and 70°. No reddened early M stars were found in this region either. Because of the lack of sufficient data, actual spatial associations cannot be inferred. Undoubtedly, the agreement in surface distribution is, at least in part, caused by the presence of interstellar material in these areas. As remarked earlier, the selection of the reddened early M stars depends on the presence of sufficient interstellar material in the direction of the star.

The S-type stars in the near infrared show *LaO* bands and weak or no *TiO*. Since all S stars do not show the *LaO* bands (Keenan 1954) and since their detection from infrared spectra depends on these bands, the present surveys do not claim completeness in these stars. The number of S stars at different longitudes in the galactic belt 4° wide is given in the seventh column of Table 2. Data for identification have been published by Nassau, Blanco, and Morgan (1954). The latitude surveys yielded too few stars to be included in any of the foregoing tables. From the few S stars available, the following tentative conclusions may be made: (*a*) they show galactic concentration; (*b*) they avoid the anticenter region, and thus their distribution in this respect is dissimilar to that of

the N stars; (*c*) they have a tendency to form groups. The lack of similarity in the longitude distribution of the S and N stars is of interest, since both these groups have been identified as spiral-arm objects. Possible experiments for this observation include (*a*) unequal luminosities in the infrared and (*b*) differences in space distribution within the spiral arms.

## XI. COMPARING THE SURFACE DISTRIBUTION OF THE RELATIVELY COOL STARS WITH OB ASSOCIATIONS

In the present surveys, with the exception of the late M stars, the objects under discussion appear in groups, and it is of importance to investigate the manner in which they may be associated with other objects, such as the known aggregates of supergiant early-

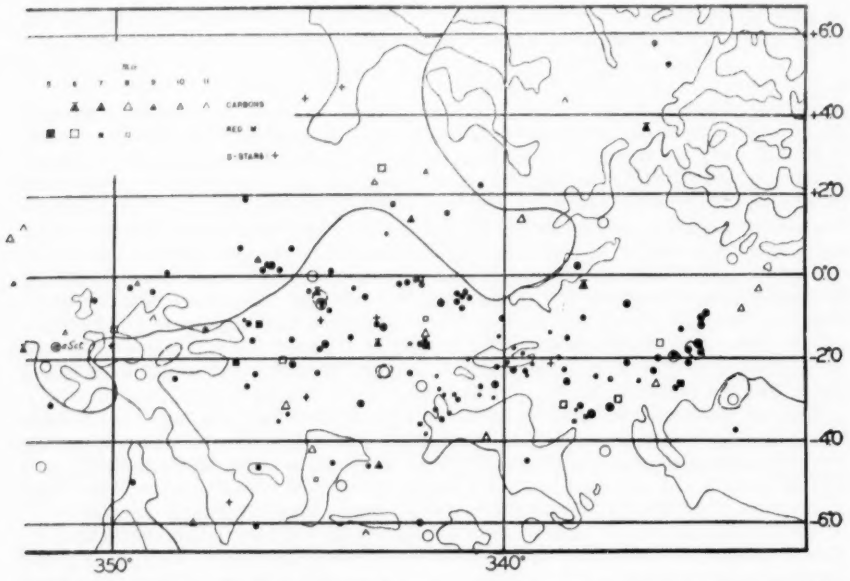


FIG. 5.—The surface distribution of the OB stars (*round dots*) and the relatively cool stars within $l = 333°$ and $l = 352°$ and $b = +6°$ to $-6°$. The star symbols are given at the upper left of the figure, while the background symbols are similar to those in Figs. 1 and 2.

type stars (Morgan, Whitford, and Code 1953) or with other apparent groupings of OB stars (Nassau and Morgan 1951). In order to do this, in a few cases the survey of the galactic zone was extended in latitude to $\pm 6°$ to correspond with the survey of the blue supergiants. The available data do not indicate that the N and R star groups are associated with regions of high surface density of OB stars or with the aggregates. On the other hand, the groups of reddened early M and S stars appear to be associated, in some cases, with groupings of OB stars, as, for example, at longitudes 338°, 41°–46°, 70°–80°, and 105°–115°. For the last two regions they seem to indicate extension into obscured regions of the areas in which OB stars are found. Early M supergiants are known to exist in aggregates. Bidelman (1947) and others have established such associations in the case of the h and $\chi$ Persei cluster. Ambarzumian (1953) and still more recently Blanco (1954) have indicated a number of other cases. The material on hand shows that a number

of other such groups may be present. However, confirmation must wait further observations.

The surface distribution of the OB stars and the relatively cool stars within $l = 333°$ to $l = 352°$ and $b = +6°$ to $b = -6°$ is shown in Figure 5. The late M stars are not shown here. The background symbols are described in Figure 3. Between $l = 335°$ and $l = 339°$, six suspected M supergiants are present which are distributed among a large group of OB stars. Similarly among the blue supergiants between $l = 341°$ and $l = 347°$, ten red suspected supergiants are present. The carbon stars within the area covered in Figure 5 are distributed more or less at random.

The support of the Office of Naval Research is gratefully acknowledged. It is also a pleasure to thank Dr. W. W. Morgan for sharing in the planning of our surveys and for his continued interest.

## REFERENCES

Ambarzumian, V. A. 1953, *Armenian Acad. Sci.*, **16**, No. 3, 73.
Bidelman, W. P. 1947, *Ap. J.*, **105**, 492.
Blanco, V. M. 1954, *A.J.* (in press).
Keenan, P. C. 1954, *Ap. J.*, **120**, 484.
Keenan, P. C., and Morgan, W. W. 1941, *Ap. J.*, **94**, 501.
Keenan, P. C., and Schroeder, L. W. 1952, *Ap. J.*, **115**, 82.
Lee, O. J., Gore, G. D., and Bartlett, T. J. 1947, *Ann. Dearborn Obs.*, Vol. **5**, Part 7.
McCuskey, S. W., and Seyfert, C. K. 1947, *Ap. J.*, **106**, 1.
Morgan, W. W., Whitford, A. E., and Code, A. D. 1953, *Ap. J.*, **118**, 318.
Nassau, J. J., and Albada, G. B. van. 1949, *Ap. J.*, **109**, 392.
Nassau, J. J., Albada, G. B. van, and Keenan, P. C. 1949, *Ap. J.*, **109**, 333.
Nassau, J. J., and Blanco, V. M. 1954*a*, *Ap. J.*, **120**, 118.
———. 1954*b*, *ibid.*, p. 129.
Nassau, J. J., Blanco, V. M., and Morgan, W. W. 1954, *Ap. J.*, **120**, 478.
Nassau, J. J., and Cameron, D. M. 1954, *Ap. J.*, **119**, 175.
Nassau, J. J., and McCuskey, S. W. 1954, unpublished.
Nassau, J. J., and Morgan, W. W. 1951, *Pub. Michigan U. Obs.*, **10**, 43.
Ohlson, J. 1932, *Lund Ann.*, Vol. **3**.
Sanford, R. F. 1944, *Ap. J.*, **99**, 145.
Sharpless, S. 1953 *Ap. J.*, **118**, 362.

# REDDENED EARLY M- AND S-TYPE STARS NEAR THE GALACTIC EQUATOR

J. J. NASSAU, V. M. BLANCO, AND W. W. MORGAN
Warner and Swasey Observatory and Yerkes Observatory

*Received March 15, 1954*

ABSTRACT

A list is given of 89 early M-type stars whose objective-prism spectra indicate abnormal reddening. The catalogue probably contains a high proportion of distant supergiants. In addition, a list of 31 new S-type stars is given which were detected by the presence of *LaO* bands in their spectra. Both groups of stars are within a galactic belt 4° wide from longitude 333° through zero to 201°. The catalogues are accompanied by a brief discussion of the distribution of these objects.

In the course of the Warner and Swasey Observatory infrared spectral surveys of the Milky Way, a number of early M-type stars were segregated which probably have higher than normal color indices, as suggested by the appearance of their spectra. The region covered in these surveys and the mode of observing have been described in previous publications (Nassau and Blanco 1954). In the unwidened spectra used, some stars of class M0–M4 show images that are wedge-shaped, with the tapering toward the shorter wave lengths. This unique appearance has been interpreted as indicative of an abnormally high color index. Photoelectric observations (Blanco 1954) of the colors of 16 such stars support this interpretation. In the same galactic region, in addition to these stars, 31 S-type stars were recognized by means of the *LaO* bands at λ 7400 and λ 7900 (Keenan 1948). The present paper presents these two groups of stars.

## EARLY M-TYPE STARS

Since spectra tapered in the manner described are also shown by the known early M supergiants in the h and χ Persei clusters, these stars were used as standards in the segregation of the reddened early M stars. The eighty-nine stars in Table 1, *a* and *b*, were segregated by direct comparison with the M supergiants of the clusters. Each of the stars listed shows a spectrum whose wedge-shaped appearance is somewhat more pronounced than the spectra of the standards of the same spectral class. The high color indices of these stars are caused principally by interstellar reddening. Photoelectric observations (Blanco 1954) of known supergiant early M stars in the blue and visual regions show that their intrinsic color index is about 0.3 mag. higher than that of the giants of the same spectral class. That the color differences between giants and supergiants are also small in the red and infrared regions follows from a comparison of the six-color photometric data of Stebbins and Whitford (1945) for α Orionis and the M2 giant HD 120933.

The stars in Table 1, *a* and *b*, may be distant supergiants or relatively near-by giants showing the effects of abnormally high obscuration. As explained later, it is also possible that a few of these stars are of S type. Since the infrared absolute magnitudes of the M supergiants are −7 or brighter and since the effect of interstellar absorption is much less in the infrared, they can be observed at great distances.

Estimates of the degree of tapering that should appear in unwidened spectra for various amounts of interstellar absorption have been made with the help of Whitford's (1948) observations of the interstellar absorption-curve. The results indicate that a total visual absorption of about 2 mag. should produce the degree of tapering used as a lower limit in the present survey. For a number of these stars it can be shown from the color excesses of the near-by O and B stars that this amount of absorption or more may exist within

TABLE 1

REDDENED EARLY M-STARS

(a)

| No. | BD | R.A. 1900 | Dec. 1900 | $m_1$ | Sp. | Group | l | b | Remarks |
|---|---|---|---|---|---|---|---|---|---|
| 1 | +58°501 | $2^h32^m3$ | +59°10' | 5.2 | M3 | A | 104° | 0° | * |
| 2 | +57 647 | 2 43.6 | +57 26 | 5.2 | M3 | A | 106 | -1 | |
| 3 | +54 651 | 3 06.5 | +54 34 | 6.9 | M3 | A | 110 | -2 | * |
| 4 | +55 778 | 3 17.2 | +56 09 | 8.0 | M1 | C | 111 | +1 | |
| 5 | +44 1005 | 4 34.0 | +44 30 | 7.5 | M3 | C | 128 | 0 | |
| 6 | +39 1070 | 4 41.6 | +39 46 | 7.6 | M1 | B | 132 | -2 | |
| 7 | +42 1065 | 4 43.1 | +42 57 | 8.5 | M2 | A | 130 | 0 | |
| 8 | +28 834 | 5 31.6 | +28 55 | 7.5 | M2 | B | 147 | 0 | |
| 9 | +19 1183 | 5 57.0 | +19 29 | 6.9 | M0 | B | 158 | +1 | |
| 10 | +13 1110 | 6 01.2 | +13 35 | 6.7 | M1 | A | 163 | -2 | |
| 11 | +10 1085 | 6 13.5 | +10 22 | 5.5 | M2 | A | 168 | -1 | |
| 12 | +13 1212 | 6 15.4 | +13 58 | 6.3 | M3 | A | 165 | +1 | |
| 13 | -12 5055 | 18 21.9 | -12 32 | 4.6 | M3 | B | 347 | -2 | * |
| 14 | + 0 4030 | 18 45.3 | + 0 40 | 6.5 | M2 | C | 1 | -1 | |
| 15 | +24 3902 | 19 45.9 | +24 41 | 5.7 | M3 | A | 29 | -2 | |
| 16 | +35 4077 | 20 17.3 | +35 18 | 6.0 | M2 | A | 42 | -2 | |
| 17 | +36 4025 | 20 17.6 | +36 37 | 4.9 | M4 | A | 43 | -1 | * |
| 18 | +37 3903 | 20 17.9 | +37 13 | 4.9 | M4 | A | 44 | 0 | * |
| 19 | +39 4208 | 20 25.2 | +39 39 | 4.7 | M4 | A | 46 | 0 | * |
| 20 | +59 2541 | 22 30.8 | +59 59 | 8.1 | M2 | C | 75 | +2 | |
| 21 | +60 2613 | 23 39.2 | +61 14 | 3.9 | M3 | A | 83 | 0 | |

(b)

| No. | BD | x | y | R.A. 1900 | Dec. 1900 | $m_1$ | Sp. | Group | l | b | Remarks |
|---|---|---|---|---|---|---|---|---|---|---|---|
| 22 | +61°153 | +1.9 | +1.0 | $0^h38^m0$ | +61°44' | 7.5 | M1 | A | 90° | 0° | |
| 23 | +63 94 | +1.9 | +0.9 | 0 43.4 | +64 13 | 6.9 | M2 | A | 90 | +2 | |
| 24 | +62 247 | +1.8 | -0.4 | 1 19.1 | +62 59 | 8.5 | M1 | C | 94 | +1 | |
| 25 | +60 312 | +3.7 | +3.8 | 1 37.7 | +61 07 | 7.1 | M1 | C | 97 | 0 | |
| 26 | +60 385 | -0.4 | -0.3 | 1 49.6 | +60 19 | 8.0 | M2 | C | 99 | -1 | |
| 27 | +59 411 | -0.5 | -0.3 | 2 00.0 | +59 46 | 7.4 | M1 | C | 100 | -1 | |
| 28 | +58 508 | +1.9 | +2.8 | 2 36.4 | +58 54 | 8.2 | M2 | C | 105 | 0 | |
| 29 | +60 574 | 0.0 | -2.2 | 2 42.0 | +60 37 | 6.7 | M1 | C | 104 | +2 | * |
| 30 | +60 588 | +5.2 | +1.6 | 2 48.7 | +60 24 | 7.7 | M1 | C | 105 | +2 | |
| 31 | +56 749 | -2.8 | -0.5 | 2 49.4 | +57 08 | 6.3 | M3 | B | 107 | -1 | |
| 32 | +59 587 | +0.9 | -0.5 | 2 55.2 | +59 26 | 7.9 | M1 | C | 107 | +2 | |
| 33 | +55 739 | -1.8 | -0.4 | 2 59.4 | +55 21 | 6.2 | M4 | A | 109 | -1 | |
| 34 | +54 655 | -0.6 | +0.1 | 3 07.7 | +54 31 | 5.9 | M2 | A | 111 | -2 | |
| 35 | +55 780 | 0.0 | -0.5 | 3 17.7 | +55 12 | 8.1 | M2 | C | 111 | 0 | |
| 36 | +52 711 | +3.5 | +2.7 | 3 39.6 | +52 46 | 6.5 | M2 | A | 115 | 0 | |
| 37 | +46 906 | +1.0 | +0.2 | 4 37.8 | +46 13 | 8.7 | M2 | C | 127 | +2 | |
| 38 | +45 987 | -3.9 | +1.4 | 4 39.5 | +45 23 | 8.9 | M1 | C | 127 | +1 | |
| 39 | +39 1085 | +1.6 | +1.6 | 4 45.1 | +39 53 | 7.8 | M2 | B | 132 | -1 | |
| 40 | +25 1011 | -0.6 | +0.4 | 5 46.0 | +25 48 | 7.4 | M0 | B | 151 | +1 | * |
| 41 | - 9 1796 | +1.0 | +0.6 | 6 57.0 | + 9 32 | 9.4 | M1 | C | 190 | -1 | |
| 42 | -14 1784 | -2.0 | -1.0 | 7 09.5 | -14 27 | 6.6 | M1 | A | 196 | 0 | |
| 43 | -15 4856 | -1.4 | +0.3 | 18 05.8 | -15 41 | 8.4 | M2 | C | 342 | 0 | |
| 44 | -16 4761 | +0.5 | +2.2 | 18 08.8 | -16 25 | 8.2 | M1 | C | 342 | -1 | |
| 45 | -16 4788 | -2.4 | +0.4 | 18 10.6 | -16 43 | 5.5 | M4 | A | 342 | -2 | |
| 46 | -16 4786 | -1.8 | -1.7 | 18 10.6 | -16 39 | 7.8 | M3 | B | 342 | -2 | |

TABLE 1 (Continued)

| No. | BD | x | y | 1900 R.A. | Dec. | $m_1$ | Sp. | Group | l | b | Remarks |
|---|---|---|---|---|---|---|---|---|---|---|---|
| 47 | -15°4911 | +0.2 | +2.8 | $18^h11^m8$ | -15°19' | 7.5 | M3 | B | 343° | -1° | |
| 48 | -12 5023 | +0.8 | -0.6 | 18 17.7 | -12 45 | 5.9 | M3 | C | 346 | -1 | * |
| 49 | -13 4973 | -0.2 | -1.7 | 18 19.9 | -13 49 | 6.9 | M3 | C | 346 | -2 | |
| 50 | - 9 4753 | +1.3 | -1.4 | 18 25.6 | - 9 27 | 6.8 | M3 | C | 350 | -1 | * |
| 51 | - 2 4686 | -0.9 | -0.7 | 18 33.8 | - 2 04 | 7.5 | M3 | C | 357 | 0 | |
| 52 | + 2 3681 | +2.8 | +2.2 | 18 42.2 | + 2 53 | 8.4 | M3 | C | 3 | +1 | |
| 53 | + 4 3900 | +2.2 | +3.1 | 18 47.7 | + 4 34 | 9.0 | M4 | C | 5 | 0 | |
| 54 | + 8 3898 | -1.2 | +0.8 | 18 50.2 | + 8 08 | 7.7 | M0 | C | 8 | +2 | |
| 55 | + 5 4002 | +0.2 | +2.4 | 18 54.5 | + 5 14 | 5.7 | M1 | B | 6 | -1 | * |
| 56 | + 7 3976 | -1.8 | -1.3 | 19 03.5 | + 7 44 | 8.5 | M2 | C | 10 | -2 | |
| 57 | +10 3796 | +0.5 | -1.3 | 19 04.0 | +10 10 | 8.9 | M1 | C | 12 | 0 | |
| 58 | +13 3984 | -0.2 | -3.0 | 19 15.4 | +13 23 | 7.1 | M1 | C | 16 | -1 | |
| 59 | +17 3977 | +1.7 | -0.2 | 19 24.0 | +17 06 | 7.5 | M2 | C | 20 | -1 | |
| 60 | +19 4103 | +0.3 | -0.9 | 19 34.9 | +19 57 | 7.0 | M4 | C | 24 | -2 | |
| 61 | +30 3854 | -0.8 | -0.5 | 19 57.0 | +30 33 | 6.7 | M2 | A | 36 | -1 | |
| 62 | +30 3854 | +1.2 | -1.2 | 19 57.6 | +30 31 | 7.2 | M2 | A | 36 | -1 | |
| 63 | +29 3869 | +0.2 | +2.6 | 19 58.9 | +30 05 | 8.4 | M3 | A | 35 | -1 | |
| 64 | +30 3866 | +0.2 | -0.4 | 19 59.6 | +30 11 | 6.9 | M4 | A | 36 | -1 | |
| 65 | +35 4010 | 0.0 | -0.8 | 20 07.6 | +35 25 | 8.0 | M4 | A | 41 | 0 | * |
| 66 | +37 3934 | -2.8 | -1.2 | 20 22.2 | +38 02 | 5.3 | M4 | A | 45 | -1 | * |
| 67 | +40 4160 | +3.0 | +2.6 | 20 22.6 | +40 48 | 8.0 | M2 | C | 47 | +1 | |
| 68 | +36 4072 | +2.0 | -0.9 | 20 23.2 | +36 13 | 5.0 | M4 | A | 43 | -2 | * |
| 69 | +40 4217 | -2.1 | +1.0 | 20 27.8 | +40 18 | 7.8 | M2 | C | 47 | 0 | |
| 70 | +40 4226 | -0.8 | +2.3 | 20 29.3 | +40 24 | 8.2 | M1 | C | 47 | 0 | * |
| 71 | +43 3708 | +0.4 | -2.6 | 20 41.9 | +43 54 | 8.2 | M1 | C | 52 | 0 | |
| 72 | +46 3140 | +0.3 | -0.1 | 20 57.4 | +46 42 | 7.6 | M4 | C | 56 | 0 | |
| 73 | +56 2739 | +1.3 | +1.3 | 22 11.8 | +57 16 | 8.1 | M2 | B | 71 | +1 | |
| 74 | +58 2436 | +2.0 | +1.1 | 22 24.7 | +58 44 | 5.8 | M3 | A | 73 | +1 | |
| 75 | +58 2450 | +2.5 | -2.6 | 22 29.8 | +58 23 | 6.1 | M1 | A | 74 | +1 | |
| 76 | +59 2549 | +2.6 | +4.4 | 22 34.1 | +59 51 | 7.3 | M2 | B | 74 | +2 | |
| 77 | +58 2473 | -1.2 | +2.0 | 22 39.4 | +59 14 | 6.6 | M4 | B | 75 | +1 | |
| 78 | +58 2485 | +1.6 | +1.4 | 22 45.4 | +58 46 | 6.7 | M2 | B | 76 | 0 | |
| 79 | +60 2452 | +2.2 | +2.0 | 22 49.3 | +60 45 | 5.7 | M3 | B | 77 | +2 | |
| 80 | +60 2492 | +1.6 | +1.5 | 23 06.0 | +60 42 | 6.1 | M3 | B | 79 | +1 | |
| 81 | +59 2675 | -1.7 | +1.0 | 23 09.2 | +59 58 | 5.9 | M0 | A | 79 | 0 | |
| 82 | +59 2676 | +0.5 | +3.0 | 23 10.3 | +60 23 | 7.2 | M1 | B | 79 | 0 | |
| 83 | +60 2512 | -1.1 | +0.9 | 23 12.0 | +60 25 | 7.1 | M2 | B | 79 | 0 | |
| 84 | +57 2718 | -1.7 | +0.1 | 23 13.0 | +58 08 | 7.9 | M1 | C | 79 | -2 | |
| 85 | +59 2727 | +0.3 | +0.3 | 23 23.0 | +59 54 | 6.7 | M3 | A | 81 | -1 | |
| 86 | +58 2598 | -0.5 | -0.2 | 23 24.3 | +59 13 | 7.7 | M2 | B | 80 | -1 | |
| 87 | +59 2734 | +1.3 | -1.0 | 23 25.6 | +59 44 | 7.3 | M4 | B | 81 | -1 | |
| 88 | +59 2738 | -0.8 | -0.2 | 23 26.2 | +59 42 | 6.4 | M3 | A | 81 | -1 | |
| 89 | +61 2466 | +2.2 | -2.6 | 23 27.7 | +61 25 | 8.0 | M2 | C | 82 | +1 | |

REMARKS TO TABLE 1

1. GP Cas, I. 3. NE star of double. 13. UY Sct. 17. BI Cyg, I. 18. BC Cyg, I. 19. RW Cyg, LP. 29. Extremely red. 40. BB Tau, I. 48. FR Sct, I. 50. BP Sct, extremely red. 55. V492 Aql, I, extremely red. 65. V430 Cyg, I? 66. KY Cyg, I. 68. V441 Cyg, LP. 70. Hα in emission

1 or 2 kiloparsecs. An effort has been made to divide the reddened early M stars into three groups in accordance with the estimated amount of absorption to various distances in the direction of each star. Group A contains stars in whose directions there is an apparent lack of near-by absorption sufficiently strong to produce the observed tapered spectra; group B contains stars for which the absorption is intermediate; and group C stars are located in regions where strong near-by absorption is suspected. The proportion of supergiant M stars is higher in groups A and B than in group C. As expected from the foregoing arguments, the stars selected by the tapered-spectrum criterion should, in general, avoid the clearer regions of the Milky Way. This agrees with observations.

Table 1, *a* and *b*, gives the reddened early M stars. These lists differ in one respect only: the first contains all stars which are in the BD catalogue; the second gives a reference BD star near the M star and co-ordinates in millimeters in the scale of the BD charts from the reference star to the M star. Positive $\Delta x$ indicates the direction of increasing R.A., while positive $\Delta y$ is in the direction of north. The infrared magnitudes designated by $m_i$ are approximate and were estimated from the spectra as described in an earlier paper (Nassau and Blanco 1954). The spectral classes are followed by a column in which the stars are assigned to one of groups A, B, or C described earlier. The last two columns give the galactic longitude and latitude to the nearest degree. In the "Remarks" column "I" designates an irregular variable, "LP" a long-period variable, and "M" a Mira type. These designations are taken from the *General Catalogue of Variable Stars* (Kukarkin and Parenago 1948). From an available red-sensitive plate, star No. 70 was found to have *Hα* in emission. In the future, for convenience, stars in this table will be designated by the letters RM-WS followed by the star's number.

## S-TYPE STARS

As has been stated, S-type stars are detected in the near infrared region of the spectrum from the presence of the *LaO* bands. However, in overexposed spectra these bands are not visible and the spectra appear similar to those of the reddened early M stars. A number of plates were taken with the 4° and 6° objective prisms, in order to remove ambiguities in the classifications. About one-third of the region of the survey was covered with these dispersions. A few S stars were found in this manner and are included in the list of S stars. However, the list of reddened early M stars may still contain stars of class S, particularly in those cases where the spectrum has been classified M0 or M1. The S stars are given in Table 2 and will be designated in the future by the letters S-WS followed by the star's number. The arrangement of the table is identical with that of Table 1, *b*, with the exception of the column designating groups A, B, and C. The present survey, which is confined within a galactic zone 4° wide from longitude 333° through zero to 201° and which has a limiting infrared magnitude of about 11, is not expected to include all the new S stars in the area. The identification was made by means of the *LaO* bands, and not all S stars show these bands (Keenan 1954).

## GALACTIC DISTRIBUTION OF S AND REDDENED M STARS

A discussion of the galactic distribution of these stars is to be included in a paper describing the results of the infrared surveys at this observatory. However, in order to point out the significance of the present lists, some brief remarks may prove appropriate. The surface distribution of these stars shows marked clustering tendencies. This is most evident for the M stars of groups A and B and for the S stars. Provisional studies at higher galactic latitudes indicate that these stars have a high degree of galactic concentration. From these observations it appears that the stars presented in this paper may be associated with the galactic spiral arms. Keenan (1953) has shown that S stars may be associated with spiral arms.

In conclusion it may be pointed out that, by means of the spectral criterion given here, early M stars were picked out and were found to be supergiants from slit spectra

TABLE 2

S STARS

| No. | BD | x | y | R.A. 1900 | Dec. | $m_1$ | l | b | Remarks |
|---|---|---|---|---|---|---|---|---|---|
| 1 | +62°147 | -1.6 | +3.2 | $0^h41^m.1$ | +63°24' | 8.3 | 90 | +1 | |
| 2 | +59 128 | + .9 | +1.6 | 0 44.8 | +59 40 | 7.9 | 91 | -2 | * |
| 3 | +61 256 | - .7 | - .8 | 1 16.4 | +61 28 | 9.8 | 94 | 0 | |
| 4 | +59 239 | +2.0 | -1.2 | 1 17.0 | +59 47 | 9.6 | 95 | -2 | |
| 5 | -19 4886 | +1.6 | - .5 | 18 05.7 | -19 53 | 9.3 | 339 | -2 | |
| 6 | -15 4902 | +1.6 | +2.5 | 18 11.1 | -15 12 | 10.7 | 343 | -1 | |
| 7 | -14 5004 | - .6 | + .6 | 18 14.8 | -14 09 | 9.0 | 345 | -1 | |
| 8 | - 9 4762 | +2.7 | -2.1 | 18 27.2 | - 9 33 | 10.0 | 350 | -2 | |
| 9 | - 4 4509 | + .7 | -1.6 | 18 31.2 | - 4 28 | 9.5 | 355 | 0 | |
| 10 | - 5 4710 | + .4 | -2.3 | 18 32.9 | - 5 31 | 8.0 | 354 | -1 | |
| 11 | - 5 4719 | -1.4 | - .1 | 18 34.8 | - 5 48 | 10.5 | 354 | -2 | |
| 12 | - 4 4559 | +1.8 | +1.2 | 18 37.7 | - 4 34 | 9.3 | 356 | -2 | |
| 13 | + 4 3936 | -2.6 | - .6 | 18 53.5 | + 4 32 | 5.0 | 6 | -1 | |
| 14 | +11 3709 | + .4 | -2.8 | 18 58.7 | +11 50 | 8.1 | 13 | +1 | |
| 15 | +10 3818 | +3.2 | + .3 | 19 07.5 | +10 45 | 8.8 | 13 | -1 | |
| 16 | +22 3675 | 0.0 | + .9 | 19 18.0 | +22 23 | 8.3 | 24 | +2 | * |
| 17 | +21 3839 | - .3 | + .9 | 19 31.4 | +22 07 | 8.1 | 25 | 0 | |
| 18 | +28 3485 | -2.4 | -1.0 | 19 44.4 | +28 31 | 9.5 | 32 | 0 | |
| 19 | +25 4000 | + .2 | - .9 | 19 47.4 | +25 52 | 9.5 | 31 | -1 | |
| 20 | +27 3561 | -1.5 | -1.3 | 19 51.6 | +27 23 | 8.6 | 32 | -1 | |
| 21 | +37 3867 | -1.6 | -2.2 | 20 13.4 | +37 48 | 9.5 | 44 | +1 | |
| 22 | +40 4243 | - .3 | + .1 | 20 32.1 | +41 01 | 9.5 | 48 | 0 | |
| 23 | +45 3297 | +1.9 | - .9 | 20 47.4 | +45 24 | 11.0 | 53 | 0 | |
| 24 | +44 3619 | +2.0 | + .3 | 20 50.6 | +44 28 | 10.4 | 53 | -1 | |
| 25 | +48 3281 | -1.6 | +2.5 | 21 01.3 | +49 05 | 9.5 | 58 | +1 | |
| 26 | +45 3429 | -1.3 | + .2 | 21 05.7 | +45 46 | 8.8 | 56 | -2 | |
| 27 | +51 3048 | +1.6 | +1.5 | 21 18.8 | +51 46 | 9.7 | 62 | +1 | |
| 28 | +60 2497 | +3.3 | +3.6 | 23 09.2 | +60 33 | 7.9 | 79 | 0 | |
| 29 | +57 2718 | + .8 | -2.6 | 23 14.0 | +58 00 | 7.4 | 79 | -2 | |
| 30 | +62 2266 | + .3 | -1.1 | 23 35.2 | +62 47 | 9.5 | 83 | +2 | |
| 31 | +62 2315 | -1.8 | - .1 | 23 46.5 | +62 18 | 8.6 | 84 | +1 | * |

REMARKS TO TABLE 2

2. 97, L. 16. 4639. 31. EO Cas, M.

taken at the Yerkes Observatory. These stars are BD 57°524 and 58°445 (near the h and $\chi$ Persei clusters) and BC Cyg. In addition, RW Cyg has been classed by Keenan (1942) as M3 I*a*.

This investigation was carried out under a grant from the Office of Naval Research.

## REFERENCES

Blanco, V. M. 1954, *A.J.* (in press).
Keenan, P. C. 1942, *Ap. J.*, **95**, 461–467.
———. 1948, *ibid.*, **107**, 420.
———. 1953, *A.J.*, **58**, 218.
———. 1954, *Ap. J.*, **120**, 484.
Kukarkin, B. V., and Parenago, P. P. 1948, *General Catalogue of Variable Stars* (Moscow).
Nassau, J. J., and Blanco, V. M. 1954, *Ap. J.*, **120**, 118.
Stebbins, J., and Whitford, A. E. 1945, *Ap. J.*, **102**, 318–346.
Whitford, A. E. 1948, *Ap. J.*, **107**, 102.

# CLASSIFICATION OF THE S-TYPE STARS

PHILIP C. KEENAN
Perkins Observatory
*Received April 13, 1954; revised June 1, 1954*

ABSTRACT

In this survey, spectra of type S are defined as those having bands of *ZrO* strong enough to be detected with low dispersion. This limitation is made because the group will be a useful one only if most or all of the members can be recognized on slitless spectrograms and if they are enough alike to give significance to their statistical properties. Stars with weaker *ZrO* bands are termed "MS" stars, and 14 of these are tabulated. Seven other stars showing neither *ZrO* nor *TiO* bands in their spectra are set aside as related more distantly to the S-type stars. The 69 S-type stars of the main catalogue are classified from the relative intensities of their *ZrO* and *TiO* bands into a two-dimensional system, in which the variables appear to be *temperature* and *chemical composition*. The lines of evidence bearing on the luminosities of the S stars—their motions and galactic distribution, as well as the classification by Feast of the faint companion of $\pi'$ Gruis—suggest that these stars belong among the giants and bright giants (luminosity classes III and II), possibly spanning a considerable range in absolute magnitude. Preliminary counts of M, MS, S, and C stars in the giant branch of the cooler stars with banded spectra show that roughly 10 per cent of them show appreciable strengthening of the S characteristics—the lines of the heavier metals and the bands of their oxides.

## PRINCIPLES OF CLASSIFICATION

Spectral class S was introduced by P. W. Merrill (1922*a*, *b*) in 1922 to designate a group of curious red stars which had not fitted well into either class M (*TiO* stars) or classes R and N (carbon stars). The original type stars of the class were the slightly variable star $\pi'$ Gruis and the two long-period variables R And and R Cyg. The history of the recognition of the peculiarities of these stars and of the early attempts to classify them has been well summarized by Merrill in his monograph *Spectra of Long-Period Variable Stars* (1940), where references to the pioneer papers will be found.

Although the members of class S have never been numerous, observers have generally agreed in assigning to it those stars whose spectra showed either or both of these features: (1) distinct bands of *ZrO* in the blue and visual regions; the strongest *TiO* bands may be practically absent (R Gem), relatively weak (AD Cyg), or stronger than the *ZrO* bands (HR 1105); (2) unusual strength of certain absorption lines in the blue-green, particularly λ 4554 (*Ba* II) and λ 4607 (*Sr* I), as compared to their intensities in normal K- or M-type stars.

There are other spectral features characteristic of the group, but characteristics 1 and 2 are the only signposts which have been consistently employed for recognition of S-type stars. An example of an additional criterion which is only occasionally useful is the strength of *Hβ* emission in long-period variables. In those of type S, *Hβ* is frequently much stronger relative to *Hγ* and *Hδ* than in typical M-type long-period variables; but this is due to the weakening of *Hβ* emission by the strong λ 4847 absorption band of *TiO* in the latter. That the effect is mainly a consequence of the absolute band strengths is shown by the failure of *Hβ* to be conspicuously strengthened in S-type variables like S Cyg, in which the *TiO* absorption remains strong.

The physical description of the stars forming type S has involved difficulties which have never been fully surmounted. In the first place, less than a hundred stars have ever been assigned to the group, and most of these have such faint apparent magnitudes that they have not been well observed spectroscopically. Consequently, we do not have reliable statistical information about such properties as mean luminosities or temperatures. Furthermore, even this small group is far from homogeneous. The differences between

individual spectra are sometimes more obvious than their similarities. Thus in R Cyg and R Gem strong bands of *ZrO* completely dominate the visual spectrum; but in some stars, especially those of the "R CMi group," which were put into class S entirely on the basis of criterion 2—enhanced atomic lines—it is difficult to detect any *ZrO* bands even on spectrograms of considerable dispersion.

The problem should become less complex if we can deal with a more homogeneous group of stars. For this reason the present investigation attempts, first, to sharpen the definition of type S and then to review critically the membership in the class. We should like to define spectral types by features which can be recognized on spectrograms of rather small scale, for the criteria will have wide usefulness only if they can be applied to surveys with slitless Schmidt spectrographs or samplings of distant fields with slit spectrograms of low dispersion. This condition is fulfilled fairly well by the strongest bands of *ZrO*, which in many known S-type stars are easily seen with a dispersion of 250 A/mm or less.

Let us, accordingly, define type S by our previous criterion 1 only—*the presence of distinct bands of ZrO in the easily observable spectral regions*. Other features, such as the strengthening of the *Ba* II 4554 line will be used only as supplementary criteria.[1]

Absorption from the ground state of the *ZrO* molecule gives rise to three band systems which are useful in classification (Lowater 1932; Afaf 1950). These bands all degrade to the red from triplet heads, of which those of the $\Delta v = 0$ sequences are the strongest and, hence, the most sensitive for detection of *ZrO* when *TiO* is also strong. The most valuable bands are discussed.

1. *α-System in the blue;* $C^3\Pi \rightarrow X^3\Pi$.— The strongest head is λ 4640.6 (0, 0 $R_1$), but it can be seen readily only when the overlapping λ 4626.1 band of *TiO* is weak. In other cases the next strongest *ZrO* band, λ 4619.8 (0, 0 $R_2$), must be used. Since this head is separated by only about 6 A from the *TiO* bands, spectrograms with a dispersion of at least 100 A/mm are needed to distinguish the bands unless the *ZrO* is quite strong. Consequently, this system is of only limited usefulness on most objective-prism plates. On the other hand, the maximum speed of blue-sensitive emulsions, such as the Eastman type O, comes just in this part of the spectrum, and, consequently, it is feasible to take slit spectrograms showing these bands in many of even the red stars.

2. *β-System in the yellow;* $B^3\Delta \rightarrow X^3\Pi$.—The bands of this system do not seem to be quite so intense as those of the α- and γ-systems, but the strongest head at λ 5551.7 is far enough away from *TiO* λ 5569 (a rather weak band) to be distinguished easily on spectrograms with a dispersion of 320 A/mm or more (Figs. 1 and 2). This spectral region has been somewhat neglected in the past, partly because it falls within the minimum of the sensitivity-curve of many panchromatic emulsions; but the Eastman type-G sensitizing is very efficient at λ 5551, and type-D sensitizing also holds up well down to λ 5500. When all factors are taken into account, *the λ 5551 head appears to be the ZrO band most useful for the marginal detection of the molecule with low dispersion*. A few of the adjacent bands, particularly λ 5718.1 (0, 0 $R_3$), are sometimes useful, but are much weaker than the main head.

3. *γ-System in the red;* $A^3\Sigma \rightarrow X^3\Pi$.—The λ 6473.7 (0, 0 $R_3$) band is one of the most persistent bands of *ZrO* and was found by Bobrovnikoff (1934) to give the best evidence for the presence of considerable amounts of *ZrO* even in such M-type stars as β Peg and ρ Per. A scale of about 130 A/mm (corresponding to about 30 A/mm at $H\gamma$ on a typical prismatic spectrogram) is required to separate the λ 6473 head from the *TiO* band at λ 6479.0. With this dispersion the strong S-type stars are easily recognizable. In stars with weak *ZrO*, however, the λ 6473 band is difficult to detect with certainty even on

[1] Observed enhancement of λ 4554 is not a necessary condition for an S-type star, for when the λ 4462 band of *TiO* is strong in very cool stars, it extends far enough to the red to overlap and weaken the *Ba* II line. Nor is the enhancement of the line a sufficient condition for membership in the class, for λ 4554 is quite strong in many of the red carbon stars also.

plates of greater dispersion, for the measurements on $\beta$ Peg carried out by D. N. Davis (1947) on Mount Wilson coudé spectrograms show that the near-by atomic lines (*Ca* I 6471.6 and *Fe* I 6475.6) are strong enough to contribute appreciably to the total absorption when blended with the still weak *ZrO* band.

These three band systems all arise from the normal electronic level of *ZrO*, and their strongest sequences originate in the lowest vibrational states also. Their behavior in absorption should, therefore, be consistent, and the observations indicate that this is so. Since the same situation holds for most of the *TiO* bands used in classification,[2] it is possible to compare the *ZrO* and *TiO* bands interchangeably in any or all of the spectral regions discussed earlier. This can be done by expressing estimates of band strengths in terms of the intensities of these bands in standard "type" stars, as is usually done in the case of line intensities in classifying stars of earlier type. In Table 1 the band intensities, in columns 8 to 10, have been carefully compared, usually on at least two good spectrograms of each star, and can be used as standards except where uncertain values are indicated by a colon. To minimize the embarrassment arising from the fact that we are necessarily dealing with a number of variable stars with variable absorption bands, we specify that in long-period variables the standard intensities and the classification refer to an average *normal maximum*.[3] Intensities at other phases also are recorded in Table 1 wherever observations are available. For semiregular and irregular variables the amplitude is small, and the standard intensity can be taken as applying to the star at *mean* brightness. In every case the normal range of brightness of the star is given in column 6, and the estimated brightness when the spectrum was observed is given in column 7. A range of magnitudes in column 7 indicates that intensity estimates from plates of different dates have been averaged.

The intensities of the bands of *TiO* are known to increase consistently with the subdivisions of type M (Adams 1925; Morgan *et al.* 1942), at least out to M8.[4] Consequently, it has been possible and convenient to define the intensity scale for *TiO* by adding one unit to the spectral subdivision of a normal M-type giant. Thus a *TiO* intensity of 4 in Table 1 indicates that these bands are as strong as in an M3 giant. The extra unit was added because at M0 the strongest bands are already strong enough to be seen clearly, even with low dispersion. For *ZrO* also the scale of intensities was chosen so that in the stars at intensity 1 the most sensitive bands are just distinctly visible on spectrograms having the dispersions suggested in the foregoing paragraphs.

In addition, intensities of the infrared bands of *lanthanum oxide* (Keenan 1948) have been added to Table 1 for the stars for which spectrograms on 1-N plates were taken. This has been done in order to bring the photographic infrared region of these very red stars into the plan of classification. In very strong S-type stars the *LaO* bands of the red system entirely dominate this part of the spectrum, and on the Perkins plates these bands have never been observed in a star which did not also show *ZrO*. Consequently, their presence appears to be another sufficient criterion for assigning a star to type S.

It happens, however, that the *LaO* bands fade out of the spectra of several long-period variables near the phase of maximum light, when the strongest sequence near $\lambda$ 7900 is replaced by some of the infrared bands of *CN*.[5] Figure 3 shows how the *LaO* bands stand

[2] The only exception among the important *TiO* bands is $\lambda$ 6479, which is a 4,2 band of the $\gamma$-system, originating in absorption by molecules in the second vibrational level.

[3] It is well known that when a long-period variable has an unusually faint maximum, the spectrum may resemble that normally observed at a phase far down the light-curve. Examples are the low maximum of Mira in 1923 as described by Joy (1926), and the one of R Gem in 1950 recorded in Table 1.

[4] Conspicuous exceptions seem to occur only near the minima of long-period variables, where overlapping band heads and the general "veiling" of the spectrum described by Merrill (1940, pp. 51 and 98) sometimes reduce the apparent intensities of even the strong *TiO* bands.

[5] The *CN* bands, just as in supergiants of types K and M, are accompanied by strong atomic lines which contribute appreciably to the blended absorption feature observed with low dispersion.

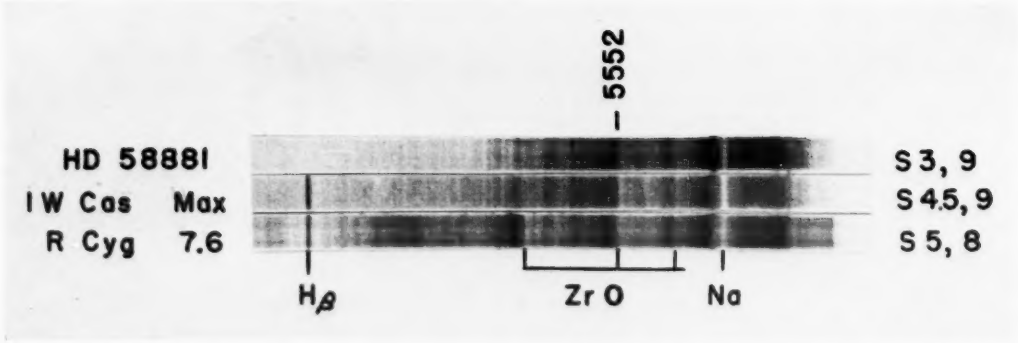


FIG. 1.—Variation of *ZrO* bands with temperature in nearly pure S-type spectra. *f*/1 camera, giving scale of 275 A/mm at λ 5600 on original negative. *Hβ* emission is conspicuous in the two long-period variables.

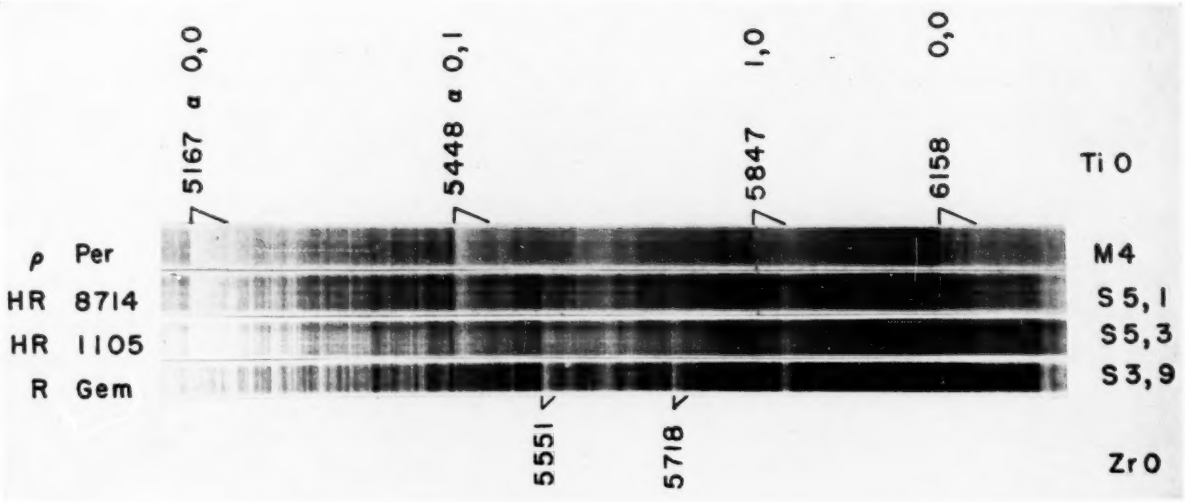


FIG. 2.—Transition from type M to type S in stars of about the same temperature. *f*/4 camera, giving scale of 80 A/mm at λ 5600 on original negative.

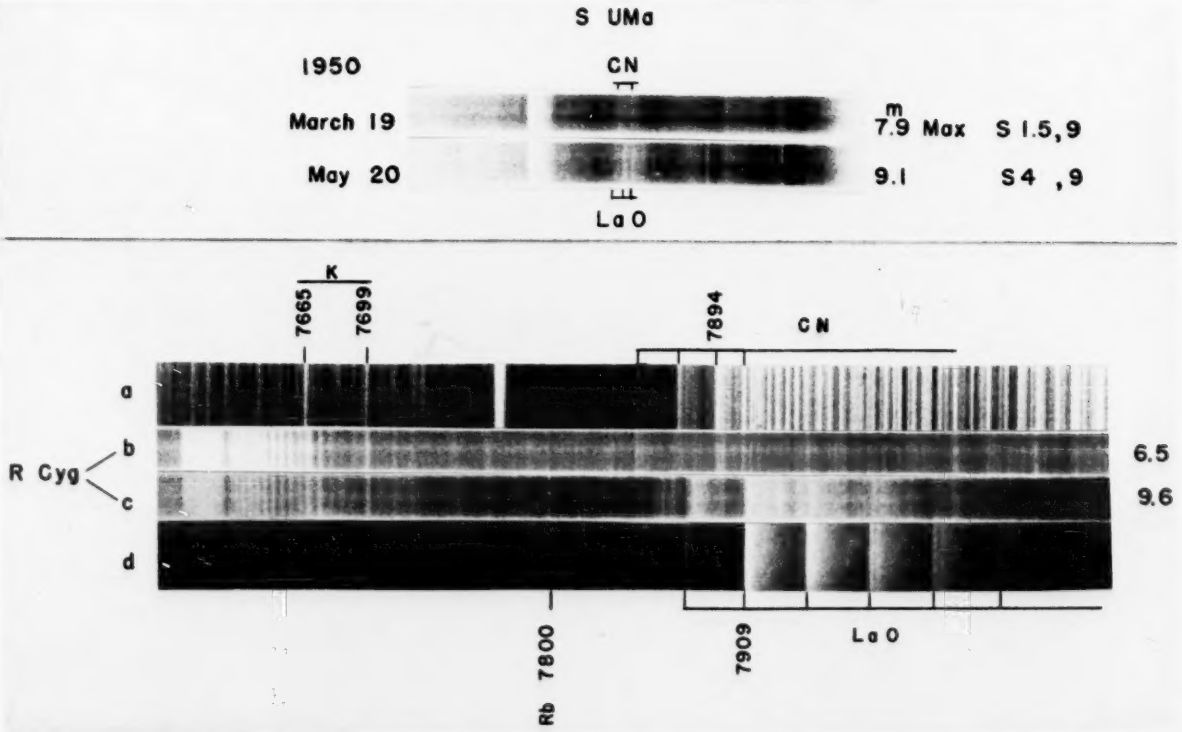


FIG. 3.—Variation of infrared *LaO* bands with temperature in long-period variables. Upper exposures on S UMa with prismatic camera, giving scale of 255 A/mm at λ 8000. Lower exposures with grating spectrograph, giving scale of 48 A/mm on original negative. Exposure *a* made with carbon arc, showing *CN* bands; *d*, with $La_2O_3$ in iron arc. Exposures *b* and *c* show R Cyg on July 9, 1950, and August 10, 1949.

TABLE 1

S-TYPE STARS BRIGHTER THAN $m_v$ = 11

| STAR | HD | BD | α(1950) | δ(1950) | $m_v$ | | INTENSITIES | | | TYPE | NOTE |
|---|---|---|---|---|---|---|---|---|---|---|---|
| | | | | | NORMAL | OBSERVED | TiO | ZrO | LaO | | |
| IW Cas | - | - | $0^h 00^m.2$ | +48°26' | 11.5-(14.7 Pg. | Max.(8.6) | 0 | 4.5 | 3: | S4.5,9e | 1 |
| X And | 1167 | +46°41a | 0 13.6 | +46°43' | 8.9-14.7 | 8.8-9.5 | 0 | 3 | Strong | S3,9e | |
| R And | 1967 | +37°58 | 0 21.4 | +38°18' | 6.8-13.9 | Max.(6.8)<br>10.5 | 3<br>5: | 4<br>4: | 1-:<br>- | S6,6e<br>S7,5e | |
| U Cas | 4350 | +47°194 | 0 43.6 | +47°59' | 8.0-14.6 | Max.(8.2)<br>8.9<br>9.0-9.6 | 3.5<br>4<br>5.5 | 3.5<br>4<br>4.5 | 0<br>0<br>- | S5,5e<br>S6,6e<br>S8,6e | |
| RR And | 4895 | +33°116a | 0 48.7 | +34°02' | 9.3-14.1 | 9.5 > | 6.5 | 2: | - | S7,2e: | 2 |
| S Cas | 7769 | +71°66 | 1 16.0 | +72°21' | 8.4-14.4 | Max.(7.7) | 2 | 3 | - | S4,6e | |
| RZ Per | - | - | 1 26.0 | +50°36' | 9.5-14 | 11.0: < | 0 | 4 | - | S4,9e | |
| - | - | +51°471 | 1 58.9 | +52°19' | Var.? | 9.4-9.9 | 5 | 2 | Weak | S6,e | 3 |
| Vys 9 | - | +31°392 | 2 15.2 | +31°31' | Var.? | 9.0-9.5 | 4.5 | 1.5 | - | S5,1 | 4 |
| BI And | - | - | 2 22.9 | +37°55' | 9.5-11.5 | 9.7-9.9 | 4 | 6 | 6 | S8,8 | 5 |
| HR 1105 | 22649 | +62°597 | 3 37.8 | +63°03' | 5.32 | 5.3 | 4 | 2.5 | Very Weak | S5,3 | |
| WX Cam | - | - | 3 45.3 | +53°03' | 10-11: | 10.0-10.5: | 1.5 | 4 | - | S5,8 | 6 |
| - | - | +24°620 | 4 02.6 | +24°36' | 9.2: | 9.2: | 3.5 | 2 | - | S4,2 | 7 |
| SX Cam | - | - | 4 19.1 | +68°07' | 11.0-14.3 Pg. | ? | 5: | 3: | ? | S6,3: | 8 |
| Vys 2 | - | +22°700 | 4 24.4 | +22°15' | 11.5 Pg. | 10: | 5 | 1.5 | - | S6,1 | 9 |
| WY Cam | - | - | 4 30.5 | +79°02' | 9.5-11.0: | - | - | - | - | - | 10 |
| Dearborn 808 | - | +12°612 | 4 32.9 | +12°33' | 10.0: | 10.0-10.5: | 5 | 1.5: | - | S6,1: | 11 |
| T Cam | 29147 | +65°422a | 4 35.2 | +66°03' | 7.7-13.5 | 9.0:<br>10.0 | 1.5<br>2: | 3<br>- | -<br>7 | S4,7e:<br>S7,8e: | |
| - | - | +79°156 | 4 46.8 | +79°55' | 9.9: | 9.9: | 3.5 | 2 | - | S4,2 | 12 |
| TV Aur | - | +48°1187 | 4 54.4 | +48°29' | 9.2-10.3 | 9.7: | 1: | 4.5 | - | S5,8: | |
| Vys 3 | 34738 | -22°1070 | 5 16.6 | -22°16' | 8.8: | 8.5 | 2.5 | 3 | - | S4,5 | 13 |
| - | 35155 | - 8°1099 | 5 19.9 | - 8°43' | 7.0 | 7.0 | 3.5 | 1.5 | - | S4,1 | |
| - | - | +15°1200 | 6 23.9 | +15°57' | 9.4: | 9.4: | 4.5 | 2 | - | S5,5,2 | 14 |
| DY Gem | - | +14°1350 | 6 33.1 | +14°14' | 11-12:pg | 10: | 5.5 | 4 | - | S8,5 | 15 |
| CX Mon | - | - | 6 34.7 | + 0°58' | 11.8-12.7 Pg. | - | - | - | - | - | 16 |
| - | 49368 | + 5°1414 | 6 45.7 | + 5°36' | 8.7: | 8.7: | 4 | 1.5 | - | S5,1 | 17 |

TABLE 1 (Con't)

| STAR | HD | BD | α(1950) | δ(1950) | $m_v$ | | INTENSITIES | | | TYPE | NOTE |
|---|---|---|---|---|---|---|---|---|---|---|---|
| | | | | | NORMAL | OBSERVED | TiO | ZrO | LaO | | |
| R Lyn | 51610 | +55°1154 | 6h57m.2 | +55°24' | 7.8-13.6 | 8.1-8.3 | 0 | 3 | - | S3,9e | |
| | | | | | | 8.7 | 0.5: | 5: | - | S5,9e: | |
| | | | | | | 9.9 | 1: | 5: | - | S6,8e: | |
| R Gem | 53791 | +22°1577 | 7 04.3 | +22°47' | 7.1-13.1 | 6.8-7.2 | 0 | 3 | 0 | S3.9e | |
| | | | | | | 7.3-7.8 | 0 | 3.5 | 4.5 | S3.5,9e | |
| | | | | | | 8 (Pt.Max) | 0 | 6 | 7.5 | S6,9e | |
| | | | | | | 8.9 | 0 | 4 | - | S4,9e | |
| RR Mon | 56567 | - | 7 15.0 | + 1°11' | 9.6-15.0 | 10.2: | 8: | 1.5 | - | S7,2e: | 18 |
| - | 58881 | -11°1941 | 7 24.7 | -11°37' | 10.0-10.7 Pg. | 9.3: | 0 | 3 | - | S3,9 | 19 |
| KZP 1098 | - | -15°1953 | 7 36.0 | -15°57' | 11-12 Pg. | 10.3 | 3: | 3.5 | - | S5,6 | 20 |
| SU Mon | 62164 | -10°2171 | 7 39.9 | -10°46' | 7.7-9.0 | 8.4-8.5 | 1 | 2.5 | - | S3,6 | |
| T Gem | 63334 | +24°1778 | 7 46.1 | +23°59' | 8.7-13.7 | 8.7 | 3 | 3 | - | S4.5,4e | |
| | | | | | | 9.0 | 4 | 4 | - | S6,6e | |
| | | | | | | 9.9 | 5 | 4 | - | S8,6e | |
| | | | | | | 10.2 | 7 | 4 | - | S9,5e | |
| - | 63733 | -18°2040 | 7 47.5 | -18°53' | 8.5 | 8.5 | 2.5 | 2 | - | S3.5,2 | |
| - | 64332 | -11°2121 | 7 50.6 | -11°30' | 8.1 | 8.1 | 5 | 2.5 | - | S6,3 | |
| BD Mon | - | - | 7 58.6 | - 5°29' | 10.3-(12.4 | - | 7: | - | - | Se? | 21 |
| V Cnc | 70276 | +17°1825 | 8 19.1 | +17°27' | 7.5-13.0 | 7.9-8.1 | 0 | 2: | - | S2,9e: | |
| - | - | -28°6970 | 9 06.9 | -28°48' | 8.4 | 8.8: | - | 4: | - | - | 22 |
| S UMa | 110813 | +61°1313 | 12 41.8 | +61°22' | 7.7-11.7 | 8.0: | 0 | 1.5 | 0 | S1.5,9e | |
| | | | | | | 8.7-9.0 | 0 | 3 | 4-: | S3,9e | |
| | | | | | | 10.0-10.6 | 0: | 5: | - | S5,9e: | |
| KZP 2016 | - | +44°2267 | 13 19.1 | +44°15' | 9.5-10.1 Pg. | 10.2: | 0: | 2.5 | - | S2.5,9: | 23 |
| R Cam | 127226 | +84°323 | 14 21.3 | +84°04' | 8.3-12.6 | 8.1 | 0 | 2: | 0: | S2,9e: | |
| ST Sco | 149511 | CD -30°13283 | 16 30.2 | -31°02' | 7.8-9.7 | - | 2: | 3.5 | - | S4,7: | |
| V635 Sco | 156957 | CD -41°11533 | 17 15.3 | -41°39' | 9.5-10.7 Pg. | 8.4: | 5 | 5: | - | S7,6: | |
| - | - | +23°3093 | 17 20.1 | +23°21' | 10.1 | 10.1 | 4 | 3 | - | S5,4 | |
| V812 Oph | - | - | 17 39.0 | + 6°45' | 11.8-12.9 Pg. | 10.9: | 5 | 2.5 | - | S6,3 | |
| V679 Oph | 172804 | + 6°3898 | 18 39.5 | + 6°45' | 9.0-9.3 | 9.0-9.3 | 1 | 4 | 1.5: | S4.5,8 | |
| ST Sgr | 176592 | - | 18 58.7 | -12°50' | 9.4-(15 | 8.9-9.2 | 3.5 | 3: | - | S5,5e: | |
| - | 177175 | +12°3780 | 19 00.8 | +12°11' | 8.7 | 8.7 | 6 | 2.5 | 0: | S7,2 | |
| W Aql | - | - | 19 12.7 | - 7°08' | 8.2-13.6 | 7.9-8.0 | 0 | 4 | 4 | S4,9: | |
| T Sgr | 180196 | -17°5546 | 19 13.4 | -17°04' | 8.0-(13.1 | 8.0-8.1 | 1+: | 4.5 | 4.5 | S5,8e: | |
| | | | | | | 8.8-9.5 | 2: | 4.5 | 7: | S5,8e: | |

TABLE 1 (Con't)

| STAR | HD | BD | α(1950) | δ(1950) | $m_v$ | | INTENSITIES | | | TYPE | NOTE |
|---|---|---|---|---|---|---|---|---|---|---|---|
| | | | | | NORMAL | OBSERVED | TiO | ZrO | LaO | | |
| CE Vul | - | - | $19^h31.^m0$ | $+23^\circ30'$ | 12-14Pg. | 10.8: | 4 | 6 | Strong | S8,7 | 24 |
| R Cyg | 185456 | $+49^\circ3064$ | 19 35.5 | $+50^\circ05'$ | 7.3-13.9 | 6.4-6.5 | 0 | 3.5 | 0 | S3.5,9e | |
| | | | | | | 7.0 | 0 | 4 | 0 | S4,9e | |
| | | | | | | 7.1-7.9 | Tr: | 5 | 7: | S5,8e: | |
| | | | | | | 8.0-8.9 | Tr: | 6 | - | S6,8e: | |
| | | | | | | 9.0-9.9 | 1: | 6: | 8 | S6,8e | |
| Vys 12 | - | - | 19 37.1 | $+67^\circ09'$ | 9.7 | 9.7 | 0.5: | 4 | 3: | S4,8 | |
| χ Cyg | 187796 | $+32^\circ3593$ | 19 48.6 | $+32^\circ47'$ | 4.9-13.3 | 5: | 7 | 0-2 | - | S7,1e: | 25 |
| | | | | | | 6: | 8 | 0-2 | 0: | S9,1e: | |
| | | | | | | 8.4 | 9 | 1-2 | 0: | S10,1e: | |
| AA Cyg | 190629 | $+36^\circ3852$ | 20 02.6 | $+36^\circ40'$ | 8.4-9.2 | 8.5-8.6 | 5 | 4 | 5 | S7,5 | |
| | | | | | | 9.0-9.9 | 5 | 5 | - | S7.5,6 | |
| S Cyg | - | - | 20 04.4 | $+57^\circ50'$ | 9.8-15.2 | 10.0 | 4 | 2 | - | S5,2e | |
| SZ Cep | 193028 | $+76^\circ784$ | 20 11.2 | $+77^\circ02'$ | 9.3-14 | - | - | - | - | Se: | 26 |
| Dearborn 6715 | - | $+0^\circ4492$ | 20 21.5 | $+0^\circ47'$ | 9.3-10.0: | 9.3 | 6 | 2.5:- | | S7,2 | 27 |
| AD Cyg | 195665 | $+32^\circ3850$ | 20 29.6 | $+32^\circ24'$ | 8.5-9.5 | 9.3 | 1.5 | 4 | 4 | S5,8 | |
| Z Del | 195763 | $+16^\circ4290$ | 20 30.4 | $+17^\circ17'$ | 9.0-14.0 | 8.6-8.9 | 4 | 2 | - | S5,2.5e | |
| | | | | | | 9.5 | 4.5 | 2 | - | S5.5,2.5e | |
| | | | | | | 10.4 | 6 | 2: | - | S7,2e: | |
| BV Vul | - | $+28^\circ3944$ | 20 55.1 | $+29^\circ08'$ | 10.5-11.5 | 10.6: | 1.5: | 6 | - | S7,8 | |
| V 471 Cyg | - | - | 21 05.1 | $+38^\circ22'$ | 11.8-13.2 Pg. | - | - | - | - | - | 28 |
| X Aqr | 211610 | - | 22 16.0 | $-21^\circ09'$ | 8.2-(14 | 8: | - | - | - | S6,3e: | 29 |
| w' Gru | 212087 | CD $-46^\circ14292$ | 22 19.7 | $-46^\circ12'$ | 5.8-6.4 | - | 2 | 3.5:- | | S5,7: | 30 |
| SX Peg | - | - | 22 47.9 | $+17^\circ38'$ | 8.7-13 | 9: | 0 | 4 | - | S4,9e | 31 |
| HR 8714 | 216672 | $+16^\circ4833$ | 22 52.1 | $+16^\circ40'$ | 6.48 | 6.48 | 4.5 | 1.5 | Tr: | S5,1 | 32 |
| BG And | - | $+42^\circ4690$ | 23 28.7 | $+42^\circ59'$ | 11.3-13.3 Pg. | 9.3: | 4.5 | 4 | 2 | S6.5,5e | |
| WY Cas | - | - | 23 55.4 | $+56^\circ13'$ | 8.8-14.6 | Near Min. | - | - | Strong | Se | 33 |
| W Cet | 224960 | $-15^\circ6531$ | 23 59.6 | $-14^\circ57'$ | 7.4-14.5 | 8: | 5.5 | 3 | 0: | S7,3e | |

NOTES TO TABLE 1

| | | |
|---|---|---|
| 1. | IW Cas | Vyssotsky 7 (1942). |
| 2. | RR And | Vyssotsky 8 (1943), confirmed by Merrill. |
| 3. | BD +61°471 | Suspected S by Merrill, Sanford and Burwell (unpublished). Position furnished by Sanford. |
| 4. | BD +31°392 | Vyssotsky 9 (1943). |
| 5. | BI And | Vyssotsky 15 (1946). In the First Supplement to the General Catalogue of Variable Stars by Kukarkin and Parenago, this star is classed as a long-period variable ( p = 220 days) of small amplitude. The Perkins spectrograms show no evidence of emission at Hβ (1 plate) or the infrared Ca II lines. |
| 6. | WX Cam | MSB 5 (1933). |
| 7. | BD +24°620 | Vyssotsky unpublished (1953). |
| 8. | SX Cam | Long-period variable usually below 11th mag. Recognized class S by Bidelman; classification from his McDonald red spectrogram of March 17, 1951. |
| 9. | BD +22°700 | Vyssotsky (1942). |
| 10. | WY Cam | Vyssotsky 10 (1943). No slit spectrograms available. Infrared CN suspected on slitless spectrogram by Blanco. |
| 11. | BD +12°612 | Lee, Baldwin and Hamlin (1943). |
| 12. | BD +79°156 | Vyssotsky unpublished (1953). |
| 13. | HD 34738 | Vyssotsky (1943). |
| 14. | BD +15°1200 | Vyssotsky unpublished (1953). |
| 15. | DY Gem | Vyssotsky unpublished (1950:). |
| 16. | CX Mon | MSB 24 (1933). No additional observations. |
| 17. | HD 49368 | MSB unpublished. (See MSB 25 in Table 3). |
| 18. | RR Mon | Not previously assigned to type S. Merrill (1941) described Sr II 4077 and 4215 as strong. |
| 19. | HD 58881 | Harvard variable 100. |
| 20. | KZP 1098 | Vyssotsky unpublished (1953). |
| 21. | BD Mon | Vyssotsky 16 (1946). Vyssotsky assigned Davis class S5e, implying TiO stronger than ZrO. Objective-prism plate in infrared by Blanco shows very TiO bands. |
| 22. | BD -28°6970 | ZrO strength estimated on McDonald spectrogram taken by Bidelman. |
| 23. | KZP 2016 | Vyssotsky unpublished (1953). Galactic latitude +72°. |
| 24. | CE Vul | ZrO bands discovered independently by three observers. Classified S by Rust (1938; MSB 67 (1942); Vys 19 (1946). No. IV: 3 in list of red stars by Hetzler (1937), who estimated IR index as $8\overline{.}0$. |

NOTES TO TABLE 1 (Con't)

| | |
|---|---|
| 25. $\chi$ Cyg | There are strong indications of differences in strength of the ZrO bands at the same phase of different maxima. T. Mao-Lin (1950) suggested that ZrO was relatively more prominent in 1948 than in 1944-5, when Merrill had observed the star. Perkins spectrograms show ZrO of approximately intensity 2 near the maximum of 1948. ZrO was apparently weaker in 1949 and almost absent at the 1947 maximum. |
| 26. SZ Cep | Infrared LaO observed as strong by Blanco. |
| 27. BD $+0^{o}4492$ | Lee et al (1943). Visual magnitude observed at Perkins as 9.3 on July 5, 1953, 10.0 on Sept. 14, and between 10.5 and 11.0 on Sept. 28. Variability of this star seems not to have been noticed previously. |
| 28. V 471 Cyg | Vyssotsky 6 (1942). Variability discovered by Ross and by Zinner. |
| 29. X Aqr | Vyssotsky (private communication, 1953) states that on a McCormick spectrogram of Sept. 28, 1945, ZrO 4640 was quite strong and that the general appearance of the bands of TiO and ZrO resembled that of HD 64332, classified as S6,3 here. On this date the visual magnitude of X Aqr was about 8 according to the AAVSO observations. The only Perkins spectrogram was taken on Aug. 19, 1953, at $m_v$ = 10.1 decreasing, and is a rather weak plate showing no clear evidence of ZrO, but very strong TiO. Possibly this star resembles $\chi$ Cyg in variability of ZrO. |
| 30. $\pi'$ Gru | Feast (1953) observed the Balmer Lines and several metallic lines in emission at times of decreasing brightness. Classified from McDonald and Radcliffe spectrograms. |
| 31. SX Peg | ZrO found by Bidelman, unpublished. |
| 32. HR 8714 | Not previously assigned to type S. |
| 33. WY Cas | ZrO bands by Nassau et al, unpublished (1952).<br>LaO bands observed as strong by Blanco. |

out in the spectrum of R Cyg at $m_v = 9.6$, only to disappear almost completely as the star brightens by 3 mag. Actually, most of the change takes place within the last magnitude of the rise to maximum of such stars as R Cyg and S UMa (Fig. 3). Thus even an S-type star with very little *TiO* may or may not show the bands; and, although these bands have been shown by Nassau and his collaborators (1948, 1954) at the Warner and Swasey Observatory to be a powerful means of detecting faint S-type stars, they do not provide so complete a census of these stars as can be made by means of the more persistent bands of *ZrO* in the visual region. The usefulness of *LaO* is further limited by the fact that in stars with *TiO* intensities of 8 or more, the *TiO* is accompanied by bands of vanadium oxide, of which the strong infrared heads near 7900 A (Keenan and Schroeder 1952) effectively blot out any *LaO* bands which might be present. This apparently happens in the spectrum of $\chi$ Cyg during part of its normal light-cycle.

Whenever the *LaO* bands *can* be observed, however, their sensitive response to small changes in brightness makes them very valuable as indicators of *temperature*. Evidently, *LaO* is starting to decompose rapidly at the pressure and temperature ($T_e \approx 2800°$ K) of an atmosphere such as that of S UMa just below maximum light, while *ZrO* is stable up to somewhat higher temperatures. The relative behavior of the bands of these two molecules is inconsistent with the published laboratory data, which indicate that the dissociation energy of *ZrO* is appreciably lower than that of *LaO*, but the laboratory estimates for these molecules may be in error by as much as 2 electron volts (Gayden 1952; Herzberg 1950).

The definition of type S can now be completed in terms of the intensity scales of Table 1. Necessarily the choice of the lower limit of intensity of *ZrO* is somewhat arbitrary. For the convenience of observers working with moderately low prismatic dispersions (100–200 A/mm at $H_\gamma$) we include in *class S all stars which have a ZrO intensity greater than 1.* There is also a marginal group of stars in which the *ZrO* bands are weaker (and usually overshadowed by the *TiO* bands) but can be seen distinctly with slightly higher dispersion. These stars are clearly intermediate in character between those of types M and S. They will be assigned the classification MS. Thus o′ Ori, which has *TiO* bands corresponding to type M4 with the addition of faint *ZrO* bands (intensity approximately 1), can be called "M4S" to indicate clearly its character. Fourteen MS stars in which the *ZrO* bands have intensities estimated between 0.2 and 1.0 are collected in Table 2.

Table 1 contains the 69 stars definitely assigned to class S. With the exception of a few southern stars for which spectrograms from McDonald or Mount Wilson were available, the table is limited to stars north of $-23°$ which attain visual magnitudes brighter than 11.0. The magnitudes in column 6 show the normal range in brightness for the stars that are known to vary in light. Column 7 gives the estimated brightness at the time of spectrographic observation. Where a range of values is given in this column the band intensities of the next three columns are means from several spectrograms taken on different dates.

For *ZrO* and *TiO* the band intensities are based chiefly upon Mount Wilson or Perkins spectrograms, but Yerkes spectrograms of the red region of several important stars were generously made available by Dr. W. B. Bidelman. The Mount Wilson plates used were those taken by Merrill between 1919 and 1945 (λ 4600 region) and a few covering the red region (taken mostly by Sanford), together with about 45 spectrograms of the yellow region taken by the author (chiefly with the Cassegrain spectrograph on the 60-inch reflector) during the winters of 1951–1952 and 1952–1953. The Perkins material consisted of prismatic spectrograms having scales of 27, 54, or 104 A/mm at $H\gamma$ and taken between 1946 and 1954. Most of the band intensities were estimated on exposures of the yellow region (chiefly on Eastman 103*a*-D plates) taken with the shortest camera, but a number of plates of the blue and red regions were taken to check doubtful cases.

Table 1 contains 24 stars not previously published as showing *ZrO* bands in their spectra. The inclusion of most of these was made possible by the generous co-operation of

TABLE 2

STARS OF TYPE MS

| STAR | HD | BD | α(1950) | δ(1950) | $m_v$ Normal | $m_v$ Observed | INTENSITIES *TiO* | INTENSITIES *ZrO* | TYPE | REMARKS |
|---|---|---|---|---|---|---|---|---|---|---|
| T Cet | 1760 | −20°50 | 0h19m2 | −20°20′ | 5.2–6.0 | ..... | 6–7 | 0.5: | M5–6Se | |
| HR 363 | 7351 | +28°196 | 1 11.3 | +28 15 | 6.63 | 6.63 | 3.5 | 1 | M2S | *Ba* II 4454 strong |
| W And | 14028 | +43°461a | 2 14.3 | +44 04 | 7.5–13.7 | 8.0: | 8 | 0.5: | M7–8Se | |
| ..... | ..... | − 2°891 | 4 21.8 | − 2 39 | 9.3: | 9.3: | 3.5 | 1 | M2S | * |
| 4o′ Ori | 30959 | +14°777 | 4 49.7 | +14 10 | 5.19 | 5.19 | 4 | 1 | M3S | |
| Vys. 5 | 49683 | −20°1589 | 6 46.7 | −20 22 | 8.9: | 8.9: | 5.5 | 1: | M4S | * |
| AA Cam | 54587 | +69°413 | 7 09.5 | +68 53 | 9.0–9.6/Pg. | 7.8 | 6 | 0.3: | M5S | |
| Y Lyn | 58521 | +46°1271 | 7 24.6 | +46 06 | 6.3–7.4 | ..... | 7 | 1: | M6S | |
| HR 2967 | 61913 | +14°1729 | 7 39.2 | +14 20 | 5.81 | 5.81 | 4 | 0.4 | M3S | |
| Dearborn 2660 | ..... | + 6°2063 | 8 53.0 | + 6 24 | 8.9: | 8.9: | 4 | 0.2: | M3S | Dearborn Sλ |
| RS Cnc | 78712 | +31°1946 | 9 07.6 | +31 10 | 5.6–6.8 | 6: | 7 | 0.5 | M6S | |
| ST Her | 142143 | +48°2334 | 15 49.3 | +48 38 | 6.8–8.5 | 7.5–8 | 7–8 | 0.8 | M6–7S | |
| HR 6702 | 163990 | +45°2627 | 17 55.3 | +45 21 | 6.22 | 6.22 | 7 | 0.3: | M6S | |
| 57 Peg | 218634 | + 7°4981 | 23 07.0 | + 8 24 | 5.41 | 5.41 | 5 | 0.5 | M4S | |

NOTES TO TABLE 2

−2°891 *ZrO* bands found by Vyssotsky (1953 unpublished).
Vys 5 *ZrO* bands found by Vyssotsky (1942).

their discoverers, W. P. Bidelman, at Yerkes; J. J. Nassau and V. Blanco, at Warner and Swasey; R. F. Sanford, at Mount Wilson; and A. N. Vyssotsky, at Leander McCormick, who furnished positions (and in some cases field charts) in advance of publication. For these stars the notes at the end of the table attempt to indicate the observer who first noted the S-type character of the spectrum, but this could not be done with certainty for some of the stars which were independently discovered by several observers.

The *LaO* intensities in column 10 of Table 1 could not be estimated for all the stars, and where values are given, they are based mostly upon Perkins infrared spectrograms. These were taken either with the grating spectrograph giving a normal dispersion of 50 A/mm or with a prismatic dispersion of about 250 A/mm at 8000 A. It was not found possible to obtain slit spectrograms of all the stars in the catalogue. This was especially true of long-period variable stars which happened to have their recent maxima at times

TABLE 3

STARS OF TYPES K AND M WHICH WERE FORMERLY CLASSIFIED AS TYPE S

| Star | HD | BD | $\alpha$(1950) | $\delta$(1950) | $m_p$ | Revised Type | Remarks |
|---|---|---|---|---|---|---|---|
| Dearborn 454 | ..... | + 7°393 | 2$^h$26$^m$.4 | + 8° 11′ | 8.9 | M4: | Dearborn S ? |
| Dearborn 794 | ..... | + 2°725 | 4 28.6 | + 2 14 | 9.8 | M3 | Dearborn S ? |
| MSB 25 | 264416 | + 5°1422 | 6 46.3 | + 5 39 | 9.1 | M | MSB S ? |
| Dearborn 2029 | ..... | ..... | 7 11.6 | + 0 10 | 9.7: | K | Dearborn S ? |
| Dearborn 2062 | ..... | − 0°1665 | 7 13.7 | − 1 08 | 9.9 | M2.5 | Dearborn S ? |
| Dearborn 3655 | ..... | ..... | 15 08.7 | + 3 33 | 10.3: | M6: | Dearborn S ? |
| RW Lib | 136734 | ..... | 15 20.1 | −23 53 | 9: | M4e | |
| Dearborn 3746 | ..... | +10°2859 | 15 26.1 | +10 39 | 9.7 | M4 | Dearborn S ? |
| Dearborn 4244 | 155819 | + 5°3352 | 17 11.3 | + 5 51 | 8.7 | M3 | Dearborn S ? |
| Dearborn 5495 | ..... | + 4°4036 | 19 12.5 | + 4 45 | 10.2: | M3.5: | Dearborn S ? |
| Dearborn 8089 | ..... | + 8°5128 | 23 49.3 | + 8 48 | 9.5 | M5.5 | Dearborn S ? |

NOTES TO TABLE 3

MSB 25 (HD Ex. 264416) Classified as M1 in *HD Extension* (*Harvard Ann.*, Vol. 100). 0.6 minutes east is the MS star HD 49368, which was suspected of S characteristics by Merrill, Sanford, and Burwell, but not included in their published lists.

Dearborn 3655 Both a Perkins slit spectrogram in the orange region and an objective-prism plate taken by Blanco in the infrared agree in showing the strong *TiO* bands, with no clear indication of either *ZrO* or *LaO*.

RW Lib Reclassified as M4e by Merrill (1952*b*) from coudé spectrogram taken with 200-inch reflector. RW Lib is of particular interest because it has the highest radial velocity ($\approx$ 135 km/sec) of any of the stars previously suspected of belonging to class S. A careful examination of the Mount Wilson prismatic spectrograms supports Merrill's reclassification; only *TiO* bands were definitely present on any of the plates of good quality.

Dearborn 5495 (BD+4°4036) Magnitude reported as variable by Dearborn observers. On the one Perkins spectrogram of the visual region the star appears rather red for its type.

when they could not be observed. For a number of these faint stars Dr. Victor Blanco kindly took slitless spectrograms on I-N plates with the 24-inch Schmidt telescope at the Warner and Swasey Observatory and lent them to the author for examination. The few remaining stars for which no band intensities are available are all stars for which published descriptions make their membership in class S fairly definite, and they have been included in order to make Table 1 a reasonably complete census of the brighter S stars.

A number of stars which have appeared in previous lists of suspected S-type stars showed no trace of *ZrO* bands on our program plates. Those which appear to belong to types K or M have been collected in Table 3, which, for completeness, includes also a few which had already been eliminated from class S by other observers. Most of the stars in this table are faint ones for which the earlier estimates of type were either based upon slitless spectrograms of extremely small scale or known to be doubtful for other reasons.

Consider, next, the problem of a more exact classification of the S-type stars of Table

1. The first introduction of subdivisions was made by D. N. Davis (1934). She divided the S stars into five groups (S1, . . . , S5) on the basis of the absolute and relative strengths of the *ZrO* and *TiO* bands. If we set aside her class S1 for the moment, the remaining four groups start with S2 for the stars with strong *ZrO* and almost no *TiO* and progress in order of decreasing relative prominence of the S-type characteristics to S5, in which the spectra have strong *TiO* and weak *ZrO*. That classification, though described by her as "necessarily preliminary," has proved of practical value because it does provide a convenient description of the most conspicuous features visible on small-scale spectrograms of the blue or visual regions.

The usefulness of Miss Davis' arrangement is limited, however, by the fact that it is a one-dimensional scheme, in which the subclasses are probably sensitive to more than one physical variable, with *chemical composition*, perhaps, the dominant one. This last characteristic is important and should not be lost in any revised classification; but, since the main subclasses for all other kinds of stars are arranged to progress in order of decreasing *temperature*, it is worth while to attempt a classification within type S which will be consistent with the others and will take into account the available evidence bearing on relative temperature differences among these stars.

Since stars can be found representing every step in the transition from pure type M (strong *TiO*, negligible *ZrO*) to extreme type S (strong *ZrO*, negligible *TiO*), it is reasonable to try an ordering which will be consistent with the subclassification of type M. This is feasible, for the *ZrO* bands also strengthen with decreasing light in long-period variables and thus are consistent with the bands of *TiO* in their dependence upon temperature.[6]

Accordingly, the *temperature class* for a star of type S will be defined by *summing* the intensities of *ZrO* and *TiO*, expressed on our standard scale. A weighted sum is desirable because the simple sum gives total intensities which are inconsistently high for spectra in which both sets of bands are strong. The exact manner of weighting is not critical, for anyone using the final classification will naturally make direct comparisons with the type stars. The formula adopted for convenience is:

Temperature class = Intensity of the stronger set of bands + half the intensity of the weaker set.

For a star with *TiO* and *ZrO* intensities both equal to 3, for example, the temperature class is 4.5. In column 11 of Table 1 the temperature class is given by the *first* figure following the letter S.

The second parameter of classification should be a measure of the relative prominence of the lines and bands due to the heavy metals (such as *Zr* and *La*) to that of the lighter metals (such as *Ti* and *V*). This parameter can be called the *abundance class* and defined by the relative intensities of *ZrO* and *TiO*. The simple ratio, Intensity *ZrO*/Intensity *TiO*, generally decreases in the spectrum of any particular long-period variable as the light of the star drops from maximum toward minimum. This effect is largely due to the fact that the bands of *TiO* are more sensitive to decreasing temperature (within this range of temperatures) than are those of *ZrO*. This temperature effect can be approximately compensated by multiplying the *ZrO*/*TiO* ratio by the temperature class. It is then convenient to relate the abundance class to this product by Table 4.

The abundance class for each of the stars in Table 1 is given by the *second* figure following the S in column 11. It will be noticed that the abundance class shows no systematic change with phase for the long-period variables in Table 1. This is what we might expect if the class is really an indicator of composition of the star's atmosphere, and it suggests that the correction for the effect of temperature works well enough to be worth keeping.

[6] The veiling effects mentioned earlier occur only near the minima of long-period variables and do not seriously affect the classification of these stars at other phases of their light-curves.

It should be emphasized, however, that in calling the second index figure an abundance class we are merely giving it a convenient label—the questions of just which elements differ in abundance and of how large the differences are remain to be investigated on spectrograms of high dispersion.

If the types of Miss Davis are plotted against either the temperature classes or the abundance classes, there is evident some correlation with each of them, except that her S4 stars show a wide scatter in the new classes. This is an added indication that her ordering involved both variables—temperature and composition.

There are two tests that can be applied immediately to our temperature classes. For two long-period S-type variables, radiometric temperatures at both maximum and mini-

TABLE 4

ABUNDANCE CLASSES

| *ZrO/TiO*×Subtype | Abundance Class | *ZrO/TiO*×Subtype | Abundance Class | *ZrO/TiO*×Subtype | Abundance Class |
|---|---|---|---|---|---|
| 1.0-1.9 | 1 | 4.0-4.9 | 4 | 7.6-9.9 | 7 |
| 2.0-2.9 | 2 | 5.0-5.9 | 5 | 10.0-50 | 8 |
| 3.0-3.9 | 3 | 6.0-7.5 | 6 | >50 | 9 |

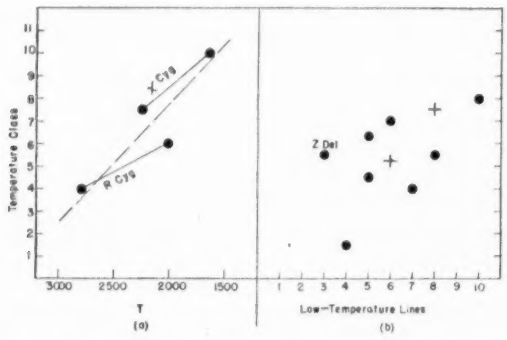


FIG. 4.—Temperature class plotted against radiometric temperatures (*a*), and intensities of low-level atomic lines (*b*).

mum were determined by Pettit and Nicholson (1933). These are plotted against temperature classes in Figure 4, *a*. A slight extrapolation was needed to give the temperature classes at minimum magnitude.

The figure shows an appreciable discrepancy between the values for $\chi$ Cyg at maximum and R Cyg at minimum; this is not surprising, for it might be expected that the calibration of the classes in terms of absolute temperatures would show some variation in passing from a nearly pure S-type star (R Cyg) to one like $\chi$ Cyg in which *TiO* is very strong and the S characteristics are quite weak. Nevertheless, the correlation is good enough to suggest use of the dashed line in the figure to estimate approximate temperatures for the stars in Table 1. Radiometric temperatures for more of the brighter S stars are badly needed.

The other test is made in Figure 4, *b*, by comparing temperature classes with the intensities of a group of "low-temperature" lines of neutral atoms as estimated by Merrill (1952) from coudé spectra of 10 S-type stars. Intensities of the blue bands of *TiO* and *ZrO* were given by Merrill for these same spectrograms and have been transferred to the

intensity scales of Table 1 in assigning temperature classes. Again the correlation is fair, with Z Del the most discrepant star in the plot.

Further refinement of the temperature classification appears unprofitable until more is known of the effective temperatures of the S stars. Ordinary colors measured through absorption filters are not reliable indicators of temperature for any of the red stars with banded spectra; a glance at Figures 2 and 3 is enough to show that an "infrared index," for example, of such stars is likely to be as much a measure of differing patterns of absorption bands as of temperature gradients in the continuous background. Radiometric temperatures, on the other hand, are significant because they are based upon integrations of such wide stretches of spectrum that even whole systems of absorption bands are averaged out.

At the other extreme it would be possible to determine fairly significant temperatures by measuring monochromatic colors at wave lengths chosen to avoid the strong bands. For this purpose "monochromatic" could be defined in practice as referring to a strip of spectrum not more than, say, 50 A in extent. Some of the most promising of such windows between terrestrial and stellar absorption bands are listed in Table 5. Even within

TABLE 5

SPECTRAL REGIONS USABLE FOR MEASUREMENT OF MONOCHROMATIC COLOR TEMPERATURES IN LATE-TYPE STARS

| Region | λλ | Remarks | Region | λλ | Remarks |
|---|---|---|---|---|---|
| Violet | 4000–4080 | Cont. absorption in carbon stars later than C4 | Yellow | 5790–5840 | Some *CN* in late carbon stars |
| Blue-green | 4900–4950 | Some *ZrO* in strong S stars; $C_2$ in strong carbon stars | Infrared | 7500–7580 | Some *CN* in carbon stars; *VO* in M7–M9 stars |
| Green | 5650–5700 | Some band absorption in late S and M stars | Infrared | 8680–8750 | Fairly strong *CN* in carbon stars |

these selected strips nothing approaching a continuum is to be found, and the remarks in the third column of the table mention the sources of the molecular absorption most likely to be present. Nevertheless, these regions are far more transparent than the average and should allow significant estimates of the very large color differences which accompany moderate temperature changes in the range below 3000° K. The regions have been chosen to avoid also the strongest emission lines occurring in the spectra of long-period variables—the lines of the Balmer series and of *Ca* II.

Up to this point the intensities of the infrared bands of *LaO* have not been used in assigning types. The extreme sensitivity of *LaO* to temperature (Fig. 3) suggests that the weighted sum *LaO* + *TiO* should correlate well with *ZrO* + *TiO*. The plot of the two sums in Figure 5, *a*, shows that *LaO* + *TiO* can be used to estimate temperature classes for any of the S-type stars in which *LaO* is observable. Reduction of the *LaO* intensity sums (strong + ½ weak) to temperature classes is given in Table 6, though again, in practice, observers will probably find it more convenient to classify by direct comparisons with spectra of standard stars.

The subdivisions of type S in which the *LaO* bands are strong enough to be observable with moderate dispersion are shown by the crosshatched area in Figure 5, *b*. The bordering zone with single hatching indicates roughly the region of ambiguity—spectra in which the *LaO* bands are close to the threshold of visibility and might or might not be seen, depending partly upon the quality of the spectrograms. The area of visibility of *LaO* has about the shape that would be expected, for in spectra with low abundance classes the *LaO* becomes increasingly hard to detect under the overlapping bands of *TiO* and *VO*, which characterize late M-type stars. In even a pure S-type star *LaO* is not observed if the temperature is greater than about 2900°.

Figure 5, *b*, was plotted from estimates on Perkins slit spectrograms, taken with either grating or prism. Fortunately, the zone of doubtful observability is relatively narrow, because the intensity of *LaO* does change so rapidly with temperature. For the same reason the area of visibility has nearly the same extent even on slitless spectrograms of very small scale. This is concluded from inspection of the Warner and Swasey I-N spectrograms taken by Nassau and Blanco. This fact is important, for it means that Figure 5, *b*, can be used by observers conducting infrared surveys of red stars with

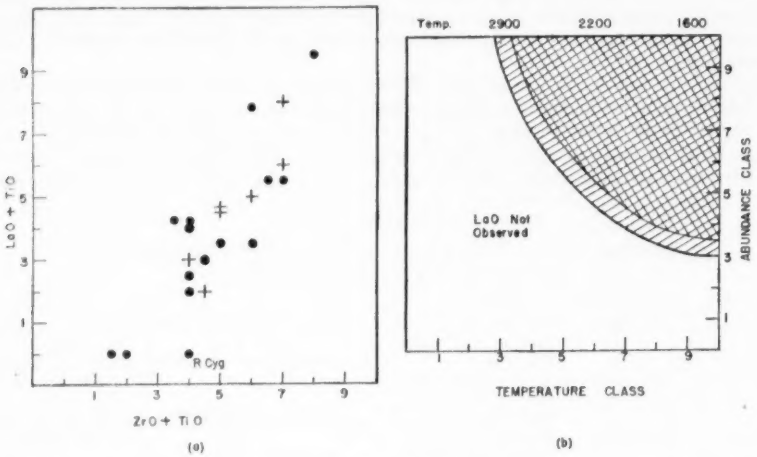


FIG. 5.—Behavior of infrared *LaO* bands. *a*, Correlation of *LaO* + *TiO* intensity with *ZrO* + *TiO*. *b*, Crosshatched area shows range of temperature and abundance classes within which *LaO* is easily observed.

TABLE 6

ESTIMATION OF TEMPERATURE CLASSES FROM INTENSITIES OF INFRARED *LaO* BANDS

| *LaO*+*TiO* | Temp. Class | *LaO*+*TiO* | Temp. Class | *LaO*+*TiO* | Temp. Class |
|---|---|---|---|---|---|
| 0.5–2.2 | 3 | 3.7–5.2 | 5 | 6.8–8.2 | 7 |
| 2.3–3.6 | 4 | 5.3–6.7 | 6 | 8.3–9.5: | 8 |

Schmidt telescopes to estimate how many subdivisions of type S they can detect. When the frequencies of occurrence of the different subdivisions have been well established, the counts on slitless spectrograms can then be used to give the total numbers of S stars in the areas surveyed.

### LUMINOSITIES

The spectroscopic criteria of luminosity which are used for M-type stars cannot be applied to S-type stars, at least not until some independent means of recalibrating them are found, for the most sensitive lines (particularly *Sr* II 4077 and 4215) are among those which appear to reflect most strongly the abundance differences among the metals. Trigonometric parallaxes fail likewise to give even group means for the luminosities of these giant stars, none of which is close enough to have an apparent magnitude brighter than 5. Nor has it proved practicable to use the method of interstellar-line intensities,

for the radial velocities of the S stars have not been found to be large enough to separate the interstellar and stellar D lines, as R. F. Sanford (1944) was able to do for several N-type stars of large velocity.

The only individual S-type star for which the luminosity has been determined is the bright southern star $\pi'$ Gruis. M. W. Feast (1953) obtained spectrograms of the companion of magnitude 10.9 at a separation of 2".7 and showed that the primary and companion had the same radial velocity within the uncertainty of measurement. The absence of any observed relative motion between the two stars over the preceding half-century was further evidence that the pair form a physical system. From Feast's classification of the companion as a G0 V star, he was able to estimate the visual absolute magnitude of $\pi'$ Gruis as between $-1$ and 0. Since no other favorable cases of S stars as members of binary systems are known, it is necessary to turn to statistical methods for average luminosities of groups of these stars.

Wilson and Merrill (1942) compared the radial velocities and proper motions of 17 long-period variables to derive their mean luminosity of $M_v = -1.0$. Their solution can now be repeated with slightly improved data. Two of their stars, R Ori and R CMi, do not show enough evidence of *ZrO* to be classed as type S under our definition. On the other hand, RR And is now included in type S, and the proper motion of W Cet is available from the Yale catalogue, giving again a total of 17 stars. Mean parallaxes were computed separately from $\tau$- and $v$-components by the usual expressions. For the $\tau$-components the mean tangential velocity of 19.3 km/sec was obtained from the radial velocities of the same stars after the contribution due to galactic rotation was removed. The results are:

$$\bar{p}_\tau = 0''.00154 , \qquad \bar{p}_v = 0''.00215 , \qquad \bar{p} = 0''.00184 ;$$

$$\bar{m}_v = 8.1 , \qquad \bar{M}_\pi = -0.5 , \qquad \bar{r} = 543 \text{ psc} .$$

After corrections for galactic absorption of $-0.3$ mag. and for dispersion of 5 (log $\bar{p}$ − log $p$) $\approx -0.2$ mag. are applied, we obtain

$$\bar{M} = -1.0 ,$$

with an uncertainty of several tenths of a magnitude, due as much to the possible systematic errors in the corrections as to scatter in the measured motions. The agreement with the mean value found by Wilson and Merrill thus implies only that the mean visual absolute magnitude of the S-type long-period variables lies in the neighborhood of $-1$ and does not appear to differ significantly from the luminosity of the average long-period variable of type M5–M8. The mean residual radial velocity of our group of S-type variables is 19.3 ± 4.1 km/sec (m.e.).

In addition to the 31 long-period variables, Table 1 contains 29 S-type stars which are either variables of small amplitude or stars for which the variability of light has not been established. For only 6 of the stars in this group are radial velocities and proper motions available. Until velocities can be measured accurately for more of these faint red stars, the best clues to their luminosity appear to be offered by their galactic distribution. In Table 7 the mean galactic latitudes for the long-period Mira-type variables and for the variables of small amplitude are shown separately for several ranges of apparent visual magnitude. The magnitudes refer to maximum light for long-period variables and to mean light for the remaining stars. The figures in parentheses are the number of stars in each group. Corresponding figures for the carbon stars, separated into types R and N, were derived for the stars in Sanford's catalogue (Sanford 1944), which have fairly well-determined visual magnitudes. Since the S stars are definitely a low-velocity group (none is known to have a radial velocity exceeding 100 km/sec), the well-known group of high-velocity carbon stars were excluded from the comparison by counting only those with $Vr < 60$ km/sec.

Although Table 7 represents a very crude way of expressing galactic concentration, it does permit suggestive comparison, and the numbers of S-type stars are too small to justify more elaborate analysis.[7] The mean latitudes of the variables of small amplitude are generally lower than those of the long-period variables. This merely shows that type S shares the known tendency of long-period variables to scatter widely from the galactic plane and is a reminder that the luminosities may differ considerably in stars showing different kinds of variability. The more significant figures are in the last three columns, which show that the galactic concentration of the small-amplitude variables of type S is probably slightly less than that of similar N-type stars but appreciably greater than the concentration of the R-type stars. Sanford (1944) brought together the evidence from radial velocities and from interstellar D-line absorption to estimate the luminosities of

TABLE 7

MEAN GALACTIC LATITUDES

| | Long-Period Variables | | | | Small-Amplitude Variables | | | |
|---|---|---|---|---|---|---|---|---|
| Type | $5^m$–$8^m$ | $8^m1$–$9^m0$ | $9^m1$–$10^m0$ | $10^m1$–$11^m0$ | $5^m$–$8^m$ | $8^m1$–$9^m0$ | $9^m1$–$10^m0$ | $10^m1$–$11^m0$ |
| S | 27° | 22° | 16° | 21° | 22° | +8° | 17° | 14° |
| | (9) | (11) | (7) | (1) | (3) | (7) | (13) | (7) |
| R | 28 | 30 | .... | .... | 17 | 26 | 21 | 27 |
| | (2) | (4) | .... | .... | (8) | (13) | (20) | (13) |
| N | 28 | 22 | 4 | .... | 21 | 9 | 7 | 8 |
| | (6) | (11) | (4) | .... | (31) | (33) | (50) | (9) |

the carbon stars. His data indicate that for type R, $\bar{M}_v \approx -0.5$, and for type N, $\bar{M}_v \approx -2.0$. The galactic concentration of the group of S stars suggests that their mean absolute magnitude lies between these two values.

A further inference which may be drawn from the similarity in the general distribution of the S stars and the late carbon stars is that the S-type variables of small amplitude are likely to be associated with the spiral arms of our galactic system. The absence of large space motions among these stars is consistent with this conclusion. Another test can be made by adopting a preliminary estimate of $-1.5$ for their mean absolute magnitude and plotting their corresponding distances as projected upon the galactic plane. In Figure 6 this has been done for all stars in the group except the two which have galactic latitudes exceeding 30°.

On the diagram can be traced roughly the spiral arm coming in between 0° and 50° longitude and extending past the sun to longitudes 180° and 220° which has been mapped by Morgan *et al.* (1953) from aggregates of supergiant stars and by Oort and his collaborators (Van de Hulst 1953) from the velocities of the 21-cm hydrogen line. In addition, there is a remarkable gap between longitudes 60° and 170°, where no S stars occur at distances between 200 and 900 parsecs. Beyond this gap lies a group of 13 or 14 stars, and it looks as though at least some of these were in the outer branch of the local arm, which, from Morgan's data, lies in the direction of the anticenter, at distances of from 900 to 1400 parsecs from the sun. The gap in Figure 6 then would correspond to the space between the two branches of the local arm. If this identification is correct, no major correction to our tentative value of $-1.5$ for $\bar{M}_v$ is indicated.

The alternative possibility that this group lies in the outer spiral arm known to cross the anticenter at a distance of about 2400 parsecs appears to be ruled out by the distribution of the S stars in galactic latitude. None of the supergiant aggregates in that arm, which have been studied by Morgan and others, lies at galactic latitudes much exceeding

[7] The statistical discussion of the distribution of S stars which was carried out by Ikaunieks (1950) is not useful for our purpose, since, out of the 88 possible S stars in his list, 17 have already been removed from the group by our classification and at least another half-dozen are of very doubtful membership. His methods may prove of value, however, when the number of known S stars becomes much larger as a result of surveys with Schmidt telescopes.

5°. Several of the S stars in our group, however, are considerably farther from the galactic plane; and a few, such as the three stars in Taurus (+24°620, +22°700, +12°612), at latitudes of −17° to −21°, may be in the nearer parts of the local arm. These latter stars, then, would have luminosities appreciably below the mean and close to the estimates made by Feast for $\pi'$ Gru. This is the first evidence indicating the real dispersion in absolute magnitudes which probably exists within type S. Another star which may have a low luminosity is BD+44°2267 ($m_v \approx 10$; type S recognized by Vyssotsky 1953, unpublished), which is remarkable for its situation only 18° from the galactic pole. It will be important to determine the space motion of this exceptional star, which would lie more than 1300 parsecs above the galactic plane if its absolute magnitude were −1.5. A plot of the long-period variables of type S projected on the galactic plane as in Figure 6 shows little more than a random scatter.

The evidence bearing on the luminosities of the S-type stars as a whole is still too scanty for final conclusions but suggests that most of them belong among the giants and

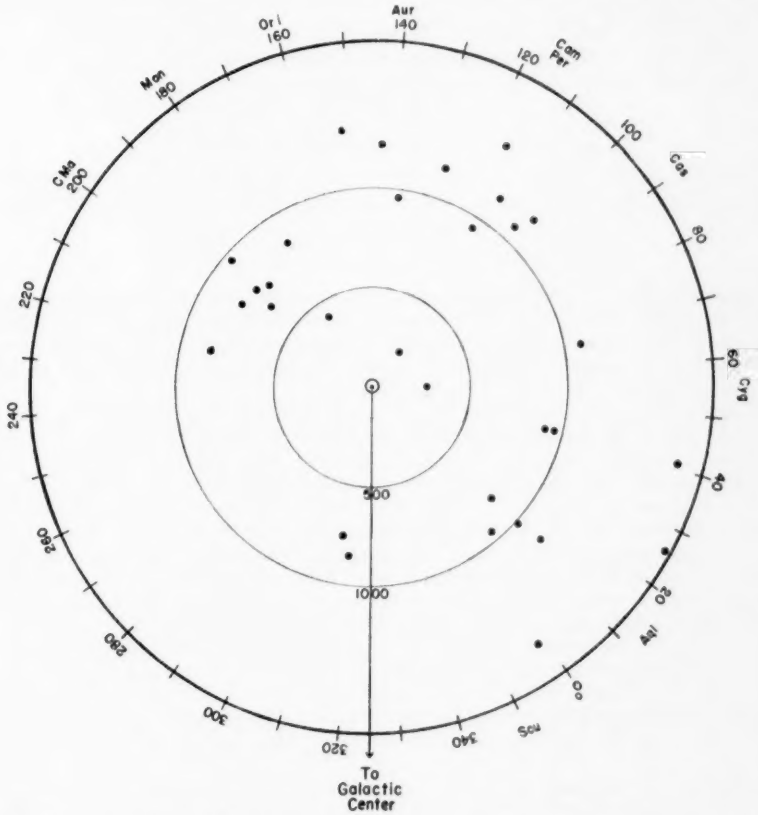


FIG. 6.—Projected distribution of S stars on galactic plane (long-period variables omitted). The blank sector from 230° to 310° is the part inaccessible to observation from northern latitudes. Distances are given in parsecs on the assumption that $\overline{M}_v = -1.5$.

bright giants (luminosity classes III and II) rather than among the supergiants, where earlier ideas (present author's included) had placed them.

## FREQUENCY OF OCCURRENCE

The S-type stars are recognized as relatively young on the galactic time scale because of their similarity to other "population I" objects in distribution and motions. In addition, the considerable strength in their spectra of the lines of *Tc* I (Merrill 1952*a*, p. 23), which has a half-life of the order of a quarter of a million years, suggests that they represent a relatively short-lived stage of evolution. The presence of MS transition stars shows their close relationship to type M. The relative frequency of occurrence of types M and S will therefore provide an important datum for testing any evolutionary theory seeking to explain their presence.

Since we lack precise knowledge of the masses and luminosities of the S-type stars, the best that can be done at this time is to compare them with the whole giant branch of type M. This is the more necessary, since individual luminosities are known for only a portion of the M-type stars.

TABLE 8

RELATIVE NUMBERS OF LATE-TYPE STARS

| | Long-Period Variables | Others | |
|---|---|---|---|
| Types | ($m_v$<10) | $m_v$<8 | 8.0≦$m_v$<10 |
| M3–M8 | 76 | 121 | 61 |
| MS | 4 | 8 | 3 |
| M | 82 (59) | 308 (84) | 155 (45) |
| MS | 4 (3) | 20 (5) | 8 (2) |
| S | 25 (18) | 3 (1) | 26 (8) |
| C | 27 (20) | 37 (10) | 156 (45) |

A search for MS stars was carried out on the prismatic spectrograms of the Mount Wilson and Perkins collections. The survey of the Mount Wilson plates covered the first 18 hours of right ascension and was limited to those negatives on blue-sensitive emulsions which had moderate density in the 4600 A region, plus a few additional spectrograms covering the yellow part of the spectrum.

In making the search for MS stars, it soon became apparent that they could be detected efficiently only in stars cool enough to develop the more intense *TiO* bands to at least the strength corresponding to an M3 giant. Otherwise, the still fainter *ZrO* bands would remain below the threshold of visibility on these spectrograms of only moderate dispersion. For this reason the counts of types M and MS in the first two rows of Table 8 were limited to the range M3–M8. In order to compare these figures with all the known S-type stars, which, of course, include many with very weak *TiO* bands, they must be corrected for the fraction of M0–M2 stars in type M. This has been done for the next two rows of Table 8, where the percentages of the totals in each column have been given also (in parentheses). The correction factor for the first two columns was 2.55, obtained by counting the numbers in each subdivision of type M in the Mount Wilson catalogue of spectroscopic absolute magnitudes (Adams *et al.* 1935). For the long-period variables the much smaller correction factor, 1.08, obtained directly from Table 4 of Merrill (1941), reflects the relative scarcity of long-period variables in the early subdivisions of type M. Counts of carbon stars in Sanford's catalogue (1944) have been added in the last row of the table.

In the last two rows of Table 8 no distinction has been made between nonvariable stars and variables of small amplitude, since among these cool stars many not yet listed as variable will eventually be found to show changes in their light. Below the eighth magnitude the percentage of variables included in the sample is greater, for many of the spectrograms in both collections were taken in the course of studies of the semiregular and irregular variable stars.

Serious selection effects undoubtedly remain in Table 8. The last column has little significance, for the ease of discovery of even the faint carbon stars has made the count relatively complete for them, while the spectrograms of only a small fraction of the M-type stars were available for examination. The same overemphasis is present in the figures for type S, but to a lesser extent, since these stars are not so easily discovered on slitless search spectrograms. These effects are much less pronounced in the second and third columns of Table 8, though the percentages of carbon stars are somewhat too high even there.

The percentages for the stars brighter than the eighth magnitude are more significant. Besides confirming the known infrequency of S stars compared to carbon stars, they show that an appreciable fraction of the stars have the intermediate MS characteristics. The actual figures for the MS group depend upon our somewhat arbitrary definition of the limiting *ZrO* intensity and would be larger if all the spectra in which the *ZrO* bands can be definitely seen with moderately high dispersion were included; but the important point is that the tendency toward strengthening of the bands of the heavy oxides is not rare among the cool stars.

In striking contrast, the long-period variables, among which definite S-type stars are relatively common, as has been shown by other counts (Merrill 1940), include only about the same percentage of MS stars as are found in the other groups, as nearly as can be judged from such a small sample population.

## STARS WITH SPECTRA RELATED TO TYPE S

In Table 9 are collected seven red stars whose spectra show some similarity to type S in the intensity of their atomic lines, but without any positive indications of bands of

TABLE 9

STARS WITH SPECTRA RELATED TO TYPE S

| Star | HD | BD | $\alpha$(1950) | $\delta$(1950) | $m_v$ Normal | $m_v$ Observed | $\Gamma_V$ | *Ba* II 4554 | *Sr* 4607 | *Na* D | *CN* (IR) |
|---|---|---|---|---|---|---|---|---|---|---|---|
| W Cas | 5235 | +57°165 | 0h51m9 | +58°17′ | 8.5–11.8 | 8.0 | −.59 | 5 | 3 | ... | ... |
| | | | | | | 8.5 | | ... | ... | ... | 8 |
| | | | | | | 9.9 | | ... | ... | 7: | ... |
| R Ori | 31798 | + 7°768 | 4 55.7 | + 8 03 | 8.7–13.5 | ..... | | | | | |
| GP Ori | ..... | +15°726 | 4 59.9 | +15 14 | 11.8–13.6 /Pg. | 9.8–9.9 | +.79 | 4: | 12: | 10 | 5.5 |
| FU Mon | 44544 | + 3°1214 | 6 19.8 | + 3 28 | 11.6–12.7 /Pg. | 8.6–9.0 | ... | 5: | 10: | 8 | ... |
| R CMi | 54300 | +10°1428 | 7 06.0 | +10 06 | 7.5–10.8 | 8.2: | +.48 | 5: | 3: | 4 | ... |
| | | | | | | 8.7 | | ... | ... | ... | 6 |
| | | | | | | 9.4 | | ... | ... | 10 | ... |
| ..... | 121447 | −17°3961 | 13 53.1 | −18 03 | 8.1 | 8.1 | | 7: | 4 | 5 | 4: |
| CY Cyg | 198164 | +45°3271 | 20 45.2 | +45 52 | 9.9–11.7 /Pg. | 8.6–8.9 | + .4 | 4: | 4 | 7 | 5 |

## NOTES TO TABLE 9

W Cas Infrared *CN* bands and Swan bands of $C_2$ observed by Bidelman at Yerkes and by Keenan at Perkins (1950).

R Ori Carbon features, including the $C_2$ band at 4737 A, noted as strong by Vyssotsky in report to Tonanzintla symposium (1942).

GP Ori Remarkably strong D lines noted by Baldwin and Hamlin (1940, Pl. 4). A low-dispersion slit spectrogram taken by Morgan, reproduced in Pl. 55 of the Yerkes *Atlas of Stellar Spectra*, shows the differences between this spectrum and typical ones of types S and N. The observations of its spectrum have been summarized by Bidelman (1950), who tentatively assigned it to type S. McKellar and Stillwell (1944) and Sanford (1949), however, considered it a late carbon star on the basis of the strong *CN* bands. A Perkins infrared grating spectrogram (scale 100 A/mm) taken at $m_p$ = 10.0: on December 7, 1952, shows no evidence of *LaO*. The band absorption between λ 7500 and λ 8700 appeared to be entirely due to *CN*, except for an absorption feature near λ 8610, which showed some similarity to the unidentified band observed at that position in very cool S-type stars.

FU Mon Strong D lines observed by Baldwin and Hamlin (1940, Pl. 3). Similarity to GP Ori discussed by Bidelman (1950). Prismatic spectrogram on 103a-G emulsion, February 22, 1953, with 18-inch camera on Mount Wilson 60-inch reflector, shows a number of strong lines in the region of λ 5590, but the *ZrO* band was not seen.

R CMi *CN* bands and Swan bands of $C_2$ observed by Bidelman at Yerkes and by Keenan at Perkins (1950).

BD 121447 Similarities to R CMi noted by Merrill (1927). Considered by Bidelman and Keenan (1951) as an unusually red member of the *Ba* II group, which show relatively strong bands of *CN* and *CH*. My examination of the Mount Wilson spectrograms, including two additional ones taken in 1952, indicated that *ZrO* had never been strong enough to be definitely established as present. Five Perkins plates of the yellow region also fail to show *ZrO*.

CY Cyg Nearly all recent observers of this red star, including Vyssotsky, Sanford, and Keenan (all unpublished), have doubted that it belongs with the S-type stars. The only bands which have been definitely recognized are those of the red and infrared systems of *CN*. On a coudé spectrogram of the red region, which Dr. Sanford kindly permitted me to measure, no *ZrO* bands were identified. When this plate was matched in a comparator against a spectrogram of the M2 *Ib* star 119 Tau, nearly all the metallic lines between 5850 and 6720 A were found to be slightly stronger in CY Cyg. The enhancement was least for the *Fe* lines and greatest for *Y*, *Zr*, and the *Li* resonance line at 6707. The radial velocity of +3.8 km/sec was measured by Sanford on this plate (1943, unpublished).

*ZrO* (or of *LaO*) on the plates at Mount Wilson or Perkins. They all show some affinity to the carbon stars, in that their infrared *CN* bands are stronger than those of the S stars but weaker than those of most of the recognized carbon stars. The table gives estimated intensities of the infrared *CN* bands and of several of the atomic lines which are most strongly enhanced in these spectra. The intensities for the *Na* D lines were estimated near the longward end of the prismatic spectrograms, where the dispersion is much less than for the lines in the blue, and the intensity scale is correspondingly compressed for sodium.

The *Ba* II line at 4554 is as prominent in this group as in the S stars; this is one of the reasons that each of these stars had been assigned to type S at one time or another. The absence from their spectra, however, of the *TiO* and *ZrO* bands which overlie the neutral lines of *Sr* and *Na* in types M or S brings out the extreme sensitivity of these resonance lines to temperature. Near minimum phase of the variables in Table 9, both *Sr* 4607 and the D lines become stronger than in even the coolest of the normal S-type stars. In GP Ori the measurements of McKellar and Stillwell (1944) gave an integrated total absorption for the D lines of 56 A, equaled only by WZ Cas among the carbon stars covered by their survey.

The three stars R CMi, W Cas, and R Ori are known also to have the Swan bands of $C_2$ present with enough strength to be recognizable with moderate dispersion (see the notes to Table 9). The resemblances of these three R CMi stars had been remarked by Merrill (1927). They were grouped by Davis (1934) to form her entire subclass S1. They are closely allied to the carbon stars; W Cas in particular has such strong *CN* bands that it can well be counted among the carbon stars.

The question of the nature of the stars of Table 9 is part of the broader problem of the relationship of the stars of type S to the other classes of cool stars. We can hope for answers to these questions only when estimates of the relative abundances of the atoms and molecules in their atmospheres become available. It will only be mentioned here that measurements of the infrared bands indicate that, in an S-type star, *CN* is more abundant than in one of type K or M but less abundant than in the transitional stars of Table 9.

Grateful acknowledgment is made to all the observers who have been mentioned as allowing their spectrograms or data to be used in assembling the tables of this paper. To Dr. Bowen and the staff of the Mount Wilson Observatory my thanks are given for the opportunity of spending two quarters as a guest observer there. The first of these, in the winter of 1951–1952, was supported in part from funds granted to the Ohio State University by the OSU Research Foundation for aid in fundamental research.

## REFERENCES

Adams, W. S. 1925, *Trans. I.A.U.*, **2**, 119.
Adams, W. S., Joy, A. H., Humason, M. L., and Brayton, A. M. 1935, *Ap. J.*, **81**, 187; *Mt. W. Contr.*, No. 51.
Afaf, M. 1950, *Proc. Phys. Soc. London*, **63**, 1156.
Baldwin, R. J., and Hamlin, D. W. 1940, *Ann. Dearborn Obs.*, Vol. **4**, Part 15.
Bidelman, W. P. 1950, *Ap. J.*, **112**, 219.
Bidelman, W. P., and Keenan, P. C. 1951, *Ap. J.*, **114**, 473.
Bobrovnikoff, N. T. 1934, *Ap. J.*, **79**, 483.
Davis, D. N. 1934, *Pub. A.S.P.*, **46**, 267.
———. 1947, *Ap. J.*, **106**, 28; *Mt. W. Contr.*, No. 733.
Feast, M. W. 1953, *M.N.*, **113**, 510.
Gaydon, A. G. 1952, *Dissociation Energies and Spectra of Diatomic Molecules* (2d ed.; London: Chapman & Hall).
Herzberg, G. 1950, *Molecular Spectra and Molecular Structure*, Vol. 1: *Spectra of Diatomic Molecules* (2d ed.; New York: D. Van Nostrand Co).
Hetzler, C. 1937, *Ap. J.*, **86**, 509.
Ikaunieks, J. 1950. *Trudy Latvian Inst. Phys. Math., Riga*, **2**, 101.
Joy, A. H. 1926, *Ap. J.*, **63**, 281.

Keenan, P. C. 1948, *Ap. J.*, **107,** 420; *Perkins Contr.*, No. 25.
———. 1950, *A.J.*, **55,** 172.
Keenan, P. C., and Schroeder, L. W. 1952, *Ap. J.*, **115,** 82; *Perkins Contr.*, No. 32.
Lee, O. J., Baldwin, R. J., and Hamlin, D. W. 1943, *Ann. Dearborn Obs.*, Vol. **5.**
Lowater, F. 1932, *Proc. Phys. Soc. London*, **44,** 51.
McKellar, A., and Stillwell, W. H. 1944, *J.R.A.S. Canada*, **38,** 237.
MaO-Lin, T. 1950, *Ann. d'ap.*, **13,** 57.
Merrill, P. W. 1922*a*. *Trans. I.A.U.*, **1,** 98.
———. 1922*b*, *Ap. J.*, **56,** 457; *Mt. W. Contr.*, No. 252.
———. 1927, *Ap. J.*, **65,** 23; *Mt. W. Contr.*, No. 325.
———. 1940, *The Spectra of Long-Period Variable Stars* (Chicago: University of Chicago Press).
———. 1941, *Ap. J.*, **94,** 171; *Mt. W. Contr.*, No. 649.
———. 1952*a*, *ibid.*, **116,** 21.
———. 1952*b*, *ibid.*, p. 523.
Merrill, P. W., Sanford, R. F., and Burwell, C. G. 1933, *Pub. A.S.P.*, **45,** 306.
———. 1942, *ibid.*, **54,** 107.
Morgan, W. W., Keenan, P. C., and Kellman, E. 1943, *An Atlas of Stellar Spectra* (Chicago: University of Chicago Press).
Morgan, W. W., Whitford, A. E., and Code, A. D. 1953, *Ap. J.*, **118,** 318.
Nassau, J. J., and van Albada, G. B. 1948, *Ap. J.*, **107,** 418.
Nassau, J. J., Blanco., V. M., and Morgan, W. W. 1954, *Ap. J.*, **120,** 478.
Pettit, E., and Nicholson, S. G. 1933, *Ap. J.*, **78,** 320; *Mt. W. Contr.*, No. 478.
Rust, C. F. 1938, *Ap. J.*, **88,** 525.
Sanford, R. F. 1944, *Ap. J.*, **99,** 145; *Mt. W. Contr.*, No. 689.
———. 1949, *Pub. A.S.P.*, **61,** 43.
Van de Hulst, H. C. 1953, *Observatory*, **73,** 129.
Vyssotsky, A. N. 1942, *Pub. A.S.P.*, **54,** 153.
———. 1943, *ibid.*, **55,** 245.
Wilson, R. E., and Merrill, P. W. 1942, *Ap. J.*, **95,** 248; *Mt. W. Contr.*, No. 648.

# SPECTRAL CLASSIFICATION WITH EXCEEDINGLY LOW DISPERSION

W. W. Morgan, A. B. Meinel, and Hugh M. Johnson
Yerkes Observatory
*Received June 17, 1954*

ABSTRACT

A method is described for the segregation of reddened O and B stars from objective-prism plates having a dispersion of the order of 30,000 A/mm. The instrument used is a Schmidt camera of 8 inches focal length and an effective aperture of 2 inches, in conjunction with an objective prism of 1° angle. A finding list of 19 stars in the γ Cygni region is given; the majority of these stars are probably of early type and are between photographic magnitudes 12.0 and 13.0.

## INTRODUCTION

The O and early B stars constitute the most important stellar group for investigations of spiral structure; observation of such stars for the determination of distance consists of three steps: (1) the segregation of the group from the general stellar population; (2) observation for the determination of accurate spectroscopic absolute magnitudes; and (3) photometric observations for magnitudes and colors, to determine the correction for interstellar absorption.

For stars brighter than the ninth magnitude the *Henry Draper Catalogue* furnishes a satisfactory finding list, although the stars of highest luminosity can be most efficiently separated by means of the classification system described a short time ago (Morgan 1950). The "natural-group" classification of early-type stars of high luminosity outlined in Morgan's article has been intensively used in the case of the stars of magnitudes 9–12 at the Warner and Swasey and Tonantzintla Observatories. The dispersion employed is around 270 A/mm in the photographic region; when widened spectra are obtained, it is possible to segregate the blue giants with an accuracy of around 90 per cent; the remaining 10 per cent consist of main-sequence B2–B5 stars having strong emission lines of hydrogen.

At the present time it appears that the practicable limit with 24–36-inch Schmidt cameras is near photographic magnitude 12.5. Since the surveys now in progress indicate that the complete galactic belt will be surveyed in this manner within the next few years, it is of interest to investigate possible ways of discovering early-type stars of fainter apparent magnitudes. The present paper describes a method which seems to promise satisfactory results for stars fainter than magnitude 12.5.

## INSTRUMENTAL EQUIPMENT

The instrument used was a Meinel-Pearson Schmidt camera of 8 inches focal length and a correcting plate 8 inches in diameter; the optical resolution of this camera is exceeding high. For experimental reasons, a 2-inch diaphragm, which was mounted eccentrically over the correcting plate, was used throughout. An objective prism having an angle of 1° was the dispersing medium. Eastman 103*a*-F3 plates were used, with exposures ranging from 2 to 20 minutes. The spectra were unwidened; their total length was between 100 and 200 $\mu$; the width for faint spectra was of the order of 8–10 $\mu$. All the plates were obtained by Hugh M. Johnson.

The best plate quality was obtained with the use of the metolsulfite developer which

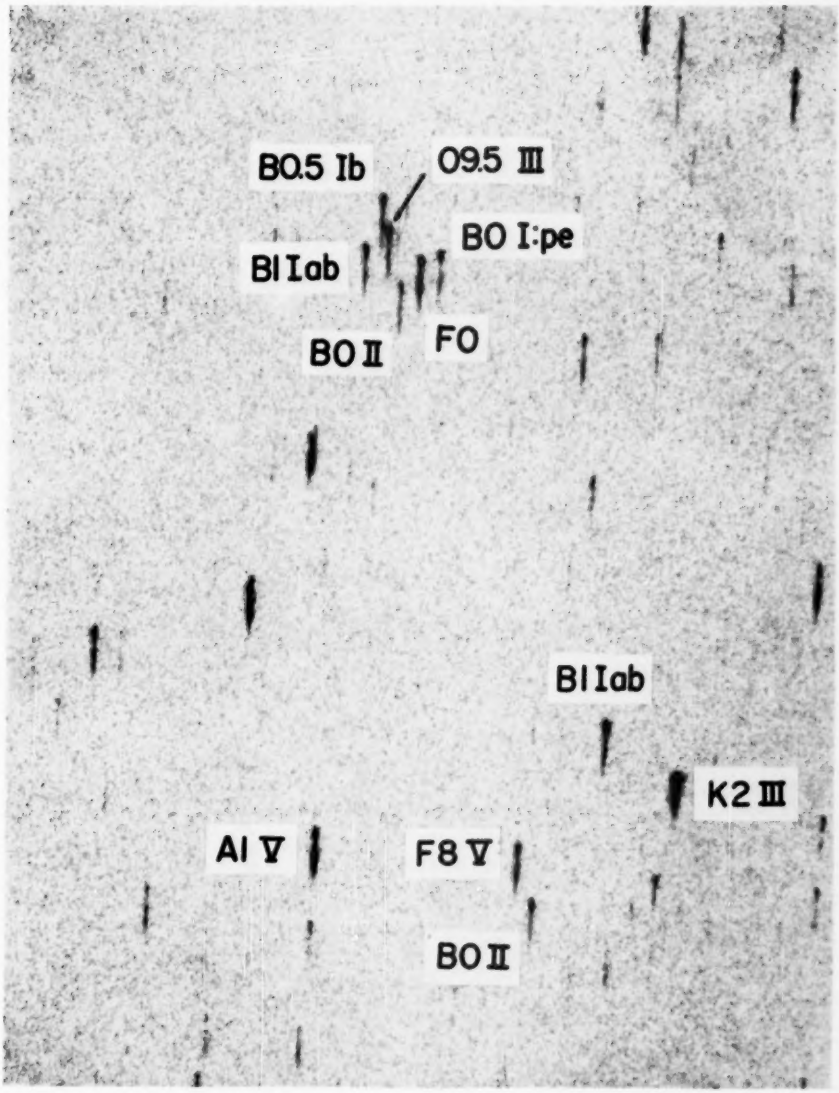


FIG. 1.—Section of objective-prism plate including NGC 6913 (*top*). The approximate wave-length limits of the spectra are 7300 A (*top*) and 3500 A (*bottom*). Eastman 103*a*-F3 plate. Exposure 2 minutes North is at top; the vertical field is about 1°. The length of the spectra on the original plate is around 0.15 mm.

has been in use for spectrograms at the Yerkes Observatory for a number of years. The formula is:

| | |
|---|---|
| Metol | 10 gm |
| Sodium sulfite (dry) | 100 gm |
| Water to | 1000 cc |

Develop 12 minutes at 65°

### THE IMAGE CHARACTERISTICS

From investigations in multicolor photometry (see Morgan, Harris, and Johnson 1953) it could be predicted that the spectra of reddened early-type stars would have a different appearance from those of the yellow giants; the ultraviolet would be considerably stronger than the blue and red. In addition, for main-sequence stars near type A0, the ultraviolet would be expected to be weakened, because of the higher members of the Balmer series and the effect of the Balmer continuum. This would result in the spectrum being shortened; a main-sequence early A star unaffected by interstellar reddening would therefore appear blue, from a comparison of the red and blue parts of the spectrum, but would not have a strong ultraviolet extension, because of the effects of Balmer lines and continuum.

FIG. 2.—Schematic drawings of standard spectra. Red is at the top. The gap in the upper part of the dA0 spectrum is due to a sensitivity dip in the emulsion. The length of the dA0 spectrum on the original plate is about 100 $\mu$. The optimum conditions for classifying these small spectra are for a total length of between 100 and 160 $\mu$, or about fifteen times the diameter of faint focal images.

Part of a plate including the region of NGC 6913 is illustrated in Figure 1. The cluster itself is located in the upper part of the illustration. The spectral types marked are from Yerkes slit spectrograms, which were obtained with the 40-inch parallax spectrograph. The long violet extension of the reddened early-type stars is apparent; there is a marked difference in appearance between the K giant and the early B stars; in addition, the A1 star shows the predicted blunting of the violet end, due to the Balmer lines and continuum.

Figure 2 illustrates characteristic images which were sketched from the original plate. The length of the dA0 image is 100 $\mu$; its maximum width is around 20 $\mu$. The break in the upper part of the spectrum is due to the dip in sensitivity of the emulsion used. The yellow O star illustrated has a visual interstellar absorption of around $1\frac{1}{2}$ mag.; the red O star has a visual absorption of around 3 mag.

An inspection of Figures 1 and 2 indicates that it should be feasible to recognize reddened early-type stars on objective-prism plates similar to the one illustrated. The principal source of uncertainty is in the separation of reddened early-type stars from giants of spectral types G0–G5 and from dwarfs of spectral types G8–K2. However, in spite of a certain amount of ambiguity, it appears that a finding list based on these criteria and covering regions of the sky near the galactic equator should include at least 50 per cent reddened B stars; if great care is used and only plates of the highest quality are included, the percentage of early B stars may be as high as 70–80 per cent. Even if the percentage of successful recognitions were as low as 30 per cent, the method would still be a most

useful one, since it is probable that no more efficient method is known for detecting such stars fainter than the twelfth magnitude.

### A FINDING LIST OF FAINT REDDENED STARS NEAR $\gamma$ CYGNI

In spite of the small aperture of 2 inches which was employed for the objective-prism camera, it was found possible to recognize the reddened O and B stars published earlier in this region by Nassau and Morgan (1951) and Nassau and Harris (1952). Exposures of 5 minutes in length were sufficient to detect the heavily reddened early-type stars in the Nassau-Harris catalogue. Exposures of 10 and 20 minutes showed a number of additional fainter stars which are probably of early type. Figures 3, 4, and 5 illustrate regions near $\gamma$ Cygni, with the newly classified stars marked. With the exception of No. 5, they are all probably between photographic magnitudes 12.5 and 13.0; No. 5 is somewhat brighter. Numbers 6 and 7 form a double star having approximately equal components separated by a distance of around 17″. Numbers 13–19 are probably fainter members of the O-type cluster described by Johnson and Morgan (1954).

A Schmidt camera with a correcting plate 7 inches in diameter and 28 inches in focal length is now under construction, which should make possible the classification of reddened early-type stars by the method described to around photographic magnitude 14–15. A survey of the galactic equatorial region is planned with this instrument. If the survey is successful, the principal problem will pass from one of the discovery of distant reddened stars to the devising of methods for their observation for the determination of accurate spectroscopic parallaxes.

### REFERENCES

Johnson, H. L., and Morgan, W. W. 1954, *Ap. J.*, **119**, 344.
Morgan, W. W. 1950, *Pub. Obs. U. Michigan*, **10**, 33.
Morgan, W. W., Harris, D. L., and Johnson, H. L. 1953, *Ap. J.*, **118**, 92.
Nassau, J. J., and Harris, D. L. 1952, *Ap. J.*, **115**, 459.
Nassau, J. J., and Morgan, W. W. 1951, *Ap. J.*, **113**, 141.

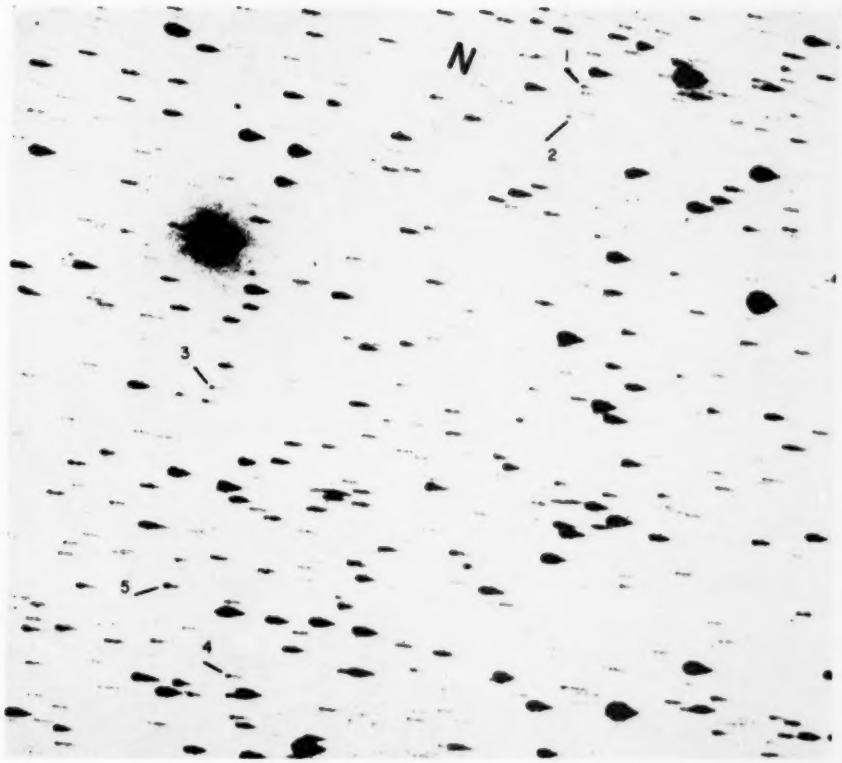


FIG. 3.—Identification chart for probable reddened early-type stars in Cygnus. Red is toward the left. The bright star in the upper left region is $\gamma$ Cygni ($20^h18^m6$; $+39°56'$ [1900]). The vertical extension of the field is around $1\frac{1}{3}°$. The contrast of Figs. 3–5 is higher than the original plate, and the ultraviolet tails are not clearly visible.

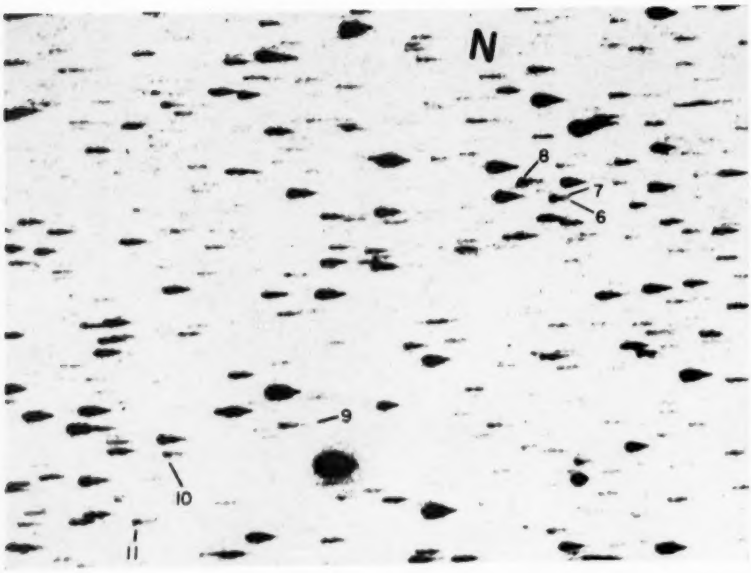


FIG. 4.—Probable reddened early-type stars in Cygnus. The bright star in lower part of field is HD 194335 ($20^h20^m0$; $+37°10'$ [1900]). The vertical extension of the field is about 1°.

FIG. 5.—Probable reddened early-type stars in Cygnus. The bright star directly above No. 17 is HD 195988 ($20^h29^m4$; $+41°7'$ [1900]). The vertical extension of the field is around $1\frac{1}{2}°$.

# IDENTIFICATION OF THE YELLOW CORONAL LINE*

CHARLOTTE PECKER,† DONALD E. BILLINGS, AND WALTER ORR ROBERTS

High Altitude Observatory, Boulder, Colorado

*Received April 29, 1954; revised July 15, 1954*

## ABSTRACT

Confirmation of Edlén's tentative identification of *Ca* XV as the atom responsible for the yellow coronal emission line λ 5694 is given. From line-profile analysis, the atomic weight of the responsible atom is shown to be close to 40. The existence of an additional emission line at about λ 5446, demanded by theory and previously reported by Waldmeier, is verified. The ratio of the intensities λ 5694/λ 5446 is found to be in agreement with theoretical values for *Ca* XV emission.

## INTRODUCTION

Among the identifications proposed by Edlén (1942) for different coronal emission lines, that for the yellow line λ 5694, which Edlén regarded as only tentative, has been the most controversial. Numerous authors have doubted that *Ca* XV was responsible for the line because of its high ionization potential (814 volts) and because the companion line expected to be present was not found or was too low in intensity (Shklovsky 1950) or because it was not at the proper wave length for agreement with theory (Garstang 1952). Other authors have advanced arguments supporting the *Ca* XV identification. Waldmeier (1951), from the discovery of a companion line, and Lyot and Dollfus (1953), from arguments based on ionization-potential groupings, supported Edlén's initial identification.

For some time the High Altitude Observatory has carried out the practice of obtaining special spectra of the yellow line whenever possible, in order to study its close association with solar flares and other active-region phenomena (Roberts 1952; Dolder, Roberts, and Billings 1954). A number of spectrograms taken with the Climax coronagraph by W. N. Fleming on February 2, 1950, show the yellow coronal line with great intensity and are well suited for microphotometric analysis. The work reported in this paper and in a previous note (Pecker, Billings, and Roberts 1954) was done entirely from these spectrograms.

The Climax coronagraph is equipped with a Littrow spectrograph of 210 cm in focal length. The first-order grating has 600 lines/mm and uses an aperture of 7.5 cm. A curved slit, 50 $\mu$ wide, parallels the image of the sun's limb. In the spectrograms the slit undergoes a 1:1 magnification, and the dispersion of the spectra is approximately 8 A/mm at 6000 A. When the spectrograph is in good adjustment, two photospheric absorption lines, spaced 0.3 A apart, appear to be just resolved.

## STUDY OF THE YELLOW-LINE PROFILE

With the new High Altitude Observatory null-method microphotometer we made tracings of deflection versus wave length from each of the several spectra of February 2, 1950, in the vicinity of the red (λ 6374), green (λ 5303), and yellow (λ 5694) coronal lines and at the position angle where the yellow coronal-line emission was strongest. One such set is shown in Figure 1. For each spectrogram we traced all three lines with the same run of the microphotometer carriage, with the same slit-width, orientation, and solar position angle. In addition, we traced, in the same carriage runs, the vicinity of the

* This work was supported by the Office of Naval Research.

† On leave from the Institut d'Astrophysique, Paris.

sodium D lines, whose profiles in absorption we used to correct our coronal-line profiles for instrumental smearing, as described below.

As a first step in analysis we converted the experimental microphotometer profiles into intensity profiles, using the intensity calibrations that are impressed on all Climax coronal spectra, also smoothing the tracings for the small film-grain fluctuations at the same time. From these profiles we measured the uncorrected half-widths (widths at half

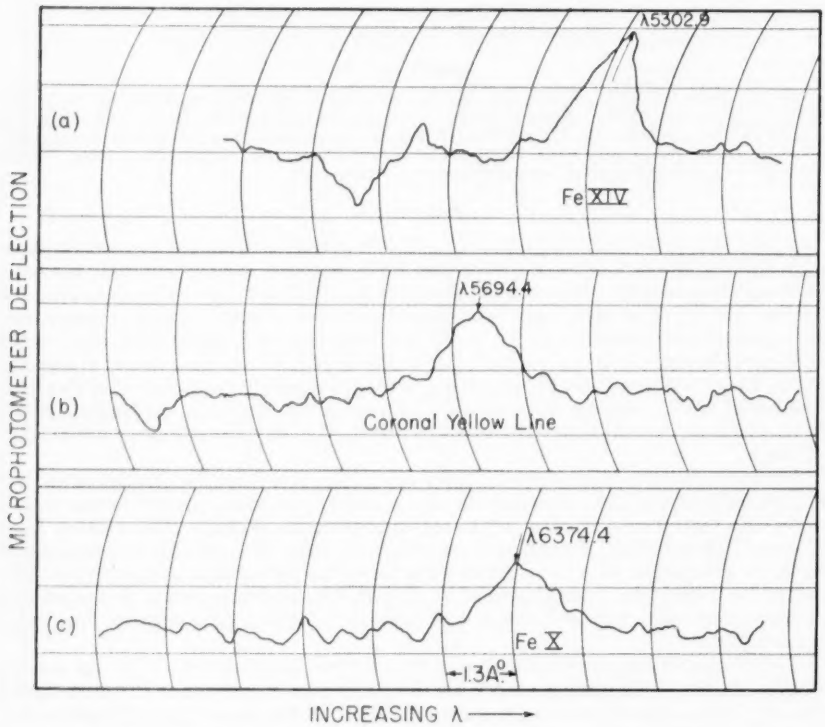


FIG. 1. – Microphotometer tracings of the green, yellow, and red coronal lines, at 0.6 A/inch. Tracings are made on Climax coronal plate No. 3076, exposure 3, of February 2, 1950, 290° heliographic position.

of maximum intensity) that are given in Table 1, column 4. We noted immediately that the yellow-line profile resembled a Gaussian profile, as shown in Figure 2. We thus confirmed for the yellow line what Lyot (1937) and Waldmeier (1941) had already found for the green and red coronal lines.

The combined effect on line widths of the finite resolution of the spectrograph and microphotometer differs from one spectrogram to another and from one tracing to another, depending on the focusing of the spectrograph and the microphotometer and the exactness of alignment of the curved microphotometer slit with the curved arc of the lines on the spectrograms. Consequently, we determined an instrument profile for each tracing, from the continuum lines of the scattered photospheric light. We then used this value in correcting the measured half-widths of the coronal lines. We tested the validity

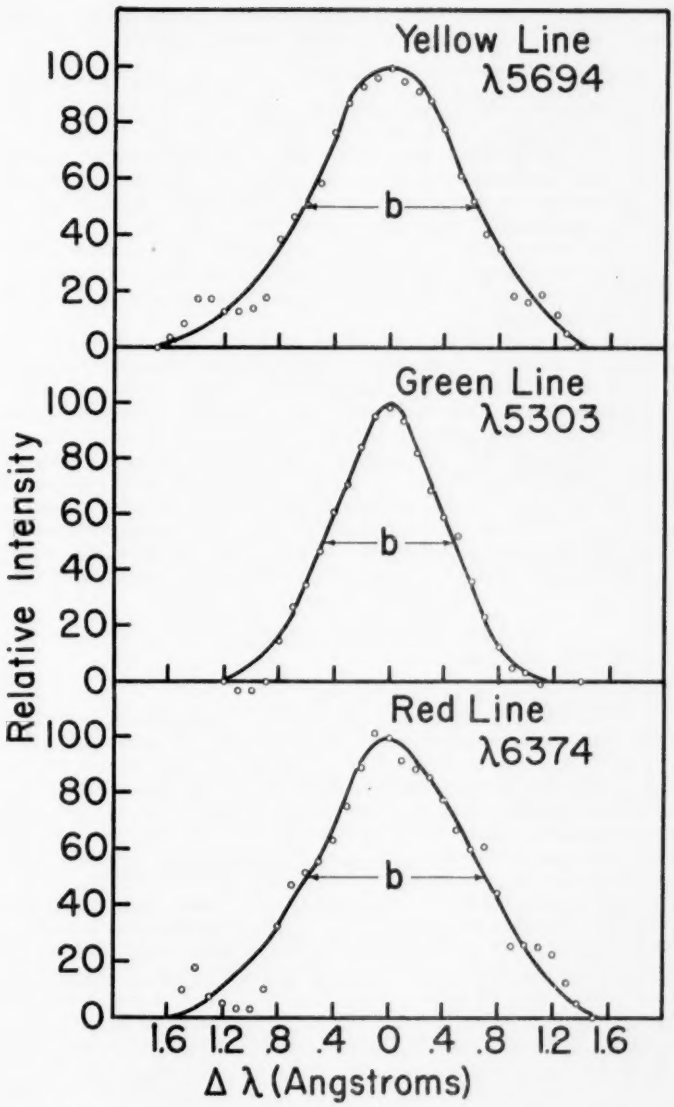


FIG. 2.—Relative intensity profiles of the yellow, green, and red coronal lines, February 2, 1950. To obtain these profiles, microphotometer tracings were first smoothed through film grain, then deflections were changed to intensities, using the calibrating spots on the plate. Each intensity is expressed as a percentage of the maximum intensity in the line profile. Points are unsmoothed microphotometer deflections converted into relative intensities.

of this process on a special spectrographic plate obtained by placing a neon glow lamp at the occulting disk of the coronagraph and superimposing its spectrum on the spectrum of the corona and scattered photospheric light. We found that neon lines had a consistent half-width of 0.45 A, and that their shape differed from Gaussian only slightly, in the direction of rectangular, rather than dispersion, profiles. By comparing the absorption lines on the same test plate with those of the Utrecht solar atlas (1940), we computed an instrumental profile of $0.51 \pm 0.06$ (p.e.) A. Hence we concluded that the absorption lines on the coronal spectrograms could be depended upon as a suitable measure of instrumental broadening on our actual yellow coronal-line spectra. Furthermore, we found that, in case the instrumental half-width was less than half of the half-width of the line being studied, the instrumental broadening of a Gaussian line was essentially the same for a Gaussian or a rectangular instrument profile. In the few cases where the instrumental profiles did not meet this standard, we increased the tabulated probable errors of the results appropriately.

If we assume that the Doppler form of the experimentally determined coronal-line profiles results from thermal broadening, a number of steps in analysis are possible. The regularity of the profiles supports the assumption, but the assumption also confronts us with some difficulties, as we point out later. For this work we have made the assumption, but we are aware of possible alternatives. Comparison of the broadened theoretical profiles and our experimental red- and green-line profiles gives us coronal temperatures, if we admit the validity of the assumption. We have given in Table 1, column 2, the temperatures of the coronal gas so derived from different spectra. Moreover, the experimental half-widths of the yellow coronal line allow us to find the ratio of temperature to atomic weight for the atom responsible for the line, since the half-widths, $b$, of Doppler profile lines are related to the temperature, $T$, and the atomic weight, $\mu$, of the emitting atoms by

$$b = \text{Const. } \lambda \sqrt{\frac{T}{\mu}},$$

where $\lambda$ is the wave length of the emission line.

We found from our better-resolution spectra the surprising result that the temperatures derived from the application of the foregoing equation to the half-widths of the green and red coronal lines (*Fe* XIV and *Fe* XV) were nearly the same for the two lines, even though they were not the same for different elevations in the coronal region. We have good reason to believe that, in the regions we studied, all three coronal lines were emitted from a relatively small locality in the corona. Figure 3 shows, for example, how the red and green coronal-line emission showed concentrated maxima localized in the same place where the yellow-line emission was most intense. In another study (Billings, Liebenberg, and Roberts 1953) which we shall report in detail later, we argue that it is difficult to explain the observed evolution of regions of coronal-line emission unless we consider the distribution of emission intensities to represent concentration in density of the gases near the active centers rather than simply differences of temperature.

Thus we consider that all three coronal lines originate in a concentrated region of denser corona, where the temperature of the gas giving rise to all three lines is the same and is above $3.5 \times 10^6$, as shown in Table 1. We are, of course, aware of the dilemma that the foregoing considerations lead us to, since the red-line emission should maximize at a lower temperature than the green, and the *Fe* X ion responsible for it should scarcely be present at all at as high a temperature as the profiles suggest.

If we therefore now assume that the yellow coronal line is emitted from gas at the same temperature as the red and green lines, we can from the foregoing equation determine from each ratio of the half-widths of red to yellow and green to yellow lines the atomic weight of the atom responsible for the yellow line, the green and red lines being known to originate in iron, with atomic weight 56. Eight such values from four separate

coronal spectrum exposures appear in columns 6 and 7 of Table 1. In column 8 we give the measure of agreement of temperatures derived from green- and red-line half-widths.

On plate 3076, exposure 3 was closer to the sun than exposure 2. The reverse was true on plate 3077. We are not able to fix the heights of the exposures precisely, but it appears that the temperature increased upward in the region studied.

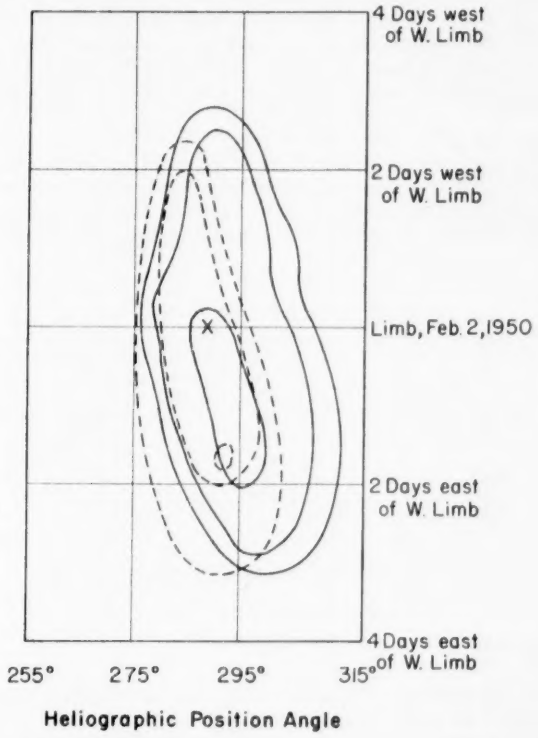


FIG. 3.—Isophotal contours of red (– – – – –) and green (————) coronal-line emission at and near the West Limb on February 2, 1950. These closed contours show that red- and green-line intensities had approximately the same spatial distribution in the region, with strong maxima at the approximate position of the most intense yellow-line emission, indicated by *X*. Contours are at intervals of five units on the Climax scale of intensities, with higher values toward the centers of the closed contours.

Table 1 thus gives us eight values for the atomic weight of the atom responsible for the yellow coronal line, with a mean value of $40.2 \pm 2.5$(p.e.). An alternative method of computation, suggested by D. H. Menzel, was also employed, in which atomic weights were determined from the ratios of abscissae in the completely unsmoothed profiles of the yellow line to the abscissae at corresponding ordinates in the green and red lines. These atomic weights (144 in all) were combined statistically, giving $40.3 \pm 0.9$ (p.e.). Our value of atomic weight definitely eliminates the identification of the yellow line proposed by Shklovsky (1950) of *Ne* X, with atomic weight 20.2, if, of course, we make the assumption that the broadenings of the profile are thermal Doppler broadenings.

Elements having atomic weights between 36 and 44 include calcium, argon, potas-

sium, and chlorine. The value of atomic weight, we found, provides a favorable argument for the original *Ca* XV identification of Edlén or for argon, since potassium is not considered to be a likely source of coronal radiation (Edlén 1942).

We show, in Figure 4, the three coronal-line profiles from one of the spectra superimposed after multiplying the abscissae by $5303/\lambda\sqrt{m/56}$. The resulting yellow-line profiles, using values for $m$ of 20, 40, and 56, are shown in the figure. The yellow-line profile, which nearly coincides with the green- and red-line profiles, is obtained by using $m = 40$. A profile with Gaussian wings is drawn underneath for comparison. From the figure we observe that the profiles using $m = 40$ for the yellow line agree within the limitations of random film-grain fluctuations and do not differ markedly from Gaussian profiles.

## STUDY OF THE CORONAL LINE λ 5446

Waldmeier (1951) reported six observations of a coronal line in the vicinity of λ 5445 at points of intense activity on the solar limb and closely associated with the yellow coronal line. He considered its existence to be evidence that the source of the yellow coronal line was *Ca* XV, since two visible lines from *Ca* XV have been predicted by theory.

TABLE 1

SUMMARY OF LINE-WIDTH ANALYSIS*

| Spectrogram No. (1) | Temp. (° K) (2) | Coronal Line (3) | Uncorrected Half-widths (A) (4) | Corrected Half-width (5) | $\mu$ Derived from $b_G/b_Y$ (6) | $\mu$ Derived from $b_Y/b_R$ (7) | $T_G/T_R$ (8) |
|---|---|---|---|---|---|---|---|
| *3076:* | | | | | | | |
| Exp. 3 | $3.6\times10^6$ | G | $1.00\pm0.02$ | 0.92 | $39\pm4$ | $42\pm5$ | 1.00 |
| | | R | $1.21\pm.05$ | 1.11 | | | |
| | | Y | $1.26\pm.05$ | 1.19 | | | |
| Exp. 2 | $6\times10^6$ | G | $1.26\pm.07$ | 1.19 | $42\pm10$ | $42\pm7$ | 0.98 |
| | | R | $1.52\pm.06$ | 1.47 | | | |
| | | Y | $1.56\pm.08$ | 1.48 | | | |
| *3077:* | | | | | | | |
| Exp. 2 | $3.8\times10^6$ | G | $1.10\pm.10$ | 0.93 | $39\pm10$ | $40\pm20$ | 0.95 |
| | | R | $1.30\pm.10$ | 1.15 | | | |
| | | Y | $1.32\pm.20$ | 1.19 | | | |
| Exp. 3 | $4.1\times10^6$ | G | $1.12\pm.10$ | 0.94 | $35\pm10$ | $42\pm15$ | 0.82 |
| | | R | $1.37\pm.15$ | 1.25 | | | |
| | | Y | $1.39\pm0.10$ | 1.27 | | | |

* Errors listed are estimated probable errors.

Shklovsky (1950) and Garstang (1952) objected to the use of λ 5445 as evidence of the *Ca* XV identification of the yellow line, pointing out that the two lines from *Ca* XV should be of very nearly the same intensity, whereas Waldmeier had reported that λ 5445 was one-sixth the intensity of λ 5694, and Lyot, being unable to find the line at all, deduced that its intensity was less than one-sixth that of the yellow line. Furthermore, Garstang computed that the wave lengths of the two *Ca* XV lines should be considerably shorter than λ 5694 and λ 5445.

We therefore examined our spectrograms of February 2, 1950, for λ 5445, which, if it was the expected companion line of λ 5694, should also be comparatively strong. Figure 5 shows a small-scale microphotometer tracing (6 A/inch) of one of the Climax spectrograms. A weak emission line at λ 5446 appears between the two strong photospheric absorption lines λ 5445.0 and λ 5446.9.

We then undertook a detailed study of this line, making large-scale microphotometer tracings (0.6 A/inch) on several spectrograms taken on February 2, 1950. We also made tracings of a Climax spectrogram taken by W. N. Fleming and D. S. Johnson on December 3, 1948. By subtracting tracings made at points on the limb outside the yellow-line emission region from tracings made on the same spectra at the points where the yellow-line emission was a maximum, we found evidence of a coronal line associated with the

yellow line, with maximum at approximately λ 5446.5 ± 0.3 on all the spectrograms. The proximity of the two strong absorption lines made a study of the line profile difficult. We were able, nevertheless, to determine the ratio of the intensity of the line to that of λ 5694.

On each of the spectrograms we traced the neighborhood of λ 5446 and λ 5694 at two points on the limb. One of the points was that of maximum yellow-line emission; the other was as close as possible, but at a point of much fainter yellow-line emission. Then, using the solar absorption lines as a guide, we superimposed the two tracings from each plate, as shown in Figure 6. Next we subdivided the area lying between the two curves

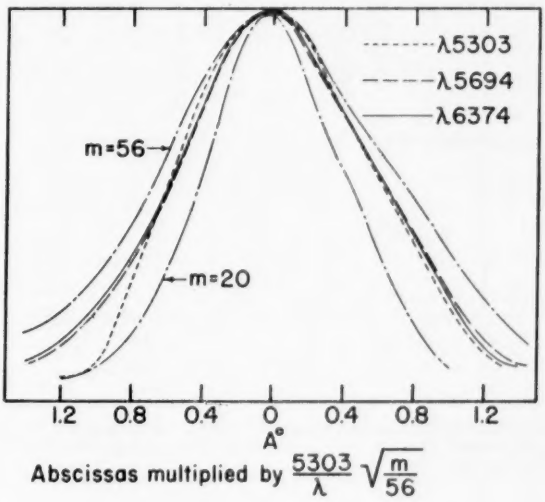


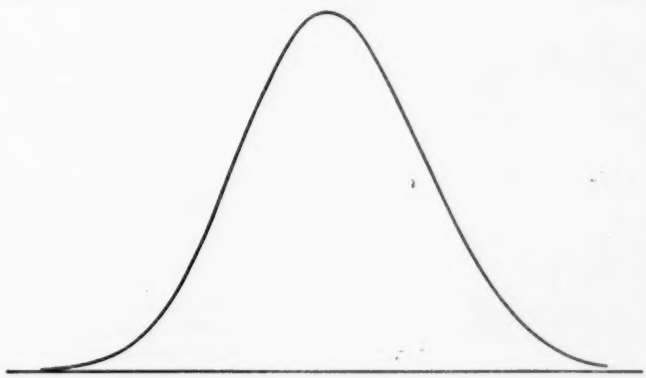

FIG. 4.—Coronal-line profiles adjusted to same maximum intensity, wave length, and atomic weight. Abscissae are multiplied by $(5303/\lambda)\sqrt{(m/56)}$, with values of $m$ of 20, 40, and 56 being applied to the yellow-line profile. The 5303 profile shows the effect of the photospheric absorption line in the extreme left-hand wing. A profile with Gaussian wings is drawn underneath for comparison.

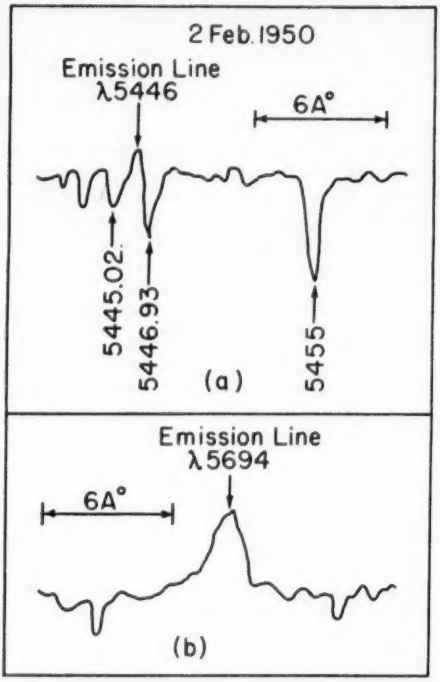


FIG. 5.—Sections from a small-scale microphotometer tracing (6 A/inch) of Climax coronal plate No. 3076, exposure 2, at the point on the limb of most intense yellow-line emission. *a* is from the vicinity of λ 5446, and *b* shows the yellow line.

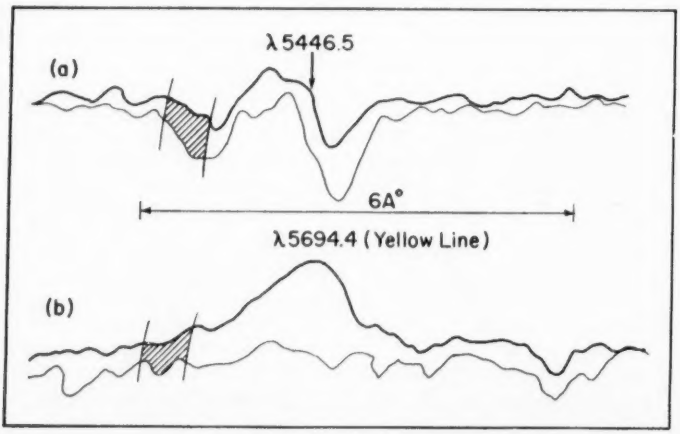


FIG. 6.—Microphotometer tracings with dispersion of 0.6 A/inch from Climax coronal plate No. 3076, exposure 3. The upper of the tracings in both *a* and *b* is through the point on the limb of most intense yellow-line emission. The lower is through a point very near, but where the yellow-line intensity is very low. *a* shows the vicinity of λ 5446; *b*, the vicinity of λ 5694. The shaded areas lying between the two curves were measured, then converted to intensity units for the plotting of points on the curves of Fig. 7.

into short sections, one of these sections being shaded in Figure 6, *a* and *b*. We measured the area of each of these sections with a planimeter, then converted each area into an integrated intensity by dividing by the slope of the calibration-curve (microphotometer deflection versus intensity) at the deflection corresponding to the center of gravity of the section. Figure 7 shows the integrated intensities of the sections plotted as a function of the wave lengths of their centers for two of the best tracings of February 2, 1950. Figure 8 shows a composite of the integrated intensities from the four best spectrograms of that date. Since the two curves of Figure 6 lie quite close together and the sections are short,

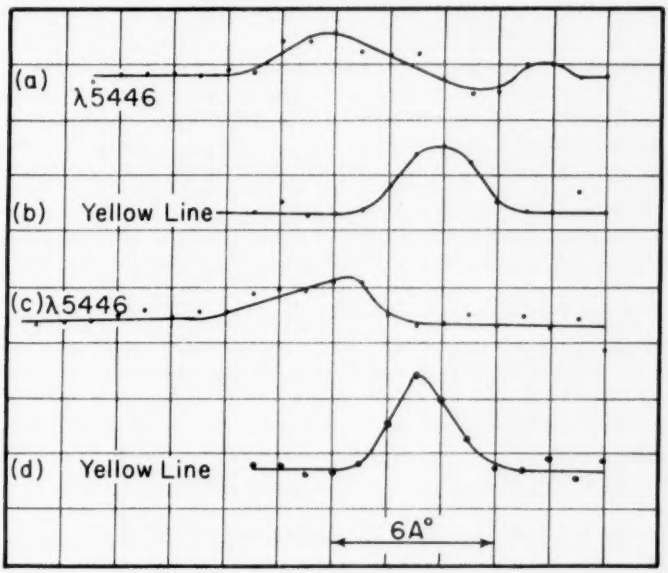


FIG. 7.—Integrated intensities corresponding to the areas of the ½-inch-long sections lying between the pairs of microphotometer tracings of Fig. 6, plotted against the wave-length positions of the sections. *a* and *b* are plotted from the vicinities of λ 5446 and λ 5694 on Climax coronal plate 3076, exposure 2; *c* and *d* are corresponding curves from exposure 3 of the same plate. The intensities are given on a relative scale the same for all curves. The scale is derived from the standard photometric spots applied in green light to all Climax coronal plates.

the slope of a single calibration-curve accurately characterizes all deflections in the curves bounding any one section.

Finally, we obtained integrated intensities for the two lines, λ 5446 and λ 5694, by measuring the areas under the curves of Figures 7 and 8. The background level in each case was determined by studying 100 A or more of small-scale microphotometer tracings, as shown in Figure 5. The above method is well suited for determining the integrated intensity of a line, since it averages over the film grain in a purely objective manner; but it is not suitable for a study of line profiles.

Table 2 gives the ratio of the intensities of the two lines, $I_{5694}/I_{5446}$, for three of the most intense yellow-line spectra, as well as for the composite from the four spectra studied. Although the coronal line λ 5446 was evident on the spectrogram of December 3, 1948, it was not of sufficient intensity for measurement.

From this study we have thus verified Waldmeier's (1951) observation of the line λ 5446 in association with the yellow coronal line λ 5694. It seems probable that Lyot was unable to find the line because of the strong absorption line λ 5446.9 almost superimposed upon it. Furthermore, we found the ratio of the intensities of the two coronal lines λ 5694 and λ 5446 to be approximately 1.6, whereas Waldmeier found a ratio of 6. The discrepancy may reasonably be explained by the influence of the neighboring absorption lines.

TABLE 2

LINE-INTENSITY RATIOS

| Plate | Spectrum (Exposure No.) | $I_{5694}/I_{5446}$ | Plate | Spectrum (Exposure No.) | $I_{5694}/I_{5446}$ |
|---|---|---|---|---|---|
| 3076 | 2 | 1.3 | 3077 | 3 | 2 |
| 3076 | 3 | 1.6 | Composite of four spectra | | 1.6 |

These results combine with the results of our study of the profile of the yellow line to support the original identification of the yellow line by Edlén. The *Ca* XV transitions responsible for the two lines should then be: λ 5694 corresponding to the transition $2s^2\ 2p^2\ {}^3P_1 - {}^3P_0$ and λ 5446 corresponding to the companion transition ${}^3P_2 - {}^3P_1$. Shklovsky (1950) calculated the relative emission probabilities of the two lines; assuming the coronal temperature to be of the order of $10^6$ degrees, he found that the ratio of the in-

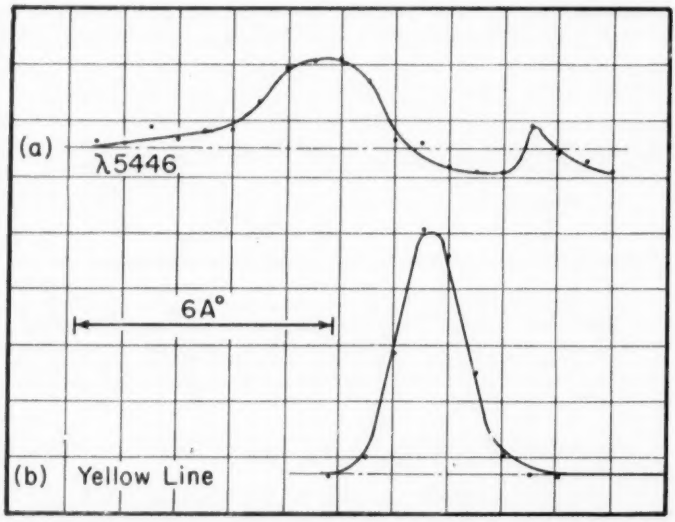


FIG. 8.—*a*, A composite of four curves: *a* and *c* of Fig. 7 and similar curves from Climax coronal plate 3077, exposures 2 and 3; wave lengths in the vicinity of λ 5446. *b*, Composite from the same exposures as Fig 8*a*, wave lengths in the vicinity of λ 5694. Areas under the curves of Figs. 7 and 8 give integrated line intensities. The small, sharp peak at the right of λ 5446 may be a prominence emission line. Mitchell reports a chromospheric emission line at λ 5448.4. The depression lying between it and the line is due entirely to an emulsion flaw in exposure 2, plate 3076, on the nonyellow-line trace. It should be emphasized that the curves of Figs. 7 and 8 are not line profiles and that the shapes of the curves do not necessarily represent the true shapes of the lines. Only the total energy in the lines, not the distribution with wave length, can be determined by methods used in plotting these curves.

tensities should lie near 1–1.5 if they are actually from these *Ca* XV transitions. Shklovsky considered the ratio measurements of Waldmeier of about 6 as strong arguments against the identification; our value of this ratio reverses the argument. The discrepancy between the observed line wave lengths and those predicted for *Ca* XV by Garstang remains unresolved.

## MEANING OF RESULTS

In the interpretation of the results of these measurements we are confronted with a serious dilemma: we first postulated that the line breadths arose from thermal Doppler broadening and that the gases emitting the yellow, red, and green lines were all at the same high temperature of several million degrees. Working from this hypothesis, we derived evidence in favor of a *Ca* XV identification of the yellow line. But *Ca* XV is an ion of such high ionization potential (814 volts) that its existence in an equilibrium situation appears incompatible with the presence of *Fe* X (with an ionization potential of 233 volts), to say nothing of the strong prominence lines that generally accompany the yellow coronal line.

The very short life of yellow-line emission (a few hours) (Dollfus 1953; Dolder, Roberts, and Billings 1954) suggests that the *Ca* XV does not exist in an equilibrium condition but that the ionization is brought about by a transient phenomenon—perhaps a flash of ionizing radiation—after which recombination reduces the ion population in a few hours. Goldberg and Menzel (1948) have shown that all three ions can coexist in the presence of an appropriate radiation field.

Certain aspects of the February 2, 1950, spectra may throw some light on the physical conditions associated with yellow-line emission:

1. In the high-intensity red- and green-line coronal region, which extended over several times as great an arc length at the solar limb as did the yellow-line-emitting region, the temperature, as measured by red- and green-line profiles, was considerably higher than the temperature of the corona of the quiet sun, a point we shall discuss in a forthcoming paper.

2. The red line showed a small, sharp secondary minimum near, but not coincident with, the yellow-line maximum, superimposed on the broader strong maximum over the general region of yellow-line emission.

3. The green line did not show any significant intensity changes near the yellow-line maximum.

4. Two limb flares were observed in the yellow-line region on February 1, 1950 (Dolder *et al.* 1954, case 39).

5. Knots of prominence material at the elevation above the sun at which we observed the yellow line were highly dispersed and of low intensity, but the profiles of the prominence lines were quite wide.

From a consideration of these circumstances, we suggest that, shortly before our yellow-line observations, some transient event occurred that left in its wake ions covering a wide range of ionization potentials and that at the time of our observations the temperature of the entire coronal region was such that the *Fe* XIV population was relatively stable, the *Fe* X population was decreasing by ionization, and the *Ca* XV population was decreasing by recombination.

We must consider the alternative hypothesis, that the greater part of the widths of the coronal lines in active regions arises, as Waldmeier (1953) has suggested, from macroscopic rather than thermal motion. According to such a model, the widths we observe for the red and green coronal lines indicate that the *Fe* X and *Fe* XIV ions are undergoing the same degree of agitation, whereas the ions that emit the yellow line are observed along the same line of sight but in a more agitated region of the corona, the degree of agitation being just sufficient to give a line width corresponding to an atomic weight of 40 by our temperature hypothesis. An analysis of the red, yellow, and green coronal-line

profiles in a number of instances of intense yellow-line emission should make possible a clear choice between the two hypotheses. This is true because the weight of the atom that emits the yellow line is the same in all cases, whereas it would be very unlikely that the degree of agitation of the region emitting the yellow line would always have the same relation to that of the region or regions emitting the red and green lines.

We acknowledge with gratitude the excellent observational work of Mr. Fleming and Mr. Johnson in obtaining these spectra and the many valuable discussions we have had with Drs. Jean-Claude Pecker and R. G. Athay during the course of this work. We also thank Dr. Leo Goldberg for advice concerning the method of determination of the line profiles, and Dr. D. H. Menzel for aid in the interpretation of our results.

## REFERENCES

Billings, D. E., Liebenberg, D. H., and Roberts, W. O. 1953, *A.J.*, **58**, 211.
Dolder, F. P., Roberts, W. O., and Billings, D. E. 1954, *Ap. J.*, **119**, 120.
Dollfus, A. 1953, *Convegno di scienze fisiche matematiche e naturali, 14–19 Settembre, 1952* (Rome: Accademia nationale dei Lincei), pp. 219–220.
Edlén, B. 1942, *Zs. f. Ap.*, **22**, 30.
Garstang, R. H. 1952, *Ap. J.*, **115**, 569.
Goldberg, L., and Menzel, D. H. 1948, *Centennial Symposia* ("Harvard Observatory Monographs," No. 7 [Cambridge, Mass.: The Observatory]), pp. 279–297.
Lyot, B. 1937, *L'Astronomie*, **51**, 203.
Lyot, B., and Dollfus, A. 1953, *C.R. Acad. sci., Paris*, **237**, 854.
Minnaert, M., Mulders, G. F. W., and Houtgast, J. 1940, *Photometric Atlas of the Solar Spectrum* (Amsterdam: D. Schnable and Kampert & Helm).
Pecker, C., Billings, D. E., and Roberts, W. O. 1954, *C.R. Acad. sci., Paris*, **238**, 1101–1103.
Roberts, W. O. 1952, *Ap. J.*, **115**, 488.
Shklovsky, I. S. 1950, *Ann. Crimean Ap. Obs.*, **5**, 109.
Waldmeier, M. 1941, *Zs. f. Ap.*, **20**, 323.
———. 1951, *ibid.*, **29**, 29.
———, 1953, *Convegno di scienze fisiche matematiche e naturali, 14–19 Settembre, 1952* (Rome: Accademia nationale dei Lincei), pp. 171–184.

# THE SOLAR PHOTOSPHERIC GRADIENT

S. W. Henriksen
Army Map Service, Washington, D.C.
*Received July 14, 1953; revised July 19, 1954*

ABSTRACT

From microdensitometer measurements on solar-spectrum photographs of the 1945 eclipse, a value of $-7.6 \times 10^{-8} + 0.6 \times 10^{-8}$ cm$^{-1}$ was derived for the photospheric gradient, a value which corresponds to 4400° C for the region measured.

## I. INTRODUCTION

The path of totality of the July 9, 1945, solar eclipse extended about 40° N., 70° E. in western Siberia to about 45° N., 115° W. at Boise, Idaho. The flash spectrum of the sun at this eclipse was photographed by at least two parties in Europe and by one party in central Canada. This last party was from the Milwaukee Astronomical Society under the direction of E. A. Halbach, and set up its observational equipment at Pine River, Canada (5°42′ N., 100°30′ W.). The photographic results of this expedition were later sent to Dr. B. Lindblad, of the Stockholm Observatory, for use, in conjunction with the film of the Lund and the Stockholm Observatories' expeditions, in a large-scale geodetic program. Because the Pine River film was considered to be much too overexposed to have much geodetic value, no work along this line was done on the film in Sweden. It was received at the Army Map Service, Washington, D.C., early in 1952, and a series of microphotometric measurements was made on the film.

## II. DESCRIPTION OF PROCEDURE

The solar-flash spectrum had been photographed on 16-mm Kodak panchromatic sound film, using an F-6 24-inch focal length lens in conjunction with a 25° $4\frac{3}{4}$-inch prism, both lens and prism being fluoride-coated. Time signals from station WWV had been impressed upon the sound-track portion of the film during the entire period of the photography. Also, with the same camera and the same exposure time ($\frac{1}{50}$ second), there had been photographed upon the tail-end of the film a series of density graduation scales made by placing a wedge-slit, steps in 2:1 ratio, at the focus of a 24-inch collimator lens and illuminating the slit with a blue photoflood lamp. The density scales so made were developed along with the original film.

For the microphotometric measurements, a Moll microphotometer was modified by substituting an RCA 1P21 photomultiplier tube for the thermoelectric element. The entire thermoelectric assembly, with the exception of the slit-condenser unit, was replaced by the 1P21 tube and housing; the slit-condenser unit was mounted about 9.5 cm from the illuminated cathode, to give maximum coverage of the cathode area. A Brush amplifier and oscillograph combination gave deflection readings proportional to the film density, while an auxiliary circuit wired through contacts on the carriage-traversing mechanism produced deflections on the oscillograph 4-cm tape indicative of the portion of the spectral arc being scanned.

Preliminary tests with Kodak Wratten neutral filters of densities 0.50, 1.00, and 1.50 and with Bureau of Standards calibrated 13-step density scales indicated linearity of response of the apparatus over the entire range of densities measured, the error of the measured densities being less than 2 per cent. In addition, tracings were made frequently of the wedge-slit spectrograms, to provide a check upon the reproducibility and con-

tinued linearity of the system. Since measurements were made from the film rather than directly from the sun and since the rate of traverse of the film through the probing light-beam was small compared to the frequency-response characteristics of the apparatus, it was possible to proceed so as to make the system's response time immaterial, and no special tests were made to determine its quantity.

A characteristic curve for the film was determined by measurements on the density scales already on the film, these measurements being carried out at the same wave lengths as those made later on the flash spectrum; this was at approximately 6000 A. The characteristic curve is shown in Figure 1.

Geodetic considerations made it necessary to take the measurements at a wave length

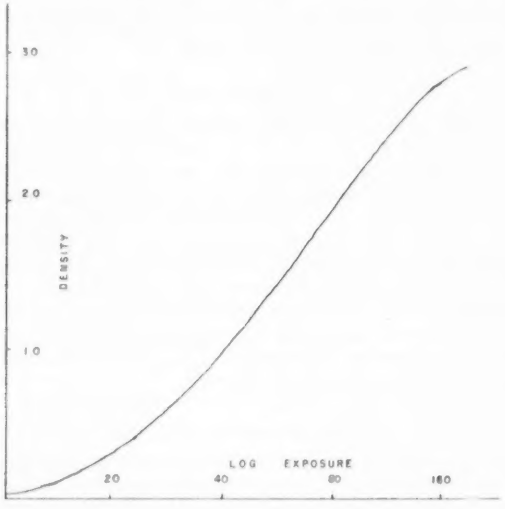


FIG. 1.—Film characteristic curve

which was present on the film at both second and third contact. Only that portion of the spectrum between the Hα at 6563 A and the helium $D_3$ line at 5876 A was present on the film both before and after conjunction (most of the blue end of the spectrum being absent at third contact and even part of the $D_3$ line being missing there); a wave length of 6030 A was finally selected as being farthest removed from disturbing influences, especially the coronal line at 6374 A, while still being present at both contacts.

During the photometry of the flash spectrum, the light-beam was displaced relative to the film, in a direction perpendicular to the direction of dispersion and crossing the line of centers (the locus of the centers of the overlapping crescent images) at 6030 A (see Fig. 2). The continued placement of this wave length on the slit at successive tracings on successive frames was insured by registration of the images of the H and $D_3$ lines onto correctly spaced lines drawn on the screen in the plane of the slit. Measurement of an interval of about 20° on either side of the line of centers was considered sufficient, since identification of lunar features became difficult at more than 45° from the line of centers.

Since the edge of the sun for a particular wave length is represented by a semicircle, it follows that the tracing light-beam should have followed the arc of the sun's limb; practically, this was not feasible with the available motions, and the tracing was done along

a tangent to the limb. The linear difference between the tangent and the arc (the so-called "ordinate of curvature") amounted, when converted to wave lengths by multiplication by the linear dispersion at 6030 A, to 95 A, the same within a few per cent at both contacts. The variation in sensitivity resulting from variation in wave length from this cause was neglected, because measurements made on and/or parallel to the line of centers indicated that the spectral sensitivity within the region in question was uniform to

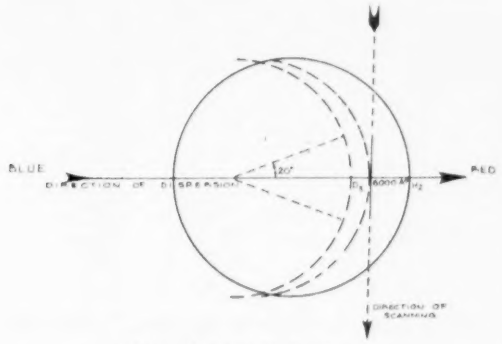


FIG. 2.—Scanning procedure used in making tracings

within the limits of error (Fig. 3). This bore out the findings of H. Kristenson (1951), who adopted the same procedure in his work.

A typical recording was a ½-meter-long tracing of the moon's profile between position angles 63° and 103° for the second contact, and of the profile between 250° and 290° for the third. Portions of the tracings corresponding to times $12^h17^m44.995^s$ at second contact and $12^h18^m19.218^s$ at third contact are shown in Figures 4 and 5.

There was, as may be seen in the figures, some distortion present at large distances from the line of centers. The principal cause of this was, of course, the continually changing direction of motion of the scanning path with respect to the moon's rim, so that, e.g., at the ends of the scanning path the beads or valleys were being explored along a normal

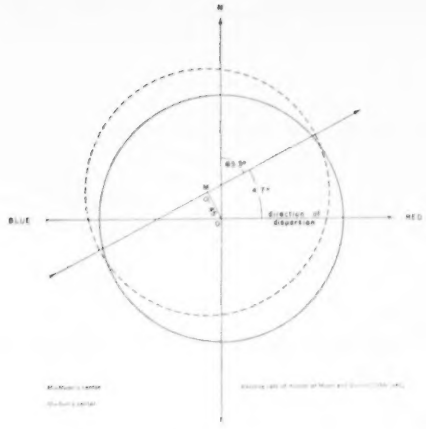


FIG. 3.—Geometric relation between solar and lunar limbs

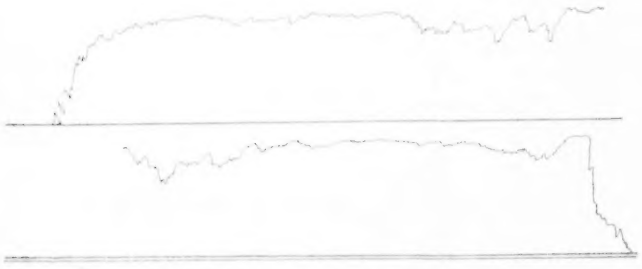

FIG. 4.—Tracing at 6030 A of moon's profile, second contact

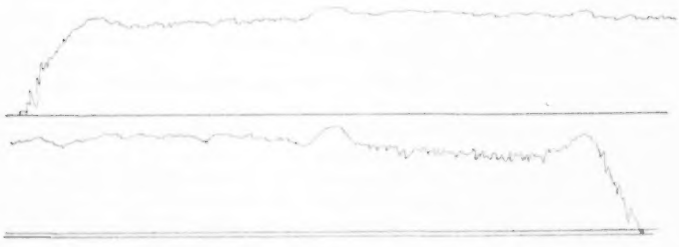

FIG. 5.—Tracing at 6030 A of moon's profile, third contact

to the lunar surface. A second contributing factor was the "smearing-out of the profile" due to overlapping of images along the direction of dispersion, while still a third was the variation in integrated brightness with distance from the central lines of dispersion. The restriction of measurements to an angular distance of 20° on either side of the line of centers effectively reduced the first two possible sources of error, and the last was eliminated by the introduction of a correcting factor, sec $\theta$, into the calculations. Figure 6 shows the method used.

Comparison of the photometrically recorded profile with profiles constructed from Hayn's charts and Kristenson's tracings made possible the identification of lunar features practically to the ends of the tracing path, although the correspondence was not perfect,

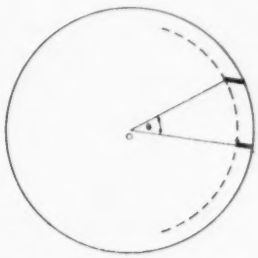

FIG. 6.—Correction for off-axis beads

many features at a distance of more than 45° from the line of centers being unrecognizable.

As was mentioned at the beginning of this section, a series of density spectrograms had been photographed on the same film as the flash spectrum, using almost the same optical setup but with the substitution of a lamp-collimator-slit combination for the lunisolar source. The spectrograms were used for the construction of the characteristic curve by tracing across each spectrogram perpendicularly to the direction of dispersion and along the 6030 A line. Figures 7 and 8 give examples taken from the eclipse film.

### III. REDUCTION OF DATA

As stated above, the relation between pen deflection and density was found to remain essentially constant throughout the series of measurements. The pen deflections were therefore converted to film density without trouble. The variation of the film density with frame number, as derived from the tape records of deflection of pen versus position on the flash spectrum (position angle on the moon's limb), was plotted for each identifiable and measurable bead in the flash spectrum, within the angular limits given above. These densities were then converted to total integrated brightness in arbitrary units through the characteristic curve found from the density spectrograms and shown in Figure 2. From a table kindly supplied by Professor E. A. Halbach (1946), these frame numbers were converted to the corresponding U.T. By the method of least squares, a straight line was then fitted to the plot for each bead on the log intensity versus time, and the quantity $dM/dh$, the rate of change of magnitude with height in seconds (of arc), calculated therefrom. Tables 1 and 2 give the various values of this quantity at different positions along the moon's limb for second and third contacts, respectively. Also given are the values of $1/kn$, the rate of change of intensity per frame. For second contact, the average value is $-6.0 \pm 0.7$ mag/sec; while for the third contact the average value is $-5.5 \pm 1.0$ mag/sec. The average value over both contacts is $-5.7 \pm 1.0$ mag/sec. These values of $dM/dh$ may be compared with those of Lindblad and of Lundmark

TABLE 1

DENSITY GRADIENT AT VARIOUS POSITION ANGLES FOR THE SECOND CONTACT

| Position Angle | $1/kn$ | Mag/Sec | $-\alpha\times10^{8}$ Cm$^{-1}$ | Probable Error |
|---|---|---|---|---|
| 63 | −24.514 | −5.1 | 7.0 | ±0.59 |
| 66.5 | −20.960 | −4.4 | 6.0 | ±0.59 |
| 71 | −30.337 | −6.3 | 8.7 | ±0.77 |
| 74 | −35.090 | −7.3 | 10.1 | ±0.70 |
| 76 | −29.412 | −6.1 | 8.5 | ±0.53 |
| 80 | −23.109 | −4.8 | 6.6 | ±0.79 |
| 81 | −34.854 | −7.3 | 10.0 | ±1.75 |
| 82 | −23.652 | −4.9 | 6.8 | ±0.61 |
| 83 | −25.596 | −5.3 | 7.4 | ±1.05 |
| 84 | −44.617 | −9.3 | 12.8 | ±1.77 |
| 88.5 | −17.037 | −3.6 | 4.9 | ±0.69 |
| 93.8 | −21.753 | −4.5 | 6.3 | ±1.11 |
| 96 | −36.461 | −7.6 | 10.5 | ±0.88 |
| 97 | −23.681 | −4.9 | 6.8 | ±0.96 |
| 103.7 | −47.137 | −9.8 | 13.6 | ±0.96 |

TABLE 2

DENSITY GRADIENT AT VARIOUS POSITION ANGLES FOR THE THIRD CONTACT

| Position Angle | $1/kn$ | Mag/Sec | $-\alpha\times10^{8}$ Cm$^{-1}$ | Probable Error |
|---|---|---|---|---|
| 243.5 | −31.747 | −6.6 | 9.1 | ±1.3 |
| 246.5 | −19.931 | −4.2 | 5.7 | ±1.0 |
| 247.4 | −26.302 | −5.5 | 7.6 | ±0.8 |
| 248.2 | −18.062 | −3.8 | 5.2 | ±2.4 |
| 250.2 | −23.286 | −4.9 | 6.7 | ±1.1 |
| 252 | −13.756 | −2.9 | 4.0 | ±1.8 |
| 254.2 | −29.064 | −6.1 | 8.3 | ±1.2 |
| 255.8 | −23.062 | −4.8 | 6.6 | ±0.8 |
| 256.6 | −19.549 | −4.1 | 5.6 | ±0.3 |
| 257.9 | −13.906 | −2.9 | 4.0 | ±0.9 |
| 259.2 | −16.655 | −3.5 | 4.8 | ±2.4 |
| 260.5 | −29.870 | −6.2 | 8.6 | ±3.2 |
| 264.2 | −35.364 | −7.4 | 10.1 | ±1.7 |
| 267.4 | −39.355 | −8.2 | 11.3 | ±1.7 |
| 268.2 | −25.732 | −5.4 | 7.4 | ±1.4 |
| 270.0 | −30.195 | −6.3 | 8.7 | ±0.9 |
| 271 | −18.974 | −4.0 | 5.5 | ±0.9 |
| 272 | −16.060 | −3.4 | 4.6 | ±2.1 |
| 273 | −8.733 | −1.8 | 2.5 | ±1.0 |
| 275.1 | −30.051 | −6.3 | 8.6 | ±1.4 |
| 276.6 | −27.356 | −5.7 | 7.9 | ±0.9 |
| 277.6 | −22.003 | −4.6 | 6.3 | ±0.9 |
| 280.9 | −18.407 | −3.8 | 5.3 | ±0.6 |
| 282.2 | −35.998 | −7.5 | 10.4 | ±0.6 |
| 283 | −33.109 | −6.9 | 9.5 | ±1.2 |
| 284 | −33.896 | −7.1 | 9.8 | ±1.7 |
| 286.5 | −28.117 | −5.9 | 8.1 | ±1.1 |
| 287.5 | −39.486 | −8.2 | 11.4 | ±1.0 |
| 288.7 | −27.723 | −5.8 | 8.0 | ±1.2 |
| 289.5 | −25.847 | −5.4 | 7.4 | ±1.0 |
| 290.9 | −40.028 | −8.4 | 11.5 | ±3.1 |

TABLE 3

COMPARISON OF MAGNITUDE GRADIENTS AND ERRORS

| Location | Wave Length (A) | Mag/Sec | Probable Error |
|---|---|---|---|
| Brattås | 4800 | −4.86 | ..... |
| Sävenäs | 4100 | −5.69 | ±0.11 |
| Pine River | 6030 | −5.71 | ±0.98 |

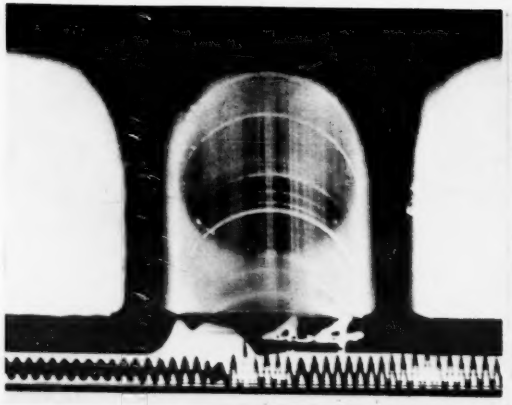

Fig. 7

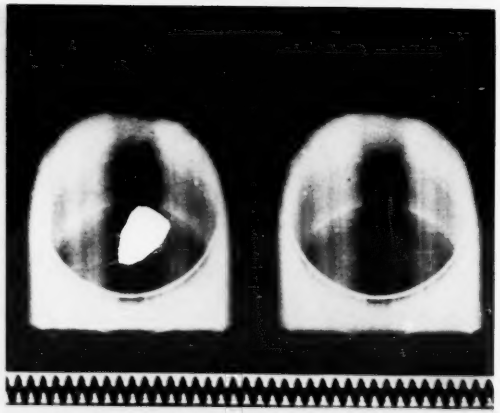

Fig. 8

FIGS. 7 and 8.—Fig. 7, frame 200 (second contact) of the 1945 eclipse film. Fig. 8, frames 929 and 930 (third contact) of the 1945 eclipse film.

(Kristenson 1951), which were obtained from observations on the same eclipse on July 9, 1945, at Brattås and Sävenäs, respectively, in Sweden.

The intensity is given by the equation

$$I = I_0 (1 - e^{-\tau'}),$$

where $\tau'$ is the optical depth and is given by

$$\tau' = K e^{(n+1)\alpha h}.$$

From this we can easily find that

$$\frac{I}{I_0} = e^{(n+1)\alpha h} (1 - K' e^{K'' \alpha})$$

(see Unsöld 1938, chap. xvii), and therefore

$$\frac{d \log I/I_0}{dh} = \alpha (n+1).$$

By means of this relation, the value of $\alpha$, the photospheric density gradient, was calculated from the values of $1/kn$ and $dM/dh$, taking account of the fact that the surface brightness is the derivative of the integrated brightness (Kristenson 1951). Its values so calculated for the second and third contacts at different position angles are given in Tables 1 and 2, together with the probable errors. An over-all estimate was made of $\alpha$, weighting the data of the second contact by a factor of 3 to take account of the heavy overexposure at the third contact. This over-all calculation gave

$$\alpha = -7.56 \times 10^{-8} \pm 0.61 \times 10^{-8}.$$

Since the value of the chromospheric gradient, as derived by R. Wildt (1946) from a study of the heights of the Balmer line, is

$$\alpha = 0.92 \times 10^{-8} \text{ cm}^{-1}$$

and since the corresponding gradient which would theoretically exist in a pure hydrogen atmosphere in hydrostatic equilibrium is

$$\alpha = 6.9 \times 10^{-8} \text{ cm}^{-1},$$

as given by the formula

$$\alpha = \frac{g m}{k T_0}$$

for an atmosphere in hydrostatic equilibrium, there can be little doubt that, within the region to which these measurements pertain, there was at least approximate hydrostatic equilibrium, as indicated by the values found in the foregoing manner by Lindblad, Kristenson, and the Army Map Service. It should be noted that the theoretical value $-6.9 \times 10^{-8}$ cm$^{-1}$ given earlier is for a boundary temperature of 4839° A and that this value would increase with decreasing temperature. Another observation which might be made is that the value $-7.6 \times 10^{-8} \pm 0.6 \times 10^{-8}$ cm$^{-1}$ was derived as an average of all measured beads, including even those for which there were valid reasons to doubt the reliability. If, as a reasonable criterion for differentiating between reliable and unreliable values, a probable error of 20 per cent had been taken as the dividing point, then, with the resulting decreased probable error, there would have been a corresponding increase in the value of the density gradient rather than a decrease, as might have been expected.

## IV. CONCLUSION

In the expression for the density gradient,

$$a = \frac{m_0 g}{kT_0},$$

only the effective atomic weight $m_0$ and the boundary temperature $T_0$ can be varied. At a temperature of 4830° A, which is the temperature assumed by Unsöld (1938) and Wildt (1947) in their calculations, the Army Map Service value of $a$ leads to an effective atomic weight of $1.83 \times 10^{-24}$ gm $\pm$ $0.2 \times 10^{-24}$, a weight approximately 1.5 times that of pure hydrogen. Neglecting entirely the heavier elements, this would correspond to a relative hydrogen-helium abundance (by weight) of 1:5. On the other hand, if we follow Wildt (1947) in using a pure hydrogen region as solely responsible for the observed gradient, so that the effective atomic weight is $1.67 \times 10^{-24}$ gm, then the corresponding temperature would be 4400° $\pm$ 355° A.

In conclusion, therefore, it may be stated that the values derived above from measurements from the Pine River, Canada, film tend to confirm those found with a similar method by Lindblad and by Kristenson and that to that extent they support the hypothesis of a solar photosphere in hydrostatic equilibrium near the boundary with no considerable amount of turbulence present.

The writer wishes to express his thanks to Miss Pamelia Anderson and Mr. Marvin L. White, both of the Army Map Service, by whom most of the work was done, and to Mr. John A. O'Keefe for his helpful corrections and comments.

## REFERENCES

Halbach, E. A. 1946, private communications to B. Lindblad.
Kristenson, H. 1951, *Stockholm Obs. Ann.*, Vol. **17**, No. 1.
Unsöld, A. 1938, *Physik der Sternatmosphären* (Berlin: Julius Springer), chaps. v and xvii.
Wildt, R. 1947, *Ap. J.* **105**, 36–84.

# PHOTOMETRIC STUDIES OF ASTEROIDS. II*

INGRID GROENEVELD AND GERARD P. KUIPER
Yerkes and McDonald Observatories
*Received May 10, 1954*

ABSTRACT

This paper gives twelve light-curves of asteroids, determined during eighteen nights, and a number of color determinations. The principal derived quantities are found in Table 1 and the figures. The arrangement of the material follows that of Paper I.

## I. PLAN OF INVESTIGATION

The present investigation is in all respects a continuation and extension of Paper I in this series (Groeneveld and Kuiper 1954). It is based on photoelectric observation with the 82-inch telescope made mostly during January, 1954. Two earlier series are included, for Pallas and Laetitia, which were observed in collaboration with Messrs. Harris and Shatzel. The record of the observations and the principal results are contained in Table 1. As the table shows, Mr. Harris collaborated also during four nights of the recent series; for this aid we are deeply indebted to him. The magnitude and color system used is again that of Johnson and Morgan. We wish to acknowledge the valuable aid which Mr. Hiltner gave us during reductions.

## THE LIGHT-CURVES

The presentation of the data follows in its essentials the arrangement of Paper I. The times given in the legends of the light-curves are U.T. as observed, uncorrected for light-time. The magnitudes are all visual ($V$) values, relative to the maximum of the curve; the $V$-value of the zero so defined is inserted in each figure (except for Laetitia, for which no standard had been observed). Uncertain values are plotted as open circles.

Table 1 resembles closely Table 1 of Paper I, but $m_0$ has been omitted, since its computation is readily made from $g$. Furthermore, the phase angle and the light-time have been added. The values of $r$, $\rho$, and $\phi$ have been taken from the Russian ephemeris, except for asteroids 2, 9, 14, and 44, for which the data were kindly computed by Dr. Rabe. For asteroids 9 and 44 the ephemeris position showed large O − C values, so that a new computation was desirable.

*2 Pallas.*—A single night's run of 4.2 hours was obtained in 1951. The results are shown in Figure 1. The phase angle was 13°.1. With Müller's average phase coefficient of 0.037 mag/degree and the known distances, the $g$-value of Table 1 was derived. The amplitude of the observed part is 0.13 mag. A half-period (or whole period, if only *one* maximum occurs per cycle) of 5–6 hours is suspected, which would confirm the provisional value of 5.7 hours derived by O. Günther (1951, 1953), obtained from photographic estimates.

*3 Juno.*—Observations of Juno were made on January 10, 11, 17, 27, and 28, 1954, but only the runs of January 10 and 17 are several hours long. On the other nights clouds cut off observations, while a few clouds interfered even on January 10. The two long runs define a period of about 7 hours and a light-curve having two unequal maxima and minima each. Examination showed that only one period is compatible with all our data; that period is $7^h12^m6$. On this basis the light-curves of Figures 2, 3, and 4 were constructed. Figure 4 combines the results of January 27 and 28, reduced to January 28. The

* *Contributions from the McDonald Observatory, University of Texas*, No. 242.

## TABLE 1

### SUMMARY OF PHOTOMETRIC RESULTS

| No. | Obs. | Date | Obs. | $V$ of Zero | $B-V$ | $U-B$ | Amp. | Period | Mean $V$* | $\varepsilon$ | Phase Coeff.† | $\phi$ | Light-Time | R.A. | Dec. | Fig. |
|---|---|---|---|---|---|---|---|---|---|---|---|---|---|---|---|---|
| 1 | 16 | Jan. 54 | G, K | $8^m17$ | $+0^m73$ | $+0^m45$ | ..... | ..... | ..... | $3^m40$ | 0.049H | 21°9 | $-17^m8$ | $13^h01^m$ | + 7?3 | ..... |
| 2 | 30 | June 51 | H, K | 9.66 | + .67 | ..... | $0^m13$ | $5\text{–}6^h$ or $10\text{–}12^h$ | $9^m71a$ | 4.38 | .037M | 13.1 | −22.1 | 20 12 | +19.5 | 1 |
| 3 | 10 | Jan. 54 | G | 8.61 | + .86 | + .44 | .15 | | 8.861*b* | 5.634 | .025 | 15.5 | −12.2 | 9 34 | + 0.4 | 2 |
| | 11 | Jan. 54 | G | 8.63 | + .85 | + .43 | ..... | | ..... | ..... | ..... | 15.0 | −12.2 | 9 34 | + 0.5 | ..... |
| | 17 | Jan. 54 | G, K | 8.51 | + .83 | + .43 | .14 | $7^h12^m6 \pm 0^m1$ | 8.580*b* | 5.634 | ..... | 12.5 | −12.0 | 9 30 | + 1.0 | 3 |
| | 27 | Jan. 54 | K | ..... | ..... | ..... | ..... | | ..... | ..... | ..... | 8.3 | −11.8 | 9 23 | + 2.2 | 4 |
| | 28 | Jan. 54 | K | 8.39 | ..... | ..... | ..... | | 8.462*b* | 5.636 | ..... | 7.9 | −11.8 | 9 23 | + 2.3 | |
| 9 | 3 | Jan. 54 | G | 8.54 | + .84 | + .50 | .26 | | 8.67*b* | 6.61 | .049 | 2.9 | − 9.5 | 6 39 | +28.7 | 5 |
| | 5 | Jan. 54 | G | 8.61 | + .85 | + .51 | .26 | | ..... | ..... | ..... | 3.6 | − 9.5 | 6 36 | +28.7 | 6 |
| | 8 | Jan. 54 | G | 8.70 | + .85 | + .49 | ..... | 5 04.6 ± 0.02 | ..... | ..... | ..... | 5.3 | − 9.6 | 6 33 | +28.9 | |
| | 16 | Jan. 54 | G, K | 8.95 | + .85 | + .48 | .25 | | 9.08*b* | 6.62 | ..... | 9.4 | − 9.8 | 6 25 | +29.2 | 7 |
| 10 | 31 | Dec. 53 | G, H | 10.27 | + .69 | + .36 | .09 | 18? | 10.32*c* | 5.656 | (.030) | 5.3 | −19.8 | 7 56 | +20.1 | 8 |
| | 1 | Jan. 54 | G, H | 10.24 | + .68 | + .37 | .10 | | 10.29*c* | 5.641 | ..... | 5.0 | −19.8 | 7 55 | +20.1 | 9 |
| 14 | 30 | Dec. 53 | G, H | 10.10 | + .81 | + .40 | .035 | 11? | 10.12*d* | 6.59 | .034M | 9.9 | −13.9 | 4 39 | +20.8 | 10 |
| | 4 | Jan. 54 | G | 10.23 | + .82 | + .39 | ..... | | 10.23*d* | 6.60 | ..... | 12.1 | −14.2 | 4 34 | +21.0 | |
| 39 | 9 | May 49 | K, S | ..... | ..... | ..... | .43 | ..... | ..... | ..... | .022M | 6.1 | −16.5 | 15 34 | −03.8 | 11 |
| 40 | 10 | Jan. 54 | G | 10.68 | + .88 | + .43 | .04 | ..... | ..... | ..... | .018M | 22.4 | −13.0 | 3 07 | +15.2 | ..... |
| 44 | 6 | Jan. 54 | G | 9.85 | + .70 | + .24 | .40 | | 10.04*b* | 7.12 | .025M | 21.9 | −11.6 | 3 22 | +13.5 | 12 |
| | 7 | Jan. 54 | G | 9.87 | + .70 | + .24 | .35 | 6 25.2 ± 0.1 | ..... | ..... | ..... | 22.2 | −11.7 | 3 22 | +13.6 | 13 |
| | 11 | Jan. 54 | G | 9.91 | + .69 | + .24 | .41 | | 10.11*b* | 7.10 | ..... | 23.3 | −12.0 | 3 22 | +13.8 | 14 |
| 354 | 2 | Jan. 54 | G, H | ..... | + .94 | + .58 | ..... | | ..... | ..... | (.030) | 17.5 | −14.4 | 10 06 | + 8.0 | ..... |
| | 5 | Jan. 54 | G | 10.09 | + .95 | + .53 | .15 | 4 16 ±1 | 10.15*b* | 6.53 | ..... | 16.6 | −14.1 | 10 04 | + 8.3 | 15 |
| | 6 | Jan. 54 | G | 10.10 | + .95 | + .58 | .12 | | ..... | ..... | ..... | 16.3 | −14.0 | 10 04 | + 8.4 | 16 |
| 433 | 2 | Jan. 54 | G, H | 12.13 | + .96 | + .56 | ..... | ..... | ..... | 10.9: | .024B | 57.2 | ..... | 13 12 | −13.5 | ..... |
| 532 | 2 | Jan. 54 | G, H | 9.42 | +0.83 | +0.44 | 0.08 | $16\text{–}17^h$? | 9.46*c* | 7.07 | (0.030) | 4.5 | −14.1 | 6 07 | +17.5 | 17 |

* The letters have the following meanings: *a* = mean over half or quarter-period (see text); *b* = mean over full period; *c* = mean over quarter period; *d* = mean over night's run.

† B = M. Beyer (1938); H = Haupt (1953); M = Müller (1897); values in ( ) are adopted; the two remaining values are derived here.

figures define the following epochs of primary minimum:

| 1954 | U.T. |
|---|---|
| January 10 | $8^h35^m \pm 3^m$ |
| January 17 | 6 30 ±4 |
| January 28 | 9 11 ±6 |

The first and last epoch, separated by 60 periods, give $P = 7^h12^m.6 \pm 0^m.1$. This value predicts the January 17 epoch as $6^h25^m \pm 4^m$, compatible with the observed value. The two principal light-curves show evidence of changes within the week elapsed. For this reason the unobserved parts in Figure 4 are somewhat hypothetical.

The mean magnitudes over one period were derived from all three curves and are given in Table 1. To give consistent $g$-values, they require a phase coefficient of 0.025

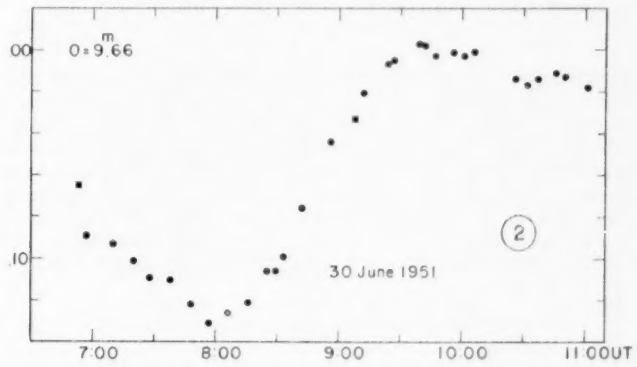


FIG. 1.—Observations of 2 Pallas

mag/degree. This figure appears well determined and is slightly less than the values of Müller (1897), 0.030; Günther (1951), who found 0.039 for phase angles smaller than 11° but a smaller value for larger angles; and Haupt (1953), 0.036. However, comparison with Haupt's plot shows no real contradiction between our value and his observations.

*9 Metis.*—In Paper I it was found that the 1949 observations gave a period of $5^h03^m \pm 2^m$. The 1954 observations were made on January 3, 5, 8, and 16, and covered 6, 2, $1\frac{1}{2}$, and $7\frac{1}{2}$ hours, respectively. The first 2 hours of the last night were disturbed by a small discontinuity in the apparent sensitivity and are not plotted here. The other data are shown in Figures 5, 6, and 7. Because of the complexity of the variation, all available evidence was combined in drawing the light-curves in Figures 5–7. The shapes differ in detail between the three figures. We find later that the epochs are also slightly variable if compared to a linear formula.

Müller's phase coefficient for Metis is 0.041 mag/degree, but a slightly larger value, of 0.049 mag/degree, fits our observations better. The phase angle on January 5 was 2°.9 and on January 16, 9°.4, so that our coefficient should be well determined. The remaining quantities are found in Table 1. It is noted that the amplitude of 0.26 mag. is considerably greater than that of the 1949 observations, which was 0.12 mag. The light-curves define the epochs given in the table on p. 532. These epochs give the intervals

$$\underset{1^h14^m}{I(m)\text{–}I(M)}\text{–}\underset{1^h43^m}{II(m)}\text{–}\underset{0^h56^m}{II(M)}\text{–}\underset{1^h11^m}{I(m)}\,,$$

| 1954 | | U.T. | 1954 | | U.T. |
|---|---|---|---|---|---|
| Jan. 3 | IIMin. | $5^h01^m$ | Jan. 8 | IIMin. | $6^h51^m$ |
| | IIMax. | 5 53 | | | |
| | IMin. | 7 04 | Jan. 16 | IIMax. | 3 38: |
| | IMax. | 8 19 | | IMin. | 4 49 |
| | IIMin. | 9 57 | | IMax. | 6 03 |
| | | | | IIMin. | 7 50 |
| Jan. 5 | IMin. | 4 45 | | IIMax. | 8 49 |
| | IMax. | 5 59 | | | |

making the total period $5^h04^m$. With the aid of these data four epochs of primary maximum are derived, as shown in the accompanying table.

| 1954 | U.T. | | Light-time |
|---|---|---|---|
| Jan. 3 | $8^h18^m4$ | $\pm 0^m5$ | $-9^m5$ |
| 5 | 5 59 | $\pm 0.5$ | $-9.5$ |
| 8 | 5 08 | $\pm 3$ | $-9.6$ |
| 16 | 6 04 | $\pm 1$ | $-9.8$ |

The interval January 3–5, which is 2740.6 ± 0.7 minutes, is about nine times the 1949 period of 303 ± 2 minutes. The improved period is then 304.5 ± 0.1 min. This shows that the interval January 3–16 is 61 cycles; it leads to the mean synodic period of 304.68 ± 0.02 minutes or 0.2115833 ± 0.000014 day. The interval 1949–1954 is 1523 days, or about 7200 periods. The uncertainty of the period carried back over this interval is nearly half a cycle, so that our observations do not suffice to bridge the gap with certainty. This situation is not changed by inclusion of the photoelectric observations published by Giclas (1950), since they happen to be nearly simultaneous with our 1949 epoch. For future reference all 1949 data are collected in Table 2.

TABLE 2

EPOCHS OF THE MAXIMA AND MINIMA OF 9 METIS

| 1949 | | U.T. | | |
|---|---|---|---|---|
| Nov. 2 | IIMax. | $5^h41^m \pm 2^m$ | | |
| | IIMin. | 6 32 ±2 | | |
| | IMax. | 7 47 ±1 | | |
| | IMin. | 9 21 ±3 | | |
| Nov. 16 | IIMax. phase | 0.07 ± 0.01 = | Nov. 16.198 ± 0.002 day U.T. | |
| | IIMin. | .26 ± .02 = | .238 ± .004 | |
| | IMax. | .51 ± .01 = | .291 ± .002 | |
| | IMin. | .84 ± .03 = | .360 ± .006 | |
| Dec. 21 | IIMax. | .13 ± .03 = | Dec. 21.122 ± .006 | |
| | IIMin. | .34 ± .03 = | .167 ± .006 | |
| | IMax. | .57 ± .03 = | .215 ± .006 | |
| | IMin. | 0.90 ± 0.03 = | .285 ± 0.006 | |

Giclas listed 74 measures each in blue and yellow, running from October 27, 1949, to January 10, 1950. He deduced a provisonal period of 0.213 days and a phase coefficient of 0.040 mag/degree for the yellow and 0.043 mag/degree for the blue. We have replotted the yellow measures against our accurate period, with the material divided into three groups, October 27–November 1 (18 measures); November 13–19 (32 measures); and November 29–January 10 (24 measures). The magnitudes used were those listed in the last column of Giclas' Table II, which are corrected to the distances of mean opposition and with the phase coefficient of 0.045 mag/degree. These plots did not give consistent mean magnitudes, and new plots were made with the corrected phase coefficient, 0.037 mag/degree, found from the first plots. Of the three groups, the first has much scatter, but the second and third show the light-variation well; they are reproduced in our Figure 8. The November 16 group defines a light-curve quite similar to that of our November 2 run (Fig. 5 of Paper I). In both cases the primary minimum is broad and flat, with the

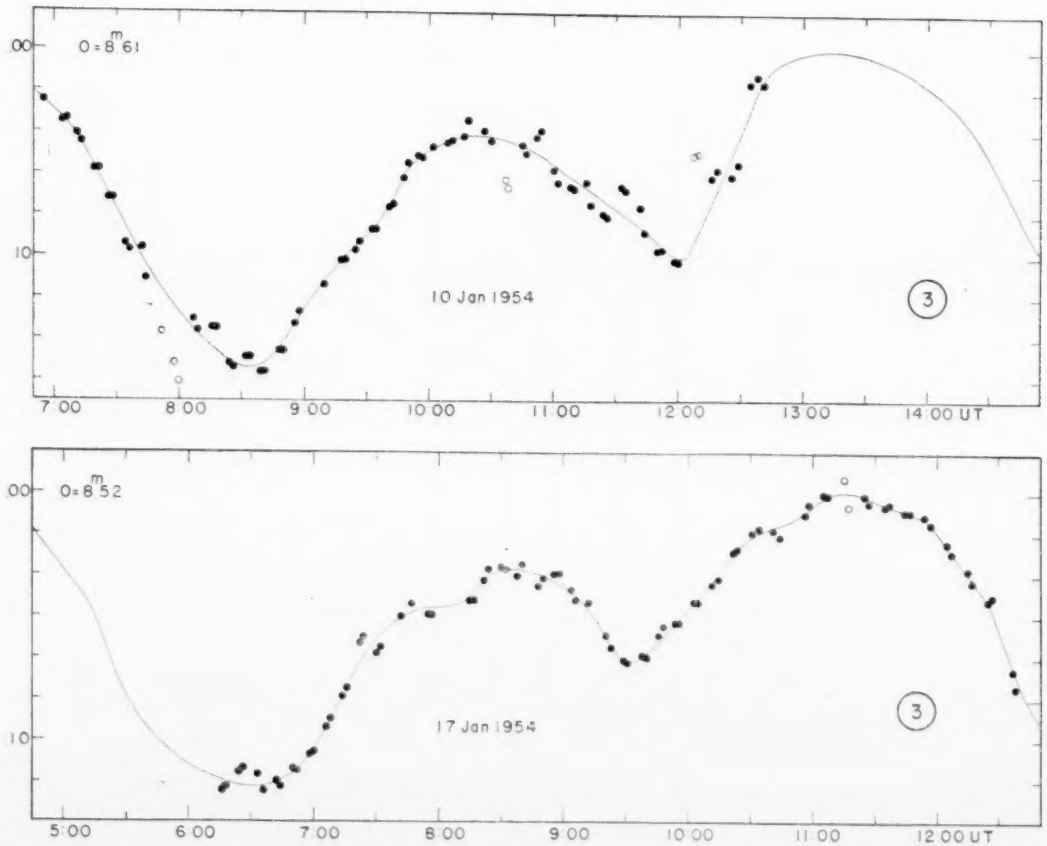


FIGS. 2 (*above*) and 3 (*below*).—Light-curves of 3 Juno

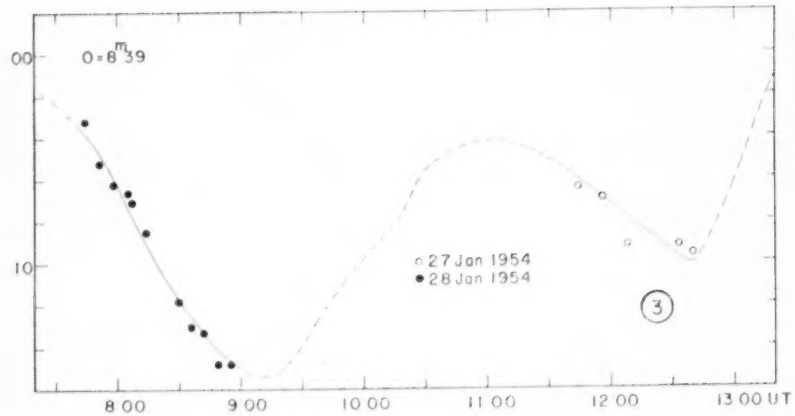


FIG. 4.—Observations of 3 Juno

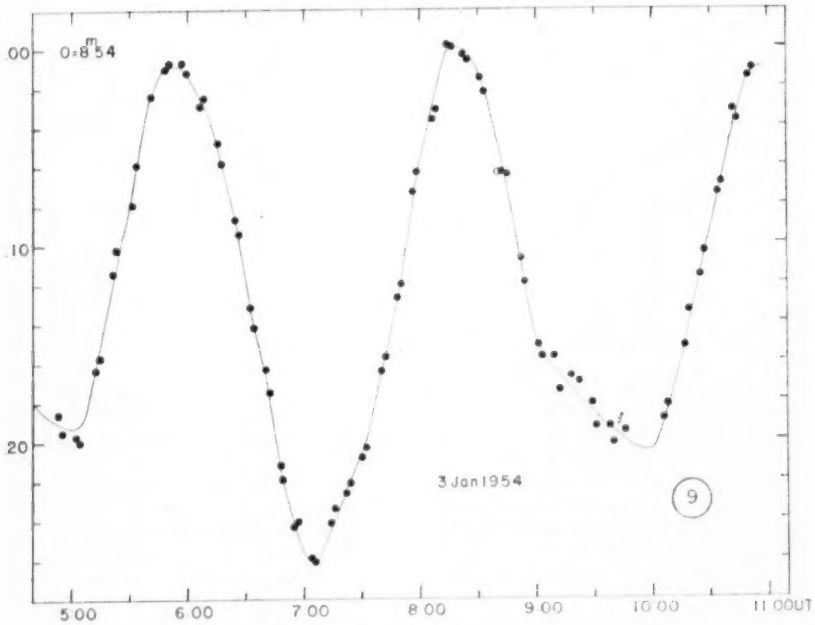


FIG. 5.—Light-curve of 9 Metis

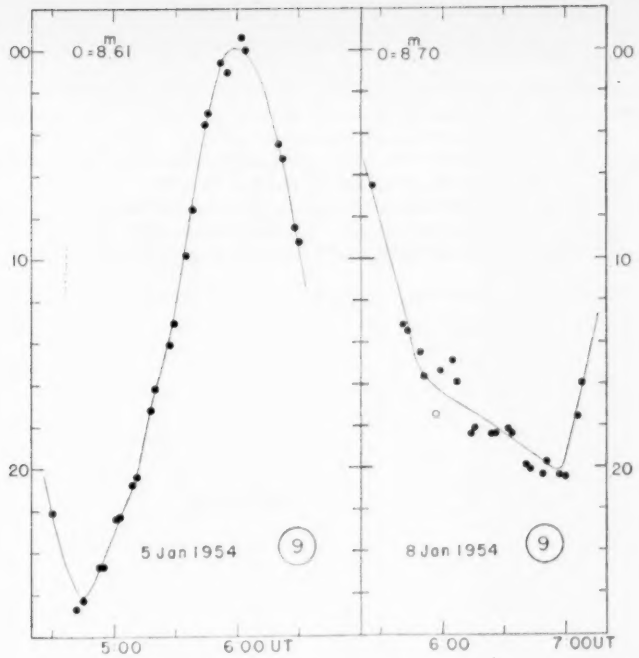


FIG. 6.—Observations of 9 Metis

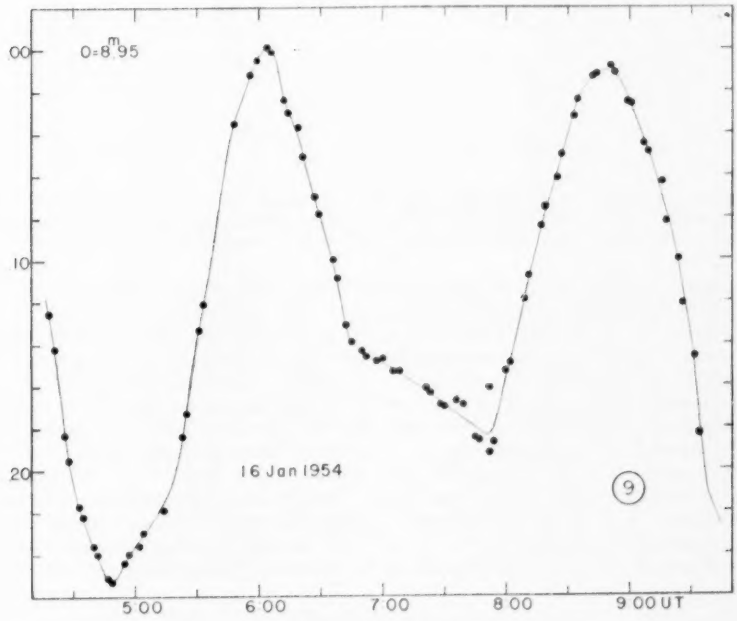


FIG. 7.—Light-curve of 9 Metis

primary maximum 0.11 mag. above it. The curve drawn in Figure 8 is based on this similarity and leads to good epochs of maximum and minimum. The December group is more uncertain, and the primary minimum seems to be skew, somewhat like the secondary minimum in January, 1954 (with which it is probably identical; see next paragraph). The amplitude appears to have increased to about 0.18 mag.

The three 1949 light-curves define the epochs, uncorrected for light-time, as given in Table 2. Comparison of the intervals fixed by these epochs with those previously listed for 1954 makes it probable that the primary maxima of the two sets of data refer to the

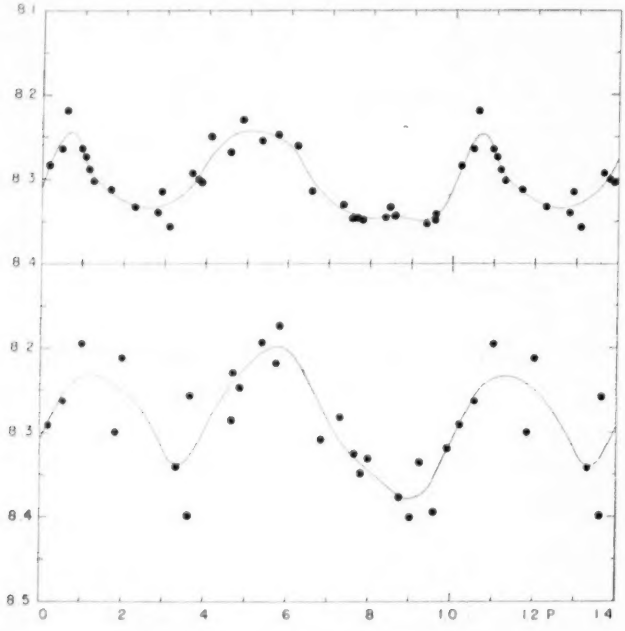


FIG. 8.—Light-curves of 9 Metis based on measures by Giclas (1950). *Abscissae:* phases (with zero on October 0.0000, 1949); *ordinates:* visual magnitudes reduced to mean opposition and phase zero with the coefficient 0.037 mag/degree. When comparing with Figs. 5–7, note that $0.20P$ is nearly 1 hour.

same event but that the primary and secondary minima have interchanged. A third epoch will clarify this relation and also determine the sense of rotation.

Examination of the individual 1954 curves shows that the period of $5^h04^m.7$ does not always fit precisely between corresponding features in successive cycles. A lack of strict periodicity is thus indicated but requires confirmation. It is further noted that the somewhat divergent values found for the phase coefficient are not necessarily due to errors of measurement; the results may have been distorted by an admixture of an independent effect, namely, a simultaneous change of aspect (or mean projected area).

*10 Hygeia.*—Two runs on consecutive nights, of 7.1 and 7.6 hours, respectively, failed to cover the entire period (see Fig. 9). The first run suggests a minimum between 6 and 7 hours, U.T., if the peculiar feature during the first 20 minutes is ignored. A maximum appears to occur about $11^h10^m$ or $20^m$ U.T. If this interval is considered to be one-quarter period, the total period would be 18–20 hours. This is compatible with the next

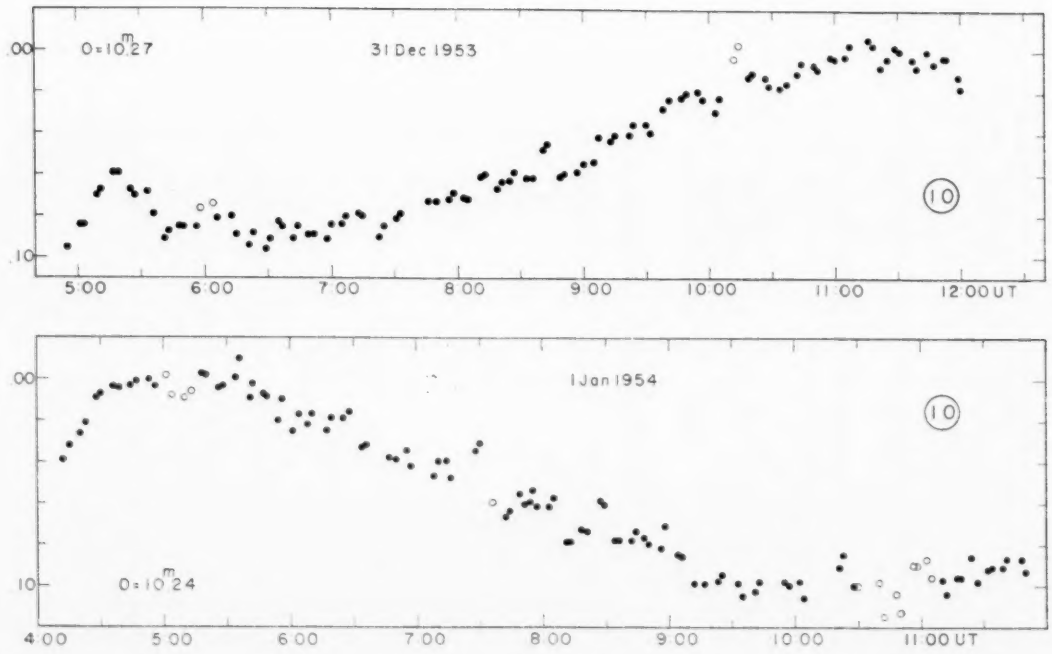


FIG. 9.—Observations of 10 Hygeia

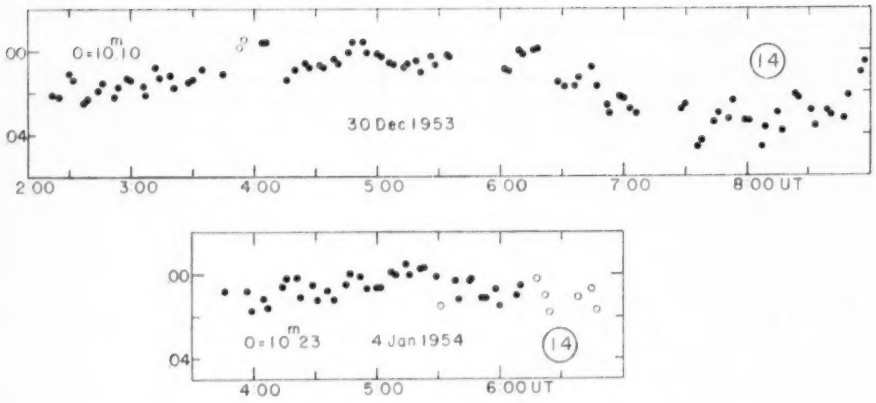


FIG. 10.—Observations of 14 Irene

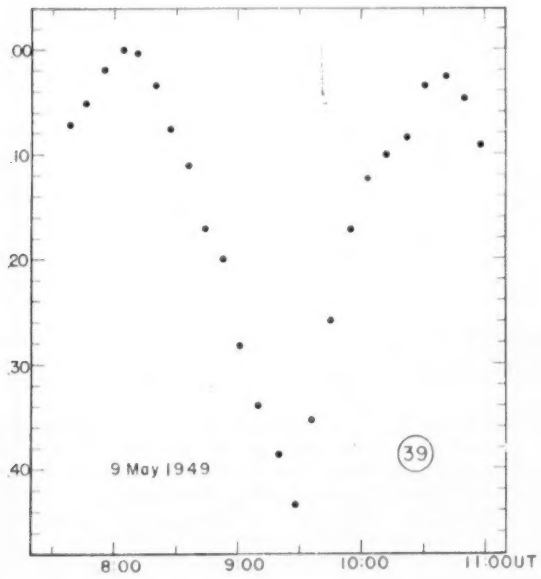


FIG. 11.—Observations of 39 Laetitia

night's maximum, which occurs 18 hours later than the first. A period of 18 hours may, therefore, be provisionally adopted. On this basis the two nights represent slightly more than half the total light-curve, with both minima but only one maximum shown. The minima are 0.09 and 0.10 mag. deep. The mean magnitude, each for a quarter-period, derived from the two nights, if corrected for changes in phase and distance, agree within 0.015 mag., if the phase coefficient 0.03 mag/degree is used.

*14 Irene.*—This object was observed on December 30, 1953, and January 4, 1954, U.T. The results are plotted in Figure 10. The December 30 run was nearly 7 hours and suggests two minima and one maximum. However, the total amplitude is only 0.035 mag., and the suggested half-period of perhaps $5\frac{1}{2}$ hours must be taken with great reserve. On this interpretation, the secondary minimum is only 0.02 mag. deep. Some irregularities are indicated which likewise need confirmation.

The mean magnitudes, corrected for changes in distance and phase, bring the two nights into good accord, as is seen from Table 1; the phase coefficient used is Müller's value, 0.034 mag/degree.

*39 Laetitia.*—The 1949 observations, plotted in Figure 11, supplement the 1952 and 1953 observations of Paper I. The amplitude in 1949 was twice that of the later observations, 0.43 mag. We shall see below that the 1949 minimum is the secondary one; it is so listed in Table 3, which gives all epochs now at hand.

TABLE 3

EPOCHS OF MAXIMA AND MINIMA OF 39 LAETITIA

| | | U.T. |
|---|---|---|
| 1949 May 9 | IMax. | $8^h08^m \pm 2^m$ |
| | IIMin. | 9 29 ±1 |
| | IIMax. | 10 40 ±2 |
| 1952 Jan. 29 | IMax. | 3 40 ±2 |
| | IIMin. | 4 56 ±2 |
| | IIMax. | 6 00 ±2 |
| | IMin. | 7 07 ±2 |
| | IMax. | 8 52 ±2 |
| 1953 Apr. 4 | IIMax. | 7 00 ±5 |
| 1953 Apr. 10 | IMax. | 4 28 ±2 |
| | IIMin. | 5 37 ±2 |
| | IIMax. | 6 54 ±3 |
| | IMin. | 7 53 ±4 |
| | IMax. | 9 37 ±4 |

The 1952 and 1953 observations give the following intervals between the cardinal points of the light-curve:

$$\underset{1^h17^m5}{I(M)}\text{–}\underset{1^h05^m5}{II(m)}\text{–}\underset{1^h03^m}{II(M)}\text{–}\underset{1^h44^m5}{I(m)}\text{–}I(M)\ ,$$

adding up to a period of $5^h10^m5$. According to the 1949 observations, the first two intervals are $1^h21^m$ and $1^h11^m$. There are apparently small differences in these intervals, probably connected with the great changes in the shape of the light-curve; but the data are incompatible with a shift of half a period. The assignment in Table 3 is therefore correct.

Table 3 may be condensed into four epochs of the secondary minimum; this minimum has the most regular shape and was directly observed in 1949 (see accompanying table).

| | | U.T. | | | U.T. |
|---|---|---|---|---|---|
| 1949 | May 9 | $9^h29^m \pm 1^m$ | 1953 | Apr. 4 | $5^h53^m \pm 5^m$ |
| 1952 | Jan. 29 | 4 56 ±1½ | 1953 | Apr. 10 | 6 54 ±3 |

In Table 4 these times are expressed in terms of Julian days (−2430000). The third

column gives values corrected for light-time. Epochs 3 and 4 lead to the period $5^h10^m75 \pm 0^m2 = 0.21580 \pm 0.00014$ day, already mentioned in Paper I. This period must now be combined with epochs 1, 2, and 4.

The varying amplitude of the light-curve shows that the pole of rotation is not at right angles to the ecliptic. There is no assurance, therefore, that the sense of rotation can be determined from the three principal epochs, which, moreover, are separated by long intervals of time. The interval 1–2 is 4609 ± 3 periods, while the interval 2–3 is 2025 ± 1½ periods. If the discussion is carried out along the lines used in Paper I on 15 Eunomia, one may consider the first interval to consist of any integral number of cycles between 4616 and 4600. Then, for *direct* rotation, the best representation of the second interval

TABLE 4

EPOCHS OF SECONDARY MINIMUM, 39 LAETITIA

| | JD | JD(c) | R.A. | Dec. | λ | β |
|---|---|---|---|---|---|---|
| 1 | 3045.8951 ± 0.0007 | 3045.8837 | $15^h34^m$ | − 3°8 | 232° | +15° |
| 2 | 4040.7056 ± .0011 | 4040.6945 | 06 26 | +11.6 | 96 | −12 |
| 3 | 4471.7451 ± .0035 | 4471.7330 | 12 15 | + 6.2 | 181 | + 7 |
| 4 | 4477.7875 ± 0.0021 | 4477.7752 | 12 11 | + 6.8 | 180 | + 7 |

is obtained by assuming the first interval to be 4609 cycles. The second interval is then 2025.037 cycles, giving a residual of 0.008 days. For *retrograde* rotation, reasonable residuals for the second interval are obtained by assuming the first interval to be 4616, 4609, or 4600 cycles. The residuals for the second interval are then, respectively, 0.006, 0.011, and 0.0006 days. While the last residual is, of course, satisfactorily small (see Table 4), it would require the period found from epochs 3 and 4 to be in error by three times the estimated uncertainty. Clearly, an accurate additional epoch is needed to settle this question.

*40 Harmonia.*—A short run, of only 1.1 hours, was obtained when clouds interrupted further work. The observations define a maximum on January 10, 1954, $1^h45^m$ U.T.; the magnitude was 10.68. The total variation observed was 0.04 mag. No *g*-value is entered in Table 1 because the mean magnitude could not be determined; the *g*-value corresponding to the *maximum* is 7.57 mag. if Müller's phase coefficient of 0.018 mag/degree is used (the phase angle was 22°4).

*44 Nysa.*—Reference is made to Shatzel's paper, No. III of this series (this issue) on the 1949 observations, in which he found a beautiful light-curve with a period of $6^h25^m$. Our observations were made on January 6, 7, and 11, 1954, and are shown in Figures 12, 13, and 14. Figure 12 also shows the observations of January 7 reduced to January 6, so as to complete the cycle. The reduction applied is 0.018 mag., 0.010 for change in the distances and 0.008 for phase (Müller's coefficient of 0.025 mag/degree was used). The light-curves define the epochs given in the accompanying table. These may be combined

| | | U.T. | | | U.T. |
|---|---|---|---|---|---|
| IMax | January 6 | $2^h10^m$ | IMax | January 7 | $3^h46^m$ |
| IMin | January 6 | 3 41 | IIMin | January 11 | 2 19 |
| IIMax | January 6 | 5 20 | IMax | January 11 | 4 08 |
| IIMin | January 6 | 6 46 | IMin | January 11 | 5 42 |
| IIMin | January 7 | 1 57 | IIMax | January 11 | 7 22 |

into epochs of primary maximum:

| 1954 | Wt. |
|---|---|
| Jan. $6^d2^h10^m$ | 1 |
| 7 3 46 | ½ |
| 11 4 09 | 1 |

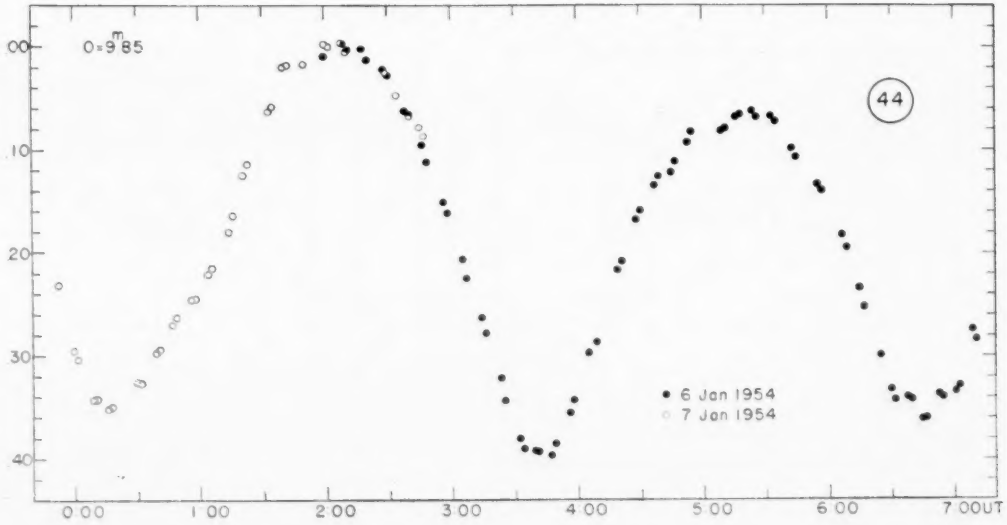


FIG. 12.—Light-curve of 44 Nysa

This will lead to a synodic period of $6^h25^m.2 \pm 0^m.1$. This period is identical with that derived by Shatzel. The interval between the two sets of data is 1522 days, or roughly 6000 periods. Clearly, a good epoch on a third opposition is needed to define the precise number of cycles and the sense of the rotation.

The shape of the light-curve in 1954 was similar, although different in detail from 1949; in particular, the minima were not flat, as in 1949. The 1954 amplitude was 0.40 mag., against 0.46 in 1949.

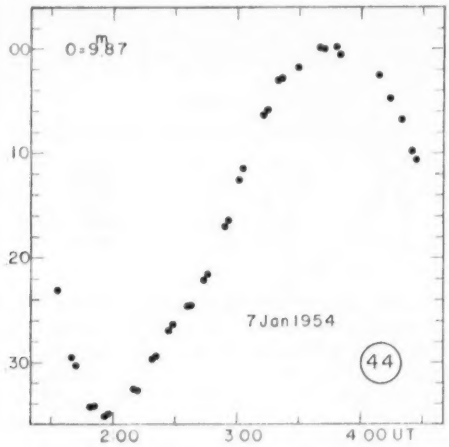


FIG. 13.—Observations of 44 Nysa

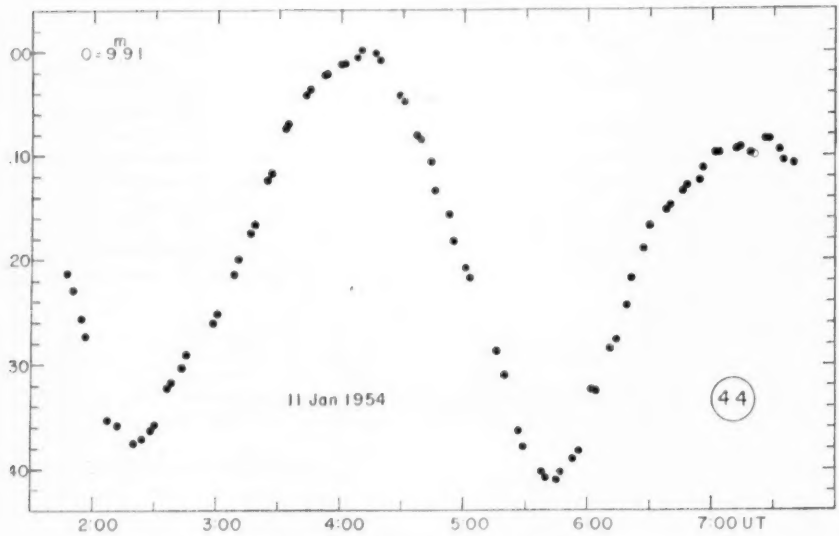


FIG. 14.—Light-curve of 44 Nysa

*354 Elenora.*—The observations on January 5, 1954, shown in Figure 15, define a light-curve of curious complexity. The first and last third of the run appear to cover the same phase of the cycle. They were combined to derive the shape of this part of the light-curve, which resulted in the full-drawn curves. The period so found is $4^h11^m$. As usual, two maxima and two minima are present in one complete cycle, and the total amplitude is 0.15 mag.

Observations on the next night were made during $2\frac{1}{2}$ hours (see Fig. 16). They are less accordant than those on January 5 but define the steep slope following the primary minimum and also the secondary maximum. The curve of January 5 is drawn in for comparison. The magnitude of the secondary maximum is then 10.10 on January 6 and 10.12 on January 5. The total reduction of January 6 to January 5 is +0.023 mag. if the phase coefficient 0.03 mag/degree is used. Therefore, the agreement between the two nights is complete.

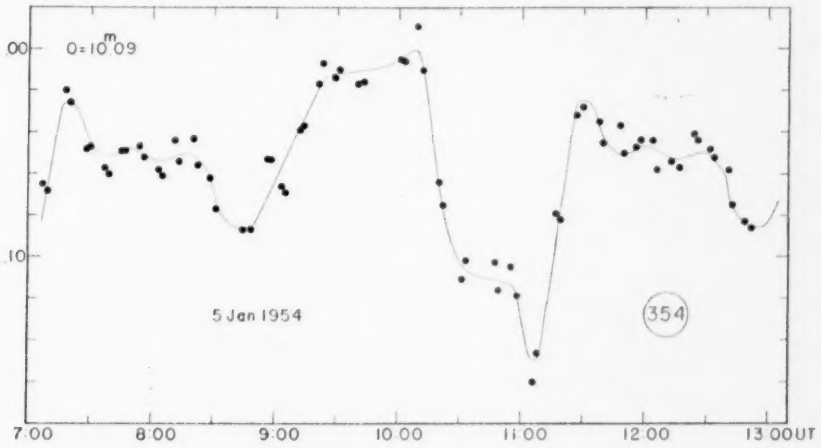


FIG. 15.—Light-curve of 354 Elenora

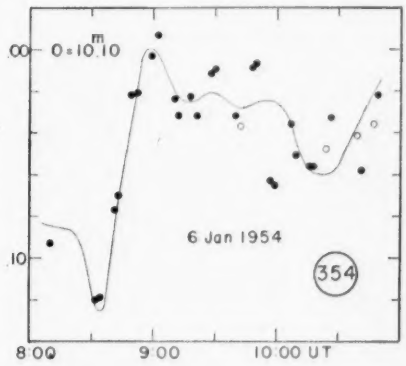


FIG. 16.—Observations of 354 Elenora

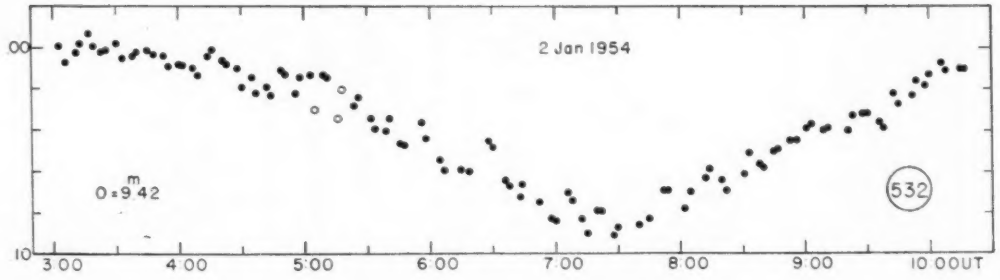


FIG. 17.—Observations of 532 Herculina

The steep slope on January 6, combined with the first slope on January 5, must be separated by six periods, making each period $4^h16^m$. This is 5 minutes more than the period found from January 5 alone, a discrepancy somewhat larger than expected. One suspects a lack of strict periodicity, but this requires confirmation. A color measurement was made on a third night, as is shown in Table 1.

*532 Herculina.*—A single night's run, of 7.3 hours, shown in Figure 17, gives a well-

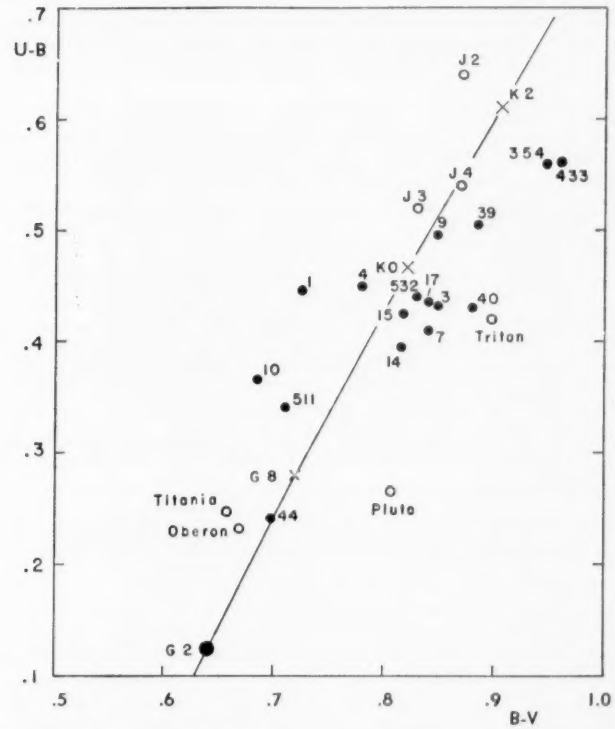


FIG. 18.—Colors, $B - V$ and $U - B$, of asteroids (*black dots*) compared to main-sequence stars (*line*) and selected satellites (*open circles*). Approximate position of sun is at *G2*.

defined variation, with an amplitude of 0.08 mag. and a suggested quarter-period of $4^h10^m \pm 10^m$. Accordingly, a period of some 16–17 hours is indicated.

## THE COLORS

The measures of color, both $B - V$ and $U - B$, are listed in Table 1. The combined color data of Paper I and this paper are shown graphically in Figure 18; the averages for each asteroid were used. The main sequence is indicated by the line and the symbols G2, G8, K0, and K2; the values are slightly smoothed means computed from the measures listed by Morgan, Harris, and Johnson (1953). Three of the Galilean satellites of Jupiter and two Uranus satellites are included for comparison. Jupiter I, at $B - V = 1.19$ and

$U - B = 1.11$ is well off the diagram; its colors correspond almost exactly to 61 Cygni A, dK5. The color of the moon is roughly $B - V = 0.98$. The Saturn satellite Dione is nearly as white as Oberon and Titania; Iapetus, Tethys, and Rhea follow, in order of increasing yellowness.

The precision of the dots in Figure 18 may be determined from the differences between nightly means for asteroids measured on more than one night. One thus finds that the p.e. per nightly result is $\pm 0.008$ mag. in $B - V$ and $\pm 0.012$ mag. in $U - B$. Since, on the average, 2 nights were combined in each dot, their average probable errors are about $\pm 0.006$ and $\pm 0.008$ mag. This proves that the asteroids shown in Figure 18 do not have identical colors. This conclusion cannot be reached from a list of photographically determined colors (Recht 1934), as is shown by a comparison of that list with the photoelectric data.

The asteroids are, on the average, slightly yellow, somewhat like a K0 main-sequence star, though they are slightly stronger in the ultraviolet than dK0. These results are of great interest in connection with studies of the presence of tenuous atmospheres for bodies like Pluto, Triton, etc., on the basis of their ultraviolet excess. This matter will be more fully discussed elsewhere; but it may be stated here that if the asteroids are used as a basis for comparison, Titan ($B - V = 1.28$, $U - B = 0.74$), Triton, and Pluto show such an excess, while the Jupiter satellites do not (cf. Fig. 18). On the contrary, the latter are slightly deficient in ultraviolet when compared to the asteroids; this fact adds to the interest of the three objects deviating from the asteroids in the opposite sense.

Figure 18 shows no evidence of a close relation between asteroid color and dimension. It is true that Eros is somewhat yellower than Ceres and Vesta, but objects of intermediate size exist both whiter and yellower than these large objects. One might perhaps expect some correlation between albedo and color, since a pulverized surface might be both brighter and whiter than the original one. Yet the proximity of Ceres and Vesta in Figure 18, in spite of their difference in albedo, indicates that such a correlation, if present, must be weak. This matter will be examined more fully upon completion of diameter measurements now in progress.

We are indebted to Dr. H. Kienle, Director of the Sternwarte Königstuhl, Heidelberg, for having made this collaboration possible by arranging the leave of absence of one of us (I. G.).

## REFERENCES

Beyer, M. 1938, *A.N.*, **267**, 27.
Giclas, H. L. 1950, *The Project for the Study of Planetary Atmospheres* (Annual Report, 1950), pp. 51, 52.
Groeneveld, I., and Kuiper, G. P. 1954, *Ap. J.*, **120**, 200.
Günther, O. 1951, *A.N.*, **280**, 83.
———. 1953, *ibid.*, **281**, 131.
Haupt, H. 1953, *Documentation des observateurs* (Inst. d'Ap. Paris, Bull. No. 8, Fasc. 1).
Morgan, W. W., Harris, D. L., and Johnson, H. L. 1953, *Ap. J.*, **118**, 82, Table 1.
Müller, G. 1897, *Die Photometrie der Gestirne* (Leipzig: Engelmann), p. 378.
Recht, A. W. 1934, *A.J.*, **44**, 25.

# PHOTOMETRIC STUDIES OF ASTEROIDS. III

## THE LIGHT-CURVE OF 44 NYSA*

ALBERT V. SHATZEL†
Yerkes and McDonald Observatories
*Received June 5, 1954*

ABSTRACT

Photoelectric observations of Nysa are presented which were made at the McDonald Observatory on November 6 and 7, 1949. The light-variation is periodic, with a period of $6^h25^m$. Two maxima and two minima are present; the latter have a peculiar, angular appearance.

The asteroid Nysa was the first object in the current photometric program to be observed on two consecutive nights and to show a large variation in brightness that was repeated precisely in consecutive cycles. The observations were made jointly with Mr. Kuiper, who initiated this program, while the reductions were carried out by the writer. We are indebted to Mr. Hiltner for the use of his photoelectric photometer. The runs were 6 and $6\frac{1}{3}$ hours, respectively. The comparison star used on both nights was BD+0°218, 9.3 mag BD, which was subsequently tied in with the Johnson-Morgan system on four nights, two by Mr. Hiltner and two by Miss Groeneveld. The results of these calibrations are

$$\text{BD}+0°218,\ V = 10.170 \text{ mag.},\ B - V = +0.499 \text{ mag., and } U - B = -0.056 \text{ mag.}$$

These colors correspond to about dwarf F7, so that the star was quite suitable for comparison purposes. The relative measures, asteroid − comparison, were made with a yellow filter which gave an effective wave length of about 5300 A.

The results of the two nights, November 6 and 7, 1949, are shown in Figures 1 and 2, plotted on the same scale as the figures in Papers I and II by Groeneveld and Kuiper. Each dot is the average of three readings of about 45 seconds each. Because of the rapid variation of the asteroid, the individual readings usually show the trend of the variation. This is seen in Figures 3 and 4, in which the individual readings of both nights are plotted, reduced to the phase of November 6. An empirical reduction of 0.02 mag. was used between the nights in Figure 3, where the interval is about 26 hours, and 0.01 mag. in Figure 4, where the interval is 19 hours. These amounts are consistent with the small change in phase, from 10°.5 to 10°.9, and Müller's phase coefficient of 0.025 mag/degree, and the changes in the distances which account for a change of 0.004 mag. The total reduction, 0.014 mag., applies to a 24-hour interval. Figures 3 and 4 show that the light-curve was identical in the two nights within the accuracy of observation.

The aspect of the asteroid depends on the co-ordinates:

$$\text{November 6, } \alpha = 1^h16^m,\ \delta = +1°.6;\ \text{November 7, } \alpha = 1^h17^m,\ \delta = +1°.5\ .$$

The mean magnitude for a complete cycle was 10.12 on November 6 and 10.14 on November 7. The mean value of $g$ is then 7.26 mag. on both nights. No color measurements were made. The period follows from the superposition of the two light-curves; it is $6^h25^m$.

* *Contributions from the McDonald Observatory, University of Texas*, No. 243.

† Now assistant director, Adler Planetarium, Chicago.

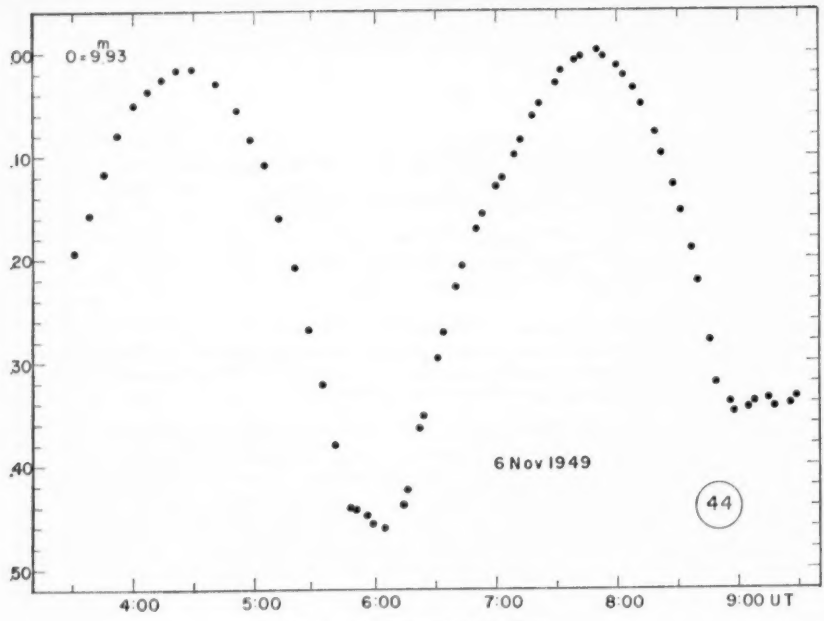


FIG. 1.—Observations of 44 Nysa

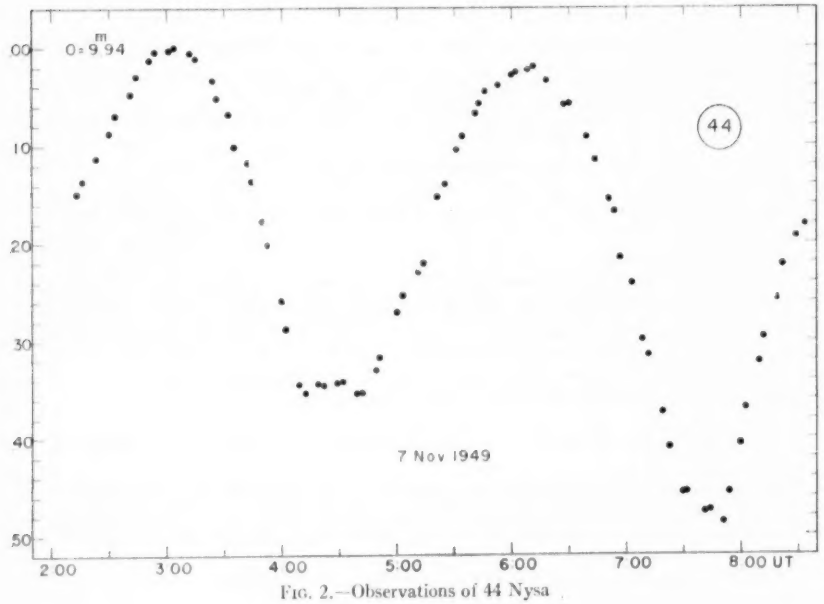


FIG. 2.—Observations of 44 Nysa

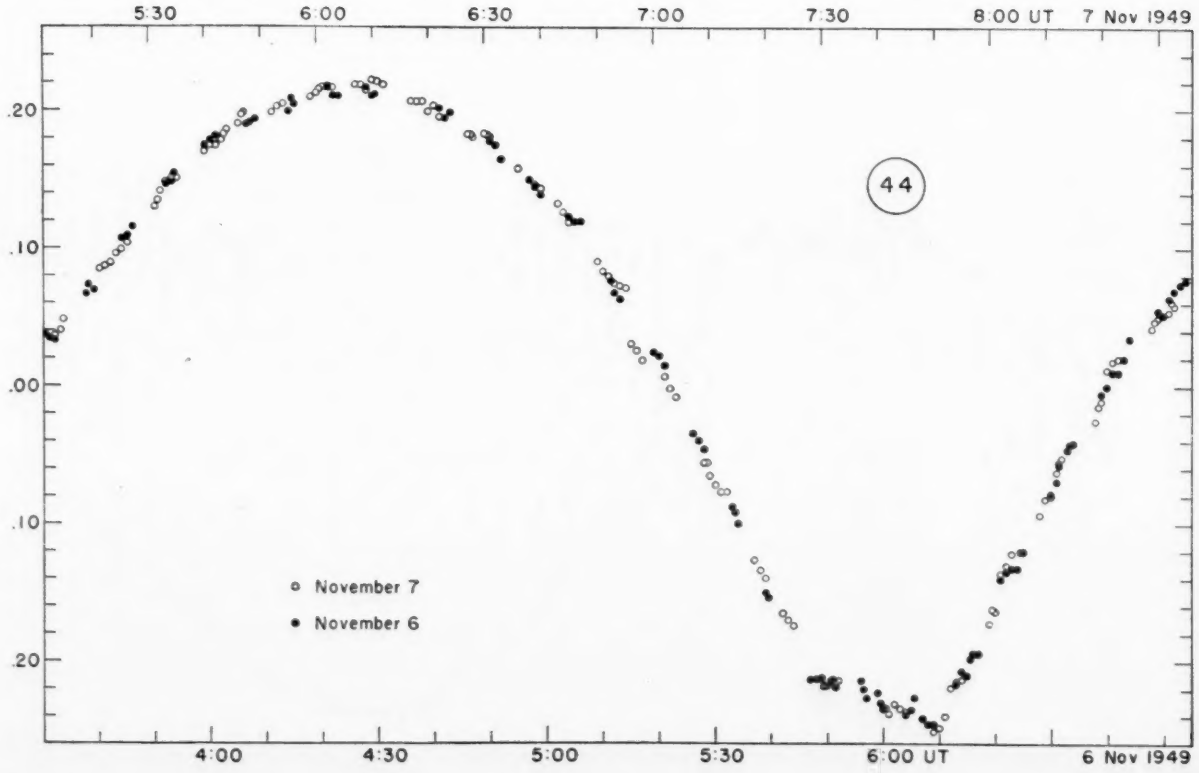


FIG. 3.—Light-curve of 44 Nysa, Part I

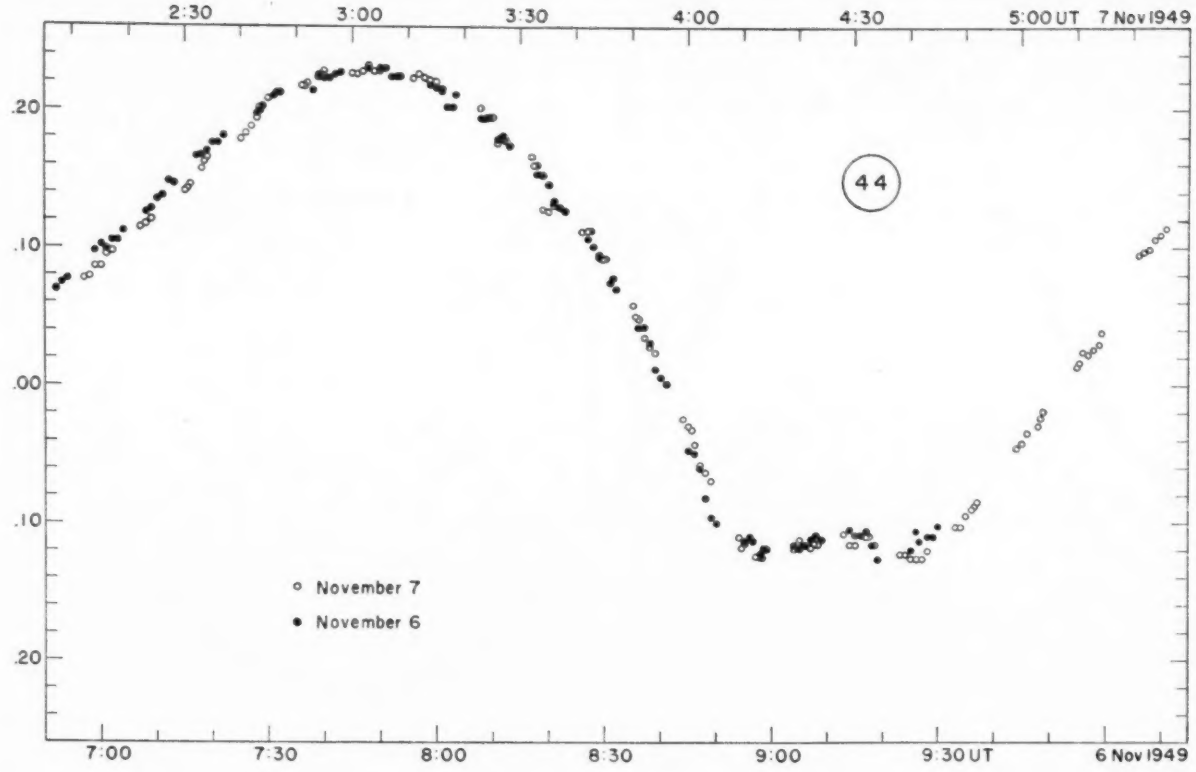


FIG. 4.—Light-curve of 44 Nysa, Part II

# PHOTOMETRIC STUDIES OF ASTEROIDS. IV. THE LIGHT-CURVES OF CERES, HEBE, FLORA, AND KALLIOPE*

IMAM I. AHMAD
Yerkes Observatory

*Received June 16, 1954*

ABSTRACT

The variation of the magnitudes of four asteroids—Ceres, Hebe, Flora, and Kalliope—has been investigated with the photoelectric photometers on the 82-inch reflector at the McDonald Observatory and on the 12-inch refractor of the Yerkes Observatory. The magnitude of Flora was nearly constant at the epoch of observation; for the other three asteroids the light varied, and the period of variation was determined. Ceres showed a range of 0.04 mag., with a period of $9^h04^m7$; Hebe a range of 0.16 mag. and a period of $7^h16^m5$; Kalliope a range of 0.14 mag. and a period of $4^h08^m8$. The latter is the shortest period that has been definitely established for an asteroid. All three asteroids show two maxima and minima. Hebe is the only asteroid observed by us over a long enough interval to establish the phase factor; the value is 0.045 mag/degree.

## I. INTRODUCTION

Short-period variations in the light of asteroids were first detected about the turn of the century, although the rather large variation in the light with phase angle had been established by Müller and Parkhurst. A compilation of the early results is given by Miss Harwood (1924). The early observations were made photographically or visually, and the accuracy was rarely sufficient to establish the period. This is particularly true if the asteroid has two nearly equal maxima and minima, as in the case of 15 Eunomia, where the correct period is exactly twice that announced earlier (Kuiper, Harris, and Ahmad 1953). Photoelectric observations of asteroids were first made by W. Calder in 1935. His observations of Ceres are discussed later.

In order to obtain information regarding the light-variations of asteroids, a program was initiated by Dr. G. P. Kuiper to observe a number of objects with high precision, using the photoelectric technique (Groeneveld and Kuiper 1954). The light-curve of Vesta has been published by B. Stephenson (1951), and a preliminary report on the results for several other asteroids was given at the Amherst meeting of the American Astronomical Society (Kuiper, Harris, and Ahmad 1953). The present paper gives the results of four asteroids investigated by the writer in 1953 with the 82-inch reflector of the McDonald Observatory and the 12-inch refractor of the Yerkes Observatory.

## II. PHOTOMETERS AND OBSERVING PROCEDURE

A description of the McDonald photometer and the modifications added in 1952 has been published by Johnson and Morgan (1951, 1953). It employs a 1P21 photomultiplier with a cast-iron shield to reduce interference from any existing magnetic field. The cell is refrigerated with dry ice to minimize the effect of dark currents. The focal-plane diaphragms are $\frac{1}{2}$, 1, 2, 3, 4, and 8 mm in diameter. A Fabry field lens is used to minimize guiding errors. The effective wave length with the yellow filter (Corning 3384 filter) is about 5550 A. The amplifier has very high stability, with a linear relationship between input and output and a high gain, which depends only on the ratios of the resistances of wire-wound resistors. An offset mechanism allows quick changes from star to sky and back. A short description of the Yerkes photometer has been published by S. Provin (1953). The same types of cell and filters as used at McDonald are employed, though the multiplier is not refrigerated.

* *Contributions from the McDonald Observatory, University of Texas*, No. 244.

An observation consists of two deflections on a comparison star (generally very close to the asteroid, to minimize the effect of extinction); one deflection on the adjacent sky; two or three deflections on the asteroid and sky; and then two deflections on the comparison star. The mean of the asteroid deflections is compared with the mean of the comparison deflections. Differential extinction was applied when necessary, though it rarely exceeded 0.002 mag. All the observations were made through the yellow filters only. Experience shows that the yellow measures give less scatter than the blue, because of the smaller extinction coefficient which is, furthermore, practically independent of color. Since asteroids do not show appreciable variations in colors (Kuiper, Harris, and Ahmad 1953; Groeneveld and Kuiper 1954*b*), little is gained by observing in more than one

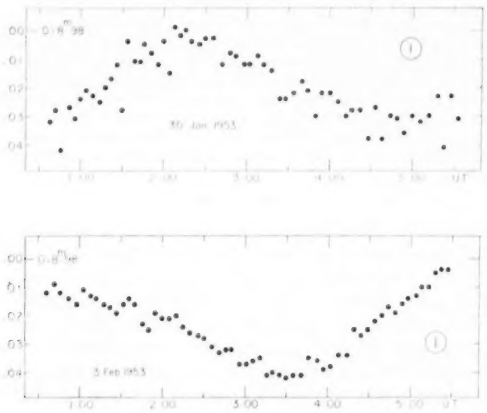

FIG. 1.—Single night's runs on 1 Ceres

color. This procedure also has the advantage of providing a large number of points as closely spaced as possible on the light-curves.

## III. THE LIGHT-CURVES

### CERES (NO. 1)

Ceres was announced to be variable, with a range of 0.2 mag., by Bailey and Campbell (1904), but they did not establish a period. In 1935 Calder observed Ceres photoelectrically and obtained a variation of 0.03 mag. He interpreted his observations as giving a period of $3^h36^m$. His observations extended over a sufficiently long interval of time to establish the phase coefficient of 0.050 mag/degree, a value which we have adopted in our reductions.

Ceres was observed on six nights at the McDonald Observatory, beginning on January 26, 1953. The main comparison star used was BD+20°703. The Yale zone catalogue gives its spectral type as F8; and its magnitude and colors as observed on Johnson's system (1953) are $V = 9.18$ mag.; $B - V = +0.63$ mag., and $U - B = +0.13$ mag. Other comparison stars used were reduced to this one differentially.

The individual observations amounted to 272 in all. The longest runs, made on January 30 and February 1, 3, and 8, consist of about 60 observations each, over $4\frac{1}{2}$–5-hour intervals, and are plotted in Figures 1 and 2. The individual observations were all re-

duced to mean opposition by applying corrections for the distances from the earth and sun,

$$\Delta m = 5 \log \frac{a\,(a-1)}{r\Delta},$$

where $r$ and $\Delta$ are the distances of the asteroid from the sun and earth and $a$ is the semi-major axis of the asteroid, 2.7674 A.U. (1947). The observations were also corrected for phase angle to January 30, 1953, with Calder's coefficient of 0.050 mag/degree.

Comparison of the observations made on different nights showed that the asteroid had a period of $9^h04^m7$. The observed times were then reduced to January 30, and the mean magnitudes were determined for every five observations consecutive in phase. These normal points are plotted in Figure 3. The range is found to be only 0.037 mag. There are two maxima, differing by 0.014 mag., and two minima, whose difference is negligible. From the mean light-curve we find that Ceres − comparison star = −1.377 mag., corrected for distance changes and phase changes with respect to January 30, 1953. With

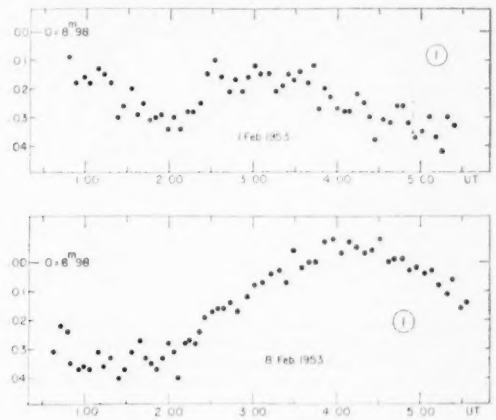


FIG. 2.—Single night's runs on 1 Ceres

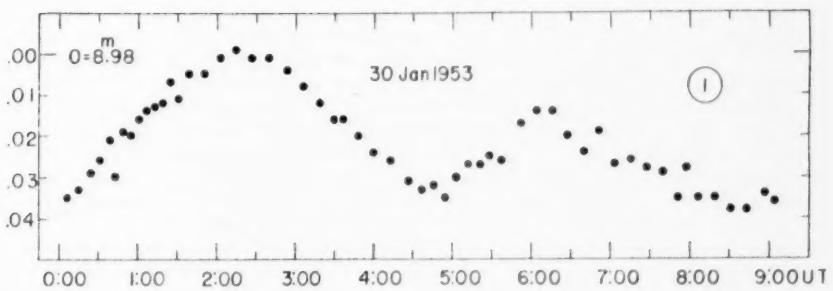


FIG. 3.—Light-curve of 1 Ceres

$V = 9.18$ mag. for the comparison star, we find Ceres = 7.803 mag. on January 30, 1953. As the phase angle was 19°.7, the correction required to reduce to zero phase angle is about −0.985 mag. Therefore, the magnitude at mean opposition is about 6.82 on Johnson's system. We can express the magnitude of Ceres as follows:

$$\text{Ceres} = 6^{m}82 + 0.05i + 5 \log r\Delta - 3.447 + \Delta m ,$$

where $\Delta m$ is dependent on the rotation phase. Calder's photoelectric observations were reduced to January 13, 1935, with our period of $9^{h}04^{m}7$ and the Calder's phase coefficient of 0.050 mag/degree. These observations are plotted in Figure 4.

As the amplitude of the rotational variations is only about 0.03 mag., it may be neg-

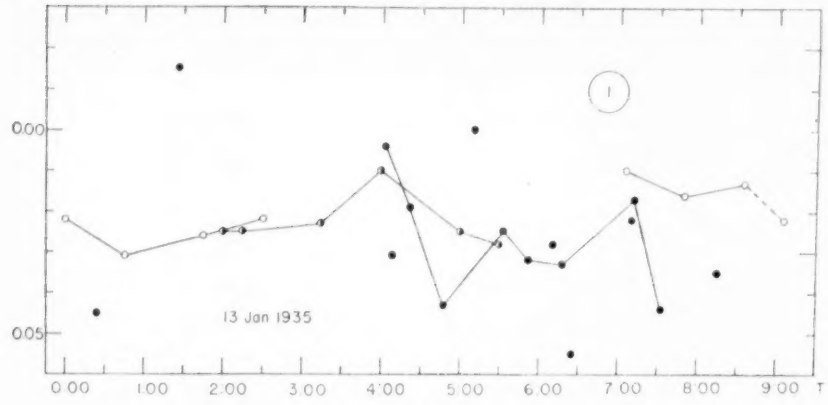


FIG. 4.—Calder's observations on 1 Ceres with the present period of $9^{h}04^{m}7$. The connected filled circles are observations on December 15, 1934, U.T.; the half-filled circles on January 12, 1935; the open circles on January 13, 1935; and the individual filled circles are observations on other dates. The zero corresponds to Ceres *minus* the mean of the two comparison stars, HD 69786 and HD 69866 = −1.28 mag. $T$ = E.S.T., January 13, 1935.

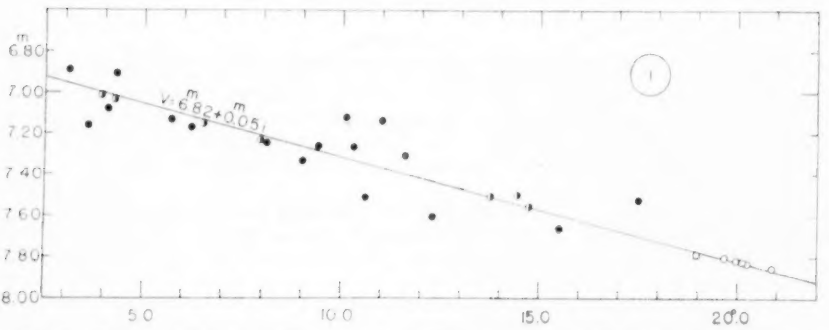


FIG. 5.—The magnitude phase relation of 1 Ceres. The open circles are the present observations; the half-filled circles represent Calder's observations; and the filled circles are Müller's observations.

lected in the determination of the phase coefficient. Applying a zero-point correction to Calder's and Müller's observations (1893), all the observations may be plotted as in Figure 5. It is seen that the present observations, as well as Calder's, fit the magnitude-phase relation very well. Müller's observations show considerable scatter but are not in disagreement with the adopted phase coefficient of 0.050 mag/degree. Müller's value of 0.042 mag/degree is obviously of considerably lower weight. Furthermore, phase coefficients determined from different oppositions may actually differ somewhat (Groeneveld and Kuiper 1954*b*).

### HEBE (NO. 6)

The variability of Hebe was reported by E. Bianchi and E. Padova in 1921. From visual observations on three nights they announced that the asteroid varied by 0.15 mag. in a period of $3^h14^m$.

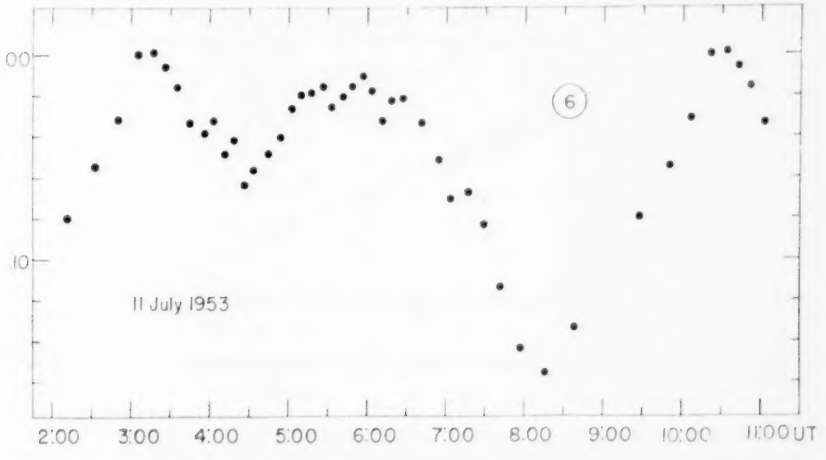


FIG. 6.—Light-curve of 6 Hebe. The zero corresponds to Hebe − (BD + 9°5203) = + 0.103 mag.

The writer observed Hebe on eight nights, beginning June 14, 1953, with the 12-inch refractor of the Yerkes Observatory. The main comparison star to which the others were reduced is BD − 9°5203. The Yale zone catalogue gives its spectral type as F2 and its magnitude as 8.3. The individual observations totaled 186 in all. By superposing plots of the observations made on different nights, we found a period of $7^h16^m5$. With this period the individual observations were reduced to July 11, 1953, and normal points for each five consecutive observations in phase were formed. The normal points are plotted in Figure 6. It is seen that the asteroid varies through a range of 0.156 mag. The curve has two maxima, differing by only 0.011 mag., while the two minima differ by 0.100 mag.

The observations extend over a range in phase angle large enough for a determination of the phase coefficient. On July 11, 1953, the mean difference Hebe − comparison star was 0.163 mag. The corresponding observed magnitude differences on the other nights were corrected for distance to mean opposition, with $a = 2.4254$ (1947). A plot of the magnitude differences against phase angle gives 0.045 mag/degree for the phase coefficient of Hebe.

To obtain the magnitude of Hebe at mean opposition, we have used Müller's (1893)

observations. These have been corrected by +0.04 mag., based on the magnitude of Müller's comparison star, BD −4°4376 as determined recently by Harris on the Johnson-Morgan $V$ system. Combining these observations with the phase coefficient determined above, we obtain $V_0 = 8.45$ for the magnitude of Hebe at mean opposition.

Assuming $V_0 = 8.45$, the zero point of our observed magnitude differences is reduced to the $V$ system. Figure 7 shows a plot of our reduced magnitudes, as well as the observations of Müller versus phase angle. The line $V = 8.45 + 0.045i$ appears to represent the observations fairly well, except for the night of June 23, which deviates by 0.08 mag.

FLORA (NO. 8)

In 1921 E. Padova obtained a variation of 0.12 mag. for 8 Flora. In 1950 R. Rigollet observed no variation. No period has been announced for the suspected variability.

Flora was observed at the McDonald Observatory for 2 hours on February 11, 1953,

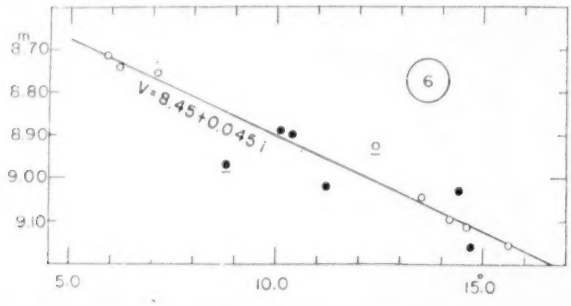


FIG. 7.—The magnitude-phase relation of 6 Hebe. Open circles are the present observations and filled circles those of Müller.

after which the observations were interrupted by clouds. On the next night a 6-hour run was obtained, with BD+15°2249 used as comparison star. The 6-hour run is plotted in Figure 8 and shows that there was no appreciable variation during the interval. If the asteroid is assumed to be constant in light over this interval, the probable error of a single observation is found to be ±0.0028 mag.

The constancy of the light of Flora can, of course, be interpreted as due to a spherical object or to the circumstance that the axis of rotation was directed toward the earth at the epoch of observations. The observations made by Kuiper and Groeneveld on March 27, also plotted in Figure 8, still fail to show decided variation, although the aspect of the asteroid had changed. It is desirable that this asteroid be investigated further, as it is the only one so far observed photoelectrically which was found constant in light within the accuracy of measurement.

KALLIOPE (NO. 22)

A light-variation of (22) Kalliope was announced by S. Bailey in 1904, who reported a range of 0.3 mag. from seven observations on three nights.

Kalliope was observed for 2 hours on February 13, 1953, when the observations were interrupted by clouds. On February 15 a run of over 6 hours showed that this asteroid has the very short period of variation of $4^h08^m8$. This is the shortest period so far determined in the current investigation of asteroids. The observations of February 15 are plotted in Figure 9 as filled circles; the observations of February 13 are plotted as open

circles after a zero-point adjustment of +0.356 mag. was made. The comparison star on February 15 was BD+30°2078.

The amplitude is 0.141 mag.; the two maxima differ by 0.016 mag. and the two minima by 0.028 mag.

## IV. DISCUSSION

The periods of the light-variation of several asteroids have been published. Except for Eros, the period has been determined from observations made during a relatively short interval of time, so that the changing distance and orientation of the asteroid with respect to the sun and the earth may be neglected. These changes must be taken into consideration when the observations cover a long interval or when we discuss light-curves at different oppositions (Huruhata 1940).

By combining light-curves made at different epochs, H. N. Russell (1906) has shown

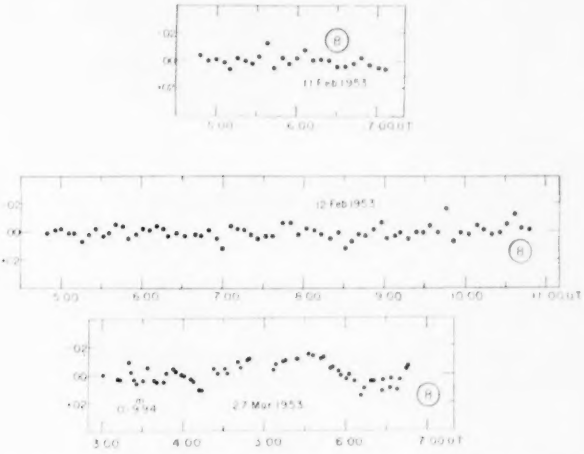


FIG. 8.—Single night's runs on 8 Flora. The zero represents Flora−(BD+15°2249) = −0.061 and −0.262 mag. on February 11 and 12, respectively.

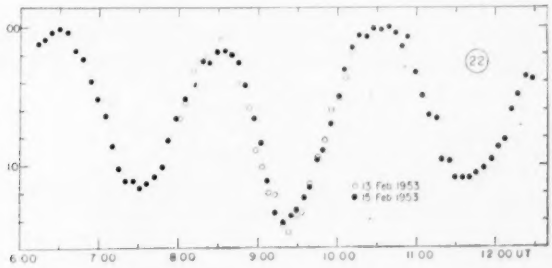


FIG. 9.—Light-curve of 22 Kalliope. Filled circles represent observations on February 15, 1953, U.T., and open circles observations on February 13, 1953, U.T. The zero corresponds to Kalliope−(BD+30°2078) = +0.394 mag.

that it is possible to determine the position of the asteroid's equator. However, the sign of the inclination remains unknown. It is also impossible to determine the shape of the asteroid unambiguously or the distribution of brightness over the surface. If any continuous convex form is possible, then many other such forms are possible too; also, a great variety of brightness distributions on the surface may give rise to the same light-curve.

A list of asteroids with known periods and the observed ranges is given in Table 1,

TABLE 1

PERIODS AND AMPLITUDES OF ASTEROIDS

| Asteroid | Period | Amplitude | Reference* | Asteroid | Period | Amplitude | Reference* |
|---|---|---|---|---|---|---|---|
| 22 Kalliope | $4^h09^m$ | $0^m14$ | a | 3 Juno | $7^h13^m$ | $0^m15$ | b |
| 354 Elenora | 4 16 | .15 | b | 6 Hebe | 7 17 | .16 | a |
| 9 Metis | 5 05 | .11 | b | 1 Ceres | 9 05 | .04 | a |
| 511 Davida | 5 10 | .06 | c, b | 25 Phocaea | 9 57 | .18 | b |
| 39 Laetitia | 5 11 | .18 | c, b | 14 Irene | 11? | .04 | b |
| 433 Eros | 5 16 | .0–1.5 | d | 17 Thetis | 12 17 | .32–0.36 | b |
| 4 Vesta | 5 20† | .10–0.12 | e, c, b | 532 Herculina | 16–17? | .08 | b |
| 15 Eunomia | 6 05 | .49 | c, b | 10 Hygiea | 18? | .10 | b |
| 44 Nysa | 6 25 | .41 | b | 8 Flora | | ≤0.01 | a |
| 7 Iris | 7 07 | 0.22 | c, b | | | | |

* References are as follows:

a: Present paper.
b: Groeneveld I., and Kuiper, G. P. 1954, *Ap. J.* **120,** 200 and 529.
c: Kuiper, G. P.; Harris, D. L.; and Ahmad, I. I. 1953, *Sky and Telescope,* **12,** 129.
d: Watson, F. 1937, *Harvard Circ.*, No. 419; Huruhata, M. 1940, *Harvard Circ.*, No. 442.
e: Stephenson, B. 1951, *Ap. J.*, **114,** 500.

† Period may be $10^h41^m$.

arranged by the length of the period. All the asteroids are intrinsically bright, except for Eros. The larger range observed for Eros is undoubtedly due to its being an elongated irregular object.

The minimum rotation period may be estimated from the results given by Jeans (1919) for an incompressible and homogeneous mass of fluid,

$$P^2 = \frac{2\pi}{0.187G\rho},$$

which gives $P = 12{,}000$ seconds or 3.3 hours for a density of 3.5. The smallest rotation period so far observed of $4^h09^m$ is 5/4 times this predicted minimum.

I wish to thank Dr. D. L. Harris for suggesting this problem and for his general guidance; Dr. G. P. Kuiper for valuable discussions; and Drs. Kuiper and Groeneveld for making available for Section IV their unpublished data. I am indebted to Miss Delphine Jehoulet, Miss Lucille Schott, Mrs. Beverly Negaard, and Mrs. Phyllis Erikson for technical help.

REFERENCES

Bailey, S., and Campbell, L. 1904, *Harvard Ann.*, **72,** 165.
Bianchi, E., and Padova, E. 1921, *Soc. astr. ital.*, ser. 2, p. 47.
Calder, W. A. 1935, *Harvard Bull.*, No. 904.
Cincinnati Observatory. 1947, *Elements and Opposition Ephemerides of Minor Planets,* p. 1.
Groeneveld, I., and Kuiper, G. P. 1954*a*, *Ap. J.*, **120,** 200.
———. 1954*b*, *ibid.*, **120,** 529.
Harwood, M. 1924, *Harvard Circ.*, No. 269.
Huruhata, M. 1940, *Harvard Circ.*, No. 442.
Jeans, J. H. 1919, *Problems of Cosmogony and Stellar Dynamics* (Cambridge: At the University Press), p. 269.
Johnson, H. L., and Morgan, W. W. 1951, *Ap. J.*, **114,** 552.
———. 1953, *ibid.*, **117,** 314.

Kuiper, G. P.; Harris, D. L.; and Ahmad, I. I. 1953, *Sky and Telescope*, **12**, 129.
Müller, G. 1893, *Publ. Astr. Obs. Potsdam*, **8**, 289 and 295.
Padova, E. 1921, *Soc. astr. ital.*, Ser. 2, p. 90.
Provin, S. 1953, *Ap. J.*, **117**, 21.
Rigollet, R. 1950, *C.R. Acad. sci., Paris*, **230**, 2077.
Russell, H. N. 1906, *Ap. J.*, **24**, 1.
Stephenson, B. 1951, *Ap. J.*, **114**, 500.

# A NEW $O_2$ BAND IN THE INFRARED AURORAL SPECTRUM*

J. W. CHAMBERLAIN, C. Y. FAN, AND A. B. MEINEL
Yerkes Observatory

*Received July 1, 1954*

ABSTRACT

A strong, but heretofore undetected, auroral emission has been identified as the 1–1 band of the forbidden Atmospheric system of $O_2$. Only transitions from $v' = 0$ have been previously observed in aurorae. The degree of excitation in the rotational and vibrational levels of the upper electronic state is discussed.

## IDENTIFICATION

One of the strongest features in the infrared auroral spectrum has remained undetected for many years. This feature, which lies on the shortward side of the 2–0 First Positive band of $N_2$, was discovered by two independent means from spectra obtained during the aurora of April 11–12, 1954: (1) A comparison of low-dispersion auroral spectra with those of "laboratory aurorae" produced by electronic and ionic impact experiments (Fan and Meinel 1953; Fan 1954) clearly showed a new emission distinct from the 2–0 First Positive band (see Fig. 1). (2) A comparison of the structure of different First Positive bands on a high-resolution auroral spectrum demonstrated that the feature with a maximum at 7688 A could not be part of the neighboring $N_2$ band (see Fig. 2).

Although the new feature appears strong and sharp under low dispersion and, in fact, resembles λ 7774 *O* I in appearance, its wave length is not appropriate for any reasonable atomic identification. The (*R*-branch) head of the 1–1 transition in the $O_2$ Atmospheric system ($b\ ^1\Sigma_g^+ \rightarrow X\ ^3\Sigma_g^-$), on the other hand, lies at 7684 A, only 4 A different from the observed emission. The origin for this band at 7708 A, moreover, coincides with a minimum in the auroral spectrum. The broader *P* branch of the 1–1 band is superimposed upon the First Positive 2–0 band of $N_2$ and consequently is difficult to distinguish. Appreciable differences in appearance of the 1–1 band from the 0–1 emission (which has similar *P* and *R* branches) are due to the change in $B_{v'} - B_{v''}$ from 0.04883 to 0.03065, respectively. As a consequence, the head (which gives rise to the sharp maximum at 7688 A) is much more prominent in the $\Delta v = 0$ sequence; the $\Delta v = -1$ bands possess a more open structure, with little difference, under low dispersion and at low temperatures, between the *R*- and *P*-form branches.

Re-examination of a long series of auroral spectra has shown that this new $O_2$ band is consistently present. It is generally somewhat brighter than λ 7774 *O* I, but its intensity varies. The 0–1 band of this system has previously been identified in both the airglow (Meinel 1950) and the aurora (Meinel 1951). In the emitting regions, the 0–0 band will be about 23 times the intensity of 0–1, according to the vibrational transition probabilities of Fraser, Jarmain, and Nicholls (1954) shown in Table 1. The 0–0 radiation, however, is rapidly converted into 0–1, 0–2, . . . , transitions, so that the 0–0 band is extinguished long before reaching the troposphere. In the troposphere the great quantity of $O_2$ produces intense wings in the 0–0 absorption (Fraunhofer A band). Thus all emissions in the region of 7600 A are absorbed, with the exception of a small window around the zero gap at 7619 A. Hence neither the strong 0–0 emission nor that portion of the strong 3–1 First Positive band with $\lambda > 7594$ A appears in the auroral spectra (cf. Figs. 1 and 2).

* The research reported in this paper was supported in part by the Geophysics Research Directorate of the Air Force Cambridge Research Center under Contract AF 19(122)-480.

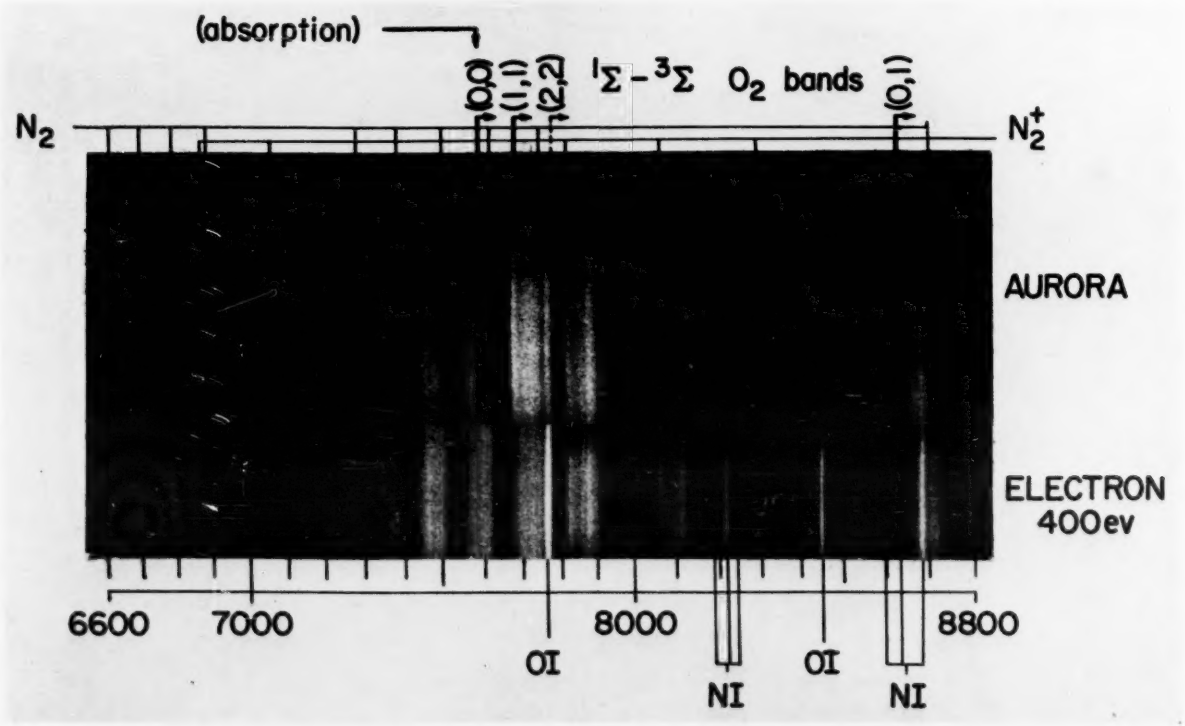


FIG. 1.—Auroral spectrum from 2.5-inch, $F$ 0.65 patrol spectrograph, April 11–12, 1954, obtained by Fan. Dispersion on the plate is 400 A/mm. Note that the 1–1 $O_2$ band extends into the upper regions of the auroral arc. The lower spectrum, shown for comparison, is air excited by monoenergetic electrons. In the laboratory spectrum, the $^1\Sigma \rightarrow {}^3\Sigma$ $O_2$ bands are absent because of the long lifetime for the upper state.

ROTATIONAL TEMPERATURE

The moderately long lifetime (~7 sec) of the $b\,^1\Sigma_g^+$ state suggests that the populations of the rotational levels will be thoroughly redistributed by inelastic and superelastic collisions before the downward transitions occur. Therefore, even if the excited molecule *initially* possesses relative populations that are not in equilibrium with the kinetic temperature of the gas, we would nevertheless expect the intensities of the rotational lines to give an accurate indication of the gas temperature.

Unfortunately, only the 0–1 band in this system is sufficiently strong and unblended for an accurate determination of the auroral temperature. Using line strengths computed by Schlapp (1937), we have estimated the temperature, from the positions of the *P*- and

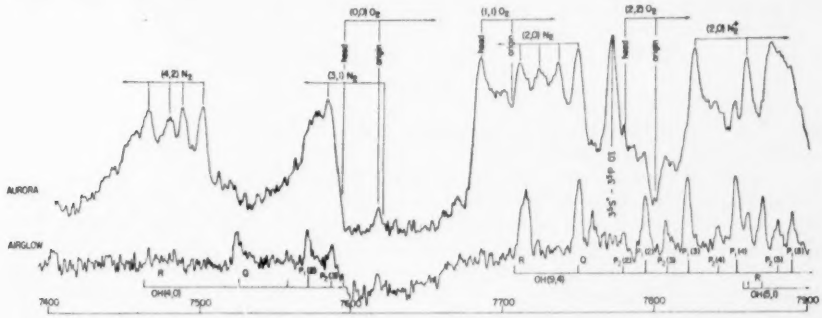


FIG. 2.—Auroral spectrum from 9-inch, *F*/0.8 spectrograph, April 11–12, 1954, obtained by Chamberlain. Dispersion on the plate is 70 A/mm. The airglow spectrum is shown for comparison. Very little *OH* contamination occurs in this region of the auroral spectrogram.

TABLE 1

ATMOSPHERIC SYSTEM OF $O_2$

| $v'-v''$ | λ(A) Origin | Δλ(A) Origin − Head | $p(v'v'')$ | $v'-v''$ | λ(A) Origin | Δλ(A) Origin − Head | $p(v'v'')$ |
|---|---|---|---|---|---|---|---|
| 0–0 ..... | 7619 | 25 | 0.933 | 0–1 ..... | 8645 | 47 | 0.065 |
| 1–1 ..... | 7708 | 24 | .802 | 1–2 ..... | 8742 | 44 | .126 |
| 2–2 ..... | 7802 | 23 | 0.675 | 1–0 ..... | 6882 | 15 | 0.065 |

*R*-branch maxima on the high-resolution spectrum, to be about 200° K. The dispersion and resolution on our numerous other infrared patrol spectra are too small for quantitative band-profile studies, in view of the complex blending of emissions near 8680 A.

The height at which the $O_2$ bands are emitted during an aurora is unknown. Oxygen probably becomes dissociated between 80 and 120 km, although convection may carry an appreciable amount of $O_2$ much higher (e.g., see Nicolet 1954). The 0–1 Atmospheric band is strong in the airglow, and it is possible that the auroral emission arises from the same regions as the airglow band. Estimates of the airglow height have been made, but Chamberlain (1954) has shown that fluorescent scattering probably exerts a large effect on the deduced emitting height, and thus the region where the primary excitation occurs is still unknown. At any rate, the temperature of 200° K is not inconsistent with a height in the neighborhood of 100 km—i.e., in the lower auroral region.

It is of interest in this respect that although the airglow $O_2$ rotational temperature is about 150° K, Meinel (1950) on one occasion observed a greatly enhanced 0–1 band in the absence of any auroral emissions, which indicated a temperature of 200° K. Since the

0–0 emission will undergo numerous resonant scatterings in the upper atmosphere before it is transformed into 0–1 by fluorescence (Chamberlain 1954), it is possible that an auroral glow could be seen in the light of $O_2$ while other emissions are still beyond the horizon; however, the enhanced 0–1 airglow band showed no concentration toward the north that would indicate this mechanism as the explanation of Meinel's enhancement.

## VIBRATIONAL EXCITATION

In the airglow, where the sky is more or less uniformly illuminated, an important source of the 0–1 band is fluorescence of reabsorbed 0–0 emission. For an aurora that covers only a small portion of the sky, however, multiple scattering will rapidly diminish that effect, and we may safely neglect it for the aurora recorded in Figure 2. Thus the relative intensities of the bands will be given by

$$I(v'v'') = \text{Const.}\ \frac{N_{v'}\, p\,(v'v'')}{\lambda^4_{v'v''}},$$

where $N_{v'}$ is the population of the upper level and $p$ is the square of the overlap integral (Fraser, Jarmain, and Nicholls 1954).

We estimate from the total emission in the $R$-form branches that $I(1\text{–}1)/I(0\text{–}1) \approx \frac{1}{2}$. The uncertainty is appreciable, since the plate was not calibrated; however, the estimate appears to be reasonable in view of the sensitivity characteristics of the Eastman I-N emulsion. This leads to a population ratio $N_1/N_0 = 0.025$, which would be obtained with a temperature of 550° K. We emphasize, however, that this "vibrational temperature" should not be construed as reflecting the kinetic temperature, since the excitation is probably nonthermal and the populations of vibrational levels do not readily come into equilibrium with the gas temperature (e.g., see Chamberlain and Meinel 1954). If the populations of higher levels continue to decrease at this same rate, we would have $I(2\text{–}2)/I(1\text{–}1) = 0.022$. Figure 2 shows a questionable feature between 7779 and 7802 A which could be due in part to the 2–2 band. However, the expected relative intensity suggests that the 2–2 band is actually much too weak to be detected.

## REFERENCES

Chamberlain, J. W. 1954, *Ap. J.*, **119**, 328.
Chamberlain, J. W., and Meinel, A. B. 1954, *The Earth as a Planet*, ed. G. P. Kuiper (Chicago: University of Chicago Press), chap. xi.
Fan, C. Y. 1954, *Ap. J.*, **119**, 294.
Fan, C. Y., and Meinel, A. B. 1952, *Ap. J.*, **118**, 205.
Fraser, P. A., Jarmain, W. R., and Nicholls, R. W. 1954, *Ap. J.*, **119**, 286.
Meinel, A. B. 1950, *Ap. J.* **112**, 464.
———. 1951, *ibid.*, **113**, 583.
Nicolet, M. 1954, *The Earth as a Planet*, ed. G. P. Kuiper (Chicago: University of Chicago Press), chap. xiii.
Schlapp, R. J. 1937, *Phys. Rev.*, **51**, 342.

# VARIATIONS IN THE AURORAL SPECTRUM*

C. Y. Fan and D. H. Schulte
Yerkes Observatory
*Received June 28, 1954*

ABSTRACT

A patrol study of auroral emissions was made with a fast grating spectrograph at the Yerkes Observatory. It was found that (1) all quiet arcs showed a very intense *Hα* line, whereas rayed features never showed *Hα*; (2) the Meinel system of $N_2^+$ underwent little variation relative to the First Positive system of $N_2$. The implications of these findings are discussed.

## INTRODUCTION

A patrol study of auroral emissions has been in progress at the Yerkes Observatory since June, 1953. The grating spectrograph, previously used at the McDonald Observatory for nebular spectra, provides a dispersion of approximately 400 A/mm in the first order with an $F/0.65$ solid Schmidt camera. It is pointed north, about 10° above the horizon, with its slit aligned vertically. An image of the sky, subtending approximately 20°, is focused upon this slit. A clock-operated shutter automatically initiates and terminates each exposure. Thus the spectrum of any aurora appearing in the north within 20° of the horizon, including faint displays normally unnoticed, is recorded. The auroral forms are determined from the records of a 16-mm wide-angle sequence camera, which takes from 15 to 60 pictures of the sky per hour (Meinel and Schulte 1953). During strong displays, as many as 4 or 5 spectra have been obtained in one night, which makes it possible to ascertain variations in the spectra as the visible auroral forms change.

From June 1 to September 20, 1953, the spectrograph was operated in the spectral range 3800–6800 A with Eastman 103*a*-F film. Subsequent to September 20, hypersensitized I-N film was used in the region 6300–9000 A. The infrared observations were made to obtain data on the behavior of the *Hα* line and the Meinel system of $N_2^+$ bands, since laboratory studies have indicated that these two are characteristic features of excitation by protons and by electrons, respectively (Fan and Meinel 1953; Fan 1954). Thus the intensity variations of *Hα* and the Meinel bands relative to those of other features, such as the First Positive system of $N_2$, for different auroral forms should give some insight into the excitation mechanisms.

## OBSERVATIONAL RESULTS

The observations during the past year have indicated the following general conclusions regarding auroral spectra:

1. *All quiet arcs show very intense Hα lines, whereas rayed features never show Hα.*—Over the one-year period, seven arcs were recorded at the Yerkes Observatory. All the arcs showed very intense *Hα* lines, as shown in Figure 1. The Doppler broadening of the lines, resulting from high-energy protons impinging upon the upper atmosphere, is conspicuous. The first spectrum is from the aurora of August 13, 1953. The arc was very faint and lasted only $1\frac{1}{2}$ hours; however, *Hα* was very intense (note the photograph in Fig. 1). The average proton flux was estimated to be $5 \times 10^6/\text{cm}^2/\text{sec}$ (see appendix).

The second is the bright aurora of September 5, 1953. In its first phase it was a quiet arc without appreciable rayed structure. One and a half hours later, intense ray structures developed, superimposed on the arc, and frequently the arc was pulsating. During

* The research reported in this paper was supported in part by the Geophysics Research Directorate of the Air Force Cambridge Research Center under Contract AF 19(122)-480.

this phase the aurora was very bright, but the Balmer lines were weaker than in the first phase. In the third phase the arc moved toward the north, and at one time only a glow could be seen above the horizon. Finally, the arc reappeared and lasted for the rest of the night. The average proton flux during this aurora was estimated to be $5 \times 10^7/\text{cm}^2/\text{sec}$. The flux of the heavier ions, presumably α-particles, was about one-tenth of the proton flux as estimated from the intensity ratio of λ 5004 due to *N* II to λ 5228 due to $N_2^+$ (Fan and Meinel 1953).

From June 1, 1953, to May 31, 1954, there were about thirty cases in which only rays could be seen above the horizon at the Yerkes Observatory. None of their spectra show Balmer lines with appreciable intensities. Figure 2 shows the aurora of September 6, 1953, as an example. The aurora appeared from 0300 to 0600 G.C.T. It reappeared from 0700 to 1000 G.C.T. and attained its maximum brightness at 0730. The spectrum is contaminated with *Hg* and *Ne* lines from near-by city lights.

2. *The Meinel system of $N_2^+$ undergoes little variation relative to the First Positive system of $N_2$.*—Laboratory experiments (Fan 1954) indicate that electrons are the only particles that can excite the Meinel system of $N_2^+$. Furthermore, the intensity of this system relative to the First Positive system of $N_2$ depends strongly upon the energy of the electrons. An examination of a long series of auroral spectra in the infrared region shows that the relative intensity is surprisingly constant. The relative intensity is comparable to spectra excited in the laboratory by electrons with energies of several hundred electron volts. It is not possible for such energetic electrons to be the result of ionization, since only a few tens of volts can be transferred in such events. On the other hand, such energy is not enough for extra-terrestrial electrons to penetrate to the average auroral height—about 105 km. Thus local electric fields induced in the ionosphere during the auroral displays seem to be required for the acceleration of the electrons (Fan 1954).

*The great aurora of April 12, 1954.*—A rather spectacular aurora occurred on the night of April 12, 1954 (shown in Fig. 3). The aurora began at 0115 G.C.T. as a low arc with occasional rays in the vicinity of the main body. The arc moved quite rapidly toward higher elevation, and the first spectrum was taken during this phase. Then the arc became stationary for 45 minutes at an elevation of 50°. The second spectrum was taken with the spectrograph pointing at the main body of the arc. The average proton flux as estimated from the intensity of the *Hα* line is $10^7/\text{cm}^2/\text{sec}$. Very abruptly the arc broke into active rays. It was brilliant, but the *Hα* line had faded away. At times the aurora again had an arclike appearance about 10° above the horizon, but it was nevertheless active and rayed. Toward morning an auroral glow filled the northern horizon, with no predominant structure being apparent. These spectra do not show *Hα*, and the Meinel bands of $N_2^+$ appear to undergo little change through the series.

In summary, these observations suggest that the formation of a quiet arc by protons is a primary event, whereas the development of rayed structures or moving displays of other types is produced by electrons and may be a phenomenon induced in the ionosphere.

The author wishes to express his sincere thanks to Dr. A. B. Meinel for his encouragement and guidance and his appreciation to Dr. J. W. Chamberlain for reading the manuscript and offering several suggestions.

## APPENDIX

### THE DETERMINATION OF THE PROTON FLUX IN A QUIET ARC

Let $I_\alpha$ = Intensity of *Hα*, averaged over different angular heights, and $I_{6300}$ = Intensity of the λ 6300 [*O* I] line in the airglow at the angular height $\theta$. The ratio of $I_\alpha/I_{6300}$ can be determined photographically.

The average number of λ 6300 [*O* I] quanta emitted per square centimeter column at angle $\theta$ in the airglow is approximately equal to the number of photons emitted per vertical square

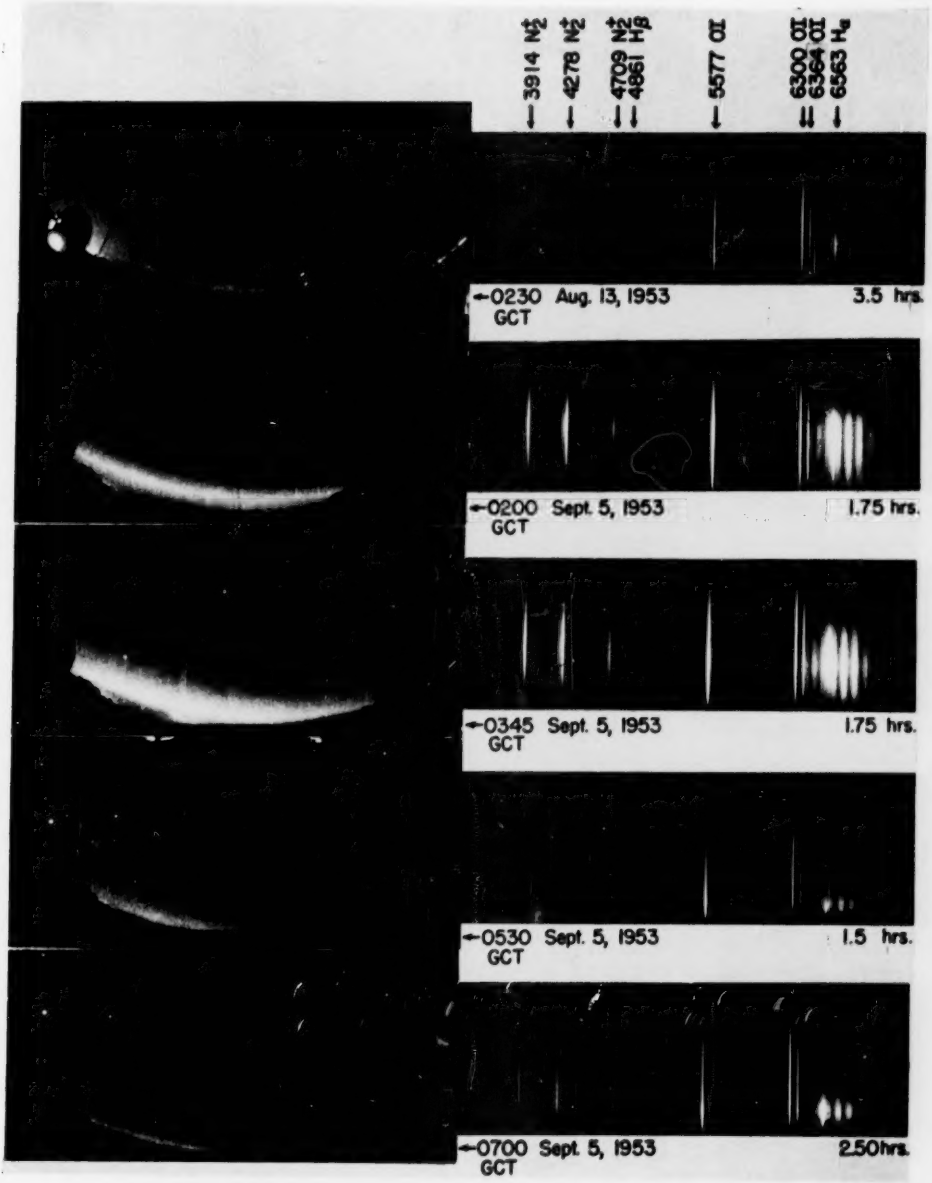


FIG. 1.—Sequence photographs and spectra of arcs. Note the intense *Hα* line in the weak arc of August 13, 1953

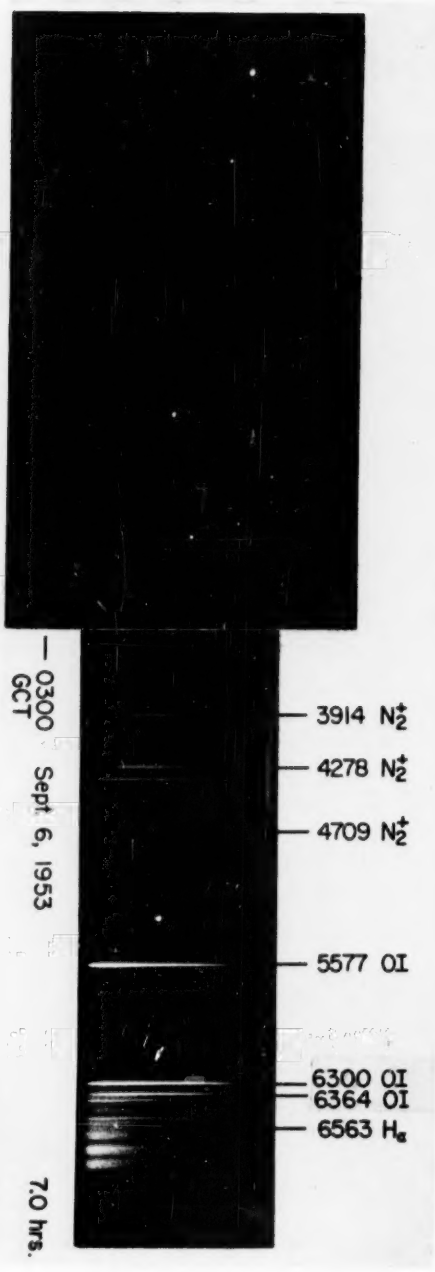


FIG. 2.—Photograph and spectrum of rays

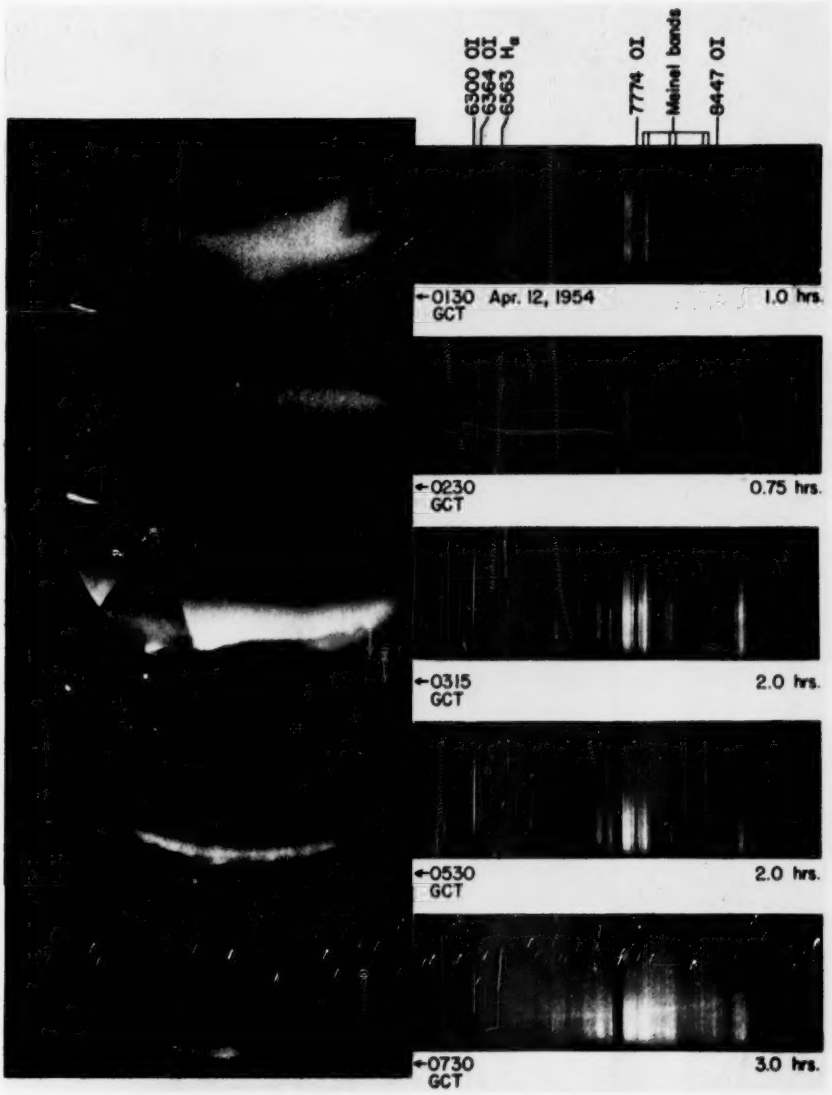


FIG. 3.—Sequence photographs and spectra of the aurora of April 12, 1954

centimeter column ($\sim 10^8$/cm$^2$/sec) multiplied by a factor $4/(1 + 15 \sin^2 \theta)^{1/2}$ if the height of the emitting layer is taken to be 150 km, with a scale height of 50 km. In order to avoid the correction of the atmospheric absorption, $\theta$ should be chosen to be the average angular height of the arc. From the ratio of $I_a$ (from the auroral plates) to $I_{6300}$ (from airglow plates reduced to the same exposure time as the auroral plate) and the value of $\theta$, one obtains the average number of $H\alpha$ lines emitted per square centimeter column at angle $\theta$. The number of $H\alpha$ per *vertical* square centimeter column should be of the same order of magnitude, because the scale height of the emitting layer of $H\alpha$ is, in general, comparable to the depth of the layer. Taking the specific yield of $H\alpha$ (number of $H\alpha$ emitted per one incoming proton) to be $\sim 50$, as estimated by Chamberlain (1954), we obtain, for the flux,

$$F = \frac{I_a}{I_{6300}} \frac{4 \times 10^8}{(1 + 15 \sin^2 \theta)^{1/2}} \frac{1}{50}.$$

It should be emphasized that this estimate is more accurate for aurorae near the zenith, i.e., $\theta = 90°$, than for low-altitude ones.

## REFERENCES

Chamberlain, J. W. 1954, *Ap. J.*, **120**, 360.
Fan, C. Y. 1954, *Ap. J.*, **119**, 294.
Fan, C. Y., and Meinel, A. B. 1953, *Ap. J.*, **118**, 205.
Meinel, A. B., and Schulte, D. H. 1953, *Ap. J.*, **117**, 454.

# ON THE PRODUCTION OF AURORAL ARCS BY INCIDENT PROTONS*

JOSEPH W. CHAMBERLAIN
Yerkes Observatory
*Received July 2, 1954*

ABSTRACT

A theory of the production of auroral arcs is extended to take account of a dispersion in directions for the incident protons. Earlier calculations of the *Hα* profile (by the author) and of the luminosity distributions (by Bates and Griffing), for the case of protons entering from only one direction, were considerably different from the observed curves. In this paper the angular distribution of incident protons is obtained by comparing the computed profile and luminosity-curves with the observational data. Essentially the same angular distribution gives a satisfactory representation of both the profile and the luminosity, which suggests that an angular dispersion may indeed be an important effect.

## I. INTRODUCTION

In a recent paper (Chamberlain 1954; referred to hereafter as "Paper I") the author discussed the penetration of protons through the atmosphere during the quiet-arc stage of an aurora. In that paper an *Hα* profile, computed for protons entering the atmosphere along the line of sight, was shown to differ considerably from Meinel's (1951) observed profile obtained for an arc in the magnetic zenith.

The *Hα* luminosity distribution with height was also obtained in Paper I, but there are no accurate observations of arcs in the light of the Balmer lines with which one can make a comparison. Bates and Griffing (1953), however, have computed auroral luminosity-curves for protons arriving in the vertical direction, by considering the ionization produced by protons in air. These calculations, also, are discordant with the observed data (Harang 1946), the theoretical curves being too narrow.

Several possibilities exist for reconciling these theoretical and observed curves: (1) There are appreciable uncertainties in the data used in the calculations; e.g., errors in the adopted cross-sections could affect the profile, and the luminosity curves are rather sensitive to the assumed model for the atmosphere. (2) The discrepancies may arise in part from errors in the observations. Only one spectrum with a Doppler-shifted profile has been published, and the need for more and accurate data on profiles is self-evident. Griffing and Stewart (1954) have examined the possibility that the observed luminosity-curves are distorted by foreshortening. They concluded that an aurora would have to possess an improbably large extent in latitude for the curve to be greatly affected. Actually, very little is known about the north-south extent of arcs, but the fact that the measured arcs (Harang 1946) show very little variation for a given height tends to support their conclusion. (3) Finally, the assumptions made in the theoretical treatments may have been oversimplified. Bates and Griffing suggested, for example, that the incident protons may not be mono-energetic, as they had assumed in their calculations, but may actually possess a dispersion of velocities. This would certainly broaden their computed arcs. The *Hα* profile would *not* be affected, however, since it is determined by the velocities at which the protons are most likely to capture electrons and radiate, rather than by the incident velocities. In Paper I it was pointed out that a dispersion in directions for the protons would affect both the *Hα* profile and the luminosity-curve in the desired directions. In this paper we shall examine this suggestion in detail.

* The research reported in this paper was supported in part by the Geophysics Research Directorate of the Air Force Cambridge Research Center under Contract AF 19(122)–480.

In the next two sections, equations and computations are presented for the profile and for the luminosity-curve when an angular distribution of particles is considered. Then in Section IV we discuss a particular distribution of directions that would reconcile both the profile and the luminosity-curves.

## II. THE *Hα* PROFILE IN THE ZENITH

The *Hα* profile computed in Paper I, for protons entering the atmosphere along the line of sight, was obtained by evaluating *numerically* the relative amounts of emission produced within equal velocity intervals. This intensity profile may be well represented, however, by an analytic expression of the following form:

$$I_0(v) = c_1 \frac{v^2}{\beta^2} \exp\left(-\frac{v^2}{\beta^2}\right). \tag{1}$$

For the best fit, the constant $\beta$ is about 1700 km/sec, when $v$ is measured in the same units. Throughout this paper, $c_i$ will denote constants of proportionality and $v$ will represent the component of velocity along the line of sight. When the protons enter along straight paths in a direction inclined at an angle $\psi$ to the line of sight, it is clear that the profile will be

$$I_\psi(v) = I_0(v \sec\psi) \sec\psi. \tag{2}$$

As a working hypothesis, we neglect any azimuth dependence of the proton directions and take the variation with zenith distance, $\theta$, to be

$$N(\theta) = c_2 \exp\left(-\frac{\tan^2\theta}{a^2}\right), \tag{3}$$

where $N(\theta)$ is the number of protons per unit solid angle. The constant $a$ in equation (3) is left undetermined for the present.

Thus for a plane-parallel atmosphere the profile observed at the zenith will be

$$\mathfrak{I}(v) = c_3 \frac{v^2}{\beta^2} \int_0^{\pi/2} \sec^3\theta \sin\theta \exp\left(-\frac{v^2 \sec^2\theta}{\beta^2} - \frac{\tan^2\theta}{a^2}\right) d\theta. \tag{4}$$

Equation (4) is readily integrated and gives

$$\mathfrak{I}(v) = c_4 \frac{v^2/\beta^2}{v^2/\beta^2 + 1/a^2} \exp\left(-\frac{v^2}{\beta^2}\right). \tag{5}$$

Meinel's (1951) published profile for the magnetic zenith (which is close to the astronomical zenith at auroral latitudes) was not corrected for the characteristic curve of the plate or for instrumental broadening (which is due primarily to the finite width of the spectrograph slit). The broadening function for the spectrum has been obtained by tracing over λ 6364 [*O* I] and using this profile to correct *Hα*.[1] [The method for obtaining the corrected *Hα* profile is that used by Wilson and Aller (1951, p. 422)]. The intensity scale, however, is still rather uncertain, and too much weight should not be given the exact shape of the profile.

Therefore, to derive a provisional value for $a$ (cf. eq. [3]), the observed and computed (eq. [5]) profiles have been fitted at their maxima. The resulting curves are shown in Figure 1, where the adopted value of $a$ is 8.5. The angular distribution of particles thus obtained is shown in Figure 3 and will be discussed in Section IV.

[1] I am deeply indebted to Dr. Meinel for the loan of his now-famous plate.

### III. THE LUMINOSITY DISTRIBUTION WITH HEIGHT

In treating the luminosity distribution, it is convenient to express the model atmosphere in terms of the *equivalent depth*, $\xi$ (measured in centimeters of air at S.T.P.), at each height (see Bates and Griffing 1954, Fig. 1). Then, having obtained luminosity curves for air at constant density, we may readily make a transformation to the model atmosphere.

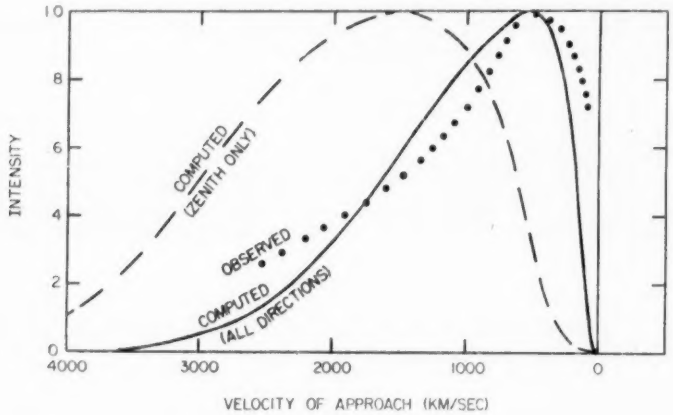


FIG. 1.—*Hα* profiles. *Dashed curve:* computed for protons entering only along the line of sight. *Solid curve:* computed for protons entering from all zenith angles according to eq. (3). *Dotted curve:* Meinel's observed profile for an arc in the magnetic zenith, corrected as described in text.

For protons arriving vertically with sufficient energy to penetrate to the 120-km level or below, the luminosity may be closely represented by

$$L_0(\xi) = c_5\left(\frac{h_0^2 - \xi^2}{b^2}\right) \exp\left(\frac{-h_0^2 + \xi^2}{b^2}\right). \tag{6}$$

Here $h_0$ is the maximum depth of penetration for these protons and $b$ is a constant characterizing the luminosity-curve at any altitude. Values of $b$ for aurorae whose bottom edges are at 100, 110, and 120 km have been derived from a comparison of equation (6) with the curves calculated numerically by Bates and Griffing. Analogous to equation (2), luminosity-curves for protons entering from zenith distance $\theta$ are given by

$$L_\theta(\xi) = L_0(\xi \sec\theta) \sec\theta. \tag{7}$$

We neglect any spiraling of the particles caused by the earth's magnetic field.

If we again adopt an angular distribution of the form of equation (3), the resulting luminosity distribution is

$$Y(\xi) = c_6 \int_0^{\theta_{\max}} \sec\theta \sin\theta \left(\frac{h_0^2 - \xi^2 \sec^2\theta}{b^2}\right) \exp\left(\frac{\xi^2 \sec^2\theta}{b^2} - \frac{\tan^2\theta}{a^2}\right) d\theta, \tag{8}$$

where $\theta_{\max}$ is the maximum angle at which protons can enter and still penetrate to the level $\xi$; thus $\sec\theta_{\max} = h_0/\xi$.

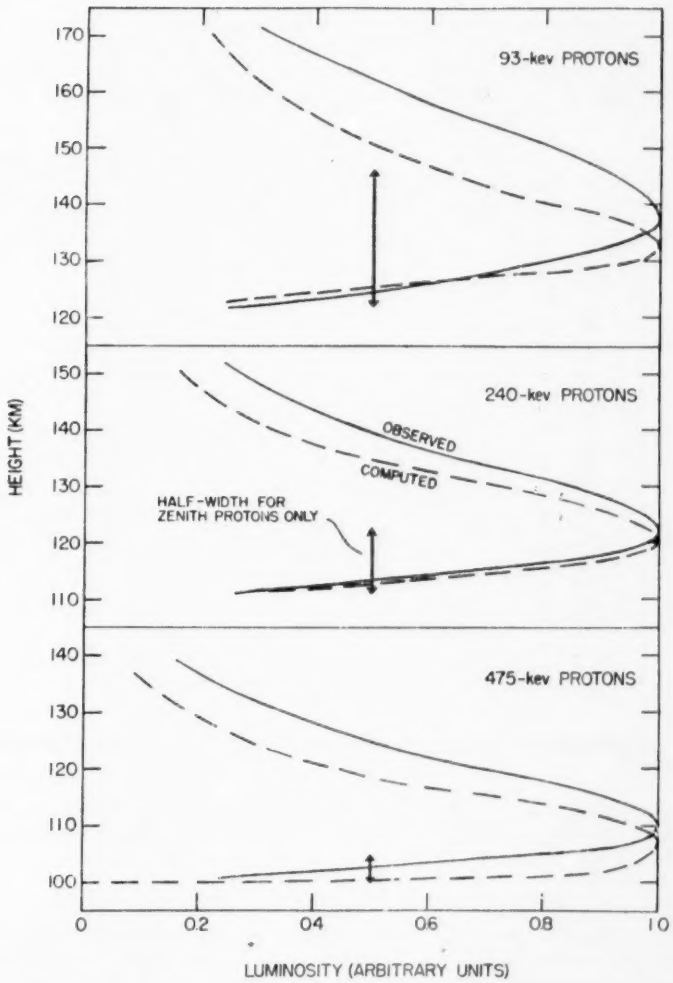


FIG. 2.—Luminosity-curves for aurorae at three heights. *Solid curves:* observed arcs (Harang 1946). *Dashed curves:* computed for protons entering from all zenith angles according to eq. (3). The arrow at the bottom of each arc indicates the half-width of the curve computed by Bates and Griffing (1953) for zenith protons only.

Evaluation of the integral in equation (8) gives

$$\mathfrak{L}(\xi) = c_7\left\{\frac{1}{\tau}(e^{-\tau} - e^{-\sigma}) + \ln\frac{h_0^2}{\xi^2} - (\tau - \sigma) + \frac{(\tau^2 - \sigma^2)}{2 \cdot 2!} - \frac{(\tau^3 - \sigma^3)}{3 \cdot 3!} + \cdots\right\}, \quad (9)$$

where

$$\sigma = \frac{1}{a^2} - \frac{\xi^2}{b^2} \qquad \text{and} \qquad \tau = \frac{h_0^2}{a^2\xi^2} - \frac{h_0^2}{b^2}. \quad (10)$$

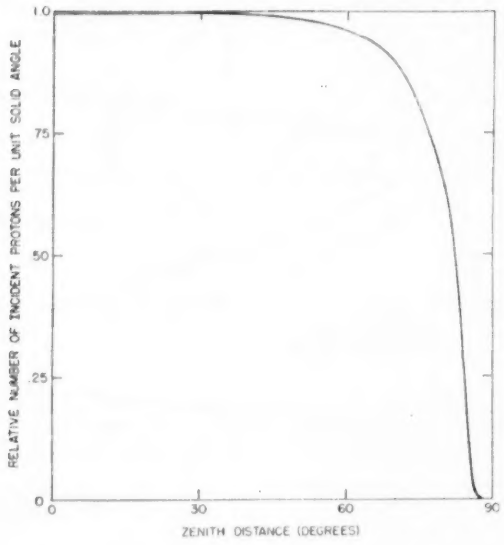


FIG. 3.—Angular distribution of incident protons used to compute the profile and luminosity-curves in Figs 1 and 2.

Curves computed from equation (9), in which the value of $a$ was obtained from fitting the observed and computed $H\alpha$ profiles as described in Section II, are compared in Figure 2 with observational data.

## IV. THE ANGULAR DISTRIBUTION OF THE INCIDENT PROTONS

Figure 3 shows the angular distribution of protons, $N(\theta)$, used in the computed profile and luminosity-curves (Figs. 1 and 2, respectively). The $N(\theta)$-curve is very broad, and it would be of considerable interest to auroral theories for us to ascertain whether this distribution is, in fact, real. The agreement of the computed profile and luminosity-curves with the observational data seems adequate, in view of all the uncertainties involved. The fact that the same angular distribution predicts with reasonable accuracy two independent types of observations is some support for its reality. As Bates and Griffing pointed out, their curves for the higher aurorae agreed fairly well with the observed ones. For these broad, high arcs there is relatively little difference between the luminosity-curves for protons entering from different directions; hence the dispersion in directions has less effect on these arcs than on low-lying aurorae. That is, the present

calculations also give a good representation of high aurorae, as well as of the lower ones.

It would be quite difficult to determine observationally how much the function $N(\theta)$ varies with altitude. A small part of the angular dispersion could originate from scattering by collisions within the atmosphere, and this portion would increase with depth. A much more important effect, however, is likely to be a dispersion in directions possessed by the protons prior to their penetrating the atmosphere. Auroral theories are too insufficiently developed, however, to predict the orbits of the incident particles.

## REFERENCES

Bates, D. R., and Griffing, G. W. 1953, *J. Atm. Terr. Phys.*, **3**, 212.
Chamberlain, J. W. 1954, *Ap. J.*, **120**, 360.
Griffing, G. W., and Stewart, A. L. 1954, *J. Atm. Terr. Phys.*, **4**, 339.
Harang, L. 1946, *Geofys. Pub.*, Vol. **16**, No. 13.
Meinel, A. B. 1951, *Ap. J.*, **113**, 50.
Wilson, O. C., and Aller, L. H. 1951, *Ap. J.*, **114**, 421.

# THE PHYSICAL THEORY OF METEORS. VI. THE LIGHT-CURVE*

ALLAN F. COOK
Harvard College Observatory
*Received May 24, 1954*

ABSTRACT

The conventional theory for predicting the light-curve of a meteor is applied to a bright meteor photographed with the Super-Schmidt cameras of the Harvard Meteor Expedition and is shown to be inadequate over the faint early portion of the trail, the meteor being fainter than predicted. An improved theory, based on the reaction-zone model and including thermal radiation from the body, provides a completely satisfactory fit to the observed light-curve.

## I. OBSERVATIONS

The Super-Schmidt cameras can reach to some 3 or more mag. fainter than the conventional cameras and thus make available not only fainter meteors but also the fainter early portions of the trails of bright meteors. The extension at the ends of the trails is not nearly so pronounced, owing to the very rapid decline in brightness occurring there. A very bright meteor with a smooth light-curve is required for the study of the early part, and one such meteor has been photographed from both stations of the Harvard Meteor Expedition. It was No. 5688, occurred on March 19–20, 1953, had a velocity outside the atmosphere of 68.64 km/sec, appeared at a height of 114 km at photographic absolute magnitude +1.9, reached −5.7 at maximum light near 84 km, and disappeared at a height of 78 km, the least measured photographic absolute magnitude being −2.6. The reduction for this meteor was performed by the Meteor Analysis Project, Harvard College Observatory, under the direction of Dr. L. Jacchia.

## II. THE PREDICTED LIGHT-CURVE

A brief résumé of the conventional theory is required. The equations of motion of a meteor are

$$m \frac{dV}{dt} = -\Gamma A m^{2/3} \rho_a V^2 , \tag{1}$$

$$\frac{dm}{dt} = -\frac{\Lambda}{2\zeta} A m^{2/3} \rho_a V^3 , \tag{2}$$

where $m$ denotes the mass of the meteor, $V$ its velocity, $t$ the time, $\Gamma$ the drag coefficient, $A$ a dimensionless shape-density factor, $\rho_a$ the atmospheric density, $\Lambda$ the heat-transfer coefficient, and $\zeta$ the heat of ablation. The first equation is the drag equation, the second the ablation equation. The intensity, $I$, is given by

$$I = -\frac{\tau}{2} \frac{dm}{dt} V^2 , \tag{3}$$

where $\tau$ denotes the luminous efficiency. There is observational evidence for bright meteors (Jacchia 1948) to support the form suggested by Öpik,

$$\tau = \tau_0 V . \tag{4}$$

* This research has been supported by the U.S. Office of Naval Research, under Contract No. N5ori-07647.

The observable quantities for a meteor are $s$, the distance along the trail from an arbitrary zero point; $H$, the height above sea-level; and $I$, the intensity, all being observed as functions of time, $t$. From these data the acceleration $dV/dt$ is derivable and also the integral,

$$\int_t^\infty \frac{I}{V^3}\,dt' = \frac{\tau_0}{2}\,m\,, \tag{5}$$

the expression on the right being found by substitution of equation (4) in equation (3), division by $V^3$ and subsequent integration between the indicated limits, $m$ ($\infty$) being assumed to be negligible. Also $\rho_a(H)$ is known from the Rocket Panel (1952) atmosphere. By substitution of equation (5) in equations (1), (2), and (3), along with substitution of the second of the resulting equations in the third, we obtain

$$\frac{\left[\int_t^\infty \frac{I}{V^3}\,dt'\right]^{1/3}}{\rho_a V^2}\,\frac{dV}{dt} = -\frac{1}{K}\,, \qquad K = \frac{2^{1/3}}{\Gamma\tau_0^{1/3}A}\,, \tag{6}$$

$$\frac{I}{\rho_a V^6\left[\int_t^\infty \frac{I}{V^3}\,dt'\right]^{2/3}} = \frac{\sigma}{K}\,, \qquad \sigma = \frac{\Lambda}{2\Gamma\zeta}\,; \tag{7}$$

$\sigma$ and $K$ are known for each meteor, $\sigma$ being observed to be essentially constant over the trail of a nonflaring meteor and $K$ constant for bright meteors but not for faint meteors (Jacchia 1954). In the case of a bright meteor, if a computed light-curve is desired, there is little point in solving equations (6) for $dV/dt$ and evaluating $V$, $s$, and $H$, along with a corresponding expression based on equation (2), because the observed constancy of $K$ implies the accuracy of the observed values of $s$ and $H$ and the tabulated values of $\rho_a(H)$. Thus $V$ is also an immediately derived quantity. By equations (7) the intensity will be

$$I = \frac{\sigma}{K}\,\rho_a V^6\left[\int_t^\infty \frac{I}{V^3}\,dt'\right]^{2/3}. \tag{8}$$

The only quantity not already available is a computed value of the integral. By substitution of equation (5) in equation (2) and rearranging slightly, we have

$$\frac{d}{dt}\left[\int_t^\infty \frac{I}{V^3}\,dt'\right]^{1/3} = -\frac{1}{3}\,\frac{\Lambda\tau_0^{1/3}A}{2^{4/3}\zeta}\,\rho_a V^3 = -\frac{1}{3}\,\frac{\sigma}{K}\,\rho_a V^3\,. \tag{9}$$

Let $t_0$ denote a standard epoch at which the observed value of equation (5) is adopted. Then, by integration of equation (9), we obtain

$$\left[\int_t^\infty \frac{I}{V^3}\,dt'\right]^{1/3} = \left[\int_{t_0}^\infty \frac{I}{V^3}\,dt'\right]^{1/3} - \frac{1}{3}\,\frac{\sigma}{K}\int_{t_0}^{t}\rho_a V^3\,dt'\,. \tag{10}$$

The result of equation (10) is thus a computed value of equation (5). Then equation (8) is used to find $I$.

The computed light-curve in Figure 1 was prepared by the Meteor Analysis Project under the direction of Dr. L. Jacchia using $\log K = 6.163$, $\log \sigma = -11.80$, and starting from the observed value of the integral (5) at $t_0 = 0^s.507$, $t = 0^s$ being taken to correspond to the appearance of the meteor. There is a large discrepancy between the early parts of the curves.

### III. AN IMPROVED THEORY

It appears obvious to try to remove the foregoing disagreement by including a term for loss of energy by thermal radiation in the heat-balance equation for the reaction-zone

theory of Cook, Eyring, and Thomas (1951). Then equation (16), given by Thomas (1952), may be transformed into

$$\left\{\sigma_1 T^4 + \frac{3}{4}\frac{k\Theta_s}{h}\, e^{-\epsilon/kT}\left[\epsilon + \tfrac{5}{2}kT\right]\left(\frac{\rho_m}{\mu m_A}\right)^{2/3}\right\}\frac{\mathfrak{S}}{\mathfrak{A}} = \frac{\Lambda}{2}\,\rho_a V^3\,, \tag{11}$$

where $\sigma_1$ is the Stefan-Boltzmann constant, $k$ is Boltzmann's constant, $h$ is Planck's constant, $\Theta_s$ is the Debye temperature of the meteoric material, $T$ the absolute temperature, $\rho_m$ the density of the meteoric material, $\mu$ its mean molecular weight, $m_A$ one-sixteenth of the mass of the oxygen atom, $\mathfrak{S}$ the surface area from which ablation is occurring, and $\mathfrak{A}$ the cross-sectional area of the meteor.

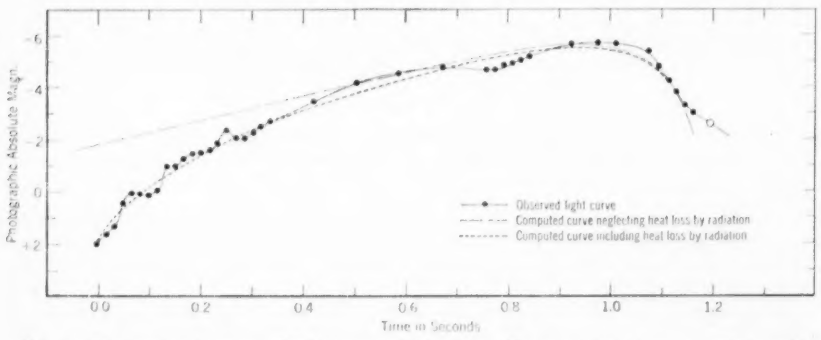


FIG. 1.—Observed and computed light-curves of the meteor. The open circle denotes a diffuse residue traveling beyond the end of the meteor.

The observed results are at hand. First, if the discrepancy is due to neglect of the thermal radiation, then the two terms on the left are equal when the observed curve falls at an intensity one-half the predicted value, or 0.75 mag. fainter. This happens at $t = 0.324$, $H = 104.2$, $\log \rho_a = 0.668 - 10$, $\log V = 6.837$, $\log (\frac{1}{2}\rho_a V^3) = 10.878$. Then

$$5.67 \times 10^{-5} T_1^4 \frac{\mathfrak{S}}{\mathfrak{A}} = 1.89 \times 10^{10}\Lambda\,, \tag{12}$$

where $T_1$ is the absolute temperature at this point. Also

$$\frac{3}{4}\frac{k\Theta_s}{h}\, e^{-\epsilon/kT_1}\left[\epsilon + \tfrac{5}{2}kT_1\right]\left(\frac{\rho_m}{\mu m_A}\right)^{2/3}\frac{\mathfrak{S}}{\mathfrak{A}} = 1.89 \times 10^{10}\Lambda\,. \tag{13}$$

Second, at the beginning of the trail the observed curve is 3.75 mag. fainter than the computed curve, showing that 0.0316 of the energy was used in ablation and 0.9684 in radiation. In this case, $t = 0^s.000$, $H = 114.4$ km, $\log \rho_a = 0.054 - 10$, $\log V = 6.837$, $\log (\frac{1}{2}\rho_a V^3) = 10.264$. Then

$$5.67 \times 10^{-5} T_2^4 \frac{\mathfrak{S}}{\mathfrak{A}} = 8.885 \times 10^9\Lambda\,, \tag{14}$$

$$\frac{3}{4}\frac{k\Theta_s}{h}\, e^{-\epsilon/kT_2}\left[\epsilon + \tfrac{5}{2}kT_2\right]\left(\frac{\rho_m}{\mu m_A}\right)^{2/3}\frac{\mathfrak{S}}{\mathfrak{A}} = 2.902 \times 10^8\Lambda\,, \tag{15}$$

where $T_2$ is the absolute temperature at this point. Dividing equation (12) by equation

(14) and equation (13) by equation (15) gives

$$\left(\frac{T_1}{T_2}\right)^4 = 2.128\,, \tag{16}$$

$$\frac{\epsilon + \frac{5}{2}kT_1}{\epsilon + \frac{5}{2}kT_2} \exp\left\{-\frac{\epsilon}{k}\left(\frac{1}{T_1} - \frac{1}{T_2}\right)\right\} = 65.15\,. \tag{17}$$

By substitution of equation (16) in equation (17) and solution for $\epsilon/kT_1$, we have

$$\frac{\epsilon}{kT_1} = 20.23\,. \tag{18}$$

Now, if $T/T_1$ is given in order to find the fraction of the incoming energy being used to ablate meteoric material together with $\rho_a V^3$, then, by equation (12),

$$\sigma_1 T^4 \frac{\mathfrak{S}}{\mathfrak{A}} = 5.67 \times 10^{-5} T_1^4 \left(\frac{T}{T_1}\right)^4 \frac{\mathfrak{S}}{\mathfrak{A}} = 1.89 \times 10^{10} \Lambda \left(\frac{T}{T_1}\right)^4; \tag{19}$$

and, by equation (13),

$$\frac{3}{4}\frac{k\Theta_s}{h}\, e^{-\epsilon/kT}\left[\epsilon + \tfrac{5}{2}kT\right]\left(\frac{\rho_m}{\mu m_A}\right)^{2/3}\frac{\mathfrak{S}}{\mathfrak{A}}$$

$$= 1.89 \times 10^{10} \Lambda \frac{\epsilon/kT_1 + \frac{5}{2}T/T_1}{\epsilon/kT_1 + \frac{5}{2}} \exp\left\{\frac{\epsilon}{kT_1}\left(1 - \frac{T_1}{T}\right)\right\}. \tag{20}$$

By addition, substitution in equation (11), and solution for $\rho_a V^3$, we obtain

$$\rho_a V^3 = 3.78 \times 10^{10}\left[\left(\frac{T}{T_1}\right)^4 + 10^{8.795(1 - T_1/T)}\,\frac{20.23 + 2.5T/T_1}{22.73}\right]. \tag{21}$$

The first term within the brackets is proportional to the energy loss by radiation, and the second term is proportional to the energy loss by ablation. Therefore, the correction to the predicted intensity by equation (8), expressed in stellar magnitudes, is

$$\Delta M = 2.5 \log \frac{22.73\,(T/T_1)^4 + (20.23 + 2.5T/T_1)\,10^{8.795(1 - T_1/T)}}{(20.23 + 2.5T/T_1)\,10^{8.795(1 - T_1/T)}}. \tag{22}$$

The correction to equation (10) is a correction to an already nearly negligible increment to the integral and thus may be ignored. The corrected curve is exhibited in Figure 1 and is seen to provide a satisfactory fit.

## IV. THE PHYSICAL CONSTANTS

The physical constants available for this meteor will now be discussed in some detail. The observed constants are $\log K = 6.163$, $\log \sigma = -11.80$, $\epsilon/kT_1 = 20.23$. Of the various component constants given in equations (6) and (7), perhaps the most promising for theoretical evaluation is $\zeta$. For vaporization at the reaction-zone temperature,

$$\zeta = \frac{1}{\mu m_A}\left(\epsilon + \tfrac{5}{2}\,kT\right). \tag{23}$$

In general, this will be a slowly varying function of position on the trail, since the second term depends on the local temperature. A suitable mean value of $T/T_1$ will be that at which about half the initial mass has been ablated. This value is $T/T_1 = 1.06$, which

is adopted for finding $\zeta$, which is henceforth regarded as constant, its variation over the trail being small. Then

$$\zeta = \frac{kT_1}{\mu m_A}\left(\frac{\epsilon}{kT_1} + \frac{5}{2}\frac{T}{T_1}\right) = 22.88\,\frac{kT_1}{\mu m_A}, \tag{24}$$

$$\zeta = \frac{1}{\mu m_A}(\epsilon + 2.65kT_1). \tag{25}$$

To evaluate $\epsilon$ and $\mu$, only the four major meteoric constituents *Fe*, *Mg*, *Si*, and *O* will be considered. Using the composition of meteorites according to H. Brown and C. Patterson (1947) quoted by H. E. Suess and J. H. D. Jensen (1952), the relative values given for *Fe*, *Mg*, and *Si* are adopted, and complete oxidation is assumed to get the abundance of *O*, which agrees very closely with the observed value. The adopted composition is then as given in the following table:

| Element | Fraction by No. | Fraction by Wt. | Atomic Wt. |
|---|---|---|---|
| *Fe* | 0.0668 | 0.1692 | 55.84 |
| *Mg* | .1551 | .1710 | 24.32 |
| *Si* | .1743 | .2218 | 28.06 |
| *O* | 0.6038 | 0.4380 | 16.00 |

For the heats of formation the following values (*Handbook of Chemistry and Physics* [1949]) are employed:

| Compound | Heat of Formation E.V. | Heat of Formation Ergs $Gm^{-1}$ |
|---|---|---|
| $Fe_2O_3$ | 19.31 | $1.670\times10^{11}$ |
| $MgO$ | 9.855 | $3.914\times10^{11}$ |
| $SiO_2$ | 15.67 | $5.39\times10^{11}$ |

From these values the following values are obtained for the heat of sublimation and dissociation, $\zeta'$, the activation energy, $\epsilon$, and the mean molecular weight, $\mu$:

$$\zeta' = \frac{\epsilon}{\mu m_A} = 2.148\times10^{11}\ \text{ergs gm}^{-1}, \tag{26}$$

$$\mu = 22.04, \qquad \epsilon = 7.92\times10^{-12}\ \text{ergs}, \tag{27}$$

since $m_A = 1.673\times10^{-24}$ gm. Then, by equations (24) and (25),

$$\zeta = 8.58\times10^{7}T_1 = 2.148\times10^{11} + 9.96\times10^{6}T_1, \tag{28}$$

$$T_1 = 2834\,^{\circ}\text{K},$$

$$\zeta = 2.430\times10^{11}\ \text{ergs gm}^{-1}. \tag{29}$$

Calling upon the observed value of $\sigma$ gives

$$\frac{\Lambda}{\Gamma} = 2\sigma\zeta = 0.770. \tag{30}$$

For $\Lambda/\Gamma \approx 1$, it is to be expected that $\Gamma \approx 1$, whence, by equation (30), $\Lambda \approx 0.77$. Putting this quantity and $T_1$ by equation (28) into equation (12) gives

$$\frac{\mathfrak{S}}{\mathfrak{A}} \approx 4. \tag{31}$$

This is to be compared with a value of 1 for a square-on plate and 2 for a hemisphere. Little emphasis is to be placed on the above value. From the equality of equations (12) and (13) for $T = T_1$, it follows that

$$\frac{3}{4}\frac{k\Theta_s}{h}\left(\frac{\rho_m}{\mu m_A}\right)^{2/3} = 3.112 \times 10^{29}\ \text{cm}^{-2}\ \text{sec}^{-1}. \tag{32}$$

It should be pointed out that reliance upon only about the first digit in all the foregoing numbers is reasonable, i.e.,

$$\epsilon = 8 \times 10^{-12}\ \text{ergs}; \qquad \zeta = 2.4 \times 10^{11}\ \text{ergs gm}^{-1}; \qquad \frac{\Lambda}{\Gamma} = 0.8; \qquad \frac{\mathfrak{S}}{\mathfrak{A}} \approx 4;$$

$$\frac{3}{4}\frac{k\Theta_s}{h}\left(\frac{\rho_m}{\mu m_A}\right)^{2/3} = 3 \times 10^{29}\ \text{cm}^{-2}\ \text{sec}^{-1}.$$

The possibility of ablation by melting may be dealt with briefly. In such a case, $\zeta'$ and $\epsilon$ would be about one-tenth the values in equations (24) and (25), and $T$ would be about 300° K. Then $\Lambda/\Gamma$ would be of the order of 0.1, and $\Lambda$ also of that order, leading to an $\mathfrak{S}/\mathfrak{A}$ of the order of $10^3$. Both this last value and melting at 300° K are absurd, so that vaporization is quite clearly the process dealt with here. The consideration concerning the temperature alone has already been put forward for iron meteors by R. N. Thomas (1952).

## VI. CONCLUSIONS

From the good fit of the computed light-curve to the observed curve, it appears that the reaction-zone theory developed by Cook, Eyring, and Thomas (1951), with the additional inclusion of the radiation term, is adequate. The zone temperature indicated, on the basis of complete vaporization and dissociation on ablation, ranges from 2340° K at the beginning of the trail to about 3600° K at the end. The assumption of ablation by melting leads to absurdly low surface temperatures of about 300° K and to absurdly high ratios of ablating area to cross-section of the order of 1000. Thus vaporization seems reasonably well established as the process occurring in the ablation of very bright meteors in the absence of flares.

The author's thanks are due to Dr. Richard N. Thomas for suggesting this investigation and to Dr. Luigi G. Jacchia and the staff of the Meteor Analysis Project for computation of the original light-curve and supplying of the observational data.

## REFERENCES

Brown, H., and Patterson, C. 1947, *J. Geol.*, **55**, 405.
Cook, M. A.; Eyring, H.; and Thomas, R. N. 1951, *Ap. J.*, **113**, 475.
*Handbook of Chemistry and Physics* (31st ed.; Cleveland, Ohio: Chemical Rubber Publishing Co., 1949), pp. 1505–1514.
Jacchia, L. G. 1948, Harvard College Observatory and Center of Analysis, Massachusetts Institute of Technology, *Technical Report No. 2* (Harvard Reprint, Ser. II, No. 26).
Jacchia, L. G. 1954, private communication.
Rocket Panel, The, 1952, *Phys. Rev.*, **88**, 1027.
Suess, H. E., and Jensen, J. H. D. 1952, *Landolt-Börnstein, Zahlenwerte und Funktionen*, Vol. **3**: *Astronomie und Geophysik* (6th ed.; Berlin, Göttingen, and Heidelberg: Springer-Verlag), p. 53.
Thomas, R. N. 1952, *Ap. J.*, **116**, 203.

# RADIATIVE EQUILIBRIUM IN A HYDROGEN ATMOSPHERE. I*

ALLAN F. COOK
Princeton University Observatory†

*Received January 13, 1954; revised July 19, 1954*

ABSTRACT

The optical properties of neutral hydrogen atoms are discussed, the Gaunt factors being taken into account. Absorption cross-sections per atom in the second quantum level at the short-wave-length side of the Balmer limit are evaluated. The ratio of the absorption cross-section at a specific wave length to that at the short-wave-length side of the Balmer limit is tabulated for a number of wave lengths and temperatures. The Rosseland mean opacity coefficient is calculated, and an integral occurring in the equation of radiative equilibrium is tabulated.

## I. INTRODUCTION

A new method has been developed for computing the temperature distribution in a hydrogen atmosphere in radiative equilibrium. The purpose of the present paper is the preparation of tables necessary for the application of the method. The method itself will be presented in a second paper.

A brief outline of the equations in which the optical properties of neutral hydrogen play a role is in order. The first of these is the definition of the monochromatic optical depth,

$$\tau_\nu = \int_z^\infty \kappa_\nu \rho \, dz \,, \tag{1}$$

where $z$ is the elevation in a stellar atmosphere assumed to be stratified in plane-parallel layers; $\kappa_\nu$ is the mass absorption coefficient at the frequency $\nu$; and $\rho$ is the density.

Another relation is the equation of radiative equilibrium or equation of continuity for radiation. Let $I_\nu$ denote the monochromatic intensity; the monochromatic mean intensity, $J_\nu$, is then defined as the average of $I_\nu$ over all solid angles. The Planck intensity or the monochromatic intensity of cavity radiation at a particular temperature $T$ is represented by $B_\nu$. If it is assumed that a state of local thermodynamic equilibrium exists (the validity of Kirchhoff's law), then the equation of radiative equilibrium takes the form

$$\int_0^\infty \kappa_\nu J_\nu d\nu = \int_0^\infty \kappa_\nu B_\nu d\nu \,. \tag{2}$$

Owing to the very pronounced jump in $\kappa_\nu$ at the Lyman limit, it will develop that in the practical application of this equation the approximation may always be made that $J_\nu \approx B_\nu$ at all temperatures at which significant contributions occur to the two integrals in equation (2) beyond the Lyman limit. The accuracy of this approximation will be discussed further in the next paper. Thus subtraction of these equal contributions from both sides leaves integrals which terminate at $\nu_L$, the frequency at the Lyman limit.

In an atmosphere in which only neutral hydrogen atoms play a role in radiative transfer it will prove convenient to use $\tau_{Ba,\nu}$, the optical depth at the short-wave-length side of the Balmer limit, as an independent variable instead of the height in the atmosphere $z$. Differentiation of equation (1) at any frequency and at the standard frequency, fol-

* This paper is based on a thesis submitted in partial fulfilment of the requirements for the degree of Doctor of Philosophy at Princeton University.

† Now at Harvard College Observatory.

lowed by formation of the ratio of the two results and subsequent integration, gives

$$\tau_\nu = \int_0^{\tau_{Ba,\,s}} \frac{\kappa_\nu}{\kappa_{Ba,\,s}}\, d\tau_{Ba,\,s}\,, \tag{3}$$

where $\kappa_{Ba,s}$ is the mass absorption coefficient at the short-wave-length side of the Balmer limit. The corresponding form of the equation of radiative equilibrium (2) with upper limit $\nu_L$ is obtained by division by $\kappa_{Ba,s}$:

$$\int_0^{\nu_L} \frac{\kappa_\nu}{\kappa_{Ba,\,s}} J_\nu d\nu = \int_0^{\nu_L} \frac{\kappa_\nu}{\kappa_{Ba,\,s}} B_\nu d\nu\,. \tag{4}$$

The quantity $\kappa_\nu/\kappa_{Ba,s}$ and the integral on the right-hand side of equation (4) are two optical properties which will receive special attention below.

A third optical property of importance may be introduced by considering the equation of radiative transfer for the case of pure absorption,

$$\cos\theta \frac{dI_\nu}{\rho dz} = -\kappa_\nu (I_\nu - B_\nu)\,, \tag{5}$$

where $\theta$ is the angle between the outward normal to the plane of stratification and the direction of travel of the pencil of radiation considered. Implicit in the expression are the two assumptions of plane-parallel stratification and local thermodynamic equilibrium. At optical depths sufficiently great that it is permissible to put $J_\nu \approx B_\nu$ over a sufficiently large range of frequency, then also $J \approx B$, where $I$, $J$, and $B$ represent, as usual, the integrals of $I_\nu$, $J_\nu$, and $B_\nu$ over the frequency. Hence, if equation (5) is divided by $\kappa_\nu$ and integrated over the frequency, we get

$$-\cos\theta \int_0^\infty \frac{dI_\nu}{\kappa_\nu \rho dz}\, d\nu = I - J\,. \tag{6}$$

The *opacity coefficient* $\bar{\kappa}$ was defined by Eddington by

$$\int_0^\infty \frac{dI_\nu}{\kappa_\nu \rho dz}\, d\nu = \frac{dI}{\bar{\kappa}\rho dz}\,. \tag{7}$$

At a sufficiently great depth $I_\nu \approx J_\nu$ may be assumed, whence $I \approx J$ by integration over all $\nu$, and the previous assumption $J_\nu \approx B_\nu$ gives $I \approx B$. Equation (7) may then be transformed by replacing derivatives of $B_\nu$ and $B$ with respect to $z$ by the products of their derivatives with respect to $T$ and the derivatives of $T$ with respect to $z$, whence the *Rosseland mean opacity coefficient* is obtained:

$$\bar{\kappa}_R = \frac{dB/dT}{\int_0^\infty (dB_\nu/\kappa_\nu dT)\, d\nu}\,. \tag{8}$$

As is well known, when these assumptions are all valid, it is very convenient to work with the total radiation, using the equation of radiative transfer found by substitution of equation (7) in equation (6). Thus the tabulation of $\bar{\kappa}_R$ is useful. In the present case, in which $\kappa_{Ba,s}$ is the independent variable, the convenient form of this equation is found by division by $\kappa_{Ba,s}$, differentiation of equation (1) for the short-wave-length side of the Balmer limit, and subsitution of the latter result on the left side of the former equation; whence

$$\cos\theta \frac{dI}{d\tau_{Ba,\,s}} = \frac{\bar{\kappa}}{\kappa_{Ba,\,s}} (I - J)\,. \tag{9}$$

Thus particular attention will be directed to the quantity $\bar{\kappa}_R/\kappa_{Ba,s}$, along with the quantity $\kappa_\nu/\kappa_{Ba,s}$ and the integral on the right-hand side of equation (4).

## II. RATIO OF MONOCHROMATIC ABSORPTION COEFFICIENT TO THAT AT SHORT-WAVE-LENGTH SIDE OF BALMER LIMIT

Attention must initially be directed to the monochromatic absorption. Let $h$ denote Planck's constant, $k$ Boltzmann's constant, $m$ the electronic mass, $\epsilon$ the electronic charge, $c$ the velocity of light, $m_H$ the mass of the neutral hydrogen atom, and $g$ the Gaunt factors. Then Kramers' absorption law, including the Gaunt factors for the bound-free transitions from the first four quantum levels and the effect of induced emission, is (Unsöld 1938*b*)

$$u = \frac{h\nu}{kT}, \tag{10}$$

$$F = \frac{64\pi^4}{3^{3/2}} \frac{m\epsilon^{10}}{ch^3 m_H k^3} \frac{e^{-u_1}}{T^3}, \tag{11}$$

$$\kappa_\nu = F \frac{1}{u^3} \left( \sum_{u_n < u}^{u_5} g_n \frac{e^{u_n}}{n^3} + \frac{e^{u_{5.5}}}{2u_1} \right) (1 - e^{-u}) \qquad (u > u_5), \tag{12}$$

$$\kappa_\nu = F \frac{1}{u^3} \frac{e^{u_{n-0.5}}}{2u_1} (1 - e^{-u}) \qquad (u_{n-1} > u > u_n ; \; n \geqslant 5), \tag{13}$$

where the subscripts denote the absorption edges from the states with the corresponding principal quantum number.[1] The Gaunt factors are given by

$$g_1 = 8\pi^{1/2} \frac{\kappa^2 \exp(-4\kappa \arctan \kappa^{-1})}{(\kappa^2+1)(1-e^{-2\pi\kappa})}, \tag{14}$$

$$g_2 = 32\pi 3^{1/2} \frac{\kappa^2 \exp(-4\kappa \arctan 2\kappa^{-1})}{(\kappa^2+4)^3 (1-e^{-2\pi\kappa})} (3\kappa^2+4)(5\kappa^2+4), \tag{15}$$

$$g_3 = 72\pi 3^{1/2} \frac{\kappa^2 \exp(-4\kappa \arctan 3\kappa^{-1})}{(\kappa^2+9)^5 (1-e^{-2\pi\kappa})} \times (13\kappa^4+78\kappa^2+81)(29\kappa^4+126\kappa^2+81), \tag{16}$$

$$g_4 = 128\pi 3^{1/2} \frac{\kappa^2 \exp(-4\kappa \arctan 4\kappa^{-1})}{9(\kappa^2+16)^7 (1-e^{-2\pi\kappa})} (197\kappa^6+3152\kappa^4+13056\kappa^2 + 12288)(539\kappa^6+6800\kappa^4+20736\kappa^2+12288), \tag{17}$$

where $\kappa$ is related to the frequency by

$$h\nu = \chi_1 \left( \frac{1}{n^2} + \frac{1}{\kappa^2} \right) \tag{18}$$

and where $\chi_1$ is the ionization potential of hydrogen from the ground state. Equations (14), (15), (16), and (17) may be written down from analytical expressions given by Menzel and Pekeris (1935). The neglect of the Gaunt factors for the states with principal quantum number greater than 5 and for the free-free transitions is justified by their

[1] It should be noted that Unsöld (1938*a*) uses the integral value of $n$ for the limit in approximating the sum in eq. (12) above over all terms with $n \geqslant 5$, when, in fact, the half-integral value, or 4.5, should be used for the limit in his eq. (34, 10). The same consideration governs in eq. (13) above.

closeness to unity and the relative unimportance of these transitions in establishing radiative equilibrium.

The units involved in expressions (10), (11), (12), (13), (14), (15), (16), (17), and (18) are $\text{sec}^{-1}$ for frequency; gm for mass; e.s.u. for charge; cm $\text{sec}^{-1}$ for the velocity of light; erg sec for Planck's constant; erg $\text{deg}^{-1}$ for Boltzmann's constant; $\text{cm}^2$ $\text{gm}^{-1}$ for the mass absorption coefficient, $\kappa_\nu$; ergs for ionization potentials; and degrees for temperature. For practical calculations it will be more convenient to use electron volts for frequency and ionization potentials whence a new variable is required to replace the temperature. It should be noted that equation (18) may be replaced by

$$\chi = \chi_1 \left( \frac{1}{n^2} + \frac{1}{\kappa^2} \right), \tag{19}$$

where $\chi$ is the energy of radiation in electron volts corresponding to the frequency $\nu$. Then equations (14), (15), (16), and (17) may be used to compute the Gaunt factors. For the new variable to replace the temperature, it should be recalled that powers of 10 are appropriate for use with energies in electron volts rather than powers of $e$ used with ergs; hence the well-known relation

$$e^{h\nu/\kappa T} = 10^{\chi\theta}; \qquad \theta = \frac{5040}{T}, \tag{20}$$

may be written down. For $\lambda$ the wave length in angstroms rather than in centimeters,

$$\lambda_n = 911.8 n^2 . \tag{21}$$

To obtain the cross-section per neutral hydrogen atom, $\kappa_\nu$ must be multiplied by $m_H$. To obtain $a_\nu$, the cross-section per neutral hydrogen atom in the second quantum level, it is necessary to divide by the Boltzmann factor,

$$\frac{n_2}{n_1} = \frac{\varpi_2}{\varpi_1} e^{-E_2/\kappa T} = 4 \times 10^{-(\chi_1 - \chi_2)\theta} = 4 \times 10^{-(\chi_1 - 1/4\chi_1)\theta} = 4.10^{-10.20\theta},$$

where $E_2$ is the excitation potential of the second quantum level and $\varpi_1$ and $\varpi_2$ are the statistical weights of the first and second quantum levels. Substitution of equations (10), (11), and (20) in (12) and (13), while it is remembered that $\nu = c/\lambda$, $\chi_1 = 13.60$ e.v., $\chi_n = \chi_1/n^2$, conversion of $\lambda$ to angstroms, division by the Boltzmann factor, multiplication by $m_H$, and insertion of all the numerical constants give

$$a_\nu = 2.612 \times 10^{-27} \lambda^3 \left( \sum_{\chi_n < \chi}^{n=4} g_n n^2 \times 10^{-(3.399 - 13.60/n^2)\theta} + 0.01597\, \theta^{-1} \times 10^{-2.728\theta} \right) (1 - 10^{-\chi\theta}) \qquad (\lambda < \lambda_0), \tag{22}$$

$$a_\nu = 2.612 \times 10^{-27} \lambda^3 \times 0.01597\, \theta^{-1} \times 10^{-2.728\theta} (1 - 10^{-\chi\theta}) \qquad (\lambda_{n-1} < \lambda < \lambda_n;\ n \geq 5). \tag{23}$$

The quantity (22) is tabulated in Table 1 for the short-wave-length side of the Balmer limit for the range $0.50 \geq \theta \geq 0.10$. Expression in terms of an atom in the second quantum level reduces the exponents involved and facilitates interpolation. If $\kappa_{Ba,s}$, the absorption coefficient per gram of neutral hydrogen, is desired, the Boltzmann factor is merely applied, followed by division by the mass of the hydrogen atom; whence

$$\kappa_{Ba,s} = \frac{4 \times 10^{-(\chi_1 - 1/4\chi_1)\theta}}{m_H} a_{Ba,s} = 2.391 \times 10^{24 - 10.20\theta} a_{Ba,s}. \tag{24}$$

Quantities (22) and (23) are next computed for various standard frequencies. These frequencies are chosen for use in forming integrals over frequency by means of Cotes's formula,

$$\int_a^b f(x)\,dx = \tfrac{1}{90}(b-a)\left[7f(a)+32f\left(a+\frac{b-a}{4}\right)+12f\left(a+\frac{b-a}{2}\right)\right.$$
$$\left.+32f\left(a+\frac{3(b-a)}{4}\right)+7f(b)\right]. \tag{25}$$

They must therefore be five equidistant frequencies over the chosen range of integration. These ranges are as follows: first, from the Lyman limit to a frequency midway between

TABLE 1

ABSORPTION CROSS-SECTION PER NEUTRAL HYDROGEN ATOM IN SECOND QUANTUM LEVEL, FOR RADIATION AT SHORT-WAVE-LENGTH SIDE OF BALMER LIMIT

| $\theta$ | $a_{\nu Ba,\,s}$ cm$^2$ | $\theta$ | $a_{\nu Ba,\,s}$ cm$^2$ | $\theta$ | $a_{\nu Ba,\,s}$ cm$^2$ | $\theta$ | $a_{\nu Ba,\,s}$ cm$^2$ |
|---|---|---|---|---|---|---|---|
| 0.50 | $1.440\cdot10^{-17}$ | 0.38 | $1.469\cdot10^{-17}$ | 0.28 | $1.502\cdot10^{-17}$ | 0.18 | $1.538\cdot10^{-17}$ |
| .48 | $1.444\cdot10^{-17}$ | .36 | $1.475\cdot10^{-17}$ | .26 | $1.509\cdot10^{-17}$ | .16 | $1.545\cdot10^{-17}$ |
| .46 | $1.449\cdot10^{-17}$ | .34 | $1.481\cdot10^{-17}$ | .24 | $1.516\cdot10^{-17}$ | .14 | $1.552\cdot10^{-17}$ |
| .44 | $1.453\cdot10^{-17}$ | .32 | $1.488\cdot10^{-17}$ | .22 | $1.523\cdot10^{-17}$ | .12 | $1.559\cdot10^{-17}$ |
| .42 | $1.458\cdot10^{-17}$ | 0.30 | $1.495\cdot10^{-17}$ | 0.20 | $1.531\cdot10^{-17}$ | 0.10 | $1.565\cdot10^{-17}$ |
| 0.40 | $1.464\cdot10^{-17}$ | | | | | | |

the Lyman and Balmer limits; second, from the latter point to the Balmer limit; third, over the Paschen continuum; fourth, over the Brackett continuum; fifth, from the Brackett limit to zero frequency. From equation (22) or equation (23) for each frequency and $a_{Ba,\,s}$ the ratios

$$\frac{\kappa_\nu}{\kappa_{Ba,\,s}} = \frac{a_\nu}{a_{Ba,\,s}} \tag{26}$$

are formed. Table 2 gives these quantities as functions of $\lambda$ and $\theta$, covering the same range of $\theta$ as Table 1.

### III. INTEGRAL OCCURRING IN EQUATION OF RADIATIVE EQUILIBRIUM

The integral on the right-hand side of the equation of radiative equilibrium (4) may be dealt with by a number of expedients. Planck's law may be transformed by equation (10) from its usual form to

$$B_\nu = \frac{2k^3T^3}{h^2c^2}\,\frac{u^3e^{-u}}{1-e^{-u}}. \tag{27}$$

Differentiation of equation (10) gives

$$d\nu = \frac{kT}{h}\,du\,; \tag{28}$$

whence, by multiplication of equations (27) and (28) and then by (12), we obtain

$$G = F\,\frac{2k^4T^4}{h^3c^2}, \tag{29}$$

$$\kappa_\nu B_\nu d\nu = G\left(\sum_{u_n<u}^{u_4}\frac{e^{u_n}}{n^3}+\frac{e^{u_{4,\,s}}}{2u_4}\right)e^{-u}du + G\left[\sum_{u_n<u}^{u_4}(g_n-1)\,\frac{e^{u_n}}{n^3}\right]e^{-u}du \qquad (u>u_5)\,. \tag{30}$$

## TABLE 2

### Ratio of Absorption Coefficient of Neutral Hydrogen to That at Short-Wave-Length Side of Balmer Limit

| | | | λ | | |
|---|---|---|---|---|---|
| θ | 912 A | 1006 A | 1122 A | 1269 A | 1459 A |
| 0.50 | 0.01879 | 0.02506 | 0.03451 | 0.04944 | 0.07424 |
| .48 | .01884 | .02513 | .03461 | .04960 | .07445 |
| .46 | .01890 | .02522 | .03473 | .04977 | .07471 |
| .44 | .01898 | .02532 | .03487 | .04996 | .07502 |
| .42 | .01907 | .02544 | .03503 | .05019 | .07538 |
| .40 | .01918 | .02558 | .03522 | .05048 | .07580 |
| .38 | .01931 | .02574 | .03546 | .05082 | .07629 |
| .36 | .01946 | .02594 | .03575 | .05122 | .07688 |
| .34 | .01964 | .02618 | .03608 | .05170 | .07758 |
| 0.32 | 0.01985 | 0.02647 | 0.03647 | 0.05226 | 0.07841 |

| | | | λ | | |
|---|---|---|---|---|---|
| θ | 912 A | 1006 A | 1122 A | 1269 A | 1459 A |
| 0.30 | 0.02010 | 0.02682 | 0.03694 | 0.05293 | 0.07939 |
| .28 | .02041 | .02724 | .03752 | .05374 | .08056 |
| .26 | .02080 | .02775 | .03822 | .05472 | .08197 |
| .24 | .02127 | .02837 | .03907 | .05591 | .08365 |
| .22 | .02185 | .02913 | .04010 | .05734 | .08565 |
| .20 | .02257 | .03007 | .04136 | .05907 | .08805 |
| .18 | .02347 | .03125 | .04292 | .06118 | .09093 |
| .16 | .02460 | .03273 | .04485 | .06375 | .09437 |
| .14 | .02605 | .03459 | .04725 | .06688 | .09845 |
| .12 | .02792 | .03693 | .05023 | .07069 | .1033 |
| 0.10 | 0.03036 | 0.03996 | 0.05400 | 0.07540 | 0.1091 |

| | | | λ | | |
|---|---|---|---|---|---|
| θ | 1716 A | 2084 A | 2652 A | 3647 A *I* | 4235 A |
| 0.50 | 0.1187 | 0.2079 | 0.4127 | 0.05619 | 0.08590 |
| .48 | .1190 | .2085 | .4136 | .06223 | .09501 |
| .46 | .1194 | .2092 | .4147 | .06896 | .1051 |
| .44 | .1199 | .2100 | .4159 | .07646 | .1164 |
| .42 | .1205 | .2109 | .4172 | .08484 | .1289 |
| .40 | .1212 | .2119 | .4187 | .09419 | .1428 |
| .38 | .1219 | .2131 | .4204 | .1047 | .1583 |
| .36 | .1228 | .2145 | .4224 | .1165 | .1756 |
| .34 | .1239 | .2162 | .4245 | .1297 | .1950 |
| .32 | .1252 | .2181 | .4268 | .1446 | .2166 |
| 0.30 | 0.1267 | 0.2203 | 0.4295 | 0.1614 | 0.2408 |

| | | | λ | | |
|---|---|---|---|---|---|
| θ | 1716 A | 2084 A | 2652 A | 3647 A *I* | 4235 A |
| 0.28 | 0.1284 | 0.2228 | 0.4326 | 0.1803 | 0.2680 |
| .26 | .1305 | .2257 | .4361 | .2017 | .2985 |
| .24 | .1329 | .2291 | .4401 | .2259 | .3328 |
| .22 | .1357 | .2330 | .4444 | .2533 | .3714 |
| .20 | .1390 | .2374 | .4493 | .2844 | .4148 |
| .18 | .1429 | .2424 | .4548 | .3199 | .4638 |
| .16 | .1474 | .2480 | .4608 | .3604 | .5192 |
| .14 | .1527 | .2544 | .4673 | .4067 | .5821 |
| .12 | .1588 | .2617 | .4743 | .4597 | .6536 |
| 0.10 | 0.1659 | 0.2700 | 0.4820 | 0.5206 | 0.7348 |

| | | | λ | | |
|---|---|---|---|---|---|
| θ | 5050 A | 6250 A | 8206 A *S* | 8206 A *I* | 9214 A |
| 0.50 | 0.1400 | 0.2490 | 0.5033 | 0.1844 | 0.2485 |
| .48 | .1544 | .2738 | 0.5515 | .2100 | .2823 |
| .46 | .1704 | .3011 | 0.6041 | .2391 | .3207 |
| .44 | .1881 | .3313 | 0.6617 | .2723 | .3645 |
| .42 | .2078 | .3646 | 0.7247 | .3101 | .4143 |
| .40 | .2296 | .4013 | 0.7937 | .3531 | .4709 |
| .38 | .2537 | .4417 | 0.8693 | .4022 | .5353 |
| .36 | .2805 | .4862 | 0.9519 | .4581 | .6085 |
| .34 | .3102 | .5353 | 1.043 | .5218 | .6917 |
| .32 | .3433 | .5895 | 1.142 | .5945 | .7863 |
| 0.30 | 0.3801 | 0.6494 | 1.251 | 0.6775 | 0.8936 |

TABLE 2—*Continued*

| | λ | | | | |
|---|---|---|---|---|---|
| θ | 5050 A | 6250 A | 8206 A *s* | 8206 A *l* | 9214 A |
| 0.28 | 0.4211 | 0.7155 | 1.370 | 0.7723 | 1.016 |
| .26 | 0.4668 | 0.7885 | 1.501 | 0.8807 | 1.156 |
| .24 | 0.5177 | 0.8694 | 1.645 | 1.005 | 1.316 |
| .22 | 0.5745 | 0.9593 | 1.802 | 1.146 | 1.497 |
| .20 | 0.6380 | 1.058 | 1.975 | 1.308 | 1.703 |
| .18 | 0.7092 | 1.168 | 2.165 | 1.494 | 1.938 |
| .16 | 0.7889 | 1.290 | 2.374 | 1.706 | 2.207 |
| .14 | 0.8782 | 1.426 | 2.604 | 1.949 | 2.515 |
| .12 | 0.9782 | 1.577 | 2.858 | 2.228 | 2.867 |
| 0.10 | 1.091 | 1.746 | 3.139 | 2.550 | 3.270 |

| | λ | | | |
|---|---|---|---|---|
| θ | 10503 A | 12213 A | 14588 A *s* | 14588 A *l* |
| 0.50 | 0.3453 | 0.5010 | 0.7688 | 0.4944 |
| .48 | 0.3918 | 0.5671 | 0.8670 | 0.5680 |
| .46 | 0.4444 | 0.6420 | 0.9779 | 0.6526 |
| .44 | 0.5039 | 0.7268 | 1.104 | 0.7497 |
| .42 | 0.5713 | 0.8224 | 1.247 | 0.8608 |
| .40 | 0.6477 | 0.9296 | 1.407 | 0.9877 |
| .38 | 0.7345 | 1.052 | 1.587 | 1.134 |
| .36 | 0.8332 | 1.190 | 1.791 | 1.302 |
| .34 | 0.9453 | 1.346 | 2.021 | 1.495 |
| .32 | 1.072 | 1.522 | 2.280 | 1.716 |
| 0.30 | 1.215 | 1.721 | 2.572 | 1.970 |

| | λ | | | |
|---|---|---|---|---|
| θ | 10503 A | 12213 A | 14588 A *s* | 14588 A *l* |
| 0.28 | 1.378 | 1.947 | 2.901 | 2.261 |
| .26 | 1.563 | 2.203 | 3.272 | 2.596 |
| .24 | 1.774 | 2.492 | 3.691 | 2.980 |
| .22 | 2.013 | 2.819 | 4.163 | 3.421 |
| .20 | 2.283 | 3.189 | 4.696 | 3.928 |
| .18 | 2.590 | 3.609 | 5.299 | 4.513 |
| .16 | 2.941 | 4.085 | 5.983 | 5.186 |
| .14 | 3.341 | 4.626 | 6.757 | 5.960 |
| .12 | 3.797 | 5.241 | 7.633 | 6.851 |
| 0.10 | 4.318 | 5.941 | 8.626 | 7.879 |

| | λ | | |
|---|---|---|---|
| θ | 19450 A | 29176 A | 58353 A |
| 0.50 | 0.9757 | 1.900 | 6.490 |
| .48 | 1.117 | 2.187 | 7.528 |
| .46 | 1.278 | 2.519 | 8.723 |
| .44 | 1.463 | 2.901 | 10.12 |
| .42 | 1.674 | 3.340 | 11.72 |
| .40 | 1.915 | 3.844 | 13.57 |
| .38 | 2.190 | 4.423 | 15.72 |
| .36 | 2.504 | 5.088 | 18.20 |
| .34 | 2.864 | 5.853 | 21.08 |
| .32 | 3.275 | 6.733 | 24.40 |
| 0.30 | 3.744 | 7.745 | 28.24 |

| | λ | | |
|---|---|---|---|
| θ | 19450 A | 29176 A | 58353 A |
| 0.28 | 4.280 | 8.908 | 32.68 |
| .26 | 4.893 | 10.25 | 37.83 |
| .24 | 5.594 | 11.79 | 43.77 |
| .22 | 6.396 | 13.55 | 50.67 |
| .20 | 7.315 | 15.58 | 58.64 |
| .18 | 8.368 | 17.91 | 67.86 |
| .16 | 9.573 | 20.60 | 78.51 |
| .14 | 10.94 | 23.71 | 90.85 |
| .12 | 12.52 | 27.29 | 105.2 |
| 0.10 | 14.35 | 31.42 | 122.0 |

58353 A is the absorption edge for the quantum level $n = 8$. The values tabulated above are the means of the shortward and longward ratios.

Repetition of the process, except that equation (13) is used instead of equation (12), gives

$$\kappa_\nu B_\nu d\nu = G\,\frac{e^{-(u-u_{n-0.5})}}{2u_1}\,du \qquad (u_{n-1} < u < u_n;\ n \geq 5)\,. \tag{31}$$

A digression is in order to note that in deriving equations (12) and (13) Unsöld (1938*a*) replaces a sum over $n > 4$ by an integral and also includes an integral over the free states:

$$\frac{e^{u_{n-0.5}}}{2u_1} \approx e^{u_1}\sum_{m=n}^{\infty}\frac{1}{m^3}\,e^{-(u_1-u_m)} - \frac{1}{2u_1}\int_0^{-\infty} e^{u_m}du_m = \sum_{m=n}^{\infty}\frac{e^{u_m}}{m^3} + \frac{1}{2u_1}, \tag{32}$$

where the second term is the contribution of the free-free transitions. It is more convenient to invert this process here and return to the use of the full sum. By substitution of (32) in (30) and (31) and integration to the Lyman limit, the following result is obtained:

$$\int_0^{\nu_L}\kappa_\nu B_\nu d\nu = G\Big[\sum_{n=2}^{\infty}\frac{1}{n^3}(1 - e^{-[u_1-u_n]}) + \frac{1}{2u_1}(1 - e^{-u_1})\Big] + G\sum_{n=2}^{4}\frac{e^{u_n}}{n^3}\int_{u_n}^{u_1}(g_n - 1)\,e^{-u}du\,. \tag{33}$$

The expression within the brackets may be written,

$$\sum_{n=2}^{\infty}\frac{1}{n^3} - e^{-u_1}\sum_{n=2}^{4}\frac{e^{u_n}}{n^3} + \frac{1-e^{-u_1}}{2u_1} - \sum_{n=5}^{\infty}\frac{1}{n^3}\,e^{-(u_1-u_n)}\,;$$

and approximation of the last sum by an integral gives

$$\sum_{n=5}^{\infty}\frac{1}{n^3}\,e^{-(u_1-u_n)} \approx -\frac{e^{-u_1}}{2u_1}\int_{u_{4.5}}^{0} e^{u_n}du_n = \frac{e^{-u_1}}{2u_1}(e^{u_{4.5}} - 1)\,,$$

where use has been made of the relations

$$u_n = \frac{u_1}{n^2}, \qquad d\left(\frac{1}{n^2}\right) = -\frac{2}{n^3}\,dn\,.$$

Equation (33) may thus be written in the form

$$\int_0^{\nu_L}\kappa_\nu B_\nu d\nu = G\Big[0.202 + \frac{1}{2u_1} - e^{-u_1}\Big(\sum_{n=2}^{4}\frac{e^{u_n}}{n^3} + \frac{e^{u_{4.5}}}{2u_1}\Big)\Big] + G\sum_{n=2}^{4}\frac{e^{u_n}}{n^3}\int_{u_n}^{u_1}(g_n - 1)\,e^{-u}du \tag{34}$$

There remains the problem of evaluation of the integrals on the right-hand side of equation (34). To this end Cotes's formula (25) is employed.

To put equation (34) into a form for practical calculations, it must first be recalled that the quantity desired is

$$\int_0^{\nu_L}\frac{\kappa_\nu}{\kappa_{Ba,\,s}}B_\nu d\nu = \frac{1}{\kappa_{Ba,\,s}}\int_0^{\nu_L}\kappa_\nu B_\nu d\nu = \frac{1}{a_{Ba,\,s}}\int_0^{\nu_L}a_\nu B_\nu d\nu \tag{35}$$

and that

$$a_\nu = m_H \frac{\varpi_1}{\varpi_2} e^{u_1 - u_2} \kappa_\nu ;$$

whence employment of $\varpi_1 = 1$ and $\varpi_2 = 4$ gives

$$\int_0^{\nu L} a_\nu B_\nu d\nu = \frac{m_H}{4} e^{u_1 - u_2} \int_0^{\nu L} \kappa_\nu B_\nu d\nu .$$

Substitution of equation (34) in this expression, subsequent substitution in equation (35), evaluation of the constant, and conversion from powers of $e$ to powers of 10 give

$$\int_0^{\nu L} \frac{\kappa_\nu}{\kappa_{Ba,\,s}} B_\nu d\nu = 2.162 \times 10^{-8} \frac{T}{a_{Ba,\,s}} \times 10^{-3.399\theta} \Big\{ \Big[ 0.202 + 0.01597\,\theta^{-1} - 10^{-10.20\theta} \Big( \sum_{n=2}^{4} n^{-3} \times 10^{-[3.399 - 13.60/n^2]\theta} + 0.01597\,\theta^{-1} \times 10^{-2.728\theta} \Big) \Big] + \sum_{n=2}^{4} n^{-3} \times 10^{(13.60/n^2)\theta} \int_{u_n}^{u_1} (g_n - 1)\, e^{-u} du \Big\} . \tag{36}$$

The integrals appearing in the second sum of equation (36) must now be considered. Here it is convenient to use powers of 10 when exponents are involved, but otherwise to use the quantity $u$. Recourse is had to equation (20) and $\chi_n = \chi_1/n^2$, whence

$$\begin{aligned} \int_{u_2}^{u_1} (g_2 - 1)\, e^{-u} du &= \int_{7.826\theta}^{31.31\theta} (g_2 - 1)\, 10^{-x\theta} dx , \\ \int_{u_3}^{u_1} (g_3 - 1)\, e^{-u} du &= \int_{3.478\theta}^{31.31\theta} (g_3 - 1)\, 10^{-x\theta} dx , \\ \int_{u_4}^{u_1} (g_4 - 1)\, e^{-u} du &= \int_{1.957\theta}^{31.31\theta} (g_4 - 1)\, 10^{-x\theta} dx . \end{aligned} \tag{37}$$

The integrals are to be evaluated by Cotes's formula (25), using the intervals described in the discussion of its application. Table 3 gives the integral (36) as a function of $\theta$ for the range $0.50 \geq \theta \geq 0.22$.

TABLE 3

INTEGRAL OCCURRING IN EQUATION OF RADIATIVE EQUILIBRIUM

| $\theta$ | $\int_0^{\nu L} B_\nu d\nu \kappa_\nu / \kappa_{Ba,\,s}$ | $\theta$ | $\int_0^{\nu L} B_\nu d\nu \kappa_\nu / \kappa_{Ba,\,s}$ | $\theta$ | $\int_0^{\nu L} B_\nu d\nu \kappa_\nu / \kappa_{Ba,\,s}$ |
|---|---|---|---|---|---|
| | erg cm$^{-2}$ sec$^{-1}$ | | erg cm$^{-2}$ sec$^{-1}$ | | erg cm$^{-2}$ sec$^{-1}$ |
| 0.50 | $6.438 \cdot 10^{10}$ | 0.40 | $1.811 \cdot 10^{11}$ | 0.30 | $5.537 \cdot 10^{11}$ |
| .48 | $7.878 \cdot 10^{10}$ | .38 | $2.245 \cdot 10^{11}$ | .28 | $7.025 \cdot 10^{11}$ |
| .46 | $9.667 \cdot 10^{10}$ | .36 | $2.796 \cdot 10^{11}$ | .26 | $8.991 \cdot 10^{11}$ |
| .44 | $1.189 \cdot 10^{11}$ | .34 | $3.495 \cdot 10^{11}$ | .24 | $1.160 \cdot 10^{12}$ |
| 0.42 | $1.466 \cdot 10^{11}$ | 0.32 | $4.388 \cdot 10^{11}$ | 0.22 | $1.513 \cdot 10^{12}$ |

## IV. ROSSELAND MEAN OPACITY COEFFICIENT

The Rosseland mean (8) is also more conveniently evaluated in terms of $\theta$ and $\chi$ than in terms of $T$ and $\nu$. Furthermore, what is really desired is the ratio $\bar{\kappa}_R / \kappa_{Ba,\,s}$. It may

easily be shown that the Planck intensity per electron volt is

$$B_\chi = 5.028 \times 10^{10} \chi^3 \frac{10^{-\chi\theta}}{1 - 10^{-\chi\theta}}. \tag{38}$$

The Stefan-Boltzmann law is

$$B = \frac{\sigma}{\pi} T^4 = 1.805 \times 10^{-5} T^4 = \frac{1.165 \times 10^{10}}{\theta^4}, \tag{39}$$

where use is made of equation (20). Substitution of $dT$ by equation (20) and equations (38) and (39) in equation (8), together with the expression of the integral over $\chi$ rather than $\nu$, and division of $\kappa_{Ba,\,s}$ give

$$\frac{\bar{\kappa}_R}{\kappa_{Ba,\,s}} = \frac{dB/d\theta}{\int_0^\infty (\kappa_{Ba,\,s}/\kappa_\nu)(dB_\chi/d\theta)\, d\chi} = \frac{0.4024}{\theta \int_0^\infty (\kappa_{Ba,\,s}/\kappa_\nu)[(\chi\theta)^4 10^{-\chi\theta}/(1 - 10^{-\chi\theta})^2]\, d\chi}. \tag{40}$$

To evaluate the integral, consideration is first given to the contribution from the range $0 \leq \chi \leq 13.60$ e.v. As was done by Strömgren (1932), Cotes's formula (25) is employed for each successive five values of $\chi$. For the range $13.60 \leq \chi \leq \infty$, the approximation is made of putting all the Gaunt factors equal to unity. The contribution of this range to the integral is sufficiently small that the error involved in this assumption is less than one-half of 1 per cent of the entire integral. This assumption is applied to equation (12), followed by division by the Boltzmann factor and multiplication by $m_H$; whence

$$a_\nu = \frac{16\pi^4}{3^{3/2}} \frac{m\epsilon^{10}}{ch^6} \frac{1}{\nu^3} \left( \sum_{n=1}^{4} \frac{10^{-(3.392 - 13.60/n^2)\theta}}{n^3} + \frac{10^{-2.728\theta}}{62.61\,\theta} \right) (1 - 10^{-\chi\theta}), \tag{41}$$

where all powers of $e$ have been converted to powers of 10 but $\nu$ has been retained instead of converting to $\lambda$. The integral to be considered is

$$\theta \int_{13.60}^\infty \frac{\kappa_{Ba,\,s}}{\kappa_\nu} \frac{(\chi\theta)^4 10^{-\chi\theta}}{(1 - 10^{-\chi\theta})^2}\, d\chi = a_{Ba,\,s}\, \theta \int_{13.60}^\infty \frac{1}{a_\nu} \frac{(\chi\theta)^4 10^{-\chi\theta}}{(1 - 10^{-\chi\theta})^2}\, d\chi .$$

Substitution of equation (41), recourse to equations (10) and (20), conversion back to powers of $e$ under the integral sign, and introduction of numerical values of the constants give

$$\psi = \sum_{n=1}^{4} \frac{10^{-(3.399 - 13.60/n^2)\theta}}{n^3} + \frac{10^{-2.728\theta}}{62.61\,\theta}, \tag{42}$$

$$\theta \int_{13.60}^\infty \frac{\kappa_{Ba,\,s}}{\kappa_\nu} \frac{(\chi\theta)^4 10^{-\chi\theta}}{(1 - 10^{-\chi\theta})^2}\, d\chi = 6.607 \times 10^{12} \frac{1}{\theta^3} \frac{a_{Ba,\,s}}{\psi} [\phi(\infty) - \phi(u_1)], \tag{43}$$

where

$$\phi(u) = \frac{15}{4\pi^4} \int_0^u \frac{u^7 e^{-u}}{(1 - e^{-u})^3}\, du \tag{44}$$

is a function defined and tabulated by Strömgren (1932), his table also being given by Unsöld (1938*c*). From the table $\phi(\infty) = 196.5$. Table 4 tabulates $\bar{\kappa}_R/\kappa_{Ba,\,s}$ as a function of $\theta$ for the range $0.34 \geq \theta \geq 0.18$.

## V. ACCURACY OF THE TABLES

Tables 1 and 2, giving $a_\nu$ and $\kappa_\nu/\kappa_{Ba,\,s}$, are accurate to somewhat better than one-half of 1 per cent for all wave lengths shortward of the Brackett limit. Beyond the Brackett limit the accuracy is only about one-half of 1 per cent except at 58353 A, which is the series limit for principal quantum number $n = 8$. Here, at worst, a 5 per cent error is introduced by ignoring the difference between the two sides at the absorption limit and putting $n - 0.5 = 8$ in equation (23). If the Gaunt factor for the free-free transitions is

TABLE 4

RATIO OF ROSSELAND MEAN OPACITY COEFFICIENT TO OPACITY COEFFICIENT AT SHORT-WAVE-LENGTH SIDE OF BALMER LIMIT

| $\theta$ | $\bar{\kappa}/\kappa_{\nu Ba,\,s}$ | $\theta$ | $\bar{\kappa}/\kappa_{\nu Ba,\,s}$ | $\theta$ | $\bar{\kappa}/\kappa_{\nu Ba,\,s}$ |
|---|---|---|---|---|---|
| 0.34 | 0.1279 | 0.28 | 0.1012 | 0.22 | 0.0901 |
| .32 | .1178 | .26 | .0954 | .20 | .0915 |
| 0.30 | 0.1088 | 0.24 | 0.0916 | 0.18 | 0.0967 |

considered, these errors become larger, particularly in the far infrared, but the effect on a model atmosphere will remain small.

Table 3, tabulating the integral on the right-hand side of the equation of radiative equilibrium (4), is valid to within less than one-half of 1 per cent throughout.

Table 4, tabulating the Rosseland mean $\bar{\kappa}_R/\kappa_{Ba,\,s}$, has a computational accuracy of better than one-half of 1 per cent.

## REFERENCES

Menzel, D. H., and Pekeris, C. L. 1935, *M.N.* **96**, 77; see eqs. (1, 23), (1, 24), (1, 25), (1, 26), and (1, 36).
Strömgren, B. 1932, *Zs. f. Ap.*, **4**, 118.
———. 1944, *Pub. Kobenhavns Obs.*, No. 138, pp. 18–19.
Unsöld, A. 1938*a*, *Physik der Sternatmosphären* (Berlin: Julius Springer), pp. 118–119; see eqs. (34, 10) and (34, 11).
———. 1938*b*, *ibid.*, p. 119; see eqs. (34, 12) and (34, 13).
———. 1938*c*, *ibid.*, p. 120.

# ON THE DYNAMICAL STABILITY OF MAGNETIC STARS

G. R. BURBIDGE
Yerkes Observatory*

*Received June 24, 1953; revised July 20, 1954*

ABSTRACT

The condition for dynamical stability in a star having a decaying magnetic field has been investigated for two models: (*a*) a stellar model computed by Schwarzschild which has a given conductivity distribution, and (*b*) the uniform sphere. The magnetic energies and the critical fields for instability have been tabulated.

## I. INTRODUCTION

In a recent paper Chandrasekhar and Fermi (1953) have shown that, for a star having a magnetic field, the extension of the virial theorem to take into account the magnetic energy leads to the condition that, for the dynamical stability of the configuration,

$$(3\gamma - 4)\ (|\Omega| - \mathfrak{M}) > 0\ , \tag{1}$$

where $\mathfrak{M}$ is the total magnetic energy of the configuration. Thus, even when $\gamma$ is greater than $\frac{4}{3}$, which is the condition for dynamical stability in the absence of a magnetic field, a sufficiently strong internal magnetic field can induce dynamical instability.

In this paper we shall determine the magnetic energies and critical magnetic fields for dynamical instability for two models having decaying magnetic fields. We shall consider (*a*) a stellar model computed by M. Schwarzschild (1946), which has an electrical conductivity distribution which is a function of the temperature, and (*b*) a uniform sphere, which has a constant conductivity.

## II. THE MAGNETIC ENERGY; THE SCHWARZSCHILD MODEL

M. Wrubel (1952) has considered the decay of a primeval magnetic field, using the Schwarzschild model and the conductivity distribution given by the equation of Cowling (1945). For a decay field we have the well-known equation for the electric field

$$\nabla^2 \boldsymbol{E} = 4\pi\sigma \frac{\partial \boldsymbol{E}}{\partial t}\ , \tag{2}$$

and we consider solutions which have axial symmetry with currents traveling in circles about the axis. The solutions are of the form

$$E_\phi = A\, g(r)\, P_n^1(\mu)\ e^{-t/\tau}\ . \tag{3}$$

Wrubel has solved equation (2) numerically and has expressed the solution in the following form:

$$H_r = \frac{A}{R}\frac{g(x)}{x}\left\{\frac{\mu}{\sqrt{(1-\mu^2)}}\, P_n^1(\mu) - \sqrt{(1-\mu^2)}\,\frac{dP_n^1(\mu)}{d\mu}\right\}\tau\, e^{-t/\tau}\ , \tag{4}$$

$$H_\theta = -\frac{A}{R}\left(\frac{dg}{dx} + \frac{g}{x}\right)P_n^1(\mu)\ \tau\, e^{-t/\tau} \qquad \text{and} \qquad H_\phi = 0\ ,$$

* Now at the Cavendish Laboratory, Cambridge, England.

where $A$ is an undetermined constant and $g(x)$ and $dg/dx$ ($x = r/R$) have been tabulated for the modes $n = 1$ with no node; $n = 1$ with one node; $n = 3$ with no node. Also the natural decay times, $\tau$, have been given for these three cases.

The internal magnetic energy of the star is given by the expression

$$\mathfrak{M}_{\text{int}} = \frac{1}{8\pi}\int_0^1\int_{-1}^{+1}\int_0^{2\pi} |\boldsymbol{H}|^2 R^3 x^2 dx\, d\mu\, d\phi\,. \tag{5}$$

If we substitute equation (4) in equation (5), we find that

$$\mathfrak{M}_{\text{int}} = e^{-2t/\tau}\left(\frac{A\tau}{2R}\right)^2 R^3 \int_0^1\int_{-1}^{+1}\left[\left\{\frac{g^2}{x^2}\right\}\left\{\frac{\mu}{\sqrt{(1-\mu^2)}}P_n^1(\mu) - \sqrt{(1-\mu^2)}\frac{dP_n^1(\mu)}{d\mu}\right\}^2 + \left(\frac{dg}{dx}+\frac{g}{x}\right)^2\left\{P_n^1(\mu)\right\}^2\right] x^2 dx\, d\mu\,. \tag{6}$$

Now

$$\int_{-1}^{+1}\left\{\frac{\mu}{\sqrt{(1-\mu^2)}}P_n^1(\mu) - \sqrt{(1-\mu^2)}\frac{dP_n^1(\mu)}{d\mu}\right\}^2 d\mu = \frac{2n^2(n+1)^2}{2n+1} \tag{7}$$

and

$$\int_{-1}^{+1}\{P_n^1(\mu)\}^2 d\mu = \frac{2n(n+1)}{2n+1}\,. \tag{8}$$

These relations follow from the well-known properties of the Legendre functions. Then, combining equations (6), (7), and (8), we have

$$\mathfrak{M}_{\text{int}} = e^{-2t/\tau}\left(\frac{A\tau}{2}\right)^2 R\left\{\frac{2n(n+1)(n^2+n+1)}{2n+1}\int_0^1 g^2 dx + \frac{2n(n+1)}{2n+1}\int_0^1 x^2\left(\frac{dg}{dx}\right)^2 dx + \frac{4n(n+1)}{2n+1}\int_0^1 gx\left(\frac{dg}{dx}\right)dx\right\}. \tag{9}$$

Using the tables of $g$ and $dg/dx$ given by Wrubel, the integrals which occur in the foregoing equation have been evaluated numerically. The final result can be expressed in the form

$$\mathfrak{M}_{\text{int}} = C e^{-2t/\tau} R (A\tau)^2\,, \tag{10}$$

where the constant $C$ has the values

$$C = 11.044,\ 10.792,\ \text{and}\ 1060.410 \tag{11}$$

for the three cases,

$$n = 1,\ \text{no node};\ n = 1,\ \text{one node};\ \text{and}\ n = 3,\ \text{no node}\,, \tag{11'}$$

respectively. The external magnetic energy of the star is obtained as follows. In general, the magnetic potential outside a magnetic sphere can be written in the form

$$\Omega = \sum_{n=0}^{\infty}\sum_{m=0}^{\infty}\frac{P_n^m(\mu)}{r^{n+1}}\{A_{n,m}\cos m\phi + B_{n,m}\sin m\phi\}\,; \tag{12}$$

and since

$$\boldsymbol{H} = \text{grad}\ \Omega\,, \tag{13}$$

we find that, for a particular mode corresponding to the internal excited mode,

$$H_r(\text{ext.}) = -\frac{(n+1)P_n(\mu)}{r^{n+2}} A_n ,$$

$$H_\theta(\text{ext.}) = \frac{P_n^1(\mu)}{r^{n+2}} A_n \quad \text{and} \quad H_\phi(\text{ext.}) = 0 , \tag{14}$$

where $A_n$ is determined by the boundary conditions

$$H_r(\text{int.}) = H_r(\text{ext.}) \quad \text{at} \quad r = R . \tag{15}$$

From equations (4) and (14) and Wrubel's table we find that

$$\begin{aligned} A_1 &= -e^{-t/\tau} R^2 (A\tau) && (n = 1, \text{ no node}) , \\ A_1 &= -e^{-t/\tau} R^2 (A\tau) && (n = 1, \text{ one node}) , \\ A_3 &= -e^{-t/\tau} (3R^4) (A\tau) && (n = 3, \text{ no node}) . \end{aligned} \tag{16}$$

The external magnetic energy is given by

$$\begin{aligned} \mathfrak{M}_{ext} &= e^{-2t/\tau} \frac{1}{4} \int_R^\infty \int_{-1}^{+1} (H_r^2 + H_\theta^2) r^2 dr d\mu \\ &= \tfrac{1}{2} e^{-2t/\tau} A_n^2 \frac{n+1}{2n+1} R^{-(2n+1)} . \end{aligned} \tag{17}$$

Finally, combining equations (10) and (17) (and making further use of eq. [16]), we obtain

$$\begin{aligned} \mathfrak{M} &= e^{-2t/\tau} R (A\tau)^2 \times 11.38 && (n = 1, \text{ no node}) , \\ \mathfrak{M} &= e^{-2t/\tau} R (A\tau)^2 \times 11.12 && (n = 1, \text{ one node}) , \\ \mathfrak{M} &= e^{-2t/\tau} R (A\tau)^2 \times 1063 && (n = 3, \text{ no node}) . \end{aligned} \tag{18}$$

In terms of the polar magnetic field,

$$y = \frac{A\tau}{R} \left[ \frac{g(x)}{x} \right]_{x=1} n(n+1) , \tag{19}$$

at time $t = 0$, we can express equations (18) alternatively in the forms

$$\begin{aligned} \mathfrak{M} &= e^{-2t/\tau} R^3 y^2 \times 2.844 && (n = 1, \text{ no node}) , \\ \mathfrak{M} &= e^{-2t/\tau} R^3 y^2 \times 2.781 && (n = 1, \text{ one node}) , \\ \mathfrak{M} &= e^{-2t/\tau} R^3 y^2 \times 7.382 && (n = 3, \text{ no node}) . \end{aligned} \tag{20}$$

### III. THE UNIFORM SPHERE OF CONSTANT CONDUCTIVITY

In this case it is well known that the solution for $E_\phi$ (eq. [37]) is expressible in terms of the Bessel function $J_{n+1/2}(\beta r)$, where $\beta R$ is a zero of the function of order $n - \frac{1}{2}$. Thus

$$g(r) = \frac{1}{\sqrt{r}} J_{n+1/2}(\beta r) \quad \text{and} \quad J_{n-1/2}(\beta R) = 0 . \tag{21}$$

The corresponding expressions for the components of the magnetic field are

$$H_r = -\frac{A}{r^{3/2}}\left\{\frac{\mu}{\sqrt{(1-\mu^2)}}P_n^1(\mu) - \sqrt{(1-\mu^2)}\frac{dP_n^1(\mu)}{d\mu}\right\}J_{n+1/2}(\beta r)\,\tau\,e^{-t/\tau}, \tag{22}$$

$$H_\theta = \frac{A}{r^{3/2}}\left\{\tfrac{1}{2}J_{n+1/2}(\beta r) + rJ'_{n+1/2}(\beta r)\right\}P_n^1(\mu)\,\tau\,e^{-t/\tau} \quad \text{and} \quad H_\phi = 0\,.$$

With $H_r$ and $H_\theta$ given by equation (22), the expression for the internal magnetic energy (cf. eq. [6]) becomes

$$\mathfrak{M}_{int} = e^{-2t/\tau}(A\tau)^2\frac{n(n+1)}{2(2n+1)}\int_0^R\left[\frac{n(n+1)}{r}J^2_{n+1/2}(\beta r) + \frac{1}{r}\left\{\tfrac{1}{2}J_{n+1/2}(\beta r) + rJ'_{n+1/2}(\beta r)\right\}^2\right]dr\,. \tag{23}$$

The various integrals over the Bessel functions which occur in equation (23) can be evaluated if proper use is made of the various recurrence relations satisfied by these functions. We find that

$$\mathfrak{M}_{int} = e^{-2t/\tau}(A\tau)^2\frac{n(n+1)}{4(2n+1)}(\beta^2R^2 - 2n)J^2_{n+1/2}(\beta R)\,. \tag{24}$$

The external magnetic field is again given in equation (14); but the constant $A_n$ is now given by

$$A_n = (A\tau)R^{n+1/2}nJ_{n+1/2}(\beta R)\,. \tag{25}$$

Hence (cf. eq. [17])

$$\mathfrak{M}_{ext} = e^{-2t/\tau}(A\tau)^2\frac{2n^2(n+1)}{4(2n+1)}\beta^2R^2J^2_{n+1/2}(\beta R)\,. \tag{26}$$

Combining equations (24) and (26), we finally obtain

$$\mathfrak{M} = e^{-2t/\tau}(A\tau)^2\frac{n(n+1)}{4(2n+1)}\beta^2R^2J^2_{n+1/2}(\beta R)\,. \tag{27}$$

For the case in hand the polar magnetic field at time $t = 0$ is given by

$$y = \frac{A\tau}{R^{3/2}}n(n+1)J_{n+1/2}(\beta R)\,; \tag{28}$$

and we can rewrite equation (27) in the form

$$\mathfrak{M} = \frac{y^2R^3}{4n(n+1)(2n+1)}\beta^2R^2e^{-2t/\tau}. \tag{29}$$

Denoting the zeros of $J_{n-1/2}(x)$ by $j_{n,s}$, we have, in an obvious notation,

$$j_{n,s} = \beta R = \left(\frac{4\pi\sigma}{\tau}\right)^{1/2}R \quad \text{and} \quad \tau = \frac{4\pi\sigma}{j^2_{n,s}}R^2. \tag{30}$$

The zeros of these Bessel functions and the values of $J_{n+1/2}(j_{n,s})$ which must be substituted in equation (30) have been obtained from the *Tables of Spherical Bessel Functions* ("Mathematical Tables Project, N.B.S." [New York: Columbia University Press, 1947]), Vols. 1 and 2.

In order to tabulate the magnetic energies and the decay times in the various modes for the uniform sphere, we have to determine a value of the electrical conductivity which is reasonable from the astrophysical viewpoint. We have estimated this by substituting the decay times given by Wrubel for case $a$ in equation (20) for the two lowest modes. We have put $R = R_\odot$.

We find that

$$n = 1, s = 1; \qquad \sigma = 2.093 \times 10^{-5}; \qquad (31)$$

$$n = 3, s = 1; \qquad \sigma = 1.718 \times 10^{-5}.$$

In our calculations we have therefore taken

$$\sigma = 1.5 \times 10^{-5} \qquad (32)$$

to be a reasonable value.

In Table 1 we have tabulated the primitive magnetic energies in units of $(y_{11}^2 R^3/16\pi)$

TABLE 1

THE MAGNETIC ENERGIES IN SOME MODES FOR THE UNIFORM SPHERE

| $n$ | $s$ | Decay Time $t\times10^{-9}$ Years | Magnetic Energy (in Units $y_{11}^2R^3/16\pi$) | $n$ | $s$ | Decay Time $t\times10^{-9}$ Years | Magnetic Energys (in Units $y_{11}^2R^3/16\pi$) |
|---|---|---|---|---|---|---|---|
| 1 | 1 | 0.931 | 20.21 | 9 | 1 | 0.056 | 1.57 |
| 1 | 2 | .233 | 2.53 | 9 | 2 | .033 | 0.88 |
| 1 | 3 | .104 | 0.75 | | | | |
| 1 | 4 | .058 | 0.31 | 11 | 1 | .041 | 1.20 |
| | | | | 11 | 2 | .025 | 0.68 |
| 3 | 1 | .277 | 7.68 | | | | |
| 3 | 2 | .111 | 2.05 | 13 | 1 | .031 | 0.85 |
| 3 | 3 | .061 | 0.86 | 13 | 2 | .020 | 0.51 |
| 3 | 4 | .038 | 0.43 | | | | |
| | | | | 15 | 1 | .024 | 0.72 |
| 5 | 1 | .137 | 3.95 | 15 | 2 | .016 | 0.43 |
| 5 | 2 | .067 | 1.49 | | | | |
| 5 | 3 | .041 | 0.74 | 17 | 1 | .020 | 0.56 |
| 5 | 4 | .027 | 0.41 | | | | |
| | | | | 19 | 1 | 0.016 | 0.43 |
| 7 | 1 | .083 | 2.44 | | | | |
| 7 | 2 | .046 | 1.10 | | | | |
| 7 | 3 | .029 | 0.62 | | | | |
| 7 | 4 | 0.021 | 0.36 | | | | |

and the decay times for values of $n$ up to 19 and for some values of $s$. In order to compute this table, we have made the assumption that the constant $A$ is the same for all modes and have eliminated it in terms of the polar field in the case $n = 1$, $s = 1$. This polar field has been denoted by $y_{11}$.

## IV. THE GRAVITATIONAL POTENTIAL ENERGY

It is well known that the gravitational potential energy of a uniform sphere is given by

$$|\Omega| = \frac{3}{5}\frac{GM^2}{R}. \qquad (33)$$

For the Schwarzschild model the appropriate integral defining $\Omega$ was evaluated numerically, and the result,

$$|\Omega| = 1.812\,\frac{GM^2}{R}, \qquad (34)$$

was obtained.

## V. THE CRITERIA FOR INSTABILITY

From equation (1) we find that for $\gamma = \frac{4}{3}$ the configuration will be dynamically unstable when $\mathfrak{W} > |\Omega|$. For Schwarzschild's model this criterion (at $t = 0$) becomes

$$y > 2.060 \times 10^{-4} \frac{M}{R^2}, \quad y > 2.083 \times 10^{-4} \frac{M}{R^2}, \quad \text{and} \quad y > 1.279 \times 10^{-4} \frac{M}{R^2} \tag{35}$$

for the three cases $n = 1$, no node; $n = 1$, one node; and $n = 3$, no node, respectively, for instability. To obtain this result we have used equations (20 and (34). For a star having solar dimensions, the critical primitive surface fields are

$$8.46 \times 10^7 \text{ gauss}; \quad 8.56 \times 10^7 \text{ gauss}; \quad \text{and} \quad 5.25 \times 10^7 \text{ gauss} \tag{36}$$

for the three cases considered.

For the model having a constant conductivity, the condition for instability becomes

$$y > [\tfrac{3}{5} n (n+1) (2n+1) G]^{1/2} \frac{2M}{R^3 \beta}. \tag{37}$$

Here we have used equations (29) and (34). The numerical values of the critical surface fields in the various modes for a sphere having solar dimensions are tabulated in Table 2.

TABLE 2

CRITICAL PRIMITIVE SURFACE FIELDS FOR INSTABILITY FOR THE UNIFORM SPHERE HAVING SOLAR DIMENSIONS

| $n$ | $s$ | $y \times 10^{-8}$ Gauss | $n$ | $s$ | $y \times 10^{-8}$ Gauss |
|---|---|---|---|---|---|
| 1 | 1 | 1.28 | 9 | 1 | 5.31 |
| 1 | 2 | 0.64 | 9 | 2 | 4.08 |
| 1 | 3 | 0.43 | 11 | 1 | 6.02 |
| 1 | 4 | 0.32 | 11 | 2 | 4.76 |
| 3 | 1 | 2.61 | 13 | 1 | 6.68 |
| 3 | 2 | 1.66 | 13 | 2 | 5.39 |
| 3 | 3 | 1.22 | 15 | 1 | 7.29 |
| 3 | 4 | 0.97 | 15 | 2 | 5.98 |
| 5 | 1 | 3.65 | 17 | 1 | 7.86 |
| 5 | 2 | 2.55 | 19 | 1 | 8.40 |
| 5 | 3 | 1.98 | | | |
| 5 | 4 | 1.63 | | | |
| 7 | 1 | 4.53 | | | |
| 7 | 2 | 3.35 | | | |
| 7 | 3 | 2.70 | | | |
| 7 | 4 | 2.27 | | | |

## VI. THE CRITICAL SURFACE FIELD FOR A WHITE DWARF STAR

It is of interest to estimate the critical primitive field for instability in a white dwarf. We can consider case *b*, that of a uniform sphere, and use the values (Chandrasekhar 1939) $\rho$ mean $= 1.34 \times 10^6$ gm/cc, $R = 1.93 \times 10^9$ cm. We have, in the nonrelativistic case for a completely degenerate configuration,

$$|\Omega| = \frac{6}{7} \frac{GM^2}{R}, \tag{38}$$

so that the condition for instability is

$$v > [\tfrac{6}{7} n (n+1) (2n+1) G]^{1/2} \frac{2M}{R^3 \beta}. \tag{39}$$

Here we have used equations (29) and (37). Substituting the numerical values, we find that, for instability,

$$y > 4.0 \times 10^{11} \tag{40}$$

for the mode $n = 1$, $s = 1$.

The decay time for this magnetic field is given by equation (30). An estimate of the electrical conductivity of degenerate matter can be made from the work of Kothari (1932). For a density $\rho \backsim 10^6$ gm/cc, $\sigma = 10^{-2}$; and for the lowest mode

$$\tau \simeq 1.5 \times 10^9 \text{ years} . \tag{41}$$

## VII. DISCUSSION

Our lack of knowledge concerning the importance of decaying magnetic fields in the evolution of stars precludes anything other than speculative discussion. The primitive fields necessary for dynamical instability are very large as compared with the surface fields in stars which have been measured by Babcock (1947, 1948, and 1951), although the decay times in the lowest modes for both models are of the same order, though less than the estimated ages, i.e., of order $10^9$ years. From the order of magnitude of our results for the uniform sphere, it would appear that the higher modes, if initially present, will be damped out. Even this argument may be oversimplified, since a star in its evolutionary path will vary in temperature, and such a variation will mean that it will have a varying electrical conductivity corresponding to a natural decay time which is itself a function of time.

The work of Chandrasekhar and Fermi (1953) has shown that an idealized model consisting of a sphere with infinite conductivity and having a uniform magnetic field inside and a dipole field outside will be distorted and will tend to become flattened, the degree of flattening depending on the strength of the internal magnetic field. For a decay field and a star having a finite conductivity, it is reasonable to suppose that the same effect will tend to occur for fields smaller than those calculated in this paper for dynamical instability, but it will be necessary to investigate such a model in detail in order to determine the magnitude of the effect.

I am deeply indebted to Dr. S. Chandrasekhar for suggestions and help and for many stimulating discussions, both privately and in his theoretical seminars. I am also indebted to Dr. E. Jensen and to Dr. E. M. Burbidge for many enlightening discussions.

## REFERENCES

Babcock, H. W. 1947, *Ap. J.*, **105**, 105.
———. 1948, *ibid.*, **108**, 191.
———. 1951, *ibid.*, **114**, 1.
Chandrasekhar, S. 1939, *Introduction to the Theory of Stellar Structure* (Chicago: University of Chicago Press), p. 427.
Chandrasekhar, S., and Fermi, E. 1953, *Ap. J.*, **118**, 116.
Cowling, T. G. 1945, *M.N.*, **105**, 166.
Kothari, D. 1932, *Phil. Mag.*, **13**, 361.
Schwarzschild, M. 1946, *Ap. J.*, **104**, 203.
Wrubel, M. 1952, *Ap. J.*, **116**, 291.

# NOTES

## SPECTRUM OF NOVA OPHIUCHUS 1952*

At the time that a telegram was received reporting a faint nova in Ophiuchus, the Cassegrain spectrograph was attached to the 82-inch reflector of the McDonald Observatory. Spectrograms were obtained on this and following nights; but, since it was immediately obvious that the nova had been discovered well past maximum light, no attempt was made to obtain a series of spectrograms for an exhaustive study of the nova. Five spectrograms with a dispersion of 113 A/mm at $H\gamma$ were obtained and are reproduced in Figure 1. The plate numbers and dates of the spectrograms are recorded in the table below. The spectral region 3900–4600 A is in good focus.

| Plate No. | Date (U.T.) 1952 | Exposure Time (Minutes) |
|---|---|---|
| H 68 | Aug. 26.11 | 25 |
| H 69 | Aug. 26.17 | 99 |
| H 71 | Aug. 27.12 | 60 |
| H 74 | Aug. 28.18 | 60 |
| H 84 | Sept. 9.14 | 123 (clouds) |

The nova, at the time of the first spectrograms, was in the stage of broad emission bands of *H*, *Fe* II, and *Ca* II. The first four spectrograms are very similar to Nova Persei 1901, on February 27–28, 1901, when it was approximately 2 mag. below maximum light. The emission has a width of about 2000 km/sec, and the $H\gamma$ violet absorption edge is displaced about −860 km/sec. The spectrogram on September 9, 1952, suggests some advancement of the spectrum. For example, it can be seen in the figure that the $H\gamma$ absorption is significantly more narrow than on previous spectrograms. Also, the *Fe* II emission 4630 and 4667 is beginning to be submerged by the *N* II–*O* II blend of the "4640" region of the Orion stage.

Photometric observations were made on two occasions with a photoelectric photometer. The magnitudes and colors are given in the accompanying table. It is seen that the

| Date (U.T.) 1952 | *V* | *B*−*V* | *U*−*B* |
|---|---|---|---|
| Sept. 2.11 | 10.94 | +0.83 | −0.27 |
| Sept. 6.10 | 11.27 | +0.82 | −0.25 |

nova was fading rapidly and was no doubt significantly fainter than photographic magnitude 12 when the last spectrogram was obtained on September 9, 1952.

W. A. Hiltner

Yerkes and McDonald Observatories
June 25, 1954

* *Contributions from the McDonald Observatory, University of Texas*, No. 245.

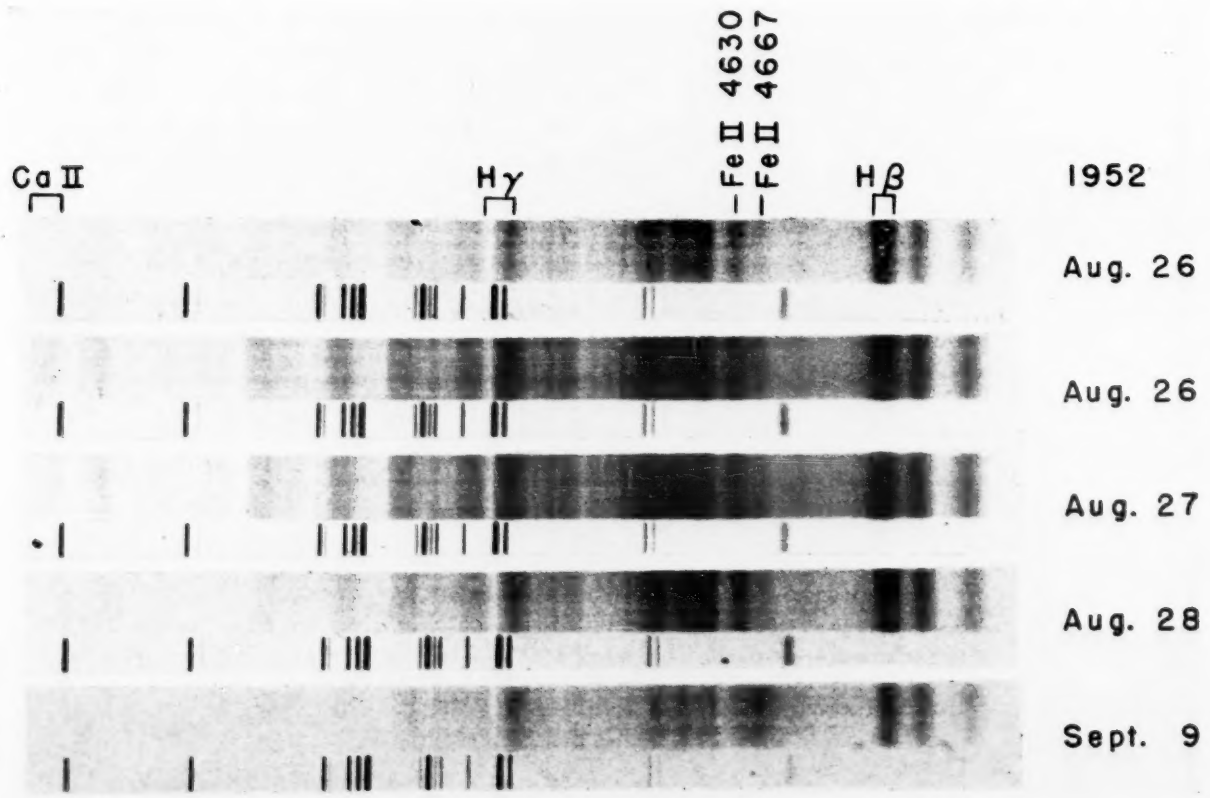


FIG. 1.—The spectrum of Nova Ophiuchus 1952

## A NOTE ON THE REPORTED COLOR-INDEX EFFECT OF DISTANT GALAXIES

In 1948 Stebbins and Whitford (1948) published a paper giving the results of a two-color photometric study of elliptical galaxies of known red shift. In order to determine the intrinsic color of these galaxies, they applied a correction for the effect of red shift on color index. This correction accounted for only part of the excess reddening which they observed. The remaining excess they interpreted as a linear correlation between color index and distance. More recently, Whitford (1953) has suggested that this effect is absent for spirals.

Observations of this kind are of the greatest importance to cosmology and also to the interpretation of the classical observations of the expanding universe. It is therefore desirable to review the existing data critically, so as to ascertain their precise information content. For this purpose we shall consider the significance of the data in terms of each one of a number of hypotheses.

### I. THAT THE EFFECT IS ENTIRELY DUE TO CHANCE IF THE STEBBINS-WHITFORD SHIFT CORRECTION IS APPROPRIATE

This can be ruled out for the excess reddening of the most distant E galaxies observed. Figure 1 gives the points after the Stebbins-Whitford corrections have been applied. Despite the scatter, the Boötes galaxies appear to be significantly redder than average.

The recent statement by Whitford (1953) that the effect appears to be absent for spirals is not based on such good statistical data, for the intrinsic scatter in the color index of spirals is much greater than for E galaxies (Stebbins and Whitford 1952), and the number of observations quoted is smaller. Thus for spirals it does not yet seem justifiable to draw even tentative conclusions from the data.

### II. THAT THE CORRECTION FACTOR IS INAPPROPRIATE

Stebbins and Whitford have evaluated the correction factor arising from the known amount of the translation of the spectrum to the red. For this purpose they used the energy-curve obtained in six colors from one particular E galaxy, namely, M32. Ideally, one should derive a correction factor for each case by using the energy-curve of a precisely similar galaxy. This implies that the result of the calculation should give an index equal to that used for deriving the correction factor. This condition was very far from satisfied in the calculations of Stebbins and Whitford, who state that M32 has a two-color index near the mean of its class (presumably about 0.86), while the values for the Boötes galaxies after correction are 1.17, 1.14, 1.09, and 0.95. Since the correction factor will be greater, the greater the proportion of red light, the intrinsic color indices of the Boötes galaxies will be smaller than those derived by Stebbins and Whitford. The data would not bear a large change of this sort without then admitting an explanation in terms of a random effect.

An underestimate of the correction factor may also arise from an overestimate of the unknown ultraviolet light of these galaxies. For the most distant galaxies observed, the light through the blue filter is derived to a significant extent from intrinsic ultraviolet light beyond the reach of the six-color photometry of near galaxies. The correction factor must therefore include a guess about the intrinsic ultraviolet emission of the type of galaxy observed.

Very little is known to make such a guess at all reliable. If, indeed, there had not been the suggestion of an unexplained reddening with distance (the Stebbins-Whitford effect), then one might well have suggested that the multicolor photometry of distant red-shifted galaxies provided a means of discovering the intrinsic ultraviolet spectra of these objects. Such knowledge would be of the greatest importance, since it is required in the estimation of their distance (via the "K term").

### III. THAT THE REDDENING IS CORRELATED WITH CLUSTERING OF GALAXIES

It will be seen from Figure 1 that the statistical quality of the data is quite inadequate to establish that the law is a linear one with distance, rather than any other dependence that gives approximately the required change for the most distant objects. It is therefore necessary to inquire whether a quantity other than distance exists which changes in the same sense for the observed objects. The size of clusters of galaxies is indeed such a quantity, and in Figure 2 the observed data are replotted as a function of the number of galaxies in each cluster (Becker 1950). Although little significance can be attached to the numbers themselves, the arrangement of the clusters in order of richness is almost certainly correct. It will be seen that these data can be interpreted in terms of a dependence of the properties of galaxies on their surroundings. Indeed, in those cosmological theories that do not require galaxies to be formed all at one time, an age effect of this sort may be expected. The age differences involved may be much greater than the light-transit times, and some statistical correlation between the real ages and the cluster size might well be suggested.

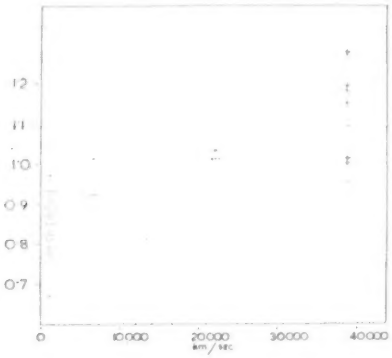


FIG. 1.—The Stebbins-Whitford observational data (*1*, *3*), corrected for the effect of the spectral shift with the coefficient adopted by Stebbins and Whitford (*1*). The corrected color index is plotted against the observed spectral shift, expressed in km/sec. — represents different objects; + represents different measures of the same object.

FIG. 2.—The Stebbins-Whitford observational data, corrected for the effect of the spectral shift with the coefficient adopted by Stebbins and Whitford (*1*). The data are arranged according to the estimated number of members of the parent-cluster (*4*), to demonstrate the monotonic dependence. — represents the different objects; + represents different measures of the same object.

Before observational results could distinguish between such widely differing interpretations, it would be necessary to observe at each range a number of galaxies taken from clusters of greatly differing sizes.

IV. THAT THERE EXISTS A CORRELATION BETWEEN BRIGHTNESS AND COLOR

The choice of galaxies suitable for the investigation results in a selection factor which favors galaxies of greater intrinsic brightness at the greater ranges. Now galaxies may possess a correlation between redness and intrinsic brightness (due, for example, to the presence of red giant stars). There are indications of such a correlation in Stebbins and Whitford's (1952) observations of the Virgo cluster. If this is the case, the selection factor would result in an apparent increase of redness with distance.

It will be seen from this discussion that the interesting observations of Stebbins and Whitford are at present quite inadequate to be of assistance in cosmological theory or in the evaluation of observations of distant galaxies. They constitute, however, the beginning of an observational method which is of an importance comparable to the classical expanding-universe observations of distance, spectral shift, and mean density.

H. BONDI

HARVARD COLLEGE OBSERVATORY, CAMBRIDGE, MASS.

T. GOLD

ROYAL GREENWICH OBSERVATORY, ENGLAND

D. W. SCIAMA

TRINITY COLLEGE, CAMBRIDGE, ENGLAND

REFERENCES

Becker, W. 1950, *Sterne und Sternsysteme* (2d ed.; Berlin: J. Steinkopf).
Stebbins, J. L. 1950, *M.N.*, **110**, 416.
Stebbins, J. L., and Whitford, A. E. 1948, *Ap. J.*, **108**, 413.
———. 1952, *ibid.*, **115**, 284.
Whitford, A. E. 1953, *A.J.*, **58**, 49.

## OBSERVATIONAL STATUS OF THE COLOR-EXCESS EFFECT IN DISTANT GALAXIES*

A color-excess effect in distant galaxies can be considered established only after the observations and analysis have stood up to healthy doubts and criticisms of the sort offered by Bondi, Gold, and Sciama (BGS) (1954). Since the first publication by Stebbins and Whitford (1948), new radial velocities of galaxies have been observed by Humason (1951) with the 200-inch Hale telescope. These velocities, which now include members of both well-known and new, more distant clusters, provide a wealth of material for additional color measurements. Two-color results obtained with the 100-inch telescope in the years 1948–1952 (Whitford 1953) are combined with older data to form the color-velocity plot shown in Figure 1. Identification of the clusters is explained in the caption. In the light of present information the following comments may be made concerning the five hypotheses suggested by BGS:

1. G. C. McVittie (1950) also raised the question of whether eight galaxies outside the Virgo cluster provided sufficient evidence of a systematic effect. The new observations strengthen the BGS conclusion that the color-excess effect can hardly be the result of observational selection among objects showing a moderate intrinsic dispersion in color. Remeasurement of all the Boötes objects has reduced the discordance (Stebbins 1950) of No. 4, and the scatter is now small.

Colors of four late-type spirals are admittedly not adequate for establishing the absence

* This note is based in part on observations made at the Mount Wilson and Palomar Observatories.

of the color-excess effect in type I systems. One must guard against a spurious bluing effect resulting from comparison of selected bluer-than-average spirals in the distant group with average spirals in the near-by sample objects. There may be some significance in the fact that the zero excess persists for the four spirals if one starts from the bluest near-by spirals in making the red-shift calculation. Fortunately, the number of spirals with a large measured red shift is growing rapidly, and the test can soon be made with a much better range of material.

2. The 1948 calculation (Stebbins and Whitford 1948) of a color excess depended on a comparison of the observed two-color index of a distant galaxy with the predicted two-color index of M32 transferred by a suitable red-shift correction to the distant velocity frame. Since the composite nature of galaxies is clearly evident on the six-color plots, the calculation must be based on empirical knowledge of an absolute energy-curve. Only M32 was observed in sufficient detail to derive an absolute energy-curve. This dictated the direction of the transfer from the local to the distant velocity frame and the two-color comparison in the latter frame. The procedure was a straightforward application of the available information about galaxies.

Although attempts thus far have not produced definitive results (Whitford 1953), it

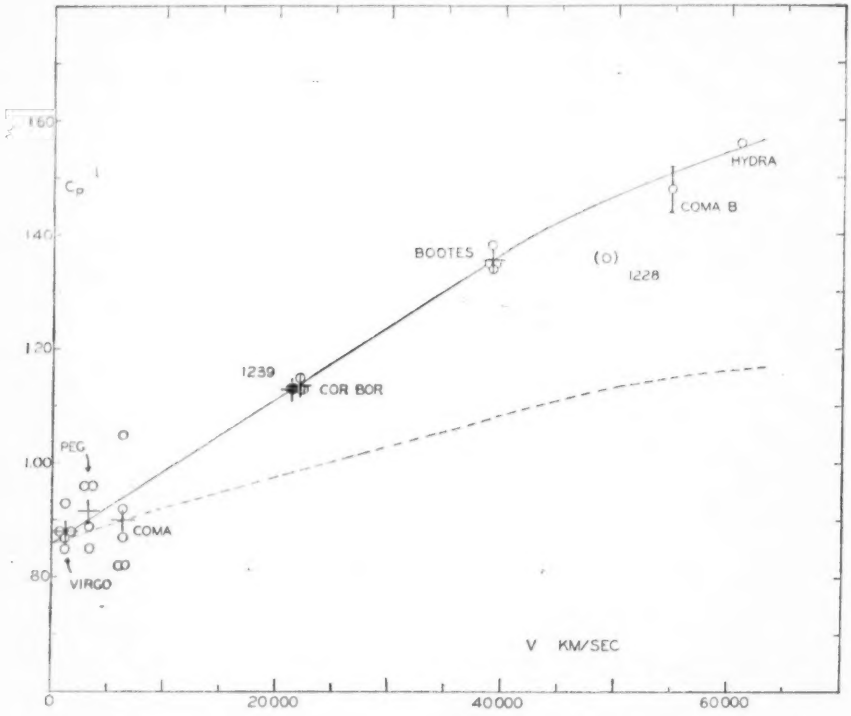


FIG. 1.—Photoelectric colors of cluster galaxies versus radial velocity. Colors are reduced to the International system. Figures refer to right ascension on Humason's list (1951). Hydra is 0855 on that list; Coma B is 1303. Single point marked 1228 could be foreground object in field of cluster; radial velocity of other measured members is assumed. Dotted line shows the expected reddening of M32 as a result of the red shift.

may be assumed that multicolor measures of faint galaxies will in time give an absolute energy-curve that can be used for the reverse calculation of the intrinsic energy-curve of a distant system in the local velocity frame. The present two-color index is clearly inadequate as a starting point. Such a calculation would determine from observations the properties of what BGS term a "precisely similar galaxy" (i.e., similar to the distant galaxy). It is difficult to understand the BGS suggestion that this galaxy would, when compared with M32, show a two-color excess in the local velocity frame differing from that already derived in the distant velocity frame. Until the necessary multicolor observations become available, the field is open for the construction of hypothetical "precisely similar galaxies." Presumably, one could be devised which would give a red-shift correction large enough to eliminate the two-color excess entirely. Such an energy-curve would not resemble that of M32; it would later have to pass the test of predicting the entire run of the multicolor measures of the distant system. It seems preferable to base calculations on the observed properties of real galaxies.

For red shifts no larger than that of the Boötes cluster ($\lambda/\Delta\lambda = 0.13$) the unknown ultraviolet light coming under the blue filter is not an appreciable factor in determining the two-color index. The initial calculations were made on the assumption that the effective wave length of each of the six-color and two-color filter bands could be used as a monochromatic substitute for the entire band. B. Strömgren (1937), A. J. Wesselink (1950), and I. King (1952) have shown that this is a remarkably good approximation if there is no discontinuity or violent asymmetry under each filter response-curve. The six-color plots (Stebbins and Whitford 1948) indicate that stars with a large Balmer jump are unimportant in the composite light of galaxies. Since the blue effective wave length for the two-color filters used in 1949 and thereafter (H. L. Johnson 1950) came at 4215 A, and the six-color ultraviolet wave length at 3530 A was shifted to 3990 A in making the two-color red-shift calculation, there was still a margin of safety; extrapolation was not necessary. If the shifted ultraviolet curve is plotted over the unshifted two-color blue curve, only 2.5 per cent of the area under the blue curve is on the shortward side of the ultraviolet curve and may therefore be said to be completely unobserved. For the 1947 blue filter the figure is 9 per cent. The two filter systems showed no systematic differences in excess of probable error (Stebbins, Whitford, and Johnson 1950). It is therefore difficult to see how even the most extreme assumptions about the ultraviolet energy of M32 can alter the red-shift correction by an amount approaching the calculated color excess.

For galaxies with red shifts larger than that of the Boötes cluster the ultraviolet problem rapidly becomes serious, and more extended analysis than that obtainable from the two-color yellow-blue filters will be necessary. The dotted line for calculated color in Figure 1 involves extrapolation at the high-velocity end.

3. Color measures of 32 bright elliptical galaxies (Stebbins and Whitford 1952), mostly taken from the Shapley-Ames catalogue, showed them to be quite homogeneous, with $C_p = +0.86 \pm 0.06$ (m.e.). Elliptical members of the local group, certainly a very small cluster, did not differ significantly from ellipticals in the very large and rich Virgo cluster. Comparisons between compact clusters with few spirals also fail to show a consistent correlation with number of members. The relatively small Pegasus cluster (100 members), which, according to the trend suggested by BGS, should be red, shows no discordance at the low-velocity end of Figure 1. At the high-velocity end the most distant clusters appear, from inspection of photographs, to be normal clusters of several hundred members, in contrast to the Boötes cluster with only 150 members.

4. The influence of a possible color-luminosity correlation was avoided in preparing Figure 1 by restricting the material to the four or five brightest members of each near-by cluster; measurements at the faint end are necessarily confined to the brightest members. This selection of data produces no significant change in the over-all result.

The foregoing discussion is not intended to indicate that the author considers the

color-excess effect established beyond all reasonable doubt. There are other possible objections, perhaps more serious than those raised by Bondi, Gold, and Sciama, which need to be explored before skepticism can be put aside. Among these may be mentioned the following:

1. The typical elliptical system used for the red-shift calculation ought to be an average bright member of a compact cluster, rather than M32. The two-color similarity of M32 to these cluster members is not sufficient to prove over-all identity of the energy-curves.

2. The six-color measures ought to be tied to an absolute energy standard by a more direct route than the assumption that the sun is an average dG2 star.

Programs in progress are designed to provide definitive answers to these doubts.

A. E. Whitford

Washburn Observatory
University of Wisconsin

REFERENCES

Bondi, H., Gold, T., and Sciama, D. W. 1954, *Ap. J.*, **120**, 597.
Humason, M. L. 1951, *Pub. A.S.P.*, **63**, 232.
Johnson, H. L. 1950, *Ap. J.*, **112**, 240.
King, I. 1952, *Ap. J.*, **115**, 580.
McVittie, G. C. 1950, *M.N.*, **110**, 590.
Stebbins, J. 1950, *M.N.*, **110**, 416.
Stebbins, J., and Whitford, A. E. 1948, *Ap. J.*, **108**, 413.
———. 1952, *ibid.*, **115**, 284.
Stebbins, J., Whitford, A. E., and Johnson, H. L. 1950, *Ap. J.*, **112**, 469.
Strömgren, B. 1937, *Handbuch der Experimentalphysik* (Leipzig: Akademische Verlag), **26**, 392.
Wesselink, A. J. 1950, *Trans. I.A.U.*, **7**, 269.
Whitford, A. E. 1953, *A.J.*, **58**, 49 (abstr.).

## EAST-WEST MOTION OF AURORAE

Considering the number of workers engaged in observing aurorae during the last hundred years, one would expect that the drift motions of auroral draperies and ray structures reported by Meinel and Schulte (1953) would have been widely known. References to the east-west motion of aurorae appear to be very few. Tromholt (1885) noted that bowlike arcs, with their eastern ends connected, almost always travel in a westerly direction when moving. Sangster (1910) mentioned the "well-known" apparent rotation of the corona about the zenith. Krogness and Tønsberg (Harang 1951) have given plots of the drift of auroral clouds on one evening—an easterly motion in this case. The definite motions observed by Meinel and Schulte had not previously been noticed at Saskatoon, and it appeared worth while to check their observations.

A 16 mm camera and mirror arrangement, working on a principle similar to that of Meinel and Schulte, has been operated nightly since December, taking 2-minute exposures of the northern half of the sky. During this period (December, 1953—April, 1954, incl.) only three large auroral displays were visible with aurorae to the south of the zenith. Other displays consisted of arcs and bands in the north sky, mostly below 40° elevation. Since the auroral zone during the past year has been well north of its average position, it is likely that these records are comparable with Meinel and Schulte's observations made in 1952.

Examination of the auroral photographs shows that, out of 58 forms observed in the 5-month period, 19 exhibited a definite easterly motion, while 14 showed a westerly motion. The motion of the rest, if any, was in a north-south direction only. It is seen in Figure 1 that the 14 cases with westerly motion all took place before 2:00 A.M. The other 44 cases were scattered throughout the night. The speeds of motion could not be meas-

ured accurately but were estimated to be of the order of 200–500 meters per second, making the usual assumptions as to the height of auroral forms. During the large displays noted above, rays were observed with higher speeds than the motion of the rest of the display at the time.

We see that only just over half the auroral displays show any definite east-west motion and that, when a westward motion exists, it is likely to occur during the first half

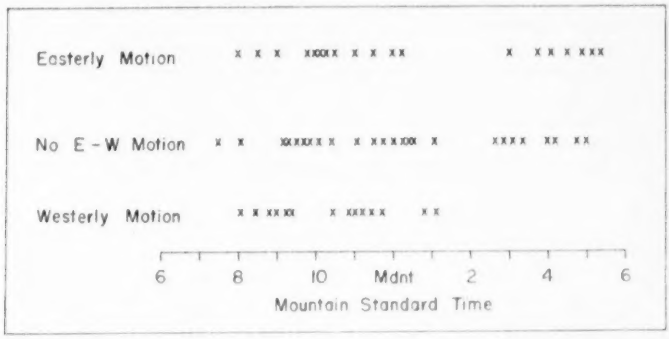


FIG. 1.—Occurrence of auroral forms at Saskatoon according to observed east-west drift motion, December, 1953, to April, 1954.

of the night. This result is not a contradiction of that of Meinel and Schulte, but it demonstrates that one cannot generalize on one's results and assign a definite drift motion to all aurorae based on local time.

This work is performed as a project of the Defence Research Board of Canada.

J. H. MEEK

UNIVERSITY OF SASKATCHEWAN
June 7, 1954

REFERENCES

Harang, L. 1951, *The Aurorae* (London: Chapman & Hall), p. 53.
Meinel, A. B., and Schulte, D. H. 1953, *Ap. J.*, **117**, 454.
Sangster, R. B. 1910, *Proc. R. Soc. London, A*, **84**, 85.
Tromholt, S. 1885, *Under the Rays of the Aurora Borealis* (London: Sampson, Low, Marston, Searle & Rivington), p. 231.

## DETERMINATION OF THE POLE OF ROTATION OF VENUS*

It is well known that photographs of Venus taken in violet light show delicate markings. The most extensive study of these markings was made by F. E. Ross (1928). As part of a systematic survey of the planets the writer photographed Venus in infrared, red, and violet light, using the 82-inch telescope equipped with an enlarging camera giving 1 mm = 2″.1. These observations are preferably made in daytime, so as to increase the altitude of the planet. This, incidentally, is an unusual strain on an observer running a full night schedule, often aggravated by poor daytime seeing or cumulus clouds around the mountain top.

* *Contributions from the McDonald Observatory, University of Texas*, No. 246.

The first good violet photographs so obtained were taken after an excellent night on the morning of April 8, 1950, when 0.48 of the Venus disk was illuminated. At that time the markings consisted of eight parallel bands, four bright and four dark, covering the entire visible planet. They were much more regular than had been anticipated on the basis of the literature. The bands had comparable width and were slightly curved, suggesting poles of rotation which were close to, but not identical with, the cusps. This obviously called for observation when Venus was near superior conjunction, at full phase. The disk is then only 10″ in size, however, and the few 1950 observations made at that phase were of insufficient quality. Better photographs were secured in June and July, 1954, with phases from 0.81 to 0.70 and disk diameters of 13″–16″. They confirm the banded structure as the normal appearance of the planet, with *usually three bright and three dark bands;* but they show that changes take place from day to day—as Ross had reported—and that at times the band system is quite irregular.

The 1954 plates, 65 in number, were exposed on 6 days between June 15 and July 20; each plate has four exposures, taken at moments of best seeing. The scale and orientation

TABLE 1

DETERMINATIONS OF POSITIONS OF POLE OF VENUS

| Date U.T. | Year | R.A. | Decl. | Weight |
|---|---|---|---|---|
| April 9.6 | 1950 | 55° | +82½° | 2 |
| June 16.0 | 1954 | 52 | +83 | 2 |
| June 26.0 | 1954 | 82 | +77½ | ½ |
| June 27.0 | 1954 | 72 | +80½ | ½ |
| July 19.0 | 1954 | 30 | +74 | 1 |

of the exposures were calibrated at night with a wide double star. No decided changes of the bands were noted during single-day runs, which lasted up to 4 hours. The best dozen or so exposures of each run were selected and combined into a single drawing for each run, except for one run, which was of inferior quality and could not be used. Thereupon preliminary measures were made as follows. A white globe with a co-ordinate grid was used as a model of the planet and illuminated from the proper direction to simulate the phase. The orientation of the globe was then changed by an assistant until the ruled circles seen from a fixed position agreed best with the orientation and shape of the bands on the drawings. The best photographs were then reinspected as checks. The co-ordinates of the pole of the globe were read off and later converted to R.A. and Dec. with the aid of the position of the planet at the time of observation. The results are given in Table 1. In judging them, it should be noted that the positions as measured varied over a good part of a hemisphere, resulting from the motions of Venus along its path. The internal agreement, found upon completion of the computations, somewhat surprised the writer. If the average of the June 26 and 27 positions is taken (weight 1), the total spread of the pole positions is within an area of the globe of 12° × 5°. The mean position, at $\alpha = 53°$ and $\delta = 81°$ has internal uncertainties of about 2° and 1°, respectively, if measured along great circles.

The pole of the Venus orbit is at $\alpha = 276°$, $\delta = +66°$, 3° from the pole of the ecliptic. *The obliquity of the Venus equator is thus about 32°*, the uncertainty being perhaps 2°. The consistency of the results in Table 1 shows that the hypothesis that the bands are formed along parallel circles is essentially correct. This seems to imply a fairly rapid rotation of the planet, of no more than a few weeks at most, and definitely not in 225 days. The argument is the same as that used by Ross, but the consistency of the pole determinations lends it greater weight. Continued studies will include the latitude distribution of the belts and its changes and a determination of the velocity of rotation at full phase.

As has been suggested before (Kuiper 1952), the dark bands are interpreted as regions where the dust, known to be yellow from the color index of the planet, is highest, while

the bright bands are regions where the dust is lower and where Rayleigh scattering of the overlying $CO_2$ contributes extra intensity in the violet. This explains why the bands are usually invisible in longer wave lengths. The meteorology on Venus should be much simpler than on the earth, where disturbances are more apparent on the weather map than the average flow. Thus Venus, without condensing water vapor or ocean basins, might show a closer approach than the earth to the three-zone circulation pattern in each hemisphere (e.g., Byers 1954), in which there would be three zones of ascending currents and four zones of descending currents, including the polar caps. On Venus the former would be dark, the latter bright. The observed bands give some general support to this view, but further work is required. Clearly, the large obliquity would cause large periodic displacements of the zones during the short Venus year of 225 days.

GERARD P. KUIPER

YERKES AND MCDONALD OBSERVATORIES

## REFERENCES

Byers, H. R. 1954, *The Earth as a Planet*, ed. G. P. Kuiper (Chicago: University of Chicago Press), chap. 7, Sec. 3.

Kuiper, G. P. 1952, *The Atmospheres of the Earth and Planets* (2d ed.; Chicago: University of Chicago Press), p. 371.

Ross, F. E. 1928, *Ap. J.*, **68**, 57.

# ABSTRACTS OF ASTROPHYSICAL JOURNAL SUPPLEMENT SERIES

Supplement No. 8, Volume I

## THE INDEX OF CLUMPINESS OF THE DISTRIBUTION OF IMAGES OF GALAXIES*

JERZY NEYMAN AND ELIZABETH L. SCOTT
Statistical Laboratory
and
C. D. SHANE
Lick Observatory, University of California

The subject of study is the index $K$ of clumpiness of the distribution of images of galaxies on a photographic plate. The index $K$ is defined as the ratio of the standard deviation of the actual number of galaxies counted in an area $\omega$ on a photographic plate, divided by the value of the same standard deviation computed on the assumption that the galaxies are distributed in space with statistical uniformity. This definition is suggested by that of a related characteristic $k(z, n)$ studied by Zwicky (1953).

Theoretical studies of $K$ assume that the actual standard deviation conforms with the recent theory (Neyman and Scott 1952; Neyman, Scott, and Shane 1953) of the distribution of galaxies in space. This theory postulates that the clumpiness of images of galaxies is due solely to the clustering of galaxies in space with no provision for extragalactic absorbing clouds. The dependence of $K$ upon the physical characteristics of the distribution of galaxies (the frequency of clusters, the variation in the number of galaxies per cluster, the compactness of clusters, and the luminosity law of the individual galaxies) and upon observational factors (size and shape of the regions $\omega$ in which counts are made and the limiting apparent magnitude of the plate) is studied. The following conclusions are drawn:

(i) The value of the index of clumpiness, $K$, is independent of the density of cluster centers in space.

(ii) $K$ is an increasing function of the ratio $\nu_2/\nu_1$ of the first two moments of the distribution of $\nu$, the number of galaxies per cluster, but does not depend on any other property of this distribution. The minimum value of $K$ is unity and is reached only when $\nu = 1$, that is, when the galaxies are not clustered.

(iii) $K$ is an increasing function of the compactness of the clusters.

(iv) If the luminosity law of the galaxies is approximately normal, then $K$ is a decreasing function of the variance in absolute magnitude.

(v) $K$ is a decreasing function of the mean absolute magnitude of the galaxies.

(vi) $K$ is a nondecreasing function of the area $\omega$ on the plate in which the galaxies are counted. When the area of $\omega$ tends to zero, then $K$ converges to unity.

(vii) The value of $K$ when $\omega$ is a square is larger than that for a rectangle of the same area.

* All computations for this paper were performed at the Statistical Laboratory, University of California, with the partial support of the Office of Naval Research. Counts of galaxies were made at the Lick Observatory by C. D. Shane and C. A. Wirtanen. This paper is a joint publication of the Statistical Laboratory and of the Lick Observatory, *Contributions from the Lick Observatory*, Ser. II, No. 54.

(viii) $K$ is an increasing function of the limiting apparent magnitude of the plate, at least over the range studied.

Conclusions (i) through (v) are mainly of theoretical interest (they may be used to estimate the various parameters involved in the distribution of galaxies in space, but this is not recommended). However, conclusions (vi) through (viii) may be verified empirically. The theoretical conclusions regarding the dependence of $K$ upon the size and shape of $\omega$ are found to contradict the conclusions implied by an alternative theory of Chandrasekhar-Münch-Limber (1952, 1953). Empirical values of $K$ obtained from counts of images of galaxies on Lick Observatory plates appear to agree with the theory of the authors. Also, the same empirical values of $K$ appear to agree qualitatively with those found by Zwicky. However, at least within the range of limiting magnitudes investigated, in order to explain the shape of the empirical curves, there is no necessity for the hypothesis of extragalactic absorbing clouds.

REFERENCES

Chandrasekhar, S., and Münch, G. 1952, *Ap. J.*, **115**, 103.
Limber, D. N. 1953, *Ap. J.*, **117**, 134.
Neyman, J., and Scott, E. L. 1952, *Ap. J.*, **116**, 144.
Neyman, J., Scott, E. L., and Shane, C. D. 1953, *Ap. J.*, **117**, 92.
Zwicky, F. 1953, *Helvet. Phys. Acta*, **26**, 241.

Supplement No. 9, Volume I

## THE SPECTRUM OF THE *CN* MOLECULE

A. E. Douglas and P. M. Routly
National Research Council

In the spectrum of a discharge through *He* mixed with a trace of $C_2N_2$, four new band systems of *CN* have been found. These four band systems arise from three new electronic states, designated as the $H^2\Pi_r$, $F^2\Delta_r$, and $D^2\Pi_i$ states. The $H^2\Pi$–$B^2\Sigma$, $F^2\Delta$–$A^2\Pi$, $D^2\Pi$–$A^2\Pi$, and the $D^2\Pi$–$X^2\Sigma$ band systems have been observed, and the rotational fine structures of bands of each system have been analyzed. The $v = 0$ levels of the H, F, and D states are 60938.7, 59682.8, and 53955.0 $cm^{-1}$ above $v = 0$ of the ground electronic state. The $B_0$ values of the H, F, and D states are 1.520, 1.374, and 1.155 $cm^{-1}$, respectively. The red ($A^2\Pi$–$X^2\Sigma$) and the violet ($B^2\Sigma$–$X^2\Sigma$) band systems have been extended by the discovery of a number of new bands of high vibrational quantum number. The rotational lines of the 0–1 sequence of the violet system have been measured. The problem of the dissociation energy of *CN* is discussed, and it is shown that the observed spectrum tends to support the high value (8.3 ev), but no definite conclusion can be reached.

## ERRATUM

On page 181 of volume **120,** line 11 from the top, *read* on the descending branch, *instead of* the ascending branch. On line 13, *read* on the ascending branch, *instead of* the descending branch.

FROM 8X10 TO

# THE OBSERVATORY

FOUNDED 1877

* * *

A Magazine presenting current developments in Astronomy by means of Articles, Correspondence, Notes on discoveries and Reviews of important astronomical books. The papers read at the Meetings (Astronomical & Geophysical) of the Royal Astronomical Society and the discussions which follow are also fully reported.

* * *

*Annual subscription for 6 issues, post free, £1 (U.S.A. and Canada, $3.00) should be sent to*

*The Editors,* ROYAL GREENWICH OBSERVATORY

Herstmonceux Castle, Hailsham, Sussex, England

# THE ASTROPHYSICAL JOURNAL

*announces the publication of*

A GENERAL INDEX, Volumes 76–100

Price: $5.00*

ORDERS NOW ACCEPTED

*Also available:*

GENERAL INDEX, Volumes 1–25 .....$2.50

GENERAL INDEX, Volumes 26–50 .....$2.50

GENERAL INDEX, Volumes 51–75 .....$2.50

* Postage $0.15 per copy extra to foreign addresses.

THE UNIVERSITY OF CHICAGO PRESS

5750 ELLIS AVENUE CHICAGO 37 · ILLINOIS

# THE SUN

## *The Solar System*

### VOLUME I

***Edited by* GERARD P. KUIPER**

*The Sun*, the first of four volumes intended to collect and systematize all significant information on the sun, the planets, the satellites, the comets, and the smaller bodies of the solar system, is written by twenty-three solar physicists from six different countries. It is designed with a dual purpose. On the one hand, it is an invaluable reference handbook for the specialist. On the other hand, it is intelligible to anyone versed in the physical sciences.

*The Sun* covers the divisions of solar physics comprehensively: the solar interior and energy production, the photosphere and the Fraunhofer spectrum; the chromosphere and the solar electrodynamics; and the many modern techniques of solar observation. All are discussed in detail. The book contains, in addition, many new illustrations and over one thousand references to the literature.

New models are given for the solar interior, based on integrations using the latest information on nuclear cross-sections. The photosphere models are critically reviewed, and a new compromise solution is proposed. Similarly, a very recent model for sunspots is reviewed. For both the chromosphere and the corona the temperature and density data are critically examined. An extensive treatment of solar radio astronomy adds significantly to the optical studies of solar phenomena treated in other chapters.

A special feature of *The Sun* is its two tables of solar observatories and their equipment, accessories, and programs. Other features include the latest results on the magnetic field and the solar component of cosmic rays, recent additions to instrumental techniques, and a record, as complete as possible, of the far-ultraviolet solar spectrum photographed on rocket flights.

*Many illustrations, 784 pages, $12.50*

---

**THE UNIVERSITY OF CHICAGO PRESS**